

Distribution Agreement:

In presenting this thesis or dissertation as a partial fulfillment of the requirements for an advanced degree from Emory University, I hereby grant to Emory University and its agents the non-exclusive license to archive, make accessible, and display my thesis or dissertation in whole or in part in all forms of media, now or hereafter known, including display on the world wide web. I understand that I may select some access restrictions as part of the online submissions of this thesis or dissertation. I retain all ownership rights to the copyright of the thesis or dissertation. I also retain the right to use in future works (such as articles or books) all or part of this thesis or dissertation.

Signature

Kathryn M. Chepiga

Date

**PRACTICAL ENHANCEMENT AND APPLICATIONS OF
DIRHODIUM CATALYZED REACTIONS OF DONOR/ACCEPTOR CARBENES**

By

Kathryn M. Chepiga
Doctor of Philosophy

Chemistry

Professor Huw M. L. Davies
Advisor

Professor Frank E. McDonald
Committee Member

Professor Simon B. Blakey
Committee Member

Accepted:

Lisa A. Tedesco, Ph.D.
Dean of the James T. Laney School of Graduate Studies

Date

**PRACTICAL ENHANCEMENT AND APPLICATIONS OF
DIRHODIUM CATALYZED REACTIONS OF DONOR/ACCEPTOR CARBENES**

By

Kathryn M. Chepiga
B.S., Wagner College, 2010

Advisor: Huw M. L. Davies, Ph.D.

An abstract of
a dissertation submitted to the Faculty of the
James T. Laney School of Graduate Studies of Emory University
in partial fulfillment of the requirements for the degree of
Doctor of Philosophy
in Chemistry
2015

Abstract

PRACTICAL ENHANCEMENT AND APPLICATIONS OF DIRHODIUM CATALYZED REACTIONS OF DONOR/ACCEPTOR CARBENES

By Kathryn M. Chepiga

Dirhodium(II) complexes are versatile catalysts for the reactions of diazo compounds, catalyzing a wide array of synthetic transformations such as cyclopropanation, dipolar additions, aromatic cycloadditions, ylide reactions, and C–H, N–H, O–H, and Si–H insertion reactions. $\text{Rh}_2(\text{S-DOSP})_4$ is the most generally effective chiral dirhodium(II) catalyst for highly enantioselective transformations involving donor/acceptor carbenoid intermediates. Several $\text{Rh}_2(\text{S-DOSP})_4$ -catalyzed transformations have been used as key steps in the syntheses of natural products.

The metal-catalyzed decomposition of diazo compounds in the presence of alkenes is a general method for the stereoselective synthesis of cyclopropanes. Rhodium-catalyzed cyclopropanation of donor/acceptor carbenoids is an effective means for the enantioselective synthesis of cyclopropanes with one or more quaternary stereogenic centers. As many cyclopropyl amines are known to have significant CNS activity, we initiated a program to use the cyclopropanation methodology developed in the Davies lab to access novel diarylcyclopropylamines as potential therapeutic agents. For the methodology to be broadly useful in drug discovery, access to a range of diarylcyclopropyl derivatives with high levels of enantioenrichment is required. In Chapter 2, a guide to choosing the optimal chiral dirhodium(II) catalyst for asymmetric cyclopropanation with various types of methyl aryldiazoacetates is presented.

Although dirhodium catalysts can be extremely effective, often giving rise to a broad range of synthetically useful products in high yields with excellent regio-, diastereo- and enantioselectivity, their cost is prohibitive and impedes to their use in pharmaceutical processes. Although considerable advances have been made in the immobilization of various dirhodium(II) catalysts, efforts to alleviate the cost associated with $\text{Rh}_2(\text{S-DOSP})_4$ by synthesis of re-usable heterogeneous derivatives have been met with limited success. Chapter 3 describes how this complication could be alleviated with the development of a broadly-applicable and highly enantioselective immobilized variant of $\text{Rh}_2(\text{S-DOSP})_4$. This $\text{Rh}_2(\text{S-DOSP})_4$ -derivative was immobilized by covalent attachment of a carboxylate ligand to a solid support. Chapter 4 describes the advances made toward increasing the efficiency of $\text{Rh}_2(\text{S-DOSP})_4$ by application of the immobilized $\text{Rh}_2(\text{S-DOSP})_4$ -derivative in continuous flow chemistry.

Finally, the application of dirhodium-stabilized donor/acceptor carbenoids the syntheses of natural products was explored in Chapter 5. As $\text{Rh}_2(\text{S-TCPTAD})_4$ has been shown to be an effective chiral catalyst for different types of C–H functionalization reactions, this catalyst was applied towards the syntheses of marine alkaloids dictyodendrins A and F which are known to possess inhibitory activity against telomerase and BACE-1 respectively, making them of interest for use as potential targets for cancer chemotherapy and treatment Alzheimer's disease respectively. Syntheses of dictyodendrin A and F were achieved by sequential C–H functionalization reactions utilizing a combination of different C–H coupling methodologies.

**PRACTICAL ENHANCEMENT AND APPLICATIONS OF
DIRHODIUM CATALYZED REACTIONS OF DONOR/ACCEPTOR CARBENES**

By

Kathryn M. Chepiga
B.S., Wagner College, 2010

Advisor: Huw M. L. Davies, Ph.D.

A dissertation submitted to the Faculty of the
James T. Laney School of Graduate Studies of Emory University
in partial fulfillment of the requirements for the degree of
Doctor of Philosophy
in Chemistry
2015

Acknowledgments

First, I would like to thank Dr. Huw Davies for accepting me to conduct my doctoral work into his laboratory. I remember how overjoyed I was when he told me I could join his lab. I cannot thank him enough for his immeasurable support and mentorship. The opportunities which he has given me throughout my graduate career have opened doors to me which have helped me to defined my future and secure the post-doctoral position of my dreams. Also, the stereoselective synthesis, organometallics, and C–H functionalization courses that he taught laid the foundation for my graduate work. I would also like to thank Dr. Davies on a personal level along with his wife, Angela Davies, for always treating me like family at Christmas parties in their home as well as at conferences in Colorado and San Francisco.

My other two committee members, Dr. Frank McDonald and Dr. Simon Blakey, also served as wonderful mentors to me throughout my time at Emory. Their feedback at my yearly reports and original research proposal was extremely helpful. Also, I am thankful for the knowledge that I gained in the courses I took with them including Dr. McDonald's synthesis course which later helped me to think through my own work on a total synthesis project as well as his organometallics course which guided me in my catalyst design projects. Additionally, Dr. Blakey's C–H functionalization course sparked my interest in this subject area which I plan to stay closely connected to. Dr. Lanny Liebeskind, who taught me spectroscopy, also served as a great mentor. I appreciate our discussions regarding my post-doctoral application and I hope to see him during my post-doctoral stay in Münster. Dr. Chris Scarborough, who taught me inorganic chemistry, provided helpful advice with my original research proposal as well as with my preparations for my post-doctoral position. I am also thankful to Dr. Cora MacBeth for career advice as well as to Dr. Patricia Marsteller for teaching me pedagogical skills during my

NSF PRISM teaching fellowship. Also, completion of my doctoral work would not have been possible without the support of the wonderful staff of the Emory University Chemistry Department including Ann Dasher, Steve Krebs, Patti Barnett, Dr. Shaoxiong Wu, Dr. Bing Wang and Dr. Fred Strobel.

My experiences in our collaboration with Dr. Kenichiro Itami have truly shaped my graduate career as well as my post-doctoral plans. Dr. Kenichiro Itami's enthusiasm for chemistry motivated me and his kind nature as well as project advice allowed for me to participate in a fruitful collaboration which resulted in the completion of a total synthesis project over a short research exchange. His support has ultimately allowed me to secure my post-doctoral position. Also, Dr. Junichiro Yamaguchi was the mastermind behind project and his expertise in the field of total synthesis amazes me. I am also thankful for my friendship with Dr. Atsushi Yamaguchi which resulted from this collaboration. His hard work and determination are inspirational. Finally, I am very grateful to Ms. Rika Kato for organizing my trip in Japan as well as taking care of me throughout my stay there. The four months that I spent in the Itami lab were some of the best times of my life and I will cherish the memories and the friendships that I formed there forever. I would like to thank the entire Itami lab for their kindness, helpfulness and for all that they taught me. They are the hardest working yet most fun-loving group of people that I have had the pleasure of meeting and I wish them the greatest success and happiness in their future.

My involvement in initiating our collaboration with Dr. Christopher Jones re-defined my graduate career. His expertise in the field of heterogeneous catalysis allowed for our ultimate goal of conducting flow chemistry to come to fruition. The post-doctoral fellows in his laboratory with whom I collaborated on this project included Dr. Yan Feng who immobilized our catalysts, Dr. Nicholas Brunelli who designed the flow reactor and Dr. Eric Moschetta who

optimized the flow conditions. They taught me more about chemical engineering than I ever imagined I would learn in an organic chemistry Ph.D. program and our efforts have resulted in groundbreaking publications which are tip of the iceberg on this continuing collaboration.

As the Davies group has been my home for almost five years, I would like to thank all Davies group members past and present for the times we spent together. First and foremost, I must sing my praises of Dr. Daniel Morton. The moment I expressed my enthusiasm for participating in the NSF SAVI program, he advocated for me and ultimately organized my trip to Japan. In my first year here, we worked in adjacent fume hoods and he spent much of his time showing me the ropes. Our original research proposal brainstorming sessions as well as his thesis corrections were invaluable. Next, I must thank my first graduate student mentor and friend in the Davies lab, Dr. Changming Qin, who imparted his knowledge of dirhodium catalysis to me. I am grateful to have had the opportunity to shadow him and our work together ultimately resulted my first publication. Another mentor of mine from my early days in the Davies lab is Dr. Fred Briones. Our friendship grew through our late nights in the lab and trips to church. Most importantly, his post-doctoral application tips were a huge help and resulted in an exciting trip to Boston for an interview. I am also thankful to several friends who completed post-doctoral fellowships in the Davies lab, including Dr. Damien Valette, Dr. Austin Smith, and Dr. Jillian Spangler, for their project advice and help with problem solving when I was studying for exams. I would like to thank former group members Dr. Felicia Fullilove, Dr. Pablo Guzman, Dr. Joshua Alford and Dr. David Guptill for all of their help in the lab as well as for their kind-heartedness and encouragement. I am very excited that Dr. Solymar Negretti continued my work in our collaborative project with Dr. Christopher Jones while I was working in Japan and am happy that her efforts led to our second publication in this collaboration. Dr. Monya Ruffin's

mentorship while I served as chair of the student advisory board to the NSF CCHF is much appreciated and her positive attitude always brightened my days. I thank Dr. Cecilia Tortoreto and Dr. Jeff Mighion for proofreading my thesis as well as all of the Davies group members including Dr. Sandeep Raikar, Dr. LaDena Bolton, Liangbing Fu, Kuangbiao Liao, Hyun Min Park, Matt Chuba, and Wenbin Liu for their help and support. My undergraduate students Michael Wade Wolfe and Wayne Chen as well as my high school students Jessie Yuan and Fatima Kamal reinvigorated my love for chemistry and I wish them all the greatest success in their future. Nina Mace Weldy, my best friend in the graduate program, has been a huge influence on me throughout graduate school from studying for exams and comes together to introducing me to Passion City Church to sharing life updates at weekly lunches. It is wonderful to see how far we have both come from our first year here and I look forward to seeing where chemistry and life take us in the future. I am grateful for my friends in other labs in the department including Dr. Santhosh Kumar and Dr. Mark Baillie as well as Dr. Rose Santangelo for serving as my graduate student mentor during my first rotation in Dr. Dennis Liotta's lab and for including me in her published work.

I am already extremely grateful to Dr. Frank Glorius for providing me with a post-doctoral position in his laboratory after graduation. His support of me over the past months has inspired me to complete my original research proposal and dissertation in a timely fashion and I very much look forward to the next step of my chemistry career under his guidance.

Christopher and Jennifer Cappelli, my best friends from Wagner College, were my original reason for visiting Emory University. I am so happy that they encouraged me to apply to this graduate program five years ago and that we were able to continue to grow our friendship after college. Also, throughout my time in Atlanta, I have made many new friends through Chris and

Jen, the best of which being my friendship with Priya D'Souza. I cannot thank Priya enough for all of the kind and thoughtful things she has done for me over these past years to keep me going through hard times. Priya, Chris and Jen are my Atlanta family and I will cherish all the memories we have made here and I am excited to make new memories overseas together soon.

My best friend from childhood who is more like a sister to me, Delia Montalbano, has maintained our friendship despite great distance. I would like to show my appreciation to her and her parents as well as to Jacki Cashin who make it as though we never spent a single day apart when I go home to visit. I thank Delia for staying a major part of my life every day. We have grown throughout life together and I am so happy to see us both now nearing the end of our formal educations and finally entering into the real world together. I am proud of the both of us and wish her the utmost success in nursing as well as all the happiness in the world in her future.

My boyfriend Thomas Özgün is my greatest inspiration. He truly puts his all into everything he does, in every aspect of his life, and makes me a better person by encouraging me to do the same. I cannot possibly begin to thank him enough for all he has done for me. His advice on my post-doctoral application and my original research proposal as well as his help in correcting this thesis have helped me immensely in completing my Ph.D. Thomas is the light of my life. I thank him for making this year the best of my life and look forward to our future together.

My loving family is the ultimate support system which fueled me to every day. Most of all, my mom and dad have supported me throughout my entire life, which has brought me to where I am today in completing my graduate education. They make time to talk to me every day, morning and night, and always encourage me to push forward no matter how difficult something may seem. They instilled in me the values of determination, diligence, persistence, perseverance and grit, without which graduate school would have been impossible.

For my parents

Table of Contents

Chapter I: Introduction to Dirhodium(II) Catalysis.....	1
1.1 Dirhodium(II) Catalysts.....	1
1.2 Application of Dirhodium(II) Catalysts.....	3
Chapter II: Guide to Enantioselective Dirhodium(II) Catalyzed Cyclopropanation of Aryldiazoacetates with Styrene Derivatives.....	9
2.1 Dirhodium(II) Binaphthylphosphate Complexes in Chiral Catalysis.....	9
2.2 3, 3' and 6,6'-Substituted Dirhodium(II) Binaphthylphosphate Derivatives.....	12
2.3 Dirhodium(II) Binaphthylphosphate Derivatives with Mixed Ligands.....	14
2.4 Donor/Acceptor Diazo Compounds in Dirhodium(II) Binaphthylphosphate Catalysis and Shortcomings of Rh ₂ (<i>S</i> -DOSP) ₄ in asymmetric cyclopropanation reactions.....	16
2.5 Introduction to Rh ₂ (<i>R</i> -BNP) ₄ -Catalyzed Cyclopropanation of Donor/Acceptor Substituted Diazo Compounds.....	18
2.6 Rh ₂ (<i>R</i> -BNP) ₄ -Catalyzed Cyclopropanation of 3,4-Dimethoxyphenyldiazoacetate and its Derivatives.....	20
2.7 Application of Rh ₂ (BNP) ₄ -Catalyzed Cyclopropanation to the Synthesis of 5-HT _{2A} Antagonist Biaryl Cyclopropylmethylamines.....	29
2.8 Development of a Guide to Choosing the Best Dirhodium(II) Catalyst to use for Enantioselective Cyclopropanation of Aryldiazoacetates with Styrene Derivatives..	31
2.9 Conclusion.....	37
2.10 Experimental Section.....	38
Chapter III: Immobilized Chiral Dirhodium(II) Catalysts for Enantioselective Carbenoid Reactions.....	91
3.1 Introduction to Supported Heterogeneous Catalysis.....	92
3.2 Design Elements of Supported Catalysts.....	93

3.3 Supported Dirhodium(II) Catalysts.....	96
3.4 Supported Dirhodium(II) Tetracarboxylate Catalysts.....	102
3.4 Introduction to Methods for the Immobilization of Rh ₂ (<i>S</i> -DOSP) ₄	110
3.5 Efforts Toward the Synthesis of a Rh ₂ (<i>S</i> -DOSP) ₄ -Derivative Immobilized by having all Four Ligands Covalently Bound to a Support.....	115
3.6 Syntheses and Testing of Rh ₂ (<i>S</i> -DOSP) ₄ -Derivatives Immobilized by a Single Ligand Covalently Bound to a Polymeric Support.....	120
3.7 Syntheses and Testing of Rh ₂ (<i>S</i> -DOSP) ₄ -Derivatives Immobilized by a Single Ligand Covalently Bound to a Silica Support.....	128
3.8 Determining the Ideal Silica Support, Recovery Method, and Catalyst Loading for Silica-Immobilized-Rh ₂ (<i>S</i> -DOSP) ₄ Catalysis.....	133
3.9 Implementing a Long Alkyl Spacer Between the Silica Support and the Active Dirhodium(II) Catalyst Core.....	138
3.10 Application of Recyclable Silica-Immobilized-Rh ₂ (<i>S</i> -DOSP) ₄ in a Broad Range of Enantioselective Reactions.....	149
3.11 Conclusion.....	154
3.12 Experimental Section.....	156
Chapter IV: The Application of Immobilized Chiral Dirhodium(II) Catalysts in Continuous Flow Processing.....	193
4.1 Introduction to Continuous Flow Chemistry.....	194
4.2 Diazo Compounds in Flow Chemistry.....	195
4.3 Dirhodium(II) Catalysis in a Continuous Flow Reactor.....	197
4.4 Exploratory Studies Conducted in Batch Toward the use of Silica-Immobilized-Rh ₂ (<i>S</i> -DOSP) ₄ -Derivatives in a Continuous Flow Reactor.....	200
4.5 The use of Cellulose Acetate Fiber-Immobilized-Rh ₂ (<i>S</i> -DOSP) ₄ -derivatives in a Continuous Flow Reactor.....	202
4.6 Composite Polymer/Oxide Hollow Fiber Contactors: Versatile and Scalable Flow Reactors for Heterogeneous Dirhodium(II) Catalyzed Reactions.....	210

4.7 Conclusion.....	216
4.8 Experimental Section.....	217
Chapter V: Concise Synthesis of Dictyodendrin A by a Sequential C–H Functionalization Strategy.....	228
5.1 Introduction to the Dictyodendrin Marine Alkaloids.....	228
5.2 Previous Total Syntheses of the Dictyodendrins.....	229
5.3 Exploratory Studies Toward the Synthesis of Dictyodendrin A.....	234
5.4 Formal Synthesis of Dictyodendrin A.....	262
5.5 Total Synthesis of Dictyodendrin F.....	276
5.6 Conclusion.....	277
5.7 Experimental Section.....	278

List of Figures

Figure 1.1 Most common rhodium(II) catalysts for the decomposition of donor/acceptor diazos.....	3
Figure 1.2 Structures of chiral dirhodium catalysts used in these studies.....	7
Figure 2.1 Types of dirhodium(II) catalysts.....	10
Figure 2.2 Dirhodium(II) tetrakisbinaphthylphosphate ($\text{Rh}_2(\text{R-BNP})_4$ and $\text{Rh}_2(\text{S-BNP})_4$).....	10
Figure 2.3 3,3'-substituted $\text{Rh}_2(\text{R-BNP})_4$ -derivative ($\text{Rh}_2(\text{R-DMBNP})_4$).....	12
Figure 2.4 6,6'-substituted $\text{Rh}_2(\text{R-BNP})_4$ -derivatives ($\text{Rh}_2(\text{R-DBBNP})_4$ and $\text{Rh}_2(\text{R-DDBNP})_4$).....	13
Figure 2.5. $\text{Rh}_2(\text{R-BNP})_4$ -derivative with mixed ligands (<i>cis</i> - $\text{Rh}_2(\text{S-BNP})_2(\text{HCO}_3)_2$).....	14
Figure 2.6 Biologically active biaryl cyclopropylmethylamine scaffold for 5-HT _{2A} receptor antagonists.....	29
Figure 2.7 Dirhodium(II) catalysts used in this study.....	32
Figure 3.1 Methods for chiral catalyst immobilization.....	93
Figure 3.2 Chiral dirhodium(II) catalysts which have been successfully immobilized.....	96
Figure 3.3 Comparison of the previously reported methods for immobilization of dirhodium(II) catalysts.....	110
Figure 3.4 Variability in enantioinduction observed with flexible polymeric $\text{Rh}_2(\text{S-DOSP})_4$ -resin.....	128
Figure 3.5 Variability in enantioinduction observed with SBA-15-supported $\text{Rh}_2(\text{S-DOSP})_4$ -derivative.....	131
Figure 3.6 Design of long-chain immobilizable $\text{Rh}_2(\text{S-DOSP})_4$ -derivative.....	140
Figure 3.7 Filtration test demonstrating lack of catalytic activity in the absence of heterogeneous catalyst.....	150
Figure 3.8 Breadth of enantioselective catalysis by recyclable silica-immobilized- $\text{Rh}_2(\text{S-DOSP})_4$ -derivative.....	155
Figure 4.1 General schematic description of a continuous flow reactor.....	194

Figure 4.2	Chiral dirhodium(II) catalysts which have been successfully derivitized, immobilized, and applied in continuous flow reactors.....	198
Figure 4.3	Ideal conditions for continuous flow processing employing immobilized– $\text{Rh}_2(\text{S-DOSP})_4$ –derivative.....	203
Figure 4.4	Continuous flow reactor design for porous hollow fiber-supported– $\text{Rh}_2(\text{S-DOSP})_4$ –derivative.....	204
Figure 4.5	Photograph of the inside of the continuous flow reactor containing porous hollow fiber-supported– $\text{Rh}_2(\text{S-DOSP})_4$ –derivative.....	208
Figure 4.6	Photograph of the stainless steel reactor, heating jacket, and solvent feed flasks and pumps.....	209
Figure 4.7	Close-up photograph of the stainless steel reactor equipped with heating jacket and HPLC valve.....	210
Figure 4.8	Schematic description of the radial flow hollow fiber flow reactor.....	211
Figure 4.9	The effect of increasing the TON on the % ee of CA- $\text{Rh}_2(\text{S-DOSP})_4$ –catalyzed intermolecular asymmetric cyclopropanation.....	216
Figure 5.1	A summary of the structures and biological activities of the dictyodendrins.....	229
Figure 5.2	Previously reported strategies for the syntheses of the dictyodendrins.....	230
Figure 5.3	Fürstner’s common intermediate for the syntheses of dictyodendrins A-E.....	231
Figure 5.4	Dirhodium(II) catalysts screened in the α -selective pyrrole functionalization.....	264
Figure 5.5	The four types of dictyodendrins: classification according to oxidation state and the C2 substituent of the central pyrrole.....	266
Figure 5.6	Summary of the formal synthesis of dictyodendrin A and total synthesis of dictyodendrin F.....	278

List of Schemes

Scheme 1.1 Synthetic routes to diazo compounds and their decomposition to metallocarbenes.....	1
Scheme 1.2 Reactivity of metallocarbenes.....	2
Scheme 1.3 Methodology development with the use of donor/acceptor metallocarbenes.....	4
Scheme 1.4 Applications of donor/acceptor metallocarbenes in drug discovery.....	5
Scheme 1.5 Applications of donor/acceptor metallocarbenes in total syntheses.....	6
Scheme 2.1 Dipolar cycloaddition catalyzed by $\text{Rh}_2(\text{S-BNP})_4$	11
Scheme 2.2 Intramolecular aziridination catalyzed by $\text{Rh}_2(\text{R-BNP})_4$	11
Scheme 2.3 Sulfur ylide/ [2,3]-sigmatropic rearrangement catalyzed by $\text{Rh}_2(\text{R-BNP})_4$	12
Scheme 2.4 [1,3]-Dipolar cycloaddition catalyzed by $\text{Rh}_2(\text{R-BNP})_4$ -derivatives.....	13
Scheme 2.5 <i>cis</i> - $\text{Rh}_2(\text{S-BNP})_2(\text{HCO}_3)_2$ -catalyzed 2,3-sigmatropic rearrangements.....	15
Scheme 2.6 <i>cis</i> - $\text{Rh}_2(\text{S-BNP})_2(\text{HCO}_3)_2$ -catalyzed intramolecular C–H insertion.....	15
Scheme 2.7 <i>cis</i> - $\text{Rh}_2(\text{S-BNP})_2(\text{HCO}_3)_2$ -catalyzed aromatic cycloaddition.....	16
Scheme 2.8 Reactivity and selectivity of $\text{Rh}_2(\text{S-DOSP})_4$ in asymmetric cyclopropanation.....	17
Scheme 2.9 Route to cyclopropyl amines from aryldiazoacetates.....	30
Scheme 2.10 Synthetic route to 5-HT _{2A} receptor antagonist analogue.....	31
Scheme 3.1 Methods for grafting the catalyst to the support and for polymerization.....	95
Scheme 3.2 Bergbreiter's route to polyethylene carboxylates.....	97
Scheme 3.3 Polyethylene-supported $\text{Rh}_2(\text{OAc})_4$	97
Scheme 3.4 First Immobilized Dirhodium System Bergbreiter's $\text{Rh}_2(\text{PE-CO}_2)_4$	98
Scheme 3.5 Immobilized (<i>S</i>)-PYCA ligand.....	98
Scheme 3.6 First immobilized chiral dirhodium(II) system: $\text{PE-Rh}_2(\text{S-PYCA})_4$	98
Scheme 3.7 Reactivity of $\text{PE-Rh}_2(\text{S-PYCA})_4$	99

Scheme 3.8	NovaSyn Tentagel immobilized Rh ₂ (<i>S</i> -MEPY) ₄ -derivative.....	100
Scheme 3.9	Merrifield immobilized Rh ₂ (<i>S</i> -MEPY) ₄ -derivative.....	100
Scheme 3.10	Comparison of NovaSyn Tentagel and Merrifield immobilized Rh ₂ (<i>S</i> -MEPY) ₄ -derivatives.....	101
Scheme 3.11	General structure of mixed ligand dirhodium(II) complexes.....	101
Scheme 3.12	Example of an immobilized azetidinone mixed ligand dirhodium(II) complex...	102
Scheme 3.13	Immobilized azetidinone mixed ligand dirhodium(II)-catalyzed C-H insertion.	102
Scheme 3.14	Argopore Wang-pyridine linker.....	103
Scheme 3.15	Coordination method of immobilization for dirhodium(II) catalysts.....	103
Scheme 3.16	Suspension copolymerization of Rh ₂ (<i>S</i> -PTTL) ₄	108
Scheme 3.17	Synthesis of immobilizable chiral salen ligand.....	111
Scheme 3.18	Free radical polymerization immobilization strategy.....	112
Scheme 3.19	Catalyst immobilization by grafting to a functionalized silica surface	113
Scheme 3.20	Free radical polymerization of functionalized catalyst, styrene, and divinylbenzene (DVB).....	114
Scheme 3.21	Late-stage modification route to immobilizable Rh ₂ (<i>S</i> -DOSP) ₄ -derivative.....	116
Scheme 3.22	Attempt towards Pd-catalyzed cross-coupling directly on dirhodium(II) tetraproline.....	116
Scheme 3.23	Attempted synthesis of allylbenzene-substituted Rh ₂ (<i>S</i> -DOSP) ₄ -derivative immobilized by all four ligands.....	117
Scheme 3.24	Attempted synthesis of Rh ₂ (<i>S</i> -DOSP) ₄ -derivative immobilized by Huisgen cycloaddition of the azide group on all four ligands with surface alkynes.....	118
Scheme 3.25	Attempted synthesis of styryl-substituted Rh ₂ (<i>S</i> -DOSP) ₄ -derivative immobilizable at all four ligands.....	119
Scheme 3.26	Possible deactivation route of Rh ₂ (<i>S</i> -DOSP) ₄ -derivative immobilized by all four ligands.....	120

Scheme 3.27	Synthesis of highly-crosslinked Rh ₂ (S-DOSP) ₄ -derivative immobilized at a single ligand by polymerization.....	125
Scheme 3.28	Synthesis of flexible polymeric Rh ₂ (S-DOSP) ₄ -derivative immobilized at a single ligand by polymerization.....	126
Scheme 3.29	Rh ₂ (S-DOSP) ₄ immobilization onto 60Å mesoporous SBA-15 silica.....	130
Scheme 3.30	Protection of the free hydroxyl groups of SBA-15 surface.....	132
Scheme 3.31	General synthetic route silica-supported Rh ₂ (S-DOSP) ₄ -derivatives.....	134
Scheme 3.32	Proposed synthetic route to long-chain immobilized Rh ₂ (S-DOSP) ₄ -derivative.....	141
Scheme 3.33	Attempted synthesis of long-chain immobilized Rh ₂ (S-DOSP) ₄ -derivative via sequential desymmetrization of a diyne.....	142
Scheme 3.34	Synthesis of long-chain immobilized Rh ₂ (S-DOSP) ₄ -derivative.....	144
Scheme 3.35	Possible deactivation route of long-chain immobilized Rh ₂ (S-DOSP) ₄ -derivative.....	147
Scheme 3.36	Cyclopropanation and cyclopropanation catalyzed by CS-2129-supported Rh ₂ (S-DOSP) ₄ -derivative.....	152
Scheme 3.37	Ylide formation / [2,3] sigmatropic rearrangement catalyzed by CS-2129-supported Rh ₂ (S-DOSP) ₄ -derivative.....	153
Scheme 3.38	C-H functionalization catalyzed by CS-2129-supported Rh ₂ (S-DOSP) ₄ -derivative.....	154
Scheme 4.1	Flow synthesis of diazoketones.....	196
Scheme 4.2	Copper-catalyzed decomposition of diazoketones in flow.....	197
Scheme 4.3	First continuous flow system with a polymer-supported dirhodium(II) catalyst and its application in cycloaddition catalysis.....	198
Scheme 4.4	Schematic set of the first continuous flow system with a polymer-supported dirhodium(II) catalyst.....	199
Scheme 4.5	Rh ₂ (S-DOSP) ₄ immobilization onto cellulose acetate hollow fibers.....	205
Scheme 4.6	Synthesis of composite polymer/oxide hollow fiber-cellulose acetate immobilized-Rh ₂ (S-DOSP) ₄ -derivative.....	206

Scheme 4.7	C–H insertion with CA-Rh ₂ (S-DOSP) ₄	215
Scheme 5.1	Tokuyama’s retrosynthetic analysis of dictyodendrin A.....	232
Scheme 5.2	Tokuyama’s benzyne-mediated one-pot indole formation / cross-coupling reaction.....	233
Scheme 5.3	Davies / Itami route to access the dictyodendrins via sequential regioselective C–H functionalizations.....	235
Scheme 5.4	Controlling factors for rhodium carbenoid selectivity in reaction with pyrroles: cyclopropanation vs. C–H functionalization.....	237
Scheme 5.5	Steglich’s synthesis of ningalin C via a rhodium carbenoid mediated α -functionalization of β,γ -diarylated <i>N</i> -alkylpyrrole.....	239
Scheme 5.6	Davies / Itami retro-synthetic route to dictyodendrin A via an α -selective double carbenoid insertion followed by a β -selective arylation.....	242
Scheme 5.7	Attempts toward the synthesis of dictyodendrin A via an α -selective double carbenoid insertion followed by a β -selective arylation.....	243
Scheme 5.8	C–H functionalization of an unsubstituted <i>N</i> -alkylpyrrole with an electron-rich methyl ester-substituted donor/acceptor-diazo compound.....	244
Scheme 5.9	Davies / Itami retro-synthetic route to dictyodendrin A via β -selective arylation followed by an initial α -selective carbenoid insertion, carbazole closure, and a final α -selective carbenoid insertion.....	245
Scheme 5.10	β -selective arylation of pyrroles by RhCl(CO){P[OCH(CF ₃) ₂] ₃ } ₂	246
Scheme 5.11	A possible mechanism of β -selective pyrrole C–H arylation by RhCl(CO){P[OCH(CF ₃) ₂] ₃ } ₂	247
Scheme 5.12	Proposed mechanism for α -selective carbenoid insertion with the use of a trichloroethyl ester-substituted donor/acceptor rhodium carbenoid.....	249
Scheme 5.13	Attempts toward the synthesis of an electron-rich trichloroethyl ester-substituted donor/acceptor-diazo compound.....	250
Scheme 5.14	Mechanistic hypothesis for problematic diazo transfer to electron-rich donor/acceptor-diazo compounds bearing a bulky ester functionality.....	251
Scheme 5.15	<i>o</i> -NBSA-mediated diazo transfer to give an electron-rich trichloroethyl ester-substituted donor/acceptor-diazo compound.....	252

Scheme 5.16	Synthesis of an electron-poor trichloroethyl ester-substituted donor/acceptor-diazo compound.....	252
Scheme 5.17	C–H functionalization of an unsubstituted <i>N</i> -alkylpyrrole with an electron-poor trichloroethyl ester-substituted donor/acceptor-diazo compound.....	254
Scheme 5.18	C–H functionalization of an arylated <i>N</i> -alkylpyrrole with an electron-poor methyl ester-substituted donor/acceptor-diazo compound.....	255
Scheme 5.19	Attempts toward the conversion of the methyl ester to a Weinreb amide for installation of the indole moiety of dictyodendrin A.....	255
Scheme 5.20	Synthesis of Weinreb amide-substituted aryldiazo.....	256
Scheme 5.21	Pyrrole C–H functionalization with Weinreb amide-substituted aryldiazo.....	257
Scheme 5.22	Modified retro-synthetic route to dictyodendrin A featuring an α -selective carbenoid insertion with an α -ketoindole aryldiazo.....	258
Scheme 5.23	Attempted conversion of the Weinreb amide to an α -ketoindole functionality for installation of the indole moiety of dictyodendrin A.....	258
Scheme 5.24	Attempted synthesis of precursor to an electron-poor α -ketoindole-substituted donor/acceptor-diazo compound.....	259
Scheme 5.25	Synthesis of an electron-poor α -ketoindole-substituted donor/acceptor-diazo compound.....	259
Scheme 5.26	Synthesis of an electron-poor α -ketophenyl-substituted donor/acceptor-diazo compound.....	261
Scheme 5.27	Attempted pyrrole C–H functionalization with an electron-poor α -ketophenyl-substituted donor/acceptor-diazo compound.....	261
Scheme 5.28	Attempted synthesis of an electron-rich α -ketoindole-substituted donor/acceptor-diazo compound.....	262
Scheme 5.29	Attempted <i>o</i> -NBSA–mediated diazo transfer to electron-rich α -ketoindole.....	262
Scheme 5.30	Davies / Itami retro-synthetic route to dictyodendrin A via β -selective arylation followed by sequential α -selective carbenoid insertions.....	263
Scheme 5.31	Davies / Itami retro-synthetic route to dictyodendrin A via β -selective arylation followed by an α -selective double carbenoid insertion.....	267

Scheme 5.32	Direct bromination and Suzuki coupling of the 4-position of the trifunctionalized <i>N</i> -alkylpyrrole.....	270
Scheme 5.33	Attempted Sc(OTf) ₃ -mediated cyclization to form the pyrrolo[2,3- <i>c</i>]carbazole core of dictyodendrin A.....	270
Scheme 5.34	Attempted 6π-electrocyclization to form the pyrrolo[2,3- <i>c</i>]carbazole core of dictyodendrin A via a (trimethylsilyl)ketene acetal intermediate.....	271
Scheme 5.35	Completion of the formal synthesis of dictyodendrin A: protection / deprotection sequence to Tokuyama intermediate.....	273
Scheme 5.36	Conversion of Tokuyama's intermediate to dictyodendrin A.....	274
Scheme 5.37	Formal synthesis of dictyodendrin A by sequential C–H functionalization strategy.....	275
Scheme 5.38	Total synthesis of dictyodendrin F from a common intermediate.....	276
Scheme 5.39	Proposed mechanism of the hydration/ retro-aldol condensation to give dictyodendrin F.....	277

List of Tables

Table 2.1 Donor/acceptor diazo compound screening in the asymmetric cyclopropanation of aryldiazoacetates with styrene by $\text{Rh}_2(\text{R-BNP})_4$..	19
Table 2.2 $\text{Rh}_2(\text{R-BNP})_4$ vs. $\text{Rh}_2(\text{R-DOSP})_4$ in the asymmetric cyclopropanation of 3,4-dimethoxyphenyldiazoacetate with styrene.....	20
Table 2.3 Influence of the position of the methoxy substituent(s) on the diazo compound on $\text{Rh}_2(\text{R-BNP})_4$ -catalyzed asymmetric cyclopropanation of aryldiazoacetates with styrene.....	21
Table 2.4 Influence of the substitution pattern of methoxy substituent(s) on the diazo compound.....	22
Table 2.5 Explorations into the governing forces behind enantioselectivity under $\text{Rh}_2(\text{R-BNP})_4$ -catalysis.....	23
Table 2.6 $\text{Rh}_2(\text{R-BNP})_4$ -catalyzed decomposition of vinyl diazoacetates.....	24
Table 2.7 The effect of added steric bulk on ester of the diazo compound.....	25
Table 2.8 Examination of $\text{Rh}_2(\text{R-BNP})_4$ loading.....	26
Table 2.9 Effect of varying the equivalents of styrene used.....	27
Table 2.10 Screening of styrene derivatives in $\text{Rh}_2(\text{R-BNP})_4$ -catalyzed cyclopropanation.....	28
Table 2.11 Examination of the influence of substitution on aryldiazoacetate.....	35
Table 2.12 A guide to chiral dirhodium(II) catalyzed cyclopropanation.....	37
Table 3.1 Immobilized $\text{Rh}_2(\text{S-TBSP})_4$ and $\text{Rh}_2(\text{S-biTISP})_4$ in cyclopropanation.....	104
Table 3.2 Catalyst recycling study in cyclopropanation with various diazoacetates.....	105
Table 3.3 C-H insertion by immobilized $\text{Rh}_2(\text{S-DOSP})_4$ -derivative.....	105
Table 3.4 Application of coordination method of immobilization to a variety of dirhodium(II) catalysts.....	106
Table 3.5 Deactivation of homogeneous dirhodium(II) catalysts by a pyridine derivative.....	107
Table 3.6 Catalyst recycling study of immobilized $\text{Rh}_2(\text{S-PTTL})_4$ -derivative.....	109
Table 3.7 Immobilization of <i>S</i> -DOSP ligand by free radical polymerization.....	121

Table 3.8 Asymmetric cyclopropanation catalyzed by a loosely cross-linked $\text{Rh}_2(\text{S-DOSP})_4$ -resin.....	123
Table 3.9 $\text{Rh}_2(\text{S-DOSP})_4$ under AIBN-initiated free radical polymerization conditions.....	124
Table 3.10 Asymmetric cyclopropanation catalyzed by a highly cross-linked $\text{Rh}_2(\text{S-DOSP})_4$ -resin.....	125
Table 3.11 Asymmetric cyclopropanation catalyzed by a flexible polymeric $\text{Rh}_2(\text{S-DOSP})_4$ -resin.....	127
Table 3.12 $\text{Rh}_2(\text{S-DOSP})_4$ performance with the addition of 60Å silica gel.....	129
Table 3.13 Asymmetric cyclopropanation catalyzed by SBA-15-supported $\text{Rh}_2(\text{S-DOSP})_4$ -derivative.....	131
Table 3.14 Asymmetric cyclopropanation catalyzed by TMS-protected SBA-15-supported $\text{Rh}_2(\text{S-DOSP})_4$ -derivative.....	133
Table 3.15 Asymmetric cyclopropanation catalyzed by CS-2129-supported $\text{Rh}_2(\text{S-DOSP})_4$ -derivative at low catalyst loading.....	135
Table 3.16 Varying the method of catalyst recovery for asymmetric cyclopropanation by CS-2129-supported $\text{Rh}_2(\text{S-DOSP})_4$ -derivative at low catalyst loading.....	136
Table 3.17 The effect of varying the method of catalyst recovery on the reactivity and selectivity of asymmetric cyclopropanation by CS-2129-supported $\text{Rh}_2(\text{S-DOSP})_4$ -derivative.....	137
Table 3.18 Varying the method of catalyst recovery and substrate for asymmetric cyclopropanation by CS-2129-supported $\text{Rh}_2(\text{S-DOSP})_4$ -derivative.....	138
Table 3.19 Asymmetric cyclopropanation catalyzed by long-chain immobilized $\text{Rh}_2(\text{S-DOSP})_4$ -derivative.....	145
Table 3.20 Asymmetric cyclopropanation catalyzed by CS-2129-supported $\text{Rh}_2(\text{S-DOSP})_4$ -derivative.....	149
Table 4.1 The effect of varying the support-system on the reactivity and selectivity of asymmetric cyclopropanation by immobilized $\text{Rh}_2(\text{S-DOSP})_4$ -derivatives.....	201
Table 4.2 Application of C803-supported- $\text{Rh}_2(\text{S-DOSP})_4$ in the synthesis of <i>S</i> -BTPCP ligand.....	202

Table 4.3 Intermolecular asymmetric cyclopropanation catalyzed by cellulose acetate immobilized-Rh ₂ (<i>S</i> -DOSP) ₄ -derivative in batch.....	207
Table 4.4 Intramolecular C–H insertion catalyzed by cellulose acetate immobilized-Rh ₂ (<i>S</i> -DOSP) ₄ -derivative in batch.....	207
Table 4.5 Intermolecular asymmetric cyclopropanation catalyzed by Torlon and cellulose acetate immobilized-Rh ₂ (<i>S</i> -DOSP) ₄ -derivatives in flow.....	212
Table 4.6 The effect of varying the sweep and reactant flow rate on intermolecular asymmetric cyclopropanation catalyzed by cellulose acetate immobilized-Rh ₂ (<i>S</i> -DOSP) ₄ -derivative in flow.....	212
Table 4.7 Preliminary catalyst recycling study of cellulose acetate immobilized-Rh ₂ (<i>S</i> -DOSP) ₄ -derivative in the asymmetric cyclopropanation of styrene with phenyldiazoacetate.....	213
Table 4.8 Scope of cyclopropanation with donor/acceptor-substituted diazo compounds using CA-Rh ₂ (<i>S</i> -DOSP) ₄ embedded in the walls of hollow fibers.....	214
Table 4.9 High turnover number and recycling study with CA-Rh ₂ (<i>S</i> -DOSP) ₄ in flow.....	215
Table 5.1 Regioselective α-functionalization of acceptor and acceptor/acceptor-substituted rhodium carbenoids with <i>N</i> -methylpyrrole.....	238
Table 5.2 Reactions of vinyl diazoacetates with substituted <i>N</i> -methylpyrroles.....	239
Table 5.3 Davies' α-selective C–H functionalization of <i>N</i> -Boc-pyrrolidine.....	240
Table 5.4 Davies' α-selective double carbenoid insertion into <i>N</i> -Boc-pyrrolidine.....	241
Table 5.5 Itami's direct C–H arylation of heteroarenes catalyzed by RhCl(CO){P[OCH(CF ₃) ₂] ₃ } ₂	246
Table 5.6 Optimization of β-selective C–H arylation of an <i>N</i> -alkylpyrrole and an electron rich aryl iodide by RhCl(CO){P[OCH(CF ₃) ₂] ₃ } ₂	248
Table 5.7 C–H functionalization of an arylated <i>N</i> -alkylpyrrole with an electron-poor trichloroethyl ester-substituted donor/acceptor-diazo compound.....	253
Table 5.8 Attempted pyrrole C–H functionalization with an electron-poor α-ketoindole aryl diazo.....	260
Table 5.9 Optimization of the α-selective rhodium carbenoid-mediated pyrrole mono-functionalization.....	265

Table 5.10	Optimization of the α -selective rhodium carbenoid-mediated pyrrole di-functionalization.....	268
Table 5.11	Attempted C–H arylation of the 4-position of trifunctionalized <i>N</i> -alkylpyrrole.....	269
Table 5.12	Attempted 6π -electrocyclization to form the pyrrolo[2,3- <i>c</i>]carbazole core of dictyodendrin A via a (triisopropylsilyl)ketene acetal intermediate.....	271
Table 5.13	6π -electrocyclization to form the pyrrolo[2,3- <i>c</i>]carbazole core of dictyodendrin A.....	272

List of Abbreviations

Ac	acetyl
Ad	adamantyl
APCI	atmospheric pressure chemical ionization
Ar	aryl
Bn	benzyl
Bu	butyl
DBU	1,8-diazabicycloundec-7-ene
COD	1,5-cyclooctadiene
Cy	cyclohexyl
dba	bis(dibenzylideneacetone)
1,2-DCE	1,2-dichloroethane
DCM	dichloromethane
DMAP	<i>N,N</i> -4-(dimethylamino)pyridine
DMB	2,2-dimethylbutane
DMF	dimethylformamide
dppf	1,1'-bis(diphenylphosphino)ferrocene
EDG	electron-donating group
ee	enantiomeric excess

Et	ethyl
equiv.	equivalents
EWG	electron-withdrawing group
HPLC	high performance liquid chromatography
HRMS	high-resolution mass spectrometry
<i>hν</i>	light
IR	infrared spectroscopy
L	ligand
LDA	lithium diisopropylamide
Me	methyl
mmol	millimoles
NMR	nuclear magnetic resonance
N.R.	no reaction
OMe	methoxy
<i>o</i>-NBSA	<i>ortho</i> -nitrobenzenesulfonyl azide
<i>p</i>-ABSA	<i>para</i> -acetamidobenzenesulfonyl azide
Ph	phenyl
Phth	phthalimide
Piv	pivaloyl
Pr	propyl

TBAF	tetrabutylammonium fluoride
TBDPS	<i>tert</i> -butyldiphenylsilyl
TBS	<i>tert</i> -butyldimethylsilyl
TEA	triethylamine
temp	temperature
Tf	trifluoromethanesulfonyl
THF	tetrahydrofuran
TIPS	triisopropylsilyl
TLC	thin layer chromatography
TMS	Trimethylsilyl
Ts	tosyl

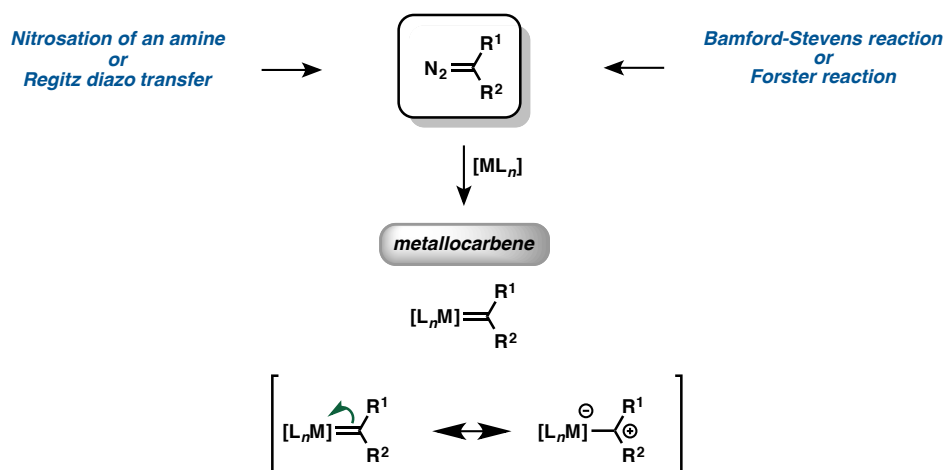
Chapter I: Introduction to Dirhodium(II) Catalysis

Advisor: Huw M. L. Davies, Ph.D.

1.1 Dirhodium(II) Catalysts

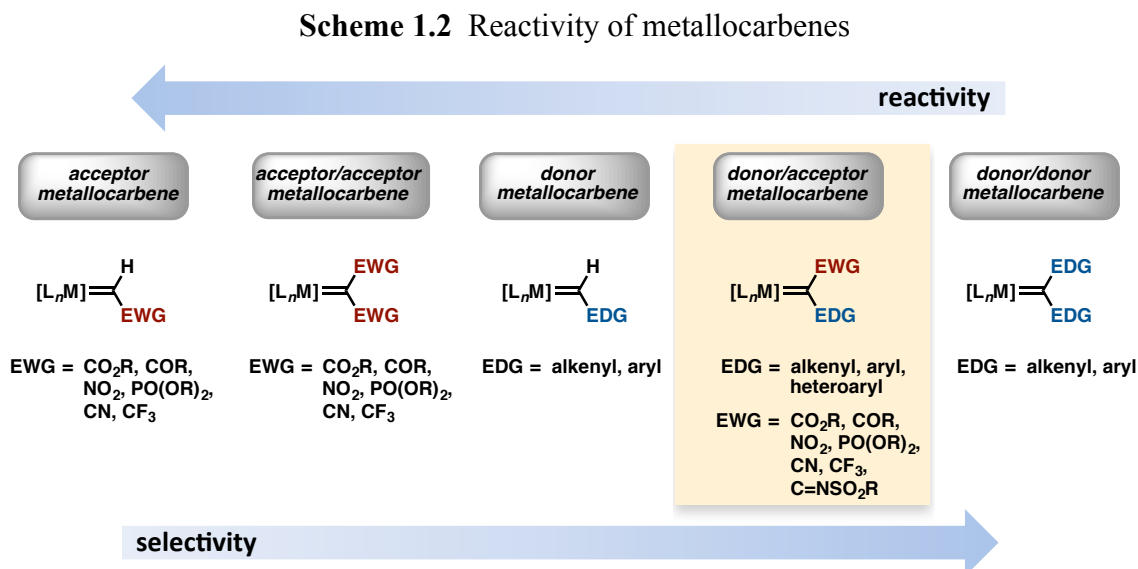
Metallocarbene scaffolds can be made by exposure of diazo compounds to various metal sources.¹ In 1952, Yates proposed that these metal carbenes, also referred to as “carbenoids”, consist of an electrophilic carbene bound to a transition metal (Scheme 1.1), rather than existing as a free carbene or an activated diazo.¹ Dirhodium(II) complexes are most commonly used to decompose diazo compounds to form a reactive rhodium carbenoid species in their axial coordination site. These rhodium carbenoids are extremely important intermediates in synthetic organic chemistry.²

Scheme 1.1 Synthetic routes to diazo compounds and their decomposition to metallocarbenes



Metallocarbenes are classified by the electronic nature of the substituents flanking the metal carbenoid. Acceptor metallocarbenes are the most reactive, but the least selective while donor/donor carbenes occupy the opposite end of the spectrum, displaying poor reactivity but good selectivity. For these reasons, donor/acceptor metallocarbenes, which display the ideal

balance of reactivity and selectivity, have found application in the broadest range of transformations to date (Scheme 1.2).³



The versatility of dirhodium(II) catalysts stems from their ability to accommodate a variety of different types of ligands which give the overall catalyst a defined symmetry. The first dirhodium(II) complex used for the decomposition of diazocarbonyl compounds was dirhodium tetraacetate (Rh₂(OAc)₄), which has four bridging ligands symmetrically positioned around the dirhodium core to provide this dimeric “paddlewheel” complex with an overall D_{4h} symmetry.⁴ Since then, a variety of dirhodium(II) tetracarboxylates and carboxamidates with chiral ligands have been synthesized and explored in asymmetric catalysis.⁵ In the early 1990’s various groups including Brunner, Doyle, and Singh explored the reactions of chiral dirhodium complexes, however, these complexes failed to provide good enantioselectivity.⁶ Further investigation by McKervey, however, provided the first highly enantioselective dirhodium(II) catalyst, Rh₂(S-BSP)₄, which employed chiral proline ligands.^{5a, 7} Since then, many different types of chiral dirhodium catalysts have been developed by Davies for the reactions of donor/acceptor

carbenoids. These catalysts include $\text{Rh}_2(\text{S-PTAD})_4$ which is most effective when the acceptor group of the donor/acceptor diazo compound is a phosphonate, trifluoromethyl or cyano group,⁸ $\text{Rh}_2(\text{S-TCPTAD})_4$ which is a sterically encumbered and rigid tetrachlorinated derivative of this catalyst,⁹ and recently $\text{Rh}_2(\text{S-BTPCP})_4$ is most promising for catalyzing primary C–H functionalization reactions.¹⁰ $\text{Rh}_2(\text{S-DOSP})_4$ and $\text{Rh}_2(\text{S-PTAD})_4$ are the most robust dirhodium(II) catalysts reported to date as they are capable of TONs as high as 850,000 and 1,800,000 respectively in asymmetric intermolecular cyclopropanation.¹¹

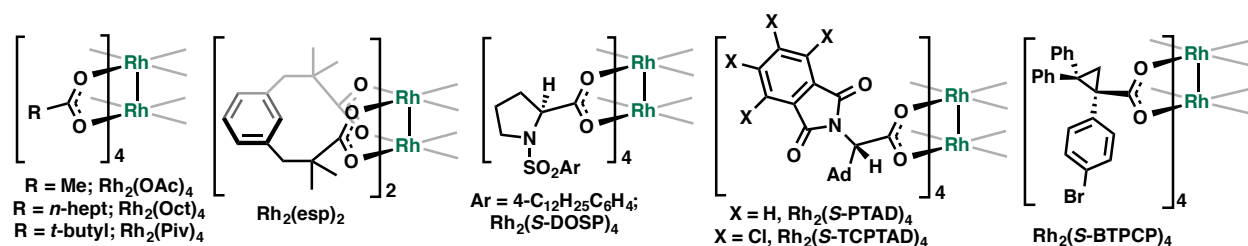


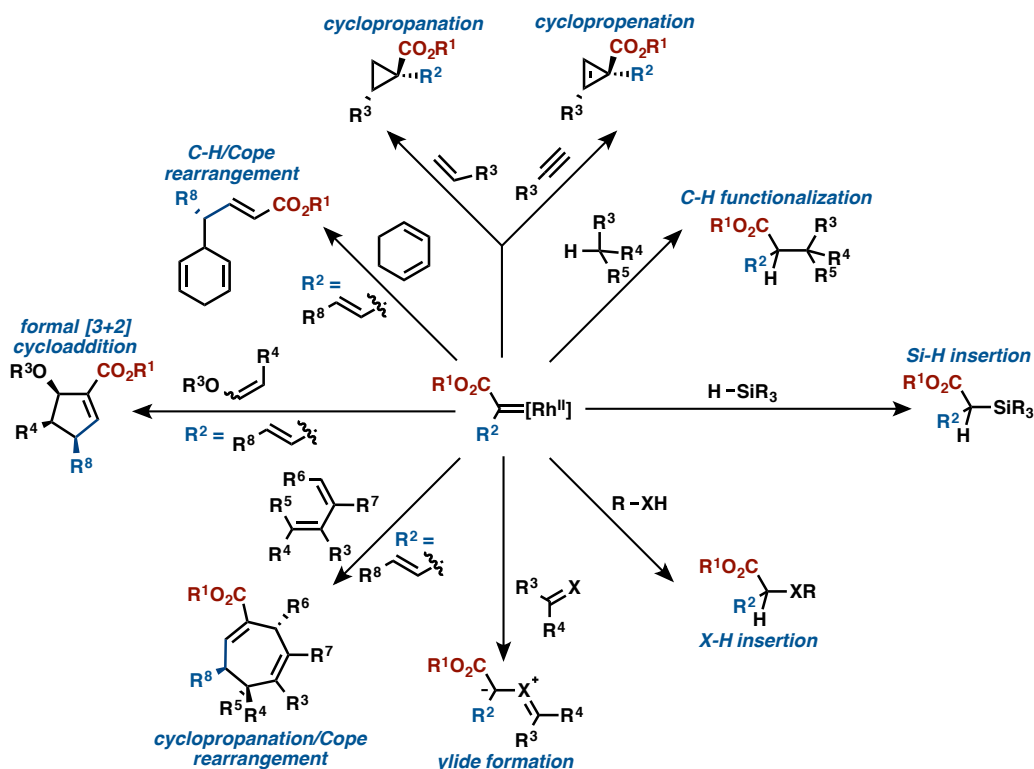
Figure 1.1 Most common rhodium(II) catalysts for the decomposition of donor/acceptor diazos

1.2 Dirhodium(II) Catalysts

Dirhodium(II) complexes are versatile and powerful catalysts for a wide array of challenging synthetic transformations of diazo compounds including enantioselective intermolecular cyclopropanations, cyclopropanations, dipolar cycloadditions, tandem ylide formation/sigmatropic rearrangements and C–H, N–H, O–H, and Si–H insertion reactions (Scheme 1.3).^{2a, 5c, 12} $\text{Rh}_2(\text{S-DOSP})_4$ is the most generally effective chiral dirhodium(II) catalyst for highly enantioselective transformations involving donor/acceptor carbenoid intermediates as this catalyst alone can catalyze highly enantioselective cyclopropanation, cyclopropanation, [3 + 4] and [3 + 2] cycloadditions, tandem carbonyl ylide formation/1,3-dipolar cycloadditions, tandem ylide formation/[2,3] sigmatropic rearrangements, C–H insertions, Si–H insertions,

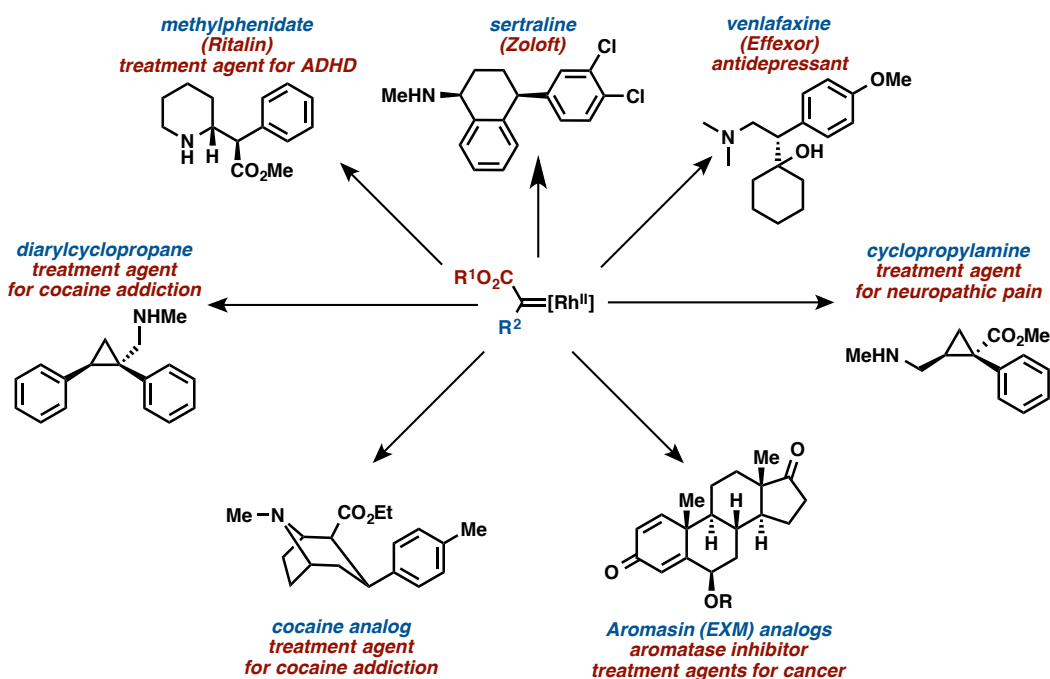
combined C–H functionalization/Cope rearrangements (CHCR), CHCR followed by retro-Cope rearrangements and CHCR followed by elimination reactions.^{2a, 5c}

Scheme 1.3 Methodology development with the use of donor/acceptor metallocarbenes



Donor/acceptor metallocarbenes have also found many applications in drug discovery (Scheme 1.4) including the syntheses of several of the most commonly used pharmaceuticals on the market today including Ritalin,¹³ Zoloft, and Effexor¹⁴ as well as several potential drug candidates still in development including analogs of cocaine for the treatment of cocaine addiction,¹⁵ Aromasin (EXM) analogs as aromatase inhibitors for treatment of cancer¹⁶ and cyclopropylamines and diarylcyclopropanes for the treatment of neuropathic pain and cocaine addiction respectively.¹⁷

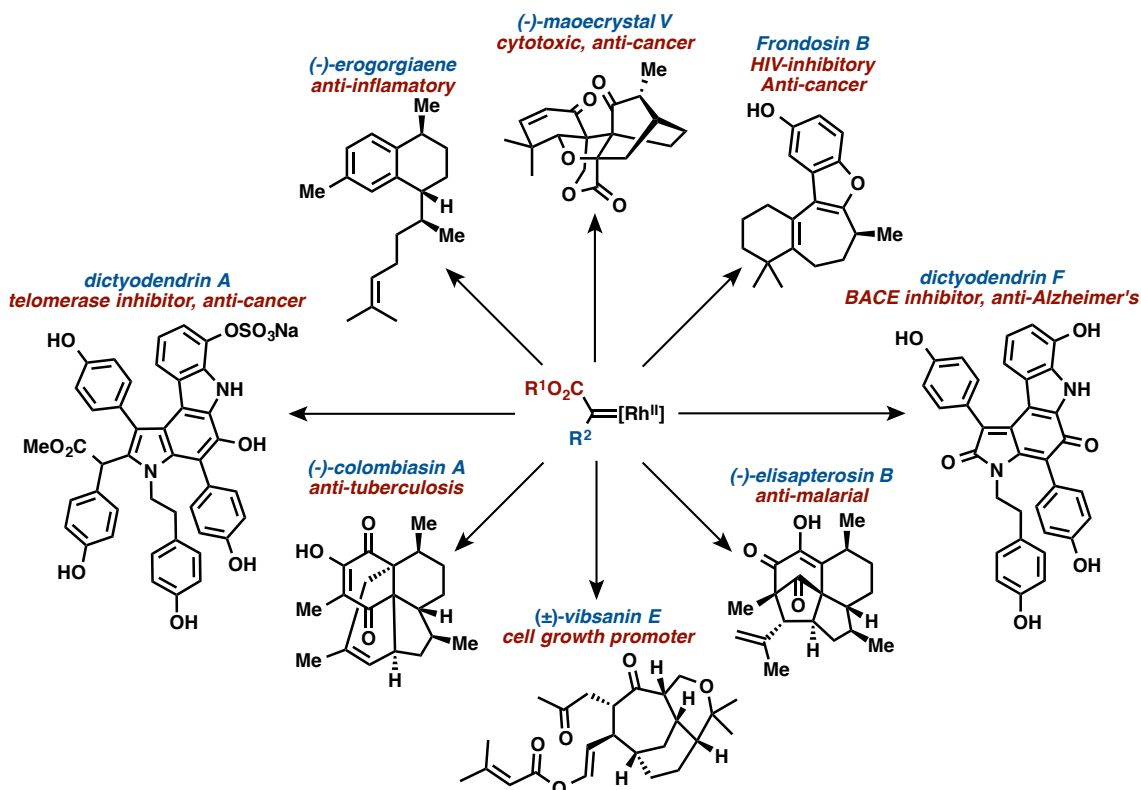
Scheme 1.4 Applications of donor/acceptor metallocarbenes in drug discovery



Donor/acceptor metallocarbenes have also found many applications in total synthesis (Scheme 1.5) including the syntheses of several different stereoisomers of vibsanin E which is a cell growth promoter,¹⁸ (-)-colombiasin A which has potential as an anti-tuberculosis agent, (-)-elisapterosin B which has potential as an anti-malarial agent, frondosin B which has potential for the treatment of both HIV and cancer,¹⁹ and (-)-erogorgiaene which has anti-inflammatory properties.²⁰ Most recently, the Davies group has been able to accomplish total syntheses of natural products with very potent anti-cancer properties through collaboration. In a recent collaboration with the Zakarian group, Davies *et al.* have accomplished the total synthesis of (-)-maoecrystal V which is extremely cytotoxic and has showed potential as an anti-cancer agent.²¹ Finally, this class of donor/acceptor metallocarbene have been used to synthesize two members of the dictyodendrin marine alkaloid family.²² Dictyodendrin A is a potent telomerase inhibitor and thus shows potential for cancer chemotherapy while dictyodendrin F exhibits significant β -

secretase (β -site APP cleaving enzyme: BACE) inhibitory activity and thus is a potential anti-Alzheimer's agent.²³

Scheme 1.5 Applications of donor/acceptor metallocarbenes in total syntheses



The focus of the projects described in this thesis is the application of dirhodium(II) tetracarboxylate and tetraphosphate (Chapter 2),¹⁷ immobilized dirhodium(II) (Chapters 3²⁴ and 4),²⁵ and bulky dirhodium(II) catalysts (Chapter 5)²² to dirhodium-stabilized donor/acceptor carbenoid reactions (Figure 1.2).

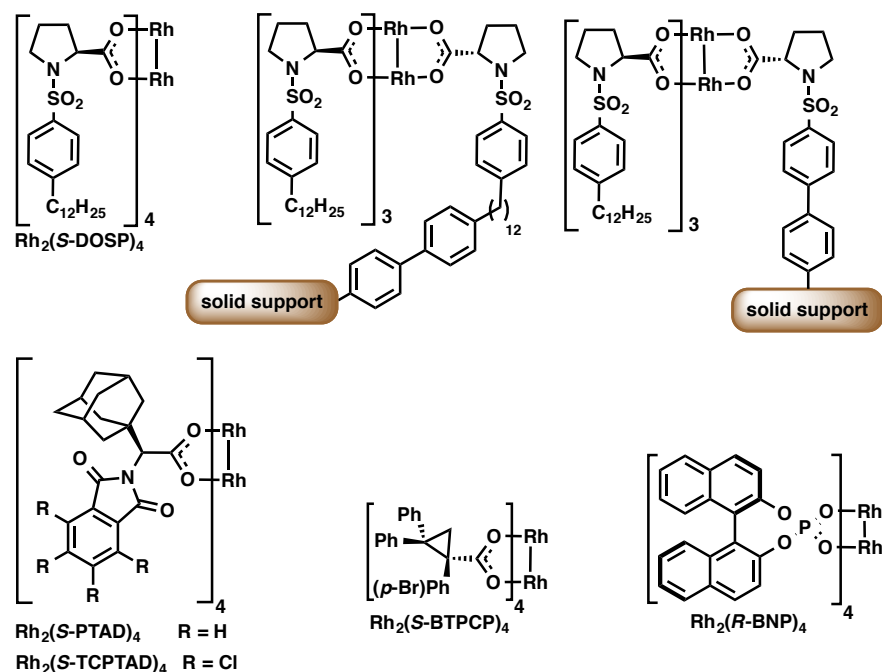


Figure 1.2 Structures of chiral dirhodium catalysts used in these studies

References:

1. Yates, P. *J. Am. Chem. Soc.* **1952**, *74*, 5376.
2. (a) Davies, H. M. L.; Beckwith, R. E. *J. Chem. Rev.* **2003**, *103*, 2861; (b) Davies, H. M. L.; Morton, D. *Chem. Soc. Rev.* **2011**, *40*, 1857.
3. Davies, H. M. L.; Panaro, S. A. *Tetrahedron* **2000**, *56*, 4871.
4. (a) Paulissen, R.; Reimlinger, H.; Hayez, E.; Hubert, A. J.; Teyssie, P. *Tetrahedron Lett.* **1973**, *24*, 2233; (b) Saegusa, T.; Ito, Y.; Kobayashi, S.; Hirota, K.; Shimizu, T. *J. Org. Chem.* **1968**, *33*, 544; (c) Cotton, F. A.; Murillo, C. A.; Walton, R. A. *Multiple Bonds Between Metal Atoms, Third Edition*. Springer: **2005**, 818.
5. (a) Kennedy, M.; McKervy, M. A.; Maguire, A. R.; Roos, G. H. P. *J. Chem. Soc., Chem. Commun.* **1990**, *5*, 361; (b) McKervy, M. A.; Ye, T. *J. Chem. Soc., Chem. Commun.* **1992**, *11*, 823; (c) Doyle, M. P.; McKervy, M. A.; Ye, T. *Modern Catalytic Methods for Organic Synthesis with Diazo Compounds: From Cyclopropanes to Ylides*. Wiley: **1998**; p 652; (d) Hodgson, D. M.; Stuppel, P. A.; Forbes, D. C. *Reactions involving metallocarbenes*, Elsevier: **2001**; pp 65.
6. (a) Brunner, H.; Kluschanzoff, H.; Wutz, K. *Bull. Soc. Chim. Belg.* **1989**, *98*, 63; (b) Singh, V. K.; DattaGupta, A.; Sekar, G. *Synthesis* **1997**, *2*, 137.
7. (a) Ye, T.; McKervy, M. A.; Brandes, B. D.; Doyle, M. P. *Tetrahedron Lett.* **1994**, *35*, 7269; (b) Ye, T.; Fernandez Garcia, C.; McKervy, M. A. *J. Chem. Soc., Perkin Trans. 1* **1995**, *11*, 1373; (c) Garcia, C. F.; McKervy, M. A.; Ye, T. *Chem. Commun.* **1996**, *12*, 1465.
8. Reddy, R. P.; Lee, G. H.; Davies, H. M. L. *Org. Lett.* **2006**, *8*, 3437.
9. Reddy, R. P.; Davies, H. M. L. *Org. Lett.* **2006**, *8*, 5013.
10. Qin, C.; Davies, H. M. L. *J. Am. Chem. Soc.* **2014**, *136*, 9792.
11. Pelphey, P.; Hansen, J.; Davies, H. M. L. *Chem. Sci.* **2010**, *1*, 254.

12. (a) Davies, H. M. L. *Compr. Asymmetric Catal., Suppl.* **2004**, *1*, 83; (b) Davies, H. M. L.; Walji, A. M. *Rhodium(II)-stabilized carbenoids containing both donor and acceptor substituents*, Wiley-VCH: **2005**; pp 301; (c) Wee, A. G. H. *Curr. Org. Synth.* **2006**, *3*, 499; (d) Zhang, Z.; Wang, J. *Tetrahedron* **2008**, *64*, 6577; (e) Davies, H. M. L.; Manning, J. R. *Nature* **2008**, *451*, 417; (f) Padwa, A. *J. Org. Chem.* **2009**, *74*, 6421; (g) Doyle, M. P. *Chem. Rev.* **1986**, *86*, 919.
13. Davies, H. M. L.; Hopper, D. W.; Hansen, T.; Liu, Q.; Childers, S. R. *Bioorg. Med. Chem. Lett.* **2004**, *14*, 1799.
14. Davies, H. M. L.; Ni, A. *Chem. Commun.* **2006**, *29*, 3110.
15. (a) Reddy, R. P.; Davies, H. M. L. *J. Am. Chem. Soc.* **2007**, *129*, 10312; (b) Sizemore, G. M.; Davies, H. M. L.; Martin, T. J.; Smith, J. E. *Drug Alcohol Depend.* **2004**, *73*, 259.
16. Ghosh, D.; Lo, J.; Morton, D.; Valette, D.; Xi, J.; Griswold, J.; Hubbell, S.; Egbuta, C.; Jiang, W.; An, J.; Davies, H. M. L. *J. Med. Chem.* **2012**, *55*, 8464.
17. Chepiga, K. M.; Qin, C.; Alford, J. S.; Chennamadhavuni, S.; Gregg, T. M.; Olson, J. P.; Davies, H. M. L. *Tetrahedron* **2013**, *69*, 5765.
18. Davies, H. M. L.; Loe, O.; Stafford, D. G. *Org. Lett.* **2005**, *7*, 5561.
19. Olson, J. P.; Davies, H. M. L. *Org. Lett.* **2010**, *12*, 1144.
20. Davies, H. M. L.; Lian, Y. *Acc. Chem. Res.* **2012**, *45*, 923.
21. Lu, P.; Mailyan, A.; Gu, Z.; Guptill, D. M.; Wang, H.; Davies, H. M. L.; Zakarian, A. *J. Am. Chem. Soc.* **2014**, *136*, 17738.
22. Yamaguchi, A. D.; Chepiga, K. M.; Yamaguchi, J.; Itami, K.; Davies, H. M. L. *J. Am. Chem. Soc.* **2015**, *137*, 644.
23. Zhang, H.; Conte, M. M.; Khalil, Z.; Huang, X.-C.; Capon, R. J. *RSC Adv.* **2012**, *2*, 4209.
24. Chepiga, K. M.; Feng, Y.; Brunelli, N. A.; Jones, C. W.; Davies, H. M. L. *Org. Lett.* **2013**, *15*, 6136.
25. Moschetta, E. G.; Negretti, S.; Chepiga, K. M.; Brunelli, N. A.; Labreche, Y.; Feng, Y.; Rezaei, F.; Lively, R. P.; Koros, W. J.; Davies, H. M. L.; Jones, C. W. *Angew. Chem. Int. Ed.* **2015**, *54*, 1.

Chapter II: Guide to Enantioselective Dirhodium(II) Catalyzed Cyclopropanation of Aryldiazoacetates with Styrene Derivatives

Advisor: Huw M. L. Davies, Ph.D.

Dirhodium(II) tetrakisbinaphthylphosphate $\text{Rh}_2(\text{BNP})_4$ stands out as unique in the family of commonly employed dirhodium(II) catalysts due to its electron-withdrawing nature and ability to impart enantioinduction from the chiral environment created by its four axially chiral ligands. This chapter will discuss the application of single enantiomers of $\text{Rh}_2(\text{BNP})_4$ to the asymmetric cyclopropanation of donor/acceptor diazo compounds. From these studies, a guide to the catalytic enantioselective generation of diverse cyclopropane libraries of long standing pharmaceutical interest was developed. This guide shows which chiral dirhodium(II) catalyst is optimal for a given cyclopropanation reaction based on the steric and electronic nature of the aryldiazoacetate at hand.



2.1 Dirhodium(II) Binaphthylphosphate Complexes in Chiral Catalysis

Although the vast majority of dirhodium(II) catalysts to date have employed carboxylate or carboxamidate ligands, a few groups have been drawn to dirhodium(II) binaphthyl phosphate complexes¹ (Figure 2.1) due to their high symmetry, longer rhodium-rhodium bond length, and because they are readily accessible as both enantiomers of the chiral ligands are commercially available.

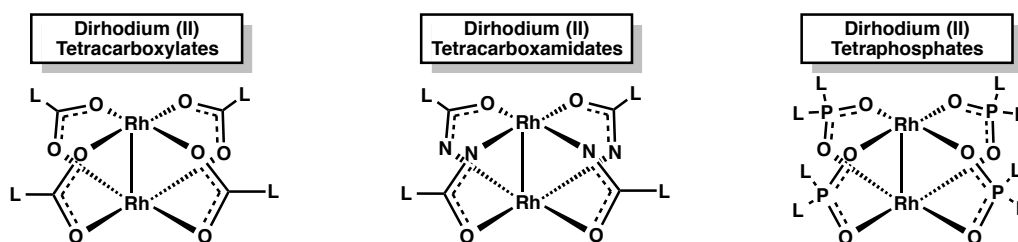


Figure 2.1 Types of dirhodium(II) catalysts

Dirhodium(II) tetrakisbinaphthylphosphate, $\text{Rh}_2(\text{S-BNP})_4$, (Figure 2.2) has four bridging C_2 -symmetric binaphthylphosphate ligands imparting an overall D_4 symmetry on the complex. This high symmetry of the ligands was predicted to give a very well-defined chiral binding pocket for the substrate. The rhodium-rhodium bond length is *ca.* 0.1 Å longer in dirhodium(II) tetrakisbinaphthylphosphate than the corresponding carboxylates which could potentially have an effect on the reactivity of these complexes.¹ Finally, another benefit of these catalysts is their ease of synthesis thanks to the commercial availability of the axially chiral binaphthylphosphoric acid ligands which are established as chiral Brønsted acid catalysts for various enantioselective reactions such as transfer hydrogenation, Friedel-Crafts, Mannich, aza-Diels-Alder, aza-ene-type, and Pictet-Spengler reactions.²

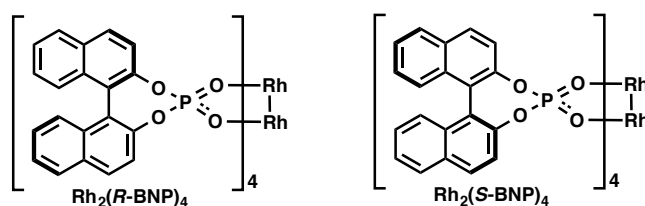
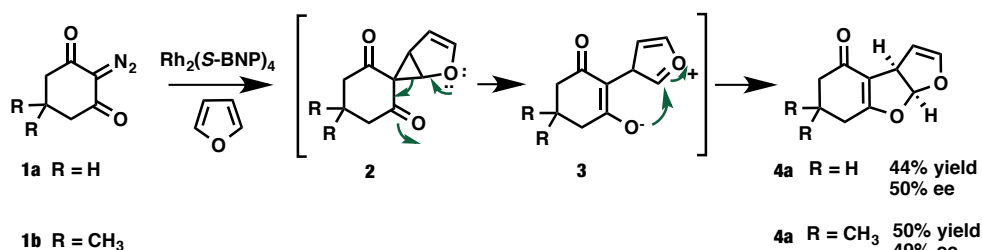


Figure 2.2 Dirhodium(II) tetrakisbinaphthylphosphate ($\text{Rh}_2(\text{R-BNP})_4$ and $\text{Rh}_2(\text{S-BNP})_4$)

In 1992 Pirrung reported the first synthesis and application of $\text{Rh}_2(\text{S-BNP})_4$ in an asymmetric dipolar cycloaddition reaction. This reaction was originally discovered in 1965 by Stetter who employed $\text{Rh}_2(\text{OAc})_4$ to catalyze the decomposition of 2-diazocyclohexane-1,3-dione (**1a**) or 2-diazodimedone (**1b**) in the presence of furan (Scheme 2.1).³ The proposed mechanism of this

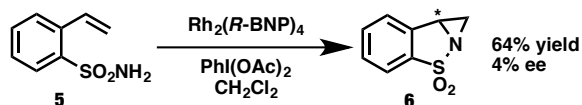
dipolar cycloaddition begins with electrophilic attack of the furan at the 2-position to give a transient cyclopropane **2** followed by ring opening to give the zwitterionic intermediate **3**, terminating with ring closure to provide the dihydrofuro[2,3]furan ring system (**4a** and **4b**). Pirrung was able to achieve moderate enantioselectivity in this reaction with the use of $\text{Rh}_2(\text{S-BNP})_4$ (Scheme 2.1, **4a**: 50% ee, **4b**: 49% ee).^{1, 4} In 1997, however, Ishitani and Achiwa reported that a dirhodium tetracarboxylate, $\text{Rh}_2(\text{S-BZP})_4$ with four benzoylated proline ligands, was able to surpass the enantioselectivity achieved with $\text{Rh}_2(\text{S-BNP})_4$ for this dipolar cycloaddition with enantioselectivity as high as 93% and even 98% ee with 4-methoxybenzoylproline ligands.⁵

Scheme 2.1 Dipolar cycloaddition catalyzed by $\text{Rh}_2(\text{S-BNP})_4$



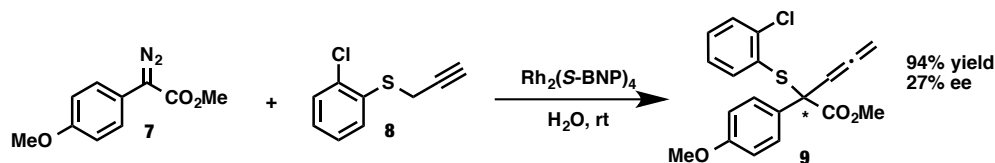
Immediately after Pirrung published synthesis of $\text{Rh}_2(\text{S-BNP})_4$, Liang was able to employ this catalyst in an intramolecular aziridination of sulfonamide **5**, obtaining **6** in modest yield (Scheme 2.2, 64 %). This transformation, however, was not enantioselective (4% ee).⁶

Scheme 2.2 Intramolecular aziridination catalyzed by $\text{Rh}_2(\text{R-BNP})_4$



In 2007, Liao *et al.* found that $\text{Rh}_2(\text{S-BNP})_4$ could catalyze a sulfur ylide/ [2,3]-sigmatropic rearrangement of **8** by decomposition of **7** to provide **9** in high yield (94%) but only moderate enantioselectivity (Scheme 2.3, 27% ee).⁷

Scheme 2.3 Sulfur ylide/ [2,3]-sigmatropic rearrangement catalyzed by $\text{Rh}_2(\text{R-BNP})_4$



2.2 3, 3' and 6,6'-Substituted Dirhodium(II) Binaphthylphosphate Derivatives

Variation of the substitution pattern around the binaphthyl framework has often been used to alter the chiral environment around catalysts containing binaphthyl ligands. In 2001, Hodgson hypothesized that slight ligand modification involving variation of the substitution pattern on the binaphthyl ring of dirhodium(II) tetrakisbinaphthylphosphate complexes could greatly influence the catalytic activity of these rigid systems and potentially give rise to new complexes capable of catalyzing a variety of transformations. Hodgson's first $\text{Rh}_2(\text{R-BNP})_4$ derivative, $\text{Rh}_2(\text{R-DMBNP})_4$, was substituted with methyl groups at the 3,3'-positions (Figure 2.3).

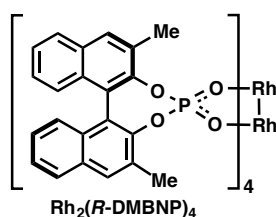
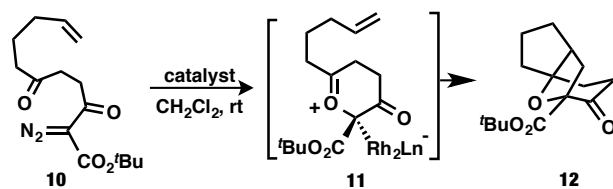


Figure 2.3 3,3'-substituted $\text{Rh}_2(\text{R-BNP})_4$ -derivative ($\text{Rh}_2(\text{R-DMBNP})_4$)

$\text{Rh}_2(\text{R-DMBNP})_4$ provided both poor reactivity and selectivity (Scheme 2.4, 50% yield, 7% ee) in the decomposition of α -diazo- β -keto ester **10** in a tandem carbonyl ylide-formation/1,3-dipolar cycloaddition. Hodgson proposed that these disappointing results were most likely due to steric congestion at the axial binding sites on the dirhodium core.⁸

Scheme 2.4 [1,3]-Dipolar cycloaddition catalyzed by $\text{Rh}_2(R\text{-BNP})_4$ -derivatives



catalyst	yield (%)	ee (%)
$\text{Rh}_2(R\text{-BNP})_4$	83	65
$\text{Rh}_2(R\text{-DMBNP})_4$	50	7
$\text{Rh}_2(R\text{-DBBNP})_4$	67	58
$\text{Rh}_2(R\text{-DDBNP})_4$	80	68
$\text{Rh}_2(R\text{-DDBNP})_4$	76	81 ^a

^a hexanes used as the solvent

Substitution at the 6,6' positions of tetrakisbinaphthylphosphate complexes, such as Mikami's Ti-BINOL catalyst derivatives⁹ and Shibasaki's La-BINOL complexes,¹⁰ has been shown to increase the selectivity of these catalytic systems. This precedence, along with the poor results obtained with $\text{Rh}_2(R\text{-DMBNP})_4$, led Hodgson to synthesize and test $\text{Rh}_2(R\text{-BNP})_4$ -derivatives substituted at 6,6'-positions. 6,6'-bromo derivative, $\text{Rh}_2(R\text{-DBBNP})_4$ (Figure 2.4), gave similar selectivity (Scheme 2.4, 66% ee) to $\text{Rh}_2(R\text{-BNP})_4$ (65% ee).

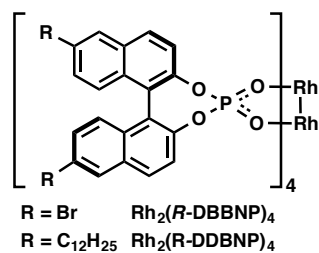


Figure 2.4 6,6'-substituted $\text{Rh}_2(R\text{-BNP})_4$ -derivatives ($\text{Rh}_2(R\text{-DBBNP})_4$ and $\text{Rh}_2(R\text{-DDBNP})_4$)

In hopes of investigating the effect of hydrocarbon solvents on the enantioselectivity, Hodgson *et al.* synthesized a more hydrocarbon-soluble catalyst, 6,6'-*n*-dodecyl-substituted derivative $\text{Rh}_2(R\text{-DDBNP})_4$ (Figure 2.4). It became apparent that solvent did greatly affect enantioselectivity when $\text{Rh}_2(R\text{-DDBNP})_4$ -catalyzed cycloaddition proved to be highly enantioselective (81% ee) in hexanes (Scheme 2.4).^{8a} Little or no influence on selectivity was

contributed by these *n*-dodecyl substituents as is seen from the similar selectivity of Rh₂(*R*-DDBNP)₄ (68% ee) to Rh₂(*R*-BNP)₄ in dichloromethane (Scheme 2.4). Furthermore, Hodgson proposed that these 6,6'-substituents were not affecting the electrophilic nature of the catalyst, or altering intra-planar (binaphthyl) torsion angles. These findings show that substitution pattern at the 6, 6'-positions of Rh₂(*R*-BNP)₄-derivatives is inconsequential to the selectivity while solvent plays a key role in the enantioselectivity of dirhodium(II) tetrakisbinaphthylphosphate catalysts.^{8b, 11}

2.3 Dirhodium(II) Binaphthylphosphate Derivatives with Mixed Ligands

At the same time that Pirrung introduced Rh₂(*S*-BNP)₄, McKervey and Doyle published a synthesis and screen of a dirhodium(II) binaphthylphosphate catalyst with mixed ligands, Rh₂(HCO₃)₂((+)-Phos)₂·5H₂O, also abbreviated as *cis*-Rh₂(*S*-BNP)₂(HCO₃)₂ (Figure 2.5).⁶

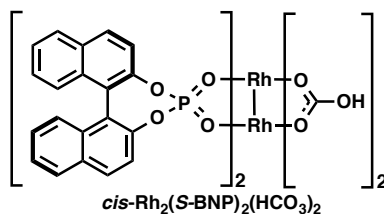
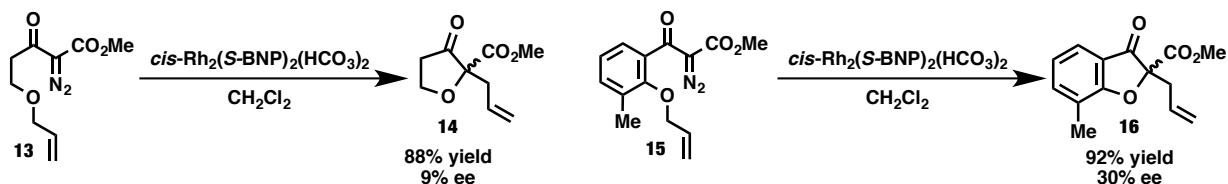


Figure 2.5. Rh₂(*R*-BNP)₄-derivative with mixed ligands (*cis*-Rh₂(*S*-BNP)₂(HCO₃)₂)

The mixed ligand Rh₂(*R*-BNP)₄-derivative, *cis*-Rh₂(*S*-BNP)₂(HCO₃)₂, was found to be an effective catalyst for 2,3-sigmatropic rearrangements, C–H insertions, and in an aromatic cycloaddition reaction. Although very low stereinduction was achieved in the two reported sigmatropic rearrangements (**14**: 88% yield, 9% ee; **16**: 92% yield, 30% ee), these *cis*-Rh₂(*S*-BNP)₂(HCO₃)₂-catalyzed 2,3-sigmatropic rearrangements represent the first example of

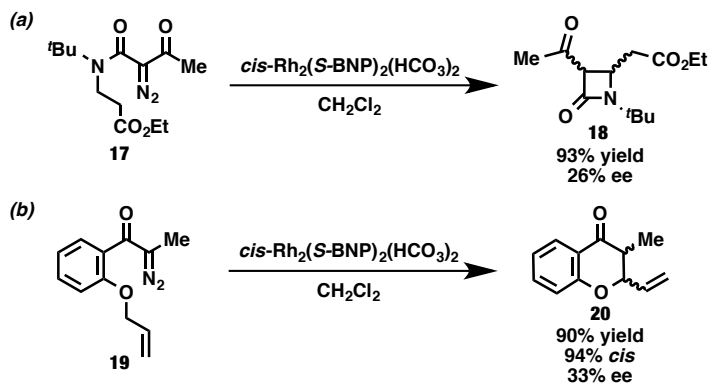
homochiral Rh(II)-catalyzed enantioselective 2,3-sigmatropic rearrangement of diazocarbonyl intermediates (Scheme 2.5).⁶

Scheme 2.5 *cis*-Rh₂(*S*-BNP)₂(HCO₃)₂-catalyzed 2,3-sigmatropic rearrangements



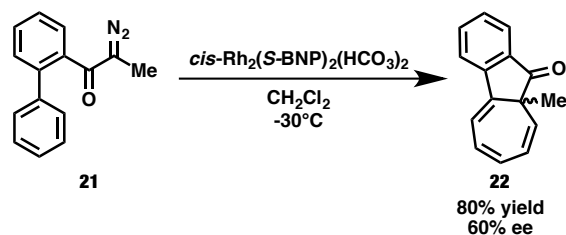
cis-Rh₂(*S*-BNP)₂(HCO₃)₂ also catalyzed cyclizations to provide 4- and 6-membered heterocycles via C–H insertion in high yields (**18**: 93%; **20**: 90%), but with minimal stereocontrol (Scheme 2.6, **18**: 26% ee; **20**: 33% ee).⁶

Scheme 2.6 *cis*-Rh₂(*S*-BNP)₂(HCO₃)₂-catalyzed intramolecular C–H insertion



The highest reported enantioselectivity employing *cis*-Rh₂(*S*-BNP)₂(HCO₃)₂ came with the decomposition of **21** in an aromatic cycloaddition providing **22** in high yield and moderate selectivity (Scheme 2.7, 80% yield, 60% ee).⁶

Scheme 2.7 *cis*-Rh₂(*S*-BNP)₂(HCO₃)₂-catalyzed aromatic cycloaddition



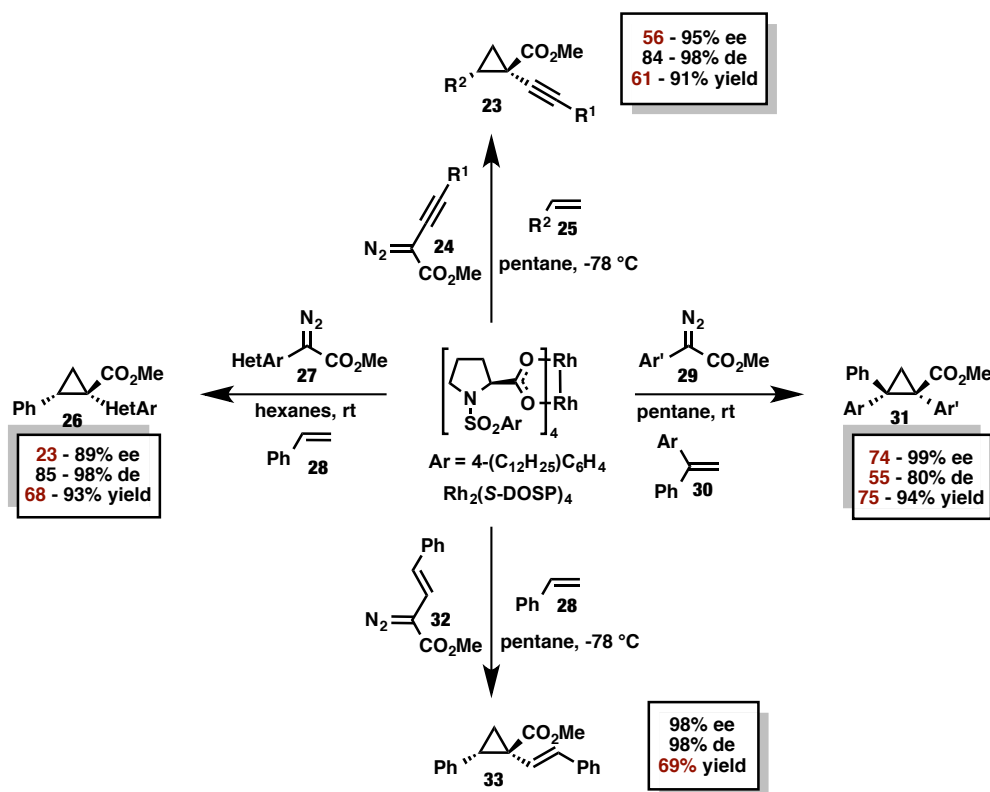
Despite these advances, dirhodium(II) tetrakisbinaphthylphosphate complexes remain relatively unexplored. Little is known about their reactivity and selectivity, especially in the reactions of donor/acceptor carbenoids. Variation of the structure of this catalyst in an organized manner and observing the corresponding enantioselectivities has begun to provide insight into the nature, reactivity, and selectivity of these catalysts. Further investigation of these complexes and their substituted derivatives is required in order to fully understand the potential and use of these complexes in asymmetric catalysis.

2.4 Donor/Acceptor Diazo Compounds in Dirhodium(II) Binaphthylphosphate Catalysis and Shortcomings of Rh₂(*S*-DOSP)₄ in Asymmetric Cyclopropanation Reactions

In most reported cases, only the “traditional carbenoids” containing one electron withdrawing group (acceptor carbenoids) or two electron withdrawing groups (acceptor/acceptor carbenoids) have been explored in the screening of Rh₂(BNP)₄. Also, most reported transformations employing Rh₂(BNP)₄ in the literature furnished products of low enantiopurity. The Davies group, therefore, was drawn to explore the reactivity of this dirhodium(II) tetrakisbinaphthylphosphate catalyst with donor/acceptor substituted diazo compounds as the increased stability of donor/acceptor substituted rhodium carbenoids has been shown to impart high levels of enantioselectivity in a wide range of transformations utilizing chiral dirhodium tetracarboxylate catalysts such as Rh₂(DOSP)₄, Rh₂(biTISP)₄, and Rh₂(PTAD)₄. The metal-catalyzed decomposition of diazo

compounds in the presence of alkenes is a general method for the stereoselective synthesis of cyclopropanes.¹² The Davies group has previously shown the dirhodium-catalyzed cyclopropanation of donor/acceptor carbenoids to be effective for the enantioselective synthesis of cyclopropanes with one or more quaternary stereogenic centers.¹³ Although dirhodium(II) carboxylate catalysts show desirable reactivity in a vast array of reactions, there are still many cyclopropanations which lie outside the capabilities of these catalysts (Scheme 2.8, highlighted in red are the areas where the Rh(II)-carboxylate catalysts underperform). It is for this reason that the Davies group set out to determine whether these binaphthylphosphate catalysts would be able to fill gaps that remain unaddressed by the well-established catalysts in the cyclopropanation of donor/acceptor substituted diazo compounds.

Scheme 2.8 Reactivity and selectivity of $\text{Rh}_2(\text{S-DOSP})_4$ in asymmetric cyclopropanation



highlighted in red are the areas where the Rh(II)-carboxylate catalysts underperform

2.5 Introduction to $\text{Rh}_2(\text{R-BNP})_4$ -Catalyzed Cyclopropanation of Donor/Acceptor Substituted Diazo Compounds

Previous studies in the Davies group conducted by Dr. Changming Qin have revealed that $\text{Rh}_2(\text{R-BNP})_4$ is capable of catalyzing the decomposition of certain donor/acceptor diazo compounds with moderate (Table 2.1, entries 5, 6 and 18) to high (Table 2.1, entries 7 and 8) levels of enantioinduction (enantiomeric excess > 80% is highlighted in red). Results of a solvent screen conducted by Dr. Changming Qin have shown that toluene is the solvent which provides products of the highest enantiopurity for $\text{Rh}_2(\text{R-BNP})_4$. For this reason, toluene was used as the solvent for all reactions in Table 2.1. Interestingly, the enantioselectivity was found to be quite dependent on the substitution of the aryl group on the carbenoid with *ortho*-methoxy-substituted aryldiazoacetates **34e-h** providing cyclopropane products of the greatest enantiopurity (entries 5-8).

Table 2.1 Donor/acceptor diazo compound screening in the asymmetric cyclopropanation of aryldiazoacetates with styrene by $\text{Rh}_2(\text{R-BNP})_4$

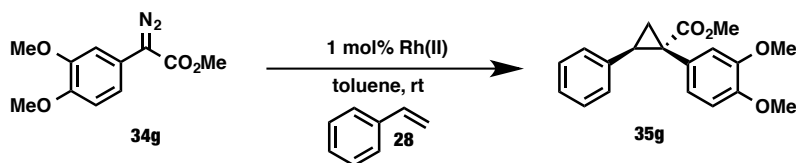
entry ^a	Ar	product	yield (%)	ee (%) ^b	entry ^a	Ar	product	yield (%)	ee (%) ^b
1		35a	42	63	10		35j	57	37
2		35b	51	42	11		35k	84	57
3		35c	67	50	12		35l	81	59
4		35d	70	58	13		35m	63	73
5		35e	82	88	14		35n	69	27
6		35f	44	82	15		35o	94	59
7		35g	93	94	16		35p	76	70
8		35h	63	90	17		35q	70	69
9		35i	82	63	18		35r	83	84

^a reactions conducted by Dr. Changming Qin

^b highlighted in red is enantiomeric excess > 80%

The high level of enantioinduction achieved in Table 2.1, entry 7 at room temperature to provide the desired cyclopropanation product **35g** in high yield (93%) with excellent enantioinduction (94% ee) was particularly intriguing because $\text{Rh}_2(\text{R-BNP})_4$ far surpassed both the reactivity (74%) and enantioselectivity (56%) achieved with $\text{Rh}_2(\text{R-DOSP})_4$ in the same reaction (Table 2.2).

Table 2.2 $\text{Rh}_2(\text{R-BNP})_4$ vs. $\text{Rh}_2(\text{R-DOSP})_4$ in the asymmetric cyclopropanation of 3,4-dimethoxyphenyldiazoacetate with styrene



entry ^a	catalyst	yield (%)	ee (%) ^b
1	$\text{Rh}_2(\text{R-BNP})_4$	93	94
2	$\text{Rh}_2(\text{R-DOSP})_4$	74	56

^a reactions conducted by Dr. Changming Qin

^b highlighted in red is enantiomeric excess > 80%

2.6 $\text{Rh}_2(\text{R-BNP})_4$ -Catalyzed Cyclopropanation of 3,4-Dimethoxyphenyldiazoacetate and its Derivatives

For those diazo compounds screened in Table 2.1, there was a great deal of variability in both yield and selectivity. It appeared that electron-rich diazo compounds gave the highest asymmetric induction but only a few substrates gave > 90% ee. Therefore, we decided to determine whether a sub-class of compounds could be identified that would routinely give high asymmetric induction. One possibility for the cause of this high level of enantioinduction observed with 3,4-dimethoxyphenyldiazoacetate could be a favorable π - π stacking interaction between the electron rich aromatic ring of the diazo compound and the naphthyl region of the electron poor dirhodium binaphthylphosphosphate catalyst. Based on this theory, many different electron rich diazo compounds with methoxy groups adorning various positions of the aromatic ring were tested under the same reactions conditions in hopes of obtaining a better understanding of the substrate scope for this reaction (Table 2.3). Methyl 2-diazo-2-(3,4,5-trimethoxyphenyl)acetate (**34h**) provided the desired product **35h** with a high level of enantioinduction (90% ee) but only moderate yield (entry 2, 63%). We then wanted to determine which position (*ortho*, *meta*, or *para*) was contributing most to these high levels of

enantioinduction. Of the three different mono-methoxy substituted isomers, only the *meta*-methoxy substituted diazo **34e** provided the corresponding cyclopropanation product **35e** in high yield (82%) with good enantioselectivity (entry 4, 88% ee) with the use of Rh₂(*R*-BNP)₄. Conversely, Rh₂(*R*-DOSP)₄ showed complementary reactivity and selectivity to Rh₂(*R*-BNP)₄ in all cases, providing the cyclopropanation products **35n** and **35k** in high yields and levels of enantioinduction when Rh₂(*R*-BNP)₄ failed (entries 3 and 5).

Table 2.3 Influence of the position of the methoxy substituent(s) on the diazo compound on Rh₂(*R*-BNP)₄-catalyzed asymmetric cyclopropanation of aryldiazoacetates with styrene

entry	-OMe	product	Rh ₂ (<i>R</i> -BNP) ₄		Rh ₂ (<i>R</i> -DOSP) ₄	
			yield (%)	ee (%) ^b	yield (%)	ee (%) ^b
1		35g	93 ^a	94 ^a	74 ^a	56 ^a
2		35h	63 ^a	90 ^a	98	34
3		35n	69 ^a	27 ^a	92 ^a	86 ^a
4		35e	82 ^a	88 ^a	78	79
5		35k	84 ^a	57 ^a	66 ^a	90 ^a

^a reactions conducted by Dr. Changming Qin

^b highlighted in red is enantiomeric excess > 80%

To further justify this trend for high level of enantioinduction with *meta*-methoxy substituted diazo compounds, we synthesized methyl 2-diazo-2-(3,5-dimethoxyphenyl)acetate (**36a**). We believed that this compound would provide the corresponding cyclopropane product **37a** with

high enantiopurity. As expected, **36a** provided **37a** with a high level of enantioinduction (92% ee) but only a moderate yield (Table 2.4, entry 1, 69%). Finally, electron rich methyl 2-diazo-2-(6-methoxynaphthalen-2-yl)acetate (**36b**) was employed with the electron donating methoxy moiety at the 6-position of the naphthyl ring. This compound provided the corresponding cyclopropane **37b** with both poor enantioselectivity (48% ee) and yield (entry 2, 22%). This example shows that the governing factors behind selectivity of this transformation are complex and not simply determined by the electronic nature of the diazo compound.

Table 2.4 Influence of the substitution pattern of methoxy substituent(s) on the diazo compound

entry	-OMe	product	Rh ₂ (<i>R</i> -BNP) ₄		Rh ₂ (<i>R</i> -DOSP) ₄	
			yield (%)	ee (%) ^a	yield (%)	ee (%) ^a
1		37a	69	92	85	28
2		37b	22	48	35	63

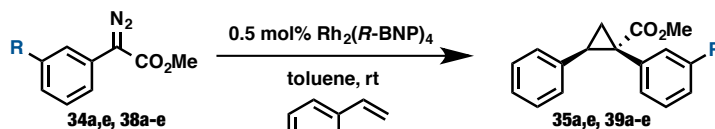
^a highlighted in red is enantiomeric excess > 80%

The realization that substitution of the donor/acceptor diazo compound at the *meta*-position with a methoxy group was the key contributor to the high levels of enantioinduction observed in Rh₂(*R*-BNP)₄-catalyzed cyclopropanation (Table 2.3, entry 4) led us to further explore *meta*-substitution on the aryl ring of the aryldiazoacetate. To determine the scope of this selectivity, donor/acceptor diazo compounds containing oxygenated substituents of varying steric bulk at the *meta*-position (**38a-e**) were synthesized and tested. To our dismay, *meta*-isopropoxy- (**38c**), benzyloxy- (**38d**), and phenoxy- (**38e**) substituted aryldiazoacetates all provided the corresponding

cyclopropanes with low levels of enantioinduction (Table 2.5, entries 5-7, **39c**: 66% ee; **39d**: 66% ee and **38e**: 33% ee).

Our next hypothesis was that this selectivity was being imparted by the steric nature of a methoxy group at the *meta*-position. To test this hypothesis, we envisioned that switching the methoxy substituent to an ethyl group at the *meta*-position (**38b**) would provide similar enantioinduction due to the similar steric environment of the two substrates. However, this reaction provided the cyclopropane **39b** with only a moderate yield and level of enantioinduction (Table 2.5, entry 3, 55% yield, 54% ee). These results indicate that a methoxy moiety at the *meta*-position is imperative to obtaining high levels on enantioinduction in cyclopropanation under $\text{Rh}_2(\text{R-BNP})_4$ -catalysis.

Table 2.5 Explorations into the governing forces behind enantioselectivity under $\text{Rh}_2(\text{R-BNP})_4$ -catalysis



entry	R	product	yield (%)	ee (%) ^a
1	H	35a	68	44
2	Me	39a	89	42
3	Et	39b	55	54
4	OMe	35e	40	88
5	O ⁱ Pr	39c	55	66
6	OBn	39d	83	66
7 ^b	OPh	39e	67	33

^a highlighted in red is enantiomeric excess > 80%

^b reaction provided the opposite enantiomer of cyclopropane product as determined by polarimeter analysis of the optical rotation

Another important type of diazo compound that had not yet been investigated with $\text{Rh}_2(\text{BNP})_4$ were styryldiazoacetates. We were interested to see whether the power of the 3,4-dimethoxy substituents on the aromatic ring of the diazo compound to provide high

enantioinduction was general for all donor/acceptor-substituted diazo compounds. For this reason, a comparative study of styryldiazoacetate (**32**) and methyl (*E*)-2-diazo-4-(3,4-dimethoxyphenyl)but-3-enoate (**40**) was conducted. Also a temperature study was conducted to determine whether higher levels of enantioinduction could be achieved at lower temperatures (Table 2.6). Unfortunately, **40** failed to provide the cyclopropanation product **41** stereoselectively (61% ee) or in high yield (entry 2, 72%). This result was similar for unsubstituted styryldiazoacetate (entry 1, **33**: 42% yield, 63% ee). Typically carbenoid reactions conducted at low-temperature and slowly allowed to warm to room temperature are more selective than those simply conducted at room temperature because they allow for the catalyst to react at an optimal temperature. Results of this temperature study, however, showed only a small increase in enantioinduction (entry 4, **41**: 66% ee).

Table 2.6 Rh₂(*R*-BNP)₄-catalyzed decomposition of vinyl diazoacetates

Reaction scheme: $\text{Ar-CH=CH-CO}_2\text{Me-N}_2 \xrightarrow[\text{Ph-CH=CH}_2 \text{ (28)}]{1 \text{ mol\% Rh}_2(\text{R-BNP})_4, \text{ toluene, rt}} \text{Cyclopropane-CO}_2\text{Me-Ar}$ (33, 41)

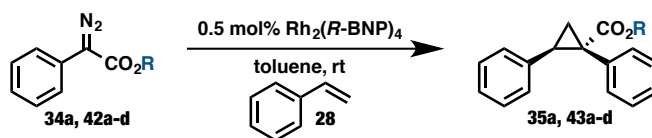
entry	Ar	temp (°C)	product	yield (%)	ee (%)
1 ^a		23	33	42	63
2 ^b		23	41	72	61
3		-78	33	38	58
4		-78	41	52	66

^a reaction conducted by Dr. Zhanjie Li and performed in CH₂Cl₂
^b reaction conducted by Dr. Changming Qin

Finally, one limitation of Rh₂(*S*-DOSP)₄ is that it has only been shown to provide high levels of enantioselectivity in decomposing donor/acceptor diazo compounds in which the carbonyl

group is a methyl ester.^{13a} Incrementally increasing the size of this ester group has been shown to cause a steady decrease in the observed enantiomeric excess of the product. For this reason, dirhodium(II) catalysts capable of tolerating an array of ester groups would be advantageous. Unfortunately screening of several different diazo compounds with varying bulk on the ester group (**42a-d**) provided primarily carbene dimerization products with only minimal conversion to the desired cyclopropanes (Table 2.7, entries 2-5, **43a-d**). Also, a very poor level of enantioinduction was observed for those products, which were isolable from the dimerization products (entries 2 and 5, **43a** and **43d**: < 5% ee).

Table 2.7 The effect of added steric bulk on ester of the diazo compound

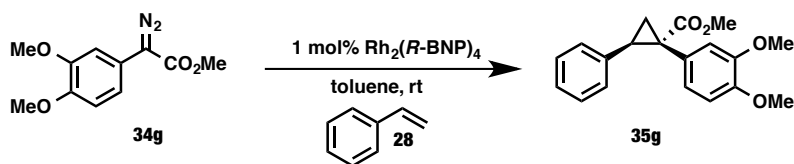


entry	R	product	yield (%)	ee (%)
1	Me	35a	68	44
2	Et	43a	39	< 5
3	<i>i</i> Pr	43b	minimal	ND
4	CH(<i>i</i> Pr) ₂	43c	minimal	ND
5	<i>t</i> Bu	43d	16	< 5

One of the most attractive features of the most commonly used dirhodium(II) catalysts (Rh₂(DOSP)₄ and Rh₂(PTAD)₄) is that they are capable of operating at low catalyst loadings.¹⁴ As Rh₂(R-BNP)₄ was found to be optimal for the cyclopropanation of 3,4-dimethoxyphenyldiazoacetate with styrene, we investigated whether it could also operate at low catalyst loading. Reactions of aryldiazoacetate **34g** with successively lower loadings of Rh₂(R-BNP)₄ are summarized in Table 2.8.¹⁵ Rh₂(R-BNP)₄ was effective at catalyzing highly enantioselective cyclopropanation with catalyst loadings of 1.0 and 0.5 mol%, providing **35g** with virtually the same level of enantioselectivity (entry 1 vs. 2, 97% ee vs. 96% ee).¹⁵ When the

catalyst loading was decreased further to 0.1 mol% a more significant drop in the level of enantioselectivity was observed (entry 3, 91% ee). Further decreasing the catalyst loading to 0.01 mol%, however, caused a dramatic decrease in enantioinduction (entry 4, 40% ee).¹⁵ These results suggest that, although $\text{Rh}_2(\text{R-BNP})_4$ is capable of moderately high turnover numbers (TONs), it may not be as robust a catalyst as $\text{Rh}_2(\text{DOSP})_4$ or $\text{Rh}_2(\text{PTAD})_4$, which are capable of TONs as high as 850,000 and 1,800,000 respectively in asymmetric intermolecular cyclopropanation.¹⁴

Table 2.8 Examination of $\text{Rh}_2(\text{R-BNP})_4$ loading¹⁵



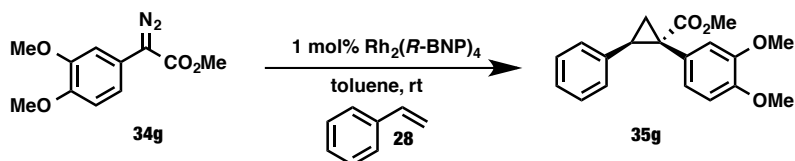
entry	styrene [equiv.]	catalyst loading (mol %)	yield (%)	ee (%) ^a
1	5	1	93	94
2	2.5	0.5	83	96
3	1.2	0.5	61	93

^a highlighted in red is enantiomeric excess > 80%

Previous studies on $\text{Rh}_2(\text{R-BNP})_4$ -catalyzed cyclopropanation conducted by Dr. Changming Qin were limited to the use of styrene as the trapping agent. Therefore, various styrene derivatives were explored in order to determine how broad the substrate scope of this highly enantioselective reaction was. In the original reaction scheme shown in Table 2.2, styrene (**28**) was used in excess (5 equiv) in relation to aryldiazoacetate **34g**. Due to the high cost of substituted styrene derivatives, however, it was desirable to decrease the amount of styrene used in the reaction. First, the minimum amount of styrene needed in order to maintain high reactivity and selectivity was explored (Table 2.9). It was found that both the amount of styrene used in the reaction as well as the catalyst loading could be reduced by half (2.5 equiv of styrene and 0.5

mol% catalyst) with no loss in enantioselectivity or reactivity (Table 2.9, entry 2). With these conditions in hand, various styrene derivatives could be tested.

Table 2.9 Effect of varying the equivalents of styrene used



entry	styrene [equiv.]	catalyst loading (mol %)	yield (%)	ee (%)
1	5	1	93	94
2	2.5	0.5	83	96
3	1.2	0.5	61	93

The impact of the nature of the substituents on the styrene component in enantioselective $\text{Rh}_2(\text{R-BNP})_4$ -catalyzed cyclopropanation with 3,4-dimethoxyphenyldiazoacetate **34g** was next determined (Table 2.10). The levels of enantioselectivity in the cyclopropanation, under $\text{Rh}_2(\text{R-BNP})_4$ -catalysis, were found to be moderately influenced by the functionality on the styrene derivative (**44a-i**), as the cyclopropanes **45a-g** were obtained with uniformly high levels of enantioinduction (80 - 90% ee). Previous studies showed that $\text{Rh}_2(\text{R-DOSP})_4$ -catalyzed cyclopropanation is also not especially influenced by the nature of the styrene^{3,4,9} and thus the $\text{Rh}_2(\text{R-DOSP})_4$ -catalyzed cyclopropanation of a range of styrenes (**44a-h**) with **34g** gave **45a-h** with modest levels of enantioselectivity (48 - 69% ee). With the exception of *p*- NO_2 -substituted styrene **44d** and 2-vinylnaphthalene **44h** (Table 2.10, entries 4 and 8, **45d** and **45h**), the enantioselectivities observed for both electron-donating (entries 1 - 3, **45a-c**) and electron-withdrawing (entries 5 - 7, **45e-g**) styrene derivatives were found to be comparable to the original reaction with unsubstituted styrene (**28**). Once again, in all cases $\text{Rh}_2(\text{R-BNP})_4$ was found to catalyze these reactions with significantly improved enantioinduction compared to $\text{Rh}_2(\text{R-DOSP})_4$. Cyclopropanation of 1-hexene (**44i**) was also tested but no cyclopropanation

product **45i** was observed in the ^1H NMR of the crude reaction mixture (entry 9). The reaction was then repeated with less highly substituted *meta*-methoxy aryldiazoacetate **35e**. Again, ^1H NMR of the crude reaction mixture showed no trace of cyclopropanation product **45i** (entry 10).

Table 2.10 Screening of styrene derivatives in $\text{Rh}_2(\text{R-BNP})_4$ -catalyzed cyclopropanation

entry	Ar	product	$\text{Rh}_2(\text{R-BNP})_4$		$\text{Rh}_2(\text{R-DOSP})_4$	
			yield (%)	ee (%) ^a	yield (%)	ee (%) ^a
1		45a	76	90	47	64
2		45b	90	88	50	67
3		45c	80	90	82	62
4		45d	94	80	28	50
5		45e	90	90	19	63
6		45f	81	89	49	67
7		45g	72	86	79	48
8		45h	87	77	93	69
9		45i	NR	NR	-	-
10 ^b		45i	NR	NR	-	-

^a highlighted in red is enantiomeric excess > 80%

^b reaction was run using methyl 2-diazo-2-(3-methoxyphenyl)acetate

2.7 Application of $\text{Rh}_2(\text{BNP})_4$ -Catalyzed Cyclopropanation to the Synthesis of 5-HT_{2A} Antagonist Biaryl Cyclopropylmethylamines

With new insight into the scope of styrene derivatives which could be successfully employed in $\text{Rh}_2(R\text{-BNP})_4$ -catalyzed decomposition of **34g**, we decided to apply this chemistry to the synthesis of a new analogue in a family of biologically active molecules. Previous results from collaborative studies between the Davies group and Prof. Steven Childers' group at Wake Forest University have shown that a series of biaryl cyclopropylmethylamine scaffolds (**I**) behave as antagonists of a particular sub-class of serotonin receptors, called 5-HT_{2A} receptors (Figure 2.6).

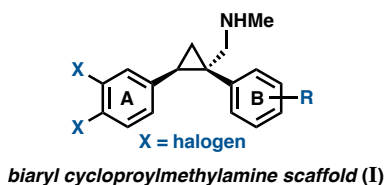
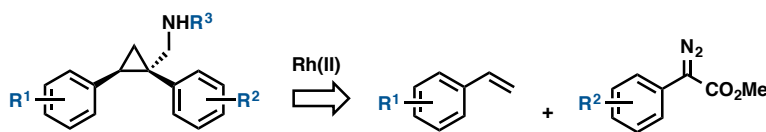


Figure 2.6 Biologically active biaryl cyclopropylmethylamine scaffold for 5-HT_{2A} receptor antagonists

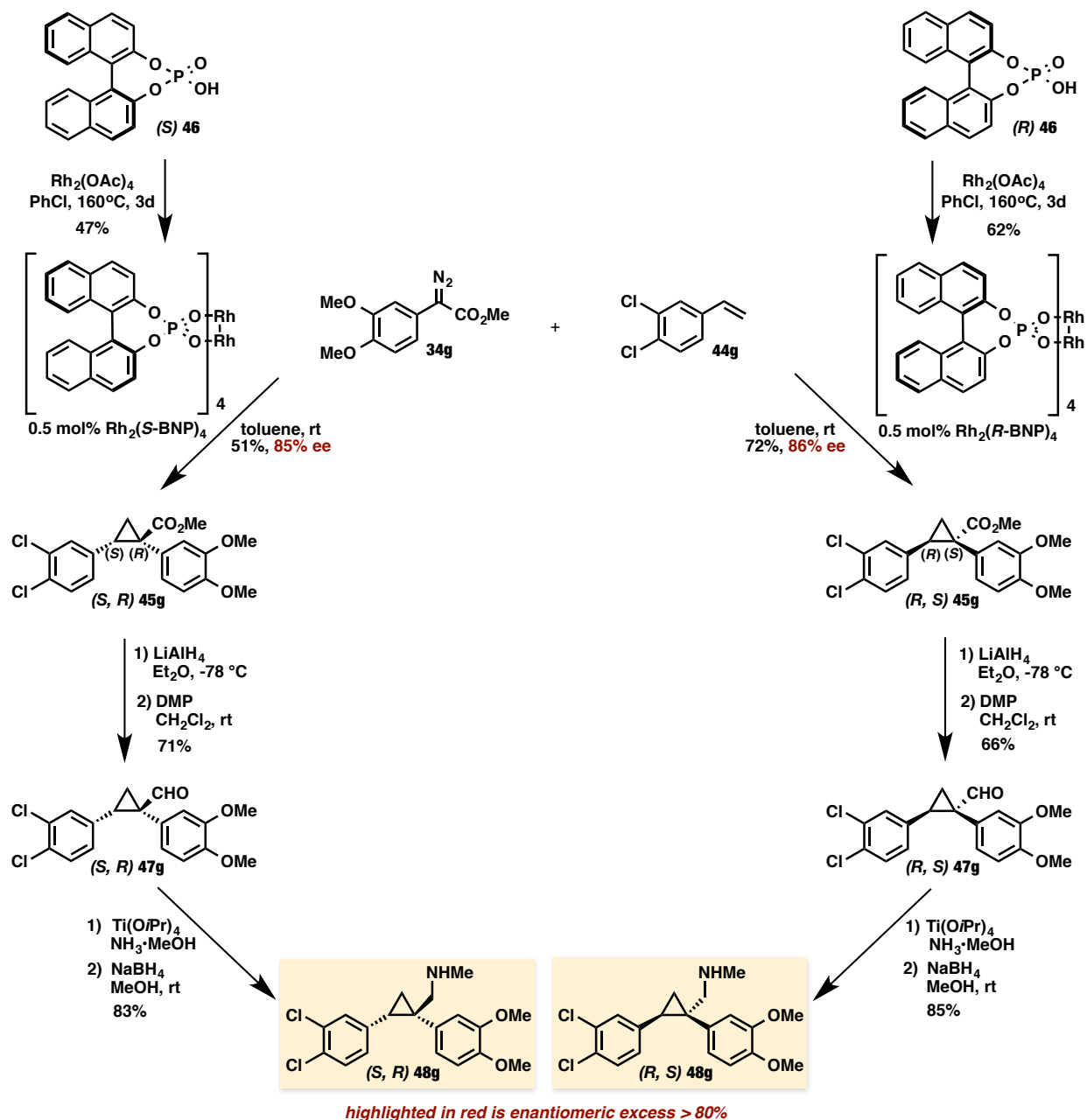
It is believed that antagonism of the 5-HT_{2A} receptor could be a viable target for the therapeutic treatment of cocaine addiction. Computational modeling studies on this system conducted by former Davies group member, Dr. Spandan Chennamadhavuni, in collaboration with the Snyder group at Emory University, have shown that oxy-halo interactions between the A-ring and the receptor site play a significant role in binding to the 5-HT_{2A} receptor.¹⁶ As these cyclopropyl amines are known to have significant CNS activity,¹⁶⁻¹⁷ Davies *et al.* initiated a program to use our cyclopropanation methodology to access novel diarylcyclopropylamines as potential therapeutic agents (Scheme 2.9).

Scheme 2.9 Route to cyclopropyl amines from aryldiazoacetates



To further probe the steric and electronic requirements of the B-ring for increased potency at the 5-HT_{2A} receptor (Figure 2.6), the previously successful cyclopropanation reaction under Rh₂(*R*-BNP)₄-catalysis was applied (Scheme 2.10). Typically, only one enantiomer will show biological activity towards the 5-HT_{2A} receptor. Which enantiomer this will be, however, is unknown until the compounds are submitted for testing. For this reason, (*S*)- and (*R*)-(+)-1,1'-Binaphthyl-2,2'-diyl hydrogenphosphate (**(*S*) 33** and **(*R*) 33**) were subjected to ligand exchange¹ with Rh₂(OAc)₄ to afford the corresponding catalysts Rh₂(*S*-BNP)₄ and Rh₂(*R*-BNP)₄ in 47% and 62% yield respectively. With both enantiomers of catalyst in hand, the syntheses of these cyclopropylmethylamines was achieved using a standard sequence developed by Dr. Spandan Chennamadhavuni. Decomposition of **34g** by Rh₂(*R*-BNP)₄, employing 1,2-dichloro-4-vinylbenzene (**44g**) as the trapping agent afforded the corresponding cyclopropane **45g** in moderate yield (72%) and stereoselectivity (86% ee). Reduction of the methyl ester moiety of cyclopropane **45g** with lithium aluminum hydride followed by Dess-Martin oxidation provided aldehyde **(*R,S*) 47g** in moderate yield over two steps (66%). Finally, reductive amination converted the aldehyde into the corresponding amine **(*R,S*) 48g** in good yield (85%). A similar synthetic sequence employing Rh₂(*S*-BNP)₄ as the catalyst was used to generate the (*S*), (*R*) cyclopropylamine **(*S,R*) 48g** (Scheme 2.10).

Scheme 2.10 Synthetic route to 5-HT_{2A} receptor antagonist analogue



2.8 Development of a Guide to Choosing the Best Dirhodium(II) Catalyst to use for Enantioselective Cyclopropanation of Aryldiazoacetates with Styrene Derivatives

For the methodology described in Scheme 2.9 to be broadly useful in drug discovery, access to a range of diarylcyclopropyl derivatives with high levels of enantioenrichment is required. For

this reason, the optimal catalysts for cyclopropanation with various types of methyl aryldiazoacetates was determined next. Three chiral dirhodium(II) catalysts were selected for this study (Figure 2.7).¹⁵ The first catalyst, $\text{Rh}_2(R\text{-DOSP})_4$, is considered to be the optimal catalyst for the reactions of donor/acceptor carbenoids when the acceptor group is a methyl ester.^{1,4} The substrate scope of $\text{Rh}_2(R\text{-DOSP})_4$ -catalyzed cyclopropanation is quite broad in terms of both the trapping agent and the donor group on the carbenoid.^{13a, 13b, 18} However, a detailed study on the influence of the aryl substituent of the aryldiazoacetate on $\text{Rh}_2(R\text{-DOSP})_4$ -catalyzed cyclopropanation has not been conducted. The second catalyst, $\text{Rh}_2(S\text{-PTAD})_4$, is the optimal chiral catalyst when the acceptor group in the donor/acceptor carbenoid is a phosphonate,¹⁹ trifluoromethyl,²⁰ cyano,²¹ or keto group.²² Due to the perceived superiority of $\text{Rh}_2(R\text{-DOSP})_4$ in the reactions of aryldiazoacetates, $\text{Rh}_2(S\text{-PTAD})_4$ has not been thoroughly evaluated in the reactions of this class of carbenoid precursor. The third catalyst, $\text{Rh}_2(R\text{-BNP})_4$, is an interesting catalyst of D_4 -symmetry that has been applied to a number of carbenoid reactions,^{1, 6-8} but prior to the aforementioned investigation, had not been previously evaluated in the cyclopropanation of donor/acceptor carbenoids.

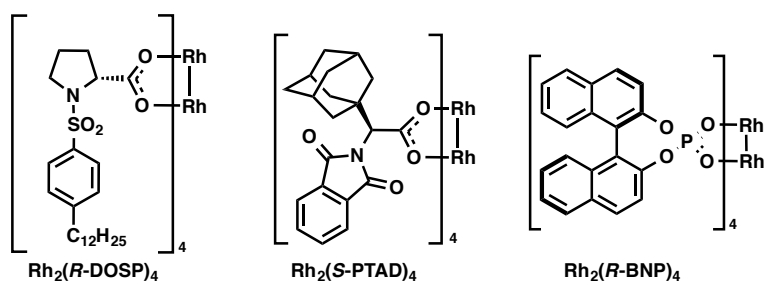


Figure 2.7 Dirhodium(II) catalysts used in this study¹⁵

The study began by exploring the effect of aryl substitution on the enantioselectivity in the cyclopropanation of styrene by aryldiazoacetates. The results for a series of aryldiazoacetates

(**34a**, **34e**, **34g-i**, **34k**, **34m-n**, **36a** and **49a-c**) using the three chiral dirhodium catalysts $\text{Rh}_2(R\text{-DOSP})_4$, $\text{Rh}_2(S\text{-PTAD})_4$ and $\text{Rh}_2(R\text{-BNP})_4$ are summarized in Table 2.11.¹⁵ Excellent levels of diastereoselectivity were achieved in all cases (> 95:5 dr) and the isolated yields of the cyclopropanes were generally high, ranging from 63 - 98%. The absolute stereochemistry of the major isomer of cyclopropane product in all cases was 1*S*, 2*R*. The absolute configuration of the cyclopropanes was determined by comparison of the optical rotation with that of an authentic sample.²³ $\text{Rh}_2(R\text{-DOSP})_4$ provided high levels of enantioinduction when unsubstituted (**34a**) or 4-substituted (**34k**, **34m** and **49a-b**) methyl aryldiazoacetates were employed as substrates (Table 2.11, entries 1 - 5, 87 - 90% ee). In general, $\text{Rh}_2(S\text{-PTAD})_4$ and $\text{Rh}_2(R\text{-BNP})_4$ gave < 60% ee in the cyclopropanation reactions of unsubstituted or 4-substituted aryldiazoacetates with these same substrates. The one exception, however, was the reaction of 4-methoxyphenyldiazoacetate **34k** with $\text{Rh}_2(S\text{-PTAD})_4$, which gave the cyclopropane **35k** in exceptionally high enantioselectivity (entry 5, 96% ee). $\text{Rh}_2(R\text{-DOSP})_4$ also performed well in the reactions of 2-substituted aryldiazoacetates **49c** (entry 6, 92% ee) and **34n** (entry 7, 86% ee), and moderately well with 3,4-dichlorophenyldiazoacetate **34i** (entry 8, 82% ee), confirming that $\text{Rh}_2(R\text{-DOSP})_4$ is the optimal catalyst for a range of aryldiazoacetates. The enantioselection with $\text{Rh}_2(S\text{-PTAD})_4$ is extremely variable. However, in certain cases, it provides exceptional levels of enantioselectivity, as is seen in the reaction with 2-chlorophenyldiazoacetate **49c**, which generates the cyclopropane **50c** in 97% ee (entry 6). Interestingly, $\text{Rh}_2(R\text{-DOSP})_4$ failed to provide high levels of enantioinduction when the aryldiazoacetate contained a 3-methoxy substituent (entries 9 - 12, **34g-h**, **34e** and **36a**), especially when the ring was polysubstituted (**34g-h** and **36a**). In these cases, the cyclopropanes **35g-h** and **37a** were produced in 28 - 56% ee (entries 9, 11 - 12). $\text{Rh}_2(S\text{-PTAD})_4$ was an effective catalyst only in the case of 3,4-

dimethoxyphenyldiazoacetate **34g**, generating the cyclopropane **35g** in 94% ee (entry 9). In contrast, $\text{Rh}_2(\text{R-BNP})_4$ was an extremely effective catalyst with all of the 3-methoxy substituted aryldiazoacetates **34g-h**, **34e** and **36a** generating the cyclopropanes **35g-h**, **35e** and **37a** in 88 - 97% ee (entries 9 - 12).¹⁵

Table 2.11 Examination of the influence of substitution on aryldiazoacetate¹⁵

$\text{Ar}-\text{C}(\text{N}_2)=\text{C}(\text{CO}_2\text{Me}) \xrightarrow[\text{solvent, rt}]{1 \text{ mol\% Rh(II)}} \text{Ph}-\text{C}(\text{Me})-\text{C}(\text{Ar})-\text{CO}_2\text{Me}$

$\text{Ph}-\text{C}(\text{Me})=\text{C} \quad \text{28}$

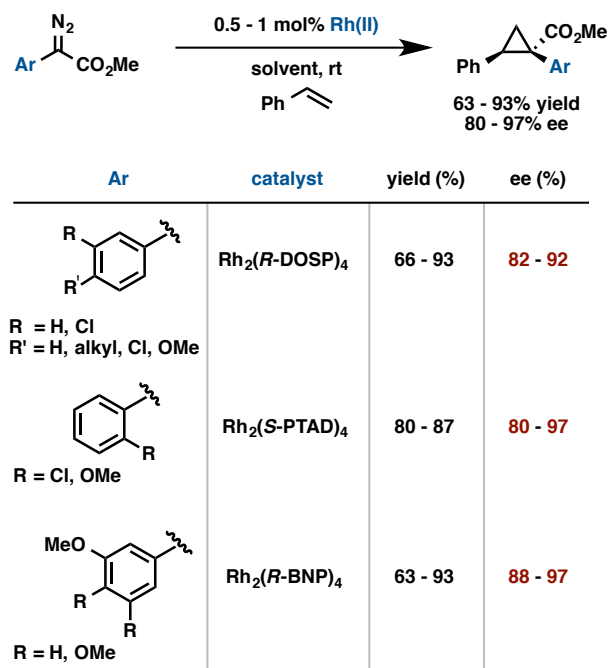
entry	Ar	product	Rh ₂ (<i>R</i> -DOSP) ₄ ^a		Rh ₂ (<i>S</i> -PTAD) ₄ ^a		Rh ₂ (<i>R</i> -BNP) ₄ ^b	
			yield (%)	ee (%) ^c	yield (%)	ee (%) ^c	yield (%)	ee (%) ^c
1		35a	85	88	87 ^b	21 ^b	72	42
2		50a	84 ^f	87 ^f	77 ^{d,f}	46 ^{d,f}	69	51
3		35m	93 ^f	87 ^f	67 ^{d,f}	77 ^{d,f}	80 ^e	57 ^e
4		50b	87 ^f	88 ^f	71 ^{d,f}	48 ^{d,f}	89	57
5		35k	66 ^f	90 ^f	93 ^{d,f}	96 ^{d,f}	84 ^e	57 ^e
6		50c	89 ^f	92 ^f	80 ^{d,f}	97 ^{d,f}	78	51
7		35n	92 ^f	86 ^f	87 ^{d,f}	80 ^{d,f}	69 ^e	27 ^e
8		35i	88 ^b	82 ^b	88 ^b	60 ^b	82 ^e	63 ^e
9		35g	74 ^f	56 ^f	70 ^{d,f}	94 ^{d,f}	93	97
10		35e	78 ^b	79 ^b	72 ^b	16 ^b	82 ^e	88 ^e
11		37a	85 ^{b,d}	28 ^{b,d}	85 ^{b,d}	3 ^{b,d}	69 ^d	92 ^d
12		35h	98 ^b	34 ^b	95 ^b	9 ^b	63 ^e	90 ^e

^a pentane, ^b toluene, ^c highlighted in red is enantiomeric excess > 80%, ^d 0.5 mol% catalyst loading,

^e reaction conducted by Dr. Changming Qin, ^f reaction conducted by Dr. Joshua S. Alford

These studies reveal subtle differences in the ability of the chiral dirhodium tetracarboxylate catalysts to induce high enantioselectivity in the cyclopropanation of styrenes, as summarized in Table 2.12. The previous expectation that $\text{Rh}_2(R\text{-DOSP})_4$ would give high asymmetric induction for all aryldiazoacetates was found not to be true, although it was found to be the most effective catalyst for the broadest range of substituted methyl aryldiazoacetates. In spite of the fact that $\text{Rh}_2(S\text{-PTAD})_4$ is the most consistent catalyst when the acceptor group of the donor/acceptor carbenoid is modified,¹⁹⁻²² the level of enantioselectivity was found to be highly variable when aryl substitution of the aryldiazoacetate was modified. In particular, $\text{Rh}_2(S\text{-PTAD})_4$ was very effective with the 2-chlorophenyl aryldiazoacetate derivative. $\text{Rh}_2(R\text{-BNP})_4$ was the most effective catalyst for 3-methoxyphenyl-substituted aryldiazoacetate derivatives. The factors behind these subtle variations, at this stage, is not well understood. There is no clear steric or electronic trend to define which catalyst will perform best in a given system, which suggests the asymmetric induction may involve a combination of factors including π -stacking interactions. Computational studies are in progress to develop a rational model to explain these trends.¹⁵

Table 2.12 A guide to chiral dirhodium(II) catalyzed cyclopropanation¹⁵



2.9 Conclusion

Catalytic enantioselective methods for the generation of cyclopropanes have been of long standing pharmaceutical interest. Chiral dirhodium(II) catalysts prove to be effective for the generation of diverse cyclopropane libraries. This study provides guidelines for choosing the optimal chiral dirhodium(II) catalyst for cyclopropanation with aryldiazoacetates. The nature of the aryl group on the aryldiazoacetate strongly affects the asymmetric induction imparted by the three catalysts studied. Depending on the aryl substituent, $\text{Rh}_2(\text{R-DOSP})_4$, $\text{Rh}_2(\text{S-PTAD})_4$, or $\text{Rh}_2(\text{R-BNP})_4$ can be utilized to obtain the desired cyclopropane with a high level of enantioinduction. $\text{Rh}_2(\text{R-DOSP})_4$ is the most effective catalyst for asymmetric intermolecular cyclopropanation of methyl aryldiazoacetates with styrene. $\text{Rh}_2(\text{S-PTAD})_4$ provides high levels of enantioinduction when the acetate group of the aryldiazoacetate precursor is varied. The less-established $\text{Rh}_2(\text{R-BNP})_4$ plays a complementary role to $\text{Rh}_2(\text{R-DOSP})_4$ and $\text{Rh}_2(\text{S-PTAD})_4$ in

catalyzing highly enantioselective cyclopropanation of alkoxy-substituted methyl aryldiazoacetates. In contrast, the functionality on the styrene has only moderate influence on the level of asymmetric induction in cyclopropanation reactions. These studies set the chemical foundation for the development of therapeutically useful diarylcyclopropylamines.¹⁵

2.10 Experimental Section

General: All reactions were conducted under anhydrous conditions in oven-dried glassware under an inert atmosphere of dry argon at room temperature, unless otherwise stated. Hexanes, pentane, and toluene were dried by a solvent purification system (passed through activated alumina columns). All solvents were degassed by bubbling argon through the solvent for a minimum of 10 minutes prior to use. Unless otherwise noted, all other reagents were obtained from commercial sources and used as received. ¹H Nuclear Magnetic Resonance (NMR) spectra were recorded at 400 MHz or 600MHz. Data presented as follows: chemical shift (in ppm on the δ scale relative to δ H 7.27 for the residual protons in CDCl₃), coupling constant (J/Hz), integration. Coupling constants were taken directly from the spectra and are uncorrected. ¹³C NMR spectra were recorded at 100 MHz and all chemical shift values are reported in ppm on the δ scale, with an internal reference of δ C 77.23 for CDCl₃. Mass spectral determinations were carried out by using APCI as ionization source. Melting points are uncorrected. Infrared spectral data are reported in units of cm⁻¹. Analytical TLC was performed on silica gel plates using UV light. Flash column chromatography was performed on silica gel 60Å (230-400 mesh). Optical rotations were measured on JASCO P-2000 polarimeters. Analytical enantioselective chromatographies were measured on Varian Prostar instrument and used isopropanol:hexane as gradient. Chiral HPLC conditions were determined by obtaining

separation of the racemic product. $\text{Rh}_2(R/S\text{-DOSP})_4$ was employed as the catalyst in the racemic reactions. Styrene (**28**) and substituted styrenes (**44a-f**) as well as styrene derivatives (**44h-i**) were commercially available and purified by pushing through a silica-filled pipette prior to use. $\text{Rh}_2(R\text{-DOSP})_4$,^{13a} $\text{Rh}_2(S\text{-PTAD})_4$,¹⁹ $\text{Rh}_2(R\text{-BNP})_4$,¹ aryldiazoacetates **32**, **34a**, **34e**, **34g-i**, **34k**, **34m-n**, **40**, **42a-b** and **49a-c**^{12b} and styrene **44g**²⁴ were all synthesized according published procedures. This experimental section also contains detailed procedures for the synthesis of $\text{Rh}_2(R\text{-DOSP})_4$, $\text{Rh}_2(S\text{-PTAD})_4$ and $\text{Rh}_2(R\text{-BNP})_4$ as well as their characterization data.

General Procedure for the Synthesis of Methyl Phenyl diazoacetates²⁵

The methyl arylacetate (1 equiv.) and *p*-ABSA (1.3 equiv.) were dissolved in acetonitrile and cooled to 0 °C using an ice bath under an argon atmosphere. 1,8-Diazabicycloundec-7-ene (DBU, 1.3 equiv.) was then added to the stirring mixture over the course of 5 minutes. After the addition of the DBU, the reaction mixture continued to stir at 0 °C for an additional 15 minutes. Once this allotted time had passed, the ice bath was removed and the reaction mixture was stirred for 24 hours at room temperature. The resulting orange solution was quenched with saturated aqueous ammonium chloride (NH_4Cl) and the aqueous layer was extracted with diethyl ether (3x). The organic layer was then washed with deionized H_2O to remove any residual salts. The combined organic layers were dried over magnesium sulfate (MgSO_4) and filtered. The organic layer was then concentrated under reduced pressure. The residue was purified via flash chromatography on silica gel (hexanes : ethyl acetate 10 : 1).

General Procedure for the Synthesis of Methyl Phenylcyclopropanecarboxylates with $\text{Rh}_2(R\text{-DOSP})_4$

In a 25-mL round bottom flask (Flask A) equipped with a magnetic stir bar, styrene (5 equiv.) and $\text{Rh}_2(R\text{-DOSP})_4$ (0.01 equiv.) were dissolved in dry, degassed pentane (3 mL). The reaction

mixture was then degassed using vacuum/argon cycles (x3). In a separate 25-mL round bottom flask (Flask B), the methyl phenyldiazoacetate (0.5 mmol, 1 equiv.) was dissolved in dry, degassed pentane (5 mL) and degassed using vacuum/argon cycles (x3). The contents in Flask B were then added to Flask A using a syringe pump for the duration of 1 hour. After the addition, the reaction mixture continued to stir for 1 additional hour. Once the allotted time had passed, the reaction mixture was concentrated under reduced pressure and purified using silica gel column chromatography (increasing gradient starting at hexanes : ethyl acetate 10 : 1).

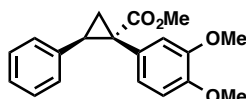
General Procedure for the Synthesis of Methyl Phenylcyclopropanecarboxylates with Rh₂(S-PTAD)₄

In a 25-mL round bottom flask (Flask A) equipped with a magnetic stir bar, styrene (5 equiv.) and Rh₂(S-PTAD)₄ (0.005 equiv.) were dissolved in dry, degassed pentane (3 mL). The reaction mixture was then degassed using vacuum/argon cycles (x3). In a separate 25-mL round bottom flask (Flask B), the methyl phenyldiazoacetate (0.5 mmol, 1 equiv.) was dissolved in dry, degassed pentane (5 mL) and degassed using vacuum/argon cycles (x3). The contents in Flask B were then added to Flask A using a syringe pump for the duration of 1 hour. After the addition, the reaction mixture continued to stir for 1 additional hour. Once the allotted time had passed, the reaction mixture was concentrated under reduced pressure and purified using silica gel column chromatography (increasing gradient starting at hexanes : ethyl acetate 10 : 1).

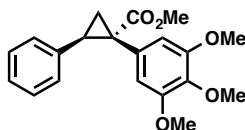
General Procedure for the Synthesis of Methyl Phenylcyclopropanecarboxylates with Rh₂(R-BNP)₄

In a 25-mL round bottom flask (Flask A) equipped with a magnetic stir bar, styrene (5 equiv.) and Rh₂(R-BNP)₄ (0.01 equiv.) were dissolved in dry, degassed toluene (3 mL). The reaction mixture was then degassed using vacuum/argon cycles (x3). In a separate 25-mL round bottom flask (Flask B), the methyl phenyldiazoacetate (0.5 mmol, 1 equiv.) was dissolved in dry,

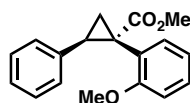
degassed toluene (5 mL) and degassed using vacuum/argon cycles (x3). The contents in Flask B were then added to Flask A using a syringe pump for the duration of 1 hour. After the addition, the reaction mixture continued to stir for 1 additional hour. Once the allotted time had passed, the reaction mixture was concentrated under reduced pressure and purified using silica gel column chromatography (increasing gradient starting at hexanes : ethyl acetate 10 : 1).



(1S,2R)-methyl 1-(3,4-dimethoxyphenyl)-2-phenylcyclopropanecarboxylate (35g): Title compound was prepared by general procedure and obtained as a white solid. 74% yield for $\text{Rh}_2(R\text{-DOSP})_4$; 70% yield for $\text{Rh}_2(S\text{-PTAD})_4$; 93% yield for 1 mol% $\text{Rh}_2(R\text{-BNP})_4$; 83% yield for 0.5 mol% $\text{Rh}_2(R\text{-BNP})_4$; 80% yield for 0.1 mol% $\text{Rh}_2(R\text{-BNP})_4$; 73% yield for 0.01 mol% $\text{Rh}_2(R\text{-BNP})_4$; HPLC: (Chiralcel OD-H, 6% *i*-PrOH in hexane, 1 mL/min, 1 mg/mL, 30 min, $\lambda = 254$ nm) retention times of 13.99 min (minor) and 17.97 min (major), 56% ee for $\text{Rh}_2(R\text{-DOSP})_4$; 94% ee for $\text{Rh}_2(S\text{-PTAD})_4$; 97% ee for 1 mol% $\text{Rh}_2(R\text{-BNP})_4$; 96% ee for 0.5 mol% $\text{Rh}_2(R\text{-BNP})_4$; 91% ee for 0.1 mol% $\text{Rh}_2(R\text{-BNP})_4$; 40% ee for 0.01 mol% $\text{Rh}_2(R\text{-BNP})_4$; $R_f = 0.20$ (hexane: ethyl acetate 4 : 1); mp 88-89 °C; $[\alpha]_D^{20} +28.4^\circ$ ($c = 1.51$, CHCl_3); ^1H NMR (400 MHz, CDCl_3) δ 7.09-7.07 (m, 3H), 6.81-6.79 (m, 2H), 6.69 (m, 2H), 6.36 (s, 1H), 3.81 (s, 3H), 3.68 (s, 3H), 3.56 (s, 3H), 3.08 (dd, $J = 9.2, 7.6$ Hz, 1H), 2.14 (dd, $J = 9.2, 4.4$ Hz, 1H), 1.84 (dd, $J = 7.6, 4.8$ Hz, 1H); ^{13}C NMR (100 MHz, CDCl_3) δ 174.5, 147.8, 136.4, 127.9, 127.7, 127.2, 126.3, 123.9, 115.3, 110.2, 55.5, 52.6, 36.9, 33.1, 20.8; IR (film): 2924, 1716, 1518, 1455, 1434, 1413, 1341, 1229, 1208, 1177; HRMS (ESI) calcd for $\text{C}_{19}\text{H}_{21}\text{O}_4$ ($\text{M}+\text{H}$) $^+$ 313.1440 found 313.1433.

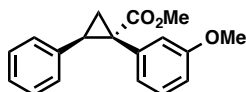


(1*S*,2*R*)-methyl 2-phenyl-1-(3,4,5-trimethoxyphenyl)cyclopropanecarboxylate (35h): Title compound was prepared by general procedure and obtained as a yellow oil. 98% yield for Rh₂(*R*-DOSP)₄; 95% yield for Rh₂(*S*-PTAD)₄; 63% yield for Rh₂(*R*-BNP)₄; HPLC: (Chiralcel OD-H, 6% *i*-PrOH in hexane, 1 mL/min, 1 mg/mL, 30 min, λ = 254 nm), retention times of 10.78 min (minor) and 11.79 min (minor), 34% ee for Rh₂(*R*-DOSP)₄; 9% ee for Rh₂(*S*-PTAD)₄; 90% ee for Rh₂(*R*-BNP)₄; *R_f* = 0.20 (hexanes : ethyl acetate 5 : 1); [α]_D²⁰ +17.5° (c = 2.02, CHCl₃); ¹H NMR (400 MHz, CDCl₃) δ 7.09-7.07 (m, 3H), 6.81-6.78 (m, 2H), 6.16 (s, 2H), 3.76 (s, 3H), 3.69 (s, 3H), 3.59 (s, 6H), 3.07 (dd, *J* = 9.2, 7.2 Hz, 1H); 2.14 (dd, *J* = 9.6, 4.8 Hz, 1H), 1.82 (dd, *J* = 7.6, 5.2 Hz, 1H); ¹³C NMR (100 MHz, CDCl₃) δ 174.2, 152.3, 136.5, 130.3, 128.1, 128.0, 127.7, 126.4, 109.4, 60.7, 55.9, 52.6, 37.4, 33.1 20.8; IR (film): 2925, 1716, 1587, 1413, 1258, 1235, 1153, 1124; HRMS (ESI) calcd for C₂₀H₂₃O₄ (M+H)⁺ 345.1485 found 345.1485.

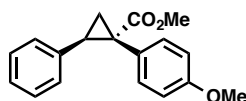


(1*S*,2*R*)-methyl 1-(2-methoxyphenyl)-2-phenylcyclopropanecarboxylate (35n): Title compound was prepared by general procedure and obtained as a white solid. 92% yield for Rh₂(*R*-DOSP)₄; 87% yield for Rh₂(*S*-PTAD)₄; 69% yield for Rh₂(*R*-BNP)₄; HPLC: (SS-WHELK column, 1% *i*-PrOH in hexanes, 1.0 mL/min, 1mg/mL, 30 min, λ = 254 nm) retention times of 11.65 min (minor) and 14.00 min (major), 86% ee for Rh₂(*R*-DOSP)₄; 80% ee for Rh₂(*S*-PTAD)₄; 27% ee for Rh₂(*R*-BNP)₄; *R_f* = 0.45 (hexanes : ethyl acetate 4 : 1); [α]_D²⁰: +133.3° (c = 1.00, CHCl₃); ¹H NMR (400 MHz; CDCl₃) δ 7.19-7.10 (m, 2H), 7.04-6.98 (m, 3H), 6.86 (td, *J* = 7.6, 1.1 Hz, 1H), 6.81-6.74 (m, 2H), 6.53 (d, *J* = 8 Hz, 1H), 3.65 (s, 3H), 3.36 (s, 3H), 3.24 (dd, *J*

= 9.6 and 7.6 Hz, 1H), 1.98 (dd, $J = 9.2$ and 4.8 Hz, 1H), 1.85 (dd, $J = 7.2$ and 4.8 Hz, 1H); ^{13}C NMR (100 MHz, CDCl_3) δ 174.7, 159.2, 137.0, 131.8, 128.9, 127.9, 127.3, 126.1, 124.1, 120.1, 110.5, 55.2, 52.7, 34.3, 32.6, 20.8; IR (film): 3030, 2950, 2835, 1716, 1496, 1242; HRMS (APCI) calcd for $\text{C}_{18}\text{H}_{19}\text{O}_3$ ($\text{M}+\text{H}$) $^+$ 283.1329 found 283.1329.

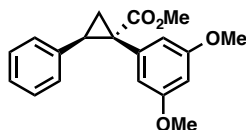


(1S,2R)-methyl 1-(3-methoxyphenyl)-2-phenylcyclopropanecarboxylate (35e): Title compound was prepared by general procedure and obtained as a yellow oil. 78% yield for $\text{Rh}_2(\text{R-DOSP})_4$; 72% yield for $\text{Rh}_2(\text{S-PTAD})_4$; 82% yield for $\text{Rh}_2(\text{R-BNP})_4$; HPLC: (Chiralcel OD-H, 0.7% *i*-PrOH in hexane, 1 mL/min, 1 mg/mL, 30 min, $\lambda = 254$ nm), retention times of 9.50 min (major) and 11.38 min (minor), 79% ee for $\text{Rh}_2(\text{R-DOSP})_4$; 16% ee for $\text{Rh}_2(\text{S-PTAD})_4$; 88% ee for $\text{Rh}_2(\text{R-BNP})_4$; $R_f = 0.25$ (hexanes : ethyl acetate 9 : 1); $[\alpha]_D^{20} +21.1^\circ$ ($c = 1.25$, CHCl_3); ^1H NMR (400 MHz, CDCl_3) δ 7.09-7.03 (m, 4H), 6.81-6.79 (m, 2H), 6.69-6.63 (m, 2H), 6.53-6.52, (m, 1H), 3.67 (s, 3H), 3.59 (s, 3H), 3.12 (dd, $J = 9.6$, 7.2 Hz, 1H), 2.12 (dd, $J = 9.2$, 4.8 Hz, 1H), 1.87 (dd, $J = 7.6$, 5.2 Hz, 1H); ^{13}C NMR (100 MHz, CDCl_3) δ 174.2, 158.8, 136.4, 136.2, 128.5, 127.9, 127.7, 126.3, 124.4, 117.5, 112.9, 55.0, 52.6, 37.3, 33.1, 20.6; IR (film): 2925, 1717, 1602, 1454, 1239, 697; HRMS (ESI) calcd for $\text{C}_{18}\text{H}_{19}\text{O}_3$ ($\text{M}+\text{H}$) $^+$ 283.1334 found 283.1329.

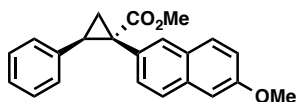


(1S,2R)-methyl 1-(4-methoxyphenyl)-2-phenylcyclopropanecarboxylate (35k): Title compound was prepared by general procedure and obtained as a white solid. 66% yield for $\text{Rh}_2(\text{R-DOSP})_4$; 93% yield for $\text{Rh}_2(\text{S-PTAD})_4$; 84% yield for $\text{Rh}_2(\text{R-BNP})_4$; HPLC: (Chiralcel OD-H, 0.7% *i*-PrOH in hexanes, 1.0 mL/min, 1mg/mL, 30 min, $\lambda = 254$ nm) retention times of

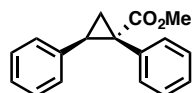
11.97 min (major) and 17.71 min (minor), 90% ee for Rh₂(*R*-DOSP)₄; 96% ee for Rh₂(*S*-PTAD)₄; 57% ee for Rh₂(*R*-BNP)₄; $R_f = 0.39$ (hexanes : ethyl acetate 4 : 1); $[\alpha]_D^{20} = +5.1^\circ$ (c = 1, chloroform); ¹H NMR (400 MHz; CDCl₃) δ 7.10-7.07 (m, 3H), 6.95 (d, $J = 8.8$ Hz, 2H), 6.80-6.77 (m, 2H), 6.68 (d, $J = 8.8$ Hz, 2H), 3.74 (s, 3H), 3.68 (s, 3H), 3.09 (dd, $J = 9.2$ and 7.6 Hz, 1H), 2.14 (dd, $J = 9.2$ and 4.8 Hz, 1H), 1.84 (dd, $J = 7.2$ and 4.8 Hz, 1H); ¹³C NMR (100 MHz, CDCl₃) δ 174.9, 158.6, 136.7, 133.1, 128.3, 127.9, 127.0, 126.5, 113.4, 55.3, 52.8, 36.9, 33.4, 21.0; IR (film): 3031, 2951, 2836, 1715, 1515, 1245; HRMS (APCI) calcd for C₁₈H₁₉O₃ (M+H)⁺ 283.1329 found 283.1328.



(1*S*,2*R*)-methyl 1-(3,5-dimethoxyphenyl)-2-phenylcyclopropanecarboxylate (37a): Title compound was prepared by general procedure and obtained as a yellow oil. 85% yield for Rh₂(*R*-DOSP)₄; 85% yield for Rh₂(*S*-PTAD)₄; 69% yield for Rh₂(*R*-BNP)₄; HPLC: (Chiralcel OD-H, 6% *i*-PrOH in hexane, 1 mL/min, 1 mg/mL, 30 min, $\lambda = 254$ nm) retention times of 7.33 min (major) and 9.07 min (minor), 28% ee for Rh₂(*R*-DOSP)₄; 3% ee for Rh₂(*S*-PTAD)₄; 92% ee for Rh₂(*R*-BNP)₄; $R_f = 0.31$ (hexanes : ethyl acetate 5 : 1); $[\alpha]_D^{20} +33.7^\circ$ (c = 1.1, CHCl₃); ¹H NMR (400 MHz, CDCl₃) δ 7.10-7.08 (m, 3H), 6.82 (dd, $J = 7.2, 2.4$ Hz, 2H), 6.24 (t, $J = 2.4$ Hz, 1H), 6.15 (d, $J = 2.4$ Hz, 2H), 3.68 (s, 3H), 3.56 (s, 6H), 3.08 (dd, $J = 9.2, 7.2$ Hz, 1H), 2.10 (dd, $J = 9.2, 4.8$ Hz, 1H), 1.84 (dd, $J = 7.2, 4.8$ Hz, 1H); ¹³C NMR (100 MHz, CDCl₃) δ 174.4, 160.1, 137.2, 136.6, 128.2, 128.0, 126.6, 110.4, 99.8, 55.4, 52.9, 37.7, 33.3, 20.9; IR (film): 2951, 2840, 1715, 1594, 1456, 1425, 1260, 1203, 1151, 1046, 715, 692; HRMS (APCI) calcd for C₁₉H₂₁O₄ (M+H)⁺ 313.1434 found 313.1435.

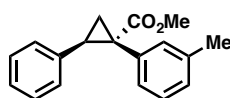


(1*S*,2*R*)-methyl 1-(3,5-dimethoxyphenyl)-2-phenylcyclopropanecarboxylate (37b): Title compound was prepared by general procedure with methyl 2-diazo-2-(6-methoxynaphthalen-2-yl)acetate (**36b**, 118 mg, 0.5 mmol, 1 equiv), styrene (**28**, 130 mg, 1.25 mmol, 2.5 equiv), and $\text{Rh}_2(\text{R-BNP})_4$ (4 mg, 0.0025 mmol, 0.005 equiv). The remaining residue was purified on silica gel eluting with hexanes : ethyl acetate (5 : 1) to afford a yellow oil. 35% yield for $\text{Rh}_2(\text{R-DOSP})_4$; 22% yield for $\text{Rh}_2(\text{R-BNP})_4$. HPLC: (Chiralcel OD-H, 6% *i*-PrOH in hexane, 1 mL/min, 1 mg/mL, 30 min, $\lambda = 254$ nm), retention times of 9.20 min (major) and 10.10 min (minor), 63% ee for $\text{Rh}_2(\text{R-DOSP})_4$, 48% ee for $\text{Rh}_2(\text{R-BNP})_4$; $R_f = 0.31$ (hexanes : ethyl acetate 5 : 1); $[\alpha]_D^{20} -16.0^\circ$ ($c = 0.7$, CHCl_3); $^1\text{H NMR}$ (400 MHz, CDCl_3) δ 7.59 (d, $J = 8.8$ Hz, 1H), 7.52 (s, 1H), 7.43 (d, $J = 8.8$ Hz, 1H), 7.07 (dd, $J = 8.8, 2.4$ Hz, 1H), 7.02-6.98 (m, 5H), 6.81-6.79 (m, 2H), 3.87 (s, 3H), 3.65 (s, 3H), 3.16 (dd, $J = 9.6, 7.4$ Hz, 1H), 2.20 (dd, $J = 9.6, 5.0$ Hz, 1H), 1.98 (dd, $J = 7.4, 5.0$ Hz, 1H); $^{13}\text{C NMR}$ (100 MHz, CDCl_3) δ 174.8, 157.8, 136.5, 133.7, 130.8, 130.5, 130.4, 129.5, 128.7, 128.3, 127.9, 126.5, 126.2, 118.7, 105.8, 55.5, 52.5, 37.6, 33.4, 21.0; IR (film): 2952, 1716, 1607, 1485, 1259, 1204, 1160, 708; HRMS (NSI) calcd for $\text{C}_{22}\text{H}_{21}\text{O}_3$ ($\text{M}+\text{H}$) $^+$ 333.1485 found 333.1483.

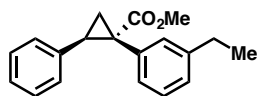


(1*R*,2*S*)-methyl 1,2-diphenylcyclopropanecarboxylate (39a): Title compound was prepared by general procedure and obtained as a white solid. 85% yield for $\text{Rh}_2(\text{R-DOSP})_4$; 87% yield for $\text{Rh}_2(\text{S-PTAD})_4$; 72% yield for $\text{Rh}_2(\text{R-BNP})_4$; HPLC: (Chiralcel SS-WHELK, 1% *i*-PrOH in hexane, 1.0 mL/min, 1 mg/mL, 30 min, $\lambda = 254$ nm) retention times of 8.62 min (major) and

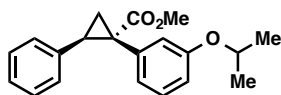
10.22 min (minor), 88% ee for Rh₂(*R*-DOSP)₄; 21% ee for Rh₂(*S*-PTAD)₄; 42% ee for Rh₂(*R*-BNP)₄; *R_f* = 0.25 (hexanes : ethyl acetate 10 : 1); ¹H NMR (600 MHz, CDCl₃) δ 7.12-7.11 (m, 3H), 7.05-7.01 (m, 5H), 6.77-6.75 (m, 2H), 3.70 (s, 3H), 3.11 (dd, *J* = 7.2, 9.3, 1H), 2.13 (dd, *J* = 4.8, 9.3, 1H), 1.88 (dd, *J* = 4.8, 7.2, 1H); ¹³C NMR (100 MHz, CDCl₃) δ 174.5, 136.5, 134.9, 132.1, 128.2, 127.9, 127.2, 126.5, 52.8, 37.6, 33.3, 20.7; Data are consistent with the literature.^{13d, 24}



(1*S*,2*R*)-methyl 2-phenyl-1-(*m*-tolyl)cyclopropanecarboxylate (39b): Title compound was prepared by general procedure with methyl 2-diazo-2-(*m*-tolyl)acetate (**38b**, 95.0 mg, 0.50 mmol, 1.00 equiv), styrene (**28**, 130 mg, 1.25 mmol, 2.50 equiv), and Rh₂(*R*-BNP)₄ (4.00 mg, 0.0025 mmol, 0.005 equiv). The remaining residue was purified on silica gel eluting hexanes : ethyl acetate (100 : 1) to afford clear oil (118 mg, 89% yield). HPLC: (Chiralcel SS-WHELK, 2% *i*-PrOH in hexane, 1 mL/min, 1 mg/mL, 30 min, λ = 254 nm) retention times of 8.35 min (major) and 9.6 min (minor), 42% ee); *R_f* = 0.24 (hexanes : ethyl acetate 20 : 1); [α]_D²⁰ +7.6° (*c* = 0.65, CHCl₃); ¹H NMR (400 MHz, CDCl₃) δ 7.08-6.94 (m, 5H), 6.86-6.77 (m, 4H), 3.68 (s, 3H), 3.12 (dd, *J* = 9.0, 7.8, 1H), 2.20 (s, 3H), 2.13 (dd, *J* = 9.0, 4.8), 1.87 (dd, *J* = 7.8, 4.8); ¹³C NMR (100 MHz, CDCl₃) δ 174.5, 137.1, 136.5, 134.5, 132.6, 129.0, 128.0, 127.8, 127.6, 127.4, 126.2, 52.6, 37.2, 33.1, 21.2, 20.6; IR (film): 2925, 1716, 1257, 1157, 702; HRMS (ESI) calcd for C₁₈H₁₉O₂ (M+H)⁺ 267.1385 found 267.1379.

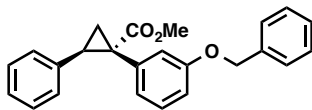


methyl (1*S*,2*R*)-1-(3-ethylphenyl)-2-phenylcyclopropane-1-carboxylate (39c): Title compound was prepared by general procedure with methyl 2-diazo-2-(3-ethylphenyl)acetate (**38c**, 69.0 mg, 0.30 mmol, 1.00 equiv), styrene (**28**, 176 mg, 1.70 mmol, 5.00 equiv), and Rh₂(*R*-BNP)₄ (4.0 mg, 0.0025 mmol, 0.005 equiv). The remaining residue was purified on silica gel eluting with hexanes : ethyl acetate (70 : 1) to afford a clear oil (52 mg, 55% yield). HPLC: (Chiralcel SS-WHELK, 0.5% *i*-PrOH in hexane, 0.5 mL/min, 1 mg/mL, 30 min, $\lambda = 254$ nm) retention times of 16.8 min (major) and 18.5 min (minor), 54% ee; $R_f = 0.15$ (hexanes : ethyl acetate 70 : 1); $[\alpha]_D^{20} +17.9^\circ$ ($c = 0.83$, CHCl₃); ¹H NMR (600 MHz, CDCl₃) δ 7.06 (m, 4H), 6.95 (d, $J = 7.5$ Hz, 1H), 6.88 (d, $J = 7.5$ Hz, 1H), 6.77 (m, 3H), 3.68 (s, 3H), 3.12 (dd, $J = 7.8$, 9.6 Hz, 1H), 2.46 (q, $J = 7.8$ Hz, 2H), 2.13 (dd, $J = 4.8$, 9.6 Hz, 1H), 1.87 (dd, $J = 4.8$, 7.8 Hz, 1H), 1.00 (t, $J = 7.8$ Hz, 3H); ¹³C NMR (100 MHz, CDCl₃) δ 174.7, 143.7, 136.7, 134.8, 132.0, 129.3, 128.3, 127.8, 127.8, 126.8, 126.4, 52.8, 37.5, 33.3, 31.2, 28.8, 20.7, 15.7; IR (film): 3029, 2963, 1717, 1456, 1433, 1259, 1158, 696; HRMS (ESI) calcd for C₁₉H₂₀O₂²³Na₁ (M+H)⁺ 303.1356 found 303.1358.



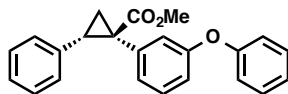
methyl (1*S*,2*R*)-1-(3-isopropoxyphenyl)-2-phenylcyclopropane-1-carboxylate (39d): Title compound was prepared by general procedure with methyl 2-diazo-2-(3-isopropoxyphenyl)acetate (**38d**, 117 mg, 0.50 mmol, 1.00 equiv), styrene (**28**, 260 mg, 2.50 mmol, 5.00 equiv), and Rh₂(*R*-BNP)₄ (4.0 mg, 0.0025 mmol, 0.005 equiv). The remaining residue was purified on silica gel eluting with hexanes : ethyl acetate (50 : 1) to afford clear oil

(85 mg, 55% yield). HPLC: (Chiralcel ADH, 1% *i*-PrOH in hexane, 1 mL/min, 1 mg/mL, 30 min, $\lambda = 230$ nm) retention times of 9.07 min (major) and 10.06 min (minor), 66% ee; $R_f = 0.55$ (hexanes : ethyl acetate 5 : 1); $[\alpha]_D^{20} +25.7^\circ$ ($c = 0.45$, CHCl_3); $^1\text{H NMR}$ (600 MHz, CDCl_3) δ 7.06 (m, 4H), 6.80 (dd, $J = 1.8, 8.4$ Hz, 2H), 6.67 (m, 2H), 6.51 (t, $J = 1.8$ Hz, 1H) 4.28 (sep, $J = 6.0$ Hz, 1H), 3.68 (s, 3H), 3.09 (dd, $J = 7.2, 9.3$ Hz, 1H), 2.13 (dd, $J = 5.1, 9.3$ Hz, 1H), 1.87 (dd, $J = 5.1, 7.2$ Hz, 1H), 1.22 (d, $J = 6.3$ Hz, 3H), 1.07 (d, $J = 6.3$ Hz, 3H); $^{13}\text{C NMR}$ (100 MHz, CDCl_3) δ 174.5, 157.4, 136.7, 136.3, 128.8, 128.2, 127.9, 126.5, 124.4, 120.0, 115.8, 70.1, 52.8, 37.6, 33.4, 22.3, 21.9, 20.8; IR (film): 2976, 2360, 2342, 1718, 1601, 1434, 1258, 1232, 1158, 1117, 698; HRMS (ESI) calcd for $\text{C}_{20}\text{H}_{22}\text{O}_3^{23}\text{Na}_1$ (M+H) $^+$ 333.1461 found 333.1463.

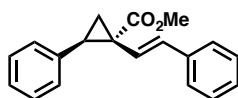


(1S,2R)-methyl 1-(3-(benzyloxy)phenyl)-2-phenylcyclopropanecarboxylate (39e): Title compound was prepared by general procedure with methyl 2-(3-(benzyloxy)phenyl)-2-diazoacetate (**38e**, 141 mg, 0.50 mmol, 1.00 equiv), styrene (**28**, 260 mg, 2.50 mmol, 5.00 equiv), and $\text{Rh}_2(\text{R-BNP})_4$ (4.0 mg, 0.0025 mmol, 0.005 equiv). The remaining residue was purified on silica gel eluting with hexanes : ethyl acetate (100 : 0 to 100 : 1.5) to afford a clear oil (125 mg, 83 % yield). HPLC: (Chiralcel ODH, 0.5% *i*-PrOH in hexane, 1 mL/min, 1 mg/mL, 30 min, $\lambda = 254$ nm) retention times of 27.94 min (minor) and 31.04 min (major), 66% ee; $R_f = 0.40$ (hexanes : ethyl acetate 5 : 1); $[\alpha]_D^{20} +0.0033^\circ$ ($c = 0.78$, CHCl_3); $^1\text{H NMR}$ (400 MHz, CDCl_3) δ 7.37-7.36 (m, 5H), 7.10-7.06 (m, 4H), 6.80 (m, 3H), 6.66-6.65 (m, 2H), 4.90 (d, $J = 11.8$ Hz, 1H), 4.81 (d, $J = 11.8$ Hz, 1H), 3.68 (s, 3H), 3.10 (dd, $J = 7.2, 9.2$ Hz, 1H), 2.11 (dd, $J = 4.8, 9.4$ Hz, 1H), 1.85 (dd, $J = 4.8, 7.2$ Hz, 1H); $^{13}\text{C NMR}$ (100 MHz, CDCl_3) δ 174.4, 158.3, 137.2, 136.6, 136.4, 128.8, 128.7, 128.2, 128.1, 127.9, 127.7, 126.5, 124.9, 118.8, 114.1, 70.0, 52.8,

37.5, 33.4, 29.9, 20.7; IR (film): 3031, 2924, 1714, 1602, 1581, 1455, 1433, 1256, 1223, 1203, 1157, 1027, 739, 695; HRMS (APCI) calcd for C₂₂H₁₉O (M+H)⁺ 299.1430 found 299.1431.

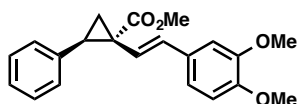


(1R,2S)-methyl 1-(3-phenoxyphenyl)-2-phenylcyclopropanecarboxylate (39f): Title compound was prepared by general procedure with methyl 2-diazo-2-(3-phenoxyphenyl)acetate (**38f**, 134 mg, 0.50 mmol, 1.00 equiv), styrene (**28**, 260 mg, 2.50 mmol, 5.00 equiv), and Rh₂(R-BNP)₄ (4.0 mg, 0.0025 mmol, 0.005 equiv). The remaining residue was purified on silica gel eluting hexanes : ethyl acetate (100 : 0.8) to afford a clear oil (83 mg, 67% yield). HPLC: (Chiralcel ODR, 0.5% *i*-PrOH in hexane, 1 mL/min, 1 mg/mL, 30 min, λ = 254 nm) retention times of 10.85 min (major) and 15.37 min (minor), 33% ee; *R*_f = 0.28 (hexanes : ethyl acetate 10 : 1); [α]_D²⁰ -4.39° (c = 3.14, CHCl₃); ¹H NMR (400 MHz, CDCl₃) δ 7.24-7.19 (ddd, *J* = 2.0, 4.0, 9.6 Hz, 2H), 7.17-7.07 (m, 4H), 6.89 (d, *J* = 8.0 Hz, 1H), 6.83-6.77 (m, 3H), 6.64-6.61 (m, 3H), 3.66 (s, 3H), 3.08 (dd, *J* = 7.2, 9.4 Hz, 1H), 2.10 (dd, *J* = 5.2, 9.4 Hz, 1H), 1.90 (dd, *J* = 5.2, 7.2 Hz, 1H); ¹³C NMR (100 MHz, CDCl₃) δ 174.1, 157.5, 156.2, 136.8, 136.4, 129.8, 129.3, 128.2, 128.1, 126.9, 126.6, 123.3, 122.9, 118.6, 118.3, 52.9, 37.5, 33.4, 20.5; IR (film): 3032, 2951, 1716, 1581, 1487, 1456, 1376, 1335, 1255, 1229, 1191, 1154, 1097; HRMS (APCI) calcd for C₂₃H₂₁O₃ (M+H)⁺ 345.1485 found 345.1485.

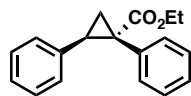


methyl (1R,2R)-2-phenyl-1-((E)-styryl)cyclopropane-1-carboxylate (33): Title compound was prepared by general procedure with (*E*)-methyl 2-diazo-4-phenylbut-3-enoate (**32**, 101 mg, 0.50 mmol, 1.00 equiv), styrene (**28**, 260 mg, 2.50 mmol, 5.00 equiv), and Rh₂(R-BNP)₄ (8.0 mg,

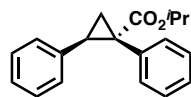
0.005 mmol, 0.01 equiv). The remaining residue was purified on silica gel eluting hexanes : ethyl acetate (15 : 1) to afford a clear oil (139 mg, 38% yield). HPLC: (Chiralcel OJH, 1.5% *i*-PrOH in hexane, 1 mL/min, 1 mg/mL, 30 min, $\lambda = 254$ nm) retention times of 15.1 min (major) and 19.9 min (minor), 66% ee. $R_f = 0.50$ (hexanes : ethyl acetate 5 : 1); $^1\text{H NMR}$ (400 MHz, CDCl_3) δ 7.25-7.21 (m, 4H), 7.19-7.13 (m, 6H), 6.35 (d, $J = 16.2$ Hz, 1H), 6.14 (d, $J = 16.2$ Hz, 1H), 3.77 (s, 3H), 3.04-2.99 (m, 1H), 2.03 (dd, $J = 9.2, 4.9$ Hz, 1H), 1.88 (dd, $J = 7.3, 5.2$ Hz, 1H); Data are consistent with the literature.²⁶



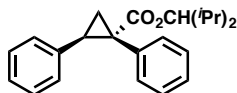
methyl (1*R*,2*R*)-1-((*E*)-3,4-dimethoxystyryl)-2-phenylcyclopropane-1-carboxylate (41): Title compound was prepared by general procedure with (*E*)-methyl 2-diazo-4-(3,4-dimethoxyphenyl)but-3-enoate (**40**, 131 mg, 0.50 mmol, 1.00 equiv), styrene (**28**, 260 mg, 2.50 mmol, 5.00 equiv), and $\text{Rh}_2(\text{R-BNP})_4$ (8 mg, 0.005 mmol, 0.01 equiv). The remaining residue was purified on silica gel eluting hexanes : ethyl acetate (2 : 1) to afford a yellow oil (176 mg, 52% yield). HPLC: (Chiralcel ODH, 6% *i*-PrOH in hexane, 1 mL/min, 1 mg/mL, 30 min, $\lambda = 254$ nm) retention times of 12.3 min (minor) and 13.4 min (major), 66% ee; $R_f = 0.13$ (hexanes : ethyl acetate 2 : 1); $^1\text{H NMR}$ (400 MHz, CDCl_3) δ 7.25-7.21 (m, 2H), 7.19-7.13 (m, 3H), 6.75-6.65 (m, 3H), 6.31 (d, $J = 15.9$ Hz, 1H), 5.97 (d, $J = 15.9$ Hz, 1H), 3.85 (s, 3H), 3.81 (s, 3H), 3.77 (s, 3H), 3.01-2.98 (m, 1H), 2.02 (dd, $J = 9.0, 5.0$ Hz, 1H), 1.82 (dd, $J = 7.3, 5.2$ Hz, 1H); $^{13}\text{C NMR}$ (100 MHz, CDCl_3) δ 174.2, 148.8, 148.6, 135.6, 132.9, 130.2, 129.0, 127.9, 126.6, 122.2, 119.2, 110.9, 108.8, 55.8, 55.7, 52.4, 34.7, 33.2, 18.6; IR (film): 2950, 1716, 1512, 1453, 1246; HRMS (APCI) calcd for $\text{C}_{21}\text{H}_{22}\text{O}_4$ ($\text{M}+\text{Na}$)⁺ 361.1416 found 361.1413.



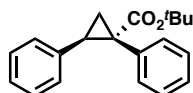
(1S,2R)-ethyl 1,2-diphenylcyclopropanecarboxylate (43a): Title compound was prepared by general procedure with ethyl 2-diazo-2-phenylacetate (**42a**, 95.0 mg, 0.50 mmol, 1.00 equiv), styrene (**28**, 260 mg, 2.50 mmol, 5.00 equiv), and $\text{Rh}_2(\text{R-BNP})_4$ (4.0 mg, 0.0025 mmol, 0.005 equiv). The remaining residue was purified on silica gel eluting with hexanes : ethyl acetate (5 : 1) to afford clear oil (104 mg, 39% yield). HPLC: (Chiralcel SS-WHELK, 1% *i*-PrOH in hexane, 1 mL/min, 1 mg/mL, 30 min, $\lambda = 254$ nm) retention times of 9.3 min (major) and 11.0 min (major), <5% ee). ^1H NMR (400 MHz, CDCl_3) δ 7.20-7.10 (m, 4H), 7.07-7.01 (m, 4H), 6.78-6.75 (m, 2H), 4.21-4.06 (m, 2H), 3.10 (dd, $J = 9.4, 7.6$ Hz, 1H), 2.12 (dd, $J = 9.4, 5.2$ Hz, 1H), 1.87 (dd, $J = 7.6, 5.2$ Hz, 1H), 1.18 (t, $J = 7.2$ Hz, 1H); Data are consistent with the literature.²⁷



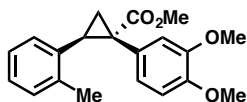
(1S,2R)-isopropyl 1,2-diphenylcyclopropanecarboxylate (43b): Title compound was prepared by general procedure with isopropyl 2-diazo-2-phenylacetate (**42b**, 102 mg, 0.50 mmol, 1.00 equiv), styrene (**28**, 260 mg, 2.50 mmol, 5.00 equiv), and $\text{Rh}_2(\text{R-BNP})_4$. The remaining residue was purified on silica gel eluting with hexanes : ethyl acetate (30 : 1) to afford crystalline white solid (9 mg, 6 % yield). ^1H NMR (600 MHz, CDCl_3) δ 7.10-7.00 (m, 8H), 6.77-6.75 (m, 2H), 4.99 (m, 1H), 3.06 (dd, $J = 9.5, 7.0$ Hz, 1H), 2.10 (dd, $J = 9.5, 5.0$ Hz, 1H), 1.85 (dd, $J = 7.0, 5.0$ Hz, 1H); Data are consistent with the literature.²⁷



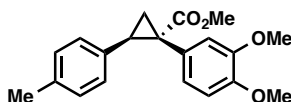
2,4-dimethylpentan-3-yl (1S,2R)-1,2-diphenylcyclopropane-1-carboxylate (43c): Title compound was prepared by general procedure with 2,4-dimethylpentan-3-yl 2-diazo-2-phenylacetate (**42c**, 130 mg, 0.50 mmol, 1.00 equiv), styrene (**28**, 260 mg, 2.50 mmol, 5.00 equiv), and $\text{Rh}_2(\text{R-BNP})_4$ (4.0 mg, 0.0025 mmol, 0.005 equiv). The remaining residue was purified on silica gel eluting with hexanes : ethyl acetate (30 : 1) to afford clear oil (7 mg, 4 % yield). $R_f = 0.22$ (pentane : diethyl ether 50 : 1); $^1\text{H NMR}$ (600 MHz, CDCl_3) δ 7.12-7.01 (m, 8H), 6.80-6.76 (m, 2H), 4.56 (t, $J = 6.2$ Hz, 1H), 3.08 (dd, $J = 9.0, 7.0$ Hz, 1H), 2.13 (dd, $J = 9.0, 4.6$ Hz, 1H), 1.84 (dd, $J = 7.0, 4.6$ Hz, 1H), 1.77 (oct, $J = 6.6$ Hz, 2H), 0.86 (d, $J = 6.8$ Hz, 3H), 0.80 (d, $J = 6.2$ Hz, 3H), 0.75 (d, $J = 6.8$ Hz, 3H), 0.66 (d, $J = 6.8$ Hz, 3H); Data are consistent with the literature.²⁷



(1S,2R)-tert-butyl 1,2-diphenylcyclopropanecarboxylate (43d): Title compound was prepared by general procedure with *tert*-butyl 2-diazo-2-phenylacetate (**42d**, 109 mg, 0.5 mmol, 1 equiv), styrene (**28**, 260 mg, 2.5 mmol, 5.0 equiv), and $\text{Rh}_2(\text{R-BNP})_4$. The remaining residue was purified on silica gel eluting with hexanes : ethyl acetate (30 : 1) to afford crystalline solid (9 mg, 6.2% yield). HPLC: (Chiralcel SS-WHELK, 2% *i*-PrOH in hexane, 1 mL/min, 1 mg/mL, 30 min, $\lambda = 254$ nm) retention times of 7.6 min (major) and 6.9min (major), <5% ee); mp 82-83°C, $R_f = 0.24$ (hexanes : ethyl acetate 60 : 1); $^1\text{H NMR}$ (600 MHz, CDCl_3) δ 7.11-7.00 (m, 8H), 6.77-7.75 (m, 2H), 4.56 (t, $J = 6.0$ Hz, 1H), 3.00 (dd, $J = 9.0, 7.5$ Hz, 1H), 2.06 (dd, $J = 9.5, 5.0$ Hz, 1H), 1.80 (dd, $J = 7.5, 5.0$ Hz, 1H), 1.39 (s, 9H); Data are consistent with the literature.²⁷

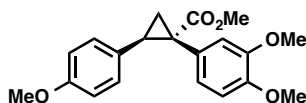


(1S,2R)-methyl 1-(3,4-dimethoxyphenyl)-2-(*m*-tolyl)cyclopropanecarboxylate (45a): Title compound was prepared by general procedure with methyl 2-diazo-2-(3,4-dimethoxyphenyl)acetate (**34g**, 118 mg, 0.50 mmol, 1.00 equiv), 2-methylstyrene (**44a**, 148 mg, 1.25 mmol, 2.50 equiv), and Rh₂(*R*-BNP)₄ (4.0 mg, 0.0025 mmol, 0.005 equiv). The remaining residue was purified on silica gel eluting with hexanes : ethyl acetate (5 : 1) to afford a yellow/green oil (114 mg, 76 % yield). HPLC: (Chiralcel OD-H, 3% *i*-PrOH in hexane, 1 mL/min, 1 mg/mL, 30 min, λ = 254 nm) retention times of 17.81 min (minor) and 19.31 min (major), 90% ee for Rh₂(*R*-BNP)₄, 64% ee for Rh₂(*R*-DOSP)₄; *R_f* = 0.12 (hexanes : ethyl acetate 5 : 1); [α]_D²⁰ +28.7° (c = 1.23, CHCl₃); ¹H NMR (400 MHz, CDCl₃) δ 7.11 (d, *J* = 7.6 Hz, 1H), 7.00 (t, *J* = 7.6 Hz, 1H), 6.83 (t, *J* = 7.6 Hz, 1H), 6.63 (m, 2H), 6.42 (d, *J* = 7.6 Hz, 1H), 6.34 (s, 1H), 3.77 (s, 3H), 3.71 (s, 3H), 3.57 (s, 3H), 3.11 (dd, *J* = 9.2, 7.6 Hz, 1H), 2.51 (s, 3H), 2.06 (dd, *J* = 9.2, 5.0 Hz, 1H), 1.99 (dd, *J* = 7.6, 5.0 Hz, 1H); ¹³C NMR (100 MHz, CDCl₃) δ 174.9, 147.9, 137.8, 134.7, 129.7, 127.8, 126.7, 126.0, 125.8, 123.7, 114.7, 110.3, 55.7, 55.6, 52.8, 36.0, 31.2, 20.2, 19.5; IR (film): 2951, 1713, 1516, 1463, 1435, 1251, 1140, 1026, 740; HRMS (APCI) calcd for C₂₀H₂₃O₄ (M+H)⁺ 327.1591 found 327.1591.



(1S,2R)-methyl 1-(3,4-dimethoxyphenyl)-2-(*p*-tolyl)cyclopropanecarboxylate (45b): Title compound was prepared by general procedure with methyl 2-diazo-2-(3,4-dimethoxyphenyl)acetate (**34g**, 118 mg, 0.50 mmol, 1.00 equiv), 4-methylstyrene (**44b**, 148 mg, 1.25 mmol, 2.50 equiv), and Rh₂(*R*-BNP)₄ (4.0 mg, 0.0025 mmol, 0.005 equiv). The remaining

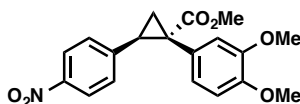
residue was purified on silica gel eluting with hexanes : ethyl acetate (5:1) to afford a yellow/green oil (147 mg, 90% yield). HPLC: (Chiralcel OD-H, 3% *i*-PrOH in hexane, 1 mL/min, 1 mg/mL, 30 min, $\lambda = 254$ nm) retention times of 17.3 min (minor) and 20.1 min (major), 88% ee for Rh₂(*R*-BNP)₄, 67% ee for Rh₂(*R*-DOSP)₄; $R_f = 0.12$ (hexanes : ethyl acetate 5:1); $[\alpha]_D^{20} +27.7^\circ$ ($c = 1.24$, CHCl₃); ¹H NMR (400 MHz, CDCl₃) δ 6.88 (d, $J = 8.0$ Hz, 2H), 6.69-6.67 (m, 4H), 6.37 (s, 1H), 3.81 (s, 3H), 3.67 (s, 3H), 3.57 (s, 3H), 3.05 (dd, $J = 9.2, 7.6$ Hz, 1H), 2.22 (s, 3H), 2.11 (dd, $J = 9.2, 4.8$ Hz, 1H), 1.80 (dd, $J = 7.6, 4.8$ Hz, 1H); ¹³C NMR (100 MHz, CDCl₃) δ 174.7, 147.9, 136.0, 133.5, 128.6, 128.0, 127.6, 124.1, 115.5, 110.3, 55.7, 55.6, 52.7, 36.9, 33.1, 21.0, 20.9; IR (film): 2951, 1714, 1589, 1516, 1435, 1413, 1341, 1315, 1250, 1228, 1155, 1027; HRMS (APCI) calcd for C₂₀H₂₃O₄ (M+H)⁺ 327.1591 found 327.1591.



(1*S*,2*R*)-methyl 1-(3,4-dimethoxyphenyl)-2-(4-methoxyphenyl)cyclopropanecarboxylate

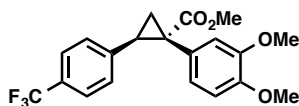
(45c): Title compound was prepared by general procedure with methyl 2-diazo-2-(3,4-dimethoxyphenyl)acetate (**34g**, 118 mg, 0.50 mmol, 1.00 equiv), 4-methoxystyrene (**44c**, 168 mg, 1.25 mmol, 2.50 equiv), and Rh₂(*R*-BNP)₄ (4.0 mg, 0.0025 mmol, 0.005 equiv). The remaining residue was purified on silica gel eluting with hexanes : ethyl acetate (5 : 1) to afford an off-white solid (137 mg, 80% yield). HPLC: (Chiralcel OD-H, 5% *i*-PrOH in hexane, 1 mL/min, 1 mg/mL, 30 min, $\lambda = 254$ nm) retention times of 19.2 min (minor) and 22.9 min (major), 90% ee for Rh₂(*R*-BNP)₄, 62% ee for Rh₂(*R*-DOSP)₄; $R_f = 0.20$ (hexanes : ethyl acetate 3 : 1); mp 123-125 °C; $[\alpha]_D^{20} +33.1^\circ$ ($c = 1.4$, CHCl₃); ¹H NMR (400 MHz, CDCl₃) δ 6.73-6.61 (m, 6H), 6.41 (s, 1H), 3.81 (s, 3H), 3.70 (s, 3H), 3.67 (s, 3H), 3.60 (s, 3H), 3.03 (dd, $J = 9.2, 7.6$ Hz, 1H), 2.10 (dd, $J = 9.2, 4.8$ Hz, 1H), 1.76 (dd, $J = 7.6, 4.8$ Hz, 1H); ¹³C NMR (100 MHz,

CDCl₃) δ 175.1, 158.6, 148.3, 129.5, 128.9, 127.9, 124.6, 115.9, 113.7, 110.7, 56.1, 55.6, 53.1, 37.1, 33.2, 21.3; IR (film): 2952, 1714, 1611, 1589, 1515, 1463, 1437, 1413, 1341, 1248, 1228, 1177, 1153; HRMS (APCI) calcd for C₂₀H₂₂O₅ (M+H)⁺ 342.1462 found 342.1459.



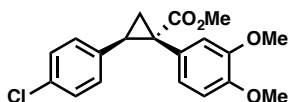
(1S,2R)-methyl 1-(3,4-dimethoxyphenyl)-2-(4-nitrophenyl)cyclopropanecarboxylate (45d):

Title compound was prepared by general procedure with methyl 2-diazo-2-(3,4-dimethoxyphenyl)acetate (**34g**, 118 mg, 0.50 mmol, 1.00 equiv), 4-nitrostyrene (**44d**, 186 mg, 1.25 mmol, 2.50 equiv), and Rh₂(*R*-BNP)₄ (4.0 mg, 0.0025 mmol, 0.005 equiv). The remaining residue was purified on silica gel eluting with hexanes : ethyl acetate (5 : 1) to afford yellow oil (168 mg, 94% yield). HPLC: (Chiralcel OD-H, 6% *i*-PrOH in hexane, 1 mL/min, 1 mg/mL, 60 min, λ = 254 nm) retention times of 30.4 min (minor) and 41.0 min (major), 80% ee for Rh₂(*R*-BNP)₄, 50% ee for Rh₂(*R*-DOSP)₄; R_f = 0.28 (hexanes : ethyl acetate 3 : 1); $[\alpha]_D^{20}$ +15.5° (c = 1.07, CHCl₃); ¹H NMR (400 MHz, CDCl₃) δ 7.94 (d, J = 8.8 Hz, 2H), 6.92 (d, J = 8.8 Hz, 2H), 6.67 (d, J = 8.2 Hz, 1H), 6.61 (dd, J = 8.2, 2.0 Hz, 1H), 6.43 (d, J = 2.0 Hz, 1H), 3.81 (s, 3H), 3.69 (s, 3H), 3.62 (s, 3H), 3.16 (dd, J = 9.2, 7.6 Hz, 1H), 2.22 (dd, J = 9.2, 5.4 Hz, 1H), 1.91 (dd, J = 7.6, 5.4 Hz, 1H); ¹³C NMR (100 MHz, CDCl₃) δ 173.9, 148.5, 145.1, 128.7, 126.2, 124.2, 123.0, 115.0, 110.6, 55.9, 55.8, 53.0, 38.4, 32.6, 29.8, 21.8; IR (film): 2924, 1717, 1597, 1515, 1463, 1415, 1342, 1229, 1206, 1156, 1141; HRMS (APCI) calcd for C₁₉H₂₀O₆N₁ (M+H)⁺ 358.1285 found 358.1284.



(1*S*,2*R*)-methyl 1-(3,4-dimethoxyphenyl)-2-(4-trifluoromethylphenyl)

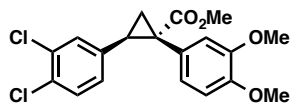
cyclopropanecarboxylate (45e): Title compound was prepared by general procedure with methyl 2-diazo-2-(3,4-dimethoxyphenyl)acetate (**34g**, 118 mg, 0.50 mmol, 1.00 equiv), 1-(trifluoromethyl)-4-vinylbenzene (**44e**, 215 mg, 1.25 mmol, 2.50 equiv), and Rh₂(*R*-BNP)₄ (4.0 mg, 0.0025 mmol, 0.005 equiv). The remaining residue was purified on silica gel eluting with hexanes : ethyl acetate (6 : 1) to afford a yellow oil (171 mg, 90% yield). HPLC: (Chiralcel OD-H, 6% *i*-PrOH in hexane, 1 mL/min, 1 mg/mL, 30 min, λ = 254 nm) retention times of 12.6 min (minor) and 15.6 min (major), 90% ee for Rh₂(*R*-BNP)₄, 63% ee for Rh₂(*R*-DOSP)₄; *R_f* = 0.24 (hexanes : ethyl acetate 4 : 1); [α]_D²⁰ +16.5° (c = 1.6, CHCl₃); ¹H NMR (400 MHz, CDCl₃) δ 7.33 (d, *J* = 8.2 Hz, 2H), 6.88 (d, *J* = 8.2 Hz, 2H), 6.70-6.65 (m, 2H), 6.35 (s, 1H), 3.81 (s, 3H), 3.68 (s, 3H), 3.56 (s, 3H), 3.11 (t, 1H), 3.12 (dd, *J* = 9.2, 7.2 Hz, 1H), 2.18 (dd, *J* = 9.2, 4.8 Hz, 1H), 1.85 (dd, *J* = 7.2, 4.8 Hz, 1H); ¹³C NMR (100 MHz, CDCl₃) δ 174.5, 148.7, 148.6, 141.5, 128.7, 127.0, 124.8, 124.7, 124.6, 124.3, 115.6, 110.9, 56.1, 53.2, 38.0, 33.0, 21.7; IR (film): 2954, 1718, 1517, 1465, 1437, 1414, 1324, 1252, 1230, 1210, 1193; HRMS (APCI) calcd for C₂₀H₁₉F₃O₄ (M+H)⁺ 380.1230 found 380.1225.



(1*S*,2*R*)-methyl 2-(4-chlorophenyl)-1-(3,4-dimethoxyphenyl)cyclopropanecarboxylate (45f):

Title compound was prepared by general procedure with methyl 2-diazo-2-(3,4-dimethoxyphenyl)acetate (**34g**, 118 mg, 0.50 mmol, 1.00 equiv), 4-chlorostyrene (**44f**, 173 mg, 1.25 mmol, 2.50 equiv), and Rh₂(*R*-BNP)₄ (4 mg, 0.0025 mmol, 0.005 equiv). The remaining

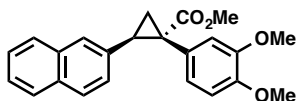
residue was purified on silica gel eluting with hexanes : ethyl acetate (6 : 1) to afford clear oil (123 mg, 89% yield). HPLC: (Chiralcel OD-H, 5% *i*-PrOH in hexane, 1 mL/min, 1 mg/mL, 30 min, $\lambda = 254$ nm) retention times of 14.9 min (minor) and 18.5 min (major), 89% ee for Rh₂(*R*-BNP)₄, 67% ee for Rh₂(*R*-DOSP)₄; $R_f = 0.30$ (hexanes : ethyl acetate 3 : 1); $[\alpha]_D^{20} +13.4^\circ$ ($c = 1.2$, CHCl₃); ¹H NMR (400 MHz, CDCl₃) δ 7.04 (d, $J = 8.4$ Hz, 2H), 6.72-6.63 (m, 4H), 6.38 (d, $J = 1.6$ Hz, 1H), 3.81 (s, 3H), 3.67 (s, 3H), 3.61 (s, 3H), 3.04 (dd, $J = 9.2, 7.2$ Hz, 1H), 2.13 (dd, $J = 9.2, 4.8$ Hz, 1H), 1.78 (dd, $J = 7.2, 4.8$ Hz, 1H); ¹³C NMR (100 MHz, CDCl₃) δ 174.4, 148.2, 148.2, 135.4, 132.3, 129.4, 128.0, 127.0, 124.2, 115.4, 110.5, 55.9, 55.8, 52.8, 37.2, 32.6, 21.2; IR (film): 2951, 1715, 1589, 1517, 1496, 1435, 1413, 1371, 1341, 1307, 1228, 1177, 1155, 1139; HRMS (APCI) calcd for C₁₉H₁₉ClO₄ (M+H)⁺ 346.0966 found 346.0963.



(1*S*,2*R*)-methyl 2-(3,4-dichlorophenyl)-1-(3,4-dimethoxyphenyl)cyclopropanecarboxylate

(45g): Methyl 2-diazo-2-(3,4-dimethoxyphenyl)acetate (**34g**, 2.70 g, 11.6 mmol, 1.00 equiv) in 153 mL dry and degassed toluene was added by syringe pump over 2 h to a solution of 1,2-dichloro-4-vinylbenzene (**44g**, 2.40 g, 13.9 mmol, 1.20 equiv) and Rh₂(*R*-BNP)₄ (92.2 mg, 0.06 mmol, 0.005 equiv) in 77 mL toluene. After addition, the solution was allowed to stir overnight and toluene was removed *in vacuo*. The remaining residue was purified on silica gel (hexanes : ethyl acetate 5 : 1) to afford a clear oil (3.2 g, 72% yield for Rh₂(*R*-BNP)₄ [enantiomer shown above]; 2.3g, 51% yield for Rh₂(*S*-BNP)₄). HPLC: (Chiralcel OD-H, 5% *i*-PrOH in hexane, 1 mL/min, 1 mg/mL, 30 min, $\lambda = 254$ nm) retention times of 15.4 min (minor) and 17.9 min (major), 86% ee for Rh₂(*R*-BNP)₄; retention times of 15.3 min (major) and 19.7 min (minor) 85% ee for Rh₂(*S*-BNP)₄, 48% ee for Rh₂(*R*-DOSP)₄; $R_f = 0.17$ (hexanes : ethyl acetate 5 : 1);

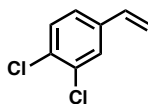
$[\alpha]_D^{20} +4.1^\circ$ ($c = 1.03$, CHCl_3) for $\text{Rh}_2(R\text{-BNP})_4$; $[\alpha]_D^{20} -6.9^\circ$ ($c = 1.05$, CHCl_3) for $\text{Rh}_2(S\text{-BNP})_4$;
 $^1\text{H NMR}$ (600 MHz, CDCl_3) δ 7.10 (d, $J = 9.0$ Hz, 1H), 7.01 (d, $J = 2.4$ Hz, 1H), 6.69 (d, $J = 9.0$ Hz, 1H), 6.63 (dd, $J = 9.0, 2.4$ Hz, 1H), 6.51 (dd, $J = 9.0, 2.4$ Hz, 1H), 6.44 (d, $J = 1.8$ Hz, 1H), 3.82 (s, 3H), 3.67 (s, 3H), 3.66 (s, 3H), 3.02 (dd, $J = 9.0, 7.2$ Hz, 1H), 2.13 (dd, $J = 9.0, 5.1$ Hz, 1H), 1.78 (dd, $J = 7.2, 5.1$ Hz, 1H); $^{13}\text{C NMR}$ (100 MHz, CDCl_3) δ 174.1, 148.4, 148.3, 137.4, 131.9, 130.5, 130.4, 129.7, 127.0, 126.6, 124.2, 115.2, 110.6, 55.9, 55.8, 52.9, 37.4, 32.1, 21.1; IR (film): 2951, 2836, 1716, 1559, 1516, 1413, 1229, 1178, 1137, 1027, 764; HRMS (APCI) calcd for $\text{C}_{19}\text{H}_{19}\text{Cl}_2\text{O}_4$ ($\text{M}+\text{H}$) $^+$ 381.2498 found 381.2498.



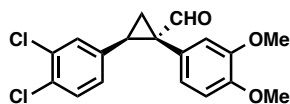
(1S,2R)-methyl 2-(4-chlorophenyl)-1-(3,4-dimethoxyphenyl)cyclopropanecarboxylate (45h):

Title compound was prepared by general procedure with methyl 2-diazo-2-(3,4-dimethoxyphenyl)acetate (**34g**, 118 mg, 0.50 mmol, 1.00 equiv), 2-vinylnaphthalene styrene (**44h**, 386 mg, 2.50 mmol, 5.00 equiv), and $\text{Rh}_2(R\text{-BNP})_4$ (4.0 mg, 0.0025 mmol, 0.005 equiv). The remaining residue was purified through silica gel eluting with hexanes : ethyl acetate (6 : 1) to afford a white oil (158 mg, 87% yield). HPLC: (Chiralcel OD-H, 6% *i*-PrOH in hexane, 1 mL/min, 1 mg/mL, 30 min, $\lambda = 254$ nm) retention times of 18.9 min (minor) and 21.2 min (major), 77% ee for $\text{Rh}_2(R\text{-BNP})_4$, 69% ee for $\text{Rh}_2(R\text{-DOSP})_4$; $R_f = 0.18$ (hexanes : ethyl acetate 4 : 1); $[\alpha]_D^{20} +1.1^\circ$ ($c = 1.5$, CHCl_3); $^1\text{H NMR}$ (600 MHz, CDCl_3) δ 7.70 (m, 1H), 7.63 (m, 1H), 7.53 (d, $J = 8.4$ Hz, 1H), 7.39 (m, 3H), 6.84 (dd, $J = 2.1, 8.4$ Hz, 1H), 6.69 (dd, $J = 2.1, 8.4$ Hz, 1H), 6.63 (d, $J = 8.4$ Hz, 1H), 6.45 (d, $J = 2.1$ Hz, 1H), 3.77 (s, 3H), 3.71 (s, 3H), 3.46 (s, 3H), 3.26 (dd, $J = 7.5, 9.0$ Hz, 1H), 2.21 (dd, $J = 4.8, 9.0$ Hz, 1H), 1.98 (dd, $J = 5.1, 7.5$ Hz, 1H); $^{13}\text{C NMR}$ (100 MHz, CDCl_3) δ 174.8, 148.1, 134.4, 133.2, 132.3, 127.7, 127.6, 127.4, 127.3, 126.2,

125.7 124.3, 115.4, 110.5, 55.7, 52.9, 37.3, 33.6, 21.3; IR (film): 3001, 2951, 2836, 2360, 2342, 1716, 1518, 1254, 1229, 1141, 1028; HRMS (ESI) calcd for C₉H₂₅O₁₀N₅ (M+H)⁺ 363.1596 found 363.1594.



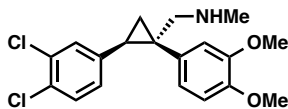
1,2-dichloro-4-vinylbenzene (44g): A 1L flask was charged with methyltriphenylphosphonium bromide (61.0 g, 171 mmol, 1.20 equiv) dissolved in tetrahydrofuran (150 mL) and cooled to 0 °C in an ice bath. Once the reaction had reached 0 °C, potassium *tert*-butoxide (24.0 g, 214 mmol, 1.50 equiv) was added. The reaction turned bright yellow and stirring was continued at 0 °C for an additional 30 minutes. In a separate flask, 3,4-dichlorobenzaldehyde (25.0 g, 143 mmol, 1.00 equiv) was dissolved in tetrahydrofuran (50 mL) and then added to the reaction mixture at 0 °C over 30 minutes and the reaction turned a dark green. Once addition was complete, the reaction was concentrated *in vacuo*, diluted with a mixture of diethyl ether (25 mL) and pentane (75 mL), and washed with deionized water (200 mL). The organic layer was then dried over MgSO₄ and concentrated *in vacuo*. Kugelrohr distillation at 3.5 x 10⁻¹ Torr and 120 °C afforded colorless oil (4.9 g, 20% yield) ¹H NMR (400 MHz, CDCl₃) δ 7.48 (d, *J* = 1.8 Hz, 1H), 7.39 (d, *J* = 8.2 Hz, 1H), 7.23 (dd, *J* = 8.2, 1.8 Hz, 1H), 6.61 (dd, *J* = 17.6, 10.8 Hz, 1H), 5.75 (d, *J* = 17.6 Hz, 1H), 5.33 (d, *J* = 17.6, 10.8 Hz, 1H). Data are consistent with the literature.²⁸



(1S,2R)-2-(3,4-dichlorophenyl)-1-(3,4-dimethoxyphenyl)cyclopropanecarbaldehyde (47g):

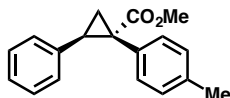
To a 500 mL flask was added **45g** (2.30 g, 5.90 mmol, 1.00 equiv) dissolved in diethyl ether (200

mL). The reaction was then cooled to -78 °C and lithium aluminum hydride (496 mg, 13.1 mmol, 2.20 equiv) was added in three portions. The reaction was then allowed to warm to room temperature overnight. The resulting mixture was then filtered through a plug of 1" plug of silica and concentrated *in vacuo*. The resulting residue was then dissolved in dichloromethane. The reaction flask was then covered in aluminum foil, Dess-Martin periodinane (1.80 g, 5.10 mmol, 1.00 equiv) was added and the reaction was allowed to stir overnight. Solvent was then removed *in vacuo* and the remaining residue was purified on silica gel (hexanes : ethyl acetate 10 : 1 to 5 : 1) to afford a clear oil (1.3 g, 66% yield for Rh₂(*R*-BNP)₄ [enantiomer shown above]; 1.5g, 71% yield for Rh₂(*S*-BNP)₄). HPLC: (Chiralcel OD-H, 1% *i*-PrOH in hexane, 1 mL/min, 1 mg/mL, 30 min, λ = 254 nm) retention times of 15.9 min (major) and 17.9 min (minor), 86% ee for Rh₂(*R*-BNP)₄; retention times of 15.3 min (minor) and 19.7 min (major) 85% ee for Rh₂(*S*-BNP)₄; *R_f* = 0.16 (hexanes : ethyl acetate 5 : 1); [α]_D²⁰ +55.84° (c = 0.97, CHCl₃) for Rh₂(*R*-BNP)₄; [α]_D²⁰ -54.4° (c = 1.13, CHCl₃) for Rh₂(*S*-BNP)₄; ¹H NMR (400 MHz, CDCl₃) δ 9.54 (s, 1H), 7.08 (d, *J* = 8.4 Hz, 1H), 6.97 (d, *J* = 2.0 Hz, 1H), 6.71 (d, *J* = 8.0 Hz, 1H), 6.61 (dd, *J* = 8.0, 2.0 Hz, 1H), 6.55 (dd, *J* = 8.4, 2.0 Hz, 1H), 6.45 (d, *J* = 2.0 Hz, 1H), 3.79 (s, 3H), 3.67 (s, 3H), 2.86 (dd, *J* = 9.0, 7.2 Hz, 1H), 2.11 (dd, *J* = 9.0, 5.0 Hz, 1H), 1.92 (dd, *J* = 7.2, 5.0 Hz, 1H); ¹³C NMR (100 MHz, CDCl₃) δ 200.5, 148.9, 148.8, 136.5, 132.0, 130.7, 130.2, 129.8, 127.0, 125.6, 123.9, 114.2, 111.2, 55.9, 55.8, 46.0, 34.0, 20.5; IR (film): 3003, 2935, 2835, 2254, 1700, 1588, 1516, 1464, 1251, 1229, 1136, 1025, 911, 730; HRMS (NSI) calcd for C₁₈H₁₇Cl₂O₃ (M+H)⁺ 351.0549 found 351.0550.



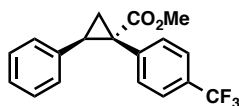
1-((1S,2R)-2-(3,4-dichlorophenyl)-1-(3,4-dimethoxyphenyl)cyclopropyl)-N-

methylmethanamine (48g): To a 1 L flask was added **47g** (1.50 g, 4.20 mmol, 1.00 equiv) dissolved in anhydrous methanol (200 mL). Titanium (IV) isopropoxide (2.20 g, 7.60 mmol, 2.00 equiv) and 2.0 M methylamine (3.80 mL, 7.60 mmol, 2.00 equiv) were then added and the reaction was allowed to stir overnight. Sodium borohydride (288 mg, 7.60 mmol, 2.00 equiv) was then added and the reaction was allowed to stir overnight. Solvent was then removed *in vacuo* and the remaining residue was purified on silica gel eluting with ethyl acetate : triethylamine (9 : 1) to afford (1.3 g, 85% yield over two steps for Rh₂(*R*-BNP)₄ [enantiomer shown above]; 1.3 g, 71% yield over two steps for Rh₂(*S*-BNP)₄). $R_f = 0.30$ (ethyl acetate : triethylamine 9 : 1); $[\alpha]_D^{20} +35.23^\circ$ (c = 1.93, CHCl₃) for Rh₂(*R*-BNP)₄; $[\alpha]_D^{20} -36.67^\circ$ (c = 1.15, CHCl₃) for Rh₂(*S*-BNP)₄; ¹H NMR (400 MHz, CDCl₃) δ 7.06 (d, $J = 8.4$ Hz, 1H), 6.97 (d, $J = 2.2$ Hz, 1H), 6.72-6.64 (m, 2H), 6.51 (d, $J = 1.6$ Hz, 1H), 6.45 (dd, $J = 8.4, 2.4$ Hz, 1H), 3.83 (s, 3H), 3.62 (s, 3H), 3.02 (d, $J = 12.0$ Hz, 1H), 2.54 (d, $J = 12.0$ Hz, 1H), 2.41 (s, 3H), 2.18 (dd, $J = 8.4, 6.0$ Hz, 1H), 1.46-1.38 (m, 2H); ¹³C NMR (100 MHz, CDCl₃) δ 148.6, 147.9, 140.1, 131.6, 130.7, 130.0, 129.5, 129.2, 128.9, 126.6, 123.2, 113.8, 111.0, 63.0, 56.0, 55.9, 36.7, 36.2, 27.6, 18.9; IR (film): 2998, 2932, 2834, 2790, 1558, 1514, 1463, 1410, 1249, 1229, 1134, 1026, 762, 733; HRMS (NSI) calcd for C₁₉H₂₂Cl₂NO₂ (M+H)⁺ 366.1022 found 366.1022.



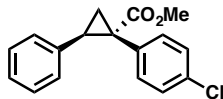
(1S,2R)-methyl 2-phenyl-1-(*p*-tolyl)cyclopropanecarboxylate (50a): Title compound was prepared by general procedure and obtained as a white solid. 84% yield for Rh₂(*R*-DOSP)₄; 77%

yield for Rh₂(*S*-PTAD)₄; 69% yield for Rh₂(*R*-BNP)₄; HPLC: (Chiralcel SS-WHELK, 1% *i*-PrOH in hexane, 1.0 mL/min, 1 mg/mL, 30 min, λ = 254 nm) retention times of 10.57 min (major) and 14.13 min (minor), 87% ee for Rh₂(*R*-DOSP)₄; 46% ee for Rh₂(*S*-PTAD)₄; 51% ee for Rh₂(*R*-BNP)₄; *R_f* = 0.44 (hexanes : ethyl acetate 4 : 1); [α]_D²⁰: +17.2° (c = 1.00, CHCl₃); ¹H NMR (400 MHz; CDCl₃) δ 7.11-7.07 (m, 3H), 6.98-6.92 (m, 4H), 6.82-6.80 (m, 2H), 3.69 (s, 3H), 3.12 (dd, *J* = 9.2 and 7.2 Hz, 1H), 2.27 (s, 3H), 2.16 (dd, *J* = 9.6 and 4.8 Hz, 1H), 1.88 (dd, *J* = 7.2 and 4.8 Hz, 1H); ¹³C NMR (100 MHz, CDCl₃) δ 174.8, 136.8, 136.7, 131.9, 131.8, 128.7, 128.3, 127.9, 126.5, 52.9, 37.3, 33.4, 21.4, 20.9; IR (film): 3028, 2950, 1716, 1255; HRMS (APCI) calcd for C₁₈H₁₉O₂ (M+H)⁺ 267.1380 found 267.1380.

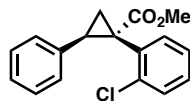


(1*S*,2*R*)-methyl 2-phenyl-1-(4-(trifluoromethyl)phenyl)cyclopropanecarboxylate (35m):

Title compound was prepared by general procedure and obtained as a transparent oil. 93% yield for Rh₂(*R*-DOSP)₄; 67% yield for Rh₂(*S*-PTAD)₄; 80% yield for Rh₂(*R*-BNP)₄; HPLC: (Chiralcel OD-H, 0.5% *i*-PrOH in hexanes, 1.0 mL/min, 1mg/mL, 30 min, λ = 254 nm) retention times of 8.27 min (minor) and 10.34 min (major), 87% ee for Rh₂(*R*-DOSP)₄; 77% ee for Rh₂(*S*-PTAD)₄; 57% ee for Rh₂(*R*-BNP)₄; *R_f* = 0.44 (hexanes : ethyl acetate 4 : 1); [α]_D²⁰: 19.1 (c = 1.00, CHCl₃); ¹H NMR (400 MHz; CDCl₃) δ 7.36 (d, *J* = 8 Hz, 2H), 7.12 (d, *J* = 8 Hz, 2H), 7.06 (m, 3H), 6.74 (m, 2H), 3.66 (s, 3H), 3.14 (dd, *J* = 9.6 and 7.6 Hz, 1H), 2.17 (dd, *J* = 9.2 and 5.2 Hz, 1H), 1.88 (dd, *J* = 7.2 and 5.2 Hz, 1H); ¹³C NMR (100 MHz, CDCl₃) δ 173.9, 139.2, 135.8, 132.4, 128.1, 126.9, 125.0, 124.9, 124.8, 124.7, 53.0, 37.2, 33.5, 20.4; IR (film): 3032, 2954, 1719, 1501, 1322, 1257; HRMS (APCI) calcd for C₁₈H₁₆O₂F₃ (M+H)⁺ 321.1097 found 321.1097.

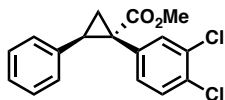


(1S,2R)-methyl 1-(4-chlorophenyl)-2-phenylcyclopropanecarboxylate (50b): Title compound was prepared by general procedure and obtained as a transparent oil. 87% yield for Rh₂(R-DOSP)₄; 71% yield for Rh₂(S-PTAD)₄; 89% yield for Rh₂(R-BNP)₄; HPLC: (Chiralcel OJ-H, 1% *i*-PrOH in hexanes, 1.0 mL/min, 1mg/mL, 30 min, λ = 254 nm) retention times of 8.62 min (minor) and 12.58 min (major), 88% ee for Rh₂(R-DOSP)₄; 48% ee for Rh₂(S-PTAD)₄; 57% ee for Rh₂(R-BNP)₄; *R_f* = 0.56 (hexanes : ethyl acetate 4 : 1); [α]_D²⁰: 4.8 (c = 1.00, CHCl₃); ¹H NMR (300 MHz; CDCl₃) δ 7.12-7.06 (m, 5H), 6.95 (d, *J* = 8.7 Hz, 2H), 6.79-6.76 (m, 2H), 3.67 (s, 3H), 3.12 (dd, *J* = 9.3 and 7.5 Hz, 1H), 2.15 (dd, *J* = 9.3 and 4.8 Hz, 1H), 1.85 (dd, *J* = 7.2 and 4.8 Hz, 1H); ¹³C NMR (100 MHz, CDCl₃) δ 174.1, 136.1, 133.7, 133.4, 133.2, 128.3, 128.2, 128.1, 126.8, 52.9, 36.9, 33.4, 20.6; IR (film): 3031, 2951, 1717, 1493, 1255; HRMS (APCI) calcd for C₁₇H₁₆O₂Cl (M+H)⁺ 287.0833 found 287.0833.

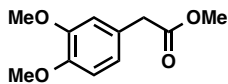


(1S,2R)-methyl 1-(2-chlorophenyl)-2-phenylcyclopropanecarboxylate (50c): Title compound was prepared by general procedure and obtained as a transparent oil. 89% yield for Rh₂(R-DOSP)₄; 80% yield for Rh₂(S-PTAD)₄; 78% yield for Rh₂(R-BNP)₄; HPLC: (Chiralcel OJ-H, 0.5% *i*-PrOH in hexanes, 1.0 mL/min, 1mg/mL, 30 min, λ = 254 nm) retention times of 11.47 min (major) and 15.27 min (major), 92% ee for Rh₂(R-DOSP)₄; 97% ee for Rh₂(S-PTAD)₄; 51% ee for Rh₂(R-BNP)₄; *R_f* = 0.43 (hexanes : ethyl acetate 4 : 1); [α]_D²⁰: 61.8 (c = 1.00, CHCl₃); ¹H NMR (300 MHz; CDCl₃) δ 7.18-7.02 (m, 7H), 6.84-6.76 (m, 2H), 3.68 (s, 3H), 3.13 (t, *J* = 8.7 Hz, 1H), 2.10 (m, 1H), 1.91 (dd, *J* = 7.2 and 5.1 Hz, 1H); ¹³C NMR (100 MHz, CDCl₃) δ 173.6,

137.5, 133.5, 129.6, 128.9, 128.2, 127.6, 126.6, 126.4, 52.9, 33.5, 29.9, 21.7; IR (film): 3031, 2950, 1718, 1251, 694; HRMS (APCI) calcd for C₁₇H₁₆O₂Cl (M+H)⁺ 287.0833 found 287.0833.

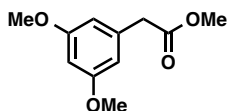


(1S,2R)-methyl 1-(3,4-dichlorophenyl)-2-phenylcyclopropanecarboxylate (35i): Title compound was prepared by general procedure and obtained as a clear oil; 88% yield for Rh₂(R-DOSP)₄; 88% yield for Rh₂(S-PTAD)₄; 82% yield for Rh₂(R-BNP)₄; HPLC: (Chiralcel OD-H, 1% *i*-PrOH in hexane, 1 mL/min, 1 mg/mL, 30 min, λ = 254 nm) retention times of 7.54 min (minor) and 9.78 min (major), 82% ee for Rh₂(R-DOSP)₄; 60% ee for Rh₂(S-PTAD)₄; 63% ee for Rh₂(R-BNP)₄; R_f = 0.23 (hexanes : ethyl acetate 7 : 1); [α]²⁰_D: -8.1° (c = 1.60, CHCl₃); ¹H NMR (400 MHz, CDCl₃): δ 7.18-7.16 (m, 2H), 7.14-7.10 (m, 3H), 6.82-6.79 (m, 3H), 3.68 (s, 3H), 3.14 (dd, *J* = 9.2, 7.6 Hz, 1H), 2.15 (dd, *J* = 9.2, 4.8 Hz, 1H), 1.84 (dd, *J* = 7.6, 5.2 Hz, 1H); ¹³C NMR (100 MHz, CDCl₃) δ 173.3, 135.3, 135.2, 133.7, 131.6, 131.4, 131.2, 129.6, 128.0, 127.9, 126.8, 52.8, 36.3, 33.3, 20.2; IR (film): 2925, 1719, 1257, 1163, 695; HRMS (ESI) calcd for C₁₇H₁₃O₂Cl₂ (M-H)⁺ 319.0293 found 319.0299.

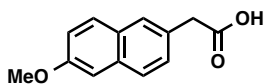


methyl 2-(3,4-dimethoxyphenyl)acetate: A 250mL flask was charged with 3,4-methoxyphenyl acetic acid (10.0 g, 60.2 mmol, 1.00 equiv) dissolved in 150 mL methanol. The reaction mixture was brought to 0 °C in an ice bath. Trimethylsilyl chloride (11.5 mL, 90.3 mmol, 1.50 equiv) was slowly added. The ice bath was removed and reaction mixture allowed to warm to room temperature overnight. Solvent was removed *in vacuo* and the remaining residue was purified through silica eluting hexanes : ethyl acetate (15 : 1 to 5 : 1) to afford clear oil (10.8 g, 85%

yield). $R_f = 0.23$ (hexanes : ethyl acetate 4 : 1); $^1\text{H NMR}$ (400 MHz, CDCl_3) δ 6.81 (m, 3H), 3.84 (d, $J = 9.2$ Hz, 6H), 3.67 (s, 3H), 3.55 (s, 2H), $^{13}\text{C NMR}$ (100 MHz, CDCl_3) δ 172.0, 148.7, 148.0, 126.3, 121.2, 112.2, 111.1, 55.6, 51.7, 40.4; IR (film): 2952, 2836, 1732, 1591, 1514, 1463, 1436, 1261, 1235, 1140, 1025, 764; Data are consistent with the literature.²⁹

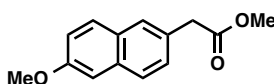


methyl 2-(3,4-dimethoxyphenyl)acetate: A 250mL flask was charged 2-(3,5-dimethoxyphenyl)acetic acid (1.03 g, 5.27 mmol, 1.00 equiv) dissolved in 25 mL methanol. The reaction mixture was brought to 0°C in an ice bath. Acetyl chloride (0.83 mL, 11.1 mmol, 2.10 equiv) was slowly added. The ice bath was removed and reaction mixture allowed to warm to room temperature overnight. The reaction was then quenched with 40mL NaHCO_3 (100 mL) and taken up in 200mL diethyl ether. Organic layer was washed with NaHCO_3 (5 x 20 mL), dried over MgSO_4 , and concentrated *in vacuo* to afford clear oil (1.0 g, quantitative yield). $^1\text{H NMR}$ (400 MHz, CDCl_3) δ 6.44 (d, $J = 2.4$ Hz, 2H), 6.38 (t, $J = 2.4, 4.8$ Hz, 1H), 3.78 (s, 6H), 3.70 (s, 3H), 3.56 (s, 2H). Data are consistent with the literature.³⁰

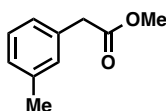


2-(6-methoxynaphthalen-2-yl)acetic acid: A 250mL flask was charged with 6'-methoxy-2'-acetoneaphthone (7.70 g, 38.4 mmol, 1.00 equiv), sulfur powder (2.46g, 76.8 mmol, 2.00 equiv), morpholine (9.96 mL, 115 mmol, 3.00 equiv) and *p*-toluene sulfonic acid (256 mg, 1.30 mmol, 0.04 equiv). The reaction mixture was then heated to reflux (129 °C) and allowed to stir overnight. The reaction was then cooled to 50°C and benzyltriethyl ammonium chloride (and NaOH solution) were then added and the reaction mixture was allowed to stir overnight. The

reaction was then cooled to room temperature and acidified to pH ~1 with 12 M HCl and filtered through glass wool. Glass wool was washed with ~2 M HCl and product was then extracted from aqueous layer with ethyl acetate until ethyl acetate layer was clear (4 x 100 mL), dried with Na₂SO₄, and concentrated *in vacuo* to afford light brown solid (503 mg, 6% yield) ¹H NMR (400 MHz, CDCl₃) δ 7.72-7.66 (m, 3H), 7.37 (d, *J*=8.4, 1H), 7.15-7.12 (m, 2H), 3.92 (s, 3H), 3.78 (s, 2H). Data are consistent with the literature.³¹

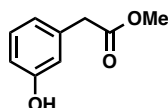


methyl 2-(3,4-dimethoxyphenyl)acetate: A 250 mL flask was charged 2-(6-methoxynaphthalen-2-yl)acetic acid (503 mg, 2.32 mmol, 1.00 equiv) dissolved in 25 mL methanol. The reaction mixture was brought to 0 °C in an ice bath. Acetyl chloride (0.19 mL, 2.56 mmol, 1.10 equiv) was slowly added. The ice bath was removed and reaction mixture allowed to warm to room temperature overnight. The reaction was then quenched with 40mL NaHCO₃ (100 mL) and taken up in 200 mL diethyl ether. Organic layer was washed with NaHCO₃ (5 x 20 mL), dried over MgSO₄, and concentrated *in vacuo* to afford clear oil (485 mg, 91% yield). ¹H NMR (400 MHz, CDCl₃) δ 7.70 (dd, *J*=4.0, 8,4 Hz, 2H), 7.65 (s, 1H), 7.37 (dd, *J*=1.6, 8.4 Hz, 1H), 7.15-7.11 (m, 2H), 3.91 (s, 3H), 3.78 (s, 2H), 3.70 (s, 3H). Data are consistent with the literature.³⁰

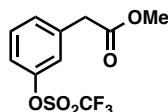


methyl 2-(*m*-tolyl)acetate: A 100mL flask was charged with *m*-tolylacetic acid (5.00 g, 33.3 mmol, 1.00 equiv) dissolved in 120 mL methanol. The reaction mixture was brought to 0°C in an ice bath. Acetyl chloride (5.20 mL, 69.9 mmol, 2.10 equiv) was slowly added. The ice bath

was removed and reaction mixture allowed to warm to room temperature overnight. The reaction was quenched with NaHCO₃ (40 mL). The mixture was taken up in diethyl ether (200 mL), washed with NaHCO₃ (5 x 20 mL), dried over MgSO₄, and then concentrated *in vacuo* to afford clear oil (4.37 g, 80% yield). ¹H NMR (400 MHz, CDCl₃) δ 7.23-7.21 (t, 1H), 7.10-7.08 (m, 3H), 3.70 (s, 3H), 3.60 (s, 2H), 2.35 (s, 3H). Data are consistent with the literature.³²

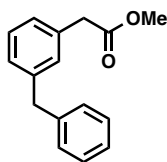


methyl 2-(3-hydroxyphenyl)acetate: Prepared according to the known literature procedure,³³ a 250 mL flask was charged with 3-hydroxyphenylacetic acid (5.00 g, 33.0 mmol, 1.00 equiv) dissolved in 125 mL methanol. 0.2 mL 12 N H₂SO₄ was then added and the reaction was allowed to stir overnight. Solvent was then removed *in vacuo*. The remaining residue was then dissolved in 100 mL dichloromethane, washed with NaHCO₃ (2 x 100 mL) followed by deionized water (3 x 150 mL), dried over Na₂SO₄ and concentrated *in vacuo* to afford 4.7 g red/brown oil (87% yield) *R*_f = 0.16 (hexanes : ethyl acetate 5 : 1); red/brown oil; ¹H NMR (400 MHz, CDCl₃) δ 7.17 (t, *J* = 8.0, 1H), 6.83-6.70 (m, 3H), 3.71 (s, 3H), 3.59 (s, 2H); ¹³C NMR (100 MHz, CDCl₃) δ 173.2, 156.2, 135.3, 129.9, 121.5, 116.4, 114.6, 52.5, 41.2; IR (film): 3385, 1712, 1589, 1490, 1455, 1436, 1277, 1215, 1011, 959, 762, 717, 689; HRMS (ESI) calcd for C₉H₁₁O₃ (M+H)⁺ 167.0703 found 167.0702.



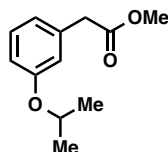
methyl 2-(3-(((trifluoromethyl)sulfonyl)oxy)phenyl)acetate: Prepared according to the known literature procedure,³³ a 250 mL flask was charged with methyl 2-(3-hydroxyphenyl)acetate

(3.90 g, 24.0 mmol, 1.00 equiv) dissolved in dry, de-gassed dichloromethane. The reaction mixture was then cooled to -15 °C in an ethylene glycol/dry ice bath. Hünig's base (4.90 mL, 28.0 mmol, 1.19 equiv) was then added dropwise over 10 min and allowed to stir for 30 minutes. Trifluoromethane sulfonic anhydride was then added and the reaction was allowed to stir for an additional hour. The reaction was warmed to room temperature and allowed to stir overnight and then washed with 1 N HCl (2 x 20 mL), 1 N NaOH (2 x 20 mL), deionized water (3 x 20 mL), dried over Na₂SO₄, and concentrated *in vacuo* to afford 5.0 g clear oil (60 % yield). $R_f = 0.15$ (hexanes : ethyl acetate 30 : 1); red/brown oil; ¹H NMR (400 MHz, CDCl₃) δ 7.43-7.39 (m, 1H), 7.33-7.31 (d, $J = 7.6$, 1H), 7.24-7.19 (m, 2H), 3.71 (s, 3H), 3.68 (s, 2H); ¹³C NMR (100 MHz, CDCl₃) δ 171.1, 149.7, 136.9, 130.4, 129.6, 122.5, 120.2, 52.4, 40.7; IR (film): 2957, 1739, 1419, 1206, 1136, 1117, 954, 928, 839, 791, 684; HRMS (ESI) calcd for C₈H₇O₄N₃F₃²³Na₁³²S₁ (M+H)⁺ 321.0002 found 321.0004.

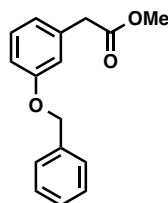


methyl 2-(3-benzylphenyl)acetate: A 100mL flask was charged with 2-benzylphenyl acetic acid (328 mg, 1.35 mmol, 1.00 equiv) dissolved in 60 mL methanol. The reaction mixture was brought to 0°C in an ice bath. Acetyl chloride (0.20 mL, 2.80 mmol, 2.10 equiv) was slowly added. The ice bath was removed and reaction mixture allowed to warm to room temperature overnight. The reaction was quenched with NaHCO₃ (40 mL). The mixture was taken up in diethyl ether (200 mL), washed with NaHCO₃ (5 x 25 mL), dried over MgSO₄, and then concentrated *in vacuo* to afford yellow oil (365 mg, quantitative yield). $R_f = 0.31$ (hexanes : ethyl

acetate 3 : 1); ^1H NMR (400 MHz, CDCl_3) δ 7.42-7.39 (m, 5H), 7.24 (m, 2H), 6.96-6.93 (m, 2H), 5.10 (s, 2H), 3.70 (s, 2H), 3.65 (s, 3H). Data are consistent with the literature.³⁴

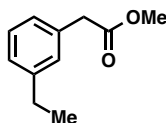


methyl 2-(3-isopropoxyphenyl)acetate: Prepared according to the known literature procedure,³⁵ a 250 mL flask was charged with methyl 2-(3-hydroxyphenyl)acetate (1.50 g, 13.0 mmol, 1.00 equiv), 2-bromopropane and K_2CO_3 (3.60 g, 26.0 mmol, 2.00 equiv) dissolved in 50 mL dry *N,N*-dimethylformamide and allowed to stir for 20 h. The reaction was quenched with 30 mL of ammonium chloride, taken up in 250 mL diethyl ether, washed with ammonium chloride (5x 30 mL), dried over MgSO_4 , and concentrated *in vacuo*. Reaction mixture was concentrated *in vacuo* and purified *via* flash column chromatograph (hexanes : ethyl acetate 10 : 1) to methyl 2-(3-isopropoxyphenyl)acetate (970 mg, 36% yield) R_f = 0.24 (hexanes : ethyl acetate 5 : 1); clear oil; ^1H NMR (600 MHz, CDCl_3) δ 7.24-7.21 (t, J = 7.8, 15.6), 6.85-6.79 (m, 3H), 4.556 (s, 1H), 3.70 (s, 3H), 3.60 (s, 2H), 1.34 (d, J = 6.0, 6H). Data are consistent with the literature.³⁵



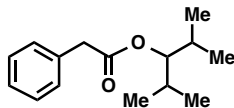
methyl 2-(3-(benzyloxy)phenyl)acetate: Prepared according to the known literature procedure,³⁶ a 250 mL flask was charged with methyl 2-(3-hydroxyphenyl)acetate (1.50 g, 13.0 mmol, 1.00 equiv), 2-bromopropane and K_2CO_3 (3.60 g, 26.0 mmol, 2.00 equiv) dissolved in 50 mL dry *N,N*-dimethylformamide and allowed to stir for 20 h. The reaction was quenched with 30 mL of ammonium chloride, taken up in 250 mL diethyl ether, washed with ammonium

chloride (5 x 30 mL), dried over MgSO₄, and concentrated *in vacuo*. Reaction mixture was concentrated *in vacuo* and purified *via* flash column chromatograph (hexanes : ethyl acetate 10 : 1) to afford clear oil (970 mg, 36% yield) $R_f = 0.24$ (hexanes : ethyl acetate 5 : 1); ¹H NMR (600 MHz, CDCl₃) δ 7.24-7.21 (t, $J = 7.8, 15.6$), 6.85-6.79 (m, 3H), 4.556 (s, 1H), 3.70 (s, 3H), 3.60 (s, 2H), 1.34 (d, $J = 6.0$, 6H). Data are consistent with the literature.³⁴

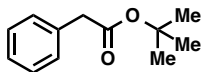


methyl 2-(3-ethylphenyl)acetate: Prepared according to the known literature procedure,³³ a 50 mL flask was charged with methyl 2-(3-(((trifluoromethyl)sulfonyl)oxy)phenyl)acetate (335 mg, 1.12 mmol, 1.00 equiv) in 3 mL anhydrous 1-methyl-2-pyrrolidinone (NMP). LiCl (142 mg, 3.37 mmol, 3.00 equiv), CuI (10.0 mg, 0.06 mmol, 0.05 equiv), AsPh₃ (27.0 mg, 0.09 mmol, 0.08 equiv), and Pd₂dba₃ (21.0 mg, 0.02 mmol, 0.02 equiv) were then added to the reaction mixture with vigorous stirring. The reaction was allowed to stir for 10 min and tetraethyl tin (0.27 mL, 1.35 mmol, 1.20 equiv) was then added and the reaction was allowed to stir for 5 h at 90 °C. The reaction was then allowed to cool to room temperature and 10 mL saturated potassium fluoride solution was then added and the mixture allowed to stir for an additional 15 min. 5 mL deionized water was then added and the product extracted with diethyl ether (3 x 10 mL). The organic layer was then washed with water (3 x 10 mL), dried over Na₂SO₄, and concentrated *in vacuo*. Purification through silica gel eluting hexane:ethyl acetate (100 : 0.8) afforded yellow oil, (396 mg, 39 % yield). $R_f = 0.31$ (hexanes : ethyl acetate 100 : 1); red/brown oil; ¹H NMR (400 MHz, CDCl₃) δ 7.43-7.39 (m, 1H), 7.33-7.31 (d, $J = 7.6$, 1H), 7.24-7.19 (m, 2H), 3.71 (s, 3H), 3.68 (s, 2H); ¹³C NMR (100 MHz, CDCl₃) δ 171.1, 149.7, 136.9, 130.4, 129.6, 122.5, 120.2, 52.4, 40.7; IR (film): 2957, 1739, 1419, 1206, 1136, 1117, 954, 928, 839, 791, 684;

HRMS (ESI) calcd for $C_8H_7O_4N_3F_3^{23}Na_1^{32}S_1$ (M+H)⁺ 321.0002 found 321.0004. Data are consistent with the literature.³³



2,4-dimethylpentan-3-yl 2-phenylacetate: Prepared according to the known literature procedure,³⁷ a 250 mL flask was charged with 2,4-dimethyl-3-pentanol dissolved in 55 mL dry tetrahydrofuran and brought to -10 °C. *n*-Butyllithium (10.6 mL, 26.6 mmol, 2.00 equiv) was then slowly added and the solution was allowed to stir for 10 minutes. Methyl phenylacetate was then dissolved in 20 mL tetrahydrofuran and slowly added to the reaction mixture. The reaction was then allowed to slowly warm to room temperature and stirred overnight. Solvent was removed *in vacuo* and the remaining residue was purified through silica eluting pentane : ether (100 : 2) to afford clear oil (2.9 g, 93% yield). $R_f = 0.40$ (pentane : ether 100 : 2); ¹H NMR (400 MHz, CDCl₃) δ 7.32-7.25 (m, 5H), 4.57 (t, $J = 6.0$ Hz, 1H), 3.64 (s, 2H), 1.85 (oct, $J = 6.8$ Hz, 2H), 0.80 (t, $J = 7.2$ Hz, 12H); ¹³C NMR (100 MHz, CDCl₃) δ 171.8, 134.7, 129.6, 128.7, 127.2, 83.3, 42.0, 29.6, 19.7, 17.3; IR (film): 3032, 2965, 2935, 2876, 2359, 1726, 1464, 1370, 1256, 1128, 973, 720, 695; Data are consistent with the literature.²⁷

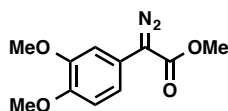


tert-butyl 2-phenylacetate: A 250 mL flask was charged with MgSO₄ (14.0 g, 0.12 mol, 4.00 equiv) in 155 mL methylene chloride. The slurry was allowed to stir for 10 minutes. 12 N H₂SO₄ (1.60 mL, 0.03 mol, 1.00 equiv), was then added dropwise. Phenyl acetic acid (4.00 g, 0.03 mol, 1.00 equiv) was then added to the solution. *Tert*-butanol (14.0 mL, 0.15 mol, 5.00 equiv) was subsequently added with syringe. Solution was then allowed to stir under argon

overnight. The reaction was quenched with 200 mL NaHCO₃ (sat.) and allowed to stir for 30 minutes until all MgSO₄ had dissolved. The organic layer was then washed with brine (2 x 100 mL), dried over MgSO₄, filtered, and evaporated under reduced pressure to afford light yellow oil (4.5 g, 81 % yield) R_f = 0.33 (hexanes : ethyl acetate 8 : 1); ¹H NMR (400 MHz, CDCl₃) δ 7.34-7.25 (m, 5H), 3.52 (s, 2H), 1.44 (s, 9H); ¹³C NMR (100 MHz, CDCl₃) δ 170.9, 134.7, 129.4, 128.7, 127.03, 80.8, 42.9, 28.2; IR (film): 3031, 2978, 2358, 1732, 1393, 136, 1141, 743, 695. Data are consistent with the literature.³⁸

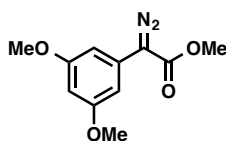
General Procedure for Diazo Transfer:

To a 250 mL round-bottomed flask was added acetate (24 mmol, 1.0 equiv) and *p*-acetamidobenzenesulfonyl azide (36 mmol, 1.5 equiv) dissolved in 250 mL acetonitrile. The reaction mixture was brought to 0°C in an ice bath. Once cool, diaza(1,3)bicyclo[5.4.0]undecane (36 mmol, 1.5 equiv) was slowly added. The ice bath was then removed and reaction mixture allowed to warm to room temperature overnight. Reaction was quenched NaHCO₃ (200 mL) and taken up in 300mL diethyl ether. The aqueous layer was washed with diethyl ether (5 x 30 mL), until organic layer was clear. The organic layer was dried over MgSO₄, filtered, and concentrated *in vacuo*. The resulting residue was purified through silica.

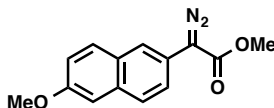


methyl 2-diazo-2-(3,4-dimethoxyphenyl)acetate (34g): Title compound was prepared by general procedure with methyl 2-(3,4-dimethoxyphenyl)acetate (5.0 g, 24 mmol, 1.0 equiv), *p*-acetamidobenzenesulfonyl azide (8.6 g, 36 mmol, 1.5 equiv), and diaza(1,3)bicyclo[5.4.0]undecane (5.3 mL, 36 mmol, 1.5 equiv). The residue was purified

through silica eluting hexane to afford orange crystalline solid (2.6 g, 45% yield); mp 85-88 °C, R_f = 0.08 (hexanes : ethyl acetate 10 : 1); ^1H NMR (400 MHz, CDCl_3) δ 7.19 (d, J = 8.4 Hz, 1H), 6.89 (m, 2H), 3.90 (s, 3H), 3.89 (s, 3H), 3.86 (s, 3H), ^{13}C NMR (100 MHz, CDCl_3) δ 166.3, 149.7, 147.6, 117.6, 116.7, 111.9, 108.6, 56.2, 56.1, 52.2; IR (film): 2993, 2949, 2842, 2085, 1617, 1517, 1438, 1318, 1254, 1192, 1136, 1022, 824, 792, 763, 736; Data are consistent with the literature.³⁹

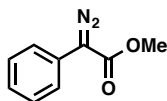


methyl 2-diazo-2-(3,5-dimethoxyphenyl)acetate (36a): Title compound was prepared by general procedure with methyl 2-(3,5-dimethoxyphenyl)acetate (1.1 g, 5.6 mmol, 1.0 equiv), *p*-acetamidobenzenesulfonyl azide (2.0 g, 8.4 mmol, 1.5 equiv), and diaza(1,3)bicyclo[5.4.0]undecane (1.3 mL, 8.4 mmol, 1.5 equiv). The residue was purified through silica eluting with pentane : diethyl ether (8 : 1 to 7 : 1) to afford orange solid (916 mg, 70% yield); mp 72-74 °C, R_f = 0.38 (pentane : diethyl ether 7 : 1); ^1H NMR (400 MHz, CDCl_3) δ 6.67 (d, J = 2.2 Hz, 2H), 6.29 (t, J = 4.4, 2.2 Hz, 1H), 3.86 (s, 3H), 3.80 (s, 6H), ^{13}C NMR (100 MHz, CDCl_3) δ 165.6, 161.3, 127.8, 102.1, 98.2, 55.6, 52.2; IR (film): 3002, 2952, 2841, 2092, 1698, 1599, 1484, 1444, 1284, 1266, 1195, 1153, 1086, 1063, 837, 756, 733; HRMS (APCI) calcd for $\text{C}_{11}\text{H}_{13}\text{O}_4$ ($\text{M}+\text{H}-\text{N}_2$)⁺ 209.0808 found 209.0808.

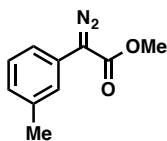


methyl 2-diazo-2-(6-methoxynaphthalen-2-yl)acetate (36b): Title compound was prepared by general procedure with methyl 2-(6-methoxynaphthalen-2-yl)acetate (485 g, 2.10 mmol, 1.00

equiv), *p*-acetamidobenzenesulfonyl azide (758 g, 3.20 mmol, 1.50 equiv), and diaza(1,3)bicyclo[5.4.0]undecane (0.47 mL, 3.20 mmol, 1.50 equiv). The residue was purified through silica eluting with pentane : diethyl ether (8.5 : 1) to afford orange solid (347 mg, 65% yield); mp 105-109°C, R_f = 0.39 (pentane : diethyl ether 8.5 : 1); ^1H NMR (400 MHz, CDCl_3) δ 7.91 (s, 2H), 7.74 (d, J = 8.8 Hz, 1H), 7.69 (d, J = 8.8 Hz, 1H), 7.47 (dd, J = 8.8, 2.2 Hz, 1H), 7.14 (dd, J = 8.8, 2.2 Hz, 1H), 7.09 (d, J = 2.2 Hz, 1H), 3.91 (s, 3H), 3.89 (s, 3H), ^{13}C NMR (100 MHz, CDCl_3) δ 166.2, 157.9, 132.9, 129.4, 129.3, 127.7, 122.9, 122.8, 120.2, 119.6, 105.8, 55.5, 52.2; IR (film): 3008, 2957, 2841, 2093, 1693, 1600, 1435, 1396, 1262, 1244, 1164, 1147, 1048, 892, 849; HRMS (APCI) calcd for $\text{C}_{14}\text{H}_{13}\text{O}_3$ ($\text{M}+\text{H}-\text{N}_2$) $^+$ 229.0859 found 229.0859.

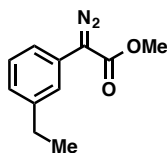


methyl 2-diazo-2-(m-tolyl)acetate (34a): Title compound was prepared by general procedure with methyl phenylacetate (10.0 g, 0.07 mol, 1.00 equiv), *p*-acetamidobenzenesulfonyl azide (24.0 g, 0.10 mol, 1.50 equiv), and diaza(1,3)bicyclo[5.4.0]undecane (14.9 mL, 0.10 mmol, 1.50 equiv). The residue was purified through silica eluting hexanes to afford an orange oil (2.60 g, 74% yield). R_f = 0.23 (hexanes : ethyl acetate 6 : 1); ^1H NMR (400 MHz, CDCl_3) δ 7.51-7.48 (m, 2H), 7.42 (m, 2H), 7.22-7.18 (m, 1H), 3.88 (s, 3H); Data are consistent with the literature.⁴⁰

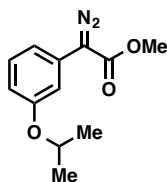


methyl 2-diazo-2-(m-tolyl)acetate (38a): Title compound was prepared by general procedure with methyl 2-(m-tolyl) acetate (4.40 g, 27.0 mmol, 1.00 equiv), *p*-acetamidobenzenesulfonyl azide (9.60 g, 40.0 mmol, 1.50 equiv.), and diaza(1,3)bicyclo[5.4.0]undecane (5.96 mL, 39.9

mmol, 1.50 equiv). The residue was purified through silica eluting hexanes : ethyl acetate (15 : 1) to afford orange oil (3.13 g, 62% yield). ^1H NMR (400 MHz, CDCl_3) δ 7.29-7.28 (m, 3 H), 7.01 (m, 1H), 3.87 (s, 3H), 2.37 (s, 3H); Data are consistent with the literature.³²

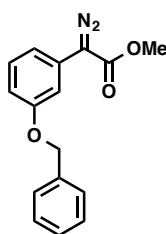


methyl 2-diazo-2-(3-ethylphenyl)acetate (38b): Prepared by general procedure with methyl 2-(3-ethylphenyl)acetate (197 mg, 1.10 mol, 1.00 equiv), *p*-acetamidobenzenesulfonyl azide (394 mg, 1.60 mmol, 1.50 equiv), and diaza(1,3)bicyclo[5.4.0]undecane (0.24 mL, 1.60 mmol, 1.50 equiv). The residue was purified through silica eluting hexanes : ethyl acetate (50 : 1) to afford an orange oil (233 mg, 58% yield). R_f = 0.63 (hexanes : ethyl acetate 5 : 1); ^1H MNR (400 MHz, CDCl_3) δ 7.32-7.28 (m, 3H), 7.02-7.00 (m, 1H), 3.84 (s, 3H), 2.63 (q, J = 7.6 Hz, 2H), 1.22 (t, J = 7.6 Hz, 3H); ^{13}C NMR (100 MHz, CDCl_3) δ 165.9, 145.2, 129.1, 126.8, 125.7, 125.4, 123.7, 121.6, 52.1, 29.1, 15.7; IR (film): 2965, 2088, 1708, 1602, 1435, 1348, 1253, 1148, 1069, 1047, 695 ; HRMS (APCI) calcd for $\text{C}_{11}\text{H}_{13}\text{O}_2$ ($\text{M}+\text{H}-\text{N}_2$)⁺ 177.0910 found 177.0910.

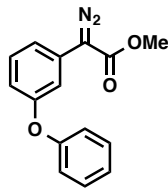


methyl 2-diazo-2-(3-isopropoxyphenyl)acetate (38c): Title compound was prepared by general procedure with methyl 2-(3-isopropoxyphenyl)acetate (970 mg, 5.00 mol, 1.00 equiv), *p*-acetamidobenzenesulfonyl azide (1.68 mg, 7.00 mmol, 1.50 equiv), and diaza(1,3)bicyclo[5.4.0]undecane (1.05 mL, 7.00 mmol, 1.50 equiv). The residue was purified through silica eluting hexanes : ethyl acetate (5 : 1) to afford an orange oil (781 mg, 71% yield).

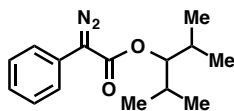
$R_f = 0.65$ (hexanes : ethyl acetate 5 : 1); $^1\text{H NMR}$ (400 MHz, CDCl_3) δ 7.30-7.26 (m, 1H), 7.14 (t, $J = 2.0$ Hz, 1H), 6.97 (ddd, $J = 1.0, 2.0, 2.4$ Hz, 1H), 6.72 (ddd, $J = 1.0, 2.4, 3.2$ Hz, 1H) 4.58 (sept, $J = 6.0$ Hz, 1H), 3.87 (s, 3H), 1.34 (d, $J = 6.0$ Hz, 6H); $^{13}\text{C NMR}$ (100 MHz, CDCl_3) δ 173.5, 165.8, 158.6, 130.1, 127.1, 116.1, 113.5, 111.9, 70.2, 52.2, 22.2; IR (film): 2977, 2083, 1702, 1597, 1575, 1250, 1229, 1144, 1116, 1052, 976, 770; HRMS (ESI) calcd for $\text{C}_{20}\text{H}_{23}\text{O}_4$ (M+H) $^+$ 207.1016 found 207.1018.



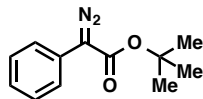
methyl 2-(3-(benzyloxy)phenyl)-2-diazoacetate (38d): Title compound was prepared by general procedure with methyl 2-(3-(benzyloxy)phenyl)acetate (1.24 mg, 5.00 mol, 1.00 equiv), *p*-acetamidobenzenesulfonyl azide (1.75 mg, 7.00 mmol, 1.50 equiv), and diaza(1,3)bicyclo[5.4.0]undecane (1.09 mL, 7.00 mmol, 1.50 equiv). The residue was purified through silica eluting hexanes : ethyl acetate (50 : 1) to afford an orange solid (870 mg, 63% yield). mp 53-58 °C, $R_f = 0.35$ (hexanes : ethyl acetate 5 : 1); $^1\text{H NMR}$ (400 MHz, CDCl_3) δ 7.47-7.25 (m, 7H), 7.04-7.01 (m, 1H), 6.82 (ddd, $J = 1.2, 2.8, 3.6$ Hz, 1 H), 5.09 (s, 2H), 3.88 (s, 3H); $^{13}\text{C NMR}$ (100 MHz, CDCl_3) δ 165.8, 159.5, 137.0, 130.2, 128.9, 128.3, 127.8, 127.3, 116.5, 112.6, 110.9, 70.3, 52.2; IR (film): 3032, 2951, 2081, 1698, 1597, 1575, 1492, 1434, 1351, 1249, 1230, 1189, 1146, 1023, 770, 736, 696, 685; HRMS (ESI) calcd for $\text{C}_{16}\text{H}_{15}\text{O}_3$ (M+H) $^+$ 255.1016 found 255.1019.



methyl 2-diazo-2-(3-phenoxyphenyl)acetate (38e): Title compound was prepared by general procedure with methyl 2-(3-phenoxyphenyl)acetate (727 mg, 3.20 mmol, 1.00 equiv), *p*-acetamidobenzenesulfonyl azide (1.10 g, 4.75 mmol, 1.50 equiv), and diaza(1,3)bicyclo[5.4.0]undecane (0.71 mL, 4.80 mmol, 1.50 equiv). The residue was purified through silica eluting hexanes to afford an orange oil (718 mg, 84% yield). $R_f = 0.43$ (hexanes : ethyl acetate 10 : 1); $^1\text{H NMR}$ (600 MHz, CDCl_3) δ 7.36-7.33 (m, 3H), 7.23-7.20 (m, 2H) 7.12 (ddd, $J = 0.6, 7.2, 8.4$ Hz, 1H), (d, $J = 8.4$ Hz, 2H), 6.80 (dt, $J = 1.2, 0.6, 7.2$ Hz, 1H), 3.86 (s, 3H).

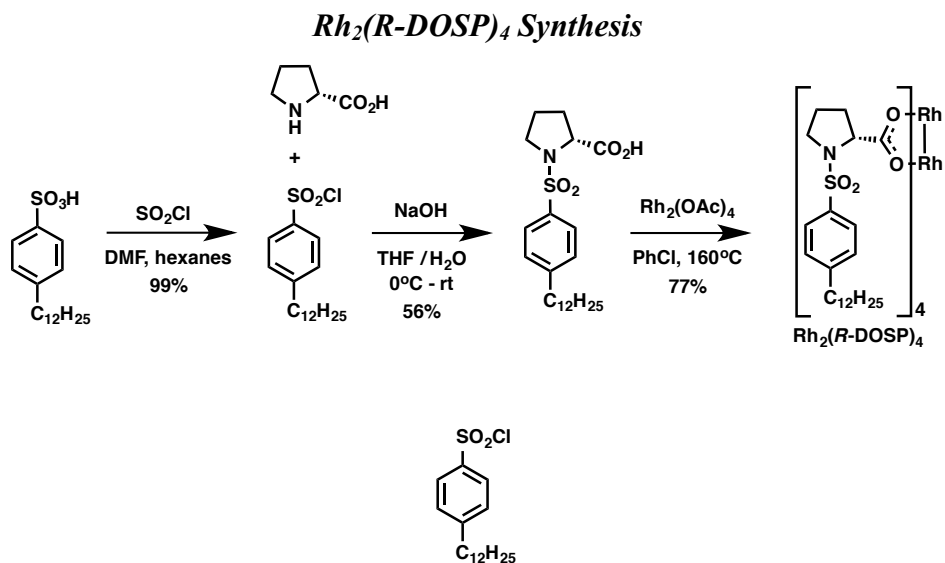


2,4-dimethylpentan-3-yl 2-diazo-2-phenylacetate (42c): Prepared by general procedure with 2,4-dimethylpentan-3-yl 2-phenylacetate (2.9 g, 12 mmol, 1.0 equiv), *p*-acetamidobenzenesulfonyl azide (6.0 g, 25 mmol, 2.0 equiv), and diaza(1,3)bicyclo[5.4.0]undecane (3.7 mL, 25 mmol, 2.0 equiv). The residue was purified through silica eluting pentane : ether (100 : 1) to afford orange crystalline solid (2.3 g, 72% yield). $R_f = 0.36$ (hexanes : ethyl acetate 15 : 1); $^1\text{H NMR}$ (400 MHz, CDCl_3) δ 7.52 (d, $J = 7.6$ Hz, 2H), 7.40 (t, $J = 7.6$ Hz, 2H), 7.19 (t, $J = 7.6$ Hz, 1H), 4.78 (t, $J = 6.2$ Hz, 1H), 1.98 (oct, $J = 6.8$ Hz, 2H), 0.96 (s, 3H), 0.94 (d, $J = 3.6$ Hz, 6H), 0.92 (s, 3H), $^{13}\text{C NMR}$ (100 MHz, CDCl_3) δ 129.1, 126.1, 125.9, 124.1, 83.7, 29.8, 19.8, 17.5; IR (film): 2965, 2078, 1699, 1370, 1240, 1163, 1010, 753; Data are consistent with the literature.²⁷



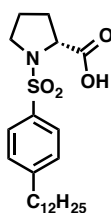
tert-butyl 2-diazo-2-phenylacetate (42d): Title compound was prepared by general procedure with tert-butyl 2-phenylacetate (4.5 g, 23 mmol, 1.0 equiv), *p*-acetamidobenzenesulfonyl azide (11 g, 47 mmol, 2.0 equiv), and diaza(1,3)bicyclo[5.4.0]undecane (7.0 mL, 47 mmol, 2.0 equiv). The residue was purified through silica eluting pentane : ether (100 : 0.5 to 100 : 1) to afford orange oil (3.4 g, 66% yield). $R_f = 0.50$ (pentane : ether 100 : 1); $^1\text{H NMR}$ (400 MHz, CDCl_3) δ 7.49-7.468 (m, 2H), 7.38 (t, $J = 7.6$ Hz, 2H), 7.17 (t, $J = 7.6$ Hz, 1H), 1.56 (s, 9H), $^{13}\text{C NMR}$ (100 MHz, CDCl_3) δ 164.8, 129.1, 126.3, 125.7, 124.2, 82.2, 28.6; IR (film): 2978, 2077, 1695, 1498, 1349, 1245, 1139, 1007, 755, 690; Data are consistent with the literature.²⁷

Dirhodium(II) Catalyst Syntheses:



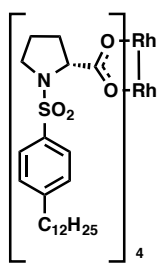
4-dodecylbenzene-1-sulfonyl chloride: 4-dodecylbenzene sulfonic acid (270 g, 1.5 equiv) was dissolved in dry hexanes (375 mL) in a 1L, 2-neck round-bottomed flask. Thionyl chloride (80 mL) was then slowly added over 45 minutes by addition funnel. *N,N*-dimethylformamide (43

mL) was then added by syringe over 5 minutes with trapping of HCl in 10% NaOH bubbler. The resulting reaction mixture was then heated to reflux (~70 °C) in an oil bath trapping the HCl gas generated by bubbling it through 10% NaOH solution and allowed to stir for six hours at reflux. After six hours, the reaction was then poured into a separatory funnel. The dark brown oil at the bottom of the funnel was then removed, carefully quenched with slow addition of bleach, and then discarded. The remaining hexanes layer was then washed with saturated aqueous NaHCO₃ solution until a pH of 8 was reached. The hexanes layer was then dried with MgSO₄ and filtered through a 1" pad of celite and concentrated *in vacuo* to give the desired product as a yellow oil (282g, 99% yield). ¹H MNR (400 MHz, CDCl₃) δ 7.97 (d, *J* = 8.0 Hz, 2H), 7.39 (d, minor rotamer, *J* = 8.5 Hz, 2H), 2.83 (quart, *J* = 7.0 Hz), 2.69-2.59 (m), 2.58-2.52 (m) (1H total), 1.71-1.54 (m, 4H), 1.28-0.76 (m, 20H). Data are consistent with the literature.⁴¹



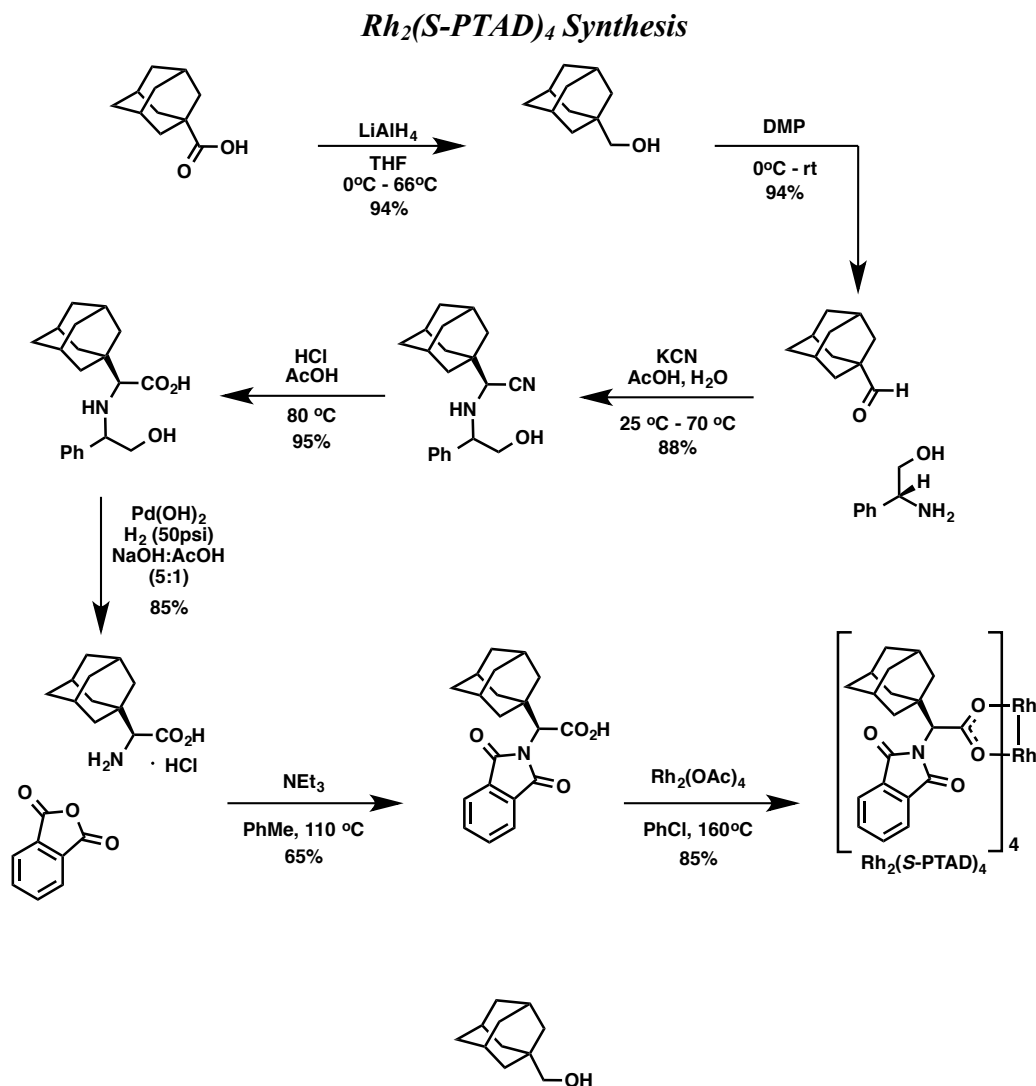
(R)-1-((4-dodecylphenyl)sulfonyl)pyrrolidine-2-carboxylic acid: *D*-proline was dissolved in 450 mL deionized water and brought to 0 °C in an ice bath. A solution of sodium hydroxide (93.5g, 2.3 mol, 3.0 equiv) dissolved in deionized water (420 mL) was then added to the reaction mixture. The reaction was then kept at 0 °C. 4-dodecylbenzene-1-sulfonyl chloride dissolved in 95 mL of tetrahydrofuran was then added dropwise over 30 minutes at 0 °C. The reaction mixture became a white suspension. The reaction mixture was then allowed to warm to room temperature and stirred over night. Concentrated HCl was then slowly added until the reaction mixture was approximately pH 2.0. The freshly acidified reaction mixture was then poured into a separatory funnel (2 L). The aqueous layer was then extracted with hexanes (6 x 500 mL) until

the organic layer was a whitish/ clear. The hexanes layer was then dried over MgSO_4 and filtered through a plug (~2 in.) silica in a fritted 2 L funnel. Solvent was then removed *in vacuo* to afford 190 g yellow oil (56% yield). ^1H MNR (400 MHz, CDCl_3) δ 7.79 (d, $J = 8.5$ Hz, 2H), 7.34 (d, minor rotamer, $J = 8.5$ Hz, 2H), 7.31 (d, major rotamer, $J = 8.5$ Hz), 4.28-4.25 (m, 1H), 3.56-3.51 (m, 1H), 3.27-3.20 (m, 1H), 2.77-2.72 (m), 2.64-2.43 (m) (1H total), 2.16-2.14 (m, 1H), 1.94-1.48 (m, 6H), 1.26-0.83 (m, 22H). Data are consistent with the literature.⁴¹



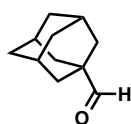
$\text{Rh}_2(\text{R-DOSP})_4$: (*R*)-1-((4-dodecylphenyl)sulfonyl)pyrrolidine-2-carboxylic acid and $\text{Rh}_2(\text{OAc})_4$ were combined in a 1 L, one-neck round-bottomed flask. Toluene (500 mL) was then added and the reaction was stirred until starting materials completely dissolved. The flask was then fitted with a long-path distillation apparatus. The reaction mixture was then brought to reflux with azeotropic removal of acetic acid/ toluene. ^1H NMR of the distillate showed no more acetic acid after collection of 5 x 1 L distillates. At this point, the reaction was diluted with 1 L of diethyl ether and poured into three separate 2 L separatory funnels. Saturated aqueous NaHCO_3 solution (1 L) was then added and the layers were allowed to separate overnight. The aqueous layer was then extracted with diethyl ether (7 x 300 mL) until the organic layer was no longer green. The ether extracts were then dried over MgSO_4 , filtered, and concentrated *in vacuo* to give the catalyst as a crude green solid. The residue was then purified on a column of silica gel using 1:1 petroleum ether/ether as eluent. The green band was then collected in 500mL fractions to afford green solid (90 g, 77% yield). ^1H NMR (400 MHz, CDCl_3) δ 7.72 (d, $J = 9.2$ Hz, 8H), 7.32 (d, J

= 9.2 Hz, 8H), 4.26 (m, 4H), 3.24 (m, 4H), 3.04 (m, 4H), 2.05 (m, 4H), 1.82 (m, 4H), 1.53 (., 8H), 1.22 (bs, 36H), 0.83 (m, 10H). Data are consistent with the literature.⁴¹

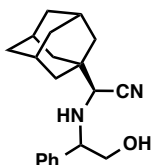


Adamantanemethanol: Lithium aluminum hydride (42.1 g, 1.11 mol, 2.0 equiv) was weighed into a 5 L three-necked round bottom flask equipped with an overhead stirrer, reflux condenser and internal thermometer. Dry tetrahydrofuran (THF) (1.85 L) was added and the solution was cooled to 0 °C. Adamantylcarboxylic acid (100 g, 0.555 mol, 1.0 equiv) was added portionwise over 30 minutes. The suspension was allowed to stir at 0 °C for an hour, then heated to reflux and stirred for 16 hours. The solution was cooled to 0 °C and sodium sulfate decahydrate

(Na₂SO₄•10 H₂O) was added portionwise until bubbling ceased. The suspension was warmed to room temperature and stirred for 30 minutes. The solids were filtered through a pad of celite and washed with dichloromethane (3 x 500 mL). The remaining solids were transferred to a 2 L Erlenmeyer flask and stirred with dichloromethane (1 L) for one hour and filtered. The combined organic layers were dried over anhydrous MgSO₄ and concentrated *in vacuo* to give the title compound as a white solid (86.7 g, 94%).⁴²

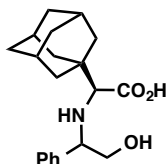


(3r,5r,7r)-adamantane-1-carbaldehyde: Adamantanemethanol (86.7 g, 0.521 mol, 1.0 equiv) was weighed into a 5 L three-necked round bottom flask equipped with an overhead stirrer and internal thermometer. Dichloromethane (1 L) was added and the solution was cooled to 0 °C. Dess-Martin periodinane (288 g, 0.678 mol, 1.3 equiv) was added portionwise over 20 minutes. The suspension was warmed to room temperature and stirred for two hours. 450 mL of saturated aqueous sodium thiosulfate (Na₂S₂O₃) and 450 mL of saturated aqueous sodium bicarbonate (NaHCO₃) were added and the mixture was allowed to stir overnight. The organic layer was taken and washed with saturated aqueous Na₂S₂O₃ (3 x 100 mL), saturated aqueous NaHCO₃ (100 mL), saturated aqueous sodium chloride (NaCl, 100 mL), and dried over anhydrous MgSO₄ and concentrated *in vacuo* to give the title compound as a pale yellow powder (80.4 g, 94%).⁴²



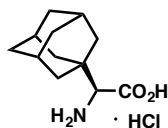
(2S)-2-((3S,5S,7S)-adamantan-1-yl)-2-((2-hydroxy-1-phenylethyl)amino)acetonitrile:

(3*r*,5*r*,7*r*)-adamantane-1-carbaldehyde (80.4 g, 0.490 mol, 1.0 equiv) was weighed into a 2 L three-necked flask equipped with a reflux condenser and two pressure equalizing addition funnels. Water (700 mL) was added followed by (*R*)-(-)-phenylglycinol (67.1 g, 0.490 mol, 1.0 equiv). The suspension was cooled to 0 °C and a solution of potassium cyanide (KCN: 33.5 g, 0.514 mol, 1.05 equiv) in water (100 mL) and acetic acid (AcOH: 29.4 mL, 0.514 mol, 1.05 equiv) were added simultaneously over 30 minutes (KCN solution and AcOH were placed into the two separate addition funnels. Mixing the two together will cause evolution of HCN gas). The reaction was allowed to stir for 30 minutes before being warmed to 70 °C where it was stirred for three hours. The reaction was then cooled to room temperature and the resulting precipitate was filtered and washed with water (3 x 500 mL). The solids were then dried to give the title compound as a pale yellow oil (134.5 g, 88%, 95 : 5 dr). $[\alpha]_D^{20}$: -5.4 (c = 2.78, CHCl₃); HRMS (NSI) calcd for C₂₀H₂₇ON₂ (M+H)⁺ 311.2118 found 311.2113. *This intermediate in the synthesis of Rh₂(S-PTAD)₄ was formed as an inseparable diastereomeric mixture and could not be resolved. The peaks in the ¹H and ¹³C NMR spectra of this compound could not be assigned. A later intermediate in the synthesis of Rh₂(S-PTAD)₄ is fully characterized.*



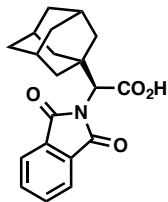
(2S)-2-((3S,5S,7S)-adamantan-1-yl)-2-((2-hydroxy-1-phenylethyl)amino)acetic acid: (2S)-2-((3S,5S,7S)-adamantan-1-yl)-2-((2-hydroxy-1-phenylethyl)amino)acetonitrile (134.5 g, 0.433

mol, 1.0 equiv) was weighed into a 2 L three-necked round bottom flask equipped with an overhead stirrer, reflux condenser and internal thermometer. Hydrochloric acid (800 mL) and acetic acid (200 mL) were added and the solution was warmed to 80 °C. The reaction was allowed to stir at 80 °C for 5 hours and cooled to room temperature. The resulting precipitate was filtered, washed with concentrated hydrochloric acid (3 x 100 mL) and dried to give the title compound as a white powder (150 g, 95%). mp 198-205 °C $[\alpha]_D^{20}$: 1.8 (c = 1.17, CHCl₃); HRMS (NSI) calcd for C₂₀H₂₈O₃N (M+H)⁺ 330.2064 found 330.2055. *This intermediate in the synthesis of Rh₂(S-PTAD)₄ was formed as an inseparable diastereomeric mixture and could not be resolved. The peaks in the ¹H and ¹³C NMR spectra of this compound could not be assigned. A later intermediate in the synthesis of Rh₂(S-PTAD)₄ is fully characterized.*

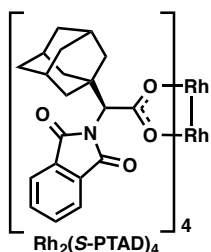


(S)-2-((3S,5S,7S)-adamantan-1-yl)-2-aminoacetic acid hydrochloride: Palladium hydroxide (Pd(OH)₂: 4.0 g, 0.10 weight %) was suspended in methanol (200 mL) and AcOH (40 mL). (2S)-2-((3S,5S,7S)-adamantan-1-yl)-2-((2-hydroxy-1-phenylethyl)amino)acetic acid (40.0 g, 0.109 mol) was added and the suspension was hydrogenated at 50 PSI for 20 hours. The solids were then filtered through celite and washed with methanol (3 x 100 mL). The solvent was removed and the residue triturated with diethyl ether (200 mL). The solids were filtered, washed with diethyl ether (3 x 150 mL) and dried to give the title compound as a white powder (22.8 g, 85%). This procedure was repeated in batches until all of the starting material was converted to the title compound. mp >260 °C $[\alpha]_D^{20}$: -0.01 (c = 1.32, CHCl₃); ¹H MNR (400 MHz, CDCl₃) δ 3.38 (s, 1H), 2.05 (t, J = 3.3 Hz, 3H), 1.87 – 1.76 (m, 6H), 1.75 – 1.58 (m, 7H); ¹³C NMR (100 MHz, CDCl₃) δ 64.5, 39.5, 37.6, 35.6, 29.8; IR (film): 3594, 3508, 2891, 2848, 2198, 1737,

1585, 1502, 1418, 1267, 1216, 838; HRMS (NSI) calcd for C₁₂H₂₀O₂N (M+H)⁺ 210.1489 found 210.1489.

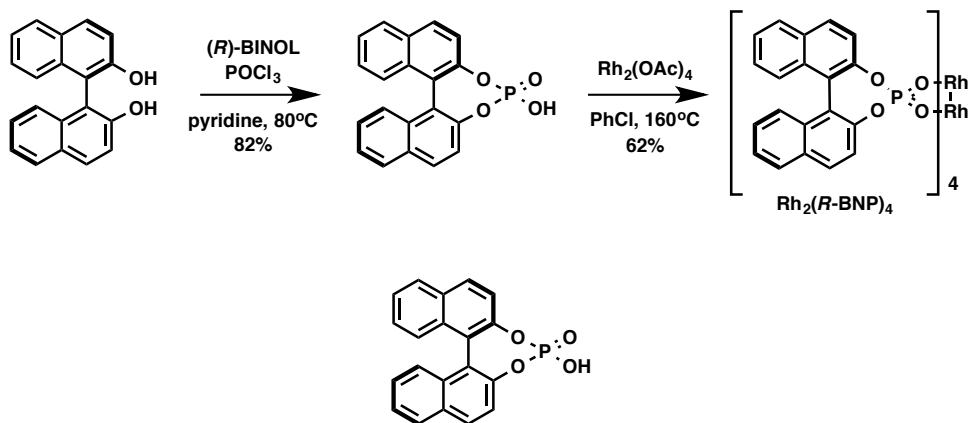


(S)-2-((3S,5S,7S)-adamantan-1-yl)-2-(1,3-dioxisoindolin-2-yl)acetic acid: (*S*)-2-((3*S*,5*S*,7*S*)-adamantan-1-yl)-2-aminoacetic acid hydrochloride (82.0 g, 0.337 mol, 1.0 equiv) was weighed into a 5 L three-necked flask equipped with an overhead stirrer, Dean-Stark trap and internal thermometer. Toluene (1.2 L) was added followed by triethylamine (NEt₃: 141 mL, 1.01 mol, 3.0 equiv). The suspension was heated to reflux and stirred for one hour. Phthalic anhydride (54.9 g, 0.370 mol, 1.1 equiv) was added and the reaction heated at reflux for 12 hours (any water generated was removed from the Dean-Stark trap). The solution was cooled to room temperature and the solvent removed under reduced pressure. The residue was dissolved in ethyl acetate (2 L) and extracted with 4% aqueous NaHCO₃ (5 x 500 mL) (using saturated NaHCO₃ causes the formation of a thick white precipitate that is not very soluble. If this happens, filter off the solid and suspend in dichloromethane. Add concentrated hydrochloric acid until pH = 2. Solids should dissolve and you can extract your product out). Aqueous layers were combined and acidified with concentrated HCl (pH = 2), then extracted with dichloromethane (6 x 500 mL). The combined organic layers were dried and concentrated to give the title compound as a white powder (75 g, 65%).¹⁹



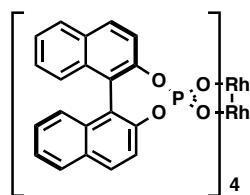
Rh₂(S-PTAD)₄: (*S*)-2-((3*S*,5*S*,7*S*)-adamantan-1-yl)-2-(1,3-dioxoisindolin-2-yl)acetic acid (74 g, 0.218 mol, 6.0 equiv) was weighed into a 3 L five-necked flask equipped with an overhead stirrer, Dean-Stark trap and internal thermometer. Toluene (1.5 L) was added followed by Rh₂(OAc)₄ (16.1 g, 0.036 mol, 1.0 equiv). The green solution was heated to reflux and stirred for 7 hours (the acetic acid that is generated is removed as an azeotrope with toluene and removed via the Dean-Stark trap). The solution was cooled to room temperature and washed with 25% NaHCO₃ (6 x 100 mL). The organic layers were dried over anhydrous MgSO₄, filtered, stirred with SiO₂ (300 g) and concentrated under reduced pressure. The dry mount was purified via flash chromatography (SiO₂, 1.5 kg) using 50% petroleum ether in ether to 100% diethyl ether as the eluent to give the title compound as a green powder (48 g, 85%).¹⁹

Rh₂(R-BNP)₄ Synthesis



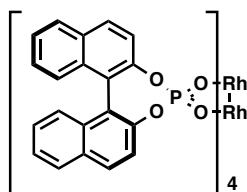
4-hydroxydinaphtho[2,1-*d*:1',2'-*f*][1,3,2]dioxaphosphepine 4-oxide (46):¹ A 50 mL flask fitted with a reflux condenser was charged with (*R*)-BINOL (12.6 g, 44.0 mmol, 1.00 equiv)

dissolved in 10 mL anhydrous pyridine. Phosphorus oxychloride (6.40 mL, 70.0 mmol, 1.60 equiv) was slowly added to the reaction mixture. The reaction was then heated to 80 °C for 2.5 hours. The reaction was then allowed to cool to room temperature and 10 mL of deionized water was added. The reaction was re-heated to 80 °C for an additional 90 minutes. The reaction was then removed from the oil bath, allowed to cool to room temperature, and concentrated *in vacuo*. To the remaining yellow oil was added 150 mL of 6 N HCl. The reaction mixture was then re-heated to 80 °C and allowed to stir for an additional two hours. The white precipitate that formed was then collected by suction filtration and washed with deionized water and dried in a vacuum desiccator over phosphorous pentoxide to afford 12.6 g white solid (82% yield). ¹H NMR (400 MHz, CD₃OD) δ 8.1 (d, *J* = 8.6, 2H), 8.0 (d, *J* = 8.6, 2H), 7.5 (d, *J* = 8.6, 2H), 7.4 (ddd, *J* = 2.0, 6.0, 8.0 2H), 7.2 (m, 4H); HRMS (ESI) calcd for C₂₀H₁₂O₄P₁ (M+H)⁺ 347.0479 found 347.0479.



(R)-dirhodium (II) binaphthyl phosphate: According to the known literature procedure,^{13d} a 100 mL two-neck flask was charged with (*R*)-1,1'-binaphthylhydrogen phosphate (5.5 g, 15.8 mmol, 14.4 equiv) and rhodium acetate (486 mg, 1.1 mmol, 1 equiv) in 52 mL dry, freshly distilled chlorobenzene. The flask was then equipped with a soxhlet extractor containing a thimble filled with sodium carbonate (Na₂CO₃): molecular sieves (1 : 1) and allowed reflux at 160 °C for 48 hours. Chlorobenzene was then removed *in vacuo* and the remaining residue was purified through silica eluting benzene : acetonitrile (100 : 1) to yield yellow-green solid (1.1 g, 62% yield). $[\alpha]_D^{20} +8.3^\circ$ (*c* = 0.77, CHCl₃); *R_f* = 0.38 (benzene : ethyl acetonitrile 100 : 1); ¹H

NMR (400 MHz, CDCl₃) δ 7.89 (d, J = 7.6 Hz, 8 H), 7.85 (d, J = 9.0 Hz, 8H), 7.61 (d, J = 9.0 Hz, 8H), 7.47 (t, J = 7.6 Hz, 16 H), 7.32 (t, J = 7.6 Hz, 8H); ¹³C NMR (100 MHz, CDCl₃) δ 148.1, 132.6, 132.0, 131.3, 128.6, 127.4, 126.6, 125.6, 121.9, 121.5; IR (film): 2970, 1738, 1365, 1231, 1216, 1058, 964 947, 884, 817, 750, 697; Data are consistent with the literature¹



(S)-dirhodium (II) binaphthyl phosphate: yellow-green solid (744 mg, 47% yield). $[\alpha]_{\text{D}}^{20}$ -4.9° (c = 0.81, CHCl₃) Data are consistent with the literature¹

References:

- Pirrung, M. C.; Zhang, J. *Tetrahedron Lett.* **1992**, *33*, 5987.
- Terada, M. *Synthesis* **2010**, *12*, 1929.
- Stetter, H.; Kiehs, K. *Chem. Ber.* **1965**, *98*, 1181.
- Pirrung, M. C.; Zhang, J.; McPhail, A. T. *J. Org. Chem.* **1991**, *56*, 6269.
- Ishitani, H.; Achiwa, K. *Heterocycles* **1997**, *46*, 153.
- McCarthy, N.; McKerverey, M. A.; Ye, T.; McCann, M.; Murphy, E.; Doyle, M. P. *Tetrahedron Lett.* **1992**, *33*, 5983.
- Liao, M.; Wang, J. *Green Chem.* **2007**, *9*, 184.
- (a) Hodgson, D. M.; Stuppel, P. A.; Johnstone, C. *Chem. Commun.* **1999**, *21*, 2185; (b) Hodgson, D. M.; Stuppel, P. A.; Pierard, F. Y. T. M.; Labande, A. H.; Johnstone, C. *Chem. – Eur. J.* **2001**, *7*, 4465.
- Terada, M.; Motoyama, Y.; Mikami, K. *Tetrahedron Lett.* **1994**, *35*, 6693.
- Sasai, H.; Tokunaga, T.; Watanabe, S.; Suzuki, T.; Itoh, N.; Shibasaki, M. *J. Org. Chem.* **1995**, *60*, 7388.
- (a) Hodgson, D. M.; Petroliaigi, M. *Tetrahedron: Asymmetry* **2001**, *12*, 877; (b) Hodgson, D. M.; Selden, D. A.; Dossetter, A. G. *Tetrahedron: Asymmetry* **2003**, *14*, 3841; (c) Hodgson, D. M.; Labande, A. H.; Glen, R.; Redgrave, A. J. *Tetrahedron: Asymmetry* **2003**, *14*, 921; (d) Hodgson, D. M.; Labande, A. H.; Pierard, F. Y. T. M.; Exposito Castro, M. A. *J. Org. Chem.* **2003**, *68*, 6153.
- (a) Lebel, H.; Marcoux, J.-F.; Molinaro, C.; Charette, A. B., *Chem. Rev.* **2003**, *103*, 977; (b) Davies, H. M. L.; Antoulinakis, E. G. *Org. React.* **2001**, *57*, 1.
- (a) Davies, H. M. L.; Bruzinski, P.; Hutcheson, D. K.; Kong, N.; Fall, M. J. *J. Am. Chem.*

- Soc.* **1996**, *118*, 6897; (b) Davies, H. M. L.; Rusiniak, L. *Tetrahedron Lett.* **1998**, *39*, 8811;
- (c) Davies, H. M. L.; Panaro, S. A. *Tetrahedron Lett.* **1999**, *40*, 5287; (d) Davies, H. M. L.; Venkataramani, C. *Org. Lett.* **2003**, *5*, 1403.
14. Pelphey, P.; Hansen, J.; Davies, H. M. L. *Chem. Sci.* **2010**, *1*, 254.
15. Chepiga, K. M.; Qin, C.; Alford, J. S.; Chennamadhavuni, S.; Gregg, T. M.; Olson, J. P.; Davies, H. M. L. *Tetrahedron* **2013**, *69*, 5765.
16. Chennamadhavuni, S. Synthesis of small molecule therapeutics utilizing rhodium carbenoid chemistry. *Ph.D. Thesis, Emory University* **2012**.
17. (a) Kozikowski, A.; Kurome, T.; Setola, V.; Roth, B. Patent Application WO2007025144A1, **2007**; (b) Cho, S. J.; Jensen, N. H.; Kurome, T.; Kadari, S.; Manzano, M. L.; Malberg, J. E.; Caldarone, B.; Roth, B. L.; Kozikowski, A. P. *J. Med. Chem.* **2009**, *52*, 1885.
18. (a) Davies, H. M. L.; Townsend, R. J. *J. Org. Chem.* **2001**, *66*, 6595; (b) Davies, H. M. L.; Nagashima, T.; Klino, J. L., III *Org. Lett.* **2000**, *2*, 823; (c) Ventura, D. L.; Li, Z.; Coleman, M. G.; Davies, H. M. L. *Tetrahedron* **2009**, *65*, 3052; (d) Davies, H. M. L.; Coleman, M. G.; Ventura, D. L. *Org. Lett.* **2007**, *9*, 4971; (e) Davies, H. M. L.; Boebel, T. A. *Tetrahedron Lett.* **2000**, *41*, 8189; (f) Hedley, S. J.; Ventura, D. L.; Dominiak, P. M.; Nygren, C. L.; Davies, H. M. L. *J. Org. Chem.* **2006**, *71*, 5349; (g) Davies, H. M. L.; Panaro, S. A. *Tetrahedron* **2000**, *56*, 4871; (h) Bonge, H. T.; Pinteá, B.; Hansen, T. *Org. Biomol. Chem.* **2008**, *6*, 3670; (i) Bonge, H. T.; Hansen, T. *J. Org. Chem.* **2010**, *75*, 2309; (j) Bonge, H. T.; Hansen, T. *Tetrahedron Lett.* **2010**, *51*, 5298.
19. Reddy, R. P.; Lee, G. H.; Davies, H. M. L. *Org. Lett.* **2006**, *8*, 3437.
20. Denton, J. R.; Sukumaran, D.; Davies, H. M. L. *Org. Lett.* **2007**, *9*, 2625.
21. Denton, J. R.; Cheng, K.; Davies, H. M. L. *Chem. Commun.* **2008**, *10*, 1238.
22. Denton, J. R.; Davies, H. M. L. *Org. Lett.* **2009**, *11*, 787.
23. Davies, H. M. L.; Huby, N. J. S.; Cantrell, W. R., Jr.; Olive, J. L. *J. Am. Chem. Soc.* **1993**, *115*, 9468.
24. Brooks, L. A. *J. Am. Chem. Soc.* **1944**, *66*, 1295.
25. Davies, H. M. L.; Cantrell, W. R., Jr.; Romines, K. R.; Baum, J. S. *Org. Synth.* **1992**, *70*, 93.
26. Davies, H. M. L., Methyl Phenyl diazoacetate. *e-EROS*, Wiley: **2001**.
27. Li, Z. Exploration of high symmetry dirhodium catalysts and the reaction of donor/acceptor carbenoids with alcohols. *Ph. D. Thesis, Emory University* **2010**.
28. Santos, L. S.; Rosso, G. B.; Pilli, R. A.; Eberlin, M. N. *J. Org. Chem.* **2007**, *72*, 5809.
29. Stearman, C. J.; Wilson, M.; Padwa, A., Conjugate Addition-Dipolar Cycloaddition Cascade for the Synthesis of Benzo[a]quinolizine and Indolo[a]quinolizine Scaffolds: Application to the Total Synthesis of (±)-Yohimbenone. *J. Org. Chem.* **2009**, *74* (9), 3491-3499.
30. Liang, Q.; Zhang, J.; Quan, W.; Sun, Y.; She, X.; Pan, X. *J. Org. Chem.* **2007**, *72*, 2694.
31. Andrus, M. B.; Harper, K. C.; Christiansen, M. A.; Binkley, M. A. *Tetrahedron Lett.* **2009**, *50*, 4541.
32. Qu, Z.; Shi, W.; Wang, J., A. *J. Org. Chem.* **2001**, *66*, 8139.
33. Allegretti, M.; Bertini, R.; Cesta, M. C.; Bizzarri, C.; Di Bitondo, R.; Di Cioccio, V.; Galliera, E.; Berdini, V.; Topai, A.; Zampella, G.; Russo, V.; Di Bello, N.; Nano, G.; Nicolini, L.; Locati, M.; Fantucci, P.; Florio, S.; Colotta, F. *J. Med. Chem.* **2005**, *48*, 4312.
34. Lee, J.; Lee, J.-H.; Kim, S. Y.; Perry, N. A.; Lewin, N. E.; Ayres, J. A.; Blumberg, P. M.

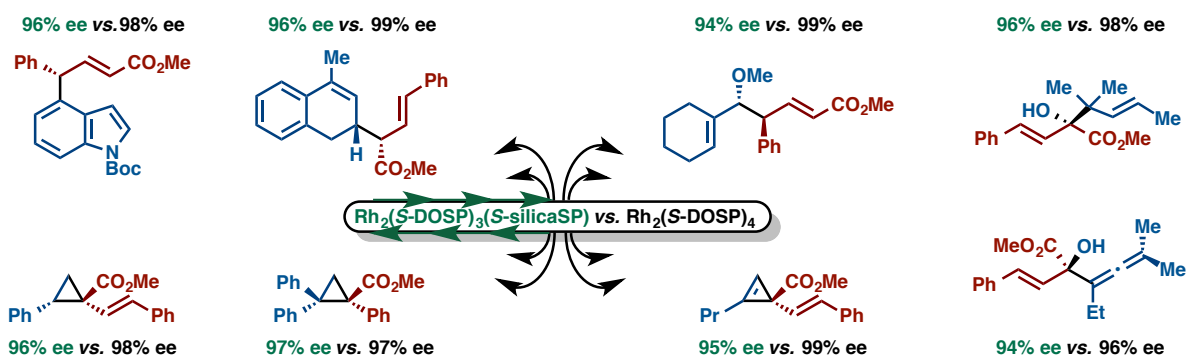
Bioorg. Med. Chem. **2006**, *14*, 2022.

35. Hashimoto, N.; Sasaki, Y.; Nakama, C.; Ishikawa, M. Preparation of phenyl-isoxazol-3-ol derivatives as GPR120 agonists. Patent Application WO2008066131A1, **2008**.
36. Sala, T.; Sargent, M. V. *J. Chem. Soc., Perkin Trans. 1* **1979**, *10*, 2593.
37. Ye, B.; Cramer, N. *Angew. Chem., Int. Ed.* **2014**, *53*, 7896.
38. Harker, W. R. R.; Carswell, E. L.; Carbery, D. R. *Org. Lett.* **2010**, *12*, 3712.
39. Wang, H.; Li, G.; Engle, K. M.; Yu, J.-Q.; Davies, H. M. L. *J. Am. Chem. Soc.* **2013**, *135*, 6774.
40. Nadeau, E.; Davies, H. M. L., Methyl (E)-4-Phenyl-2-diazo-3-butenolate. *e-EROS*, Wiley: **2001**.
41. Davies, H. M. L. Tetrakis[1-[[4-dodecylphenyl]sulfonyl]-(2S)-prolinate] Dirhodium. *e-EROS*, Wiley: **2001**.
42. Lill, A.P.; Roedl, C. B.; Steinhilber, D.; Stark, H.; Hofmann, B. *Eur. J. Med. Chem.* **2015**, *89*, 503.

Chapter III: Immobilized Chiral Dirhodium(II) Catalysts for Enantioselective Carbenoid Reactions

Advisor: Huw M. L. Davies, Ph.D.
Collaborator: Christopher W. Jones, Ph.D.

The great majority of pharmaceutical processes employ heterogeneous catalysts as they offer simplified catalyst separation and recovery. Chiral transition metal catalysts can be heterogenized by immobilization of the catalyst onto a support, which is insoluble in the reaction mixture. This chapter describes a silica-supported dirhodium(II) tetraproline catalyst, which was synthesized in four steps from L-proline and used in a range of enantioselective transformations of donor/acceptor carbenoids including cyclopropanation, cyclopropanation, tandem ylide formation/[2,3] sigmatropic rearrangement, and a variety of combined C–H functionalization/Cope rearrangement reactions. The products of these transformations were obtained in yields and levels of enantioselectivity comparable to those obtained with its homogeneous counterpart, $\text{Rh}_2(\text{S-DOSP})_4$. The silica-supported $\text{Rh}_2(\text{S-DOSP})_4$ derivative is successfully recycled over five reactions.



3.1 Introduction to Supported Heterogeneous Catalysis

A catalyst is not consumed in a particular process but rather serves to promote a thermodynamically favorable reaction pathway and is regenerated at the end of a catalytic cycle for reuse.¹ For a reaction to be practical, the catalyst cost and the level of metal contaminants in the final product become important issues to consider. Catalysts can be recovered after a reaction and reused but catalyst isolation from homogeneous reactions may not be practical for repeated recycling procedures. Depending upon the polarity of the homogeneous catalyst in relation to the polarities of the products and by-products of a given reaction, chromatographic separation of a given catalyst from the products may be troublesome and lead to loss of material. Heterogeneous catalysis offers simplified catalyst separation and recovery since it involves immobilization of the catalyst onto a support, which is typically insoluble in the reaction mixture. Separation of the catalyst from the reaction mixture involves a simple filtration or decanting of the soluble products from the reaction vessel to leave behind the catalyst ready to catalyze another reaction.²

As the breadth of chiral homogeneous catalysis increases, several interdisciplinary efforts have led to the development of chiral heterogeneous variants of the prominent homogeneous catalysts. For both academia and industry, heterogeneous chiral catalysis offers all the benefits of homogeneous chiral catalysis with the added advantage of catalyst recovery and reuse along with the potential for higher turnover numbers (TON) and high turnover frequency (TOF) as well as the potential for incorporation of the catalyst into new reactor manifolds.²

3.2 Design Elements of Supported Catalysts

The benefits of catalyst recycling have been realized in industry, as many chemical and petrochemical processes use achiral heterogeneous catalysts.² Over the past ten years, however, there has been an increased demand for immobilized chiral catalysts. The method of immobilization, the choice of support, and the point of attachment of the support to the catalyst are the three primary variables which can influence the chiral environment, turnover numbers (TONs), reaction rates, recyclability, and stereoselectivity.² Careful consideration of these variables can allow for the development of a chiral heterogeneous catalyst capable of matching the stability, activity, and stereoselectivity of its homogeneous counterpart. However, achieving this goal is difficult in most cases.²

The general approaches for chiral catalyst immobilization have been placed into four categories: (a) covalent attachment of the chiral catalyst onto a solid support, (b) adsorption of the catalyst on the support, (c) ion-pair formation between the metal complex and the solid support and (d) entrapment of the homogeneous catalysts into pores of the solid support (Figure 3.1). Immobilization via covalent attachment has been the easiest to design and develop.²

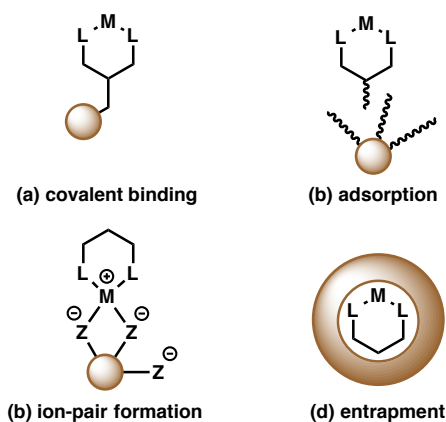
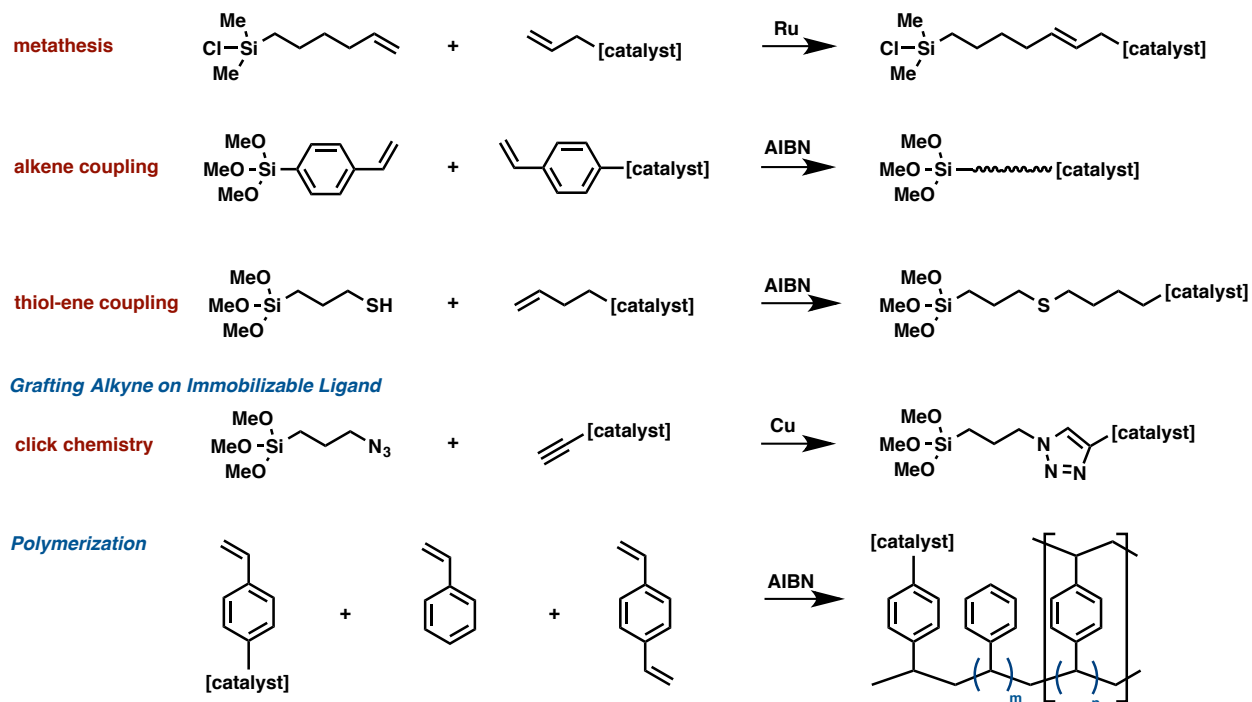


Figure 3.1 Methods for chiral catalyst immobilization

For the covalent immobilization method, there are several different ways in which the catalyst can be covalently linked to the support.² For solid supports such as SiO₂, there are several methods for grafting the catalyst to the functionalized support (Scheme 3.1). Alkene-functionalized supports undergo metathesis with an alkene attached to the catalyst to give the corresponding covalently immobilized species. Similarly, styryl-functionalized supports can undergo AIBN-initiated radical coupling with a catalyst featuring a styryl group. Surface thiols can undergo thiol-ene coupling with catalysts containing terminal alkenes. Also, surface azides can undergo copper catalyzed click chemistry to provide a catalyst covalently immobilized by a triazole linkage. Rather than being grafted to a pre-existing support, catalysts featuring a styryl group can also undergo polymerization with styrene and/or divinylbenzene (DVB) to give a catalyst immobilized by a polymeric matrix (Scheme 3.1). The rigidity of the polymer can be varied by this method by modifying the ratio of styrene : DVB employed in the polymerization step.²

Scheme 3.1 Methods for grafting the catalyst to the support and for polymerization

Grafting Alkene on Immobilizable Ligand

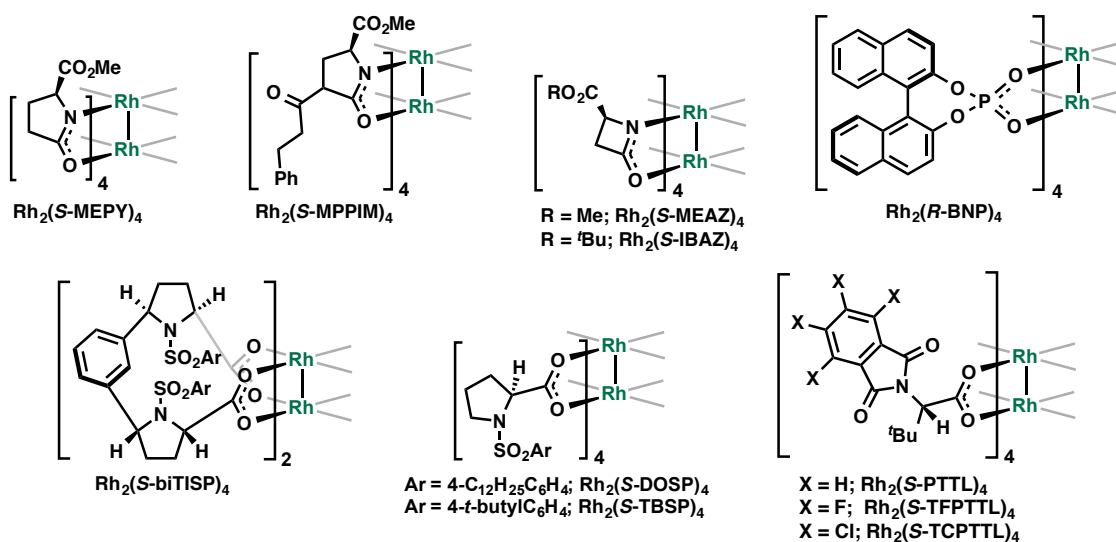


Choice of a suitable support is key to obtaining a recyclable catalyst system. The sterics and electronics of the catalyst can be fine-tuned to obtain optimal activity and stereoselectivity. The classic problem in most systems is the inevitable distortion of the chiral environment of the homogeneous catalyst. The benefits of implementing long spacers between the polymer attachment and the active site of the catalyst have been recognized.³ Soai and Wantanabe studied the effect of various alkyl spacers in polymer-supported enantioselective addition of dialkylzincs to both aromatic and aliphatic aldehydes using polymer-bound chiral catalysts with a spacer. In order to eliminate the restriction of the freedom of the catalytic site, they synthesized chiral polymer catalysts with methylene spacers that served to separate the catalytic site from the polystyrene resin.³

3.3 Supported Dirhodium(II) Catalysts

After Teyssie's initial report on the use of dirhodium(II) tetracetate ($\text{Rh}_2(\text{OAc})_4$) for generating rhodium carbenoids from diazo compounds,⁴ Brunner introduced chiral rhodium(II) catalysts from simple enantiomerically pure amino acids.⁵ The dirhodium(II) tetracarboxylate core became a new transition metal scaffold for chiral catalyst development.⁶ Davies,⁷ McKervey,⁸ and Hashimoto⁹ have developed very effective chiral amino-acid based rhodium catalysts. Doyle *et al.* have developed a family of rhodium carboxamidate catalysts by replacing the carboxylates with chiral amidate ligands.¹⁰ Several different chiral dirhodium(II) catalysts have been heterogenized in an effort to make dirhodium(II) catalysis more affordable by increasing their recyclability and thus their efficiency (Figure 3.2). The unique reactivity profile of these catalysts combined with the precious, expensive nature of rhodium makes these systems highly attractive candidates for immobilization.

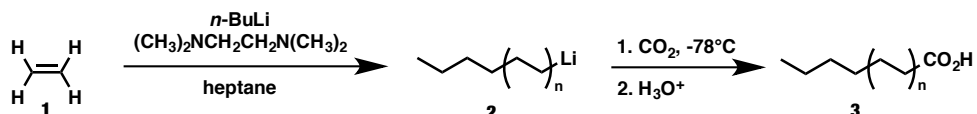
Figure 3.2 Chiral dirhodium(II) catalysts which have been successfully immobilized



Bergbreiter was the first to immobilize a dirhodium catalyst ($\text{Rh}_2(\text{OAc})_4$), using a covalent attachment through one of the acetate ligands to a polyethylene (PE) based support which

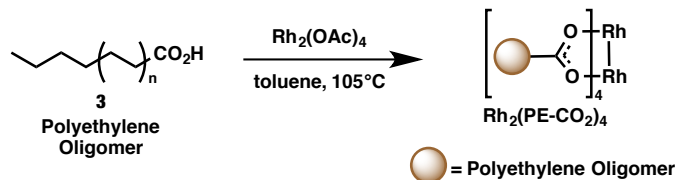
showed temperature-dependent solubility and inertness to various reactions (Scheme 3.3).¹¹ These polyethylene carboxylates (PE-CO₂) were prepared by anionic oligomerization of ethylene, then carboxylation with carbon dioxide at -78 °C, followed by acidification (Scheme 3.2).

Scheme 3.2 Bergbreiter's route to polyethylene carboxylates



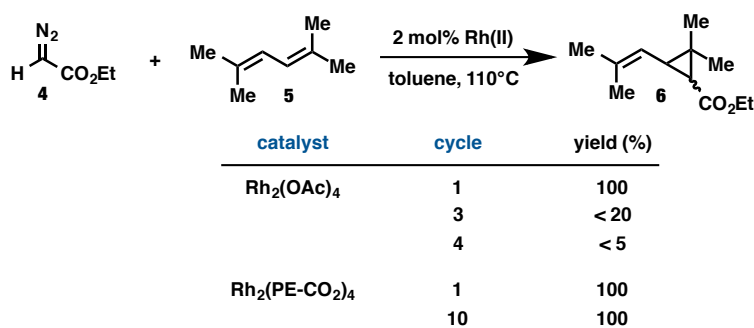
The polyethylene carboxylates were then metallated by ligand exchange with Rh₂(OAc)₄ in refluxing toluene with azeotropic removal of acetic acid generated from the exchange of acetate ligands for polyethylene carboxylate (Scheme 3.3).

Scheme 3.3 Polyethylene-supported Rh₂(OAc)₄



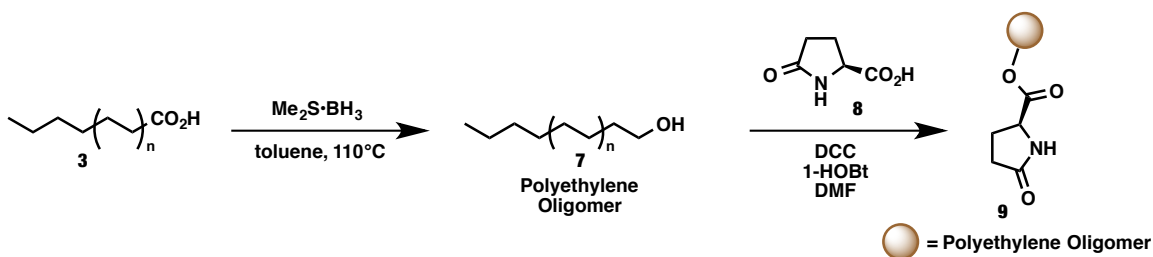
The polyethylene-bound rhodium(II) catalyst was reused up to 10 times with retention of original reactivity and essentially unchanged diastereoselectivity (Scheme 3.4, starting ratio of 2.3 : 1 (*trans* : *cis*) as compared to a final value of 2.4 : 1).

Scheme 3.4 First Immobilized Dirhodium System Bergbreiter's $\text{Rh}_2(\text{PE-CO}_2)_4$

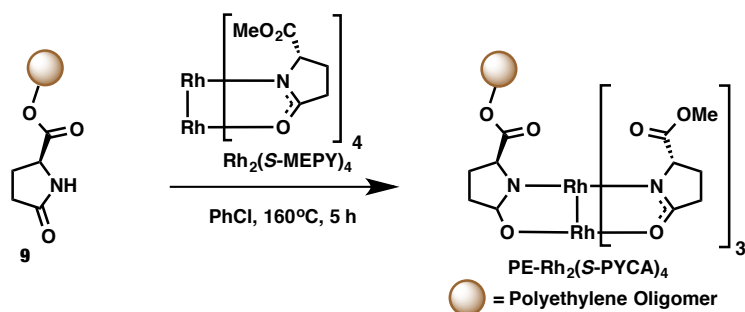


The following year, a collaborative work by the Bergbreiter and Doyle groups, applied the polyethylene based support to dirhodium(II) tetracarboxamidate catalyst $\text{Rh}_2(\text{S-MEPY})_4$ to provide the first immobilized chiral dirhodium catalyst, oligomer-bound dirhodium(II) 2-pyrrolidone-5(*S*) carboxylate ($\text{PE-Rh}_2(\text{S-PYCA})_4$). $\text{PE-Rh}_2(\text{S-PYCA})_4$ was prepared by esterification of 2-pyrrolidinone-5(*S*)-carboxylic acid with the polyethylene polymer (Scheme 3.5) followed by ligand exchange (Scheme 3.6).¹²

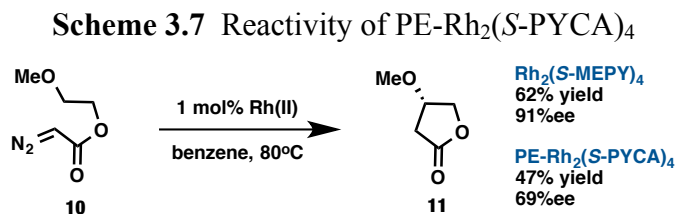
Scheme 3.5 Immobilized (*S*)-PYCA ligand



Scheme 3.6 First immobilized chiral dirhodium(II) system: $\text{PE-Rh}_2(\text{S-PYCA})_4$



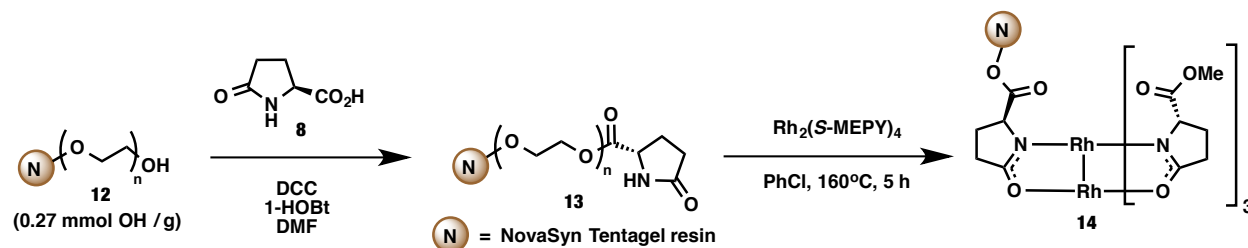
This polyethylene-supported catalyst PE-Rh₂(*S*-PYCA)₄, however, was found to be less reactive and less selective than Rh₂(*S*-MEPY)₄ (Scheme 3.7). Cyclopropanation reactions with PE-Rh₂(*S*-PYCA)₄ provided similar results.¹²



Considering that these reactions were conducted in refluxing benzene, it was believed that the noted decreases in both reactivity and selectivity were due to the displacement of chiral ligands from the dirhodium core. Enhanced recyclability was achieved by addition of a catalytic amount of chiral (*S*)-MEPY ligand to the reaction mixture. In this case, the immobilized catalyst remained active for up to eight reaction rounds with only minimal loss in enantioselectivity (5%) and yield (20%).¹²

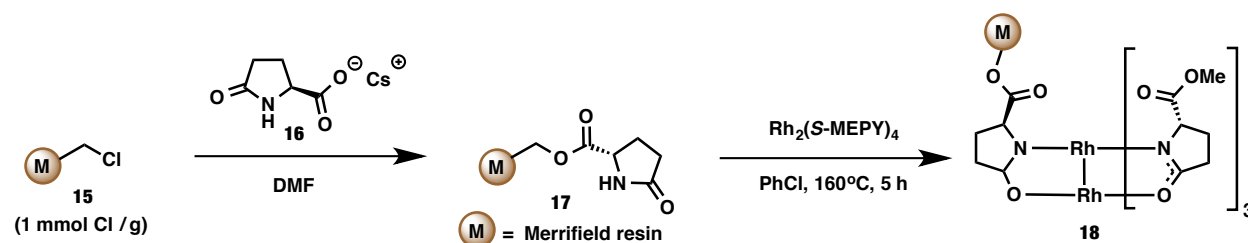
Although these seminal works on the syntheses and applications of immobilized dirhodium(II) complexes represent significant advances, many drawbacks exist in these systems. For example, all reported reactions employing these polyethylene oligomer catalysts were conducted at reflux to ensure complete solubility of the catalyst in the reaction. Doyle *et al.* reported an improved immobilized Rh₂(*S*-MEPY)₄-derivative in 2002, which did not require high reaction temperatures, by employing a NovaSyn Tentagel (TG) hydroxyl resin. As in their original paper, DCC and HOBt-mediated coupling of the hydroxyl resin with pyroglutamic acid provided the corresponding immobilized ligand (Scheme 3.8).¹⁰

Scheme 3.8 NovaSyn Tentagel immobilized $\text{Rh}_2(\text{S-MEPY})_4$ -derivative



A second immobilized $\text{Rh}_2(\text{S-MEPY})_4$ -derivative containing no polyethylene spacer between the carboxylate and the resin moiety was synthesized employing a Merrifield resin (Scheme 3.9). This ligand was used as a control to show that the long polyethylene spacer was necessary in order to prevent potential adverse reactivity that could potentially occur due to the proximity of the bound catalyst to the polymer surface and backbone. Doyle reported the immobilized $\text{Rh}_2(\text{S-MEPY})_4$ -derivatives **14** and **18** as if a single ligand exchange had been conducted in which only one ligand from $\text{Rh}_2(\text{S-MEPY})_4$ was replaced with the immobilized ligand (Schemes 3.8 and 3.9). However, in the report there is no data suggesting the number of ligands exchanged. “Single” ligand exchange was conducted for a shorter period of time (5 hours vs. 3 days) and at lower temperature (130°C vs. 160°C) than the typical tetra-ligand exchange reaction to ensure formation of mono-ligand exchange product.¹⁰

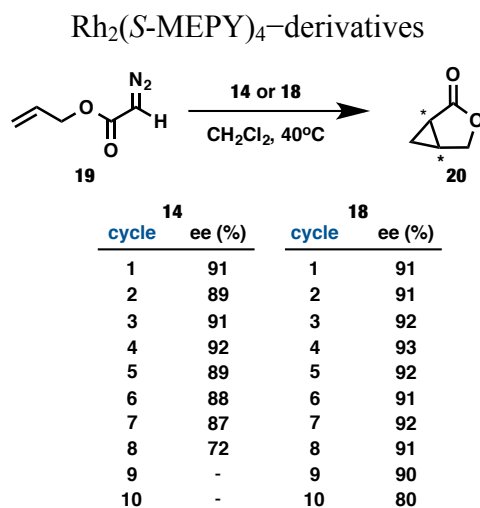
Scheme 3.9 Merrifield immobilized $\text{Rh}_2(\text{S-MEPY})_4$ -derivative



Although immobilization by covalent attachment of a resin to a single ligand differentiates one rhodium face from the other, this differentiation does not appear to have an effect on the

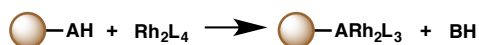
selectivity of the resulting catalyst.⁶ Both of these catalysts provided products with the same level of enantioinduction as homogeneous $\text{Rh}_2(\text{S-MEPY})_4$ in an intramolecular cyclopropanation reaction and were recyclable in up to 10 runs (Scheme 3.10). Contradictory to their original hypothesis, catalyst **18** outperformed catalyst **14** in achieving both higher levels of enantioinduction and greater catalyst recyclability. This result was attributed to the higher ligand loading of catalyst **18** (0.1 mmol Cl / g) as compared to **14** (0.27 mmol OH / g). Also, the inferior selectivity of catalyst **14** could potentially be attributed to undesirable carbene reactions occurring at the linker, poly(ethylene oxide), of **14**.¹⁰

Scheme 3.10 Comparison of NovaSyn Tentagel and Merrifield immobilized



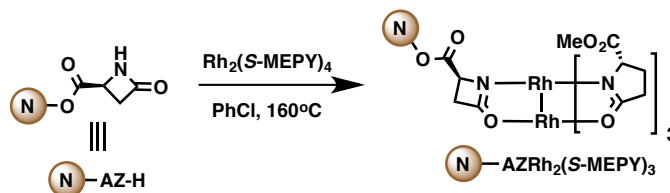
The following year, Doyle *et al.* published a follow-up report describing in more detail the significance of these mixed ligand systems (Scheme 3.11). The resulting catalyst from mono-ligand exchange was found to be significantly altered both electronically and sterically from its tetrasubstituted counterpart.¹³

Scheme 3.11 General structure of mixed ligand dirhodium(II) complexes

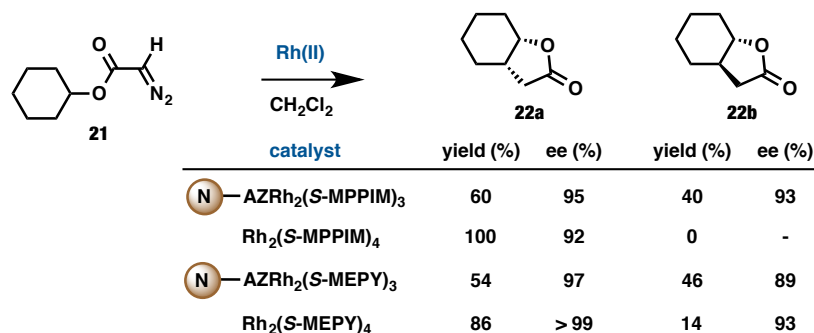


Immobilized azetidinones were employed in the “single” ligand exchange with several different chiral tetracarboxamidates ($\text{Rh}_2(\text{S-MEPY})_4$, $\text{Rh}_2(\text{S-MPPIM})_4$, $\text{Rh}_2(\text{S-MEAZ})_4$, and $\text{Rh}_2(\text{S-IBEAZ})_4$ (Scheme 3.12). Immobilized variants of $\text{Rh}_2(\text{S-MPPIM})_4$ and $\text{Rh}_2(\text{S-MEPY})_4$ were able to catalyze the first reaction round of a C–H insertion at similar levels of enantioinduction as their homogeneous counterparts. The level of diastereoselection, however, was greatly decreased in reactions catalyzed by heterogeneous catalysts and most importantly, the study failed to address the recyclability of these catalysts (Scheme 3.13).¹³

Scheme 3.12 Example of an immobilized azetidinone mixed ligand dirhodium(II) complex



Scheme 3.13 Immobilized azetidinone mixed ligand dirhodium(II)-catalyzed C–H insertion

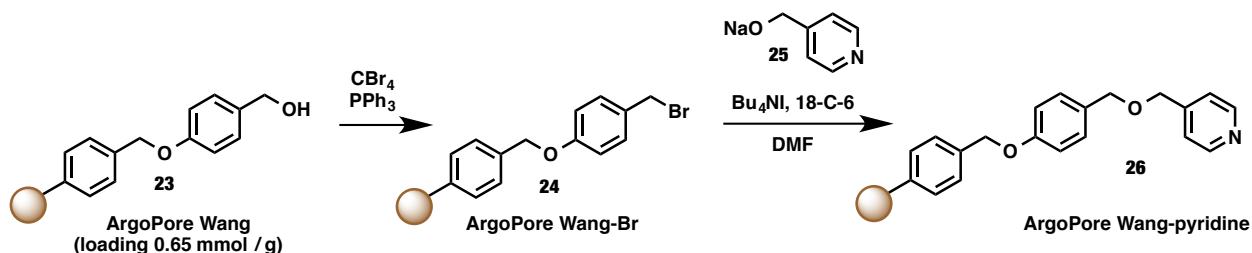


3.4 Supported Dirhodium(II) Tetracarboxylate Catalysts

The first reported dirhodium tetracarboxylate to be immobilized through a non-covalent linkage was presented by Davies *et al.* in 2002.¹⁴ Several different types of commercially available linkers were tested for their immobilization efficiency and it was found that the Argopore Wang-

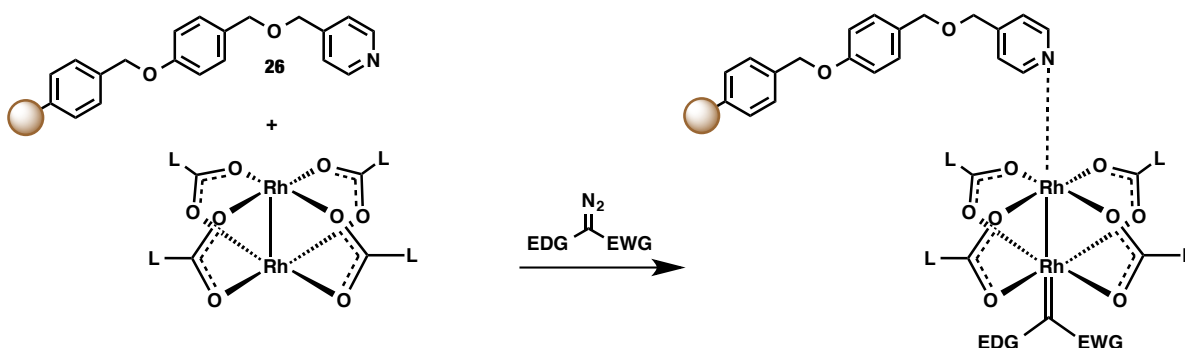
pyridine linker, shown in Scheme 3.14, gave the highest percent immobilization (86%).¹⁵ In their 2002 report, Davies and coworkers were able to utilize pyridine functionalized highly cross-linked polystyrene resins to immobilize an array of dirhodium(II) tetracarboxylates.¹⁴

Scheme 3.14 ArgoPore Wang-pyridine linker



Initially, these supports were envisioned to effect immobilization of the catalyst through coordination of the pyridyl nitrogen to one of the axial binding sites of dirhodium. The remaining axial binding site of dirhodium would remain uncoordinated and active for catalysis (Scheme 3.15).¹⁴

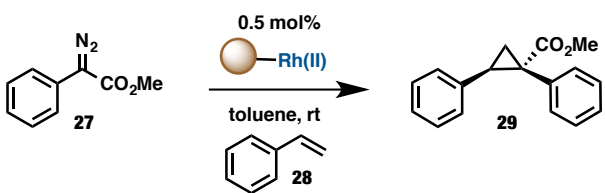
Scheme 3.15 Coordination method of immobilization for dirhodium(II) catalysts



Initial studies involved testing the catalysts immobilized by this method in a standard cyclopropanation reaction. $\text{Rh}_2(\text{S-TBSP})_4$ immobilized by ArgoPore Wang-pyridine **26** was able to effectively catalyze four cycles of cyclopropanation with minimal decrease in yield (92% to 89%) and little deterioration of enantioselectivity (82% to 70%). $\text{Rh}_2(\text{S-biTISP})_4$, however,

was found to be a much more robust catalyst than $\text{Rh}_2(\text{S-TBSP})_4$, providing fifteen cycles with similar yields and enantioselectivities to the first reaction round (Table 3.1, 91% to 89% yield; 85% to 88% ee).¹⁴

Table 3.1 Immobilized $\text{Rh}_2(\text{S-TBSP})_4$ and $\text{Rh}_2(\text{S-biTISP})_4$ in cyclopropanation



$\text{Rh}_2(\text{S-TBSP})_4$				$\text{Rh}_2(\text{S-biTISP})_4$			
cycle	time (min)	yield (%)	ee (%)	cycle	time (min)	yield (%)	ee (%)
1	10	92	82	1	18	91	85
4	14	89	70	15	92	89	88

Interestingly, Davies *et al.* showed that immobilized $\text{Rh}_2(\text{S-biTISP})_4$ was capable of catalyzing successive cyclopropanation reactions while introducing a different diazo compound each successive run. Five rounds of cyclopropanations provided the corresponding products in yields and enantioselectivities comparable to those obtained with the homogeneous catalyst. Significantly, Davies *et al.* were able to efficiently wash the product from the polymer support between reaction cycles while retaining the catalyst (Table 3.2).¹⁴

Table 3.2 Catalyst recycling study in cyclopropanation with various diazoacetates

Reaction scheme showing the cyclopropanation of diazoacetate **30a-e** (where R is a phenyl group) with styrene (**28**) using 0.5 mol% of immobilized $\text{Rh}_2(\text{S-biTISP})_4$ catalyst in toluene at room temperature (rt) to yield cyclopropane **31a-e**.

cycle	R	product	time (min)	yield (%)	ee (%)
1		31a	16	82	71
2		31b	30	86	76
3		31c	5	84	80
4		31d	30	85	80
5		31e	30	94	90

The first reported immobilization of $\text{Rh}_2(\text{S-DOSP})_4$ came the following year. In this report, Davies *et al.* were able to successfully apply $\text{Rh}_2(\text{S-DOSP})_4$ immobilized by the coordination method described in Scheme 3.15 to C–H insertion reactions. (Table 3.3) C–H insertion of phenyldiazoacetate into 1,4-cyclohexadiene with the immobilized $\text{Rh}_2(\text{S-DOSP})_4$ -derivative provided the corresponding product with no deterioration of yield (81% to 84%) and minimal loss of enantioselectivity (88% to 84%) over ten cycles (Table 3.3).¹⁶

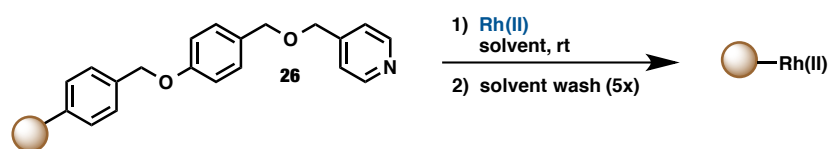
Table 3.3 C–H insertion by immobilized $\text{Rh}_2(\text{S-DOSP})_4$ -derivative

Reaction scheme showing the C–H insertion of phenyldiazoacetate **27** into 1,4-cyclohexadiene (**32**) using 0.5 mol% of immobilized $\text{Rh}_2(\text{S-DOSP})_4$ catalyst in toluene at room temperature (rt) to yield cyclohexane **33**.

cycle	time (min)	yield (%)	ee (%)
1	20	81	88
10	30	84	84

Finally, in 2005, Davies reported application of this “universal immobilization strategy” to all three types of dirhodium catalysts: tetracarboxylates, tetracarboxamides, and tetraphosphates. Inductively coupled plasma atomic emission spectroscopy (ICP-AES) analysis for percent rhodium was used to calculate the catalyst immobilization (%) for each catalyst tested. The results of this study showed that $\text{Rh}_2(\text{S-MEPY})_4$, $\text{Rh}_2(\text{S-MEAZ})_4$, $\text{Rh}_2(\text{S-PTTL})_4$, $\text{Rh}_2(\text{S-BNP})_4$ could be effectively immobilized (Table 3.4).¹⁷

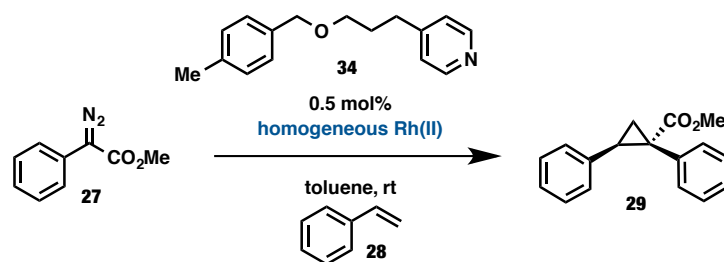
Table 3.4 Application of coordination method of immobilization to a variety of dirhodium(II) catalysts



catalyst	loading (mmol/g)	immobilization (%)
$\text{Rh}_2(\text{S-MEPY})_4$	0.12	60
$\text{Rh}_2(\text{S-MEAZ})_4$	0.12	61
$\text{Rh}_2(\text{S-PTTL})_4$	0.14	77
$\text{Rh}_2(\text{R-BNP})_4$	0.14	81

The great success of these systems, however, is surprising because donor groups such as pyridine are known have a deactivating effect on dirhodium tetracarboxylates. Control experiments employing homogeneous catalyst were conducted in the presence of a non-immobilized *para*-substituted pyridine derivative **34**. Shockingly, low yields (43% and 18%) of cyclopropanation were obtained when the reaction was doped with pyridine derivative **34**, showing that a strong deactivation of the proline catalysts was occurring (Table 3.5).¹⁷ These results, along with a few mechanistic investigations into the means of immobilization, led Davies *et al.* to attribute immobilization to a cooperative effect of microencapsulation¹⁸ and pyridine coordination.¹⁵

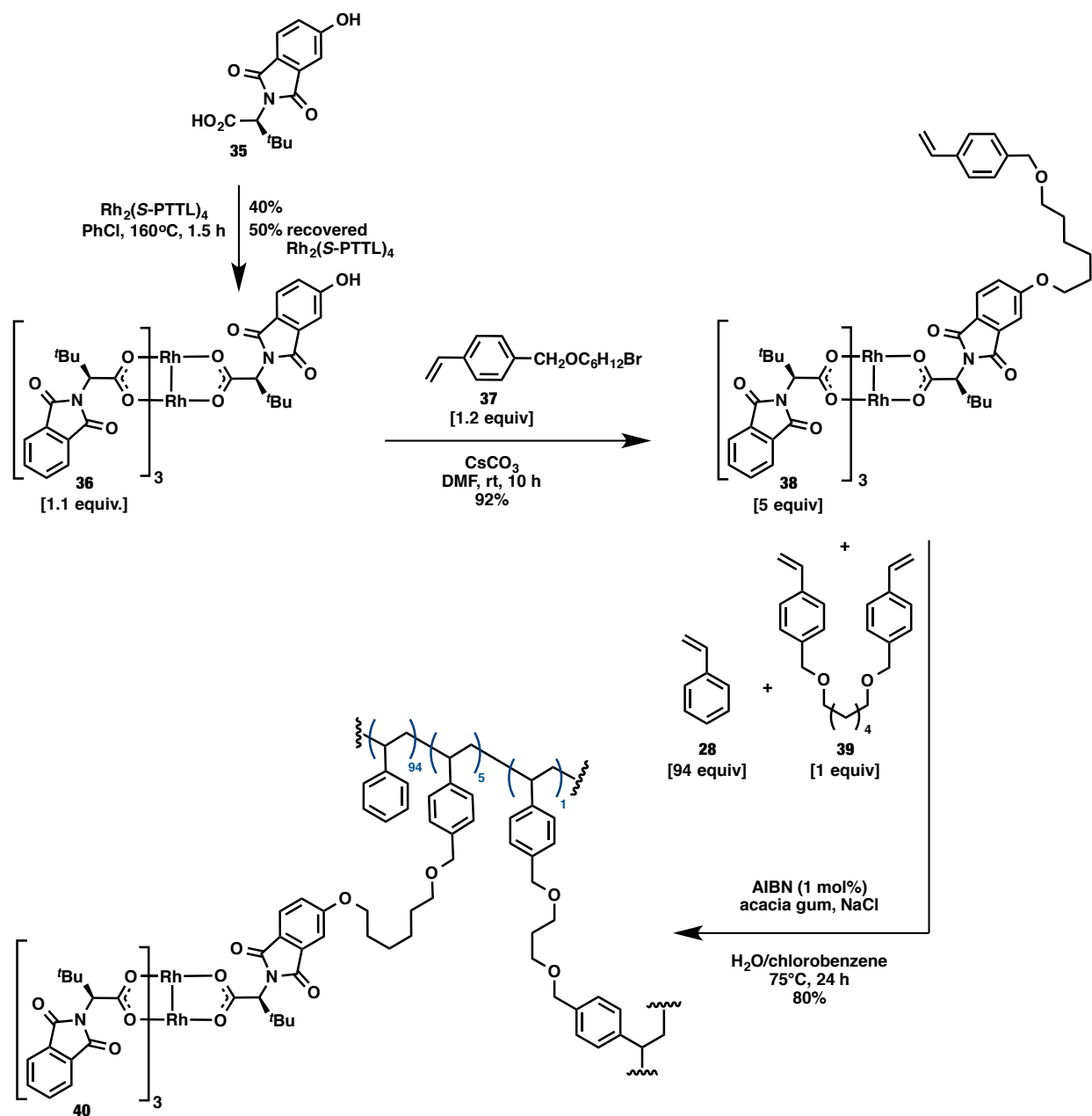
Table 3.5 Deactivation of homogeneous dirhodium(II) catalysts by a pyridine derivative



catalyst	time (min)	yield (%)	ee (%)
Rh ₂ (S-TBSP) ₄	10	43	81
Rh ₂ (S-biTISP) ₄	720	18	88

The most impressive reported results to date for immobilized dirhodium catalysis came from the Hashimoto group in 2010. In the first step of a three-step immobilization process, Hashimoto *et al.* successfully completed a single ligand exchange of *N*-4-hydroxyphthloyl-(*S*)-*tert*-leucine **35** with Rh₂(*S*-PTTL)₄ in 40% yield and 50% recovery of starting Rh₂(*S*-PTTL)₄. The product of this mono-ligand exchange was then treated with styrene-derivative **37** to afford O-alkylation product **38** in 92% yield. Suspension copolymerization of rhodium complex **38** with styrene and cross-linker **39** in a ratio of 5:94:1 provided the polymer-supported chiral dirhodium(II) catalyst **40** in 80% yield (Scheme 3.16).¹⁹ Hashimoto *et al.* applied this same immobilization strategy to the chiral fluorinated derivative of this catalyst, Rh₂(*S*-TFPTTL)₄, which was able to catalyze the amination of silyl enol ethers with [*N*-(2-nitrophenylsulfonyl)imino]phenyliodinane (NsN=IPh) to provide α -amino ketones in high yields with high levels of enantioselectivity and recycled this catalyst 20 times.²⁰

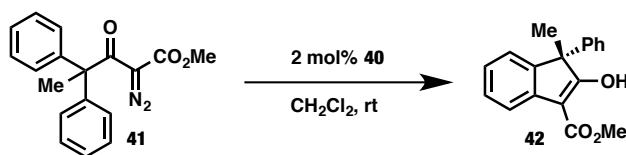
Scheme 3.16 Suspension copolymerization of $\text{Rh}_2(\text{S-PTTL})_4$



This immobilized $\text{Rh}_2(\text{S-PTTL})_4$ -derivative **40** provided unprecedented results in intramolecular C–H insertion of α -diazo- β -ketoester, providing the desired product in exactly the same yield (88%) and enantioselectivity (92%) as homogeneous catalyst after 100 reaction cycles (Table 3.6).¹⁹ The product of this reaction is a key intermediate in the asymmetric

synthesis of FR115427, a non-competitive NMDA antagonist. This extremely impressive result shows the huge impact that immobilization can have on the field of rhodium carbenoid chemistry by significantly lowering the cost of these processes.

Table 3.6 Catalyst recycling study of immobilized Rh₂(S-PTTL)₄-derivative



cycle	time (min)	yield (%)	ee (%)
1	5	86	91
10	20	90	90
50	20	90	91
100	20	88	92

Direct comparison of the method for immobilization of dirhodium(II) catalyst reveals that immobilization by covalent attachment of one of the ligands of the dirhodium(II) catalyst to a solid support provided a more robust heterogeneous catalyst which was less susceptible to rhodium leaching, or losing a percentage of the catalyst after the first reaction cycle, as determined by ICP-AES.¹⁹ Although the entrapment immobilization method by cooperative microencapsulation and pyridine coordination was both broadly applicable and involved minimal preparation, significant rhodium leaching was observed upon analysis of the reaction mixture after completion of the first cycle (Figure 3.3).¹⁴⁻¹⁷

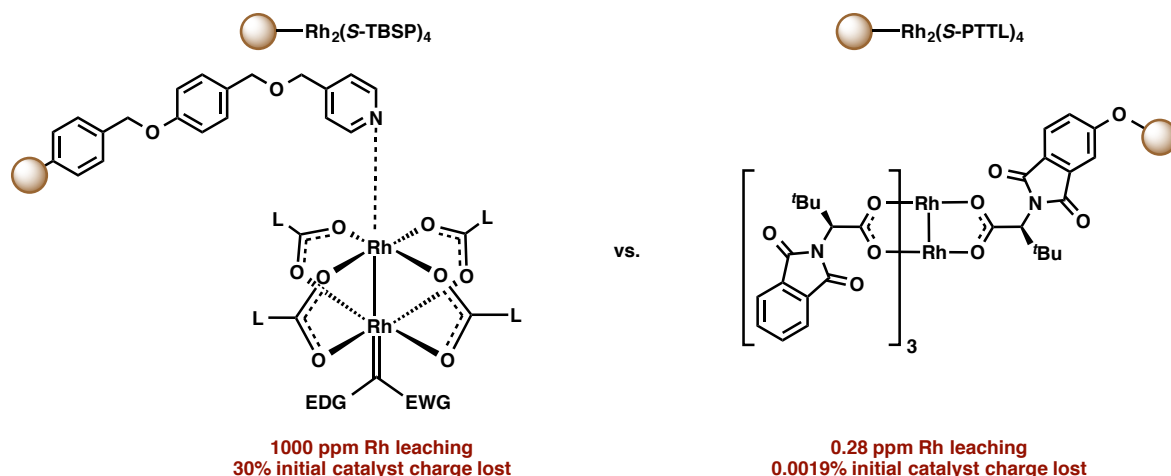


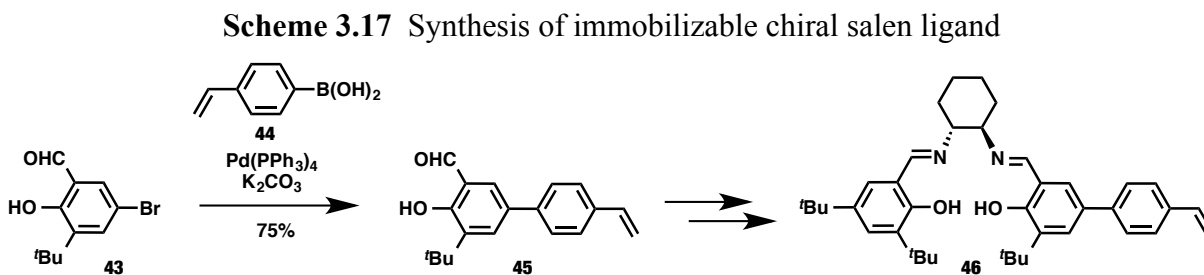
Figure 3.3 Comparison of the previously reported methods for immobilization of dirhodium(II) catalysts

3.4 Introduction to Methods for the Immobilization of $\text{Rh}_2(\text{S-DOSP})_4$

Davies *et al.* previously developed an immobilization strategy employing axially coordinated pyridyl supports. While this strategy was successful for several chiral dirhodium(II) catalysts,²¹ rhodium leaching was observed in these systems.¹⁹ This was believed to be due in part to the equilibrium between coordinated and non-coordinated states. We hypothesized that $\text{Rh}_2(\text{S-DOSP})_4$ immobilization by covalent attachment of the *S*-DOSP-ligand to a support would allow for the synthesis and application of the first robust heterogeneous $\text{Rh}_2(\text{S-DOSP})_4$ -derivative for application in a broad range of synthetically useful transformations. For these reasons, Dr. Huw Davies and Dr. Christopher Jones, a chemical engineer from Georgia Tech, initiated a collaborative effort to covalently immobilize $\text{Rh}_2(\text{S-DOSP})_4$.

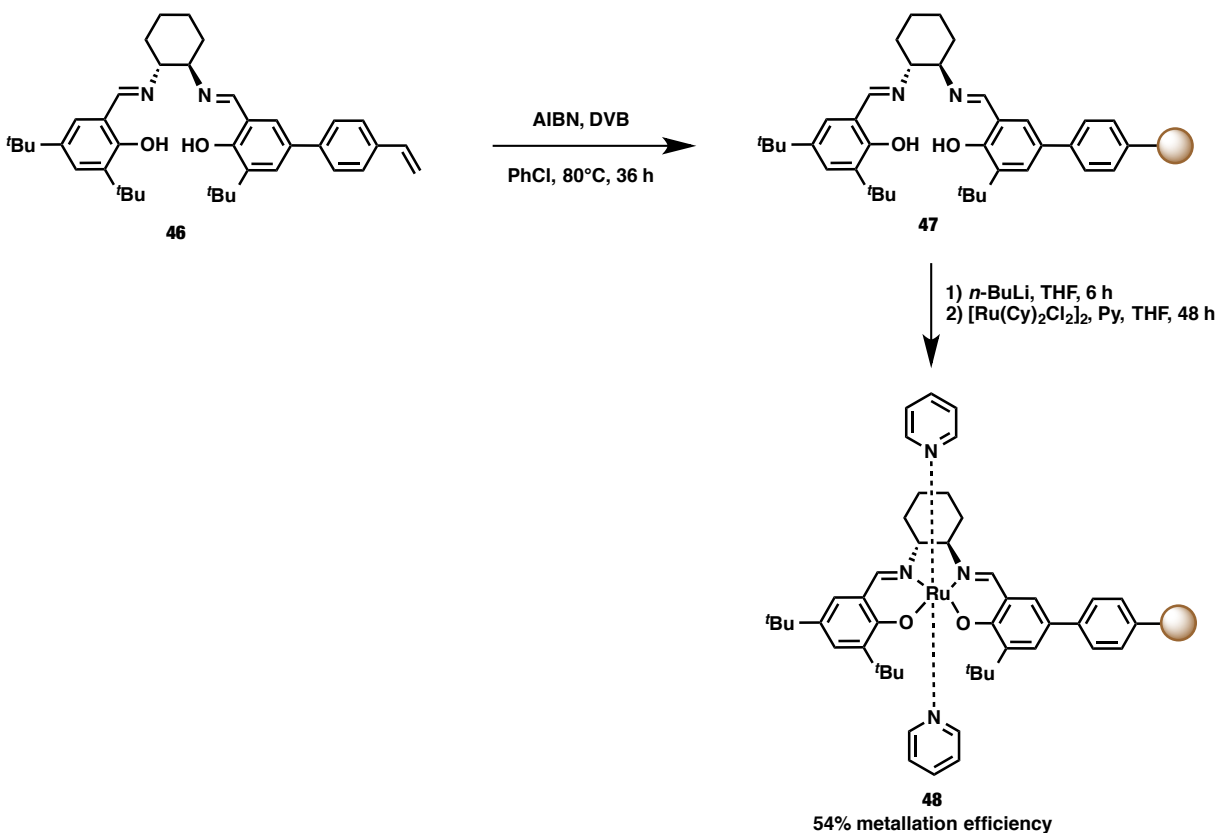
The Jones group has extensively studied the immobilization of chiral salen catalysts and successfully employed them in hydrolytic kinetic resolution of epoxides²² as well as asymmetric cyclopropanation.²³ The synthetic route to immobilized complexes used by Jones *et al.* for

asymmetric cyclopropanation involved an initial Suzuki coupling to incorporate the styryl moiety (Scheme 3.17).^{22b}



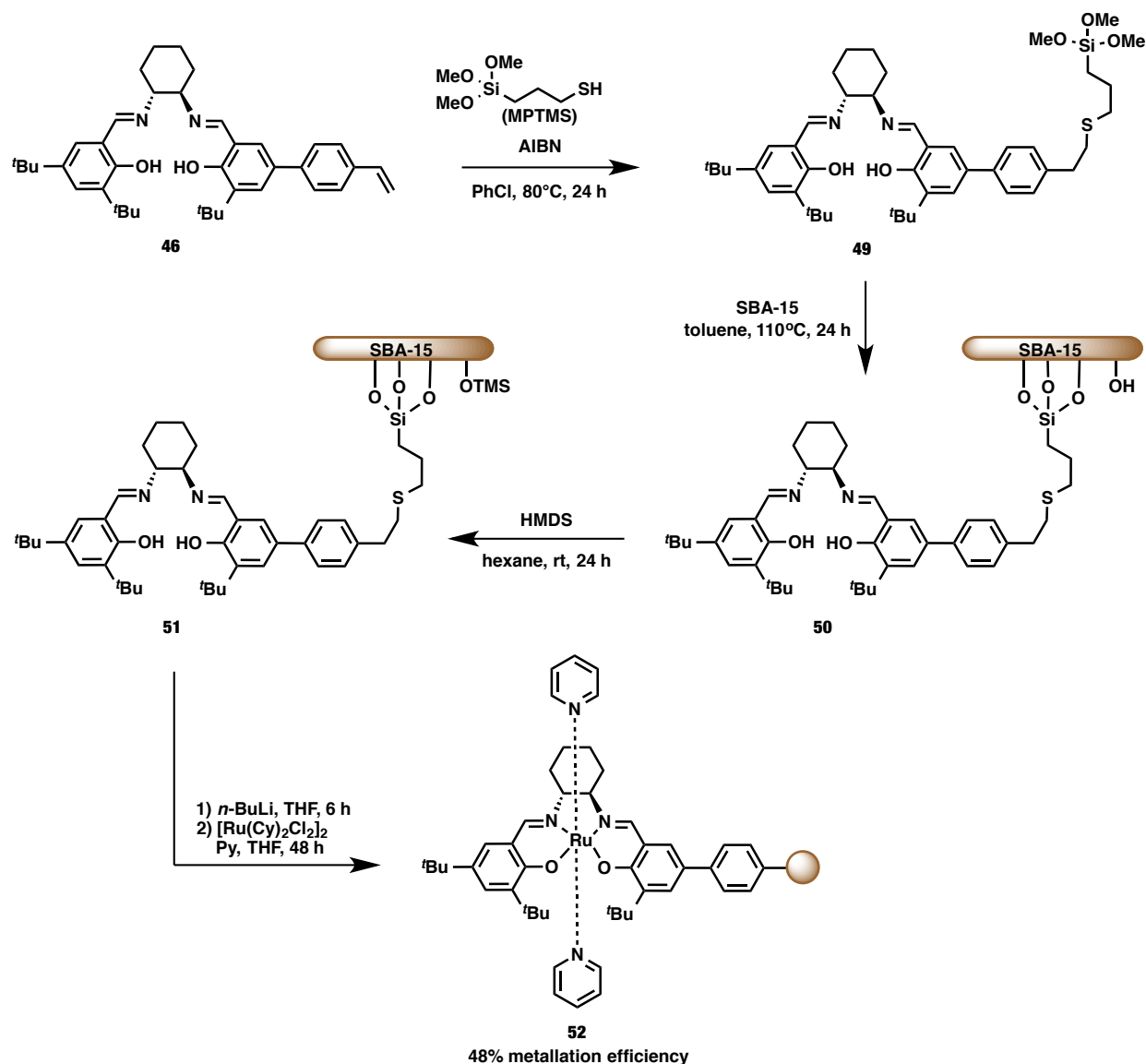
Once synthesis of the immobilizable chiral salen was complete, two routes to immobilization were explored. The first route was AIBN-initiated free radical polymerization of the styryl group of compound **46** with 1,4-divinylbenzene (DVB). Treatment of the resulting polymer **47** with *n*-butyllithium to deprotonate the phenolic protons of the salen ligand, followed by metallation with dichloro(*p*-cymene)ruthenium(II) dimer in the presence of excess pyridine provided the immobilized Ru-salen complex **48** with 53.5% metallation efficiency as determined by elemental analysis (Scheme 3.18).²³

Scheme 3.18 Free radical polymerization immobilization strategy



The second route involved AIBN-initiated grafting of the styryl group onto a surface of SBA-15 mesoporous silica. This was accomplished by thiol coupling of mercaptopropyltrimethoxysilane (*MPTMS*) with the terminal styryl moiety of compound **46** followed by immobilization on 60Å mesoporous SBA-15 silica by condensation with surface hydroxyl groups to afford immobilized **50**. The remaining free-surface hydroxyl groups of **50** were then TMS-protected with hexamethyldisilazane (HMDS) to afford **51**. Finally, metallation of **51** provided the immobilized Ru-salen complex **52** with 48% metallation efficiency (Scheme 3.19).²³

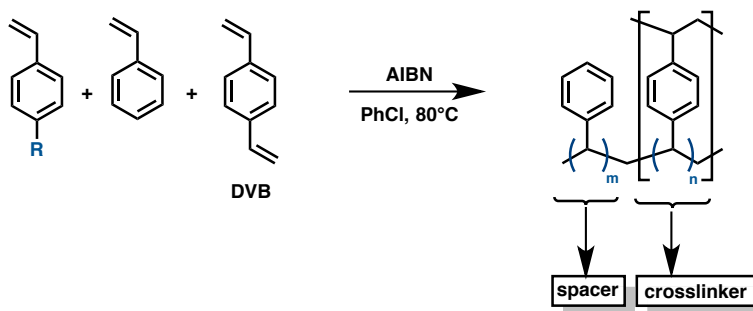
Scheme 3.19 Catalyst immobilization by grafting to a functionalized silica surface



The results of this study showed that polymer-supported Ru-salen-Py₂ catalysts were superior, in terms of activity and selectivity, as compared to the porous silica-supported catalyst. For this reason, we began by exploring polymer-supported Rh₂(S-DOSP)₄-derivatives. Polymer-supported systems are made through a process known as free radical polymerization. One method of free radical polymerization, shown in Scheme 3.20, involves treatment of a starting monomer (bearing a styryl substituent) with AIBN in the presence of styrene and 1,4-

divinylbenzene (DVB). In this polymerization AIBN serves as a radical initiator. DVB units are considered “crosslinking” units. They serve to both bind the catalyst to the resin and to hold the resin together. The styrene units add flexibility to the polymer chain, which allows the resin to impart less steric strain on the catalyst to which it is bound (Scheme 3.20).

Scheme 3.20 Free radical polymerization of functionalized catalyst, styrene, and divinylbenzene (DVB)



Loosely cross-linked resins (LCRs) are flexible with a large number of styrene units incorporated into the polymer chain. LCRs are often soluble in a number of solvents and thus reactions can be accomplished at room temperature with fully-expanded catalyst in solution, but precipitation of this type of catalyst can be complicated due to partial solubility in a number of solvents. Highly cross-linked resins (HCRs), on the other hand, are typically insoluble in most solvents and thus catalyst recovery is much easier to accomplish. A high degree of crosslinking, however, can have a deleterious effect on the reaction in terms of yield and enantioselectivity due to the greater steric congestion of the system. For this reason, the ratio of DVB : styrene : monomer is varied until a recyclable polymer with optimal solubility is achieved.

3.5 Efforts Toward the Synthesis of a $\text{Rh}_2(\text{S-DOSP})_4$ -Derivative Immobilized by having all Four Ligands Covalently Bound to a Support

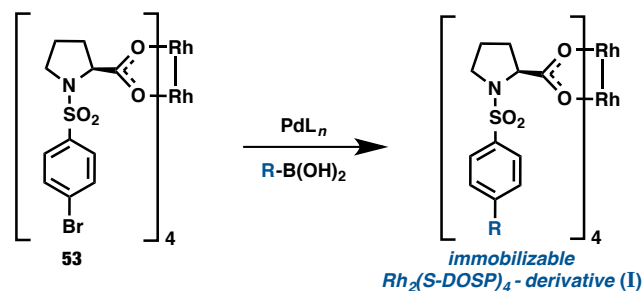
Davies *et al.* have developed catalysts such as $\text{Rh}_2(\text{S-DOSP})_4$ that are extremely active in carbenoid reactions such as C–H activation. However, their cost is often prohibitive in terms of use in pharmaceutical development as the cost of $\text{Rh}_2(\text{S-DOSP})_4$ is \$1,330.00 / g from Sigma Aldrich. Practical application of this expensive catalyst can be achieved by covalent attachment of its ligand to a solid support so that it can be easily separated from the reaction mixture and re-used. Jones *et al.* have adapted many catalysts for immobilization on solid supports. The objective of the collaboration between Jones and Davies has been to develop a recyclable dirhodium(II) catalyst on a solid support in order to alleviate the cost associated with the use of $\text{Rh}_2(\text{S-DOSP})_4$.

In this project, my role was to design and synthesize novel derivatives of $\text{Rh}_2(\text{S-DOSP})_4$ with ligands that enable immobilization on a solid support. This immobilization was then carried out by post-doctoral fellows Dr. Nicholas Brunelli, Dr. Sarah Russell, and Dr. Yan Feng in the Jones laboratory. The resulting immobilized ligands and catalysts were then sent back to me for determination of catalyst activity, selectivity, and recyclability in carbenoid reactions. Based on my findings, Dr. Brunelli, Dr. Russell and Dr. Feng then modified the support until the ideal catalyst structure, method of immobilization, support, and recovery method were determined.

Our first strategy for the synthesis of polymer supportable catalysts is shown in Scheme 3.21. We initially envisioned synthesizing catalysts of type **54** in which the R-group is a functional group that will enable subsequent polymerization (Scheme 3.21). Based on the previous studies in the Jones group,^{22b} we had envisioned that catalysts with the general structure (**I**) could come from a late stage derivatization of catalyst **53** via a Suzuki coupling reaction. If Suzuki coupling were possible, synthesis of catalyst **54** could be conducted on a large scale and late-stage

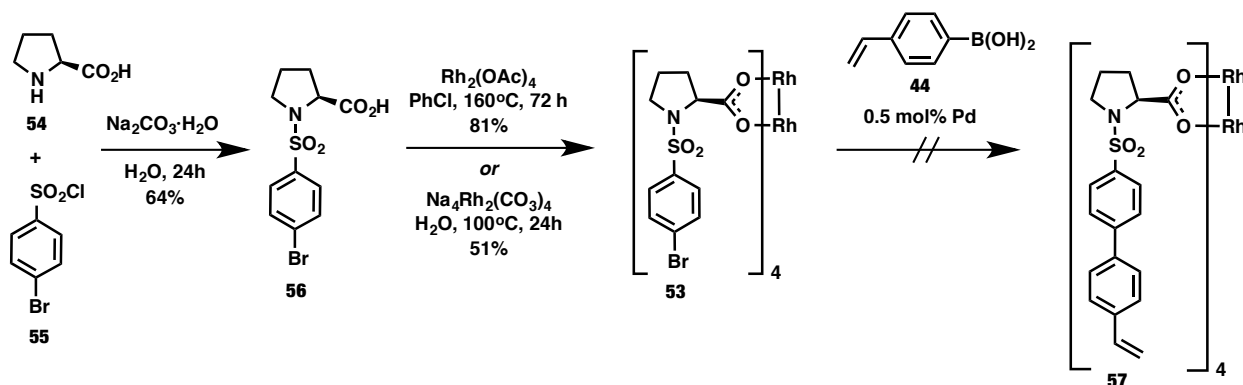
derivatization via cross-coupling could provide a catalyst library for testing.

Scheme 3.21 Late-stage modification route to immobilizable $\text{Rh}_2(\text{S-DOSP})_4$ -derivative



Palladium-catalyzed cross-coupling directly on a dirhodium complex is not precedented in the literature. Therefore, three different sets of conditions were chosen based on literature precedence for their ability to catalyze coupling of 4-bromobenzene sulfonamide derivatives with boronic acids.²⁴ However, all of the conditions screened failed to provide the desired product **57**. Instead, ^1H and ^{13}C NMR experiments conducted on purified products showed the reactions resulted in deprotection of the proline (Scheme 3.22).

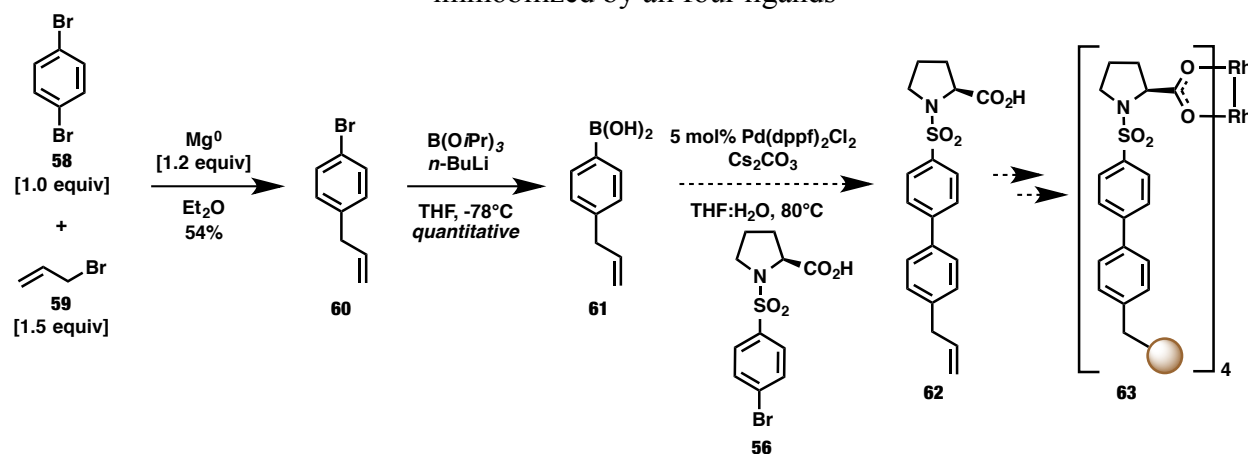
Scheme 3.22 Attempt towards Pd-catalyzed cross-coupling directly on dirhodium(II) tetraproline



catalyst	base	phase-transfer catalyst	temp (°C)	solvent	time (h)
$\text{Pd}(\text{OAc})_2$	K_2CO_3	Bu_4NBr	70	toluene : EtOH	1
$\text{Pd}(\text{PPh}_3)_4$	Na_2CO_3	-	110	$\text{H}_2\text{O} : \text{toluene} : \text{EtOH}$	3
$\text{Pd}(\text{dppf})_2\text{Cl}_2$	CsCO_3	-	80	$\text{THF}:\text{H}_2\text{O}$	24

Although derivatization of the catalyst post-ligand exchange initially seemed ideal, three new potential routes to immobilized $\text{Rh}_2(\text{S-DOSP})_4$ -derivatives were devised and simultaneously explored. The polymerized catalyst **63** in Scheme 3.23 would ultimately result from AIBN-initiated free radical polymerization onto the terminal alkene of **62**. This route began with *in situ* conversion of 1,4-dibromobenzene **58** to (4-bromophenyl)magnesium bromide followed by Grignard addition to allyl bromide **59** according to the procedure of Shi²⁵ to provide **60** in 54% yield. Conversion to the corresponding boronic acid was achieved in quantitative yield according to the procedure of Bradbury (Scheme 3.23).²⁶ The subsequent Suzuki coupling, ligand exchange, and immobilization, however, were not attempted because a higher yielding route to an immobilizable prolinolate ligand was simultaneously discovered (Scheme 3.25).

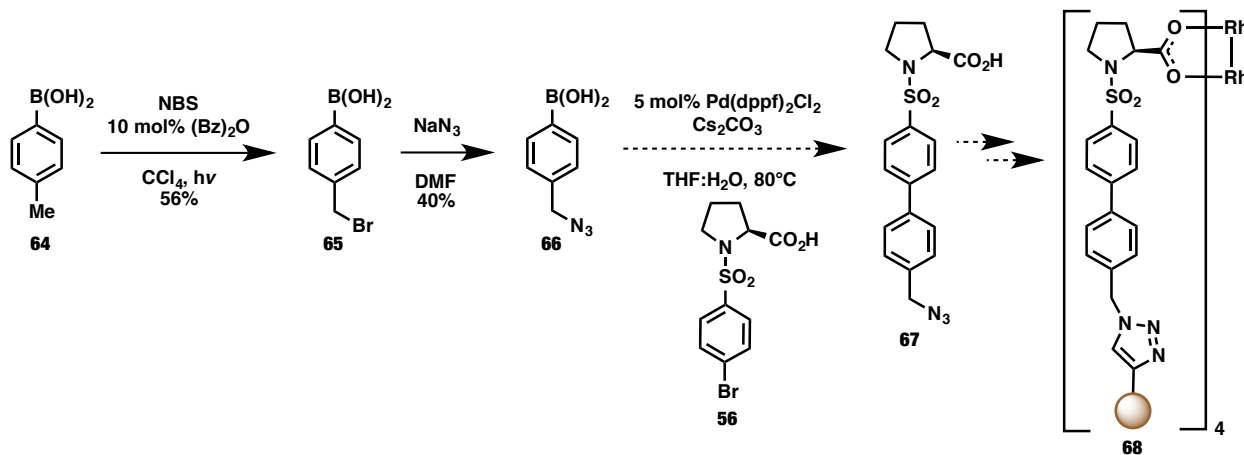
Scheme 3.23 Attempted synthesis of allylbenzene-substituted $\text{Rh}_2(\text{S-DOSP})_4$ -derivative immobilized by all four ligands



The resulting catalyst in Scheme 3.24 would come from a azide-alkyne Huisgen cycloaddition of the azide of **67** onto a resin bearing alkynes. Starting boronic acid for the route shown in Scheme 3.24 was made by radical bromination of the benzylic methyl group of **64** with NBS and 10 mol% benzoyl peroxide²⁷ to provide **65** in 56% yield. Displacement of bromine of **65** with sodium azide provided **66** in 40% yield (Scheme 3.24). The subsequent Suzuki

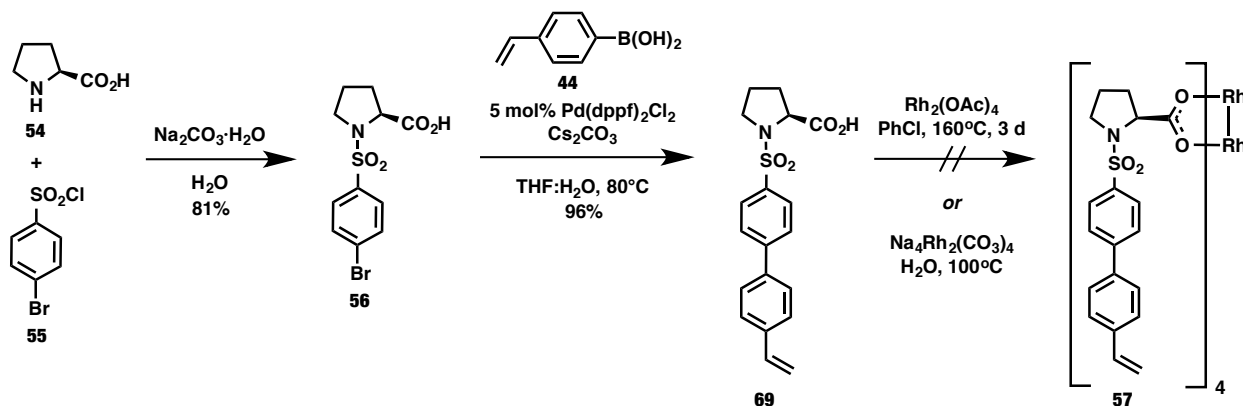
coupling, ligand exchange, and immobilization, however, were not attempted because a higher yielding route to an immobilizable prolinic ligand was simultaneously discovered (Scheme 3.25).

Scheme 3.24 Attempted synthesis of $\text{Rh}_2(\text{S-DOSP})_4$ -derivative immobilized by Huisgen cycloaddition of the azide group on all four ligands with surface alkynes



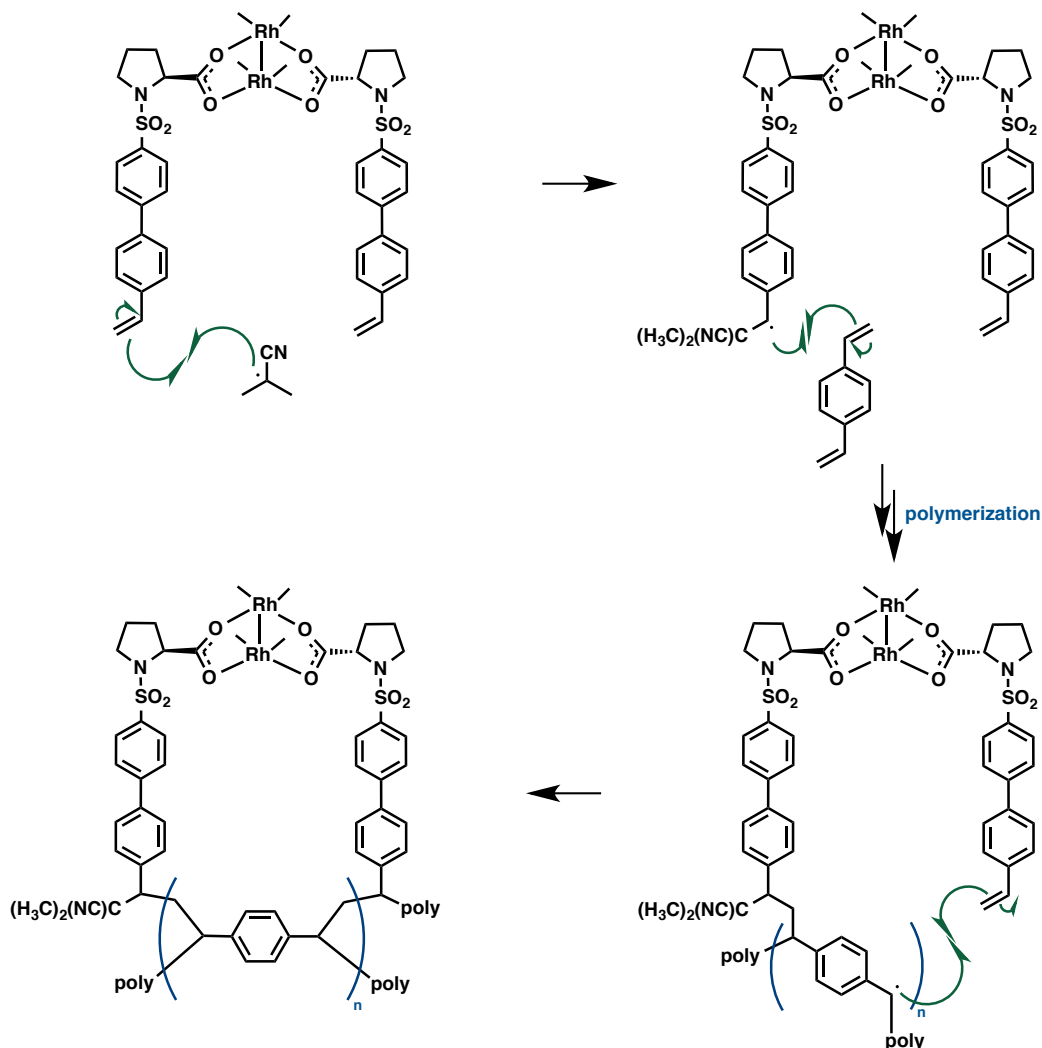
We believed that the metallated compound **53** (Scheme 3.21) was a more activated species than the free ligand **56** (Scheme 3.25). For this reason, we believed cross-coupling to be feasible on **56** despite the deprotection of pyrrolidine observed with **53** in Scheme 3.22. Therefore, coupling conditions were chosen for their ability to tolerate a carboxylic acid moiety. Employing 5 mol% $\text{Pd}(\text{dppf})_2\text{Cl}_2$ provided the desired coupling product **69** in 96% yield after recrystallization. We then moved ahead with this concise and high yielding route (Scheme 3.25). Subsequent attempts towards ligand exchange of **69** with $\text{Rh}_2(\text{OAc})_4$ yielded minimal desired product **57**. It is possible that ligand exchange with this particular substrate requires longer reaction times in order to provide better conversion to the desired product, however this was not explored.

Scheme 3.25 Attempted synthesis of styryl-substituted $\text{Rh}_2(\text{S-DOSP})_4$ -derivative immobilizable at all four ligands



It is possible that two terminal alkenes from neighboring ligands could potentially undergo the undesired polymerization of the type shown in Scheme 3.26, which would block the axial binding sites of dirhodium, causing deactivation of the catalyst. A new route to synthesize polymerizable $\text{Rh}_2(\text{S-DOSP})_4$ derivatives was next explored.

Scheme 3.26 Possible deactivation route of $\text{Rh}_2(\text{S-DOSP})_4$ -derivative immobilized by all four ligands

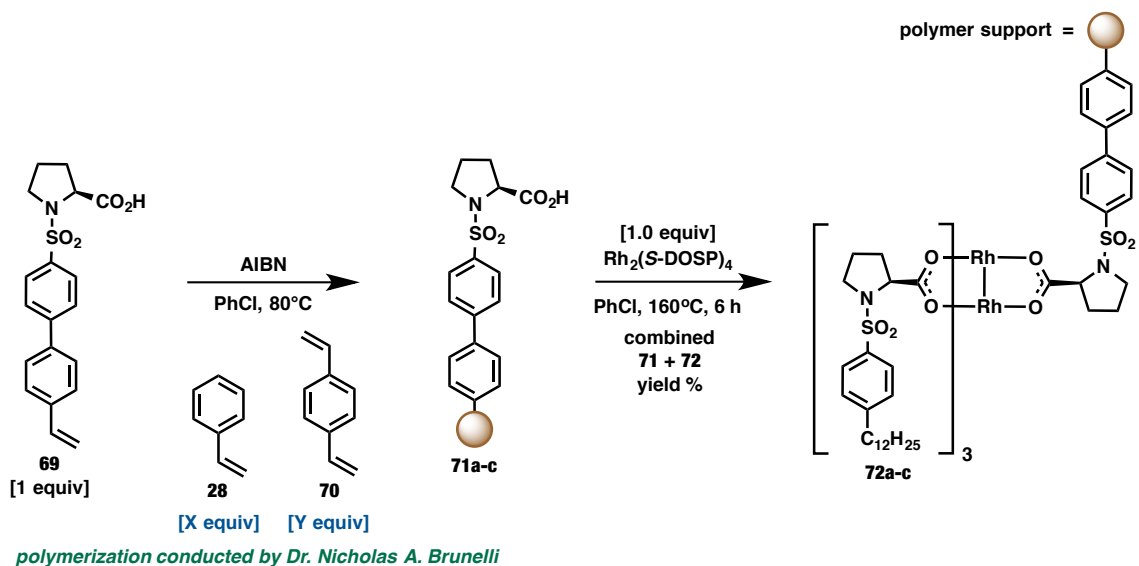


3.6 Syntheses and Testing of $\text{Rh}_2(\text{S-DOSP})_4$ -Derivatives Immobilized by a Single Ligand Covalently Bound to a Polymeric Support

At this point, we decided to directly subject **69** to free radical polymerization in order to determine whether this sulfonyl pyrrolidine could survive treatment with AIBN in chlorobenzene at 80 °C and would undergo polymerization. Dr. Nicholas Brunelli was able to successfully convert **69** into three different polymer-supported *S*-DOSP-derivatives **71a-c** (Table 3.7). The first two derivatives were loosely cross-linked resins (LCR) which incorporated styrene and

divinylbenzene (DVB) in a ratio of 100 : 1 (LCR (a)) or 50 : 1 (LCR (b)). A highly-crosslinked resin (HCR) was also synthesized which employed four DVB units to every unit of monomer (Table 3.7).

Table 3.7 Immobilization of S-DOSP ligand by free radical polymerization



71a-c	styrene [X equiv]	DVB [Y equiv]	product	mmol 69 / g	combined yield (%) (71 + 72)
LCR (a)	5	0.05	72a	0.3	27
LCR (b)	20	0.4	72b	0.4	53
HCR	0	4	72c	1.1	27

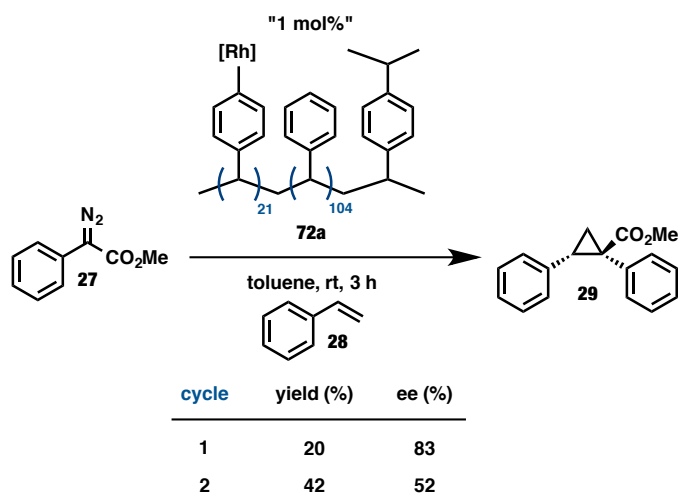
Of these three resins, only LCR(a) (**71a**) was soluble in common organic solvents (toluene, chlorobenzene, chloroform, and dichloromethane) while remaining insoluble in methanol and ethanol. Solubility in chloroform was critical and allowed for complete removal of excess starting monomeric ligand **69** from LCR (a) (**71a**). For this reason we decided to focus on LCR(a) (**71a**). Thus, solvation of the mixture of monomer **69** and polymer **71a** in dichloromethane was followed by precipitation of the polymeric **71a** by dropwise addition of methanol and removal of the monomeric counterpart **69** by decanting. This process was repeated three times to ensure removal of all residual monomeric ligand **69**. ¹H NMR of the washed

polymer showed two distinct broad singlets of equal integration at 7.97 and 7.69 ppm, corresponding to the biaryl protons of the monomer. These resonances were significantly downfield of the next closest aromatic resonance, a broad multiplet from 7.09-6.48 ppm, suggesting that the monomer **69** had been successfully incorporated to the polymer. Although the ultimate goal was to metallate prior to ligand exchange, with this immobilized material in hand, we were able to examine the possibility of post-immobilization ligand exchange. Ligand exchange according to the method of Doyle *et al.* was then attempted on these immobilized species.²² Thus **71a** and Rh₂(*S*-DOSP)₄ were refluxed in chlorobenzene for six hours. The product of ligand exchange **72a** was precipitated out of the reaction mixture by dropwise addition of methanol. Catalyst **72a** was then washed by repeated solvation into dichloromethane followed by precipitation with methanol until the washings turned clear. The precipitated solid was nearly the same color as the starting ligands with only a slightly green tinge. Although this particular ligand exchange was not extensively studied, the absence of a green hue anticipated for an immobilized rhodium catalyst suggested that ligand exchange of this type did not provide a high degree of metallation.

The polymer-supported catalyst **72a** derived from **71a** displayed similar properties to the LCR(a) ligand in that it was soluble in toluene, chlorobenzene, chloroform, and dichloromethane yet insoluble in methanol and ethanol. Toluene was chosen as the solvent, for testing the catalyst in standard cyclopropanation, in order to observe the behavior of this catalyst in its fully expanded form (Table 3.8). Elemental analysis studies were not yet conducted on these immobilized rhodium complexes due to their prohibitive cost. Percent metallation of the complexes, therefore, is unknown. Theoretical molecular weight, and thus catalyst loading, of the immobilized catalyst was approximated from the ratio of monomer : styrene : DVB

employed in the polymerization step. The results of the cyclopropanation reaction showed significant deterioration of enantioselectivity after a single reaction round (Table 3.8, cycle 1: 83% ee vs. cycle 2: 52% ee for round 2). The high level of enantioinduction observed in the first cycle is believed to be due to residual $\text{Rh}_2(\text{S-DOSP})_4$ which was not fully removed after the ligand exchange.

Table 3.8 Asymmetric cyclopropanation catalyzed by a loosely cross-linked $\text{Rh}_2(\text{S-DOSP})_4$ -resin



The limitations of this method became immediately obvious. Optimization of ligand exchange would be difficult as the reaction cannot be monitored by TLC and the extent of ligand exchange can only be confirmed by elemental analysis. Also, previous findings from the Jones group showed that higher degrees of metallation are possible if the metallation can be conducted prior to polymerization. Based upon these preliminary results, we decided to explore our next route.

First, to determine whether or not the free radical polymerization process would affect the catalyst, we subjected homogeneous $\text{Rh}_2(\text{S-DOSP})_4$ to the polymerization conditions. We found that these conditions did not show a deleterious effect on the catalyst (Table 3.9). We thus

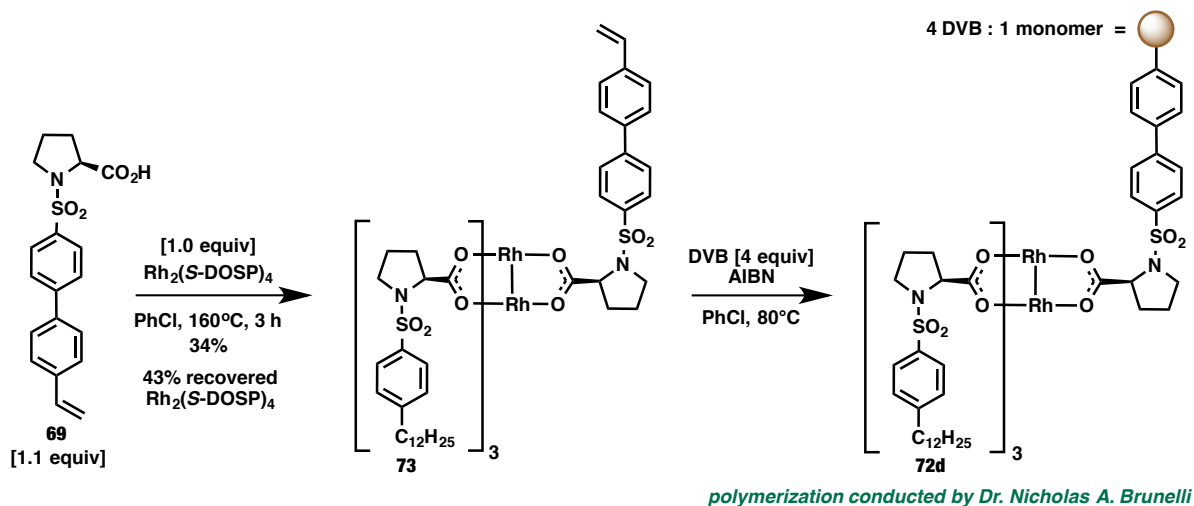
proceeded with the plan to conduct polymerization as the last stage in the synthesis of the polymer-supported catalyst. All subsequent cyclopropanation reactions were run using either pentane or hexanes as solvent as they provide the ideal nonpolar solvent systems for homogeneous $\text{Rh}_2(\text{S-DOSP})_4$ -catalysis and were also found to be ideal for reactions employing silica-immobilized $\text{Rh}_2(\text{S-DOSP})_4$ -derivatives.

Table 3.9 $\text{Rh}_2(\text{S-DOSP})_4$ under AIBN-initiated free radical polymerization conditions

$\text{Rh}_2(\text{S-DOSP})_4$	yield (%)	ee (%)
fresh $\text{Rh}_2(\text{S-DOSP})_4$	85	88
$\text{Rh}_2(\text{S-DOSP})_4$ subjected to AIBN-initiated polymerization	73	88

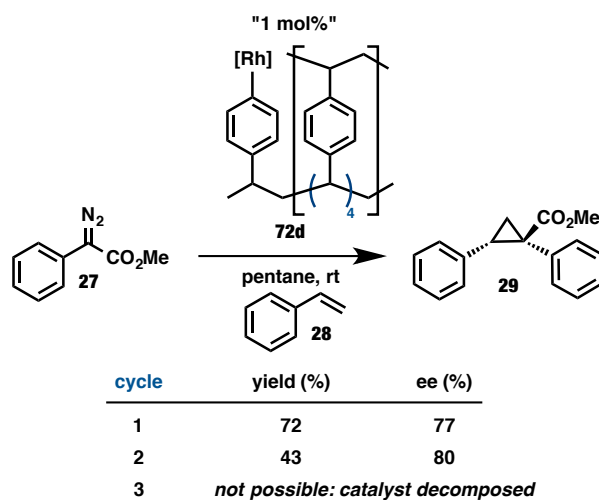
Using the reported procedure by Hashimoto *et al.*,¹⁹ three hour single-ligand exchange with polymerizable ligand **69** [1.1 equiv] and $\text{Rh}_2(\text{S-DOSP})_4$ [1.0 equiv] proceeded in low yield (34%) but with moderate recovery of $\text{Rh}_2(\text{S-DOSP})_4$ (43%). Notably, tests with recovered $\text{Rh}_2(\text{S-DOSP})_4$ in cyclopropanation showed no degradation in enantiopurity of the cyclopropanation product resulting from catalysis by recovered $\text{Rh}_2(\text{S-DOSP})_4$ which had been reused in 3 rounds of ligand exchange. A highly-crosslinked resin (4 DVB : 1 monomer) was explored in the first polymerization of **73** which was conducted by Dr. Nicholas Brunelli (Scheme 3.27). The polymerization product **72d** remained a dark-green color after extensive washing, implying a high degree of metallation was achieved.

Scheme 3.27 Synthesis of highly-crosslinked $\text{Rh}_2(\text{S-DOSP})_4$ -derivative immobilized at a single ligand by polymerization



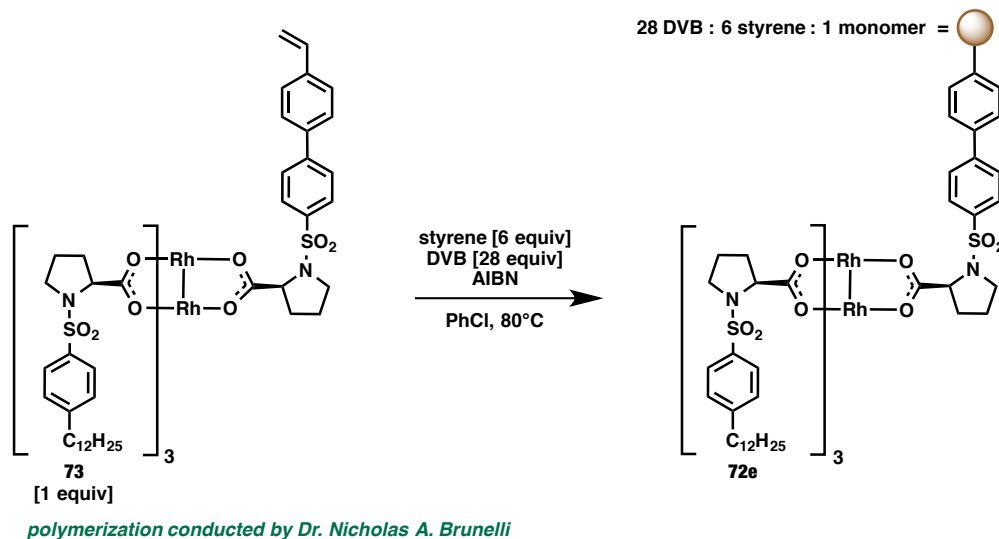
Catalyst **72d** was then screened in a standard asymmetric cyclopropanation reaction. Unfortunately, **72d** was not recyclable after the second reaction (Table 3.10, decomposition of aryldiazoacetate **27** in the third reaction cycle was not complete at $t = 48$ hours). We attributed this deterioration to the extreme rigidity of the highly crosslinked resin.

Table 3.10 Asymmetric cyclopropanation catalyzed by a highly cross-linked $\text{Rh}_2(\text{S-DOSP})_4$ -resin



At this point, we realized that on the scale at which we were working, “1 mol%” catalyst loading did not allow for effective evaluation of recyclability over multiple cycles due to substantial loss of catalyst during recycling via precipitation method. For this reason, catalyst loading was increased to “10 mol%” in the following preliminary studies to obtain an accurate depiction of catalyst recyclability. The following results, therefore, cannot be directly compared to those previously described because catalyst loading was increased substantially to allow for effective recycling of the catalyst. A more flexible polymer support was then made by incorporating styrene units into the backbone of the polymer. Catalyst **72e** was prepared by Dr. Nicholas Brunelli from **73** using a stoichiometry of 28 DVB : 6 styrene : 1 monomer (Scheme 3.28).

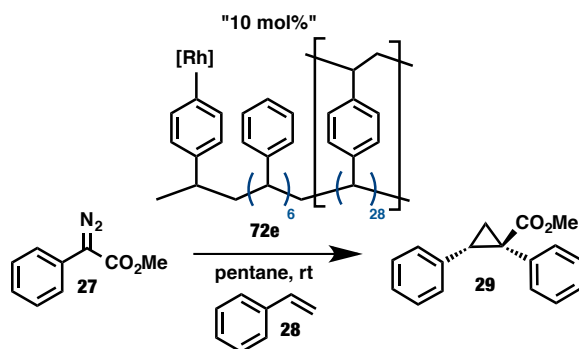
Scheme 3.28 Synthesis of flexible polymeric $\text{Rh}_2(\text{S-DOSP})_4$ -derivative immobilized at a single ligand by polymerization



Initial enantioinduction obtained with this catalyst was high (80% ee for the first two rounds) but quickly dropped off and deteriorated significantly by the eleventh reaction cycle to 24% ee (Table 3.11). The high levels of enantioinduction which were obtained initially were attributed

to residual homogeneous $\text{Rh}_2(\text{S-DOSP})_4$. Although these results were somewhat disappointing, they showed that the catalyst could be recycled up to eleven rounds (Figure 3.4). Also, to our dismay, yields of this reaction were extremely variable (33-79%). Difficulties in separation of the catalyst from the product occurred due to the physical property of catalyst **72e** to exist as a very fine particulate post-reaction. This caused variability in both the catalyst recovery and thus the yield (Table 3.11). Some variability in yield was also attributed to $-\text{OH}$ insertion into residual methanol from the precipitation process. An observation that we made with the 28 DVB : 6 styrene : 1 monomer polymer-supported catalyst **72e** was that a large weight percent of catalyst was being lost in the precipitation process after every round.

Table 3.11 Asymmetric cyclopropanation catalyzed by a flexible polymeric $\text{Rh}_2(\text{S-DOSP})_4$ -resin



cycle	yield (%)	ee(%)
1	67	80
2	39	80
3	68	68
4	79	73
5	54	66
6	33	62
7	48	58
8	73	54
9	57	47
10	60	36
11	37	24

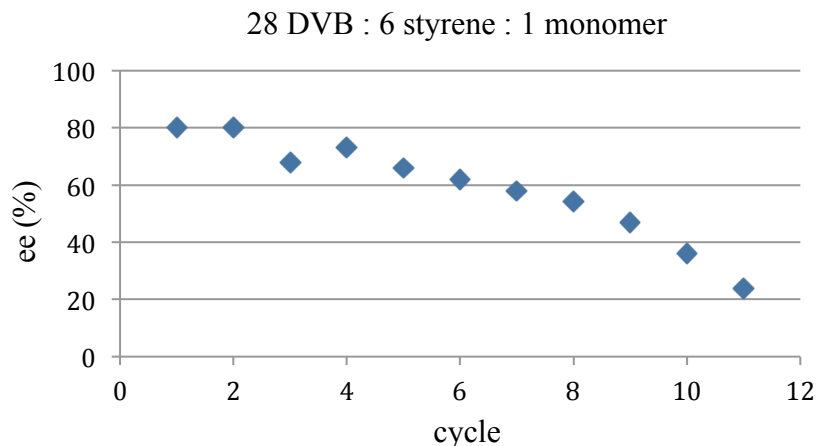


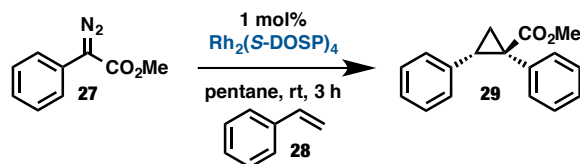
Figure 3.4 Variability in enantioinduction observed with flexible polymeric $\text{Rh}_2(\text{S-DOSP})_4$ -resin

3.7 Syntheses and Testing of $\text{Rh}_2(\text{S-DOSP})_4$ -Derivatives Immobilized by a Single Ligand Covalently Bound to a Silica Support

Silica-supported catalysts often play a complimentary role to polymer-supported²⁸ catalysts. Silica supports are typically recoverable in high yield post-reaction, do not require extensive washing, and often play a complementary role to polymer-supported catalysts.²⁹ Silica-supported catalysts can allow for faster reaction rates than conventional polymer resin-bound reagents, where the reaction is often slowed by the rate of diffusion through the polymer.²⁹ Also, silica neither swells nor shrinks in solvents, whereas, polymer-supported catalysts have the ability to swell, which can dramatically narrow the scope of solvents that can be used for a reaction.³⁰ Silica-supported systems are typically recoverable in high yield post-reaction due to the absence of static and the fact that they do not require extensive washing. Also, because the surface of silica is functionalized, it typically reacts much faster than conventional polymer-bound reagents where the reaction is slowed by the rate of diffusion through the polymer. For these reasons, catalysts grafted to SBA-15 mesoporous silica were explored next. To determine

whether the silica supports would affect the enantioinduction of the catalyst, a test reaction was run in which 60Å silica gel was added into the reaction mixture during the standard asymmetric cyclopropanation reaction. The results of this test showed that silica had no detrimental effect on the enantioinduction obtained with homogeneous $\text{Rh}_2(\text{S-DOSP})_4$, but the yield was greatly affected (Table 3.12, 47% with the addition of SiO_2 vs. 88% in the absence of SiO_2). However, we were not concerned by this result because we believed that modifications to the surface of silica could be made to provide higher reaction yields.

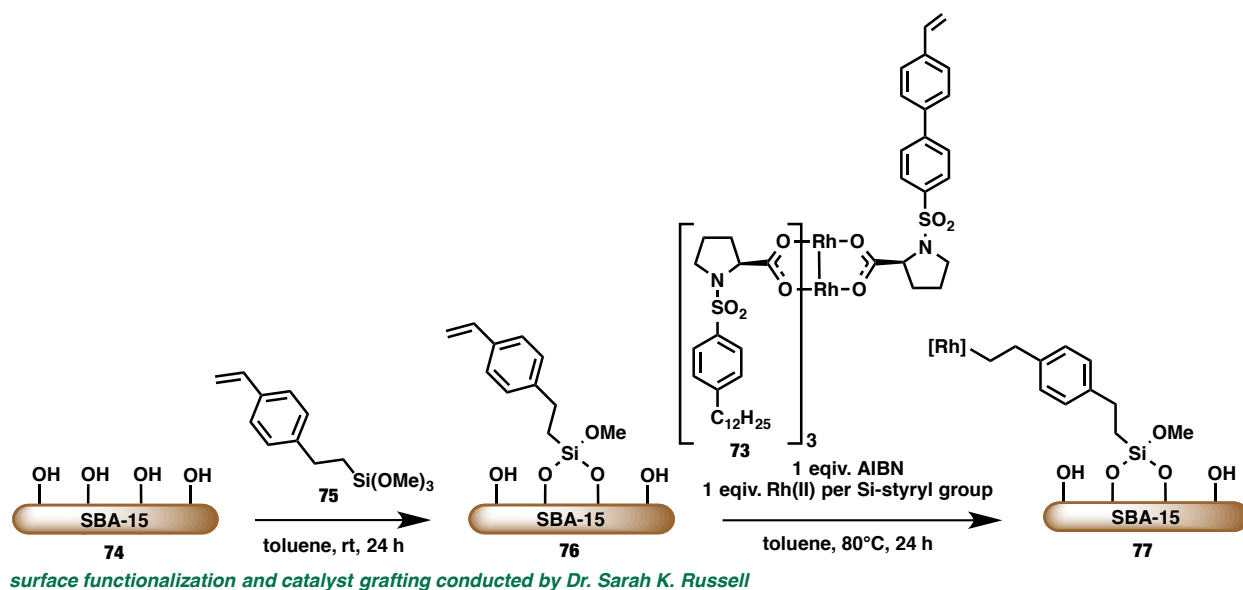
Table 3.12 $\text{Rh}_2(\text{S-DOSP})_4$ performance with the addition 60Å of silica gel



$\text{Rh}_2(\text{S-DOSP})_4$	yield (%)	ee (%)
$\text{Rh}_2(\text{S-DOSP})_4$	85	88
$\text{Rh}_2(\text{S-DOSP})_4$ + 5x catalyst mass SiO_2	47	88

Dr. Sarah Russell began the synthesis of silica-immobilized $\text{Rh}_2(\text{S-DOSP})_4$ -derivative **77** by functionalization of 60Å mesoporous SBA-15 silica by condensation of **75** with the surface hydroxyl groups of SBA-15 (**74**) to provide styryl-functionalized SBA-15 **76**. AIBN-initiated coupling of **73** with **76** provided the corresponding SBA-15 immobilized $\text{Rh}_2(\text{S-DOSP})_4$ -derivative **77** (Scheme 3.29).

Scheme 3.29 $\text{Rh}_2(\text{S-DOSP})_4$ immobilization onto 60Å mesoporous SBA-15 silica



SBA-15-supported **77** was then tested for recyclability in the standard asymmetric cyclopropanation reaction. Although the first reaction round provided the corresponding product with significantly diminished enantioinduction from homogeneous $\text{Rh}_2(\text{S-DOSP})_4$ (65% ee vs. 88% ee respectively), the yields obtained in this screening of **77** (Table 3.13, ranging from 44% to 69%) were much less variable than those observed with the polymer-supported catalyst **72e** (Table 3.11, ranging from 33 to 79%). Also enantioselectivities were more static over eleven reaction rounds with SBA-15-supported catalyst **77** (Table 3.13, 65% ee to 42% ee) as compared to polymer-supported catalyst **72e** (Table 3.11, 80% ee to 24% ee).

Table 3.13 Asymmetric cyclopropanation catalyzed by SBA-15-supported $\text{Rh}_2(\text{S-DOSP})_4$ -derivative

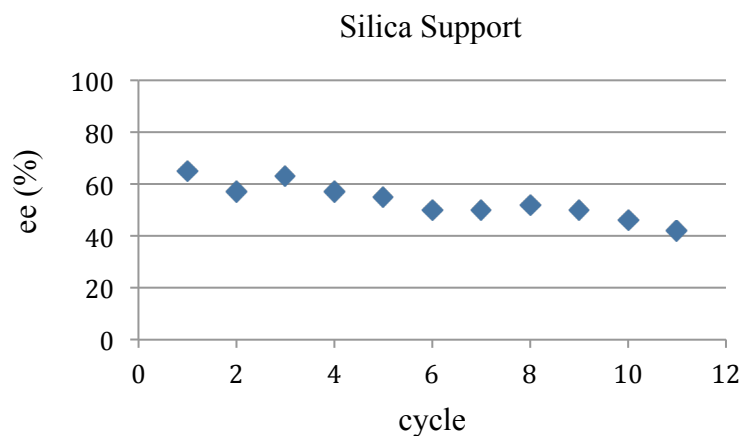
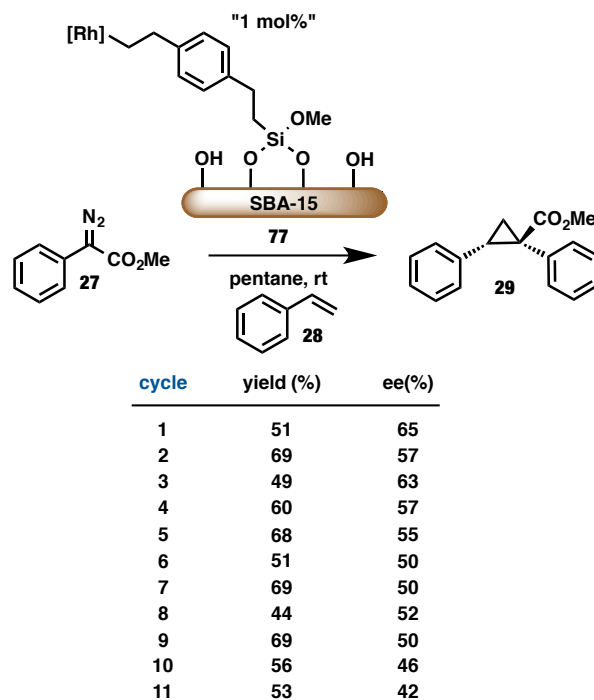
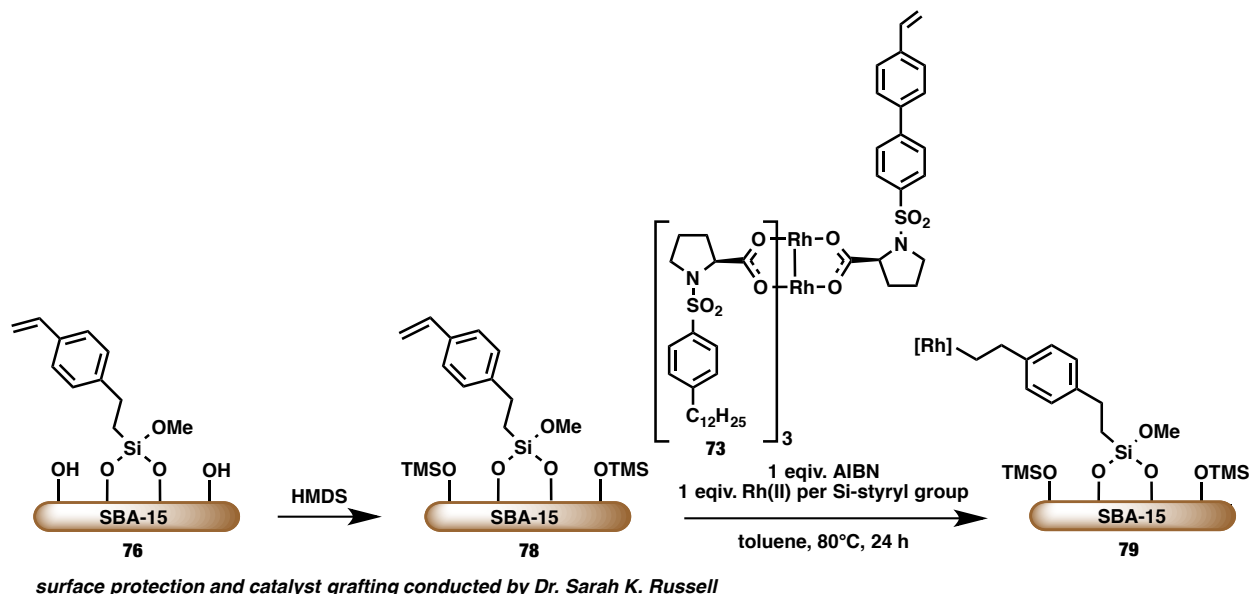


Figure 3.5 Variability in enantioinduction observed with SBA-15-supported $\text{Rh}_2(\text{S-DOSP})_4$ -derivative

We attributed the low yields obtained with the silica-supported system to -OH insertion of the aryl diazoacetate into free surface hydroxyl groups of the SBA-15 resin. For this reason Dr. Sarah Russell treated the SBA-15 resin **76** with HMDS to cap all free surface hydroxyl groups,

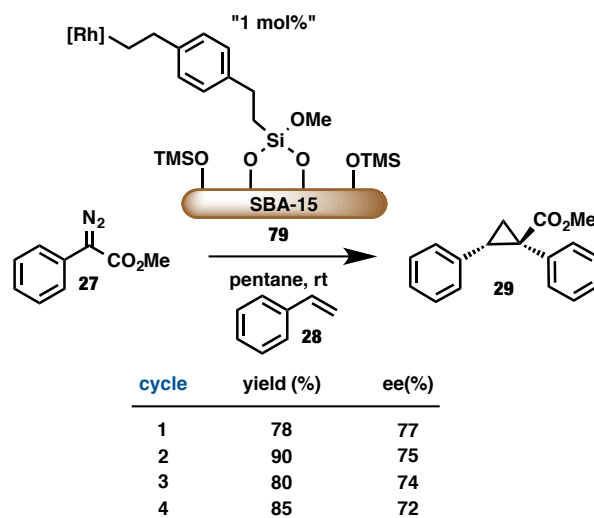
rendering them inert on the surface of functionalized silica material **78** and in catalyst **79** (Scheme 3.30).

Scheme 3.30 Protection of the free hydroxyl groups of SBA-15 surface



We next tested TMS-protected SBA-15-supported dirhodium(II) catalyst **79** for recyclability in the standard asymmetric cyclopropanation reaction and saw a clear increase in enantioselectivity as well as more stability in the enantioinduction after repeated recycling of the catalyst (Table 3.14, 77% ee gradually decreasing to 72% ee over five consecutive cycles). Similarly, higher and more stable yields were obtained throughout five consecutive reaction cycles (ranging from 78% to 90%).

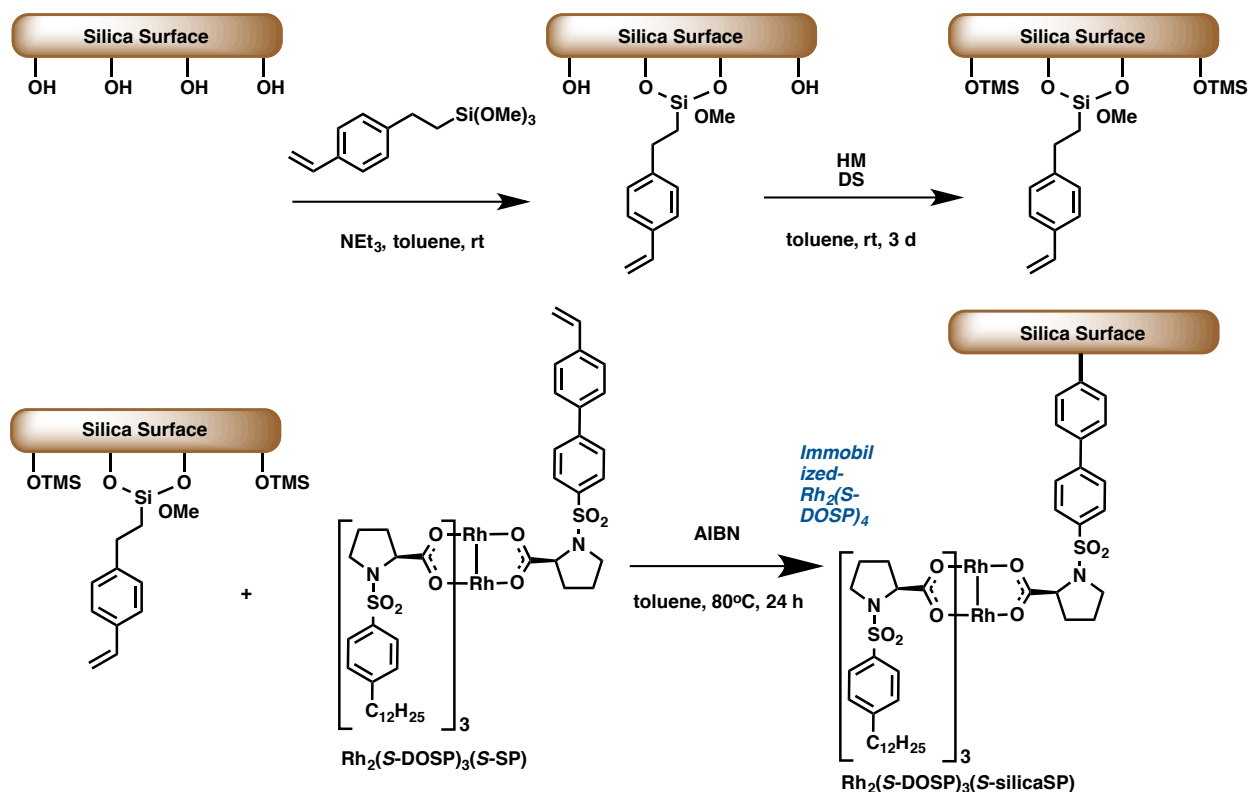
Table 3.14 Asymmetric cyclopropanation catalyzed by TMS-protected SBA-15-supported $\text{Rh}_2(\text{S-DOSP})_4$ -derivative



3.8 Determining the Ideal Silica Support, Recovery Method, and Catalyst Loading for Silica-Immobilized- $\text{Rh}_2(\text{S-DOSP})_4$ Catalysis

Once we had established an active, recyclable and enantioselective silica-supported $\text{Rh}_2(\text{S-DOSP})_4$ -derivative, we sought to optimize the catalyst further, in order to improve the recyclability and enantioselectivity imparted by the system, by changing the silica support to CS-2129 which is a commercially available silica and has both a large particle and pore size. We envisioned that a silica support with a large particle and pore size would provide more room for the large dirhodium species and the reactants to freely interact. The CS-2129-supported $\text{Rh}_2(\text{S-DOSP})_4$ -derivative was synthesized by the general route shown in Scheme 3.31.

Scheme 3.31 General synthetic route silica-supported $\text{Rh}_2(\text{S-DOSP})_4$ -derivatives

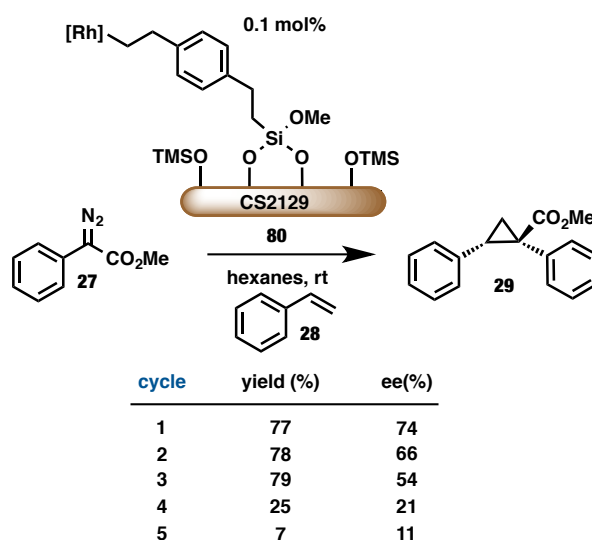


surface functionalization, protection and catalyst grafting conducted by Dr. Sarah K. Russell for SBA-15 and SBA-16 silica supports and by Dr. Yan Feng for CS-2129 and C803 silica supports

In testing this catalyst, we changed the solvent from pentane to hexanes as we found that the standard asymmetric cyclopropanation reaction gave identical results in hexanes and this is a much cheaper solvent. At first, we only obtained a small amount of the CS-2129-immobilized $\text{Rh}_2(\text{S-DOSP})_4$ -derivative from the grafting step. For this reason, we turned our efforts toward conducting the recycling study at low catalyst loading. As we know from previous homogeneous $\text{Rh}_2(\text{S-DOSP})_4$ catalyzed cyclopropanation studies, these reactions are extremely robust and can achieve over a million TON, and therefore can be conducted at extremely low catalyst loadings.³¹ For this reason, we thought it was reasonable to attempt our studies at low catalyst loadings and expected to observe the same reactivity and selectivity at 0.1 mol% as can be achieved with 1 mol%. Unfortunately, at these catalyst loadings, the level of enantioinduction

decreased significantly in each successive asymmetric cyclopropanation catalyzed by CS-2129-immobilized $\text{Rh}_2(\text{S-DOSP})_4$ -derivative **80** (Table 3.15). This observation could potentially be due to the physical loss of catalyst after each reaction. Considering there was only a very small amount of catalyst starting in the first reaction cycle, any loss of catalyst mass could depreciate the reactivity and selectivity of cyclopropanation. In an attempt to avoid physical loss of catalyst, alternate methods of recovery were next explored.

Table 3.15 Asymmetric cyclopropanation catalyzed by CS-2129-supported $\text{Rh}_2(\text{S-DOSP})_4$ -derivative at low catalyst loading



In all previous recycling studies we had employed the precipitation method of recovery to recycle the catalyst, which involves allowing the immobilized catalyst to settle to the bottom of the flask at the end of a reaction, then carefully pipet out the liquid phase without disrupting the catalyst at the bottom of the flask and subsequently wash the catalyst 5x with hexanes to ensure removal of the product and excess reagents (see general procedure for details). Unfortunately, at low catalyst loading, modifying the recovery method from precipitation to centrifugation did not

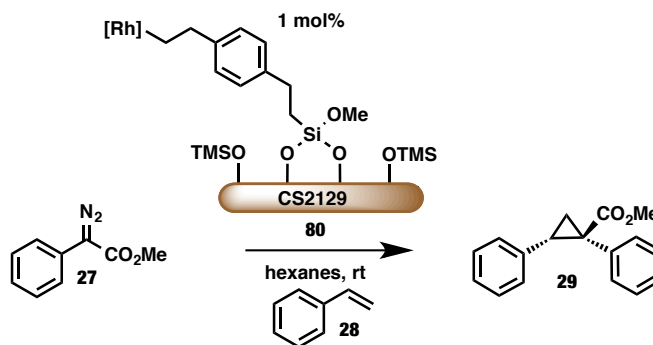
improve the recyclability of the catalyst and screening various porous membranes was unsuccessful as none of the membranes tested appeared to be hexanes permeable (Table 3.16).

Table 3.16 Varying the method of catalyst recovery for asymmetric cyclopropanation by CS-2129-supported $\text{Rh}_2(\text{S-DOSP})_4$ -derivative at low catalyst loading

precipitation			membrane	centrifugation		
cycle	yield (%)	ee(%)		cycle	yield (%)	ee(%)
1	77	74	membranes were not hexanes permeable no reaction occurred	1	81	74
2	78	66		2	76	46
3	79	54		3	61	41
4	25	21		4	63	20
5	7	11		5	19	13

In order to determine which of the two methods for catalyst recovery tested, precipitation or centrifugation, was better for the recycling of **80**, we next increased the catalyst loading to 1 mol% and repeated the test. After comparing these two methods for catalyst recovery over two reaction cycles at 1 mol%, we found that the precipitation method was more suitable for catalyst recovery as the product was obtained with a higher yield and level of enantioinduction by the second reaction cycle using this method (Table 3.17).

Table 3.17 The effect of varying the method of catalyst recovery on the reactivity and selectivity of asymmetric cyclopropanation by CS-2129–supported $\text{Rh}_2(\text{S-DOSP})_4$ –derivative



cycle	precipitation	
	yield (%)	ee(%)
1	72	80
2	78	79



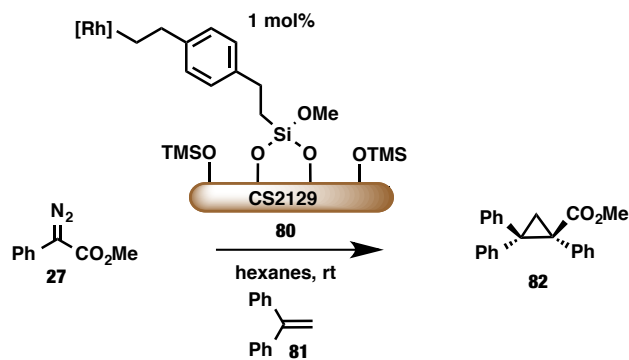
cycle	centrifugation	
	yield (%)	ee(%)
1	75	80
2	69	74



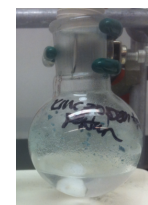
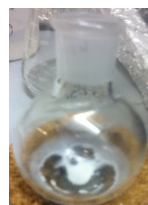
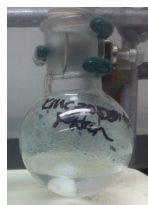
We next screened a reaction to see if the catalyst was able to achieve even higher enantioinduction in asymmetric cyclopropanation. The cyclopropanation of 1,1-diphenylethylene is known to provide extremely high levels of enantioinduction and yields with $\text{Rh}_2(\text{S-DOSP})_4$ (87% yield and 97% ee).³² For this reason, we next screened this reaction under the optimal conditions. We found that the same high % ee (97% ee) and moderate yield (73%) were obtained with the use of catalyst **80**. We then wanted to see if using a hexanes-permeable thimble made of cellulose acetate, could hold the catalyst in place while allowing the starting materials to enter and exit so as to obviate any physical loss of catalyst during the recycling step. Unfortunately, low yields (37-69%) and lower enantioselectivities (91-93%) were obtained with

this method (Table 3.18). This is believed to be due the adverse reaction of the dirhodium catalyst and the diazo substrate with the free -OH groups on the cellulose acetate thimble.

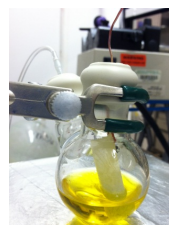
Table 3.18 Varying the method of catalyst recovery and substrate for asymmetric cyclopropanation by CS-2129-supported $\text{Rh}_2(\text{S-DOSP})_4$ -derivative



cycle	precipitation	
	yield (%)	ee(%)
1	73	97



cycle	thimble	
	yield (%)	ee(%)
1	37	93
2	69	91



3.9 Implementing a Long Alkyl Spacer Between the Silica Support and the Active Dirhodium(II) Catalyst Core

The classic problem in most immobilized systems to date is distortion of the chiral environment of the heterogeneous catalyst leading to deterioration of enantioinduction from the level obtainable with its homogeneous counterpart. The benefits of implementing long spacers between the support and the active site of the catalyst have also been recognized¹⁰ with enantioselective addition of dialkylzincs to both aromatic and aliphatic aldehydes using polymer-

bound chiral catalysts with a spacer. In order to eliminate the restriction of the freedom of the catalytic site, chiral polymer catalysts were synthesized with a methylene spacer that served to separate the catalytic site from the polystyrene resin.¹⁰ Another prime example of this was evidenced when Jacobsen's Mn(III) salen complex was heterogenized and found to catalyze epoxidation with decreased enantioinduction from that of the homogeneous catalyst. Implementation of a lengthening spacer linking the catalyst to the support, however, provided a catalyst capable of matching the enantioinduction of its homogeneous counterpart. This observed increase in enantioinduction was attributed to the spacing of the polymer away from the metal center.³³ In an effort to do the same and place the active site of our dirhodium(II) catalyst far from the solid support, we synthesized a catalyst with a twelve carbon spacer between the support and the carboxylate ligand. We believed that proximity of the polymer chain to the axial site of the dirhodium core was causing the diminished reactivities and selectivities observed. Although the spacer implemented in Hashimoto's system employed an ether linkage, it is possible that ether linkages can deteriorate over time. For this reason, we sought to explore a long alkyl spacer of similar length to the dodecyl moiety of Rh₂(*S*-DOSP)₄. We believed that this alkyl spacer would allow for sufficient spacing of the polymer chain away from the active site. Also, we believed that implementation of a long-alkyl spacer would allow the catalyst to exhibit similar conformational mobility to Rh₂(*S*-DOSP)₄ (Figure 3.6).

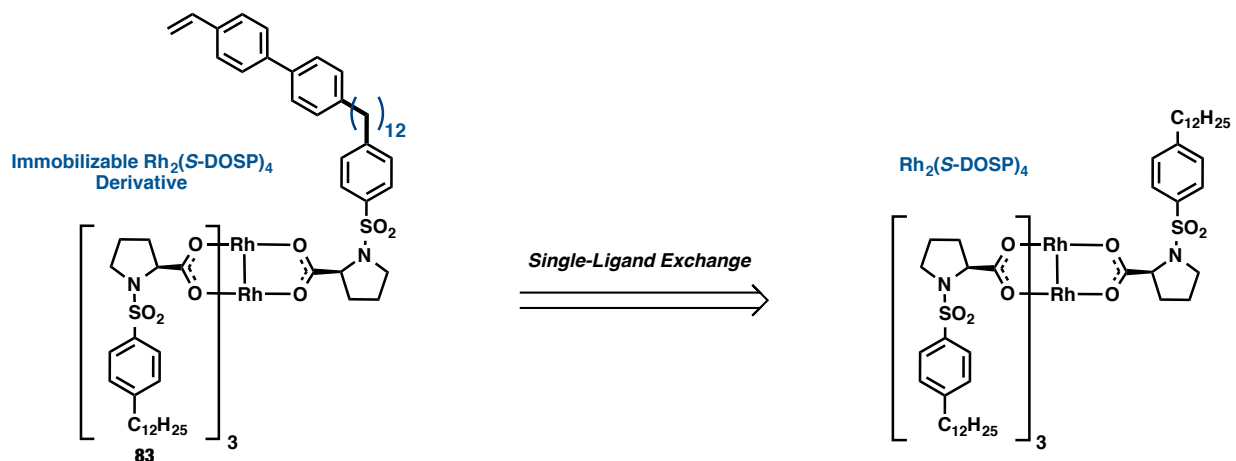
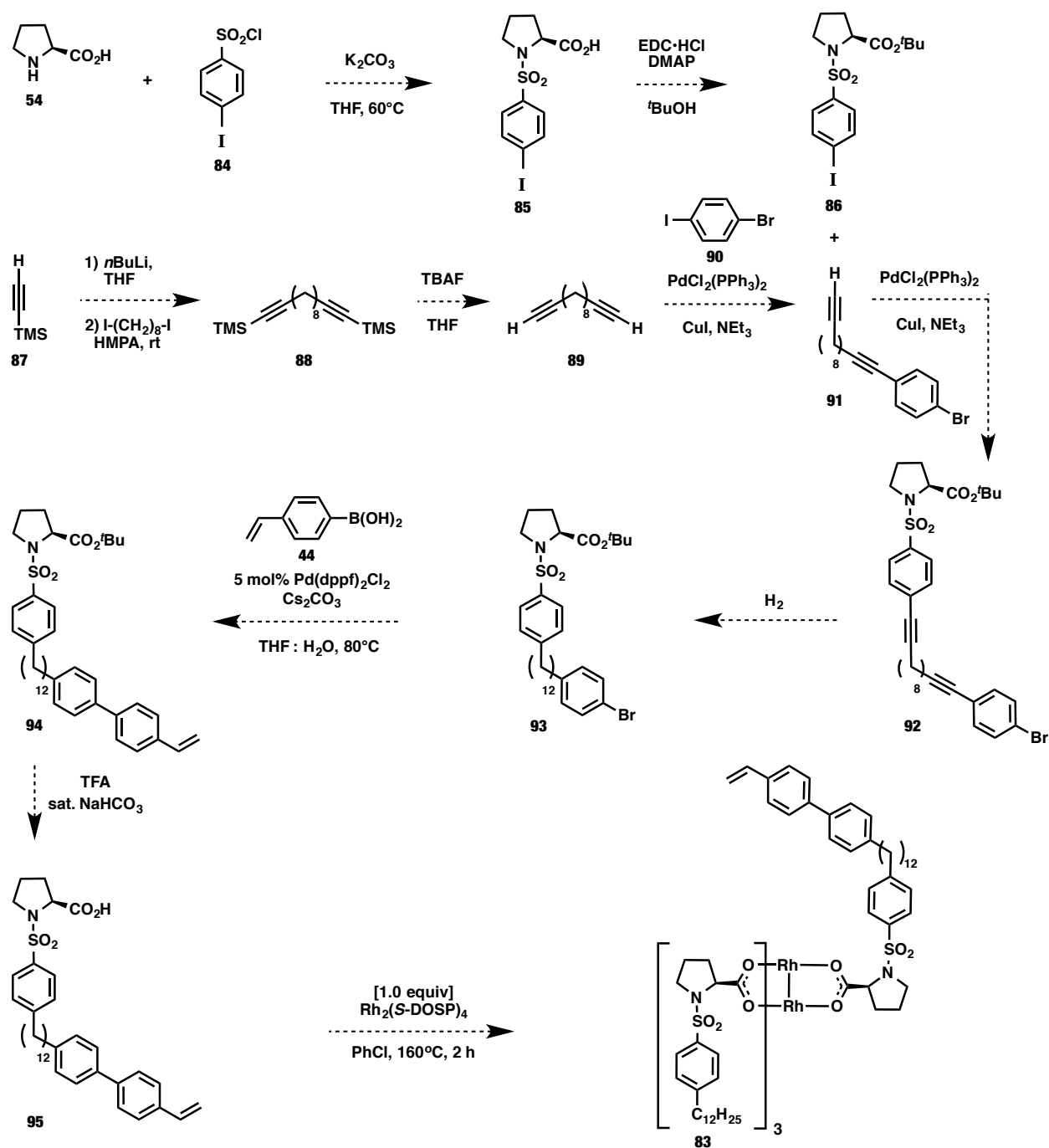


Figure 3.6 Design of long-chain immobilizable $\text{Rh}_2(\text{S-DOSP})_4$ -derivative

The forward synthesis of long-chain immobilizable $\text{Rh}_2(\text{S-DOSP})_4$ -derivative **83** was envisioned to begin with sulfation of L-proline followed by *tert*-butyl esterification to provide cross-coupling partner **86** (Scheme 3.32). After desymmetrization of diyne **89**, Sonogashira coupling of the terminal alkyne of **91** with the aryl iodide **86** would give rise the homologated ligand **92** which would undergo alkyne hydrogenation provide the 12-carbon alkyl spacer of proline **93**. Suzuki coupling of the aryl bromide **93** with boronic acid **44** followed by deprotection would give rise to the styryl-functionalized carboxylate ligand which, upon subjection to the single-ligand exchange procedure with $\text{Rh}_2(\text{S-DOSP})_4$, would provide the desired long-chain immobilizable $\text{Rh}_2(\text{S-DOSP})_4$ -derivative **83** (Scheme 3.32).

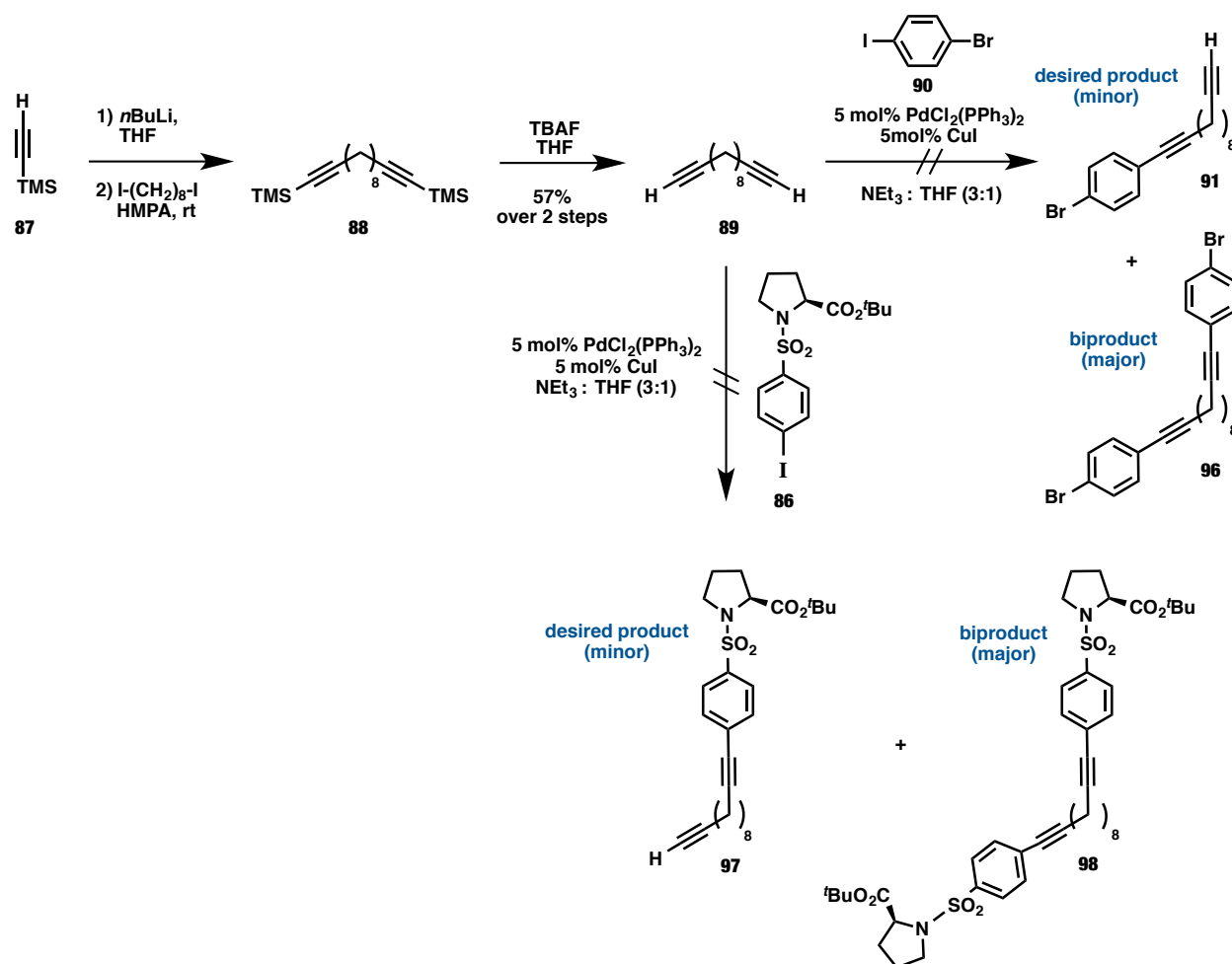
Scheme 3.32 Proposed synthetic route to long-chain immobilized $\text{Rh}_2(\text{S-DOSP})_4$ -derivative



In our first attempt to synthesize **83**, desymmetrizing Sonogashira coupling of the diyne **89** with aryl iodides **86** and **90** failed to provide the desired products of a single Sonogashira coupling at one of the alkynes (**97** or **91** respectively). Instead, the major product of these

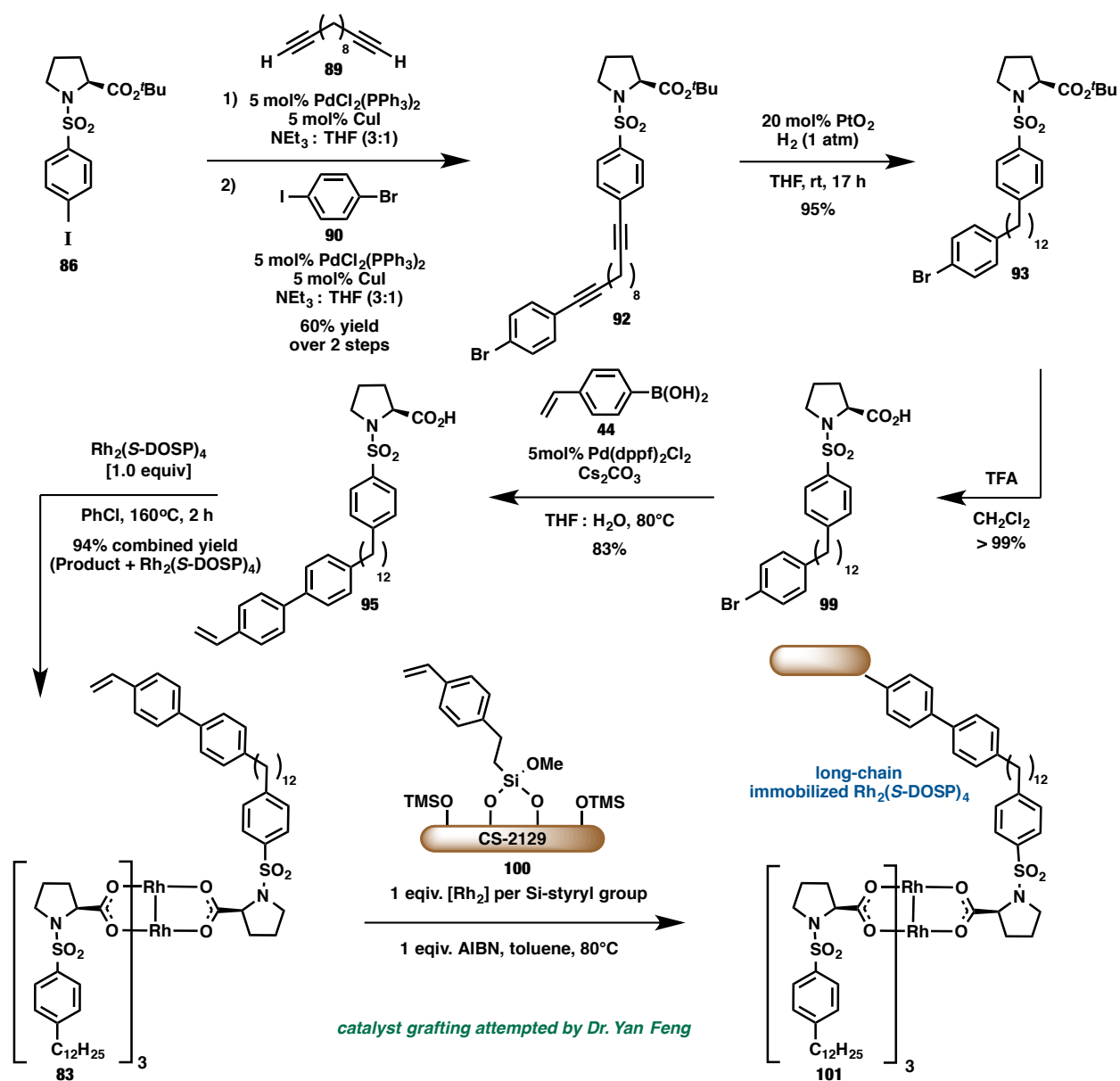
coupling reactions was the product of Sonogashira reaction of the substrate with both alkynes to give products **98** and **96** respectively. Several different reaction conditions were screened including reversing the stoichiometries of the diyne **89** and the aryl iodide (**86** or **90**), but this did not provide the desired product of a single Sonogashira coupling. Only the product of the double Sonogashira coupling products along with recovered starting materials were obtained at the end of the reaction (Scheme 3.33).

Scheme 3.33 Attempted synthesis of long-chain immobilized $\text{Rh}_2(\text{S-DOSP})_4$ -derivative via sequential desymmetrization of a diyne



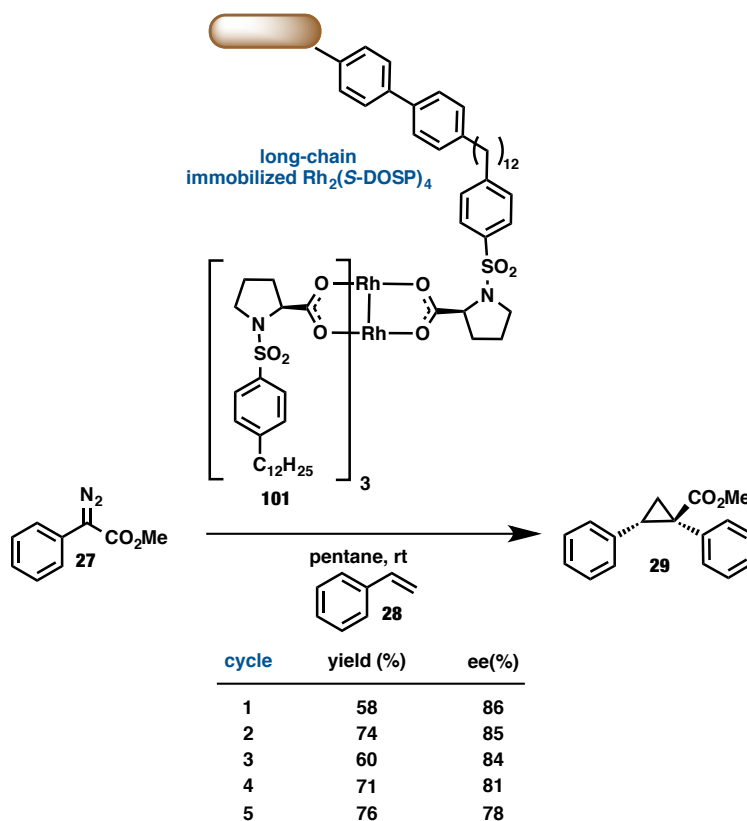
We were able to prevent formation of the doubly-coupled products by conducting the reactions sequentially but in one-pot. Reaction of aryl iodide **86** with diyne **89** was monitored by thin-layer chromatography. Once the first coupling reaction had gone to completion, the second aryl iodide **90** was added to the reaction mixture along with a second amount of catalyst to provide the desired doubly-coupled product **92**. Hydrogenation, deprotection, Suzuki coupling and ligand exchange all proceeded with excellent yields to provide the desired long-chain immobilizable $\text{Rh}_2(\text{S-DOSP})_4$ -derivative **83**. **83** was then exposed to functionalized silica **100** in the presence of AIBN radical initiator (Scheme 3.34).

Scheme 3.34 Synthesis of long-chain immobilized $\text{Rh}_2(\text{S-DOSP})_4$ -derivative



The CS-2129 immobilized $\text{Rh}_2(\text{S-DOSP})_4$ -derivative **101** was capable of catalyzing cyclopropanation of aryldiazoacetate **27** and styrene with high enantioselectivity in its first cycle (86% ee) but did not prove to be recyclable (Table 3.19, enantioselectivities decreasing from 86% ee to 78% ee over five cycles).

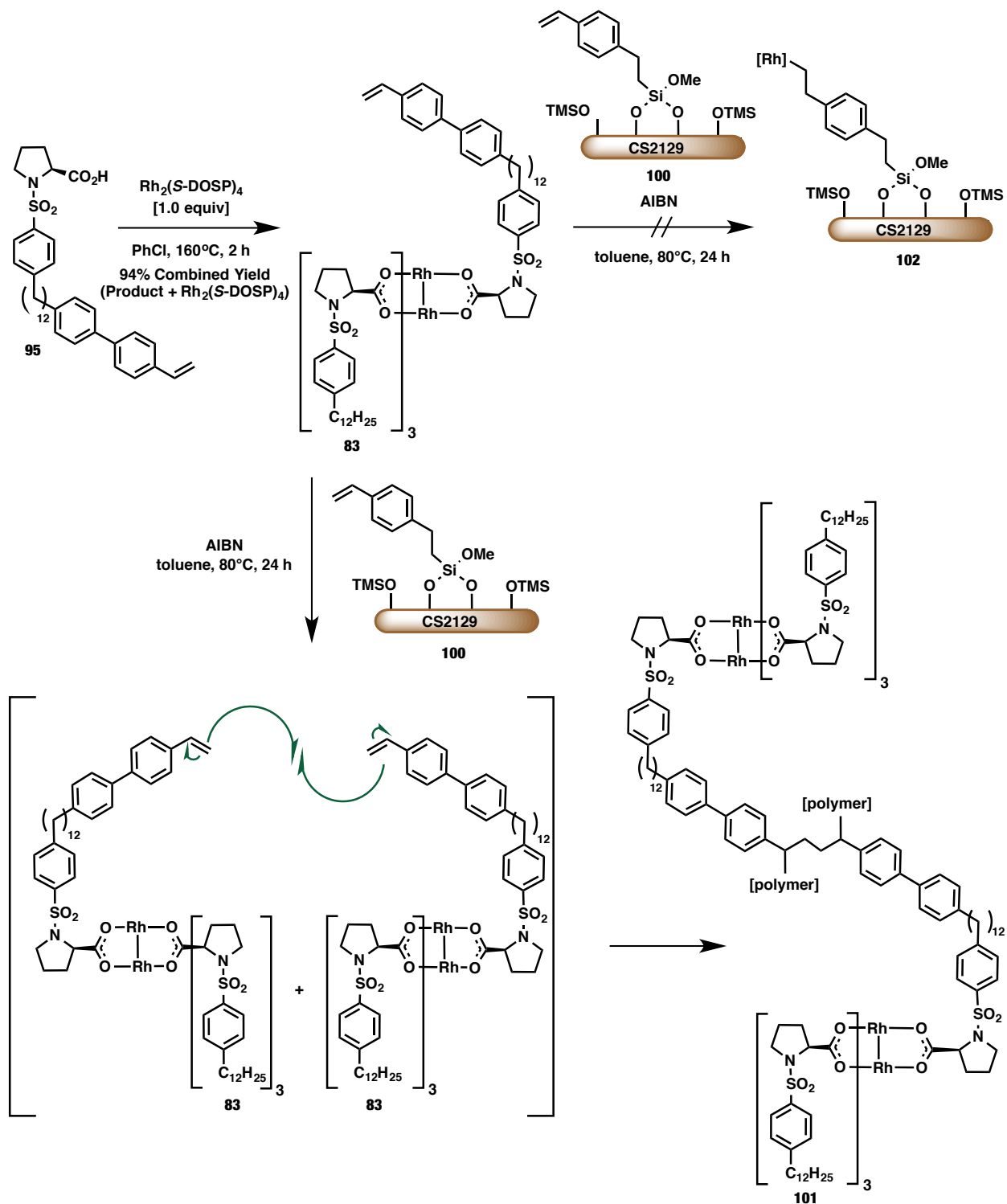
Table 3.19 Asymmetric cyclopropanation catalyzed by long-chain immobilized $\text{Rh}_2(\text{S-DOSP})_4$ -derivative



Although the short-chain ligand **69** was bench stable for extended periods of time, the long-chain ligand **95** was unstable and found to polymerize if allowed to sit at room temperature (Scheme 3.35). Long-chain immobilizable ligand **95** had to be made fresh and immediately brought through to the ligand exchange. The initial high % ee obtained in the first cycle, which rapidly deteriorated over five consecutive cycles, led us to believe that long-chain immobilizable $\text{Rh}_2(\text{S-DOSP})_4$ -derivative **83** did not graft to functionalized silica **100**, but rather polymerized by AIBN-initiated free radical polymerization of the flexible terminal styryl groups to provide polymerized $\text{Rh}_2(\text{S-DOSP})_4$ -derivative **101** (Scheme 3.35). We believed that polymeric **101**, which was stuck in pores of CS-2129, was the active catalyst system in the recycling study and that a small amount of soluble **101** was freed from CS-2129 every cycle. Once freed from CS-

2129, soluble **101** was presumed to be lost in the solvent wash during precipitation. Characterization of **101** could not be accomplished by nuclear magnetic resonance spectroscopy due to the insoluble nature of the catalyst in the presence of CS-2129.

Scheme 3.35 Possible deactivation route of long-chain immobilized $\text{Rh}_2(\text{S-DOSP})_4$ -derivative



Many lessons were learned about from the aforementioned exploratory studies on the design, synthesis, and testing of covalently immobilized-Rh₂(*S*-DOSP)₄-derivatives in catalyzing asymmetric cyclopropanation. Both polymer- and silica- supports were successfully incorporated into the catalyst structure by derivitization and immobilization of a single ligand. Also, we have found that our tetraproline derivatives could be immobilized by employing both the methods of Doyle (which involved initial polymerization followed by ligand exchange) and Hashimoto (which involved a single-ligand exchange reaction followed by polymerization). Free -OH groups on the silica surface were not tolerated and needed to be capped with TMS protecting groups in order to prevent adverse reactivity of the aryldiazoacetate with the silica surface. Low catalyst loadings (0.1 mol%), although effective in catalyzing the first cycle, did not allow for recycling due a small physical loss of catalyst every consecutive cycle. Precipitation was found to be the ideal recovery method for this system as centrifugation caused a drop-off in the reactivity and selectivity after the first reaction cycle. Membranes of different pore sizes were not permeable to hexanes and thus were not suitable for this system. Thimbles made of cellulose acetate were hexanes permeable and allowed for reactants to enter, contact the catalyst, and for product to diffuse out, but a lower yield and level of enantioinduction were observed in the second reaction cycle using this recovery method. Long-chain immobilizable catalyst **83** preferred to undergo polymerization over grafting to the silica-surface.

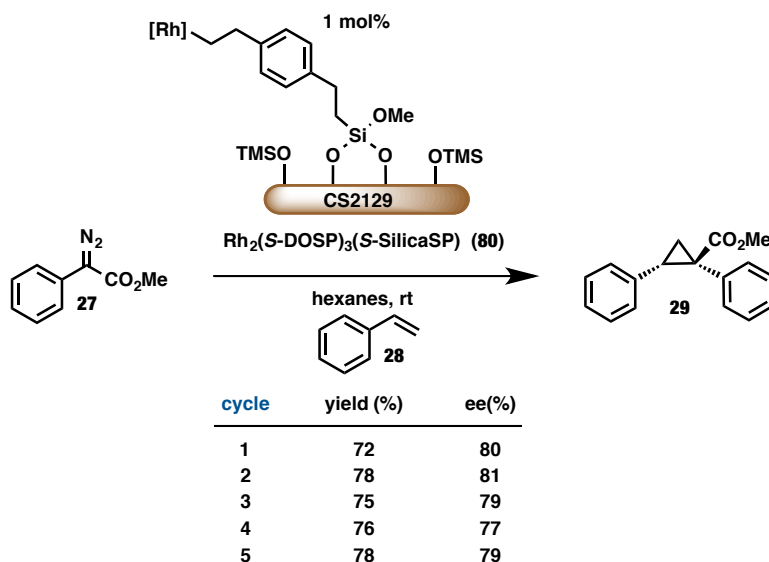
In moving forward from these findings, we know that CS-2129 was the best support owing to its large pore size providing high reactivity and selectivity of the catalyst, presumably due to open space available around the active site allowing for catalyst flexibility and reagent/product mobility. Seeing as the long-chained **83** is presumed to have formed a soluble polymerized Rh₂-

(*S*-DOSP)₄-derivative as opposed to the desired silica-grafted derivative **101**, we decided to turn out efforts back to the original CS-2129-immobilized Rh₂(*S*-DOSP)₄-scaffold.

3.10 Application of Recyclable Silica-Immobilized-Rh₂(*S*-DOSP)₄ in a Broad Range of Enantioselective Reactions

To our delight, when the catalyst loading was increased to 1 mol% with the original short-chain CS-2129-supported Rh₂(*S*-DOSP)₄-derivative, stable yields (ranging from 72-78%) and enantioselectivities (ranging from 81-77% ee) were obtained in the five consecutive cycles of the standard asymmetric cyclopropanation reaction (Table 3.20).³⁴

Table 3.20 Asymmetric cyclopropanation catalyzed by CS-2129-supported Rh₂(*S*-DOSP)₄-derivative



The promising activity and enantioselectivity of the immobilized complex led us to evaluate the robustness of the immobilization process via a filtration test, to assess catalyst heterogeneity and stability. Conversion of substrate was monitored as a function of time, removing the solid catalyst by filtration, while allowing the solid-free solution to continue to react.³⁵ Phenyl diazoacetate (**27**) was added to a mixture of **28**, Rh₂(*S*-DOSP)₃(*S*-SilicaSP) (**80**), and

mesitylene in hexanes by syringe pump, stopping at 7.5 min. After filtering **80**, the filtrate was transferred to a new flask before adding the second half of the solution of **27**. The amount of product in the filtrate remained constant after the filtration despite the additional phenyldiazoacetate addition, indicating robust immobilization of **80** on the silica surface (Figure 3.7).³⁴

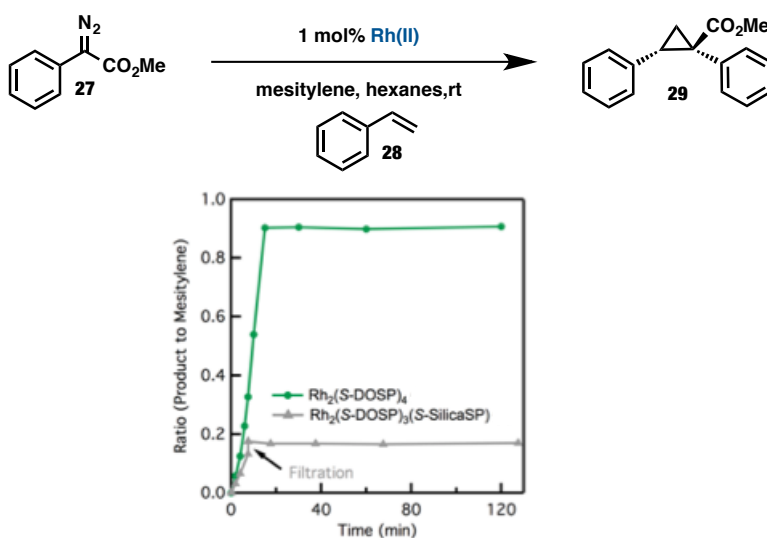


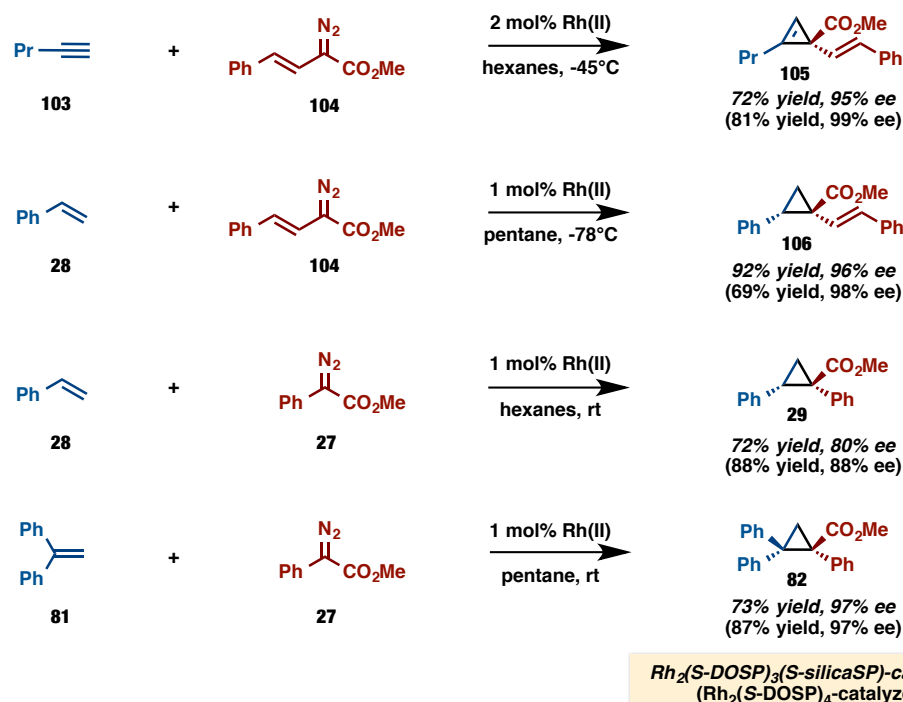
Figure 3.7 Filtration test demonstrating lack of catalytic activity in the absence of heterogeneous catalyst

$\text{Rh}_2(\text{S-DOSP})_4$ is the most generally effective chiral dirhodium(II) catalyst for highly enantioselective transformations involving donor/acceptor carbenoid intermediates including cyclopropanation,^{32, 36} cyclopropanation,³⁷ [3+4] and [3+2] cycloadditions,³⁸ tandem carbonyl ylide formation–1,3-dipolar cycloadditions,³⁹ tandem ylide formation/[2,3] sigmatropic rearrangements,⁴⁰ C–H insertions,³⁸ Si–H insertions,⁴¹ combined C–H functionalization/Cope rearrangements (CHCR),⁴² CHCR followed by retro-Cope rearrangements,⁴³ and CHCR–elimination reactions.⁴⁴ Several of these $\text{Rh}_2(\text{S-DOSP})_4$ -catalyzed transformations have been used as key steps in the syntheses of natural products.³⁸ In light of our successful immobilization

and recycling of $\text{Rh}_2(\text{S-DOSP})_4$ -derivative, we sought employ **80** in these transformations.³⁴ Our initial attempt at using substituted aryldiazoacetates with catalyst **80** provided products with diminished enantioinduction as compared to $\text{Rh}_2(\text{S-DOSP})_4$ (See experimental section 3.12 for details). For this reason, we focused these studies around the reactions of phenyldiazoacetate and styryldiazoacetate.

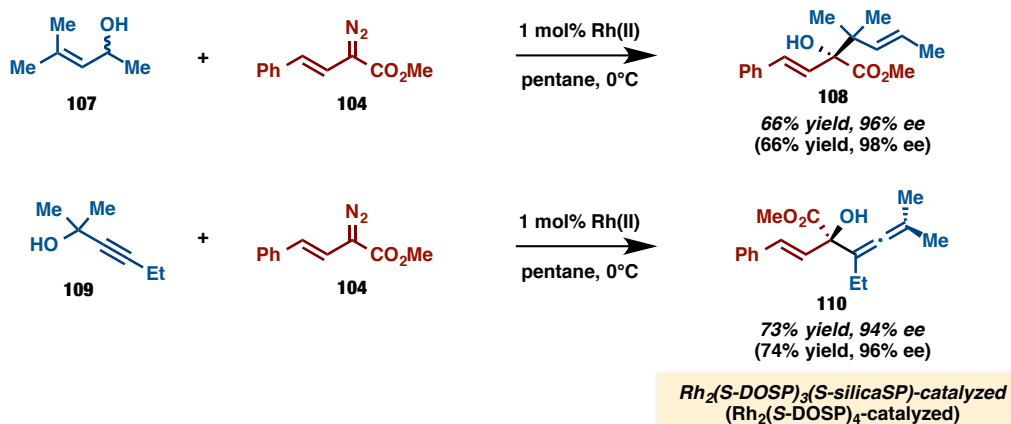
Initial comparison studies between $\text{Rh}_2(\text{S-DOSP})_3(\text{S-silicaSP})$ (**80**) and $\text{Rh}_2(\text{S-DOSP})_4$ were conducted with standard cyclopropanation and cyclopropenation reactions of donor/acceptor carbenoids. These studies were conducted with the most widely used donor/acceptor carbenoid precursors, styryldiazoacetate (**104**) and phenyldiazoacetate (**27**). The reactions were conducted using the optimal conditions developed previously for $\text{Rh}_2(\text{S-DOSP})_4$ -catalyzed reactions. $\text{Rh}_2(\text{S-DOSP})_3(\text{S-silicaSP})$ (**80**)-catalyzed cyclopropanation of 1-pentyne (**103**) and cyclopropanation of styrene (**28**) with styryldiazoacetate **104** provided the corresponding cyclopropene **105** and cyclopropane **106** in $\geq 95\%$ ee, comparable to the results obtained under $\text{Rh}_2(\text{S-DOSP})_4$ -catalyzed conditions. Similarly, **80**-catalyzed cyclopropanation of styrene (**28**) or 1,1-diphenylethylene (**81**) with phenyldiazoacetate **27** gave comparable results to the $\text{Rh}_2(\text{S-DOSP})_4$ -catalyzed reactions. Cyclopropane **29** was formed in 80% ee with $\text{Rh}_2(\text{S-DOSP})_3(\text{S-silicaSP})$ (**80**) vs. 88% ee with $\text{Rh}_2(\text{S-DOSP})_4$,^{36b} whereas cyclopropane **82** was formed in 97% ee using either the immobilized or the homogeneous catalyst (Scheme 3.36).^{32, 34}

Scheme 3.36 Cyclopropanation and cyclopropanation catalyzed by CS-2129–supported $\text{Rh}_2(\text{S-DOSP})_4$ –derivative



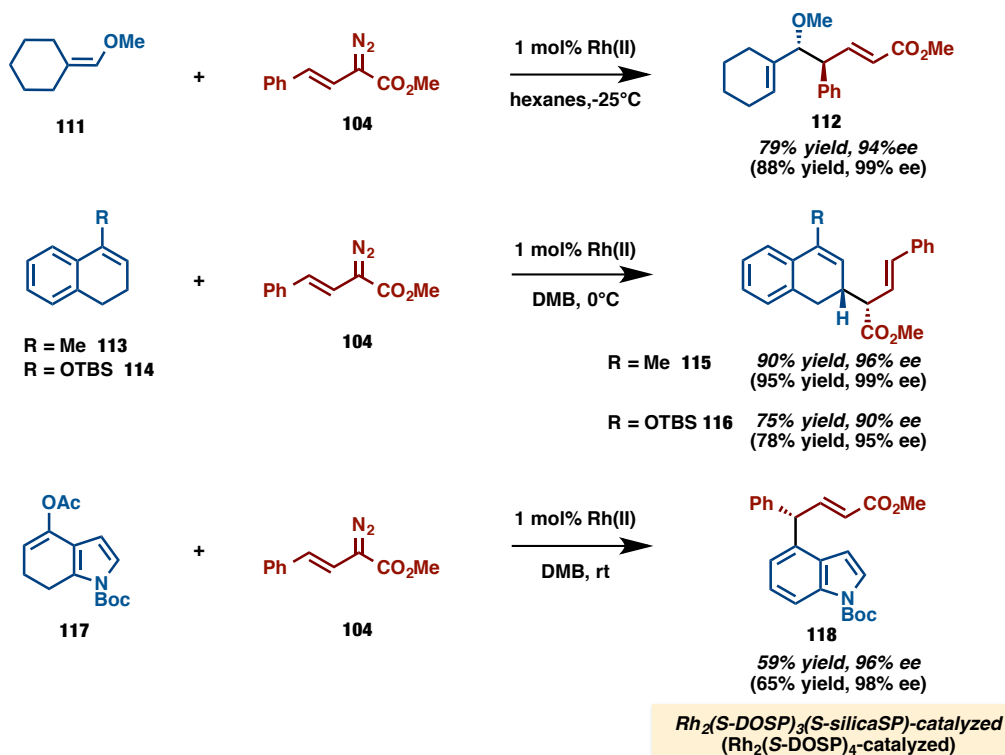
We then sought to determine the capability of $\text{Rh}_2(\text{S-DOSP})_3(\text{S-silicaSP})$ (**80**) in more exotic reactions of donor/acceptor carbenoids. A new transformation for these intermediates is the tandem ylide formation/[2,3] sigmatropic rearrangements with allylic and propargylic alcohols.⁴⁰ $\text{Rh}_2(\text{S-DOSP})_3(\text{S-silicaSP})$ -catalyzed reaction of allylic alcohol **107** with styryldiazoacetate **104** provided the corresponding rearrangement product **108** with a high level of asymmetric induction (96% ee), comparable to the results with $\text{Rh}_2(\text{S-DOSP})_4$ (Scheme 3.37, 98% ee).^{40a} Similarly, $\text{Rh}_2(\text{S-DOSP})_3(\text{S-silicaSP})$ -catalyzed ylide formation/[2,3] sigmatropic rearrangement of propargylic alcohol **109** with **104** provided **110** with a high level of enantiocontrol.^{34, 40b}

Scheme 3.37 Ylide formation / [2,3] sigmatropic rearrangement catalyzed by CS-2129-supported Rh₂(S-DOSP)₄-derivative



Donor/acceptor carbenoids have been shown to be versatile reagents for stereoselective C–H functionalization. A particularly robust transformation is the combined C–H functionalization/Cope rearrangement (CHCR). The Rh₂(S-DOSP)₃(S-silicaSP)-catalyzed reaction was applied to a range of CHCR reactions as illustrated in Scheme 3.38. The **80**-catalyzed CHCR reaction of (methoxymethylene)cyclohexane (**111**) with **104** provided **112** in 79% yield and 94% ee.⁴² The tandem CHCR/retro-Cope rearrangement of 1-methyl-3,4-dihydronaphthalene (**113**) with **104** provided **115** in 90% yield and 96% ee. The 1,2-dihydronaphthalene **114** performed similarly in the **80**-catalyzed CHCR/retro-Cope rearrangement cascade providing **116** in 75% yield and 90% ee.⁴³ Finally, the CHCR reaction–elimination cascade of 4-acetoxy-6,7-dihydroindole (**117**) with **104** provided the indole **118** in 59% yield and 96% ee.⁴⁴ All of these reactions proceeded with levels of enantioinduction close to those obtained with Rh₂(S-DOSP)₄.³⁴

Scheme 3.38 C–H functionalization catalyzed by CS-2129–supported $\text{Rh}_2(\text{S-DOSP})_4$ –derivative



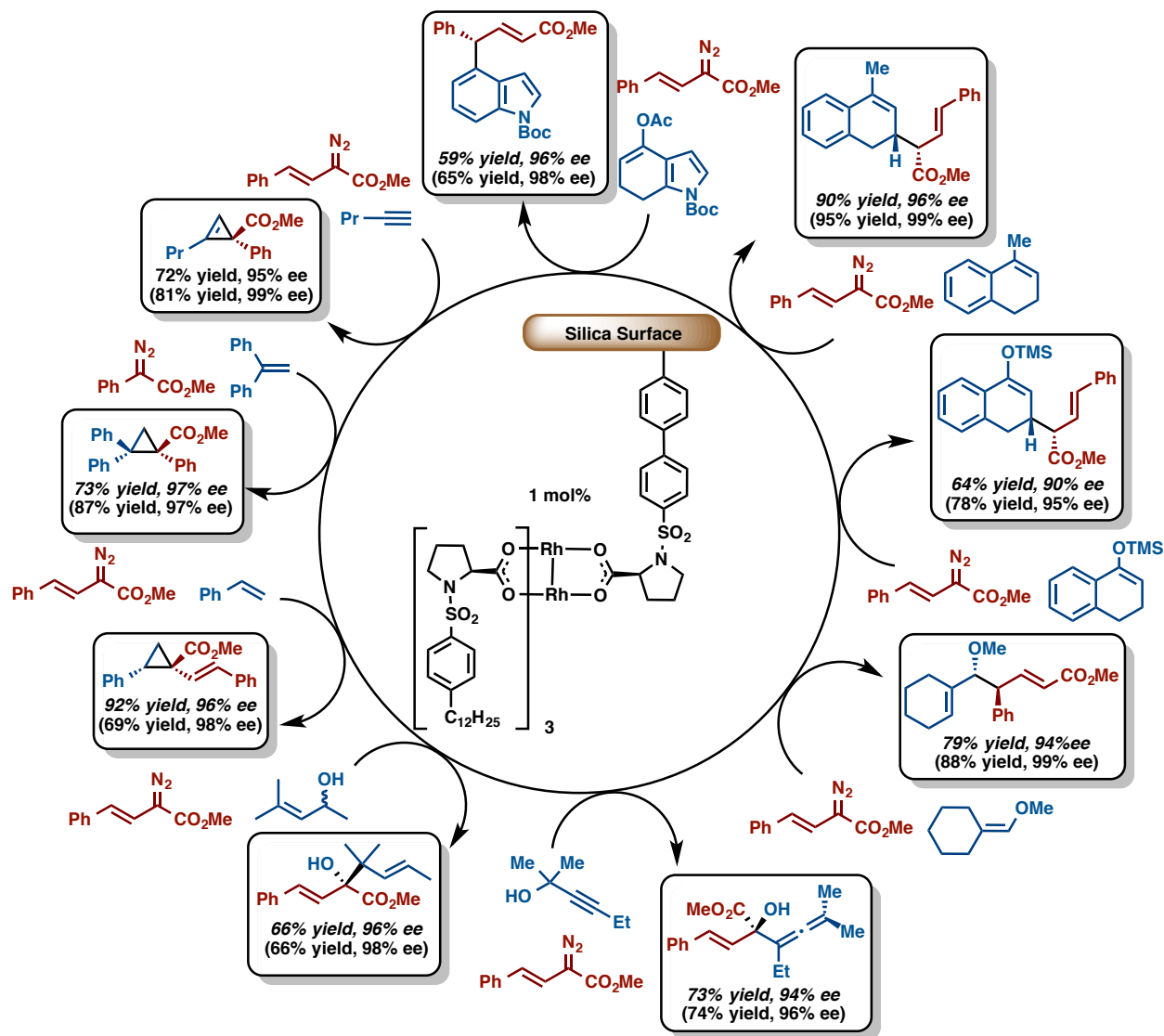
3.11 Conclusion

This study describes an effective method for covalent immobilization of a highly versatile and robust³¹ dirhodium catalyst onto a silica support. Also, this represents the first successful immobilization, recycling, and application of an immobilized $\text{Rh}_2(\text{S-DOSP})_4$ analogue in a broad range of enantioselective transformations with comparable enantioinduction to its homogeneous counterpart. It is anticipated that this catalyst may prove useful in flow reactors, which was the subject of our next investigation and is described in Chapter 4 of this thesis.

This study represents the first successful immobilization, recycling, and application of immobilized $\text{Rh}_2(\text{S-DOSP})_4$ derivatives in a broad range of enantioselective transformations. It is also the first example of the use of a styryl rhodium carbenoid in heterogeneous catalysis. In

this project, we were able to meet our collaborative goals of enhancing catalyst recovery and recyclability. We next sought to better understand the factors that contribute to catalyst deactivation and loss and to apply this catalyst system in novel flow reactors.

Figure 3.8 Breadth of enantioselective catalysis by recyclable silica-immobilized- $\text{Rh}_2(\text{S-DOSP})_4$ -derivative



3.12 Experimental Section

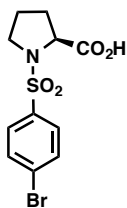
General: All reactions were conducted under anhydrous conditions in oven-dried glassware under an inert atmosphere of dry argon, unless otherwise stated. Hexanes, pentane, toluene, tetrahydrofuran (THF), and α,α,α -trifluorotoluene (TFT) were dried by a Grubbs-type solvent purification system (passed through activated alumina columns). 2,2-Dimethylbutane (DMB) was freshly distilled prior to use over sodium. Chlorobenzene was freshly distilled over calcium hydride. Unless otherwise noted, all other reagents were obtained from commercial sources and used as received. ^1H Nuclear Magnetic Resonance (NMR) spectra were recorded at 400 and 600 MHz. Data presented as follows: chemical shift (in ppm on the δ scale relative to δH 7.27 for the residual protons in CDCl_3 , coupling constant (J/Hz), integration. Coupling constants were taken directly from the spectra and are uncorrected. ^{13}C NMR spectra were recorded at 100 MHz and all chemical shift values are reported in ppm on the δ scale, with an internal reference of δC 77.23 for CDCl_3 . Mass spectral determinations were carried out on a Thermo Finnigan LTQ-FTMS spectrometer with ESI or APCI ionization. Melting points are uncorrected. Infrared spectral data are reported in units of cm^{-1} . Analytical TLC was performed on silica gel plates using UV light or *Phosphomolybdic acid (PMA) stain*. Flash column chromatography was performed on silica gel 60 Å (230-400 mesh). Optical rotations were measured on JASCO P-2000 polarimeters. Analytical enantioselective chromatographies were measured on Varian Prostar instrument and used isopropanol:hexane as gradient. All solvents were degassed by bubbling argon through the solvent for a minimum of 10 min prior to use. Enantiomeric excess was determined by high performance liquid chromatography (HPLC), using chiral analytical columns with 2-propanol in hexane as eluent. Chiral HPLC conditions were determined by

obtaining good separation of the racemic product. $\text{Rh}_2(R/S\text{-DOSP})_4$ was employed as the catalyst in the racemic reactions.

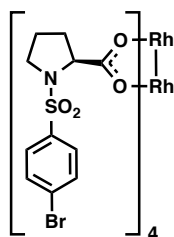
Thermogravimetric analysis (TGA) was performed on a Netzsch STA409. Samples were heated under a nitrogen diluted air stream from 30 to 900 °C at a rate of 10 °C min⁻¹, and the organic loading was estimated from relative weight loss in the range 200–800 °C. Cross-polarization magic-angle spinning (CP-MAS) solid-state NMR spectra were collected on a Bruker DSX 300 MHz instrument. Samples were packed in 7 mm zirconia rotors and spun at 10 kHz. Typical ¹³C CP-MAS parameters were 3000 scans, a 90° pulse length of 4 ms, and recycle times of 4 s. The surface area, total pore volume and pore size distributions were determined by nitrogen adsorption–desorption isotherms measured on a Micromeritics Tristar 2030 at 77 K, with the surface area determined by the Brunauer–Emmett–Teller (BET) method. Total pore volume and pore size were calculated using the Broekhoff-de Boer method with the Frenkel–Halsey–Hill (BdB-FHH) modification using the adsorption isotherm. Elemental analysis was performed by ALS Environmental Laboratories and Robertson MicroLit Laboratories.

L-proline, 4-bromobenzenesulfonyl chloride, sodium carbonate monohydrate, cesium carbonate, [1,1'-Bis(diphenylphosphino)ferrocene]dichloropalladium(II), complex with dichloromethane ($\text{Pd}(\text{dppf})_2\text{Cl}_2$), 4-vinylphenylboronic acid (**44**), styrylethyltrimethoxysilane (**75**), triethylamine, hexamethyldisilazane (HMDS), azobisisobutyronitrile (AIBN), 1-pentyne (**103**), 1,1-diphenylethylene (**81**), 1-bromo-4-iodobenzene (**90**), 2-methyl-3-hexyn-2-ol (**109**), (methoxymethyl)triphenyl phosphonium chloride, and mesitylene were all commercially available and used without further purification. The silica CS-2129 (**74**) was commercially available from PQ corporation. Styrene (**28**) was commercially available and purified by pushing through a silica-filled pipette prior to use. $\text{Rh}_2(S\text{-DOSP})_4$,^{36a} styryldiazoacetate (**104**),⁴⁵

phenyldiazoacetate (**16**),^{7a} 4-methylpent-3-en-2-ol (**107**),^{7a} 1-methyl-3,4-dihydronaphthalene (**113**),⁴⁵ and *tert*-butyl 4-acetoxy-6,7-dihydro-1H-indole-1-carboxylate (**117**)⁴⁴ were all synthesized according to published procedures. ((4-iodophenyl)sulfonyl)-*L*-proline (**86**)⁴⁶ and dodeca-1,11-diyne (**89**)⁴⁷ in the synthesis of long-chain immobilizable Rh₂(*S*-DOSP)₄-derivative were synthesized according to published procedures. Rh₂(*S*-DOSP)₄-catalyzed cyclopropanation providing **105**,³⁷ cyclopropanation providing **106**,^{36a} **29**,^{36b} and **82**,³² ylide formation/[2,3] sigmatropic rearrangements providing **108**^{40a} and **110**,^{40b} C–H functionalization/Cope rearrangement cascade (CHCR) providing **112**,⁴² CHCR/retro CHCR providing **115**⁴³ and **116**,⁴³ and CHCR/elimination providing **118**⁴⁴ were all run according to published procedures. Rh₂(*S*-DOSP)₃(*S*-silicaSP) (**80**)-carbenoid reactions were also run following the published procedures listed above. Once all of the diazo compound had been consumed and the reactions had gone to completion, Rh₂(*S*-DOSP)₃(*S*-silicaSP) (**80**) was removed from the reaction mixtures by vacuum filtration. The filtrates were collected, concentrated *in vacuo*, crude ¹H NMR obtained, and the residues purified according to the known literature procedures. Polymerization by the general procedure for single-ligand exchange of polymer with Rh₂(*S*-DOSP)₄ was conducted by Dr. Nicholas A. Brunelli. The surface functionalization and subsequent characterization of styryl silica; surface protection and subsequent characterization of styryl-TMS-silica (**100**); and catalyst grafting and subsequent characterization of Rh₂(*S*-DOSP)₃(*S*-silicaSP) (**80**) were conducted by Dr. Yan Feng.



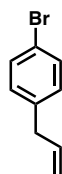
(S)-1-((4-bromophenyl)sulfonyl)pyrrolidine-2-carboxylic acid (56): According to the known literature procedure,⁴⁸ a 1 L flask was charged with L-(-)-proline (9.72 g, 0.09 mol, 1.00 equiv) and sodium carbonate monohydrate (31.4 g, 0.25 mol, 3.00 equiv) dissolved in 150 mL deionized water. 4-bromobenzene sulfonyl chloride (25.9 g, 0.10 mol, 1.20 equiv) was then added and allowed to stir for one day. The reaction mixture was then washed with ether (2 x 10 mL), acidified to pH 1.5 with 12 M HCl, saturated with sodium chloride, and extracted with ethyl acetate (10 x 20 mL). Solvent was removed *in vacuo* and the remaining red oil residue was purified on silica gel eluting with hexane : ethyl acetate (1 : 2) to afford white solid (27.3 g, 81 % yield). $R_f = 0.07$ (hexane : ethyl acetate 1 : 1); $[\alpha]_D^{20} -38.3^\circ$ (c = 2.45, CHCl₃); ¹H NMR (600 MHz, CDCl₃) δ 7.77 (d, $J = 6.6$ Hz, 2H), 7.69 (d, $J = 8.7$ Hz, 2H), 4.34 (dd, $J = 3.2, 8.7$ Hz, 1H), 3.51 (ddd, $J = 4.2, 7.5, 9.6$ Hz, 1H), 3.31 (dd, $J = 7.5, 9.6$ Hz, 1H), 2.13 (m, 2H), 2.01 (m, 1H), 1.85 (m, 1H); ¹³C NMR (100 MHz, CDCl₃) δ 177.1, 137.2, 132.7, 129.3, 128.4, 60.5, 48.8, 31.1, 24.9; IR (film): 2955, 1720, 1574, 1472, 1389, 1343, 1197, 1091, 1006, 824, 740; HRMS (ESI) calcd for C₁₁H₁₁O₄N₁⁷⁹Br₁³²S₁ (M+H)⁺ 331.9598 found 331.9601.



Catalyst 53: Ligand Exchange Procedure 1: According to the known literature procedure,^{36a} a 100 mL, two-neck flask fitted with a reflux condenser was charged with (S)-1-((4-

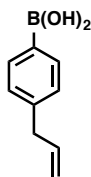
bromophenyl)sulfonyl)pyrrolidine-2-carboxylic acid (1.00 g, 3.00 mmol, 8.00 equiv) and $\text{Na}_4\text{RH}_2(\text{CO}_3)_4$ (198 mg, 0.30 mmol, 1.00 equiv) dissolved in 40 mL deionized water. The reaction was heated to reflux and allowed to stir for 24 h. The product was extracted with methylene chloride (3 x 100 mL) until the organic layer was clear, concentrated *in vacuo*, and purified through silica eluting hexane : ethyl acetate (2 : 1) and freeze-dried from benzene to afford green solid (297 mg, 51 % yield).

Ligand Exchange Procedure 2: According to the known literature procedure,⁴⁹ a 100 mL two-neck flask was charged with (S)-1-((4-bromophenyl)sulfonyl)pyrrolidine-2-carboxylic acid (2.00 g, 6.00 mmol, 10.0 equiv) and rhodium acetate (265 mg, 0.600 mmol, 1.00 equiv) in 30 mL dry, freshly distilled chlorobenzene. The flask was then equipped with a soxhlet extractor containing a thimble filled with CaCO_3 and allowed reflux at 160 °C for 48 hours. Chlorobenzene was then removed *in vacuo* and the remaining residue was purified through silica eluting hexane : ethyl acetate (2 : 1) green solid (163 mg, 81% yield). $[\alpha]_D^{20} +3.7^\circ$ (c = 0.77, CHCl_3); $R_f = 0.35$ (hexane : ethyl acetate 1 : 1); $^1\text{H NMR}$ (600 MHz, CDCl_3) δ 7.66 (dd, $J = 8.4, 7.8$ Hz, 13H), 4.31-4.29 (m, 4H), 3.25-3.22 (m, 4H), 3.13-3.10 (m, 4H), 2.02-1.96 (m, 4H), 1.91-1.81 (m, 8H), 1.62-1.57 (m, 4H); $^{13}\text{C NMR}$ (100 MHz, CDCl_3) δ 192.8, 137.8, 132.6, 129.4, 128.0, 62.0, 48.4, 31.4, 25.1; IR (film): 3089, 2955, 1600, 1574, 1417, 1154, 1091, 1067, 1006, 737; HRMS (ESI) calcd for $\text{C}_{44}\text{H}_{45}\text{O}_{11}\text{N}_5^{79}\text{Br}_4^{23}\text{Na}_4^{103}\text{Rh}_2^{32}\text{S}_4$ (M+H)⁺ 1560.6427 found 1560.6398.



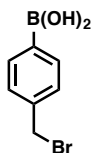
1-allyl-4-bromobenzene (60): According to the known literature procedure,²⁵ a 1 L 3-neck round bottom flask was charged with Mg^0 and a stir bar. 1,4-dibromobenzene (50.0 g, 0.21 mol,

1.00 equiv) and a small amount of iodide grain were then dissolved in dry diethyl ether (132.5 mL) to give a 1.6 M solution. A small portion (2 mL) of this solution was then added to the reaction mixture. After the color of the reaction mixture had faded from red to clear yellow, the rest of the 1.6 M 1,4-dibromobenzene solution was then added dropwise by addition funnel. Once addition was complete, the mixture was stirred at reflux for two hours. The reaction mixture was then decanted into another flask *via* syringe to another dry 1 L flask. Freshly distilled allyl bromide was then added by syringe pump at 0 °C and the reaction was allowed to stir overnight. Ammonium chloride (50 mL) was then added by syringe pump over one hour. The aqueous layer was then removed and extracted with diethyl ether (4 x 200 mL). Organic phases were combined and dried over MgSO₄. Purification by Kugelrohr distillation at 90 °C and 0.1 Torr afforded a clear oil (32.7 g, 79% yield). ¹H NMR (400 MHz, CDCl₃) δ 7.39 (d, *J* = 8.4 Hz, 2H), 7.04 (d, *J* = 8.4 Hz, 2H), 5.96-5.86 (m, 1H), 5.11-5.03 (m, 2H), 3.33 (d, *J* = 6.4 Hz, 2H). Data are consistent with the literature.²⁵

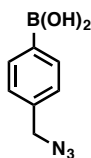


(4-allylphenyl)boronic acid (61): According to the known literature procedure,²⁶ 1-allyl-4-bromobenzene was dissolved in dry tetrahydrofuran (15 mL). The reaction mixture was then cooled to -70 °C and *n*-BuLi was added dropwise. Stirring at -70 °C was continued for an additional hour. Triisopropyl borate was then added and allowed to stir for 90 minutes at -70 °C. Ammonium chloride solution (15 mL) was then added and stirring was continued at 70 °C for an additional 10 minutes. Water (50 mL) was added and the reaction was allowed to warm to room temperature. The reaction mixture was extracted with diethyl ether (4 x 25 mL) and dried over

MgSO₄ to afford pink solid (4.2 g, quantitative yield). ¹H NMR (400 MHz, CDCl₃) δ 8.17 (d, *J* = 7.6 Hz, 2H), 7.35 (d, *J* = 7.6 Hz, 2H), 6.06-5.97 (m, 1H), 5.16-5.08 (m, 2H), 3.49 (d, *J* = 6.4 Hz, 2H). Data are consistent with the literature.²⁶

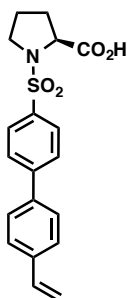


(4-allylphenyl)boronic acid (65): According to the known literature procedure,⁵⁰ a 100 mL 2-neck round-bottom flask was charged with *p*-tolylboronic acid (1.00 g, 7.36 mmol, 1.00 equiv), benzoyl peroxide (119 mg, 0.78 mmol, 0.10 equiv), and *N*-bromosuccinimide (1.39 g, 7.80 mmol, 1.0 equiv). Carbon tetrachloride (50 mL) was then added and the reaction was subjected to light (150 watt). The reaction mixture was then brought to reflux and allowed to stir there for 4.5 hours. The reaction was then cooled to 40 °C and filtered two times *via* vacuum filtration and solvent was removed *in vacuo*. The product was then washed with cold diethyl ether (14 mL) and recrystallized by dissolving in minimal dichloromethane followed by addition of an equal amount of diethyl ether and then hexanes with slow stirring until the product precipitated out of solution. The resulting solid was purified on silica gel (hexane : ethyl acetate 20 : 1 to 2 : 1) to afford white solid (8.0 g, 56% yield). ¹H NMR (400 MHz, CDCl₃) δ 8.20 (d, *J* = 7.6 Hz, 2H), 7.54 (d, *J* = 7.6 Hz, 2H), 4.57 (s, 2H). Data are consistent with the literature.⁵⁰



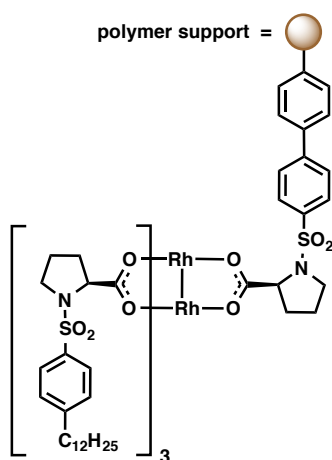
(4-allylphenyl)boronic acid (66): According to the known literature procedure,⁵⁰ a 50mL round-bottom flask was charged with (4-allylphenyl)boronic acid (160 mg, 0.74 mmol, 1.00

equiv) dissolved in dry *N*-dimethylformamide (5 mL). Sodium azide (140 mg, 2.20 mmol, 3.00 equiv) was then added and the reaction was allowed to stir at room temperature for 18 hours. Chloroform (30 mL) was then added to the reaction mixture. Organic layer was washed with water (5 x 20 mL) and dried over Na₂SO₄. Kugelrohr distillation under reduced pressure (1 Torr) at 30 °C afforded clear oil (52.5 mg, 40% yield). ¹H NMR (400 MHz, CDCl₃) δ 8.18 (d, *J* = 7.6 Hz, 2H), 7.41 (d, *J* = 7.6 Hz, 2H), 4.38 (s, 2H); IR (film): 2926, 2093, 1611, 1407, 1334, 1303, 1181, 1020, 727, 691.



(S)-1-((4'-vinyl-[1,1'-biphenyl]-4-yl)sulfonyl)pyrrolidine-2-carboxylic acid (69): An oven-dried and argon-purged 250 mL round bottom flask was charged with (S)-1-((4-bromophenyl)sulfonyl)pyrrolidine-2-carboxylic acid (**3**) (4.09 g, 12.3 mmol, 1.00 equiv), 4-vinylphenylboronic acid (**44**) (2.00 g, 13.5 mmol, 1.10 equiv), and cesium carbonate (12.0 g, 36.9 mmol, 3.00 equiv). A mixture of tetrahydrofuran : water (80 mL : 20 mL) was then added to dissolve the reactants. [1,1'-Bis(diphenylphosphino)ferrocene]dichloropalladium(II), complex with dichloromethane (Pd(dppf)₂Cl₂) (502 mg, 0.62 mmol, 0.05 equiv) was then added and reaction turned a bright red and then to a dark brown. The reaction was then brought to reflux (80 °C) and allowed to stir overnight. The reaction mixture was concentrated *in vacuo* and ~200 mL deionized water was added to the resulting residue. The aqueous wash was then acidified to pH 1.0. The aqueous layer was then extracted with ethyl acetate until the organic

washings were clear (5 x 50 mL). The organic layer was dried with Na₂SO₄ and concentrated *in vacuo*. Recrystallization of the crude product by dissolving in minimal dichloromethane (20 mL) and slowly adding a 1 : 1 mixture of hexane : diethyl ether with gentle stirring afforded solid brown product (4.21 g, 96% yield). $R_f = 0.11$ (hexane : ethyl acetate 1 : 1); $[\alpha]_D^{20} +1.8^\circ$ ($c = 1.49$, CHCl₃); ¹H NMR (600 MHz, CDCl₃) δ 7.94 (d, $J = 7.8$ Hz, 2H), 7.77 (d, $J = 7.8$ Hz, 2H), 7.60 (d, $J = 7.8$ Hz, 2H), 7.54 (d, $J = 7.8$ Hz, 2H), 6.78 (dd, $J = 10.8, 17.7$ Hz, 1H), 5.84 (d, $J = 17.7$ Hz, 1H), 5.34 (d, $J = 10.8$ Hz, 1H), 4.32-4.34 (m, 1H), 3.57-3.60 (m, 1H), 3.31-3.35 (m, 1H), 2.21-2.24 (m, 1H), 1.94-1.99 (m, 2H), 1.81-1.83 (m, 1H); ¹³C NMR (100 MHz, CDCl₃) δ 176.0, 145.7, 138.5, 138.1, 136.2, 135.9, 128.3, 127.8, 127.7, 127.1, 115.1, 60.6, 49.0, 30.8, 24.9; IR (film): 3208, 1710, 1438, 1339, 1156, 1097, 824, 743; HRMS (ESI) calcd for C₁₉H₁₈O₄N₁S₁ (M+H)⁺ 356.0964 found 356.0962.



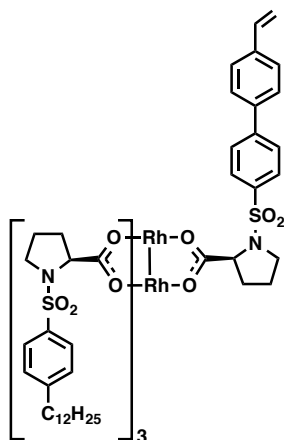
General Procedure for Single-Ligand Exchange of Polymer with Rh₂(S-DOSP)₄:

This polymerization was conducted by Dr. Nicholas A. Brunelli. Adapted from the known literature procedure,¹³ A 25 mL 3-neck round bottom flask was charged with Rh₂(S-DOSP)₄ (111 mg, 0.04 mmol, 1.50 equiv) and polymerized ligand (117 mg, 0.39 mmol, 1.00 equiv) dissolved in chlorobenzene (8 mL). The reaction mixture was then brought to reflux (160 °C) and allowed

to stir for 7 hours. The reaction mixture was then allowed to cool to room temperature and chlorobenzene was removed *in vacuo*. The residue was then washed with ethanol (500 mL) followed by methanol (500 mL) until no more green was eluting. Filtration afforded a very light green solid (70 mg, 27% yield).

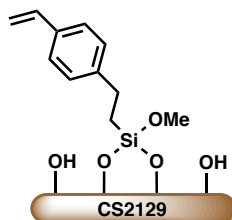


Methyl (1*R*,2*S*)-1,2-diphenylcyclopropane-1-carboxylate (29):^{36b} A mixture of styrene (**28**) (312 mg, 3.00 mmol, 2.00 equiv.) and Rh₂(*S*-DOSP)₃(*S*-silicaSP) (**80**) (250 mg, 0.02 mmol, 0.01 equiv) were added to a 25 mL dry and argon-purged round-bottom flask and stirred in dry, degassed hexanes (4 mL). Phenyl diazoacetate (**27**) (264 mg, 1.50 mmol, 1.00 equiv.) in hexanes (8 mL) was then added to the reaction mixture *via* syringe pump over 30 min. The product was then separated from the catalyst by vacuum filtration. Rh₂(*S*-DOSP)₃(*S*-silicaSP) (**80**) was then washed with dry, degassed hexanes (5 x 10 mL) and the filtrate was then concentrated *in vacuo*. The product was obtained in >20:1 dr as determined by ¹H NMR analysis of the crude reaction mixture. The residue was then purified through silica gel eluting with hexanes : ethyl acetate (100 : 4.5) to afford a white solid (271 mg, 72% yield). Enantioenrichment was determined by chiral HPLC analysis after purification: (Chiralcel (*S,S*)-WHELK, 1% *i*-PrOH in hexane, 1.0 mL/min, 1 mg/mL, 30 min, λ = 254 nm) retention times of 8.65 min (minor) and 10.08 min (major), 80% ee. The spectral data were identical to those previously reported.^{36b} The Rh₂(*S*-DOSP)₄-catalyzed reaction between **27** and **28** has been previously reported to give **29** in 88% yield and 88% ee.^{36b}

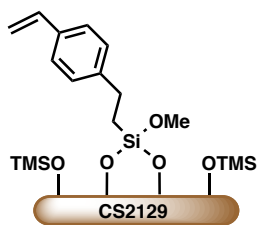


Rh₂(S-DOSP)₃(S-SP) (73): According to the known literature procedure,¹⁹ A 100 mL 3-neck round bottom flask was charged with Rh₂(S-DOSP)₄ (1.00 g, 0.53 mmol, 1.00 equiv) and (S)-1-((4'-vinyl-[1,1'-biphenyl]-4-yl)sulfonyl)pyrrolidine-2-carboxylic acid (**69**) (0.21 g, 0.21 mmol, 1.10 equiv) dissolved in chlorobenzene (20 mL). The reaction mixture was then brought to reflux (160 °C) and allowed to stir for 2 h. The reaction mixture was then allowed to cool to room temperature and chlorobenzene was removed *in vacuo*. The residue was then purified through silica gel eluting with hexane:ethyl acetate (increasing from 1 : 20 to 1 : 5) and freeze-dried from benzene to afford dark green solid (330 mg, 34% yield) along with recovered Rh₂(S-DOSP)₄ (428 mg, 43% yield). $R_f = 0.42$ (hexane : ethyl acetate 2 : 1); $[\alpha]_D^{20} +2.2^\circ$ (c = 2.45, CHCl₃); ¹H NMR (600 MHz, CDCl₃) δ 7.89 (d, $J = 7.8$ Hz, 2H), 7.77 (d, $J = 6.6$ Hz, 2H), 7.70 (d, $J = 7.2$ Hz, 6H), 7.63 (d, $J = 7.2$ Hz, 2H), 7.55 (d, $J = 7.8$ Hz, 2H), 7.25 (m, 6H), 6.92 (dd, $J = 17.7, 10.8$ Hz, 1H), 5.96 (d, $J = 17.7$ Hz, 1H), 5.49 (d, $J = 10.8$ Hz, 1H), 4.34-4.21 (m, 4H), 3.23 (s, 4H), 3.10-2.97 (m, 8H), 2.73-2.69 (m, 1H), 2.54-2.42 (m, 1H), 2.01 (bs, 4H), 1.83-1.50 (m, 27H), 1.25-1.02 (m, 54H); ¹³C NMR (100 MHz, CDCl₃) δ 192.9, 192.8, 192.7, 153.4, 152.1, 152.0, 151.8, 145.0, 138.7, 137.8, 137.4, 136.0, 135.8, 128.4, 127.8, 127.6, 127.5, 127.3, 113.4, 61.9, 48.4, 48.1, 46.3, 46.1, 40.2, 39.1, 38.3, 36.8, 36.4, 32.1, 31.9, 31.4, 29.8, 29.4, 27.8, 27.4,

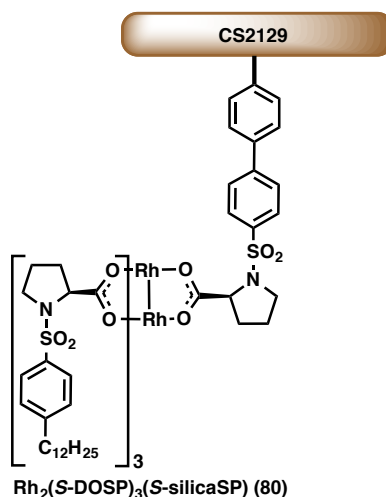
25.0, 22.8, 22.1, 20.8, 14.3, 12.3; IR (film): 2956, 2926, 2855, 1605, 1418, 1346, 1158, 1098, 1012, 656; HRMS (ESI) calcd for $C_{63}H_{125}O_{24}N_{17}^{103}Rh_2^{32}S_4$ (M+H)⁺ 1837.6069 found 1837.6071.



Styryl silica: This surface functionalization and subsequent characterization was conducted by Dr. Yan Feng. To a 250 mL two-neck flask that was purged with nitrogen for 30 min, added 5.0 g CS-2129 silica. The flask was then purged with nitrogen for another 30 min, before 1.33 g (5.00 mmol) styrylethyltrimethoxysilane (**8**) in about 75 mL anhydrous toluene taken immediately from the glovebox was injected into the flask by a syringe, and the syringe was rinsed several times with anhydrous toluene. Then 5.00 mL (36.0 mmol) triethylamine in anhydrous toluene was added in a similar way. The total volume of the reaction mixture was about 125 mL. The reaction was stirred at 25 °C under nitrogen overnight. The resulting white powder was filtered, washed with toluene (3 x 75 mL) and hexanes (3 x 75 mL), and dried under vacuum overnight. Approximately 5.0 g product was obtained. TGA: styryl loading was 0.36 mol / g. Nitrogen physisorption: BET surface area: 268 m² / g, pore volume: 1.81 cm³ / g. ¹³C-CP-MAS NMR: δ (ppm), 127.1, 45.1, 5.9.



Styryl-TMS-silica (100): This surface protection and subsequent characterization was conducted by Dr. Yan Feng. To a 250 mL two-neck flask that was purged with nitrogen for 30 min, 4.5 g styryl-silica was added. The flask was then purged with nitrogen for another 30 min, before 8.30 mL (39.6 mmol) hexamethyldisilazane in about 100 mL anhydrous toluene taken immediately from the glovebox was injected into the flask by a syringe. The syringe was rinsed several times with anhydrous toluene. The total volume of the reaction mixture was about 150 mL. The reaction was stirred at 25 °C under nitrogen for 3 days. The resulting white powder was filtered, washed with toluene (3 x 75 mL) and hexanes (3 x 75 mL), and dried under vacuum overnight. About 4.4 g product was obtained. TGA: styryl loading: 0.34 mmol / g, trimethylsilane loading: 0.44 mmol / g. Nitrogen physisorption: BET surface area: 218 m² / g, pore volume: 1.78 cm³ / g. ¹³C-CP-MAS NMR: δ (ppm), 126.6, 28.4, 14.3, 0.2.



Rh₂(S-DOSP)₃(S-silicaSP) (80): This catalyst grafting and subsequent characterization was conducted by Dr. Yan Feng. To a dry 500 mL Schlenk flask, 2.6 g styryl-TMS-silica (**100**), 4.0 g (0.88 mmol) Rh₂(S-DOSP)₃(S-SP) (**73**), 0.145 g (0.88 mmol) AIBN, and about 175 mL toluene were added. The flask was then sealed and connected to the Schlenk line. The solution was degassed by 4 freeze-thaw cycles, and then heated to 80 °C and stirred under nitrogen for 4 days. The solution was cooled to room temperature and divided into 4 portions for filtration. Large amounts of toluene (150 mL X 3) and hexanes (100 mL X 3) were used to wash away soluble components. A light green powder was obtained (2.5 g). TGA: [Rh₂]: 0.06 mmol / g. Elemental analysis: [Rh₂]: 0.055 mmol / g. Nitrogen physisorption: BET surface area: 210 m² / g, pore volume: 1.41 cm³ / g. ¹³C-CP-MAS NMR: δ (ppm), 127.6, 48.2, 27.8, 13.2, 0.7.

Elemental analysis:

	%C (mmol / g)	%H (mmol / g)	%N (mmol / g)	%Si (mmol / g)	%Rh (mmol / g)	Rh/Si
Fresh Catalyst ^a	11.77 (9.8)	1.39 (1.4)	0.52 (0.37)	32.10 (11.4)	1.16 (0.11)	0.0096
Spent Catalyst ^a	14.21 (11.8)	1.72 (1.7)	0.49 (0.35)	32.20 (11.5)	1.08 (0.10)	0.0087

^aElemental analysis performed by ALS Environmental Laboratories.

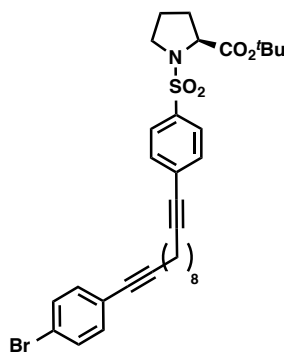
Sample	Rhodium wt% ^b	Silicon wt%
Post-Cyclopropanation Cycle 1 ^a	<0.01	0.05

^aICP-OES performed by Robertson Microлит Laboratories due to their low detection limit for Rh.

^bThe Rh level in the solution after Rh₂(*S*-DOSP)₃(*S*-silicaSP) (**80**)-catalyzed cyclopropanation is below the detection limit of ICP-OES, indicating that the subsequent reactivity is not from any leached Rh species.

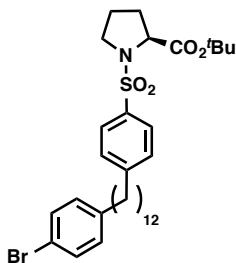


Methyl (S)-1,2,2-triphenylcyclopropane-1-carboxylate (82):³² A mixture of 1,1-diphenylethylene (**81**) (209 mg, 1.16 mmol, 2.32 equiv.) and Rh₂(*S*-DOSP)₃(*S*-silicaSP) (**80**) (89.0 mg, 0.01 mmol, 0.01 equiv) were added to a 25 mL dry and argon-purged round-bottom flask and stirred in dry, degassed pentane (6 mL). Phenyl diazoacetate (**27**) (88.0 mg, 0.50 mmol, 1.00 equiv.) in pentane (10 mL) was then added to the reaction mixture *via* syringe pump over 15 min. The product was then separated from the catalyst by vacuum filtration. Rh₂(*S*-DOSP)₃(*S*-silicaSP) (**80**) was then washed with dry, degassed pentane (5 x 10 mL) and the filtrate was then concentrated *in vacuo*. The product was obtained in >20:1 dr as determined by ¹H NMR analysis of the crude reaction mixture. The residue was then purified through silica gel eluting with pentane : diethyl ether (increasing from 10 : 1 to 5 : 1) to afford a clear oil (120 mg, 73% yield). Enantioenrichment was determined by chiral HPLC analysis after purification: (Chiralcel (*S,S*)-WHELK, 9% *i*-PrOH in hexane, 1.0 mL/min, 1 mg/mL, 30 min, λ = 254 nm) retention times of 6.89 min (minor) and 16.24 min (major), 97% ee. The spectral data were identical to those previously reported.³² The Rh₂(*S*-DOSP)₄-catalyzed reaction between **27** and **81** has been previously reported to give **82** in 87% yield and 97% ee.³²



(S)-tert-butyl 1-((4-(12-(4-bromophenyl)dodeca-1,11-diyn-1-yl)phenyl)sulfonyl)pyrrolidine-2-carboxylate (92): A dry and argon-purged 250mL round-bottom flask was charged with (S)-tert-butyl 1-((4-iodophenyl)sulfonyl)pyrrolidine-2-carboxylate (**86**) (3.96 g, 9.10 mmol, 1.00 equiv) and dodeca-1,11-diyne (**89**) (2.94 g, 18.1 mmol, 2.00 equiv) dissolved in a 3:1 mixture of triethylamine (19 mL) : dry tetrahydrofuran (6 mL). Bis(triphenylphosphine)palladium(II) dichloride (318 mg, 0.45 mmol, 0.05 equiv) was then added to the reaction mixture and stirred at room temperature for 5 minutes. Copper(I) iodide (86 mg, 0.45 mmol, 0.05 equiv) was then added and the resulting mixture was heated to 60 °C and allowed to stir there for 2.5 hours. Once the first Sonogashira coupling had gone to completion, the reaction mixture was cooled to room temperature and the reaction mixture was again charged with bis(triphenylphosphine)palladium(II) dichloride (318 mg, 0.45 mmol, 0.05 equiv) and copper(I) iodide (86 mg, 0.45 mmol, 0.05 equiv). 1-bromo-4-iodobenzene (**90**) (7.69 g, 27.2 mmol, 3.00 equiv) was then added to the reaction mixture and dissolved in a 3 : 1 mixture of triethylamine (19 mL) : dry tetrahydrofuran (6 mL). The reaction was then re-heated to 60 °C and allowed to stir there overnight. The reaction was then cooled to room temperature and extracted with diethyl ether (3 x 100 mL) and washed with sat'd. aq. ammonium chloride, dried over magnesium sulfate, filtered, and concentrated *in vacuo*. The crude product was purified by flash column chromatography eluting hexanes : ethyl acetate (6 : 1) to afford **92** as a brown oil (6.80 g,

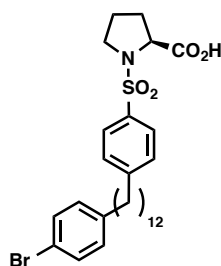
60% yield); $R_f = 0.26$ (hexane : ethyl acetate 6 : 1); $[\alpha]_D^{20} -27.9^\circ$ ($c = 1.21$, CHCl_3); $^1\text{H NMR}$ (400 MHz, CDCl_3) δ 7.80-7.77 (d, $J = 8.4$ Hz, 2H), 7.51-7.48 (d, $J = 8.4$ Hz, 2H), 7.42-7.39 (d, $J = 8.4$ Hz, 2H), 7.26-7.23 (d, $J = 8.4$ Hz, 2H), 4.20-4.17 (dd, $J = 3.6, 8.0$ Hz, 1H), 3.49-3.44 (m, 1H), 3.34-3.28 (m, 1H), 2.44-2.37 (dt, $J = 7.2, 14.8$ Hz, 4H), 2.04-1.90 (m, 3H), 1.79-1.73 (m, 1H), 1.65-1.57 (m, 8H), 1.45 (s, 9H), 1.39-1.33 (m, 4H); $^{13}\text{C NMR}$ (100 MHz, CDCl_3) δ 171.3, 137.3, 133.2, 132.1, 131.6, 129.0, 127.5, 123.2, 121.7, 94.7, 91.9, 81.9, 79.8, 79.7, 61.4, 48.5, 31.1, 29.2, 29.1, 29.0, 28.9, 28.7, 28.6, 28.5, 28.1, 24.7, 19.6, 19.5, 19.4; IR (film): 2929, 2855, 2230, 1740, 1593, 1485, 1457, 1394, 1366, 1349, 1219, 1153, 1093, 1070, 1010, 825, 743, 722; HRMS (ESI) calcd for $\text{C}_{33}\text{H}_{40}\text{O}_4\text{N}_1^{79}\text{Br}_1^{23}\text{Na}_1^{32}\text{S}_1$ ($\text{M}+\text{Na}$) $^+$ 648.1754 found 648.1762.



(S)-tert-butyl 1-((4-(12-(4-bromophenyl)dodecyl)phenyl)sulfonyl)pyrrolidine-2-carboxylate

(93): A dry and argon-purged 50mL round-bottom flask was charged with **92** (197 mg, 0.31 mmol, 1.00 equiv) and platinum (IV) oxide (7.00 mg, 0.03 mmol, 0.10 equiv). Dry tetrahydrofuran (12.5 mL) was then added and the reaction mixture was stirred at room temperature. The flask was then fitted with a balloon of hydrogen gas and the reaction mixture was allowed to stir under 1 atmosphere of hydrogen for 24 hours. At this time, more platinum (IV) oxide (7 mg, 0.03 mmol, 10 mol%) and dry tetrahydrofuran (5 mL) were added and the reaction mixture was allowed to stir under 1 atmosphere of hydrogen for an additional 24 hours. The reaction mixture was then filtered through a plug of celite. The wet celite was then washed with ~25 mL dry tetrahydrofuran and the washings were collected and concentrated *in vacuo*.

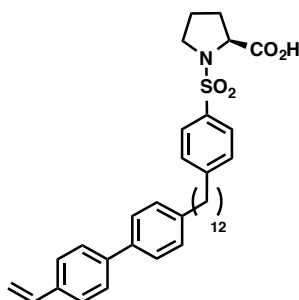
The crude product was purified by flash column chromatography eluting hexanes : ethyl acetate (6 : 1) to afford **93** as a clear oil (199 mg, 95% yield); $R_f = 0.34$ (hexane : ethyl acetate 6 : 1); $[\alpha]_D^{20} -37.5^\circ$ ($c = 1.06$, CHCl_3); $^1\text{H NMR}$ (400 MHz, CDCl_3) δ 7.79-7.77 (d, $J = 8.4$ Hz, 2H), 7.38-7.36 (d, $J = 8.0$ Hz, 2H), 7.31-7.29 (d, $J = 8.4$ Hz, 2H), 7.05-7.03 (d, $J = 8.4$ Hz, 2H), 4.21-4.18 (dd, $J = 3.6, 8.0$ Hz, 1H), 3.50-3.44 (m, 1H), 3.36-3.30 (m, 1H), 2.67-2.63 (t, $J = 7.4$ Hz, 2H), 2.56-2.52 (t, $J = 7.4$ Hz, 2H), 2.04-1.91 (m, 3H), 1.77-1.74 (m, 1H), 1.63-1.55 (m, 4H), 1.45 (s, 9H), 1.37-1.25 (m, 16H); $^{13}\text{C NMR}$ (100 MHz, CDCl_3) δ 171.5, 148.4, 142.0, 136.0, 131.4, 130.3, 129.1, 127.6, 119.3, 81.7, 61.3, 48.5, 36.0, 35.5, 31.5, 31.2, 31.1, 29.8, 29.7, 29.6, 29.5, 29.4, 29.3, 28.1, 24.7; IR (film): 2924, 2852, 1742, 1488, 1457, 1366, 1343, 1219, 1153, 1093, 1093, 1071, 1010, 831, 731, 679, 659; HRMS (ESI) calcd for $\text{C}_{33}\text{H}_{48}\text{O}_4\text{N}_1^{79}\text{Br}_1^{23}\text{Na}_1^{32}\text{S}_1$ ($\text{M}+\text{Na}$) $^+$ 656.2380 found 656.2391.



(S)-1-((4-(12-(4-bromophenyl)dodecyl)phenyl)sulfonyl)pyrrolidine-2-carboxylic acid (99):

Adapted from the known literature procedure¹, a dry and argon-purged 250mL round-bottom flask was charged with **93** (3.00 g, 4.70 mmol, 1.00 equiv) dissolved in dry dichloromethane (90 mL). Trifluoroacetic acid (2.03 mL, 26.5 mmol, 5.60 equiv) was then added and the reaction was allowed to stir at room temperature for 10 hours. At this time, more trifluoroacetic acid (0.72 mL, 9.50 mmol, 2.00 equiv) was added and the reaction was allowed to stir for another 5 hours. Again, at this time, more trifluoroacetic acid (0.72 mL, 9.50 mmol, 2.00 equiv) was added and the reaction was allowed to stir for another 5 hours. Finally, more trifluoroacetic acid

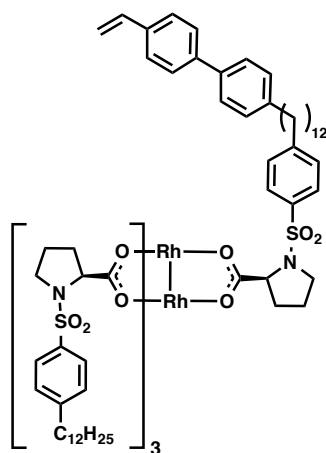
(0.36 mL, 4.70 mmol, 1.00 equiv) was added and the reaction was allowed to stir overnight. (Sequential additions of trifluoroacetic acid were necessary in order to push the reaction to completion.) Dichloromethane (~400 mL) was then added and the reaction was quenched with saturated aqueous sodium bicarbonate. Once pH \approx 14 had been reached, the aqueous layer was acidified with 20% HCl until pH \approx 0 was reached. The aqueous layer was separated and extracted with dichloromethane (3 x 200 mL). The combined organic washings were dried with sodium sulfate, filtered, and concentrated *in vacuo* to afford **99** as a white solid (3.00 g, quantitative yield). R_f = 0.04 (hexane : ethyl acetate 6 : 1); mp 43-46 °C; $[\alpha]_D^{20}$ -38.2° (c = 1.33, CHCl₃); ¹H NMR (400 MHz, CDCl₃) δ 8.78-7.90 (bs, 1H), 7.80-7.78 (d, J = 8.4 Hz, 2H), 7.39-7.37 (d, J = 8.4 Hz, 2H), 7.35-7.33 (d, J = 8.4 Hz, 2H), 7.05-7.03 (d, J = 8.0 Hz, 2H), 4.30-4.21 (dd, J = 3.6, 8.0 Hz, 1H), 3.56-3.51 (m, 1H), 3.28-3.23 (dd, J = 7.2, 16.8 Hz, 1H), 2.69-2.66 (t, J = 7.4 Hz, 2H), 2.56-2.52 (t, J = 7.4 Hz, 2H), 2.17-2.11 (m, 1H), 2.02-1.93 (m, 2H), 1.79-1.71 (m, 1H), 1.64-1.55 (m, 4H), 1.37-1.20 (m, 16H); ¹³C NMR (100 MHz, CDCl₃) δ 176.7, 149.2, 142.0, 134.5, 131.4, 130.4, 129.4, 127.8, 119.4, 60.6, 49.0, 36.1, 35.5, 31.5, 31.2, 30.8, 29.9, 29.8, 29.7, 29.6, 29.5, 29.4, 29.3, 24.9; IR (film): 2921, 2850, 1709, 1598, 1488, 1467, 1407, 1343, 1235, 1197, 1156, 1073, 1094, 1011, 840, 798, 685; HRMS (ESI) calcd for C₂₉H₄₀O₄N₁⁷⁹Br₁²³Na₁³²S₁ (M+Na)⁺ 600.1754 found 600.1758.



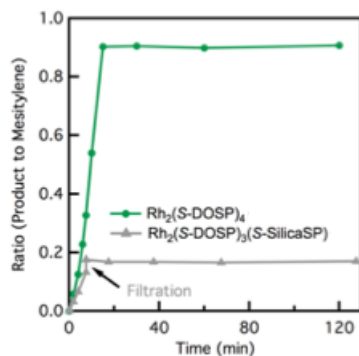
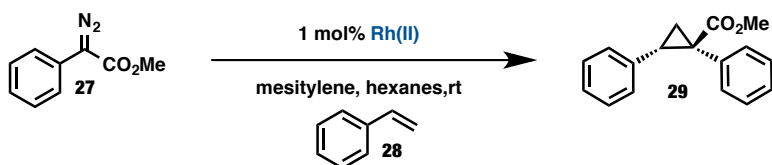
(S)-1-((4-(12-(4'-vinyl-[1,1'-biphenyl]-4-yl)dodecyl)phenyl)sulfonyl)pyrrolidine-2-carboxylic acid (95):

A dry and argon-purged 25 mL round-bottom flask was charged with **99** (400 mg, 0.69 mmol, 1.00 equiv), 4-vinylphenylboronic acid (102 mg, 0.69 mmol, 1.00 equiv), and cesium carbonate (676 mg, 2.07 mmol, 3.00 equiv) dissolved in 4 : 1 mixture of tetrahydrofuran (8 mL) : deionized water (2 mL). [1,1'-Bis(diphenylphosphino)ferrocene]dichloropalladium(II), complex with dichloromethane (28 mg, 0.03 mmol, 5 mol%) was then added to the reaction mixture and the reaction flask was fitted with a reflux condenser. The reaction mixture was then heated to 80 °C and allowed to stir there for 9 hours. The reaction was then cooled to room temperature, filtered, and concentrated *in vacuo*. Saturated aqueous sodium bicarbonate was then added along with an additional 200 mL of dichloromethane and the mixture was stirred for 10 minutes. 20% HCl (~200 mL) was then added and allowed to stir for an additional 30 minutes. The layers were then separated and the aqueous layer was extracted with dichloromethane (4 x 150 mL). The organic washings were then dried over sodium sulfate, filtered, and concentrated *in vacuo*. The crude product was purified by flash column chromatography eluting hexanes : ethyl acetate (3 : 1) with 1% acetic acid to afford **95** as a white solid (345 mg, 83% yield); $R_f = 0.18$ (hexane : ethyl acetate 2 : 1 with 1% acetic acid); mp 43-46 °C; $[\alpha]_D^{20} -38.2^\circ$ (c = 1.33, CHCl₃); ¹H NMR (400 MHz, CDCl₃) δ 9.68-8.10 (bs, 1H), 7.78-7.77 (d, $J = 7.6$ Hz, 2H), 7.57-7.55 (d, $J = 8.0$ Hz, 2H), 7.53-7.50 (d, $J = 8.4$ Hz, 2H), 7.48-7.46 (d, $J = 8.4$ Hz, 2H), 7.35-7.33 (d, $J = 8.4$ Hz, 2H), 7.26-7.24 (d, $J = 9.6$ Hz, 2H), 6.79-6.72 (dd, $J = 10.8, 17.6$ Hz, 1H), 5.81-5.76 (d, $J = 17.6$ Hz,

1H), 5.27-5.25 (d, $J = 10.8$ Hz, 1H), 4.26-4.24 (m, 1H), 3.55-3.52 (m, 1H), 3.27-3.21 (dd, $J = 7.2, 16.4$ Hz, 1H), 2.69-2.62 (ddd, $J = 8.0, 14.8, 21.6$ Hz, 4H), 2.22-2.12 (m, 1H), 2.01-1.84 (m, 2H), 1.80-1.52 (m, 5H), 1.43-1.19 (m, 16H); ^{13}C NMR (100 MHz, CDCl_3) δ 175.5, 149.3, 142.4, 140.7, 138.2, 136.6, 136.5, 134.2, 129.5, 129.1, 127.9, 127.2, 127.0, 126.8, 113.9, 60.9, 49.2, 36.1, 35.8, 31.7, 31.3, 30.6, 29.9, 29.8, 29.7, 29.6, 29.5, 29.4, 24.9; IR (film): 2921, 2850, 1709, 1598, 1488, 1467, 1407, 1343, 1235, 1197, 1156, 1073, 1094, 1011, 840, 798, 685; HRMS (ESI) calcd for $\text{C}_{29}\text{H}_{40}\text{O}_4\text{N}_1^{79}\text{Br}_1^{23}\text{Na}_1^{32}\text{S}_1$ ($\text{M}+\text{Na}$) $^+$ 600.1754 found 600.1758.



Catalyst 83: According to the known literature procedure³, A 100mL 3-neck round bottom flask was charged with $\text{Rh}_2(\text{S-DOSP})_4$ (1.00 g, 0.53 mmol, 1.00 equiv) and (S)-1-((4'-vinyl-[1,1'-biphenyl]-4-yl)sulfonyl)pyrrolidine-2-carboxylic acid (0.21 g, 0.21 mmol, 1.10 equiv) dissolved in chlorobenzene (20 mL). The reaction mixture was then brought to reflux (160 °C) and allowed to stir for 2 hours. The reaction mixture was then allowed to cool to room temperature and chlorobenzene was removed *in vacuo*. The residue was then purified through silica gel eluting hexane : ethyl acetate (increasing from 1 : 20 to 1 : 5) and freeze-dried from benzene to afford dark green solid (330 mg, 34% yield) along with recovered $\text{Rh}_2(\text{S-DOSP})_4$ (428 mg, 43% yield).



Filtration Test: General: The filtration test was evaluated using a slight modification to the standard reaction conditions for the cyclopropanation reaction. The initial reaction mixture included an internal standard 1,3,5-trimethylbenzene (mesitylene) to allow the determination of the amount of product. An initial aliquot of the internal standard, styrene, and solvent were sampled before phenyldiazoacetate addition. The sample was diluted using diethyl ether to a concentration appropriate for GC analysis. Samples were withdrawn periodically during the addition of the phenyldiazoacetate, filtering through a plug of silica to remove the catalyst. After 7.5 min (addition of half of the phenyldiazoacetate solution), the reaction mixture was filtered to remove the $\text{Rh}_2(\text{S-DOSP})_3(\text{S-silicaSP})$ (**80**). The filtrate was transferred to a new flask, and the remaining portion of the phenyldiazoacetate was added to the mixture. Sampling continued after the diazo addition stopped (15 mins) until 120 min after the reaction mixture was filtered. The samples were quantitatively analyzed on a Shimadzu GC-2010 gas chromatograph using a SHRX5 column (15 m, 0.25 lm film thickness, 0.25 mm i.d.) and detecting with a flame ionization detector using a standard analysis method.

The filtration method is considered a better method than elemental analysis to determine the potential leaching of the catalyst from the surface of the silica. The high activity of the

homogeneous $\text{Rh}_2(\text{S-DOSP})_4$ catalyst is advantageous, as small amounts of leached catalyst would result in significant conversion of the diazo substrate. Elemental analysis, on the other hand, has low sensitivity for leached Rh. Approximately 25% of the Rh added to the reaction mixture would have to leach in order for it to be above the detectable limit.

Filtration Test: *Experimental Details:* To an oven dried and argon-purged 25 mL round bottom flask charged with a stir bar was added mesitylene (84.0 mg, 0.699 mmol, 1.500 equiv.), $\text{Rh}_2(\text{S-DOSP})_3(\text{S-silicaSP})$ (**80**) (85.0 mg, 0.005 mmol, 0.010 equiv.), and styrene (99.0 mg, 0.953 mmol, 2.00 equiv.). The reactants were dissolved in hexanes (6 mL dry, degassed). A 0.01 mL aliquot was removed from the reaction mixture at reaction time point of 0 min and prepared for analysis by GC. In a separate 20 mL glass vial, phenyldiazoacetate (84 mg, 0.4766 mmol, 1.00 equiv.) was then dissolved in hexanes (10 mL dry, degassed). Half of the solution of phenyldiazoacetate in hexanes (5 mL) was then added to the reaction mixture over 7.5 min. by syringe pump. 0.01 mL aliquots were removed from the reaction mixture at reaction time points of 2 min., 4 min., 6 min., and 7.5 min. into the phenyldiazoacetate addition and prepared for analysis by GC. $\text{Rh}_2(\text{S-DOSP})_3(\text{S-silicaSP})$ (**80**) was then removed from the reaction mixture by vacuum filtration. The filtrate was then filtered then subjected to vacuum filtration three additional times to ensure complete removal of **80** from the reaction mixture. The reaction was then allowed to stir. A 0.01 mL aliquot was removed from the reaction mixture and prepared for analysis by GC (at reaction time point of 0 min. with respect to the second addition of phenyldiazoacetate). The remainder of the solution of phenyldiazoacetate in hexanes (5 mL) was then added to the reaction mixture over 7.5 min. by syringe pump. 0.01 mL aliquots were removed from the reaction mixture at reaction time points 10 min., 30 min., 60 min., 120 min.

into the second phenyldiazoacetate addition and prepared for analysis by GC. The remaining solution was concentrated *in vacuo* and sent for elemental analysis to determine the amount of Rh leaching. The filtration test was then repeated a second time to verify the results. All 0.01 mL aliquots were prepared for GC analysis by filtering the sample through a 1 cm. plug of silica eluting with diethyl ether.

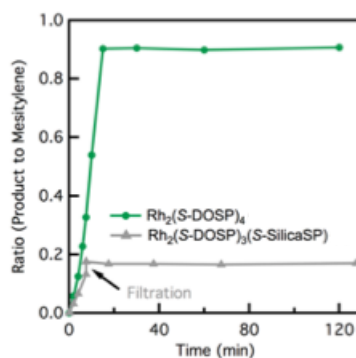
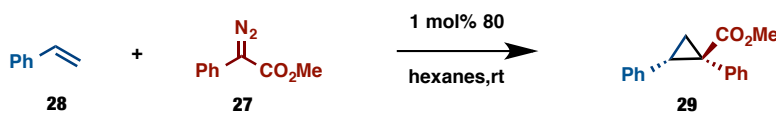


Figure S1. The amount of product produced from the cyclopropanation reaction for both the homogeneous $\text{Rh}_2(\text{S-DOSP})_4$ catalyst and the silica-immobilized complex $\text{Rh}_2(\text{S-DOSP})_3(\text{S-silicaSP})$ (**80**). The $\text{Rh}_2(\text{S-DOSP})_3(\text{S-silicaSP})$ (**80**)-catalyzed reaction mixture was filtered at 7.5 min. to remove the catalyst before adding the remaining portion of the diazo (up to 15 mins). For the homogeneous catalyst, the amount of product increased until the end of the addition of the diazo. For the heterogeneous catalyst, the amount of product did not increase after filtration, indicating the robust immobilization of the complex.

Recycling Study: *Experimental Details:*



cycle	yield (%)	ee(%)
1	72	80
2	78	81
3	75	79
4	76	77
5	78	79
$\text{Rh}_2(\text{S-DOSP})_4$	88	88

To a pre-weighed, dried and argon-purged 20 mL glass vial charged with a magnetic stir bar was added $\text{Rh}_2(\text{S-DOSP})_3(\text{S-silicaSP})$ (**80**) (250 mg, 0.02 mmol, 0.01 equiv.) and hexanes (4 mL, dry, degassed). In a separate 20 mL glass vial was added phenyldiazoacetate (**27**) (264 mg, 1.50 mmol, 1.00 equiv.) and styrene (**28**) (312 mg, 3.00 mmol, 2.00 equiv.) in hexanes (8 mL dry, degassed). The solution of phenyldiazoacetate and styrene in hexanes was then added to the catalyst slurry over 30 min. by syringe pump. Once the addition was complete and the reaction had gone to completion, **80** was washed with hexanes (3 x 5 mL dry, degassed) and the hexanes washings pipetted out and collected. The reaction mixture was then concentrated *in vacuo*. The 20 mL glass reaction vial containing **80** was then charged with additional hexanes (4 mL dry, degassed) and the reaction sequence was subsequently repeated five times using the same catalyst. The cyclopropanation products of the five cycles were purified using silica gel column chromatography (hexanes : ethyl acetate 100 : 4.5) to afford clear oil: cycle 1 (271 mg, 72% yield), cycle 2 (295 mg, 78% yield), cycle 3 (285 mg, 75% yield), cycle 4 (286 mg, 76% yield), cycle 5 (295 mg, 78% yield); HPLC: (Chiralcel SS-WHELK, 1% *i*-PrOH in hexane, 1.0 mL/min, 1 mg/mL, 30 min, $\lambda = 254$ nm) retention times of 8.62 min (major) and 10.22 min (minor), 80% ee for cycle 1; 81% ee for cycle 2; 79% ee for cycle 3, 77% ee for cycle 4, 79% ee for cycle 5;

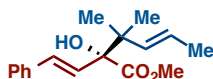
$R_f = 0.25$ (hexane: ethyl acetate 10:1); ^1H NMR (600 MHz, CDCl_3) δ 7.12-7.11 (m, 3H), 7.05-7.01 (m, 5H), 6.77-6.75 (m, 2H), 3.70 (s, 3H), 3.11 (dd, $J = 7.2, 9.3$, 1H), 2.13 (dd, $J = 4.8, 9.3$, 1H), 1.88 (dd, $J = 4.8, 7.2$, 1H); ^{13}C NMR (100 MHz, CDCl_3) δ 174.5, 136.5, 134.9, 132.1, 128.2, 127.9, 127.2, 126.5, 52.8, 37.6, 33.3, 20.7; Data are consistent with the literature.⁵¹



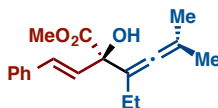
Methyl (*R,E*)-2-propyl-1-styrylcycloprop-2-ene-1-carboxylate (105):³⁷ A mixture of 1-pentyne (**103**) (34.0 mg, 0.50 mmol, 1.00 equiv.) and $\text{Rh}_2(\text{S-DOSP})_3(\text{S-silicaSP})$ (**80**) (179 mg, 0.01 mmol, 0.02 equiv.) were added to a 25 mL dry and argon-purged round-bottom flask and stirred in dry, degassed hexanes (1 mL). The reaction mixture was then cooled to $-45\text{ }^\circ\text{C}$ in an acetonitrile/ $\text{CO}_2(\text{s})$ bath under an atmosphere of argon. Styryldiazoacetate (**104**) (202 mg, 1.00 mmol, 2.00 equiv.) in hexanes (10 mL) was then added to the reaction mixture *via* syringe pump over 2 h. After the addition was complete, the mixture was stirred for an additional 20 min. The product was then separated from the catalyst by vacuum filtration. $\text{Rh}_2(\text{S-DOSP})_3(\text{S-silicaSP})$ (**80**) was then washed with dry, degassed hexanes (5 x 10 mL) and the filtrate was then concentrated *in vacuo*. The product was obtained in >20:1 dr as determined by ^1H NMR analysis of the crude reaction mixture. The residue was then purified through silica gel eluting with hexane : ether (15 : 1) to afford a yellow oil (87 mg, 72% yield). Enantioenrichment was determined by chiral HPLC analysis after purification: (Chiralcel (*R,R*)-Whelk, 5% *i*-PrOH in hexane, 1.0 mL/min, 1 mg/mL, 30 min, $\lambda = 254\text{ nm}$) retention times of 8.40 min (minor) and 10.37 min (major), 95% ee. The spectral data were identical to those previously reported.³⁷ The $\text{Rh}_2(\text{S-DOSP})_4$ -catalyzed reaction between **103** and **104** has been previously reported to give **105** in 81% yield and 99% ee.³⁷



Methyl (1S,2S)-2-phenyl-1-((E)-styryl)cyclopropane-1-carboxylate (106):^{36a} A mixture of styrene (**28**) (260.0 mg, 2.500 mmol, 5.000 equiv.) and Rh₂(S-DOSP)₃(S-silicaSP) (**80**) (89.0 mg, 0.005 mmol, 0.010 equiv) were added to a 25 mL dry and argon-purged round-bottom flask and stirred in dry, degassed pentane (4 mL). The reaction mixture was then cooled to -78 °C in an acetone/CO₂(s) bath under an atmosphere of argon. Styryldiazoacetate (**104**) (101.0 mg, 0.500 mmol, 1.000 equiv.) in pentane (8 mL) was then added to the reaction mixture *via* syringe pump over 10 min. After the addition was complete, the mixture was allowed to slowly warm to room temperature overnight. The product was then separated from the catalyst by vacuum filtration. Rh₂(S-DOSP)₃(S-silicaSP) (**80**) was then washed with dry, degassed pentane (5 x 10 mL) and the filtrate was then concentrated *in vacuo*. The product was obtained in >20:1 dr as determined by ¹H NMR analysis of the crude reaction mixture. The residue was then purified through silica gel eluting with pentane : ether (increasing from 100 : 0 to 90 : 10) to afford a white solid (127 mg, 92% yield). Enantioenrichment was determined by chiral HPLC analysis after purification: (Chiralcel OJ-H, 1.5% *i*-PrOH in hexane, 1.0 mL/min, 1 mg/mL, 30 min, λ = 254 nm) retention times of 13.17 min (major) and 17.91 min (minor), 96% ee. The spectral data were identical to those previously reported.^{36a} The Rh₂(S-DOSP)₄-catalyzed reaction between **28** and **27** has been previously reported to give **106** in 69% yield and 98% ee.^{36a}

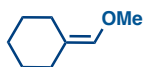


Methyl (*R,E*)-2-hydroxy-3,3-dimethyl-2-((*E*)-styryl)hex-4-enoate (108**):**^{40a} A mixture of 4-methylpent-3-en-2-ol (**107**) (50.00 mg, 0.500 mmol, 1.000 equiv.) and Rh₂(*S*-DOSP)₃(*S*-silicaSP) (**80**) (89.00 mg, 0.005 mmol, 0.010 equiv) were added to a 25 mL dry and argon-purged round-bottom flask and stirred in dry, degassed pentane (1 mL). The reaction mixture was then cooled to 0 °C in an ice bath under an atmosphere of argon. Styryldiazoacetate (**104**) (113.0 mg, 0.550 mmol, 1.100 equiv.) in pentane (5 mL) was then added to the reaction mixture *via* syringe pump over 1 h. After the addition was complete, the mixture was stirred for an additional 30 min. The product was then separated from the catalyst by vacuum filtration. Rh₂(*S*-DOSP)₃(*S*-silicaSP) (**80**) was then washed with dry, degassed pentane (5 x 10 mL) and the filtrate was then concentrated *in vacuo*. The product was obtained in >20:1 dr as determined by ¹H NMR analysis of the crude reaction mixture. The residue was then purified through silica gel eluting with pentane : diethyl ether (10 : 1) to afford a clear oil (91.0 mg, 66% yield). Enantioenrichment was determined by chiral HPLC analysis after purification: (Chiralcel (*S,S*)-WHELK-O1, 0.5% *i*-PrOH in hexane, 0.7 mL/min, 1 mg/mL, 30 min, λ = 254 nm) retention times of 12.70 min (major) and 15.00 min (minor), 96% ee. The spectral data were identical to those previously reported.^{40a} The Rh₂(*S*-DOSP)₄-catalyzed reaction between **107** and **104** has been previously reported to give **108** in 66% yield and 98% ee.^{40a}



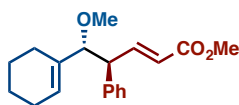
Methyl (*R,E*)-3-ethyl-2-hydroxy-5-methyl-2-styrylhexa-3,4-dienoate (110**):**^{40b} A mixture of 2-methyl-3-hexyn-2-ol (**109**) (56.00 mg, 0.500 mmol, 1.000 equiv.) and Rh₂(*S*-DOSP)₃(*S*-

silicaSP) (**80**) (89.00 mg, 0.005 mmol, 0.010 equiv) were added to a 25 mL dry and argon-purged round-bottom flask and stirred in dry, degassed pentane (1 mL). The reaction mixture was then cooled to 0 °C in an ice bath under an atmosphere of argon. Styryldiazoacetate (**104**) (209.0 mg, 1.000 mmol, 2.000 equiv.) in pentane (9 mL) was then added to the reaction mixture *via* syringe pump over 1.5 h. After the addition was complete, the mixture was stirred for an additional 2 h. The product was then separated from the catalyst by vacuum filtration. Rh₂(S-DOSP)₃(S-silicaSP) (**80**) was then washed with dry, degassed pentane (5 x 10 mL) and the filtrate was then concentrated *in vacuo*. The product was obtained in >20:1 dr as determined by ¹H NMR analysis of the crude reaction mixture. The residue was then purified through silica gel eluting with pentane : diethyl ether (5 : 1) to afford a clear oil (110.0 mg, 73% yield). Enantioenrichment was determined by chiral HPLC analysis after purification: (Chiralcel AD-H, 1% *i*-PrOH in hexane, 0.6 mL/min, 1 mg/mL, 30 min, λ = 254 nm) retention times of 21.36 min (major) and 26.69 min (minor), 94% ee. The spectral data were identical to those previously reported.^{40b} The Rh₂(S-DOSP)₄-catalyzed reaction between **109** and **104** has been previously reported to give **110** in 74% yield and 96% ee.^{40b}



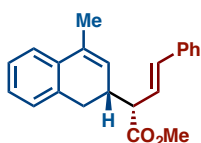
(methoxymethylene)cyclohexane (111): To a dry, argon-purged 1 L round bottom flask was added (methoxymethyl)triphenyl phosphonium chloride (37.50 g, 109.4 mmol, 1.200 equiv.) and tetrahydrofuran (THF) (500 mL). The slurry was then cooled to -78 °C in a CO₂(s)/acetone bath. Potassium *tert*-butoxide (12.30 g, 109.4 mmol, 1.200 equiv.) was then added in one portion *via* funnel. The reaction mixture was then warmed to 0 °C over 20 min. The solution was then re-cooled to -78 °C. Cyclohexanone (9.400 mL, 91.20 mmol, 1.000 equiv.) was then added dropwise to the reaction mixture. The reaction was then allowed to warm to room temperature

and stir overnight. The reaction mixture was then washed with satd. aqueous ammonium chloride (2 x 150 mL) and satd. aqueous sodium chloride (150 mL) and then dried over magnesium sulfate. The solids were removed by gravity filtration and the reaction mixture was concentrated *in vacuo*. The crude product was purified using silica gel column chromatography (pentane : diethyl ether 10:1) and then distilled by Kugelrohr at 2.0×10^1 Torr at 50 °C to afford clear oil (8.100 g, 70% yield). $R_f = 0.78$ (pentane : diethyl ether 10 : 1); $^1\text{H NMR}$ (400 MHz, CDCl_3) δ 5.75 (s, 1H), 3.54 (s, 3H), 2.17 (t, $J = 5.4$ Hz, 2H), 1.94 (t, $J = 5.4$ Hz, 2H), 1.56-1.44 (m, 6H); $^{13}\text{C NMR}$ (100 MHz, CDCl_3) δ 138.9, 118.4, 59.3, 30.7, 28.5, 27.2, 27.0, 25.6; IR (film): 3054, 2953, 2921, 2854, 1736, 1434, 1229, 1120, 743, 695; HRMS (ESI) calcd for $\text{C}_8\text{H}_{15}\text{O}_6\text{N}_4$ (M+H) $^+$ 263.0982 found 263.0986.



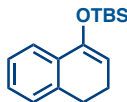
Methyl (4*S*,5*R*,*E*)-5-(cyclohex-1-en-1-yl)-5-methoxy-4-phenylpent-2-enoate (112):⁴² A mixture of (methoxymethylene)cyclohexane (**111**) (63.00 mg, 0.500 mmol, 1.000 equiv.) and $\text{Rh}_2(\text{S-DOSP})_3(\text{S-silicaSP})$ (**80**) (89.00 mg, 0.005 mmol, 0.010 equiv) were added to a 100 mL dry and argon-purged round-bottom flask and stirred in dry, degassed hexanes (10 mL). The reaction mixture was then cooled to -25 °C in an acetonitrile/ $\text{CO}_2(\text{s})$ bath under an atmosphere of argon. Styryldiazoacetate (**104**) (162.0 mg, 1.000 mmol, 2.000 equiv.) in hexanes (10 mL) was then added to the reaction mixture *via* syringe pump over 3 h. After the addition was complete, the mixture was warmed to room temperature over 2 h. The product was then separated from the catalyst by vacuum filtration. $\text{Rh}_2(\text{S-DOSP})_3(\text{S-silicaSP})$ (**80**) was then washed with dry, degassed hexanes (5 x 10 mL) and the filtrate was then concentrated *in vacuo*. The product was obtained in >20:1 dr as determined by $^1\text{H NMR}$ analysis of the crude reaction mixture. The

residue was then purified through silica gel eluting with pentane : diethyl ether (10 : 1) to afford a clear oil (119.0 mg, 79% yield). Enantioenrichment was determined by chiral HPLC analysis after purification: (Chiralcel AS-H, 1% *i*-PrOH in hexane, 0.7 mL/min, 1 mg/mL, 30 min, λ = 254 nm) retention times of 7.12 min (major) and 7.87 min (minor), 94% ee. The spectral data were identical to those previously reported.⁴² The Rh₂(*S*-DOSP)₄-catalyzed reaction between **111** and **104** has been previously reported to give **112** in 88% yield and 99% ee.⁴²

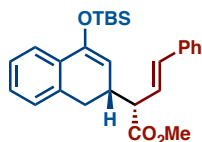


Methyl (*S,E*)-2-((*R*)-4-methyl-1,2-dihydronaphthalen-2-yl)-4-phenylbut-3-enoate (115**):**⁴³ A mixture of 1-Methyl-3,4-dihydronaphthalene (**113**) (72.0 mg, 0.500 mmol, 1.00 equiv.) and Rh₂(*S*-DOSP)₃(*S*-silicaSP) (**80**) (89.0 mg, 0.005 mmol, 0.01 equiv) were added to a 25 mL dry and argon-purged round-bottom flask and stirred in dry, degassed 2,2-dimethyl butane (DMB) (1 mL). The reaction mixture was then cooled to 0 °C in an ice bath under an atmosphere of argon. Styryldiazoacetate (**104**) (111 mg, 0.550 mmol, 1.10 equiv.) in DMB (5 mL) was then added to the reaction mixture *via* syringe pump over 45 min. After the addition was complete, the mixture was allowed to stir overnight at room temperature. The product was then separated from the catalyst by vacuum filtration. Rh₂(*S*-DOSP)₃(*S*-silicaSP) (**80**) was then washed with dry, degassed DMB (5 x 10 mL) and the filtrate was then concentrated *in vacuo*. The product was obtained in >20:1 dr as determined by ¹H NMR analysis of the crude reaction mixture. The residue was then purified through silica gel eluting with pentane : diethyl ether (20 : 1) to afford a white solid (143 mg, 90% yield). Enantioenrichment was determined by chiral HPLC analysis after purification: (Chiralcel OD-H, 2% *i*-PrOH in hexane, 0.8 mL/min, 1 mg/mL, 30 min, λ = 254 nm) retention times of 8.14 min (major) and 9.70 min (minor), 96% ee. The spectral data

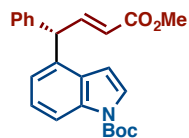
were identical to those previously reported.⁴³ The Rh₂(S-DOSP)₄-catalyzed reaction between **113** and **104** has been previously reported to give **115** in 95% yield and 99% ee.⁴³



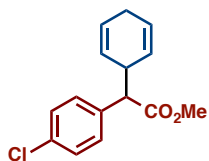
tert-butyl((3,4-dihydronaphthalen-1-yl)oxy)dimethylsilane (114): To a 500 mL dry, argon-purgen round bottom flask was added α -tetralone (9.0 g, 60 mmol, 1.0 equiv.) and dichloromethane (DCM) (70 mL). The solution was cooled to 0°C in an ice bath. Triethylamine (16.8 mL, 120 mmol, 2.00 equiv.) was then added. At this time the reaction mixture turned from a light brown to a deep brown colored solution. *Tert*-Butyldimethylsilyl trifluoromethane sulfonate (TBSOTf) (15.3 mL, 66.0 mmol, 1.10 equiv.) was then added dropwise to the reaction mixture over 30 min. The reaction was then allowed to stir for 1 h. Satd. aqueous sodium chloride (40 mL) was then added and the organic layer was separated. The aqueous layer was then extracted with DCM (3 x 150 mL). The combined organic layers were then washed with satd. aqueous ammonium chloride (150 mL) and satd. aqueous sodium chloride (150 mL) and then dried over magnesium sulfate. The solids were removed by gravity filtration and the reaction mixture was concentrated *in vacuo*. The crude product was purified using silica gel column chromatography (pentane : diethyl ether 40:1) to afford clear oil (11.4 g, 73% yield). R_f = 0.43 (pentane : diethyl ether 40 : 1); ¹H NMR (400 MHz, CDCl₃) δ 7.47 (d, J = 7.8 Hz, 1H), 7.23-7.11 (m, 3H), 5.18 (t, J = 4.4 Hz, 1H), 2.77 (t, J = 7.8 Hz, 2H), 2.34-2.29 (m, 2H), 1.03 (s, 9H), 0.22 (s, 6H); ¹³C NMR (100 MHz, CDCl₃) δ 148.5, 137.3, 133.8, 127.4, 127.1, 126.3, 122.0, 105.0, 28.4, 26.1, 22.4, 18.5; IR (film): 2929 2885, 2857, 1637, 1471, 1360, 1337, 1248, 1188, 1139, 1092, 1045, 940, 914, 835, 791, 736, 670; HRMS (APCI) calcd for C₁₆H₂₅OSi (M+H)⁺ 261.1669 found 261.1669.



Methyl (S,E)-2-((R)-4-((tert-butyldimethylsilyloxy)-1,2-dihydronaphthalen-2-yl)-4-phenylbut-3-enoate (116):⁴³ A mixture of *tert*-butyl((3,4-dihydronaphthalen-1-yl)oxy)dimethylsilane (**114**) (130.0 mg, 0.500 mmol, 1.000 equiv.) and Rh₂(*S*-DOSP)₃(*S*-silicaSP) (**80**) (89.0 mg, 0.005 mmol, 0.010 equiv.) were added to a 25 mL dry and argon-purged round-bottom flask and stirred in dry, degassed 2,2-dimethyl butane (DMB) (1 mL). The reaction mixture was then cooled to 0 °C in an ice bath under an atmosphere of argon. Styryldiazoacetate (**104**) (111.0 mg, 0.550 mmol, 1.100 equiv.) in DMB (5 mL) was then added to the reaction mixture *via* syringe pump over 45 min. After the addition was complete, the mixture was allowed to stir for an additional 2 h at room temperature. The product was then separated from the catalyst by vacuum filtration. Rh₂(*S*-DOSP)₃(*S*-silicaSP) (**80**) was then washed with dry, degassed DMB (5 x 10 mL) and the filtrate was then concentrated *in vacuo*. The product was obtained in >20:1 dr as determined by ¹H NMR analysis of the crude reaction mixture. The residue was then purified through silica gel eluting with pentane : diethyl ether (20 : 1) to afford a clear oil (163 mg, 75% yield). Enantioenrichment was determined by chiral HPLC analysis after purification: (Chiralcel OD-H, 2% *i*-PrOH in hexane, 0.8 mL/min, 1 mg/mL, 30 min, λ = 254 nm) retention times of 5.80 min (major) and 7.55 min (minor), 90% ee. The spectral data were identical to those previously reported.⁴³ The Rh₂(*S*-DOSP)₄-catalyzed reaction between **114** and **104** has been previously reported to give **116** in 78% yield and 95% ee.⁴³



***Tert*-butyl (S,E)-4-(4-methoxy-4-oxo-1-phenylbut-2-en-1-yl)-1H-indole-1-carboxylate (118):**⁴⁴ A mixture of *tert*-butyl 4-acetoxy-6,7-dihydro-1H-indole-1-carboxylate (**117**) (138.0 mg, 0.500 mmol, 1.000 equiv.) and Rh₂(*S*-DOSP)₃(*S*-silicaSP) (**80**) (89.0 mg, 0.005 mmol, 0.010 equiv) were added to a 25 mL dry and argon-purged round-bottom flask and stirred in dry, degassed 2,2-dimethyl butane (DMB) (10 mL). Styryldiazoacetate (**104**) (131.0 mg, 0.650 mmol, 1.300 equiv.) in DMB (5 mL) and anhydrous, degassed α,α,α -trifluorotoluene (TFT) (5 mL) was then added to the reaction mixture *via* syringe pump over 30 min. The product was then separated from the catalyst by vacuum filtration. Rh₂(*S*-DOSP)₃(*S*-silicaSP) (**80**) was then washed with dry, degassed DMB (5 x 10 mL) and the filtrate was then concentrated *in vacuo*. The product was obtained in >20:1 dr as determined by ¹H NMR analysis of the crude reaction mixture. The residue was then purified through silica gel eluting with pentane:diethyl ether (7:1) to afford a sticky white solid (115.0 mg, 59% yield). Enantioenrichment was determined by chiral HPLC analysis after purification: (Chiralcel OD-H, 2% *i*-PrOH in hexane, 0.8 mL/min, 1 mg/mL, 30 min, λ = 254 nm) retention times of 7.81 min (major) and 17.71 min (minor), 96% ee. The spectral data were identical to those previously reported.⁴⁴ The Rh₂(*S*-DOSP)₄-catalyzed reaction between **117** and **104** has been previously reported to give **118** in 65% yield and 98% ee.⁴⁴



Methyl 2-(4-chlorophenyl)-2-(cyclohexa-2,5-dien-1-yl)acetate:⁵² According to the known literature procedure,⁵³ a mixture of cyclohexa-1,4-diene (200.0 mg, 2.500 mmol, 5.000 equiv.) and $\text{Rh}_2(\text{S-DOSP})_3(\text{S-silicaSP})$ (**80**) (89.0 mg, 0.005 mmol, 0.010 equiv) were added to a 25 mL dry and argon-purged round-bottom flask and stirred in dry, degassed hexanes (2.5 mL). The reaction mixture was then cooled to $-50\text{ }^\circ\text{C}$ in an acetonitrile / dry ice bath under an atmosphere of argon. Methyl 2-(4-chlorophenyl)-2-diazoacetate (105.0 mg, 0.500 mmol, 1.000 equiv.) in hexanes (5 mL) was then added to the reaction mixture *via* syringe pump over 1 hour. The product was then separated from the catalyst by vacuum filtration. $\text{Rh}_2(\text{S-DOSP})_3(\text{S-silicaSP})$ (**80**) was then washed with dry, degassed hexanes (5 x 10 mL) and the filtrate was then concentrated *in vacuo*. The product was obtained in >20:1 dr as determined by ^1H NMR analysis of the crude reaction mixture. The residue was then purified through silica gel eluting with 2% ether / petroleum ether to afford a clear oil (75.0 mg, 58% yield). Enantioenrichment was determined by chiral HPLC analysis after purification: (Daicel OD, 0.5% *i*-PrOH in hexane, 1.0 mL/min, 1 mg/mL, 30 min, $\lambda = 230\text{ nm}$) retention times of 5.30 min (minor) and 7.36 min (major), 80% ee. The spectral data were identical to those previously reported.⁵² The $\text{Rh}_2(\text{S-DOSP})_4$ -catalyzed reaction between cyclohexa-1,4-diene and methyl 2-(4-chlorophenyl)-2-diazoacetate gave methyl 2-(4-chlorophenyl)-2-(cyclohexa-2,5-dien-1-yl)acetate in 84% yield and 94% ee.

References

1. Smith, M. B.; March, J. *March's Advanced Organic Chemistry: Reactions, Mechanisms, and*

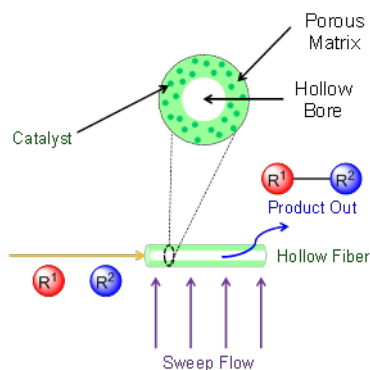
- Structure, 5th Edition*. Wiley: **2000**; p 1824.
2. De Vos, D. E.; Vankelecom, I. F. J.; Jacobs, P. A. *Chiral Catalyst Immobilization and Recycling*. Wiley: **2000**; p 32.
 3. Soai, K.; Watanabe, M. *Tetrahedron: Asymmetry* **1991**, *2*, 97.
 4. Paulissen, R.; Reimlinger, H.; Hayez, E.; Hubert, A. J.; Teyssie, P. *Tetrahedron Lett.* **1973**, *24*, 2233.
 5. Brunner, H.; Kluschanzoff, H.; Wutz, K. *Bull. Soc. Chim. Belg.* **1989**, *98*, 63.
 6. Doyle, M. P.; McKervey, M. A.; Ye, T., *Modern Catalytic Methods for Organic Synthesis with Diazo Compounds: From Cyclopropanes to Ylides*. Wiley: **1998**; p 652.
 7. (a) Davies, H. M. L.; Antoulinakis, E. G. *Org. React.* **2001**, *57*, 1; (b) Davies, H. M. L. *Eur. J. Org. Chem.* **1999**, *10*, 2459.
 8. Kennedy, M.; McKervey, M. A.; Maguire, A. R.; Roos, G. H. P. *J. Chem. Soc. Chem. Commun.* **1990**, *5*, 361.
 9. (a) Watanabe, N.; Ogawa, T.; Ohtake, Y.; Ikegami, S.; Hashimoto, S.-i. *Synlett* **1996**, *1*, 85; (b) Hashimoto, S.; Watanabe, N.; Ikegami, S. *Tetrahedron Lett.* **1990**, *31*, 5173.
 10. Doyle, M. P.; Timmons, D. J.; Tumonis, J. S.; Gau, H.-M.; Blossey, E. C. *Organometallics* **2002**, *21*, 1747.
 11. Bergbreiter, D. E.; Morvant, M.; Chen, B. *Tetrahedron Lett.* **1991**, *32*, 2731.
 12. Doyle, M. P.; Eismont, M. Y.; Bergbreiter, D. E.; Gray, H. N. *J. Org. Chem.* **1992**, *57*, 6103.
 13. Doyle, M. P.; Yan, M.; Gau, H.-M.; Blossey, E. C. *Org. Lett.* **2003**, *5*, 561.
 14. Nagashima, T.; Davies, H. M. L. *Org. Lett.* **2002**, *4*, 1989.
 15. Davies, H. M. L.; Walji, A. M.; Nagashima, T. *J. Am. Chem. Soc.* **2004**, *126*, 4271.
 16. Davies, H. M. L.; Walji, A. M. *Org. Lett.* **2003**, *5*, 479.
 17. Davies, H. M. L.; Walji, A. M. *Org. Lett.* **2005**, *7*, 2941.
 18. (a) Kobayashi, S.; Ishida, T.; Akiyama, R. *Org. Lett.* **2001**, *3*, 2649; (b) Kobayashi, S.; Endo, M.; Nagayama, S. *J. Am. Chem. Soc.* **1999**, *121*, 11229; (c) Nagayama, S.; Endo, M.; Kobayashi, S. *J. Org. Chem.* **1998**, *63*, 6094; (d) Kobayashi, S.; Nagayama, S. *J. Am. Chem. Soc.* **1998**, *120*, 2985.
 19. Takeda, K.; Oohara, T.; Anada, M.; Nambu, H.; Hashimoto, S. *Angew. Chem., Int. Ed.* **2010**, *49*, 6979.
 20. Oohara, T.; Nambu, H.; Anada, M.; Takeda, K.; Hashimoto, S. *Adv. Synth. Catal.* **2012**, *354*, 2331.
 21. (a) Van Alsten, J. G.; Reeder, L. M.; Stanchina, C. L.; Knoechel, D. J. *Org. Process Res. Dev.* **2008**, *12*, 989; (b) Kulkarni, A. A.; Kalyani, V. S.; Joshi, R. A.; Joshi, R. R. *Org. Process Res. Dev.* **2009**, *13*, 999; (c) Baumann, M.; Baxendale, I. R.; Martin, L. J.; Ley, S. V. *Tetrahedron* **2009**, *65*, 6611; (d) Baxendale, I. R.; Griffiths-Jones, C. M.; Ley, S. V.; Tranmer, G. K. *Synlett* **2006**, *3*, 427.
 22. (a) Gill, C. S.; Venkatasubbaiah, K.; Phan, N. T. S.; Weck, M.; Jones, C. W. *Chem. - Eur. J.* **2008**, *14*, 7306; (b) Zheng, X.; Jones, C. W.; Weck, M. *Chem. - Eur. J.* **2006**, *12*, 576; (c) Zheng, X.; Jones, C. W.; Weck, M. *J. Am. Chem. Soc.* **2007**, *129*, 1105; (d) Zheng, X.; Jones, C. W.; Weck, M. *Adv. Synth. Catal.* **2008**, *350*, 255; (e) Jain, S.; Zheng, X.; Jones, C. W.; Weck, M.; Davis, R. J. *Inorg. Chem.* **2007**, *46*, 8887.
 23. Gill, C. S.; Venkatasubbaiah, K.; Jones, C. W. *Adv. Synth. Catal.* **2009**, *351*, 1344.
 24. (a) Shaw, Y.-J.; Yang, Y.-T.; Garrison, J. B.; Kyprianou, N.; Chen, C.-S. *J. Med. Chem.* **2004**, *47*, 4453; (b) Greig, I. R.; Idris, A. I.; Ralston, S. H.; van't Hof, R. J. *J. Med. Chem.* **2006**, *49*, 7487.

25. Lin, S.; Song, C.-X.; Cai, G.-X.; Wang, W.-H.; Shi, Z.-J. *J. Am. Chem. Soc.* **2008**, *130*, 12901.
26. Bradbury, R. H.; Butlin, R. J.; James, R., Heterocyclic compounds. Google Patents: **1999**.
27. Fedorov, A. Y.; Shchepalov, A. A.; Bol'shakov, A. V.; Shavyrin, A. S.; Kurskii, Y. A.; Finet, J. P.; Zelentsov, S. V. *Russ. Chem. Bull.* **2004**, *53*, 370.
28. Haag, R.; Roller, S. *Top. Curr. Chem.* **2004**, *242*, 1.
29. Corma, A.; Garcia, H. *Adv. Synth. Catal.* **2006**, *348*, 1391.
30. Desikan, S.; Doraiswamy, L. K. *Ind. Eng. Chem. Res.* **1995**, *34*, 3524.
31. Pelphrey, P.; Hansen, J.; Davies, H. M. L. *Chem. Sci.* **2010**, *1*, 254.
32. Davies, H. M. L.; Nagashima, T.; Klino, J. L., III *Org. Lett.* **2000**, *2*, 823.
33. Angelino, M. D.; Laibinis, P. E. *Macromolecules* **1998**, *31*, 7581.
34. Chepiga, K. M.; Feng, Y.; Brunelli, N. A.; Jones, C. W.; Davies, H. M. L. *Org. Lett.* **2013**, *15*, 6136.
35. Hamlin, J. E.; Hirai, K.; Millan, A.; Maitlis, P. M. *J. Mol. Catal.* **1980**, *7*, 543.
36. (a) Davies, H. M. L.; Bruzinski, P.; Hutcheson, D. K.; Kong, N.; Fall, M. J. *J. Am. Chem. Soc.* **1996**, *118*, 6897; (b) Chepiga, K. M.; Qin, C.; Alford, J. S.; Chennamadhavuni, S.; Gregg, T. M.; Olson, J. P.; Davies, H. M. L. *Tetrahedron* **2013**, *69*, 5765.
37. Briones, J. F.; Hansen, J.; Hardcastle, K. I.; Autschbach, J.; Davies, H. M. L. *J. Am. Chem. Soc.* **2010**, *132*, 17211.
38. Davies, H. M. L. Tetrakis[1-[[4-dodecylphenyl]sulfonyl]-(2S)-prolinate] Dirhodium. *e-EROS*, Wiley: **2001**.
39. (a) Hodgson, D. M.; Labande, A. H.; Pierard, F. Y. T. M.; Exposito Castro, M. A. *J. Org. Chem.* **2003**, *68*, 6153; (b) Hodgson, D. M.; Labande, A. H.; Pierard, F. Y. T. M. *Synlett* **2003**, *1*, 59.
40. (a) Li, Z.; Davies, H. M. L. *J. Am. Chem. Soc.* **2010**, *132*, 396; (b) Li, Z.; Boyarskikh, V.; Hansen, J. H.; Autschbach, J.; Musaev, D. G.; Davies, H. M. L. *J. Am. Chem. Soc.* **2012**, *134*, 15497; (c) Zhang, X.; Ma, M.; Wang, J. *Tetrahedron: Asymmetry* **2003**, *14*, 891.
41. Davies, H. M. L.; Hansen, T.; Rutberg, J.; Bruzinski, P. R. *Tetrahedron Lett.* **1997**, *38*, 1741.
42. Lian, Y.; Davies, H. M. L. *J. Am. Chem. Soc.* **2011**, *133*, 11940.
43. Davies, H. M. L.; Jin, Q. *J. Am. Chem. Soc.* **2004**, *126*, 10862.
44. Davies, H. M. L.; Manning, J. R. *J. Am. Chem. Soc.* **2006**, *128*, 1060.
45. Manning, J. R.; Davies, H. M. L. *Org. Synth.* **2007**, *84*, 334.
46. Itoh, T.; Matsuya, Y.; Enomoto, Y.; Ohsawa, A. *Tetrahedron* **2001**, *57*, 7277.
47. Huang, J.; Wang, H.; Wu, C.; Wulff, W. D. *Org. Lett.* **2007**, *9*, 2799.
48. Cupps, T. L.; Boutin, R. H.; Rapoport, H. *J. Org. Chem.* **1985**, *50*, 3972.
49. Pirrung, M. C.; Zhang, J. *Tetrahedron Lett.* **1992**, *33*, 5987.
50. Mironov, Y. V.; Efremova, O. A.; Solodovnikov, S. F.; Naumov, N. G.; Sheldrick, W. S.; Perrin, A.; Fedorov, V. E. *Russ. Chem. Bull.* **2004**, *53*, 2129.
51. (a) Davies, H. M. L.; Venkataramani, C. *Org. Lett.* **2003**, *5*, 1403; (b) Brooks, L. A. *J. Am. Chem. Soc.* **1944**, *66*, 1295.
52. Owens, C. P.; Varela-Alvarez, A.; Boyarskikh, V.; Musaev, D. G.; Davies, H. M. L.; Blakey, S. B. *Chem. Sci.* **2013**, *4*, 2590.
53. Davies, H. M. L.; Stafford, D. G.; Hansen, T. *Org. Lett.* **1999**, *1*, 233.

Chapter IV: The Application of Immobilized Chiral Dirhodium(II) Catalysts in Continuous Flow Processing

Advisor: Huw M. L. Davies, Ph.D.
Collaborator: Christopher W. Jones, Ph.D.

The immobilization of expensive chiral transition metal catalysts and their application in continuous flow processing has the potential to revolutionize the pharmaceutical industry by making the use of extremely reactive and selective yet expensive transition metal catalysts practical for use on a large scale. Reactions conducted in flow can be faster, safer, more efficient and more easily scaled-up. This chapter describes the synthesis of composite polymer/oxide hollow fibers and their use as flow reactors for heterogeneous dirhodium(II)-catalyzed reactions. Fiber synthesis is scalable and thus could potentially be used for large-scale production. Incorporating heterogeneous catalysts in the walls of the fibers presents an alternative to a traditional packed bed reactor and avoids large pressure drops, which is a crucial challenge in employing microreactors. This chapter describes hollow composite fibers as a platform for dirhodium(II) catalyst immobilization and application in enantioselective rhodium carbenoid flow chemistry.



4.1 Introduction to Continuous Flow Chemistry

Continuous flow chemistry is a new and emerging strategy that can significantly decrease the time from drug discovery to production by delivering pharmaceutical compounds more quickly and supporting their subsequent scale-up. Continuous flow chemistry is performed by pumping reagents together down a temperature-controlled tube to meet at a mixing junction and then exit as product (Figure 4.1). The major advantages of flow chemistry are that the reactions are faster, safer, and more easily optimized and scaled-up. Also, the products are typically cleaner and several processes can be completed simultaneously including synthesis, work-up and in-situ analysis. Flow reactors improve product quality by carefully controlling reaction variables. They increase safety by containing and regulating reactions at high temperatures and pressures. Automated reactors eliminate the need for manual handling of dangerous (toxic and explosive) and therefore shorter processing times, precise parameter control, and higher reproducibility and selectivity can be achieved.¹ Multiple flow reactors can be used sequentially for in-line purification and reaction telescoping.²

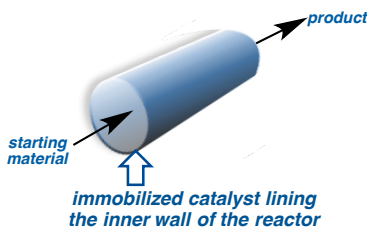


Figure 4.1 General schematic description of a continuous flow reactor

Commercial flow reactors for organic synthesis are available from numerous vendors, ranging from μL to L in volume.³ These reactors offer improved heat and mass transfer over batch reactors.^{3a, 3b, 4} As the surface area-to-volume ratio of the reactor increases, the heat and mass transfer performance of the reactor improves, which is critical for consistent product yield

and selectivity in a continuous process.^{3a}

Organic synthesis via flow chemistry is an emerging paradigm in fine chemistry and pharmaceutical production.^{3a, 3b, 4a, 5} Flow chemistry has been used by Pfizer to conduct highly exothermic reactions and/or nitrogen releasing reactions such as Curtius rearrangements or Sandmeyer reactions.²

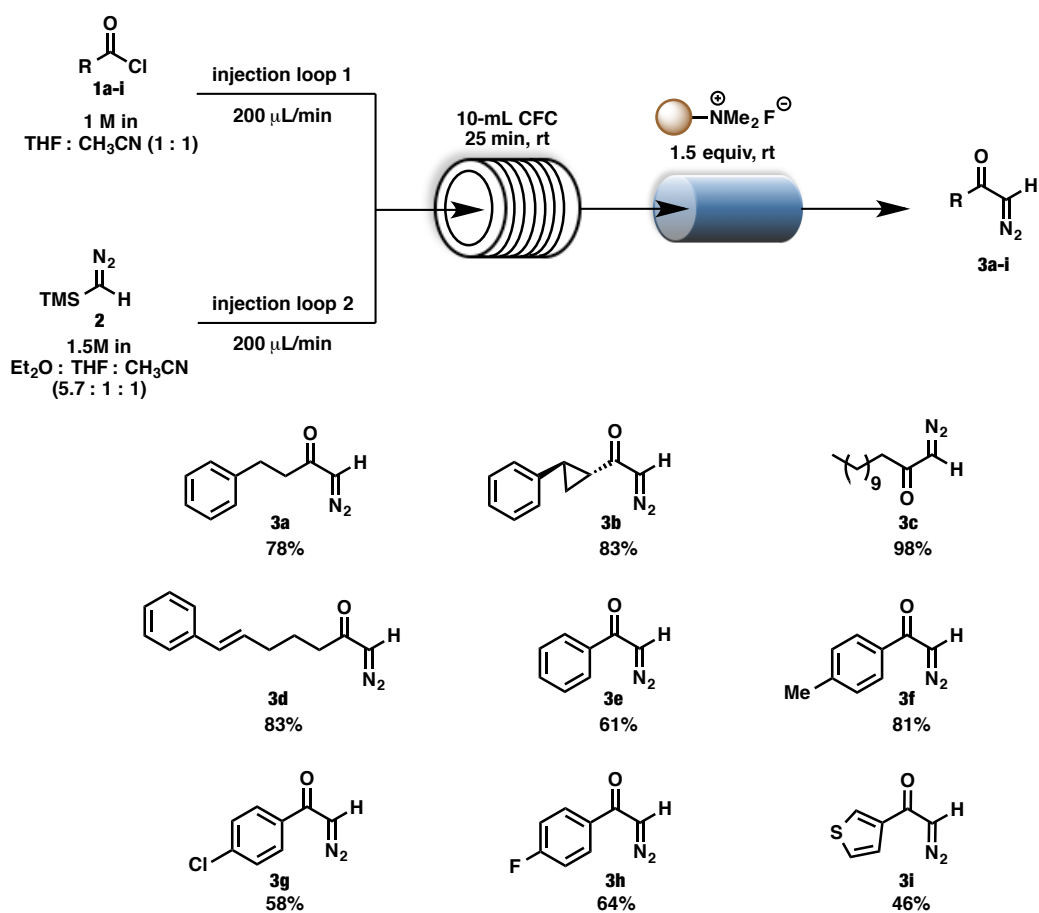
Immobilized catalysts have found use in continuous-flow processes, which adds many more benefits to this type of catalysis.⁶ Practical application of expensive catalysts can be achieved by utilization as a solid catalyst in a flow reactor.⁷ The ability of reactors to flow small volumes of reagents past a catalyst bed increases the catalyst : substrate ratio in these heterogeneously catalyzed reactions which could provide higher turnover numbers (TON) than can be achieved in typical homogeneous catalysis in batch reactions.²

4.2 Diazo Compounds in Flow Chemistry

The inherent dangers, which come with the use of diazo compounds inhibit their use on an industrial scale. Preparation and isolation of diazo compounds comes with potential risks due to their explosive nature.⁸ Flow based synthesis can potentially alleviate these problems by compartmentalizing various reagents and continuously flowing them at slow rates to a meeting point at which only a small reaction volume collects at one time. In addition, exothermic reactions involving the decomposition of diazo compounds can be carried out with ease in microreactors that allow for efficient heat and mass transfer.^{1e, 9} In a collaborative effort Ley and Baxendale were able to both produce and utilize diazo compounds in flow reactors.^{3d, 8} In these reports, they were able to overcome the ultimate challenge of using diazo compounds in flow reactors: keeping the system under a constant pressure (necessary for steady flow of reactants)

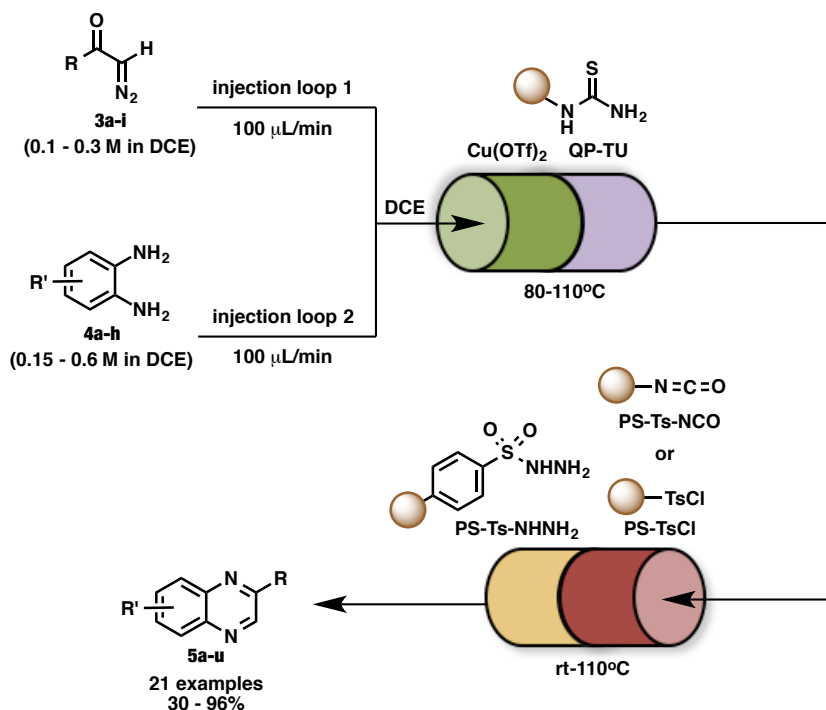
while alleviating the build up of excessive pressure resulting from extrusion of nitrogen gas during the reaction. For these reasons, a back-pressure regulator (BPR) was used to maintain a constant system pressure at 8 bar. Once a BPR was installed, continuous flow was successfully employed in a safe route to a range of acceptor diazo compounds from various acid chlorides using trimethylsilyldiazomethane as the diazotizing source.⁸ Slow addition of both the diazo compound and the acid chloride was achieved with two injection loops which only combined small volumes of reactants at any given time. Additionally, this flow process allowed for the direct purification of products with the use of polymer-supported scavengers (Scheme 4.1).⁸

Scheme 4.1 Flow Synthesis of Diazoketones



The copper-catalyzed synthesis of quinoxalines by the decomposition of diazo compounds was also achieved in flow with a variety of substituted diazo starting materials (Scheme 4.2). These two reactions (the synthesis and application of diazoketones) could be conducted as a telescoped process thus obviating the need for isolation of the unstable diazoketones.⁸

Scheme 4.2 Copper-catalyzed decomposition of diazoketones in flow



4.3 Dirhodium(II) Catalysis in a Continuous Flow Reactor

Along with the explosive nature of the diazo compounds used for rhodium carbenoid chemistry, another major limitation that hinders the use of dirhodium(II) catalysts on an industrial scale is the prohibitive cost of rhodium and its chiral ligands. These drawbacks to dirhodium catalysis can be eliminated with the application of heterogeneous catalysts in continuous flow reactors, which allows for large-scale production with very low catalyst loadings by suppressing mechanical degradation of catalyst supports. Hashimoto *et al.* recently reported the effective

immobilization of $\text{Rh}_2(\text{S-PTTL})_4$ by copolymerization. This polymer-supported $\text{Rh}_2(\text{S-PTTL})_4$ -derivative catalyzed asymmetric C–H insertions with high yields and enantioselectivities similar to those achieved with homogeneous $\text{Rh}_2(\text{S-PTTL})_4$ and could be recycled 100 times with minimal Rh leaching (See Chapter 3 for details).¹⁰ In a follow-up study, they were able to apply a similar polymer-supported dirhodium(II) complex (a mixed ligand $\text{Rh}_2(\text{S-PTTL})(\text{S-TCPTTL})_3$ -derivative (Figure 4.2) to highly enantioselective intermolecular tandem carbonyl ylide formation-1,3-dipolar cycloaddition reactions of 2-diazo-3,6-diketoesters with arylacetylene and styrene dipolarophiles under continuous flow conditions (Scheme 4.3, up to 99% ee).¹¹

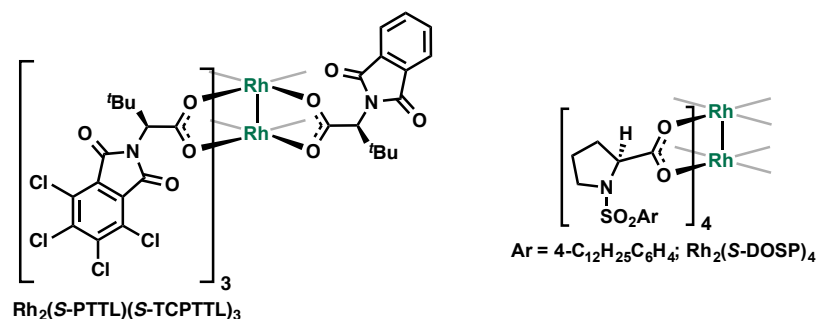
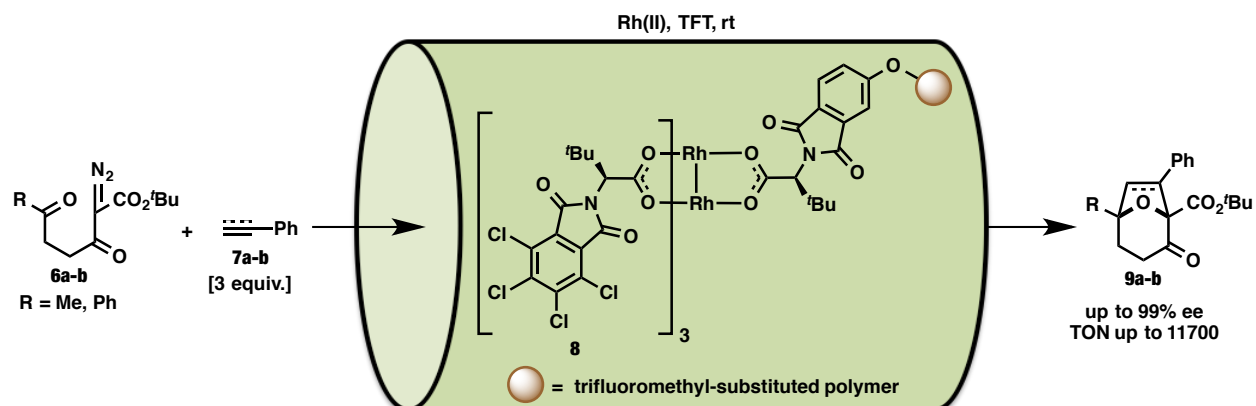


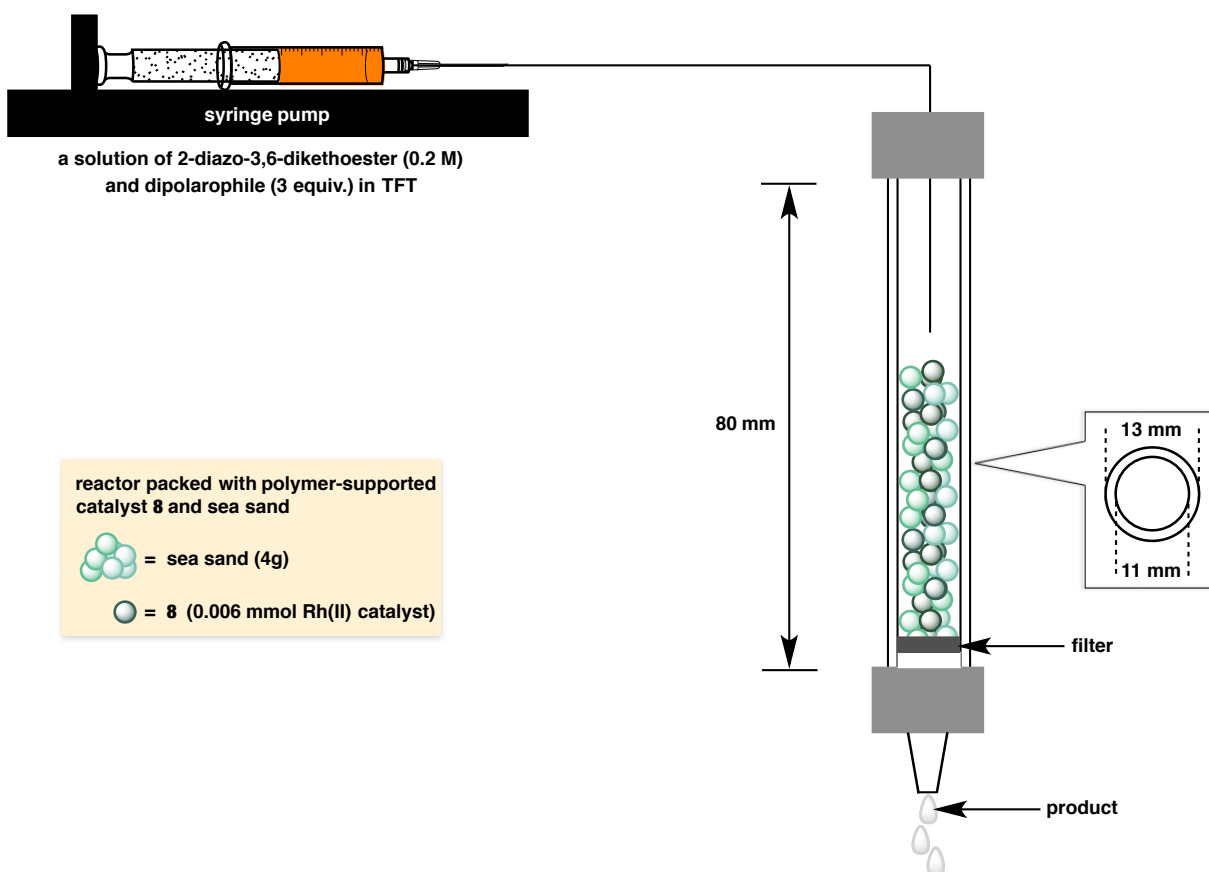
Figure 4.2 Chiral dirhodium(II) catalysts which have been successfully derivitized, immobilized, and applied in continuous flow reactors

Scheme 4.3 First continuous flow system with a polymer-supported dirhodium(II) catalyst and its application in cycloaddition catalysis



Hashimoto's flow system employed a tube packed with a slurry of catalyst **8** and sea sand in trifluorotoluene equipped with a filter. A solution of diazodiketoester (**6a-b**) and styrene or phenylacetylene (**7a-b**) was passed through the flow reactor using a syringe pump (Scheme 4.4). The continuous flow experiments gave higher yields than the reaction under batch conditions with the homogeneous counterpart to **8**, $\text{Rh}_2(\text{S-PTTL})(\text{S-TCPTTL})_3$. Also, extrusion of nitrogen gas from the decomposition of diazodiketoester did not cause complications.

Scheme 4.4 Schematic set of the first continuous flow system with a polymer-supported dirhodium(II) catalyst



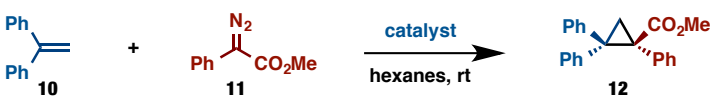
4.4 Exploratory Studies Conducted in Batch Toward the use of Silica-Immobilized-Rh₂(S-DOSP)₄-Derivatives in a Continuous Flow Reactor

The findings of Ley and Baxendale as well as Hashimoto gave us hope that intermolecular reactions of donor/acceptor diazo compounds catalyzed by our previously developed immobilized dirhodium catalyst (see Chapter 3) could be accomplished in flow. In this project, together with Jones *et al.*, we designed and developed novel flow reactors for controlling interactions of reactive diazo compounds, substrate, and catalyst in order to enhance catalyst longevity and thus increase total turnover number. In the Chapter 3, we reported an effective immobilization of Rh₂(S-DOSP)₄ which relied on single ligand exchange of Rh₂(S-DOSP)₄ with a ligand that could undergo a grafting reaction to a solid support to give an immobilizable Rh₂(S-DOSP)₄-derivative which could then be grafted to silica by AIBN initiated radical coupling. The immobilizable Rh₂(S-DOSP)₄-derivative was able to catalyze a broad range of enantioselective reactions with product yields and levels of diastereo- and enantioselectivity comparable to its homogeneous counterpart, Rh₂(S-DOSP)₄. Additionally, this catalyst system was recyclable and could be used to catalyze up to 5 consecutive reaction cycles without degradation of the yield, enantio- or diastereoselectivity and with no catalyst leaching as determined by filtration test and elemental analysis of the reaction mixture after the first cycle.¹²

We initially envisioned building a flow reactor similar to the system reported by Hashimoto *et al.* in which a tube would be either lined or filled with a silica-immobilized Rh₂(S-DOSP)₄-derivative. The commercial silica (CS-2129)-supported Rh₂(S-DOSP)₄-derivative (**13**), which was successfully employed in the system discussed in Chapter 3, is known to give high yield and levels of enantioinduction. We next wanted to see if different types of silica could be employed to give similar reactivity and selectivity. C803-supported Rh₂(S-

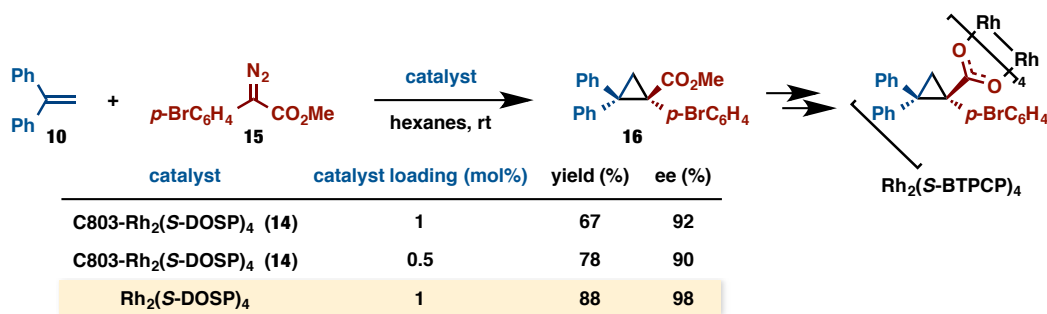
DOSP)₄-derivative (**14**) gave similar results and the catalyst loading could be decreased with only a slight resultant decrease in enantioinduction. Finally, we wanted to determine whether iron oxide supports could be used in the immobilization of Rh₂(S-DOSP)₄ as these could allow for magnetic catalyst recovery, but addition of iron oxide to the standard Rh₂(S-DOSP)₄-catalyzed reaction caused a deleterious effect on the yield of asymmetric cyclopropanation (Table 4.1).

Table 4.1 The effect of varying the support-system on the reactivity and selectivity of asymmetric cyclopropanation by immobilized Rh₂(S-DOSP)₄-derivatives



catalyst	catalyst loading (mol%)	yield (%)	ee (%)
CS2129-Rh ₂ (S-DOSP) ₄ (13)	1	73	97
C803-Rh ₂ (S-DOSP) ₄ (14)	1	72	97
C803-Rh ₂ (S-DOSP) ₄ (14)	0.5	74	94
Rh ₂ (S-DOSP) ₄ + Fe ₂ O ₃ [1 equiv.]	1	52	98
Rh ₂ (S-DOSP) ₄	1	87	97

Our ultimate goal of employing silica-immobilized Rh₂(S-DOSP)₄-derivatives in flow reactors was to be able to more efficiently produce synthetically useful compounds such as triaryl cyclopropane carboxylate **16** which is used to make a ligand for an extremely selective C–H functionalization catalyst (Rh₂(S-BTPCP)₄).¹³ Although the cyclopropanation of 1,1-diphenylethylene **10** with un-substituted phenyldiazoacetate **11** proceeded with the same selectivity as homogeneous Rh₂(S-DOSP)₄, C803-supported–Rh₂(S-DOSP)₄ catalyzed the cyclopropanation of **10** with methyl 2-(4-bromophenyl)-2-diazoacetate **15** gave the corresponding cyclopropane **16** with diminished enantioselection (Table 4.2).

Table 4.2 Application of C803-supported-Rh₂(S-DOSP)₄ in the synthesis of S-BTPCP ligand

4.5 The use of Cellulose Acetate Fiber-Immobilized-Rh₂(S-DOSP)₄-derivatives in a Continuous Flow Reactor

After thinking deeply about flow reactor design, we realized that the typical packed bed reactor, as was used by Hashimoto, may not be the best set-up for flow chemistry with extremely reactive dirhodium(II) catalysts. Upon exposure to the diazo compound, the catalyst residing at the front of the reactor would react quickly, leaving the majority of the packed bed unutilized. This could lead to deactivation of the catalyst residing at the front of the reactor as well as variability of results. We envisioned that this problem could be obviated by the use of a porous hollow fiber-immobilized catalyst system (Figure 4.3). Polymeric hollow fibers are commercially used for industrial gas separations, namely separation and purification of CO₂, and provide high surface areas at low cost.¹⁴ The small inner (~300 μm) and outer (~1100 μm) diameters of the fibers ensure that the walls are thin, which imparts excellent heat and mass transfer properties.¹⁵ In this case, the thin wall presents an extremely short reaction bed length when radial flow through the fiber wall is used. Recently, composite hollow fibers (organic polymers and inorganic fillers such as zeolites,¹⁶ silicas,¹⁷ and metal-organic frameworks (MOFs)¹⁸) have emerged as separation membranes and sorbents offering highly tunable material properties. Previous work on hollow fiber reactors focused on Pd-catalyzed reactions and alkene/alkyne hydrogenations,¹⁹

though, to the best of our knowledge, no examples of asymmetric reactions using well-defined organometallic complexes embedded in hollow fiber reactors in flow have been reported. In general, the few examples of flow catalysis using hollow fiber catalysts/reactors are for simple catalysts and reactions, with no examples in organic synthesis using well-defined asymmetric organometallic catalysts.

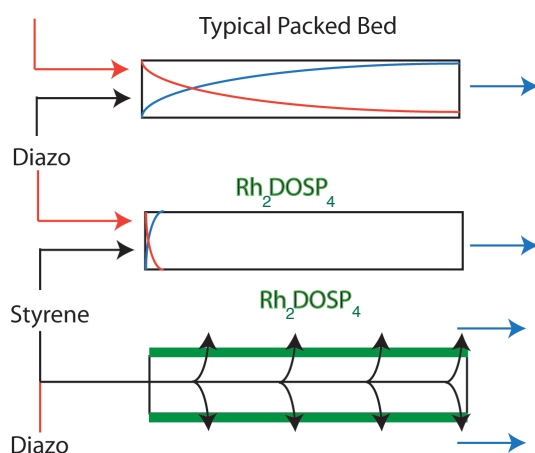


Figure 4.3 Ideal conditions for continuous flow processing employing immobilized- $\text{Rh}_2(\text{S-DOSP})_4$ -derivative

A reactor for continuous flow processing employing immobilized- $\text{Rh}_2(\text{S-DOSP})_4$ -derivative was designed by Dr. Nicholas Brunelli from the Jones laboratory. This reactor featured a small chamber in which a sweep flow of solvent could come from the front of the reactor and exit with the product at the opposite side (out flow). The porous hollow fiber-supported- $\text{Rh}_2(\text{S-DOSP})_4$ -derivative would span across the reactor and a solution of the diazo compound and trapping agent would be injected into the center of this hollow fiber. Upon contacting the catalyst, the diazo compound would decompose to the rhodium carbenoid and directly react with trapping agent in solution. The reactor would also featured spaces for nitrogen gas exhaust and for a ReactIR probe for in-situ reaction progress kinetics (Figure 4.4).

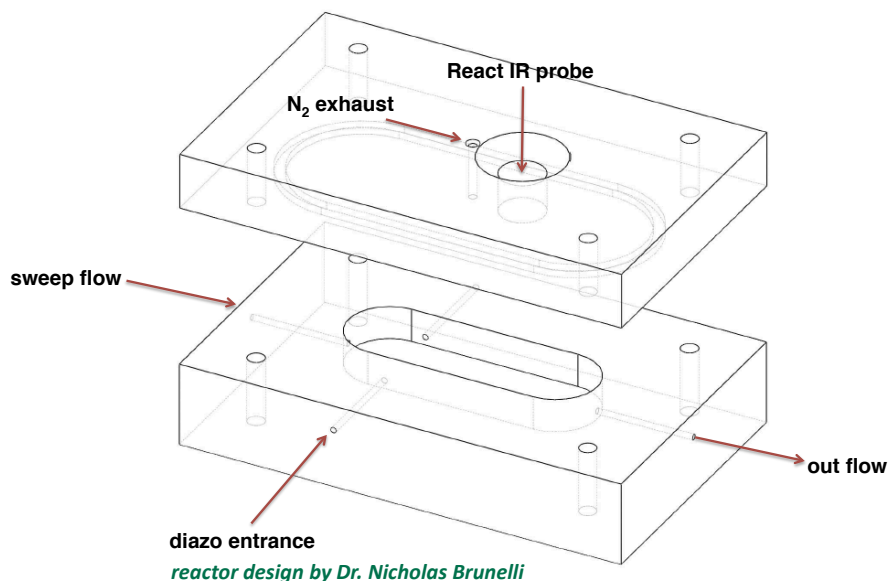
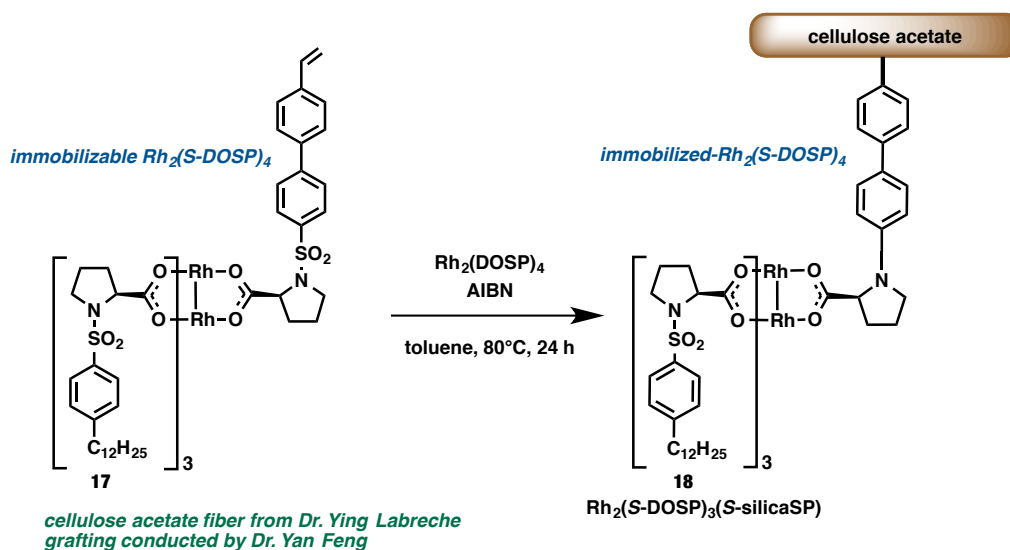


Figure 4.4 Continuous flow reactor design for porous hollow fiber-supported-Rh₂(S-DOSP)₄-derivative

The immobilizable Rh₂(S-DOSP)₄-derivative **17** used to graft Rh₂(S-DOSP)₄ to a silica surface in Chapter 3 was employed to graft Rh₂(S-DOSP)₄ to a cellulose acetate fiber. The general synthetic route to silica-supported Rh₂(S-DOSP)₄-derivatives (See Chapter 3, Scheme 3.31) was employed in the grafting Rh₂(S-DOSP)₄ to a cellulose acetate fiber. The composite polymer/oxide hollow fibers used in this study were prepared in a continuous process whereby the solid oxide particles were incorporated into the porous polymer matrix during the fiber spinning, allowing fibers to be made rapidly at low cost using commercially available materials.¹⁴ Well-established dry-jet, wet-quench, nonsolvent induced phase separation spinning method¹⁴ was used to make the fibers. This process was conducted by Dr. Ying Labreche in Prof. William J. Koros group at Georgia Institute of Technology (experts in the field of porous hollow fibers). The cellulose acetate hollow fiber contained 59 wt% silica and had a [Rh₂] loading of 0.05 mmol/g (Scheme 4.5).

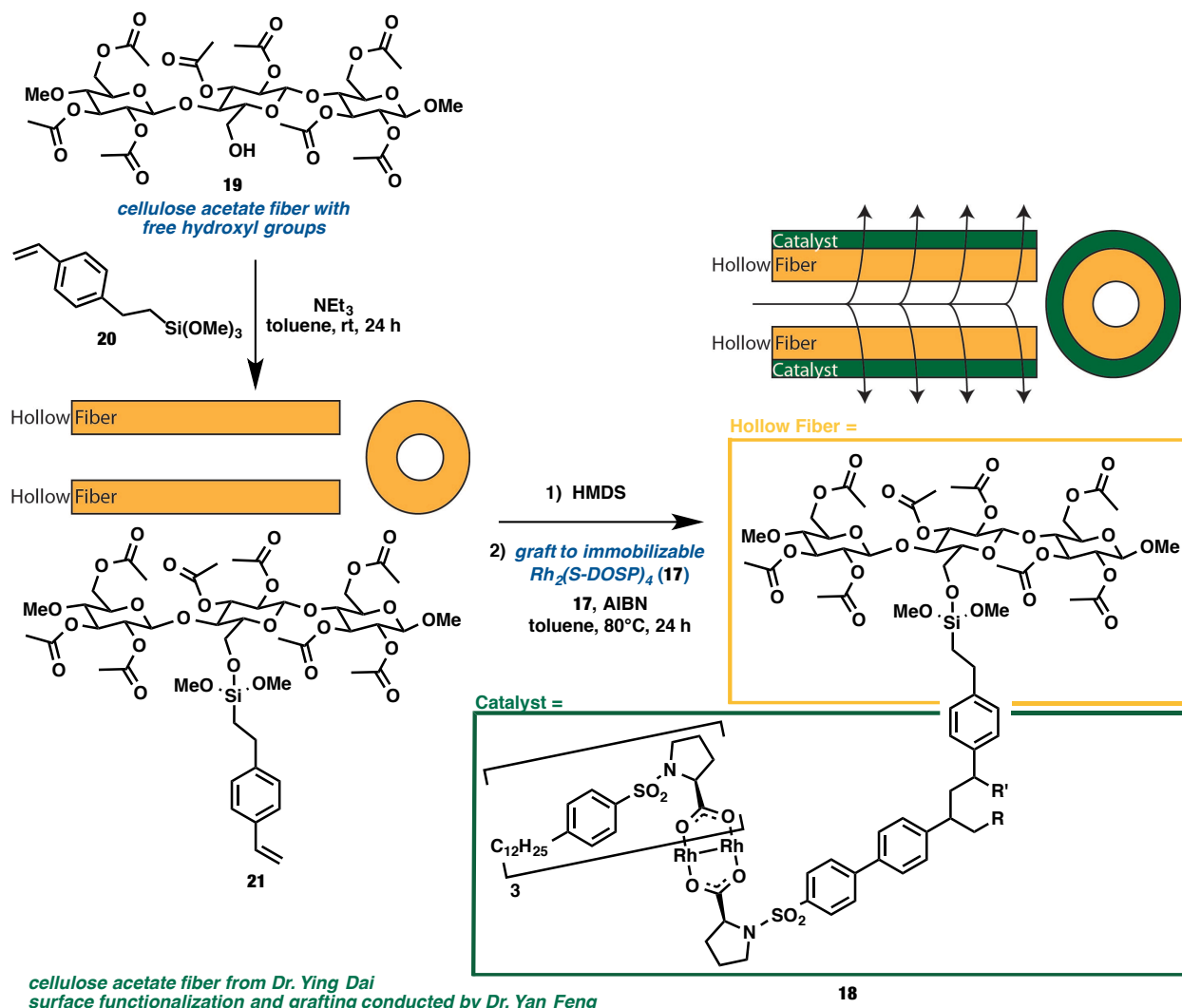
Scheme 4.5 $\text{Rh}_2(\text{S-DOSP})_4$ immobilization onto cellulose acetate hollow fibers



Immobilizable $\text{Rh}_2(\text{S-DOSP})_4$ -derivative **17** was embedded into the walls of functionalized composite polymer/oxide hollow fiber-cellulose acetate (**21**). Styryl-functionalized cellulose acetate fiber **21** was made by reaction of monomethoxysilane **20** with the free hydroxyl groups of cellulose acetate fiber **19**. Treatment of functionalized cellulose acetate fiber **21** with HMDS to TMS-protect any unreacted hydroxyl groups followed by AIBN-initiated free radical coupling of the surface styryl groups with those on immobilizable $\text{Rh}_2(\text{S-DOSP})_4$ -derivative **17** provided cellulose acetate hollow fiber-immobilized $\text{Rh}_2(\text{S-DOSP})_4$ -derivative **18** (Scheme 4.6). It is important to note that the schematic description of this catalyst shown in Scheme 4.6 is generalized and does not fully convey the structure of this catalyst system. The catalyst **17** is actually tethered to the silica in the cellulose acetate fiber (not shown) and not the cellulose acetate fiber itself.

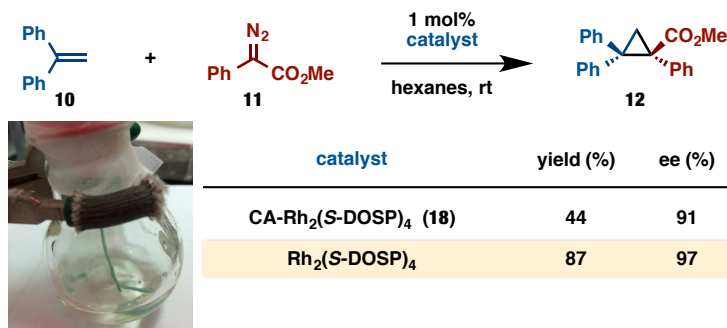
The porous nature of catalyst **18** was envisioned to prevent clogging of the flow channels (often observed in continuous flow processing with typical packed bed reactors) and provide a short catalyst bed in a flow reactor platform for heterogeneous dirhodium(II) catalyzed reactions.

Scheme 4.6 Synthesis of composite polymer/oxide hollow fiber-cellulose acetate immobilized-Rh₂(S-DOSP)₄-derivative



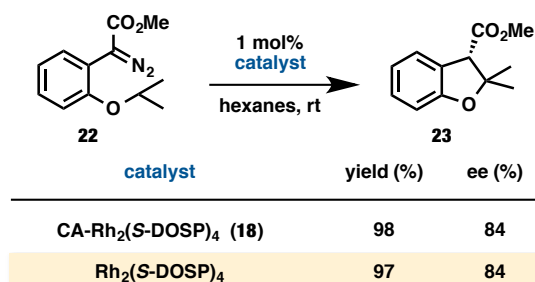
Cellulose acetate (CA) immobilized-Rh₂(S-DOSP)₄-derivative (**18**) was then tested in a standard asymmetric cyclopropanation in batch to determine its reactivity and selectivity. This catalyst provided cyclopropanation product **12** with slightly lower enantiomeric excess and much lower yield than Rh₂(S-DOSP)₄ (Table 4.3).

Table 4.3 Intermolecular asymmetric cyclopropanation catalyzed by cellulose acetate immobilized-Rh₂(S-DOSP)₄-derivative in batch



Although CA-Rh₂(S-DOSP)₄ (**18**) did not match the reactivity or selectivity of Rh₂(S-DOSP)₄ in an intermolecular reaction, we wanted to test **18** in an intramolecular C–H insertion reaction, seeing as intramolecular reactions of rhodium carbenoids were successfully conducted in a continuous flow manner with Hashimoto’s system.¹¹ To our delight, catalyst **18** displayed the same reactivity and selectivity as Rh₂(S-DOSP)₄ in intramolecular C–H insertion with methyl 2-diazo-2-(2-isopropoxyphenyl)acetate (**22**) (Table 4.4).²⁰

Table 4.4 Intramolecular C–H insertion catalyzed by cellulose acetate immobilized-Rh₂(S-DOSP)₄-derivative in batch



Inspired by these promising results, we next looked to apply catalyst **18** towards reactions of donor/acceptor carbenoids in a continuous flow manner. The flow reactor was built according to the aforementioned reactor design (Figure 4.4). A sweep flow of solvent can enter the reactor from one end and push out product on the opposite side. Rh₂(S-DOSP)₄-fiber (**18**) spans the

width of the reactor and is held in place by epoxy binding either end of the fiber to the reactor. The reactants in solution are fed through the bore of the hollow fiber. The fiber walls, composed of cellulose acetate (36-52 wt %) and inorganic particles (0.9 wt % Rh (4 wt % immobilized catalyst, 44 wt % silica)) are highly permeable. The walls are ~300-400 μm thick and can be considered an ultra-short catalyst bed through which the reactants pass. Flowing outside the fiber is a sweep flow of an organic solvent that facilitates product collection. In this initial work, reactant pulses were flowed through the fiber, though continuous flow operation can also be conducted. The fiber was capped at the opposite end to ensure the reactants flow through the walls and contact the catalyst (tubular dead-end flow) and, after reacting, exit through the pores of the fiber (Figure 4.5).

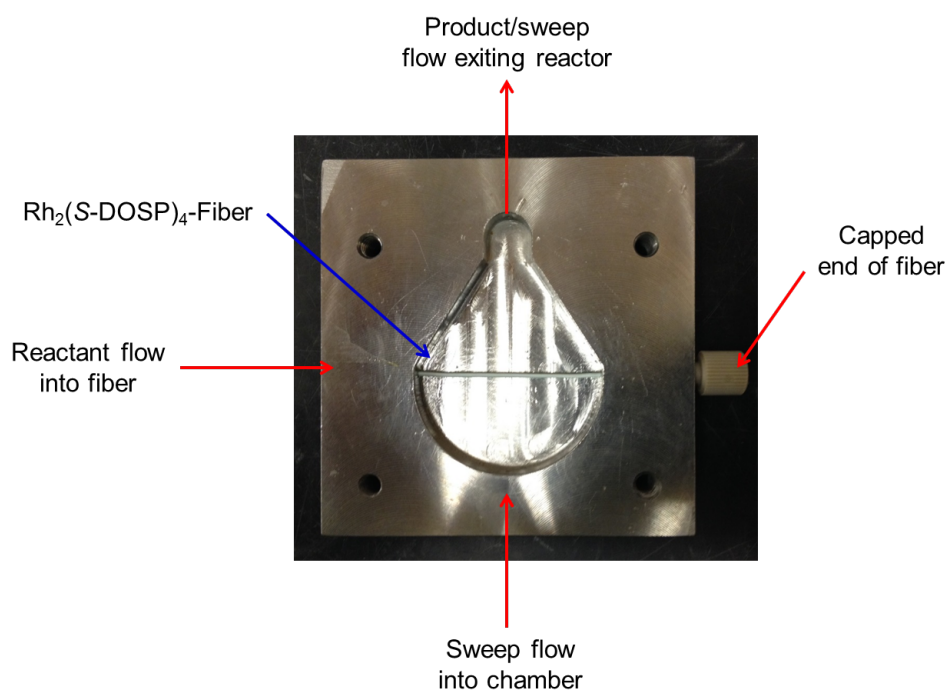


Figure 4.5 Photograph of the inside of the continuous flow reactor containing porous hollow fiber-supported- $\text{Rh}_2(\text{S-DOSP})_4$ -derivative

The reactant feed and sweep flow into the reactor are regulated with the use of peristaltic pumps. The stainless steel chamber of the reactor is equipped with a heating jacket which could allow for reactions at elevated temperatures to be carried out in this microreactor (Figure 4.6).

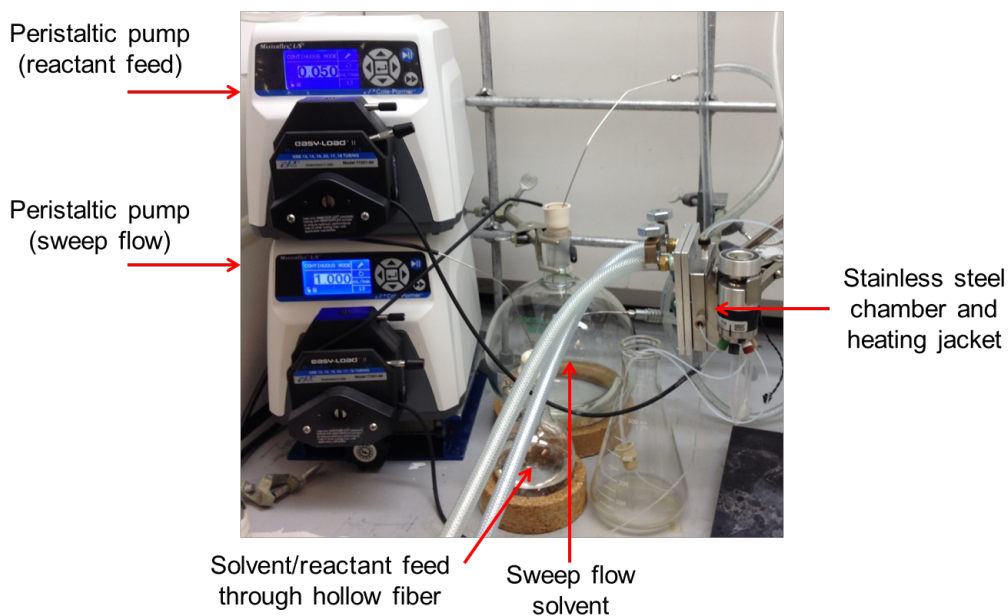


Figure 4.6 Photograph of the stainless steel reactor, heating jacket, and solvent feed flasks and pumps

The exact volume of a the solution of reactants injected into the reactor is controlled by an HPLC valve connected to a 0.5 mL sample loop. Once the 0.5 mL sample loop is full, excess solution of reatants is paped into a waste container. The 0.5 mL of reactants is then injected into the reactor and flowed through the catalyst fiber **18**. The products of the reation are then pushed out of the reactor by the sweep flow of solvent (Figure 4.7).

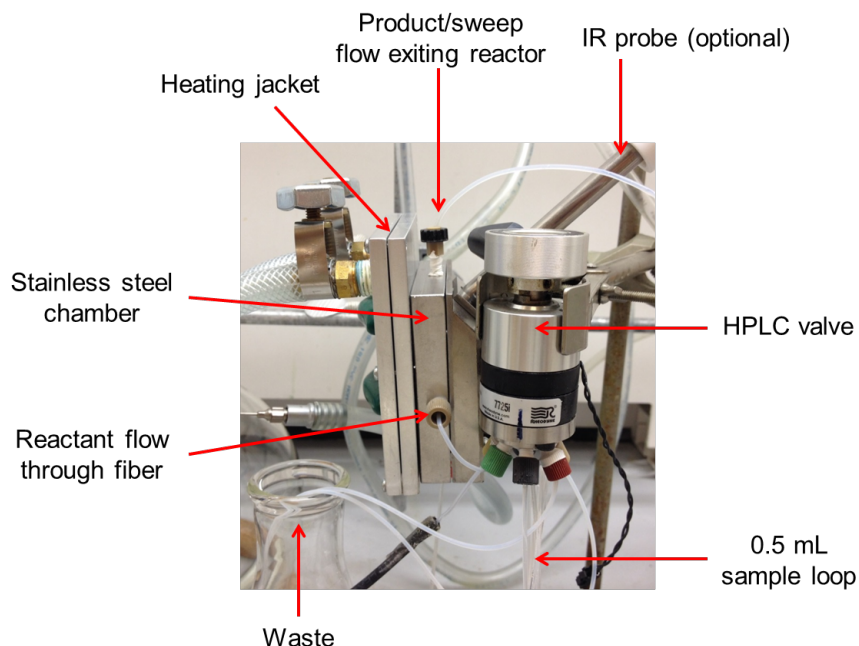


Figure 4.7 Close-up photograph of the stainless steel reactor equipped with heating jacket and HPLC valve

4.6 Composite Polymer/Oxide Hollow Fiber Contactors: Versatile and Scalable Flow Reactors for Heterogeneous Dirhodium(II) Catalyzed Reactions

Incorporating heterogeneous catalysts in the walls of the hollow fibers presents an alternative to a traditional packed bed reactor. A drawback associated with some commercially available flow reactors and microreactors is the potential for high pressure drop along the length of the reactor, due to poor handling of solid species, which can clog the flow channels and reduce the rate of production.^{4, 21} Therefore, alternate reactor types that avoid large pressure drops but accommodate supported catalysts for complex organic reactions while maintaining superior heat and mass transfer properties are desirable. Inspired by our aforementioned finding that cellulose acetate hollow fiber-immobilized $\text{Rh}_2(\text{S-DOSP})_4$ -derivative **18** displayed the same reactivity and selectivity as $\text{Rh}_2(\text{S-DOSP})_4$ in intramolecular C–H insertion, we began to explore the possibility of using flow chemistry in the emerging field of C–H functionalization. The goal of this

program is not only to demonstrate that C–H functionalization reactions can be conducted in flow,^{5c, 11, 22} but also to design new types of flow reactors to handle supported catalysts that are often used for such reactions (Figure 4.8).

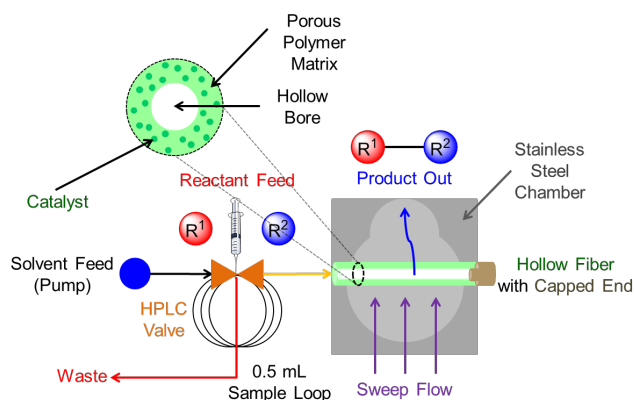


Figure 4.8 Schematic description of the radial flow hollow fiber flow reactor

In addition to cellulose acetate-supported $\text{Rh}_2(\text{S-DOSP})_4$ -derivative **18**, Torlon-supported $\text{Rh}_2(\text{S-DOSP})_4$ -derivative **26** was tested due to its stability in a broad range of solvents including dichloromethane. We imagined that stability in dichloromethane could be advantageous to our catalyst system for its application in reactions with styryldiazoacetates, which are typically used in excess due to their rapid decomposition to the corresponding pyrazole. After reaction with styryldiazoacetate, **26** could be washed with dichloromethane to remove any residual pyrazole from before injection of the next solution of reactants. Application of **26** in the standard intermolecular asymmetric cyclopropanation reaction, however, provided products with significantly lower enantio- and diastereoselectivity than **18** or $\text{Rh}_2(\text{S-DOSP})_4$ (Table 4.5).

Table 4.5 Intermolecular asymmetric cyclopropanation catalyzed by Torlon and cellulose acetate immobilized-Rh₂(S-DOSP)₄-derivatives in flow

catalyst	sweep flow	reactant flow	yield (%)	ee (%)	dr
Torlon-Rh ₂ (S-DOSP) ₄ (26)	1 mL/min	0.5 mL/min	25	59	16:1
Torlon-Rh ₂ (S-DOSP) ₄ (26)	0.1 mL/min	0.1 mL/min	70	60	16:1
CA-Rh ₂ (S-DOSP) ₄ (18)	0.1 mL/min	0.1 mL/min	60	72	> 20:1
Rh ₂ (S-DOSP) ₄	-	-	88	88	> 20:1

We next sought to determine the optimal reaction conditions in moving forward with the use of CA-Rh₂(S-DOSP)₄ (**18**) in continuous flow. Varying the sweep and reactant flow rate had no effect of on the reactivity and selectivity of intermolecular asymmetric cyclopropanation catalyzed by CA-Rh₂(S-DOSP)₄ (**18**) (Table 4.6).

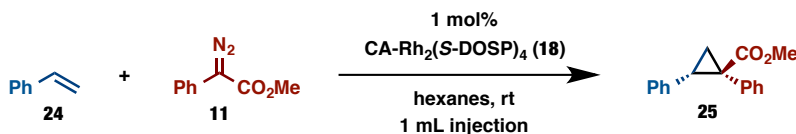
Table 4.6 The effect of varying the sweep and reactant flow rate on intermolecular asymmetric cyclopropanation catalyzed by cellulose acetate immobilized-Rh₂(S-DOSP)₄-derivative in flow

catalyst	sweep flow	reactant flow	[diazo]	[styrene]	yield (%)	ee(%)	dr
CA-Rh ₂ (S-DOSP) ₄ (18)	0.1 mL/min	0.1 mL/min	0.15 M	0.30 M [2 equiv]	74	72	> 20:1
" "	" "	" "	" "	0.60 M [4 equiv.]	72	72	> 20:1
" "	" "	" "	" "	1.20 M [8 equiv.]	75	72	> 20:1
" "	" "	" "	0.30 M	0.60 M [2 equiv.]	72	72	> 20:1
" "	" "	" "	0.45 M	0.90 M [2 equiv.]	73	72	> 20:1
Rh ₂ (S-DOSP) ₄	-	-		[2 equiv.]	88	88	> 20:1

Recyclability of CA-Rh₂(S-DOSP)₄ (**18**) was then determined by repeatedly injecting 1 mL of a mixture of **24** and **11** in hexanes into the flow reactor and monitoring change in reactivity and enantioselectivity. Under these conditions, **18** was found to deactivate (Table 4.7). (A total

injection volume of 1 mL total volume 0.5 mL was injected twice: once the first 0.5 mL passed through the sample loop, another 0.5 mL was injected.)

Table 4.7 Preliminary catalyst recycling study of cellulose acetate immobilized-Rh₂(S-DOSP)₄-derivative in the asymmetric cyclopropanation of styrene with phenyldiazoacetate



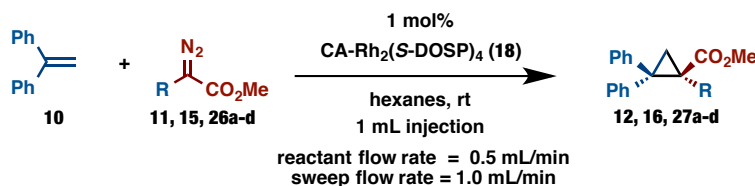
reactant flow rate = 0.1 mL/min
sweep flow rate = 0.1 mL/min

cycle	ee (%)	conversion
1	76	complete
2	70	complete
3	78	complete
4	67	complete
5	66	complete
6	63	complete
7	61	complete
8	60	complete
9	61	incomplete
10	61	incomplete
11	63	incomplete
12	55	incomplete

While cyclopropanations/cyclopropanations have been investigated using flow systems,^{11, 22c-e, 22k} no such investigations have occurred using hollow fiber reactors, nor have there been studies of dirhodium(II)-catalyzed asymmetric intermolecular C–H functionalization reactions in flow. For this reason, the main focus for the remainder of this study was directed at C–H functionalization. As described in Table 4.2, dirhodium(II)-catalysts with triarylcyclopropane carboxylate ligands have recently been reported to promote high asymmetric induction in several carbenoid reactions including selective primary C–H functionalization.^{13, 23} In hopes of conducting the synthesis of these ligands in continuous flow, we re-examined was the asymmetric cyclopropanation of 1,1-diphenylethylene (**10**) with *para*-substituted donor/acceptor-substituted diazo compound **11** as well as with various related diazo compounds (**15**, **26a-d**).²⁴ The data in Table 4.8 demonstrates the breadth of diazo compounds that were successfully used

under optimized flow conditions, giving the products with comparable, but slightly diminished, enantioselectivities and yields to the complementary $\text{Rh}_2(\text{S-DOSP})_4$ -catalyzed batch reactions.^{12,}
^{23a} (The residence time of the reactions was estimated to be 10-42 s at a flow rate of 0.05 mL min^{-1} assuming the 0.5 mL pulse permeates the entire shell of an average 4 cm-long fiber.)

Table 4.8 Scope of cyclopropanation with donor/acceptor-substituted diazo compounds using $\text{CA-Rh}_2(\text{S-DOSP})_4$ embedded in the walls of hollow fibers

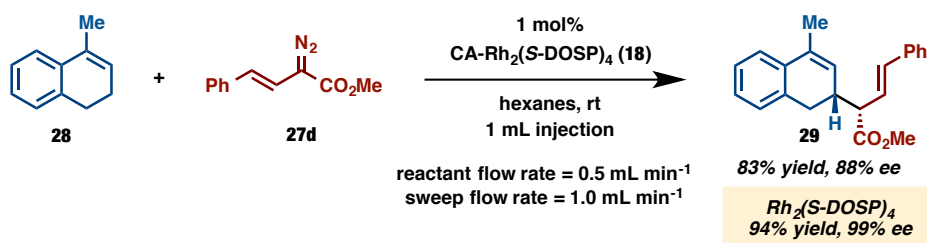


entry	R	product	$\text{CA-Rh}_2(\text{S-DOSP})_4$ (18)		$\text{Rh}_2(\text{S-DOSP})_4$	
			yield (%)	ee (%)	yield (%)	ee (%)
1 ^a	Ph	12	77	92	87	98
2 ^a	<i>p</i> -BrC ₆ H ₄	16	77	88	88	98
3 ^a	<i>p</i> -MeOC ₆ H ₄	27a	61	92	70	99
4 ^a	<i>p</i> -CF ₃ C ₆ H ₄	27b	64	94	59	98
5 ^a	<i>o</i> -ClC ₆ H ₄	27c	66	86	69	90
6	PhCH=CH ₂	27d	68	92	81	92

^areaction conducted by Dr. Eric G. Moschetta and Dr. Solymar Negretti

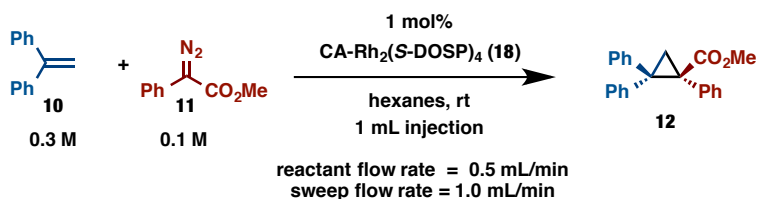
Seeing as $\text{Rh}_2(\text{S-DOSP})_4$ itself is an effective catalyst for a variety of stereoselective C–H functionalizations,²⁵ we further demonstrated the utility of the fiber-supported $\text{Rh}_2(\text{S-DOSP})_4$ -derivative **18** in a classic C–H functionalization, the combined C–H functionalization/Cope rearrangement (CHCR)²⁶/retro-Cope rearrangement²⁷ of 1-methyl-3,4-dihydronaphthalene (**28**) and styryldiazoacetate (**27d**). A similar % ee was achieved with catalyst **18** and $\text{Rh}_2(\text{S-DOSP})_4$,¹² with a slightly lower yield observed with the use of **18** in flow. Successful completion of such robust organic transformations in flow is promising for the construction of natural products and other organic compounds using the hollow fibers.²⁸

Scheme 4.7 C–H insertion with CA-Rh₂(S-DOSP)₄



To examine the stability of CA Rh₂(S-DOSP)₄ (**18**), the use of the Rh₂-functionalized fibers over multiple reactions was probed. Although dirhodium(II) catalysts are known to deactivate,²⁹ good % ee values were obtained over 1000+ turnover numbers (TON) in the cyclopropanation of methyl phenyldiazoacetate (**11**) and **10** (Figure 4.9, two different Rh₂(S-DOSP)₄-fibers were used to demonstrate reproducibility). Over the 1000+ TON achieved in 10 consecutive reaction cycles, only a small decrease in enantioselectivity was observed (Table 4.9, 92% ee gradually decreased to 84% ee).

Table 4.9 High turnover number and recycling study with CA-Rh₂(S-DOSP)₄ in flow



cycle	yield (%)	ee (%)
1	97	92
2	80	90
3	75	89
4	80	89
5	66	88
6	83	87
7	68	84
8	65	85
9	71	86
10	64	84

high TON study conducted by Dr. Eric G. Moschetta and Dr. Solymar Negretti

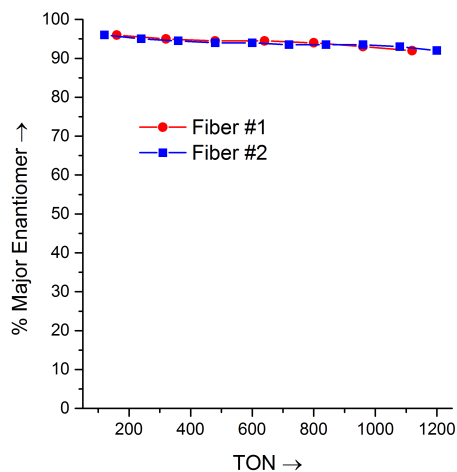


Figure 4.9 The effect of increasing the TON on the % ee of CA-Rh₂(*S*-DOSP)₄-catalyzed intermolecular asymmetric cyclopropanation

4.7 Conclusion

These studies provided new insight into the design and application of dirhodium(II)-catalysts in continuous flow processing. We were able to apply our previously reported immobilizable Rh₂(*S*-DOSP)₄-derivative to Rh₂(*S*-DOSP)₄-immobilization onto styryl-functionalized cellulose acetate and torlon supports for use in continuous flow processing. We found that a cellulose acetate supported Rh₂(*S*-DOSP)₄-derivative provided products of carbenoid reactions in good yields and with high enantio- and diastereoselectivities. We also found that an ideal flow reactor set-up involved the use of peristaltic pumps for sweep flow, an HPLC valve for sample injection, and an automated fraction collector for product collection. We were able to demonstrate that hollow composite fibers are a great platform for dirhodium(II) catalyst immobilization and application in enantioselective rhodium carbenoid flow chemistry. This was demonstrated by creating hollow fibers that contained silica-tethered dirhodium(II) catalysts and use of these fibers in synthetically useful enantioselective transformations. The reactions catalyzed within

the hollow fiber flow system demonstrates that the composite hollow fiber platform may be a useful new approach to conducting flow liquid phase synthesis of organic molecules.

4.8 Experimental Section

General: All solvents were purified and dried by a *Glass Contour Solvent System* unless otherwise stated. ^1H and ^{13}C NMR spectra were recorded at either 400 MHz (^{13}C at 100 MHz) on a Varian-400 spectrometer. NMR spectra were run in solutions of deuterated chloroform (CDCl_3) with residual chloroform taken as an internal standard (7.26 ppm for ^1H , and 77.0 ppm for ^{13}C), and were reported in parts per million (ppm). Abbreviations for signal multiplicity are as follows: s = singlet, d = doublet, t = triplet, q = quartet, p = pentet, m = multiplet, dd = doublet of doublet, app t = apparent triplet, etc. Coupling constants (J values) were calculated directly from the spectra. IR spectra were collected on a Nicolet iS10 FT-IR spectrometer. Mass spectra were taken on a Thermo Finnigan LTQ-FTMS spectrometer with APCI, ESI or NSI. Thin layer chromatographic analysis was performed with silica gel plates, visualizing with UV light and/or staining with PMA. Flash column chromatography was performed on silica gel 60Å (230-400 mesh). Analytical enantioselective chromatographies were measured on Varian Prostar instrument and used isopropanol : hexane as gradient. 1,1-diphenylethylene (**10**) was commercially available and used without further purification. Styrene (**24**) was commercially available and purified by pushing through a silica-filled pipette prior to use. $\text{Rh}_2(\text{S-DOSP})_4$,³⁰ methyl phenyldiazoacetate (**11**),³¹ methyl 2-(4-bromophenyl)-2-diazoacetate (**15**),³¹ methyl 2-diazo-2-(2-isopropoxyphenyl)acetate (**22**),²⁰ styryldiazoacetate (**27d**),³² and 1-methyl-3,4-dihydronaphthalene (**28**),³² were prepared following known literature procedures. 1,1-diphenyl ethylene was commercially available and filtered through silica prior to use. $\text{Rh}_2(\text{S-}$

DOSP)₄-catalyzed cyclopropanation providing **12**,³³ **16**,³⁴ and **25**³⁵ intramolecular C–H insertion providing **23**,²⁰ and CHCR/retro CHCR providing **29**²⁷ were all run according to published procedures. The flow reactor was designed by Dr. Nicholas Brunelli. The cellulose acetate fiber was provided by Dr. Ying Dai. Surface functionalization and grafting of the immobilizable dirhodium(II) catalyst to the surface, as shown in Scheme 4.6, was conducted by Dr. Yan Feng. The optimal flow conditions used the reactions shown in Tables 4.7 - 4.9 and Scheme 4.7 were established by Dr. Eric G. Moschetta. Cyclopropanes **12**, **16**, and **27a-c** in Table 4.8 were synthesized under continuous flow conditions by Dr. Eric G. Moschetta and characterized by Dr. Solymer Negretti.

Fiber synthesis: The synthetic strategy for immobilizing a ligand-exchanged analogue of Rh₂(S-DOSP)₄, Rh₂(S-DOSP)₃(S-SP) (**17**), on a styryl-functionalized silica surface using an AIBN-initiated free radical coupling process is described in the experimental section 3.12 of Chapter 3. Also, for full characterization of Rh₂(S-DOSP)₃(S-SP) (**17**),¹² see experimental section 3.12 of Chapter 3. The silica is embedded in the walls of the cellulose acetate fibers and the remaining surface silanols were capped with HMDS prior to immobilization of the dirhodium(II) species.

Cellulose acetate-supported Rh₂(S-DOSP)₄-fiber (18**) synthesis:** The synthesis of cellulose acetate fibers has been described previously.^{14, 36} Fresh cellulose acetate fibers containing silica particles embedded in the walls (7.0 g) were admitted to a 250 mL two-neck flask purged with nitrogen (UHP) for 30 min. The flask was then purged with nitrogen for another 30 min, then 5.0 g of styrylethyltrimethoxysilane (**20**) in about 75 mL anhydrous toluene was injected into the flask via syringe, which was rinsed several times with anhydrous toluene. Next, 20 mL triethylamine in anhydrous toluene was added in an identical manner. The total volume of the

reaction mixture was about 125 mL. The reaction was stirred at 25 °C under nitrogen overnight. The resulting fibers were filtered and washed with toluene (three 75 mL washes) and hexanes (three 75 mL washes) and dried under vacuum overnight to yield styryl-functionalized silica particles in the fibers. The styryl-functionalized fibers were placed in a 250 mL two-neck flask that was purged with nitrogen for 30 min before and after addition of the fibers. The fibers were subsequently treated with 50 mL hexamethyldisilazane (HMDS) in 100 mL anhydrous toluene via a syringe, which was washed several times with dry toluene. The mixture was stirred at 25 °C under nitrogen for 3 days. The resulting fibers were filtered and washed with toluene (three 75 mL washes) and hexanes (three 75 mL washes) and dried under vacuum overnight. The HMDS-treated fibers (7.0 g) were added to a dry 500 mL Schlenk flask, along with 4.0 g (0.88 mmol) $\text{Rh}_2(\text{S-DOSP})_3(\text{S-SP})$, 0.15 g (0.88 mmol) azobisisobutyronitrile (AIBN), and about 175 mL toluene. The flask was then sealed and connected to the Schlenk line. The solution was degassed over 4 freeze-pump-thaw cycles, heated to 80 °C, and stirred under argon (UHP) for 4 days. The solution was cooled to room temperature and filtered and washed with toluene (three 150 mL washes) and hexanes (three 100 mL washes).

General procedure A for flow reactions: (without final wash) For each reaction, a fresh cellulose acetate fiber containing the embedded catalyst (immobilized analogue of $\text{Rh}_2(\text{S-DOSP})_4$) was positioned in the bottom part of the stainless steel reactor and glued in place using a commercially available epoxy (Loctite). The epoxy was allowed to dry for 30 min before assembling the reactor. The top of the reactor was then screwed in, using a rubber O-ring to prevent the solvent from leaking out from the stainless steel frame. The ReactIR (Mettler-Toledo) probe was then inserted and the HPLC fittings were attached using Teflon tape. Hexanes was fed directly to the fiber (the reactant flow) and the reactor cell (the sweep flow) to

test for leaks and to fill the chamber with solvent prior to each reaction. Peristaltic pumps (Cole-Parmer Masterflex L/S) were used to pump the dry, degassed solvents from round-bottom flasks to the reactor. Once the reactor was free of leaks and a steady stream of solvent was exiting the reactor as the sweep flow, the HPLC valve (Rheodyne) was switched to the loading position and 0.5 mL of the reactant solution was injected. The HPLC valve was then switched to the feed position and the reaction started. The fraction collector (Varian 701 ProStar) was set to a clean, labeled test tube to collect the sweep flow containing the reaction products and the ReactIR was used to monitor the progress of the reaction. An additional 0.5 mL of reaction solution was injected immediately after the first injection went through the fiber. After enough time elapsed to allow the entire reaction solution to enter the fiber, another 45 min were allowed to pass to extract as much product from the reactor as possible. Once the reaction was over, the reactor was disassembled, the fiber was collected in a labeled container, and the epoxy was removed. The reactor was cleaned with acetone and dried in an oven before the next reaction. The products were purified through silica gel column chromatography (10% EtOAc in hexanes).

General procedure B for flow reactions: The procedure is identical to General Procedure A, with the exception of injecting a 0.5 mL pulse of isopropanol every 15 min during the 45 min elution time to increase the yield of more polar products. The products were purified through silica gel column chromatography (10% EtOAc in hexanes).

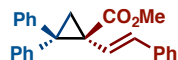


Methyl (S)-1,2,2-triphenylcyclopropane-1-carboxylate (12): Following general procedure A, phenyldiazoacetate (17.6 mg, 0.1 mmol, 1 equiv.) and 1,1-diphenylethylene (54.1 mg, 0.3 mmol, 3 equiv.) were employed to yield 25.2 mg of product (77%) after chromatography. The NMR

data was consistent with previous reports. ^1H NMR (400 MHz; CDCl_3) δ 7.52-7.50 (m, 2H), 7.36-7.32 (m, 4H), 7.26-7.23 (m, 1H), 7.16-7.10 (m, 3H), 6.98-6.94 (m, 5H), 3.36 (s, 3H), 2.70 (d, $J = 5.5$ Hz, 1H), 2.43 (d, $J = 5.5$ Hz, 1H); HPLC (*S,S*-Whelk, 9.0% isopropanol in hexane, 1.0 mL min^{-1} , 1 mg mL^{-1} , 30 min, UV 254 nm) retention times of 6.8 min (minor) and 17.4 min (major), 96:4 e.r. (92% ee).

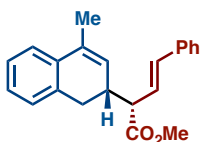


Methyl (*S*)-1-(4-bromophenyl)-2,2-diphenylcyclopropane-1-carboxylate (16): Following general procedure A, *p*-bromophenyldiazoacetate (25.5 mg, 0.1 mmol, 1 equiv.) and 1,1-diphenylethylene (54.1 mg, 0.3 mmol, 3 equiv.) were employed to yield 31.0 mg of product (77%). The NMR data was consistent with previous reports. ^1H NMR (400 MHz, CDCl_3) δ 7.48-7.47 (m, 2H), 7.35-7.31 (m, 2H), 7.27-7.18 (m, 5H), 7.02-6.97 (m, 5H), 3.34 (s, 3H), 2.68 (d, $J = 5.5$ Hz, 1H), 2.39 (d, $J = 5.9$ Hz, 1H); HPLC (*S,S*-Whelk, 5% isopropanol in hexane, 0.8 mL min^{-1} , 1 mg mL^{-1} , 60 min, UV 254 nm) retention times of 10.6 min (minor) and 50.9 min (major) 94:6 e.r. (88% ee).



Methyl (*S,E*)-2,2-diphenyl-1-styrylcyclopropane-1-carboxylate (27d):³⁷ Following general procedure A, styryldiazoacetate (20.2 mg, 0.1 mmol, 1 equiv.) and 1,1-diphenylethylene (16.4 mg, 0.9 mmol, 0.9 equiv.) were employed to yield the product in >20:1 dr as determined by ^1H NMR analysis of the crude reaction mixture. The residue was then purified through silica gel eluting with pentane:ether (increasing from 100:0 to 90:10) to afford a white solid (21 mg, 68% yield). Enantioenrichment was determined by chiral HPLC analysis after purification: (Chiralcel OJ-H, 1.5% *i*-PrOH in hexane, 1.0 mL min^{-1} , 1 mg mL^{-1} , 30 min, $\lambda = 254$ nm) retention times of

6.24 min (minor) and 13.25 min (major), 96:4 e.r. (92% ee). The spectral data were identical to those previously reported.³⁷ The $\text{Rh}_2(\text{S-DOSP})_4$ catalyzed reaction between **10** and **26d** gave **27d** in 81% yield and 96:4 e.r. (92% ee).



Methyl (S,E)-2-((R)-4-methyl-1,2-dihydronaphthalen-2-yl)-4-phenylbut-3-enoate (29):²⁷

Following general procedure A, styryldiazoacetate (20.2 mg, 0.1 mmol, 1 equiv.) and 1,1-diphenylethylene (16.4 mg, 0.9 mmol, 0.9 equiv.) were employed to yield the product in >20:1 dr as determined by ¹H NMR analysis of the crude reaction mixture. The residue was then purified through silica gel eluting with pentane:diethyl ether (20:1) to afford a white solid (24 mg, 83% yield). Enantioenrichment was determined by chiral HPLC analysis after purification: (Chiralcel OD-H, 2% *i*-PrOH in hexane, 0.8 mL min⁻¹, 1 mg mL⁻¹, 30 min, $\lambda = 254$ nm) retention times of 7.68 min (major) and 9.13 min (minor), 94:6 e.r. (88% ee). The spectral data were identical to those previously reported.²⁷ The $\text{Rh}_2(\text{S-DOSP})_4$ catalyzed reaction between **28** and **27d** has been previously reported to give **29** in 95% yield and >99:1 e.r. (99% ee).²⁷

General procedure for $\text{Rh}_2(\text{S-DOSP})_4$ -catalyzed homogeneous reactions: An oven-dried 25 mL round-bottom flask was charged with $\text{Rh}_2(\text{S-DOSP})_4$ (3.8 mg, 0.002 mmol, 0.01 equiv.), 1,1-diphenylethylene (106 μL , 0.60 mmol, 3.0 equiv.) and dry, degassed pentane (3 mL). The flask was then purged with argon. On a separate oven-dried 20 mL scintillation vial the corresponding diazoacetate (0.20 mmol, 1 equiv.) was dissolved in dry, degassed pentane (3 mL). The vial was then purged with argon. Then the solution of the diazoacetate was added to the reaction flask over 1 h via syringe pump. The reaction mixture was allowed to stir at rt at least 2 h after the

addition was complete. Then the reaction mixture was concentrated under reduced pressure and the crude residue purified through silica column chromatography (eluent: 10% EtOAc in hexanes) to yield the desired triarylcyclopropane carboxylate methyl ester.

Characterization of the hollow fibers:

Table S1. Elemental analysis of fresh and used Rh₂(*S*-DOSP)₄-fibers. Elemental analysis (ALS Environmental – Tucson, AZ) suggests that neither the sweep flow nor the cyclopropanations caused the dirhodium(II) species to be leached from the fiber walls appreciably.

	wt % Element			
	C	H	N	mol Rh/mol Si
Fiber #1 (fresh)	28.01	3.84	1.26	0.010
Fiber #1 (used)	28.73	3.75	1.23	0.012
Fiber #2 (fresh)	28.05	3.7	1.21	0.010
Fiber #2 (used)	28.44	3.67	1.21	0.010

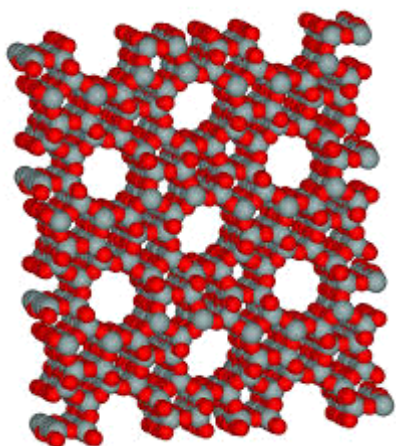
The surface area and pore volume of the fibers (Table S2) was determined by nitrogen physisorption experiments on a Micromeritics Tristar 2030 at 77 K. All samples were evacuated overnight at 110 °C. Approximately 100 mg of each sample, catalyst-containing fibers and bare cellulose acetate fibers as references, was used for the measurements. The isotherms were analyzed using the Brunauer-Emmett-Teller (BET) method to calculate the surface area of the materials and the Broekhoff-de Boer method with the Frenkel-Halsey-Hill (BdB-FHH) modification using the data from the adsorption isotherm to calculate the total pore volume. The slight decreases in surface area and total pore volume for the catalyst-containing fibers compared to the bare cellulose acetate fibers indicate successful immobilization of the catalytic species in the fiber walls.

Table S2. Surface areas and total pore volumes of the hollow fibers and the silica support.

Material	Surface area (m ² /g)	Pore volume (cm ³ /g)
C803 silica	180	0.94
Bare cellulose acetate fibers	125	0.60
ZSM-5 fibers	194	0.08 ^[a]
APS fibers	57	0.28
Rh ₂ (<i>S</i> -DOSP) ₄ -fibers	101	0.55

^[a]Low pore volume may be due to some zeolite pore blockage by polymer

(A)



(B)

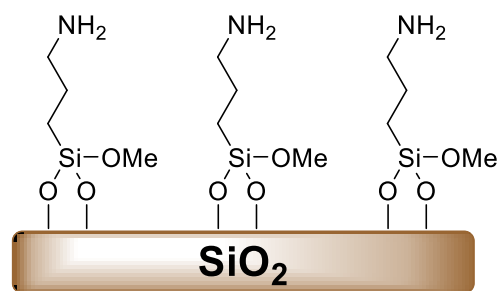


Figure S1. Structures of (A) the solid oxide Brønsted-acid catalyst, zeolite ZSM-5, and (B) the solid oxide base organocatalyst, APS-functionalized silica. For (A), the gray spheres represent either Si or Al and the red spheres represent O.

Variable-amplitude cross-polarization solid-state (VACP-MAS) ¹³C and ²⁹Si NMR spectra were recorded on a Bruker Avance III 400 spectrometer at a spinning speed of 12 kHz. Figure S2 shows the ¹³C NMR spectra for fresh Rh₂(*S*-DOSP)₄-fibers and used fibers after the same high TON experiments in flow described in the DR-UV-Vis section and Figure 3 of the main text. Both spectra exhibit the same peaks at the same chemical shifts. Peaks corresponding to the cellulose acetate polymer are marked 1-8 in the fresh fiber spectrum and a molecule of cellulose acetate is provided for reference.³⁸ Peaks marked Rh correspond to Rh₂(*S*-DOSP)₃(*S*-SP) and are in agreement with the literature values.¹² There is a slight increase in the peak area near 127 ppm for the high TON fibers, possibly due to residual 1,1-diphenylethylene.

Additional information: The cellulose acetate fibers are compatible with water, hydrocarbon solvents, and short-chain alcohols (e.g. methanol, ethanol). Halogenated solvents should be avoided and the pH of aqueous solutions should be kept between pH = 4-8 to avoid degradation of the fibers. In dry conditions, cellulose acetate has a glass transition temperature of ~200 °C, which should be considered the maximum temperature when using the fibers in chemical reactions. In addition to keeping the dirhodium(II) catalyst immobilized in the fiber for reuse, the improved heat and mass transfer of the fibers (high surface area-to-volume ratio) allow for efficient transfer of the nitrogen gas that is evolved during the reaction and the large amount of heat released in the cyclopropanations and C–H functionalizations. The sweep flow over the fiber also helps transfer the heat and nitrogen released during the reactions, providing additional benefits from using the hollow fibers to conduct the reactions in flow compared to the homogeneous batch reactions.

*The key discoveries made in this chapter were recently published.*³⁹

References:

1. (a) Anderson, N. G. *Org. Process Res. Dev.* **2001**, *5*, 613; (b) Kockmann, N.; Gottspöner, M.; Zimmermann, B.; Roberge, D. M. *Chem. -Eur. J.* **2008**, *14*, 7470; (c) Hessel, V. *Chem. Eng. Technol.* **2009**, *32*, 1655; (d) Baxendale, I. R.; Deeley, J.; Griffiths-Jones, C. M.; Ley, S. V.; Saaby, S.; Tranmer, G. K. *Chem. Commun.* **2006**, *24*, 2566; (e) Baxendale, I. R.; Griffiths-Jones, C. M.; Ley, S. V.; Tranmer, G. K. *Synlett* **2006**, *3*, 427.
2. Malet-Sanz, L.; Susanne, F., Continuous Flow Synthesis. A Pharma Perspective. *J. Med. Chem.* **2012**, *55*, 4062.
3. (a) Pastre, J. C.; Browne, D. L.; Ley, S. V. *Chem. Soc. Rev.* **2013**, *42*, 8849; (b) Myers, R. M.; Fitzpatrick, D. E.; Turner, R. M.; Ley, S. V. *Chem. -Eur. J.* **2014**, *20*, 12348; (c) Irfan, M.; Glasnov, T. N.; Kappe, C. O. *ChemSusChem* **2011**, *4*, 300; (d) Baxendale, I. R.; Ley, S. V.; Mansfield, A. C.; Smith, C. D. *Angew. Chem., Int. Ed.* **2009**, *48*, 4017.
4. (a) McQuade, D. T.; Seeberger, P. H. *J. Org. Chem.* **2013**, *78*, 6384; (b) Wegner, J.; Ceylan, S.; Kirschning, A. *Chem. Commun.* **2011**, *47*, 4583.
5. (a) Noel, T.; Buchwald, S. L. *Chem. Soc. Rev.* **2011**, *40*, 5010; (b) Cantillo, D.; Kappe, C. O. *ChemCatChem* **2014**, *6*, 3286; (c) Tsubogo, T.; Ishiwata, T.; Kobayashi, S. *Angew. Chem., Int. Ed.* **2013**, *52*, 6590.
6. (a) Davis, M. E.; Davis, R. J. *Fundamentals of chemical reaction engineering.*; McGraw-Hill: **2003**; p 368; (b) Malet-Sanz, L.; Madrzak, J.; Ley, S. V.; Baxendale, I. R. *Org. Biomol.*

- Chem.* **2010**, *8*, 5324; (c) O'Brien, M.; Baxendale, I. R.; Ley, S. V. *Org. Lett.* **2010**, *12*, 1596; (d) Mak, X. Y.; Laurino, P.; Seeberger, P. H. *Org. Chem.* **2009**, *5*, 19; (e) Fukuyama, T.; Rahman, M. T.; Sato, M.; Ryu, I. *Synlett* **2008**, *2*, 151; (f) Benito-Lopez, F.; Egberink, R. J. M.; Reinhoudt, D. N.; Verboom, W. *Tetrahedron* **2008**, *64*, 10023; (g) Jaehnisch, K.; Hessel, V.; Loewe, H.; Baerns, M. *Angew. Chem., Int. Ed.* **2004**, *43*, 406.
7. Kirschning, A.; Jas, G. *Top. Curr. Chem.* **2004**, *242*, 209.
 8. Martin, L. J.; Marzinzik, A. L.; Ley, S. V.; Baxendale, I. R. *Org. Lett.* **2011**, *13*, 320.
 9. (a) Van Alsten, J. G.; Reeder, L. M.; Stanchina, C. L.; Knoechel, D. J. *Org. Process Res. Dev.* **2008**, *12*, 989; (b) Kulkarni, A. A.; Kalyani, V. S.; Joshi, R. A.; Joshi, R. R. *Org. Process Res. Dev.* **2009**, *13*, 999; (c) Baumann, M.; Baxendale, I. R.; Martin, L. J.; Ley, S. V. *Tetrahedron* **2009**, *65*, 6611.
 10. Takeda, K.; Oohara, T.; Anada, M.; Nambu, H.; Hashimoto, S. *Angew. Chem., Int. Ed.* **2010**, *49*, 6979.
 11. Takeda, K.; Oohara, T.; Shimada, N.; Nambu, H.; Hashimoto, S. *Chem. –Eur. J.* **2011**, *17*, 13992.
 12. Chepiga, K. M.; Feng, Y.; Brunelli, N. A.; Jones, C. W.; Davies, H. M. L. *Org. Lett.* **2013**, *15*, 6136.
 13. Qin, C.; Davies, H. M. L. *J. Am. Chem. Soc.* **2014**, *136*, 9792.
 14. Lively, R. P.; Chance, R. R.; Kelley, B. T.; Deckman, H. W.; Drese, J. H.; Jones, C. W.; Koros, W. J. *Ind. Eng. Chem. Res.* **2009**, *48*, 7314.
 15. Lively, R. P.; Chance, R. R.; Mysona, J. A.; Babu, V. P.; Deckman, H. W.; Leta, D. P.; Thomann, H.; Koros, W. J. *Int. J. Greenhouse Gas Control* **2012**, *10*, 285.
 16. Lively, R. P.; Leta, D. P.; DeRites, B. A.; Chance, R. R.; Koros, W. J. *Chem. Eng. J.* **2011**, *171*, 801.
 17. Labreche, Y.; Lively, R. P.; Rezaei, F.; Chen, G.; Jones, C. W.; Koros, W. J. *Chem. Eng. J.* **2013**, *221*, 166.
 18. Brown, A. J.; Brunelli, N. A.; Eum, K.; Rashidi, F.; Johnson, J. R.; Koros, W. J.; Jones, C. W.; Nair, S. *Science* **2014**, *345*, 72.
 19. (a) Gao, H.; Xu, Y.; Liao, S.; Liu, R.; Liu, J.; Li, D.; Yu, D.; Zhao, Y.; Fan, Y. *J. Membr. Sci.* **1995**, *106*, 213; (b) Garcia-Garcia, F. R.; Kingsbury, B. F. K.; Rahman, M. A.; Li, K. *Catal. Today* **2012**, *193*, 20; (c) Liu, C.; Xu, Y.; Liao, S.; Yu, D. *Appl. Catal., A* **1998**, *172*, 23; (d) Liu, C.; Xu, Y.; Liao, S.; Yu, D.; Zhao, Y.; Fan, Y. *J. Membr. Sci.* **1997**, *137*, 139; (e) Macanas, J.; Ouyang, L.; Bruening, M. L.; Munoz, M.; Remigy, J. C.; Lahitte, J. F. *Catal. Today* **2010**, *156*, 181; (f) Rahman, M. A.; Garcia-Garcia, F. R.; Hatim, M. D. I.; Kingsbury, B. F. K.; Li, K. *J. Membr. Sci.* **2011**, *368*, 116; (g) Tan, X.; Li, K. *Ind. Eng. Chem. Res.* **2006**, *45*, 142; (h) Tan, X.; Li, K. *J. Chem. Technol. Biotechnol.* **2013**, *88*, 1771; (i) Vincent, T.; Guibal, E. *Environ. Sci. Technol.* **2004**, *38*, 4233; (j) Ziegler, S.; Theis, J.; Fritsch, D. *J. Membr. Sci.* **2001**, *187*, 71.
 20. Davies, H. M. L.; Grazini, M. V. A.; Aouad, E. *Org. Lett.* **2001**, *3*, 1475.
 21. (a) Roberge, D. M.; Ducry, L.; Bieler, N.; Cretton, P.; Zimmermann, B. *Chem. Eng. Technol.* **2005**, *28*, 318; (b) Poe, S. L.; Cummings, M. A.; Haaf, M. P.; McQuade, D. T. *Angew. Chem., Int. Ed.* **2006**, *45*, 1544; (c) Bogdan, A. R.; Mason, B. P.; Sylvester, K. T.; McQuade, D. T. *Angew. Chem., Int. Ed.* **2007**, *46*, 1698; (d) Noel, T.; Naber, J. R.; Hartman, R. L.; McMullen, J. P.; Jensen, K. F.; Buchwald, S. L. *Chem. Sci.* **2011**, *2*, 287; (e) Kuhn, S.; Noel, T.; Gu, L.; Heider, P. L.; Jensen, K. F. *Lab Chip* **2011**, *11*, 2488; (f) Hartman, R. L.; Naber, J. R.; Zaborenko, N.; Buchwald, S. L.; Jensen, K. F. *Org. Process Res. Dev.* **2010**, *14*, 1347.

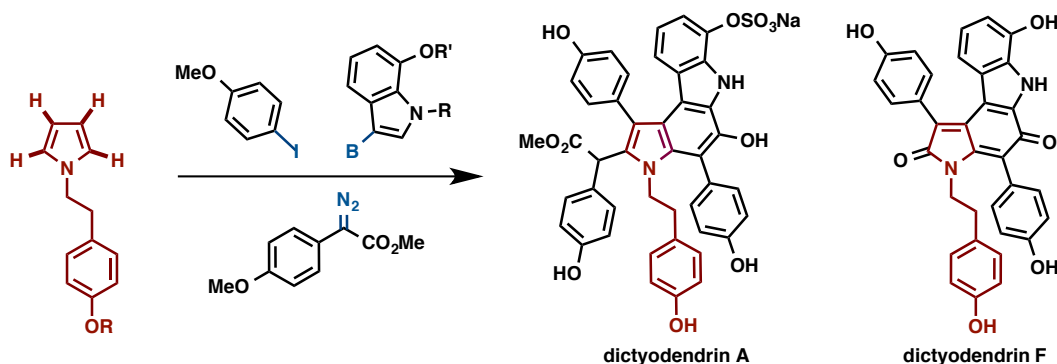
22. (a) Ushakov, D. B.; Gilmore, K.; Kopetzki, D.; McQuade, D. T.; Seeberger, P. H. *Angew. Chem., Int. Ed.* **2014**, *53*, 557; (b) Zhao, D.; Ding, K. *ACS Catal.* **2013**, *3*, 928; (c) Aranda, C.; Cornejo, A.; Fraile, J. M.; Garcia-Verdugo, E.; Gil, M. J.; Luis, S. V.; Mayoral, J. A.; Martinez-Merino, V.; Ochoa, Z. *Green Chem.* **2011**, *13*, 983; (d) Burguete, M. I.; Cornejo, A.; Garcia-Verdugo, E.; Garcia, J.; Jose Gil, M.; Luis, S. V.; Martinez-Merino, V.; Mayoral, J. A.; Sokolova, M. *Green Chem.* **2007**, *9*, 1091; (e) Burguete, M. I.; Cornejo, A.; Garcia-Verdugo, E.; Gil, M. J.; Luis, S. V.; Mayoral, J. A.; Martinez-Merino, V.; Sokolova, M. *J. Org. Chem.* **2007**, *72*, 4344; (f) Abahmane, L.; Koehler, J. M.; Gross, G. A. *Chem. -Eur. J.* **2011**, *17*, 3005; (g) Chinnusamy, T.; Yudha S, S.; Hager, M.; Kreitmeier, P.; Reiser, O. *ChemSusChem* **2012**, *5*, 247; (h) Christakakou, M.; Schoen, M.; Schnuerch, M.; Mihovilovic, M. D. *Synlett* **2013**, *24*, 2411; (i) Dieguez, M.; Pamies, O.; Mata, Y.; Teuma, E.; Gomez, M.; Ribaudó, F.; van Leeuwen, P. W. N. M. *Adv. Synth. Catal.* **2008**, *350*, 2583; (j) Kumar, G. S.; Pieber, B.; Reddy, K. R.; Kappe, C. O. *Chem. - Eur. J.* **2012**, *18*, 6124; (k) Lim, J.; Riduan, S. N.; Lee, S. S.; Ying, J. Y. *Adv. Synth. Catal.* **2008**, *350*, 1295; (l) Tagata, T.; Nishida, M.; Nishida, A. *Adv. Synth. Catal.* **2010**, *352*, 1662; (m) Rueping, M.; Vila, C.; Bootwicha, T. *ACS Catal.* **2013**, *3*, 1676; (n) Brzozowski, M.; Forni, J. A.; Paul Savage, G.; Polyzos, A. *Chem. Commun.* **2015**, *51*, 334; (o) Gemoets, H. P. L.; Hessel, V.; Noel, T. *Org. Lett.* **2014**, *16*, 5800.
23. (a) Qin, C.; Boyarskikh, V.; Hansen, J. H.; Hardcastle, K. I.; Musaev, D. G.; Davies, H. M. L. *J. Am. Chem. Soc.* **2011**, *133*, 19198; (b) Qin, C.; Davies, H. M. L. *J. Am. Chem. Soc.* **2013**, *135*, 14516.
24. Davies, H. M. L.; Manning, J. R. *Nature* **2008**, *451*, 417.
25. Davies, H. M. L.; Morton, D. *Chem. Soc. Rev.* **2011**, *40*, 1857.
26. Lian, Y.; Davies, H. M. L. *J. Am. Chem. Soc.* **2011**, *133*, 11940.
27. Davies, H. M. L.; Jin, Q. *J. Am. Chem. Soc.* **2004**, *126*, 10862-10863.
28. Davies, H. M. L.; Lian, Y. *Acc. Chem. Res.* **2012**, *45*, 923.
29. Kornecki, K. P.; Briones, J. F.; Boyarskikh, V.; Fullilove, F.; Autschbach, J.; Schrote, K. E.; Lancaster, K. M.; Davies, H. M. L.; Berry, J. F. *Science* **2013**, *342*, 351.
30. Davies, H. M. L.; Bruzinski, P.; Hutcheson, D. K.; Kong, N.; Fall, M. J. *J. Am. Chem. Soc.* **1996**, *118*, 6897.
31. Davies, H. M. L.; Antoulinakis, E. G. *Org. React.* **2001**, *57*, 1.
32. Manning, J. R.; Davies, H. M. L. *Org. Synth.* **2007**, *84*, 334-346.
33. Davies, H. M. L.; Nagashima, T.; Klino, J. L., III *Org. Lett.* **2000**, *2*, 823.
34. Qin, C.; Boyarskikh, V.; Hansen, J. H.; Hardcastle, K. I.; Musaev, D. G.; Davies, H. M. L. *J. Am. Chem. Soc.* **2011**, *133*, 19198.
35. Chepiga, K. M.; Qin, C.; Alford, J. S.; Chennamadhavuni, S.; Gregg, T. M.; Olson, J. P.; Davies, H. M. L. *Tetrahedron* **2013**, *69*, 5765.
36. Rezaei, F.; Lively, R. P.; Labreche, Y.; Chen, G.; Fan, Y.; Koros, W. J.; Jones, C. W. *ACS Appl. Mater. Interfaces* **2013**, *5*, 3921.
37. Thompson, J. L.; Davies, H. M. L. *J. Am. Chem. Soc.* **2007**, *129*, 6090.
38. (a) Ohno, T.; Yoshizawa, S.; Miyashita, Y.; Nishio, Y. *Cellulose* **2005**, *12*, 281; (b) Ohno, T.; Nishio, Y. *Cellulose* **2006**, *13*, 245; (c) Kusumi, R.; Teramoto, Y.; Nishio, Y. *Polymer* **2011**, *52*, 5912.
39. Moschetta, E. G.; Negretti, S.; Chepiga, K. M.; Brunelli, N. A.; Labreche, Y.; Feng, Y.; Rezaei, F.; Lively, R. P.; Koros, W. J.; Davies, H. M. L.; Jones, C. W. *Angew. Chem. Int. Ed.* **2015**, *54*, 1.

Chapter V: Concise Synthesis of Dictyodendrin A by a Sequential C–H Functionalization Strategy

Advisor: Huw M. L. Davies, Ph.D.

Collaborator: Kenichiro Itami, Ph.D.

The dictyodendrin marine alkaloids possess unique structures as well as notable biological activities. This chapter describes a synthetic strategy for the synthesis of dictyodendrins A and F. In this chapter a new synthetic strategy to the dictyodendrins utilizing sequential regioselective C–H functionalizations is described. This synthetic approach features a combination of regioselective C–H arylation, C–H insertion, and Suzuki-Miyaura coupling to fully functionalize the pyrrole ring in order to realize a short synthesis.



5.1 Introduction to the Dictyodendrin Marine Alkaloids

Dictyodendrins A–E (Figure 5.1, **1** – **4** and **9**), isolated in 2003 from a Japanese marine sponge, *Dictyodendrilla verongiformis* by Fusetani, Matsunaga and co-workers,¹ are the first marine alkaloids to inhibit telomerase,² giving them potential as targets for cancer chemotherapy. Dictyodendrins F–J (**5** – **8** and **10**), isolated in 2012 from a southern Australian marine sponge *Ianthella* sp. by Capon and co-workers,³ exhibit significant β -secretase (β -site APP cleaving enzyme: BACE) inhibitory activity (IC_{50} 1–2 μ M). Synthetic organic chemists have developed

new methods for the syntheses of these natural products which are synthetically challenging due to the structural complexity of their highly substituted pyrrolo[2,3-*c*]carbazole core (Figure 5.1).⁴

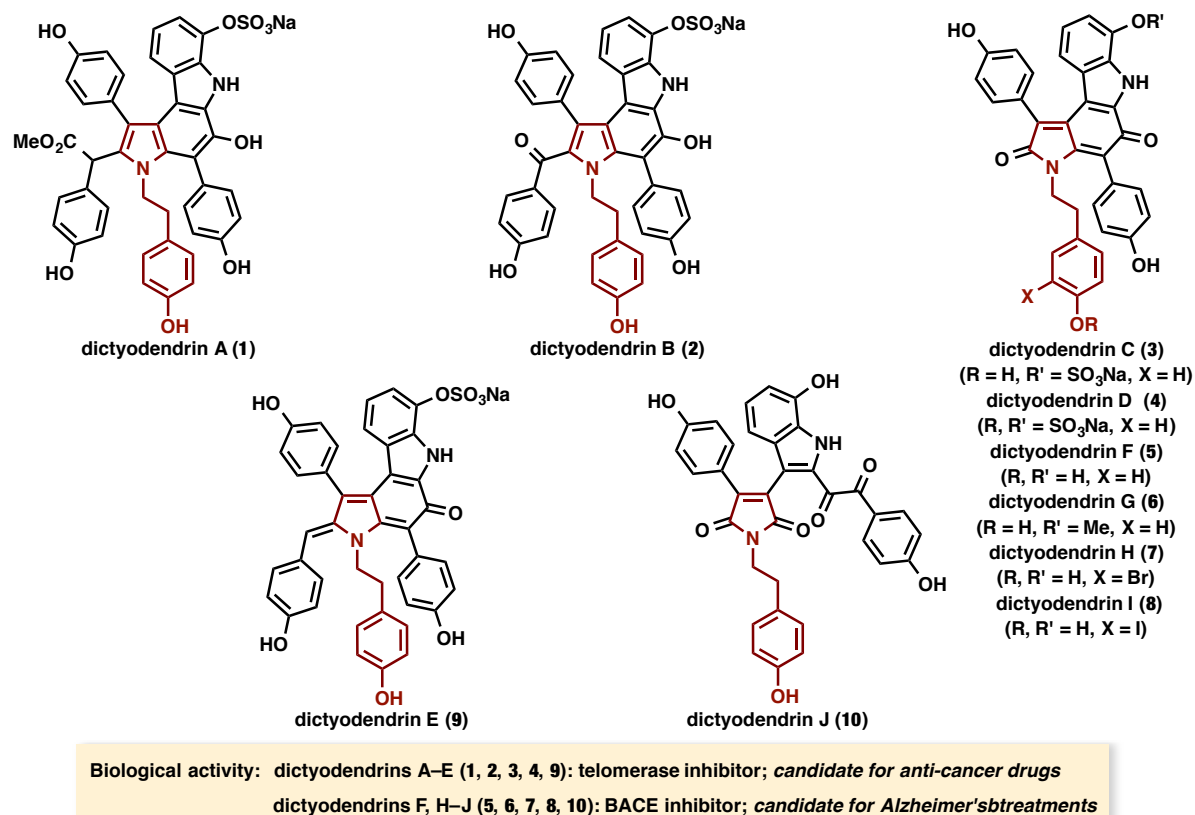


Figure 5.1 A summary of the structures and biological activities of the dictyodendrins

5.2 Previous Total Syntheses of the Dictyodendrins

Through the combined efforts of Fürstner, Ishibashi, Tokuyama, and Jia, the total syntheses of dictyodendrins A-F have been accomplished (Figure 5.2). Fürstner and Ishibashi focused on building complexity around the pyrrole core, while the Tokuyama and Jia chose the indole ring for the core structure (Figure 5.2, core structures highlighted in red). Fürstner and co-workers reported the first total syntheses of dictyodendrins B, C, E, and F in 2005 and 2006. Their

synthetic route featured a titanium-mediated reductive coupling reaction for the construction of the indole ring, followed by pyrrolo[2,3-*c*]carbazole core closure via 6π -electrocyclization.⁵ In 2010, Iwao, Ishibashi and co-workers achieved an efficient synthesis of dictyodendrin B by use of a Suzuki–Miyaura cross-coupling reaction to introduce two aromatic rings to the pyrrole core.⁶ Tokuyama and co-workers accomplished the total syntheses of dictyodendrins A–E in 2010 and 2011 utilizing an indoline formation by *in situ* generation of benzyne and a Pd-catalyzed cross-coupling.⁷ Recently, Jia and co-workers reported the total syntheses of dictyodendrins B, C and E using a one-pot Buchwald–Hartwig amination / intramolecular C–H coupling (Figure 5.2).⁸

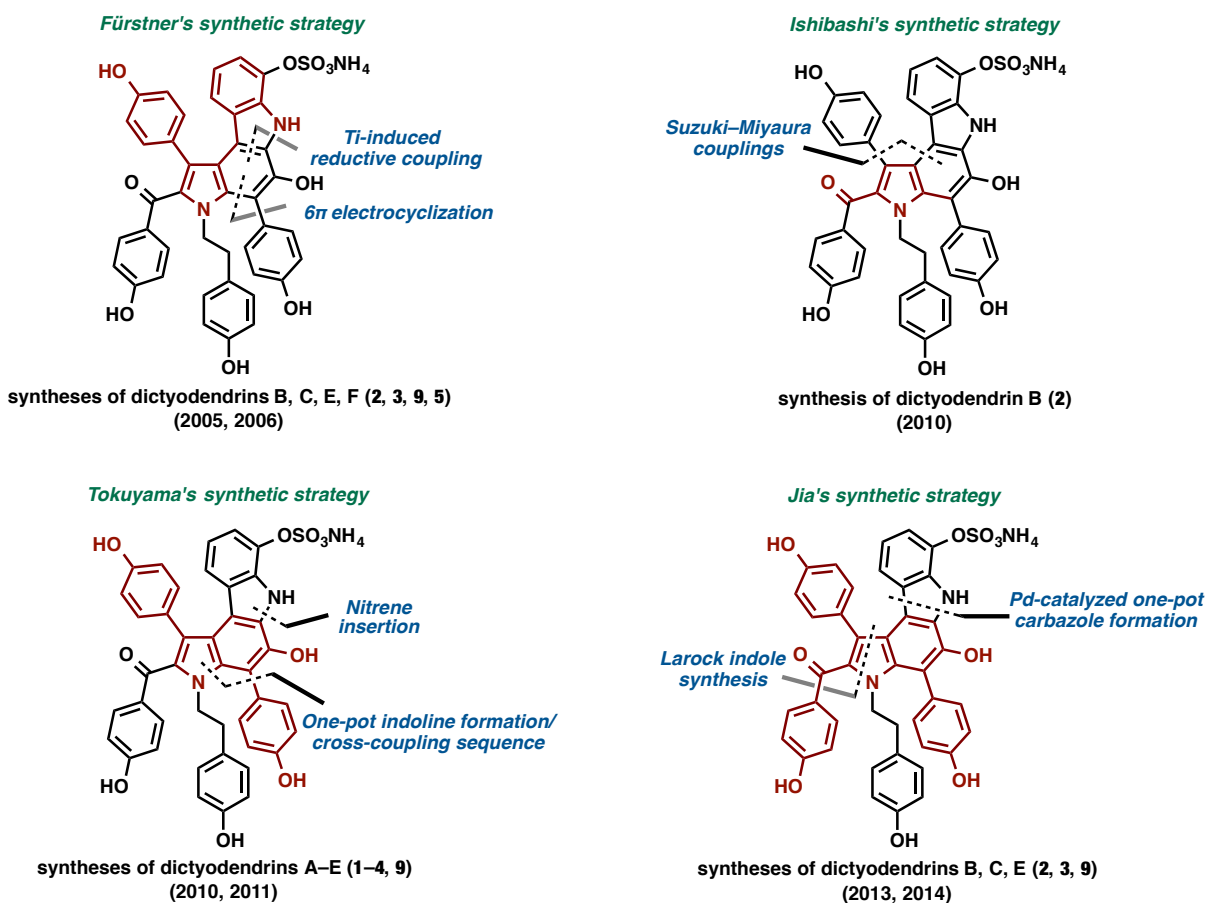


Figure 5.2 Previously reported strategies for the syntheses of the dictyodendrins

In Fürstner's report on the total syntheses of dictyodendrins B, C and E, he noted that dictyodendrins A–E differ only in their oxidation state and C2 substitution of the central pyrrole ring. For this reason, he proposed a pyrrolocarbazole as a common intermediate for the preparation of the entire dictyodendrin family (Figure 5.3). Dictyodendrins B (**2**)^{5a} and C (**3**),^{5b} E (**9**)^{5b} were synthesized from this common intermediate (**1**).^{5b} Although initially proposed in this report, the syntheses of dictyodendrins A (**1**) and D (**4**) were not accomplished in this way.

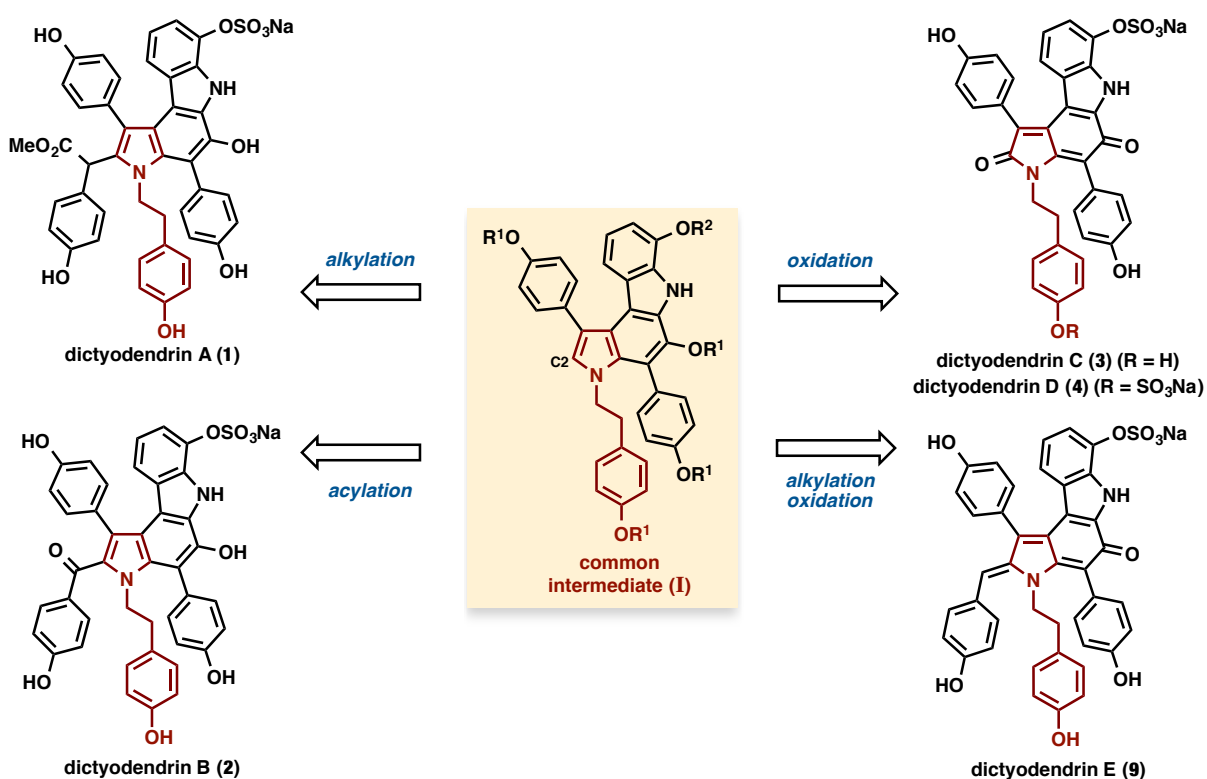
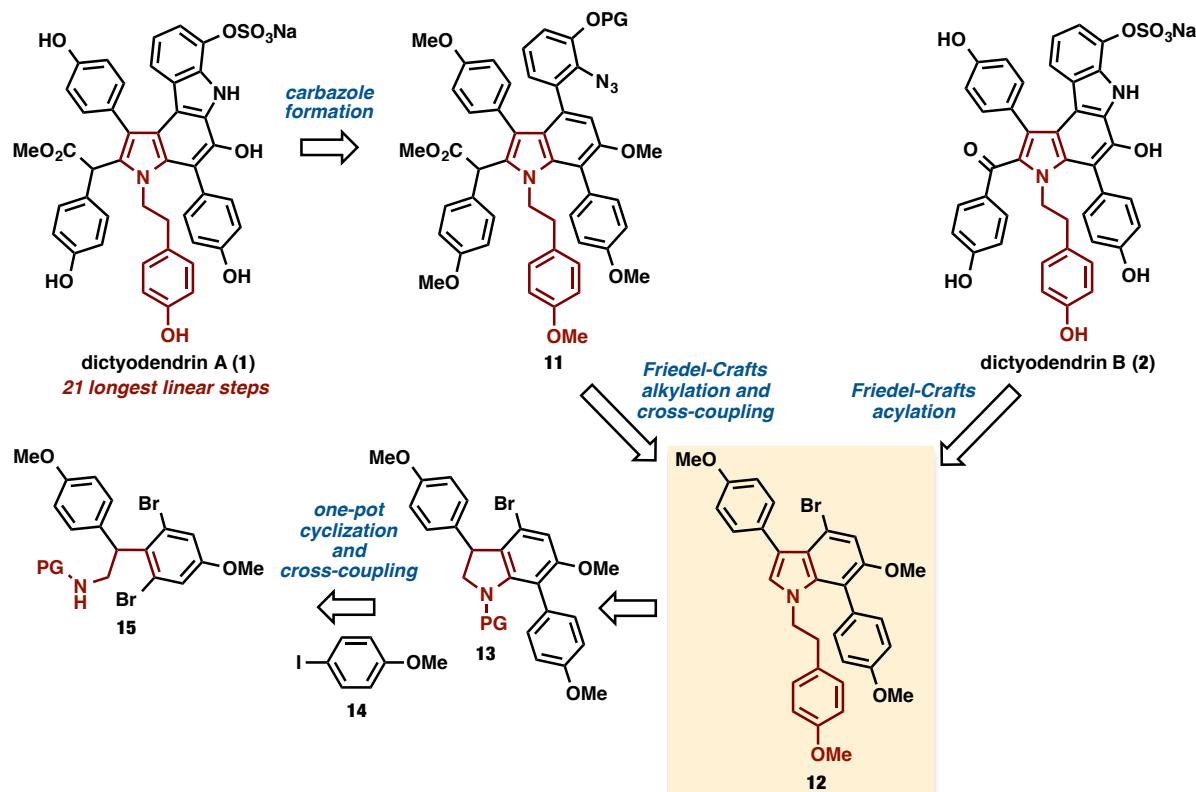


Figure 5.3 Fürstner's common intermediate for the syntheses of dictyodendrins A-E

Tokuyama's synthesis of dictyodendrin A (**1**) and a total synthesis of B (**2**) involved introduction of peripheral segments on the pivotal indoline intermediate **13**. The carbazole skeleton of the natural product was formed by installation of an aryl azide segment (**11**) and intramolecular C–H insertion via a nitrene intermediate generated by thermolysis. The *para*-

anisylacetate moiety of **11** could be introduced on a bromoindole intermediate (**12**) by regioselective Friedel–Crafts alkylation. This synthesis featured one of its initial steps, an unprecedented benzyne-mediated one-pot cyclization/cross-coupling sequence, as the key step in the synthesis (Scheme 5.1).⁷

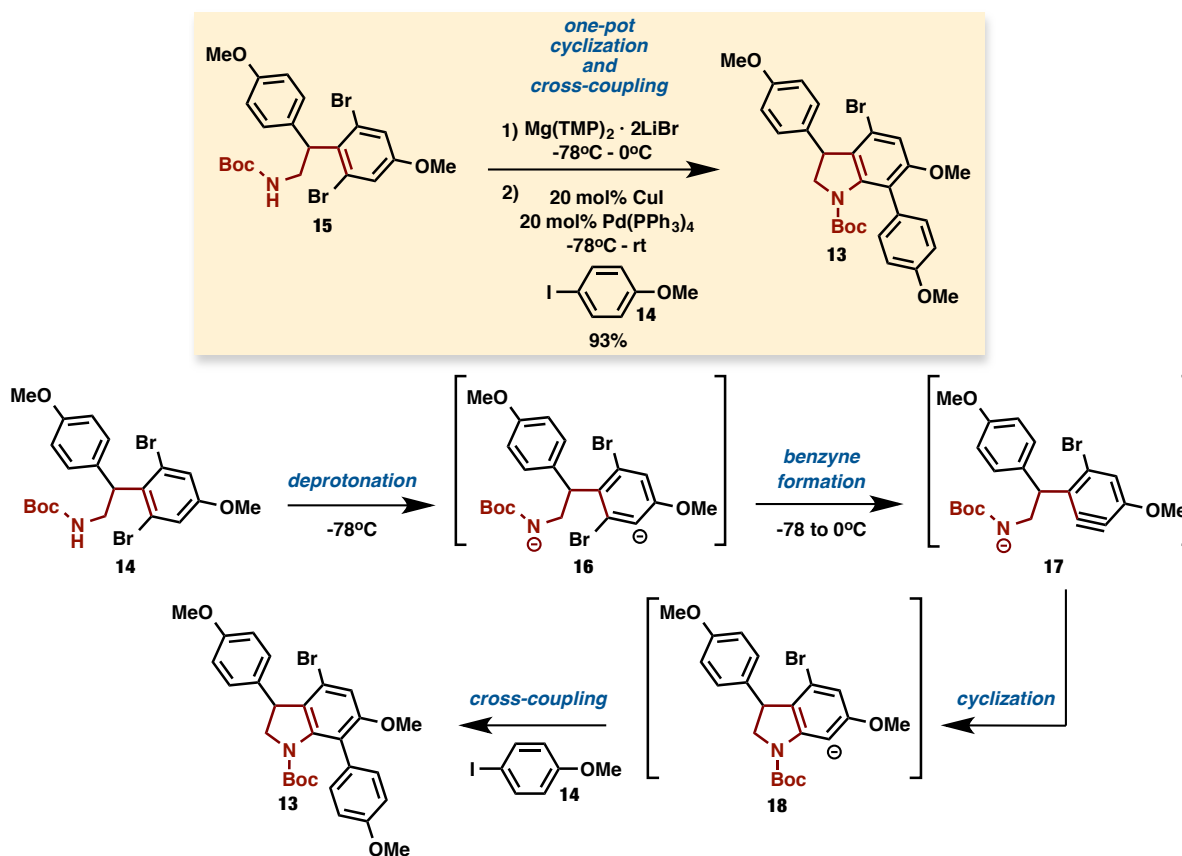
Scheme 5.1 Tokuyama's retrosynthetic analysis of dictyodendrin A



The working hypothesis for the mechanism of the benzyne-mediated one-pot indoline formation/cross-coupling reaction is initial generation of dianion species **16** at low temperature followed by elevation of the reaction temperature to induce the formation of benzyne **17** and cyclization to provide 7-metalated indoline **18**. The metalated species **18** then serves as a suitable substrate for the subsequent cross-coupling with 4-iodoanisole (**14**) to furnish the desired 7-anisyl derivative **13**. Direct coupling of 7-magnesium species **18** was examined under Kumada–

Tamao coupling conditions. Transmetalation to the copper species was crucial for a high yielding cross-coupling process (Scheme 5.2).^{7a}

Scheme 5.2 Tokuyama's benzyne-mediated one-pot indole formation / cross-coupling reaction



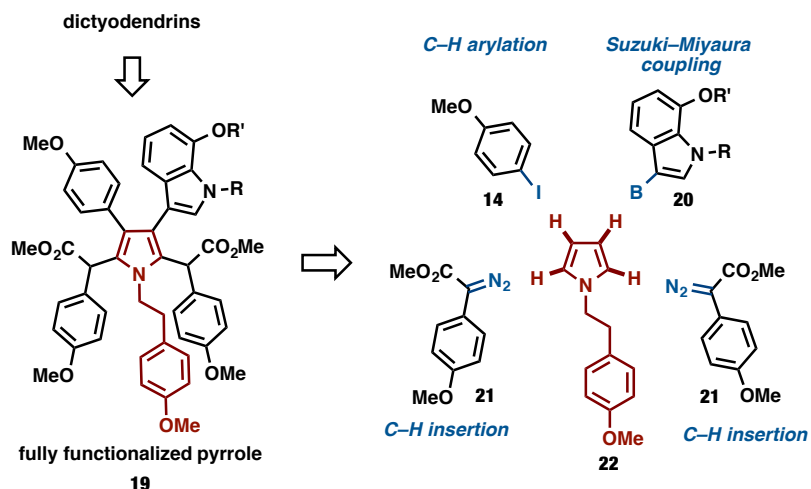
Although this was a flexible route which provided access to two of the dictyodendrins, including a total synthesis of B and the first total synthesis of dictyodendrin A, the synthesis of dictyodendrin A required 21 total steps and was only produced in 8.2% overall yield.

5.3 Exploratory Studies Toward the Synthesis of Dictyodendrin A

Jia and co-workers, who achieved the synthesis of dictyodendrins B, C and E through a C–H activation strategy, also attempted, yet failed to complete, the total synthesis of dictyodendrin A.^{8b} Their key one-pot reaction of Buchwald–Hartwig amination/intramolecular C–H coupling reaction gave only a trace amount of dictyodendrin A and they failed to convert the intermediate of the synthesis of dictyodendrin B into dictyodendrin A by means of the transformation of the C2 substituent.^{8b} Although these findings confirm that dictyodendrin A is a particularly challenging target, through a collaboration with Prof. Kenichiro Itami and Prof. Junichiro Yamaguchi from the University of Nagoya in Japan, we envisioned a streamlined retro-synthetic route to dictyodendrin A by sequential C–H functionalization reactions utilizing a combination of rhodium carbenoid C–H activation developed by Davies and co-workers and rhodium mediated aryl C–H coupling developed by Itami and co-workers.

The first synthetic route presented was investigated by Dr. Atsushi D. Yamaguchi of the Itami lab during his research exchange in the Davies lab. In this route, *N*-alkylpyrrole **22** serves as the core structure around which complexity could be built by functionalization of the four C–H bonds of the pyrrole ring. This route obviates the need for substrate prefunctionalization and thus would allow for a short and efficient synthesis of dictyodendrin A (Scheme 5.3). The order in which the C–H functionalization reactions are carried out plays a key role in controlling regioselectivity.⁹

Scheme 5.3 Davies / Itami route to access the dictyodendrins via sequential regioselective C–H functionalizations

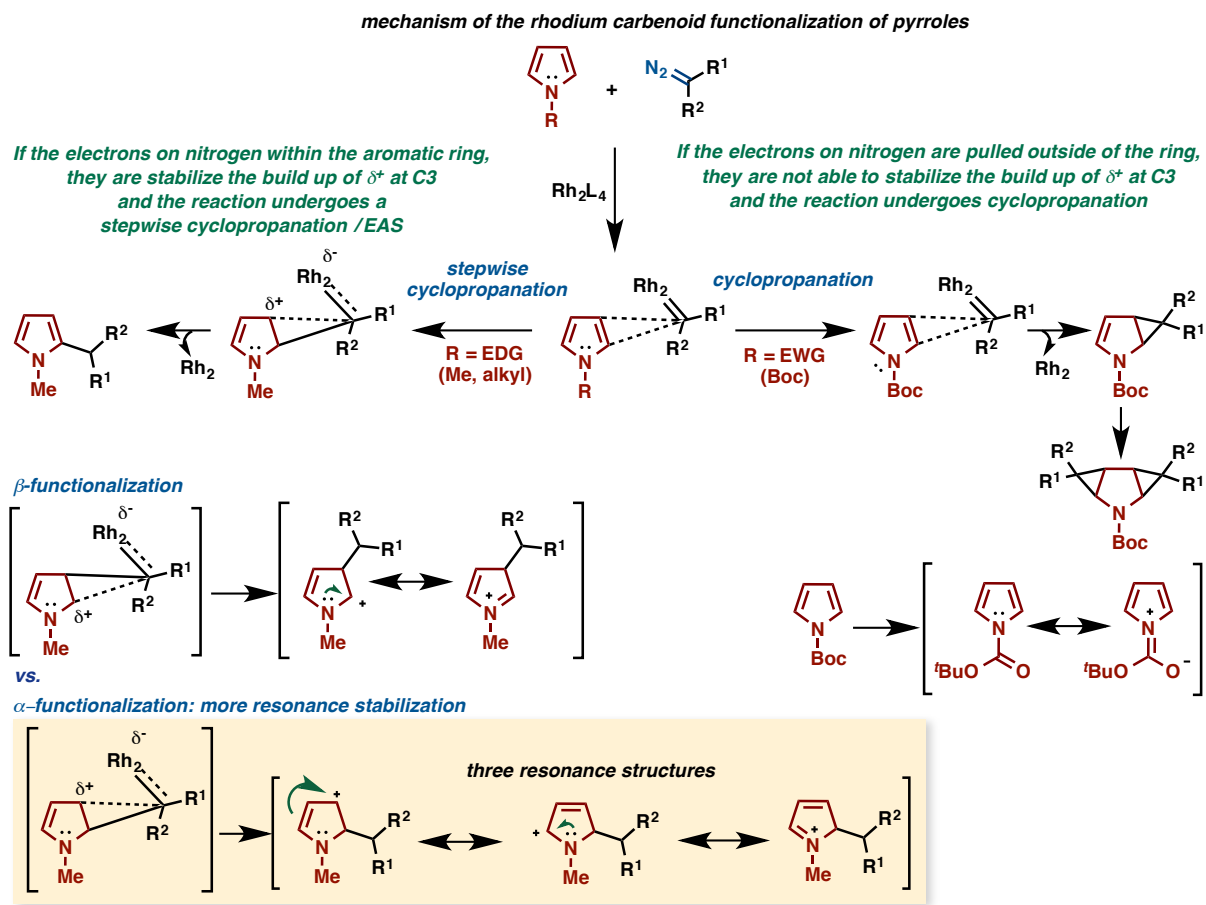


Two main reaction pathways are possible in the reaction of pyrroles with dirhodium(II) carbenoids involving either a concerted asynchronous cyclopropanation or zwitterionic intermediates. The nitrogen lone pair of *N*-acyl pyrroles is in conjugation with the carbonyl group, pulling electron density out of the aromatic ring and making them behave more like a diene towards metal carbenoids, giving rise predominantly to cyclopropane products. The reaction of carbenoids with *N*-H or *N*-alkyl pyrroles tends to proceed via zwitterionic intermediates, leading to alkylation products. The mechanism is stepwise. The size of the alkyl substituent determines whether the electrophilic carbenoid will attack at the 2- or 3-position. Smaller substituents favor 2-alkylation, while bulkier substrates give rise to the 3-alkylation product. The vinyl C–H bond is too strong to undergo a typical C–H insertion reaction or a hydride-abstraction/C–H insertion type mechanism.

The alkylation products can be considered to be derived from two possible pathways (Scheme 5.4). Donor/acceptor-substituted rhodium carbenoid intermediates could undergo a concerted asynchronous cyclopropanation in which ring opening and proton transfer gives rise to

the alkylation products. Alternatively, when acceptor/acceptor-substituted diazo starting materials are used, this transformation is presumed to proceed via an electrophilic aromatic substitution-type attack of the pyrrole on the rhodium carbenoid to generate zwitterionic intermediates which then rearrange by a 1,2-proton shift and concurrent aromatization. The preference for 2-alkylation is consistent with the electrophilic substitution reactions of pyrroles. Additionally the largest orbital coefficients on the HOMO of the pyrrole further support the preference for 2-alkylation. The most robust substrates for these reactions are those which best stabilize the anion portion of the zwitterionic intermediate. The *N*-alkyl substituent and the type of catalyst used determine the efficiency and regioselectivity of the reaction.¹⁰

Scheme 5.4 Controlling factors for rhodium carbenoid selectivity in reaction with pyrroles: cyclopropanation vs. C–H functionalization



The 2-functionalization of *N*-alkylpyrroles with the use of a rhodium-stabilized carbenoid is a well-precedented transformation. In their efforts to optimize the syntheses of tolmetin, an important nonsteroidal anti-inflammatory agent for the treatment of arthritis, and zomepirac, a potent nonnarcotic analgesic, Maryanoff explored the 2-alkylation of *N*-methylpyrrole with ethyl diazoacetate (EDA),¹¹ dimethyl diazomalonate (DMDM) and ethyl 2-diazoacetoacetate (EDAA) with the use of both copper(II)-promoting agents and rhodium(II) acetate dimer.¹² The reaction of EDA (**24a**) with *N*-methylpyrrole (**23**) failed to proceed under $\text{Rh}_2(\text{OAc})_4$ -catalysis.^{11a} When the diazo substrate was switched to DMDA (**24b**) or EDAA (**24c**), however, the selective 2-functionalization of *N*-methylpyrrole (**23**) proceeded in high yield

(**25b**: 83% and **25c**: 72%) and regioselectivity (**25b**: 9.8 : 1 and **25c**: > 10 : 1) (Table 5.1).

Table 5.1 Regioselective α -functionalization of acceptor and acceptor/acceptor-substituted rhodium carbenoids with *N*-methylpyrrole

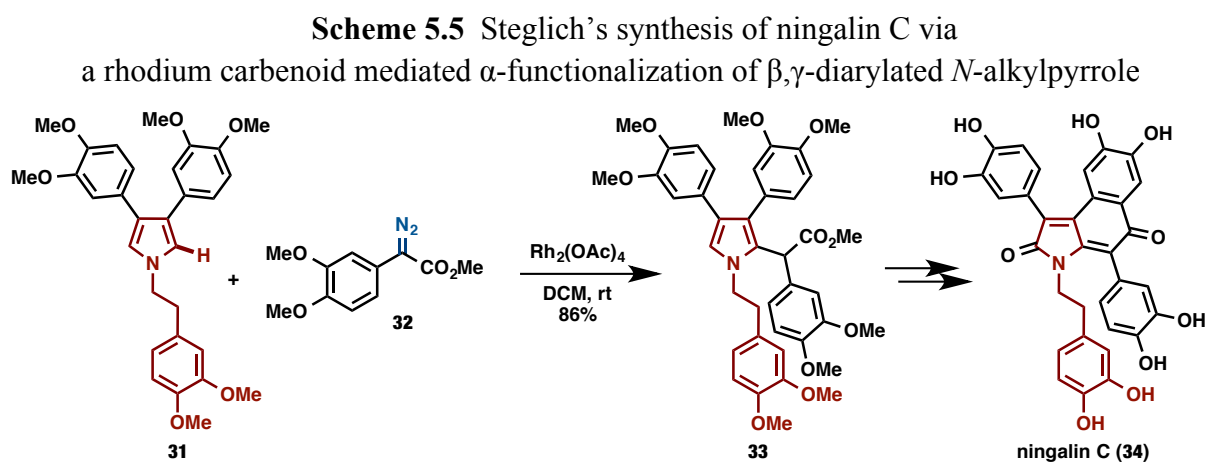
entry	diazo	R ¹	R ²	product	combined yield (%) (25 + 26)	ratio (25 : 26)	isolated yield (%) (25)
1	EDA	H	CHO ₂ C ₂ H ₅	25a + 26a	0	N/A	N/A
2	DMDA	CO ₂ CH ₃	CO ₂ CH ₃	25b + 26b	92	9.8 : 1	83
3	EDAA	C(O)CH ₃	CO ₂ C ₂ H ₅	25c + 26c	-	>10 : 1	72

Davies *et al.* have explored the reactions of rhodium stabilized donor/acceptor carbenoids with pyrroles.¹⁰ Tropanes are formed in the rhodium-catalyzed reaction of vinyldiazoacetates with *N*-Boc-pyrroles via tandem cyclopropanation/Cope rearrangement.¹³ Interestingly, when the substrate is switched to *N*-methylpyrroles, alkylation occurs rather than cyclopropanation.^{13a} In 2010, Davies and co-workers reported the functionalization of *N*-methylpyrroles with vinyldiazoacetates. This report mostly focused on the vinylogous reactivity of vinyldiazoacetates with only three examples of reactivity of the vinyldiazoacetate coming from the carbenoid site (Table 5.2).¹⁴ The reaction of aryldiazoacetates with *N*-Boc-pyrrole results in double cyclopropanation of the pyrrole rings.¹⁵ The reaction of aryldiazoacetates with *N*-methylpyrrole, however, has not been explored and there has only been one report of reaction of aryldiazoacetates with *N*-alkylpyrroles to date.¹⁶

Table 5.2 Reactions of vinyl diazoacetates with substituted *N*-methylpyrroles

entry	R	alkene geometry of vinyl diazoacetate	carbenoid reactivity yield (%)	vinylogous reactivity yield (%)
1	H	(<i>E</i>)	54	0
2	H	(<i>Z</i>)	50	5
3	CH ₃	(<i>E</i>)	50	28

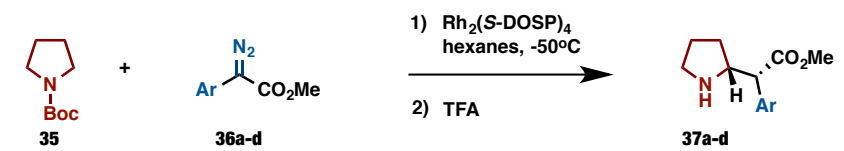
The rhodium carbenoid mediated 2-functionalization of a β -arylated *N*-alkylpyrrole with an electron-rich aryldiazoacetate is also preceded by an inhibitor (Scheme 5.5).¹⁶ In 2000, Steglich and co-workers reported the monoalkylation of 3,4-diarylated pyrrole **31** with electron-rich aryldiazoacetate **32** as a key step in the synthesis of ningalin C (**34**), a biogenetically related analogue of the marine alkaloid purpurone which is a potent ATP-citrate lyase (ACL) inhibitor (Scheme 5.5).¹⁶



Additionally, although the double carbenoid functionalization of an *N*-alkylpyrrole, as proposed in Scheme 5.3, is unprecedented, it was inspired by the work of Davies and co-workers

in the highly enantioselective C–H insertion into cycloalkanes and tetrahydrofuran. Specifically, C–H insertions of aryldiazoacetates **36a-d** into *N*-Boc-pyrrolidine (**35**) are highly regio-, diastereo-, and enantioselective (Table 5.3).¹⁷

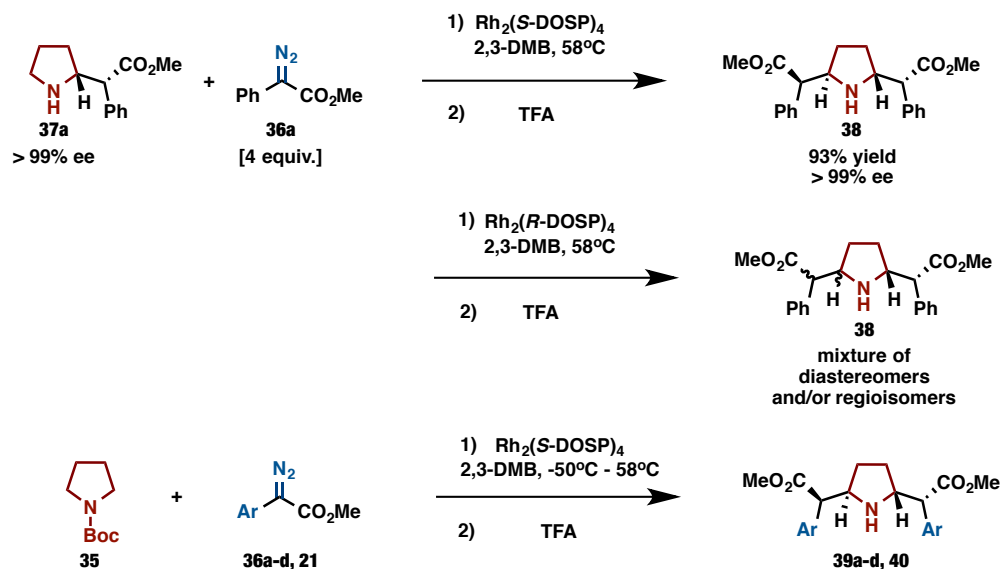
Table 5.3 Davies' α -selective C–H functionalization of *N*-Boc-pyrrolidine



entry	Ar	product	yield (%)	ee (%)	de (%)
1	Ph	37a	72	94	92
2	<i>p</i> -ClC ₆ H ₄	37b	70	94	94
3	<i>p</i> -MeC ₆ H ₄	37c	67	93	94
4	2-Naphthyl	37d	49	93	92

In this report, bis-C–H insertion reactions were also possible by Rh₂(*S*-DOSP)₄-catalyzed decomposition of aryldiazoacetates **36a-d** and **21** in the presence of *N*-Boc-pyrrolidine (**35**), followed by heating of the mixture under reflux with additional aryldiazoacetate to generate *C*2-symmetric amines **39a-d** and **40**. This second pyrrole functionalization reaction also proceeded with excellent yield and enantioselection with the use of enantiomerically pure 2-functionalized pyrrolidine **37a** (obtained from recrystallization of the product shown in Table 5.3 up to enantiopurity). In contrast, using Rh₂(*R*-DOSP)₄ as catalyst resulted in the formation of a mixture of diastereomers and/or regioisomers that were not resolvable. This difunctionalization reaction could be performed as a one-pot process with the use of Rh₂(*S*-DOSP)₄ as a catalyst and was found to be compatible with a variety of diazo substrates (Table 5.4).¹⁷ This 2, 5-difunctionalization methodology, however, has not been previously reported with the use of pyrroles as substrates.

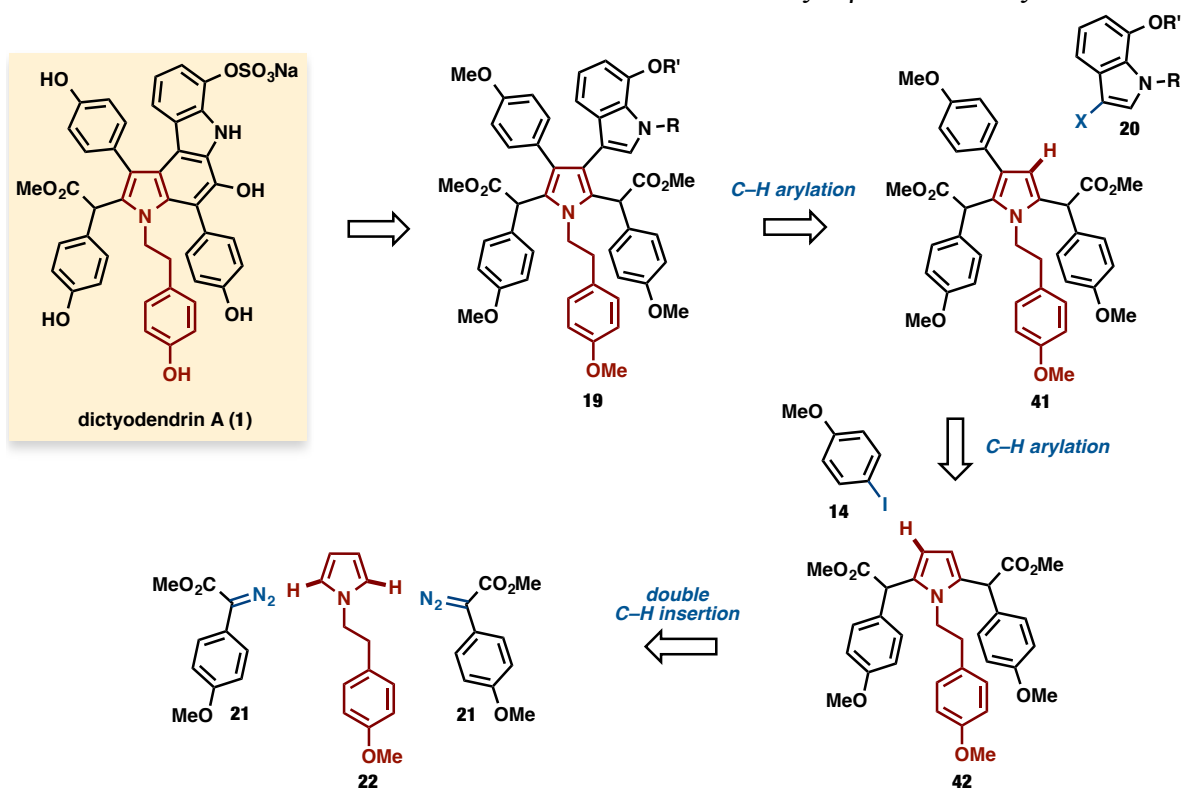
Table 5.4 Davies' α -selective double carbenoid insertion into *N*-Boc-pyrrolidine



entry	Ar	product	ee (%)	yield (%)
1	Ph	39a	97	78
2	<i>p</i> -ClC ₆ H ₄	39b	96	50
3	<i>p</i> -MeC ₆ H ₄	39c	96	51
4	2-Naphthyl	39d	88	62
5	<i>p</i> -MeOC ₆ H ₄	40	97	40

Inspired by this chemistry, the bis-functionalization of the *N*-alkylpyrrole **22** was proposed. In a collaborative effort to synthesize dictyodendrin A, the Davies and Itami groups proposed a retro-synthetic route that would proceed via an initial α -selective double carbenoid insertion followed by a β -selective arylation. This initial approach toward dictyodendrin A (**1**) was proposed based on the known regioselectivities of pyrrole functionalization chemistry. At first, double C–H insertion of *N*-alkylpyrrole **22** with aryldiazoester **21** would provide 2,5-disubstituted pyrrole **42** which could then undergo sequential C–H arylations, to introduce two different aryl moieties (**14** and **20**), and afford the fully functionalized pyrrole **19**. The arylations were expected to proceed at the β -positions of the pyrrole because the two α -positions would be blocked by the alkyl groups. Finally, dictyodendrin A (**1**) would be prepared from fully functionalized pyrrole **19** by construction of the six-membered ring (Scheme 5.6).

Scheme 5.6 Davies / Itami retro-synthetic route to dictyodendrin A via an α -selective double carbenoid insertion followed by a β -selective arylation

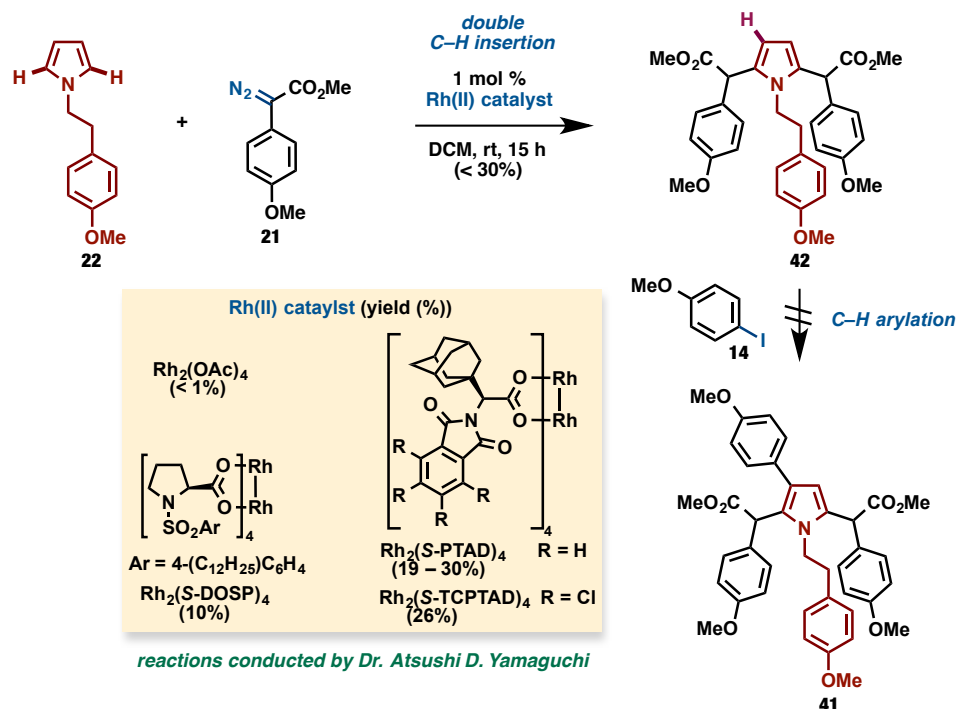


Next, the double C–H insertion of **22** with diazoester **21** was investigated by Dr. Atsushi Yamaguchi. Unfortunately, $\text{Rh}_2(\text{OAc})_4$ did not provide any alkylated pyrrole **42**. $\text{Rh}_2(\text{S-DOSP})_4$, gave the desired product **42** in less than 10% yield along with the 3,4-difunctionalized isomer. $\text{Rh}_2(\text{S-PTAD})_4$ and its tetrachlorinated and sterically hindered derivative $\text{Rh}_2(\text{S-TCPTAD})_4$ also produced **42** in low yields (Scheme 5.7). (As $\text{Rh}_2(\text{S-TCPTAD})_4$ was the best catalyst for this transformation, it was used in all subsequent attempts for the α -selective double carbenoid insertion into pyrroles). Additionally, varying the temperature of the reaction did not affect reactivity.

Once 2,5-disubstituted pyrrole **42** was obtained, the next challenge involved introduction of an aryl group to the C3 position. Different reaction conditions for direct C–H arylation of electron-rich heteroarenes previously developed in the Itami group were screened by Dr. Atsushi

Yamaguchi. Several catalyst systems were screened including $\text{RhCl}(\text{CO})\{\text{P}[\text{OCH}(\text{CF}_3)_2]_3\}_2$ which has shown a high reactivity for the C–H arylation of thiophenes and pyrroles,¹⁸ $\text{PdCl}_2/\text{P}[\text{OCH}(\text{CF}_3)_2]_3$ which has enabled a β -selective direct arylation of thiophenes,¹⁹ $\text{PdCl}_2/\text{bipy}$ which has catalyzed efficient C–H arylation of thiophenes to provide α -arylated thiophenes regioselectively,²⁰ and $[\text{Pd}(\text{OAc})_2/\text{bipy}/\text{TEMPO}]$ which has shown β -selectivity in the direct arylation of thiophenes with arylboronic acids.²¹ Unfortunately, none of these reaction conditions afforded the desired coupling product **41**. This reaction is believed to have failed due to the steric hindrance at the C3 position of **42** as well as to the electronic influence of ester groups and α -protons adjacent to carbonyl groups (Scheme 5.7).⁹

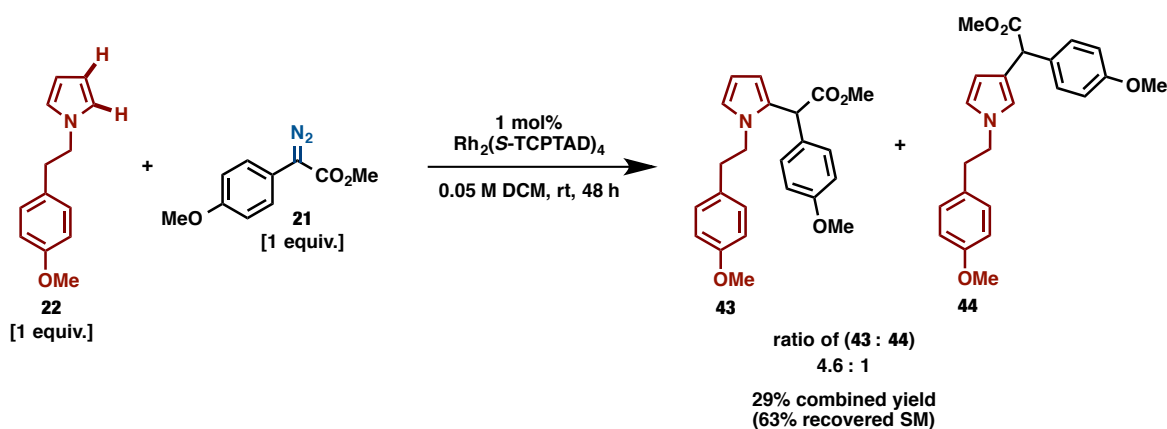
Scheme 5.7 Attempts toward the synthesis of dictyodendrin A via an α -selective double carbenoid insertion followed by a β -selective arylation



Finally, to better understand the regioselectivity of this transformation, the reaction was repeated with one equivalent of both the *N*-alkylpyrrole **22** and the aryl diazoacetate **21**. The

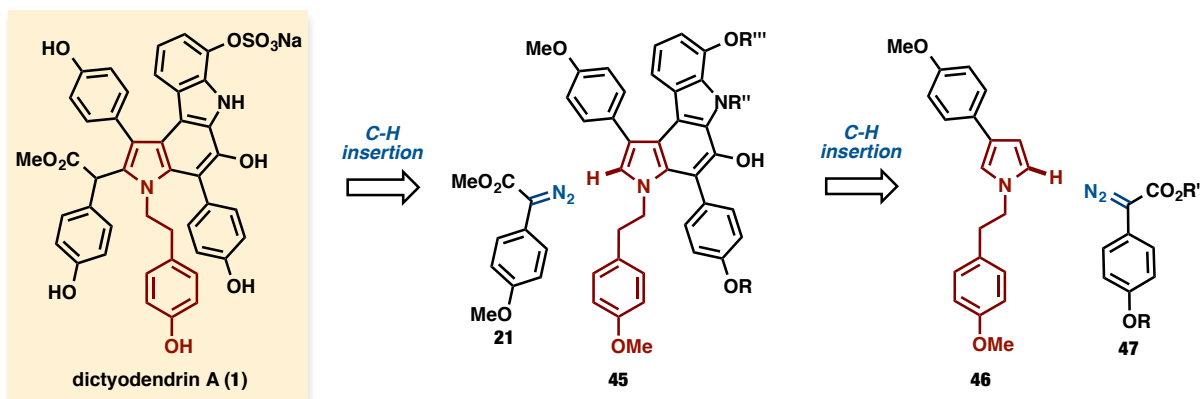
functionalization of **22** with methyl 2-diazo-2-(4-methoxyphenyl)acetate (**21**) proceeded with poor regioselectivity (4.6 : 1 ratio of **43** to **44**) and yield (29% combined yield of **43** and **44**) and a significant amount of undecomposed starting pyrrole **22** (63%) was recovered (Scheme 5.8). One possible explanation for this poor reactivity could be catalyst poisoning as a color change from green to red was observed upon addition of substrate **22** to the catalyst in solution.

Scheme 5.8 C–H functionalization of an unsubstituted *N*-alkylpyrrole with an electron-rich methyl ester-substituted donor/acceptor-diazo compound



A new synthetic route to dictyodendrin A that commences with β -selective direct arylation of pyrroles was chosen due to the difficulty in introducing the aryl group into a sterically hindered pyrrole. Inspired by Steglich's successful 2-functionalization of a β -arylated *N*-alkylpyrrole with an electron-rich aryldiazoacetate (Scheme 5.5), we decided to reverse the order of the functionalization reactions and attempt the C–H arylation of the β -position of pyrrole **22** followed by functionalization of the 2-position of **46**. To better understand the selectivity of the functionalization reactions, this synthetic route involved two sequential rhodium carbenoid C–H functionalizations (Scheme 5.9).

Scheme 5.9 Davies / Itami retro-synthetic route to dictyodendrin A via β -selective arylation followed by an initial α -selective carbenoid insertion, carbazole closure, and a final α -selective carbenoid insertion



There have been several reports of the C–H arylation of pyrroles but these almost always occur with α -selectivity.²² Itami *et al.* developed a rhodium complex bearing a strongly π -accepting ligand, $P[OCH(CF_3)_2]_3$, as an efficient catalyst precursor for C–H arylation of heteroarenes with aryl iodides. In this report, a range of five-membered heteroarenes, such as thiophenes, furans, pyrroles, and indoles, could be arylated. While thiophenes, bithiophene, and 2,3-dimethylfuran were arylated selectively at carbons adjacent to sulfur or oxygen, 1-phenylpyrrole was selectively arylated at the β -position (Table 5.5).²³

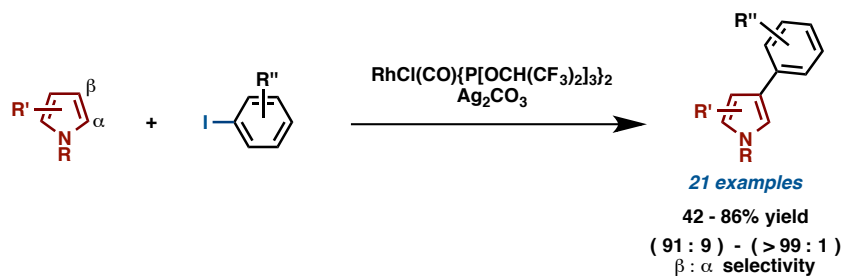
Table 5.5 Itami's direct C–H arylation of heteroarenes catalyzed by $\text{RhCl}(\text{CO})\{\text{P}[\text{OCH}(\text{CF}_3)_2]_3\}_2$

entry	product structure	product	R	yield (%)
1		50a	H	73
2		50b	Ac	94
3		50c		52
4		50d	H	76
5		50e	Ac	79
6		50f	Me	50
7				
8		50g	Ac	64
9		50h	CN	66
10		50i		58
11		50j		57% C-3 functionalized
12		50k		23% C-2 functionalized

Cl
 $\text{[(F}_3\text{C)}_2\text{HCO]}_3\text{P}-\text{Rh}-\text{P}[\text{OCH}(\text{CF}_3)_2]_3$
 CO

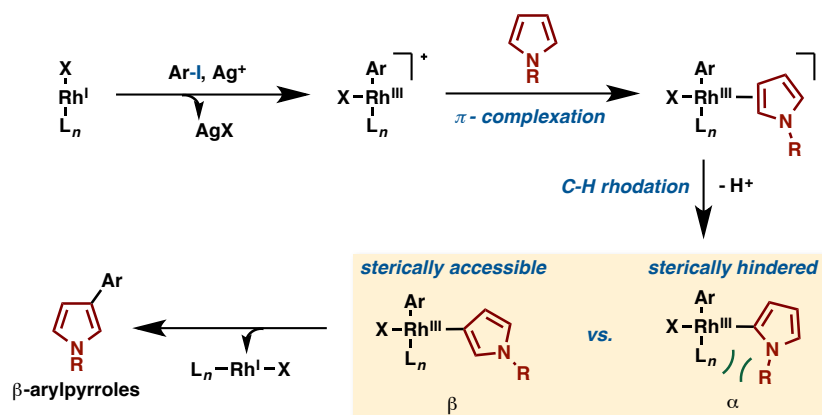
Recently, the Itami group reported this as a general method for the β -selective C–H arylation of pyrroles (Scheme 5.10).^{18, 24}

Scheme 5.10 β -selective arylation of pyrroles by $\text{RhCl}(\text{CO})\{\text{P}[\text{OCH}(\text{CF}_3)_2]_3\}_2$



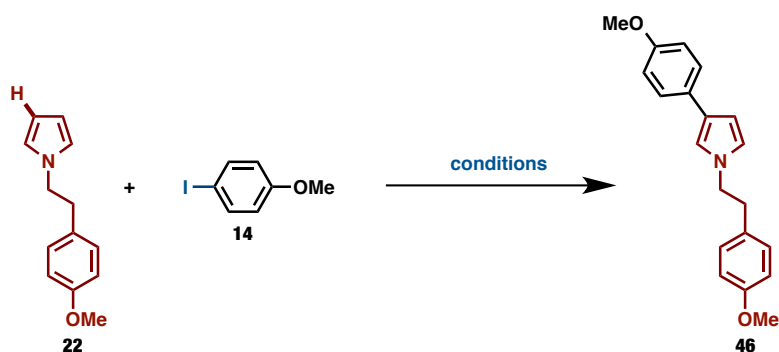
The mechanism for the β -selective pyrrole C–H arylation by $\text{RhCl}(\text{CO})\{\text{P}[\text{OCH}(\text{CF}_3)_2]_3\}_2$ is thought to proceed by the pathway shown in Scheme 5.11.²⁴ The neutral Rh(I) complex undergoes oxidative addition with the aryl iodide and halide removal with Ag_2CO_3 to generate cationic aryl-Rh(III) species followed by π -complexation of the pyrrole. C–H rhodation of this intermediate leads to the formation of the less sterically hindered diaryl-Rh(III) intermediate which, upon reductive elimination, affords the β -arylated pyrrole and regenerates the catalyst. The regioselectivity of this transformation is determined during the π -complexation and C–H rhodation steps in which the sterically more accessible C–H rhodation intermediate is preferred due to steric repulsion of the *N*-substituent of the pyrrole substrate and bulky phosphite ligand on the catalyst (Scheme 5.11). In the case of thiophenes and furans, there are no substituents on heteroatoms and thus the formation of the intermediate leading to the α -arylated products is preferred. The importance of *N*-substituents of pyrrole substrates was demonstrated by the increase in β -selectivity with increasing the steric bulk of the *N*-substituent on the pyrrole (Me < Et < Bn = TIPS). *N*-H pyrroles, however, did not react under these conditions.

Scheme 5.11 A possible mechanism of β -selective pyrrole C–H arylation by $\text{RhCl}(\text{CO})\{\text{P}[\text{OCH}(\text{CF}_3)_2]_3\}_2$



Dr. Atsushi Yamaguchi was able to employ this methodology to make key intermediate **46**, which served as the core structure in the synthesis of dictyodendrin A. $\text{RhCl}(\text{CO})\{\text{P}[\text{OCH}(\text{CF}_3)_2]_3\}_2$ -catalyzed direct β -selective C–H arylation of the *N*-alkylpyrrole (**22**) with *para*-iodoanisole (**14**) provided the corresponding 3-arylpyrrole **46** in 52% yield. Changing the solvent did not drastically effect the yield (Table 5.6).

Table 5.6 Optimization of β -selective C–H arylation of an *N*-alkylpyrrole and an electron rich aryl iodide by $\text{RhCl}(\text{CO})\{\text{P}[\text{OCH}(\text{CF}_3)_2]_3\}_2$



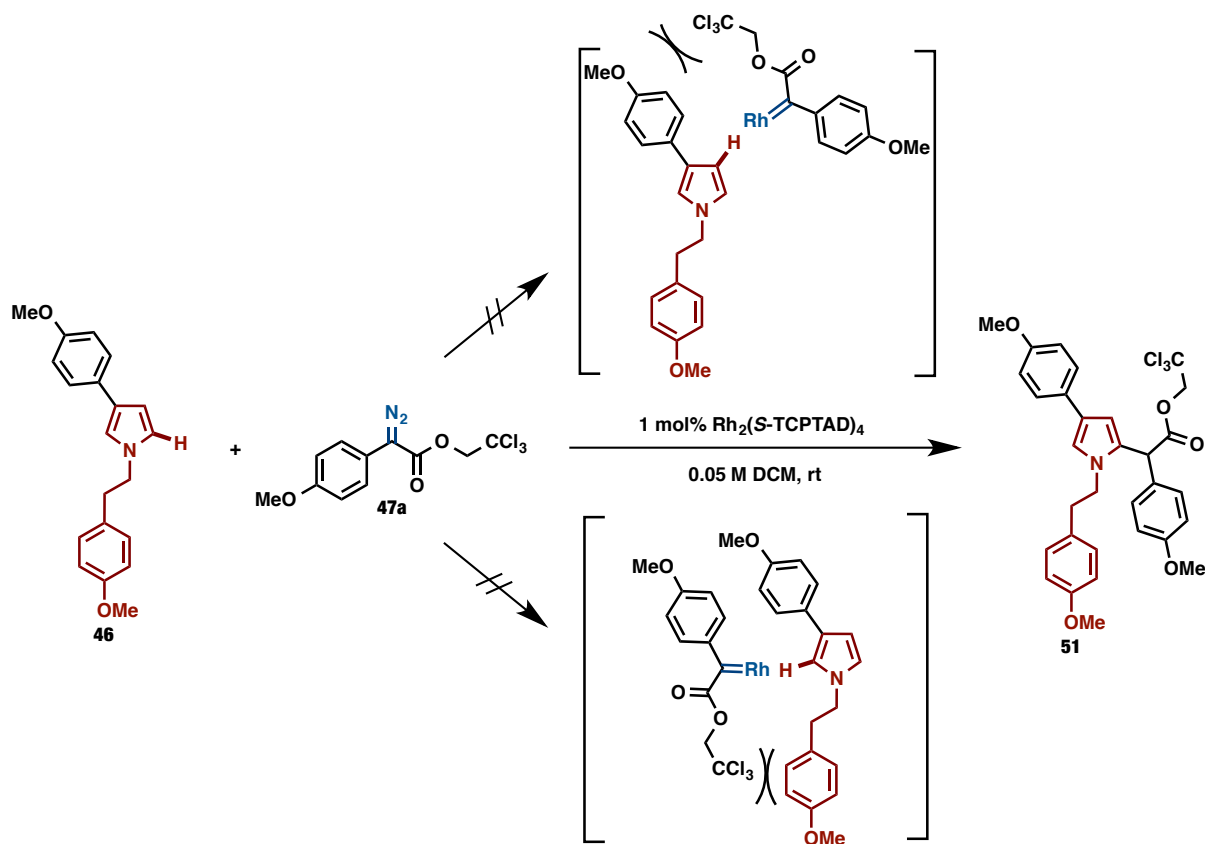
entry	conditions	time (h)	yield (%)
1	3 mol% $\text{RhCl}(\text{CO})\{\text{P}[\text{OCH}(\text{CF}_3)_2]_3\}_2$ Ag_2CO_3 [1 equiv.] 0.2 M <i>m</i> -xylene/dioxane = 2/3 150 °C	17	50
2	" "	40	25
3	3 mol% $\text{RhCl}(\text{CO})\{\text{P}[\text{OCH}(\text{CF}_3)_2]_3\}_2$ Ag_2CO_3 [1 equiv.] DME [1 equiv.] 0.25 M <i>m</i> -xylene 150 °C	40	52
4	" "	60	51

reactions conducted by Dr. Atsushi D. Yamaguchi

We originally believed that rhodium(II) carbenoid-mediated C–H functionalization would occur regioselectively at the most sterically accessible C–H bond of the pyrrole ring by using a bulky carbenoid compound containing a trichloroethyl ester moiety²⁵ along with sterically encumbered catalyst.²⁶ $\text{Rh}_2(\text{S-TCPTAD})_4$ is a very rigid catalyst due to the inflexible nature of

its chlorinated ligands which force it to adopt a *C4*-symmetric confirmation.²⁶ We presumed that use of a bulky dirhodium catalyst in combination with a 2,2,2-trichloroethyl ester adjacent to the rhodium carbenoid, would force insertion to occur exclusively at the more sterically accessible α -position (Scheme 5.12). It is important to note that 2,2,2-trichloroethyl aryldiazoacetates have been found to be robust reagents for the enantioselective C–H functionalization of methyl ethers).²⁵

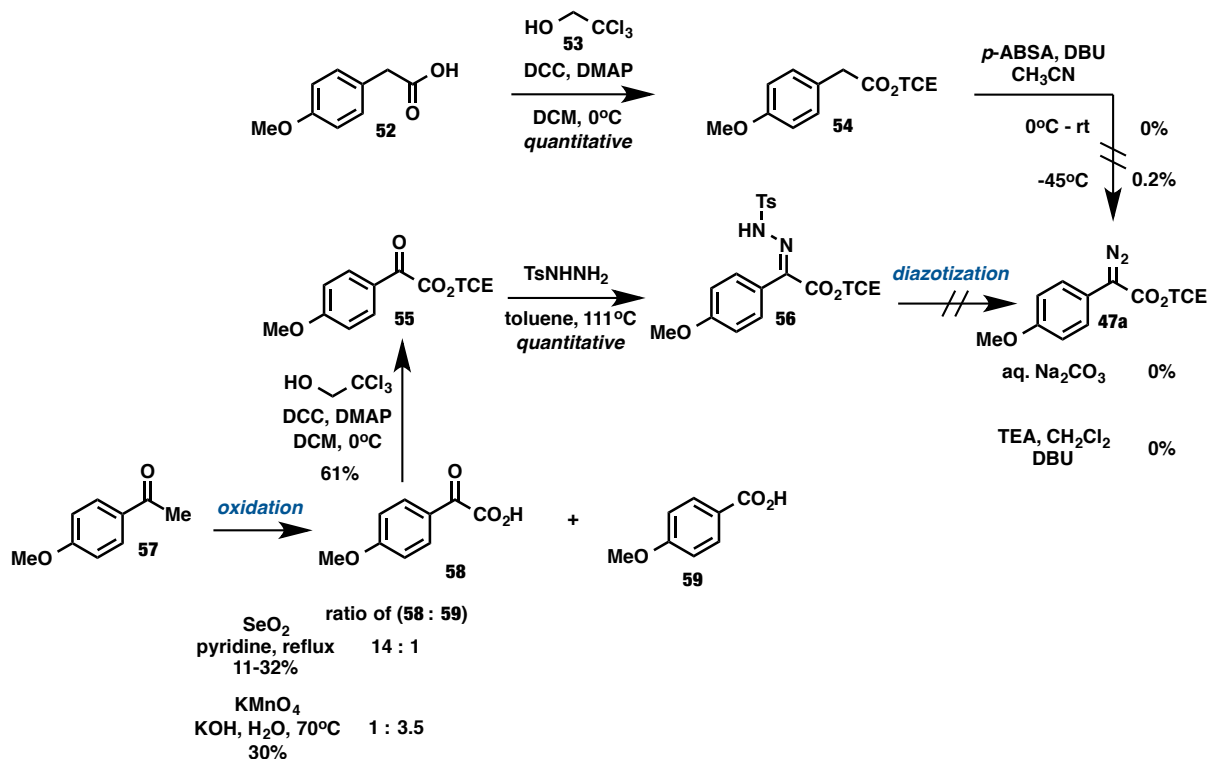
Scheme 5.12 Proposed mechanism for α -selective carbenoid insertion with the use of a trichloroethyl ester-substituted donor/acceptor rhodium carbenoid



Initially, efforts to synthesize 2,2,2-trichloroethyl 2-diazo-2-(4-methoxyphenyl)acetate (47a) were unsuccessful. Both common diazo transfer conditions and diazotization by Bamford-Stevens reaction of the *N*-tosylhydrazone 56 failed to provide the desired diazo compound 47a.

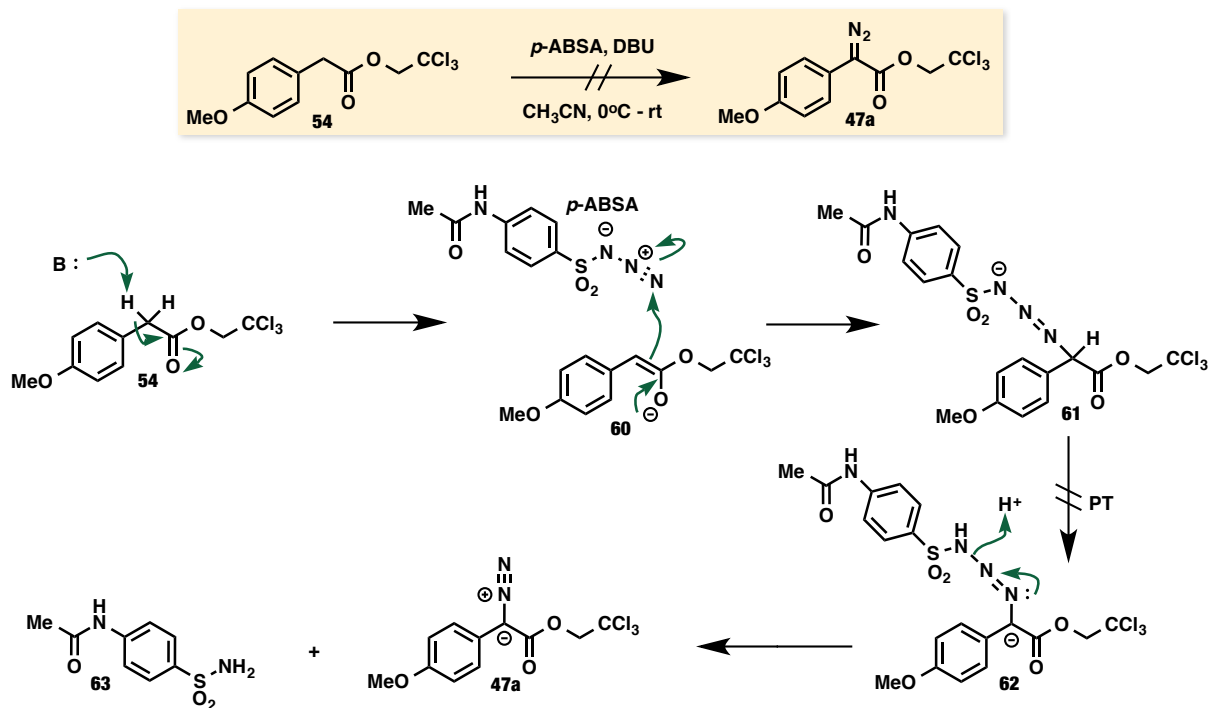
Under standard diazo transfer conditions, elimination of sulfonamide to provide the corresponding diazo compound failed presumably due to the electron-donating nature of both the *p*-ABSA and the starting material **54** (Scheme 5.13).

Scheme 5.13 Attempts toward the synthesis of an electron-rich trichloroethyl ester-substituted donor/acceptor-diazo compound



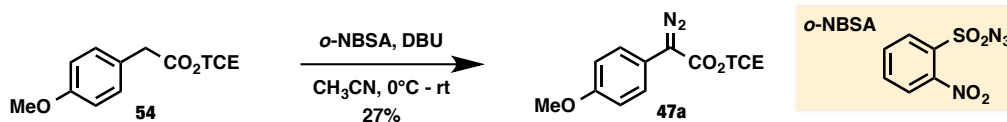
It is believed that these diazo transfer reactions employing electron rich *para*-methoxy substituted aryldiazo derivatives fail due to the electron donating nature of both diazo transfer reagent, *p*-ABSA, and the diazo precursor. Presumably, after enolate **60** attacks *p*-ABSA, intermediate **61** is forming and failing to undergo proton transfer to give intermediate **62** (Scheme 5.14).

Scheme 5.14 Mechanistic hypothesis for problematic diazo transfer to electron-rich donor/acceptor-diazo compounds bearing a bulky ester functionality



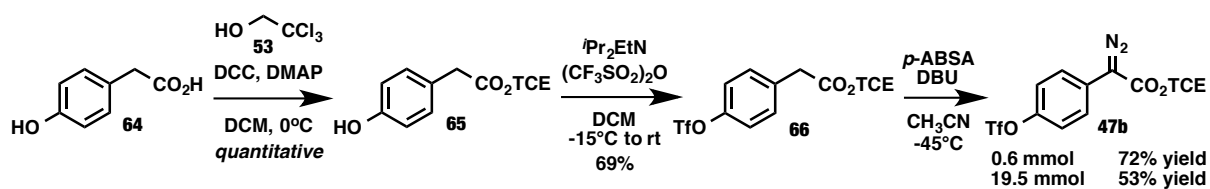
We believed that the use of electron withdrawing *o*-NBSA as a diazo transfer reagent could be a general solution to the problems that we had been facing with diazo transfer to this electron rich aryldiazoacetate bearing a trichloroethyl ester. In order to test this theory, *ortho*-nitrobenzenesulfonyl azide (*o*-NBSA) was synthesized from the corresponding sulfonyl chloride²⁷ and tested as a diazo transfer reagent. Under these conditions, diazo compound **47a** was obtained, albeit in low yield (Scheme 5.15, 27%). This diazo compound, however, was not pursued further as a substrate in the carbenoid C–H functionalization of pyrroles as the ideal route to dictyodendrin A was discovered at the same time as these ideal diazo transfer conditions were established.

Scheme 5.15 *o*-NBSA-mediated diazo transfer to give an electron-rich trichloroethyl ester-substituted donor/acceptor-diazo compound



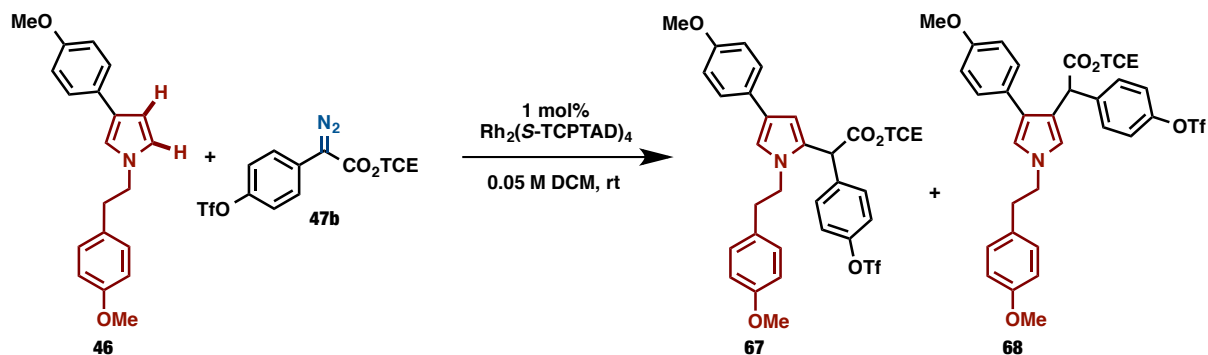
When the *para*-substituent on the aryldiazo was switched from an electron donating methoxy group to an electron-withdrawing *para*-trifluoromethanesulfonate, the corresponding diazo compound (**47b**) could be readily synthesized with the use of *p*-ABSA as the diazo transfer reagent in 72% yield. This route was scalable up to a 20 mmol scale (Scheme 5.16).

Scheme 5.16 Synthesis of an electron-poor trichloroethyl ester-substituted donor/acceptor-diazo compound



The C–H functionalization of arylated pyrrole **46** with diazo **47b** provided **67** and **68** in excellent yield (96%) but with poor regioselectivity (2.6 : 1 ratio of **67** : **68**). The poor regioselectivity of this transformation could be due to steric hindrance between the bulky trichloroethyl ester moiety and the *N*-alkyl group (Table 5.7).

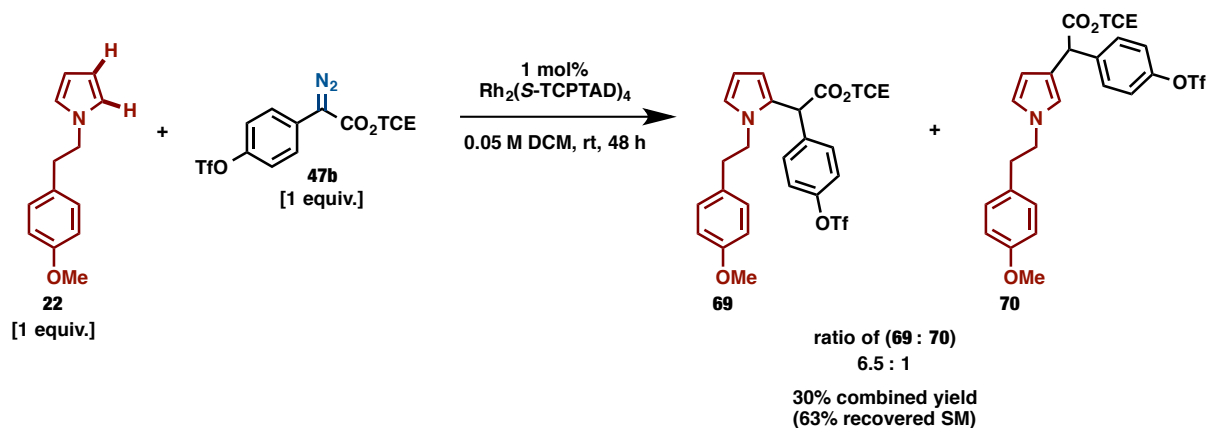
Table 5.7 C–H functionalization of an arylated *N*-alkylpyrrole with an electron-poor trichloroethyl ester-substituted donor/acceptor-diazo compound



aryl pyrrole (eq)	diazo (eq)	reaction time (h)	ratio (67 : 68)	combined yield (67 + 68) (%)
1	2	24	2.6 : 1	96
1	1	48	2.8 : 1	93

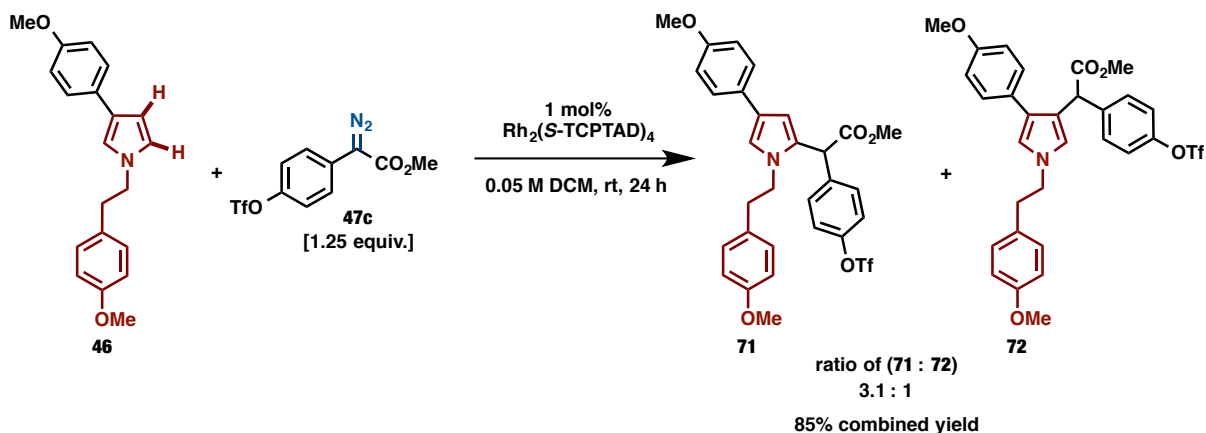
To better understand the regioselectivity of this transformation, the reaction was repeated with the unsubstituted pyrrole **22**. The regioselectivity increased to 6.5 : 1 favoring the desired α -functionalized product **69**, but the yield was greatly diminished (30%) and a significant amount of undecomposed starting pyrrole **22** was recovered (63%). The catalyst deactivated in this reaction as was observed by a color change from green to red upon addition of the solution of substrate **22** in dichloromethane to the catalyst (Scheme 5.17).

Scheme 5.17 C–H functionalization of an unsubstituted *N*-alkylpyrrole with an electron-poor trichloroethyl ester-substituted donor/acceptor-diazo compound



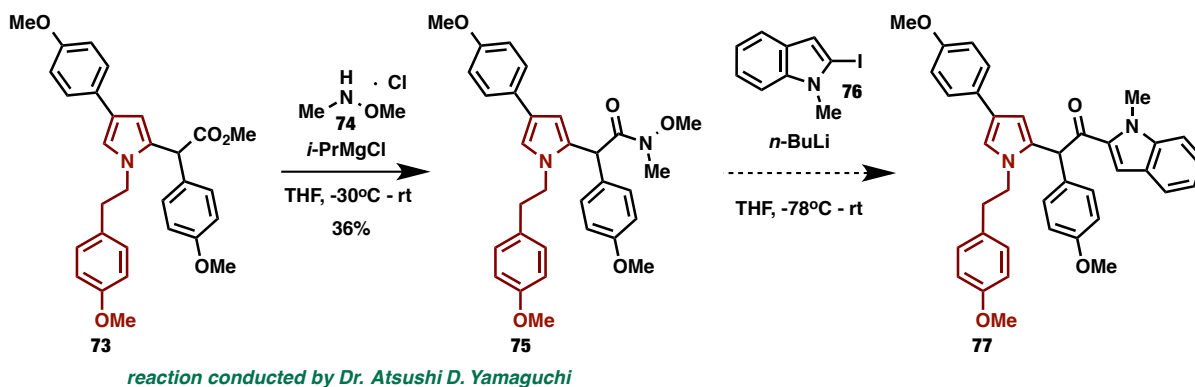
We next sought to determine whether the aryldiazoacetate could be tuned to increase the regioselectivity of this transformation while maintaining the high yields observed with the use of electron-poor trifluoromethanesulfonate-substituted aryldiazoacetate **47b**. Also, to determine if poor regioselectivity of the transformations shown in Table 5.7 and Scheme 5.17 was due to either the steric encumbrance of the trichloroethyl ester or to the electron withdrawing nature of the resulting carbenoid of this reaction, the methyl ester derivative (**47c**) of diazo compound **47b** was synthesized and tested to determine its influence on the regioselectivity in dirhodium(II)-catalyzed functionalization of 3-arylated pyrrole **46**. Similar to the functionalization of **46** with **47b** (Table 5.7), methyl ester derivative **47c** provided the corresponding C–H functionalization products **71** and **72** in good yield (85%) but showed only slightly improved regioselectivity (Scheme 5.18, 3.1 : 1 ratio of **71** : **72**) than was observed in the reaction with diazo **47b** (Table 5.7, 2.6 : 1 ratio of **67** : **68**). These results tell us that the poor regioselectivity observed in the reactions of **47b** shown in Table 5.7, although in part due to the bulky nature of the trichloroethyl ester, were primarily due to the electron withdrawing nature of the resulting rhodium carbenoid with *para*-triflate substitution on the aryl group of the aryldiazo.

Scheme 5.18 C–H functionalization of an arylated *N*-alkylpyrrole with an electron-poor methyl ester-substituted donor/acceptor-diazo compound



One route to dictyodendrin A, which was being explored in parallel to these studies by Dr. Atsushi Yamaguchi, who had synthesized **73** (as described later in this chapter in Table 5.9) and was investigating the conversion of the methyl ester of **73** to the Weinreb amide of **75**. In his studies on this synthetic route, Dr. Atsushi Yamaguchi found that this proved difficult due to a low yield of 36% (Scheme 5.19).

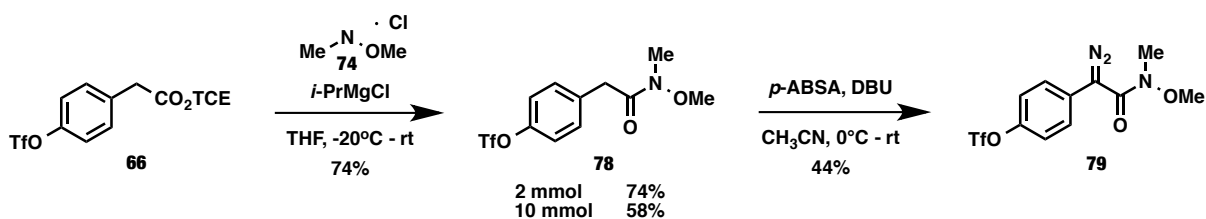
Scheme 5.19 Attempts toward the conversion of the methyl ester to a Weinreb amide for installation of the indole moiety of dictyodendrin A



To further explore how varying the diazo starting material in the rhodium carbenoid functionalization of 3-arylpyrrole **46** affects yield and regioselectivity of the transformation, the

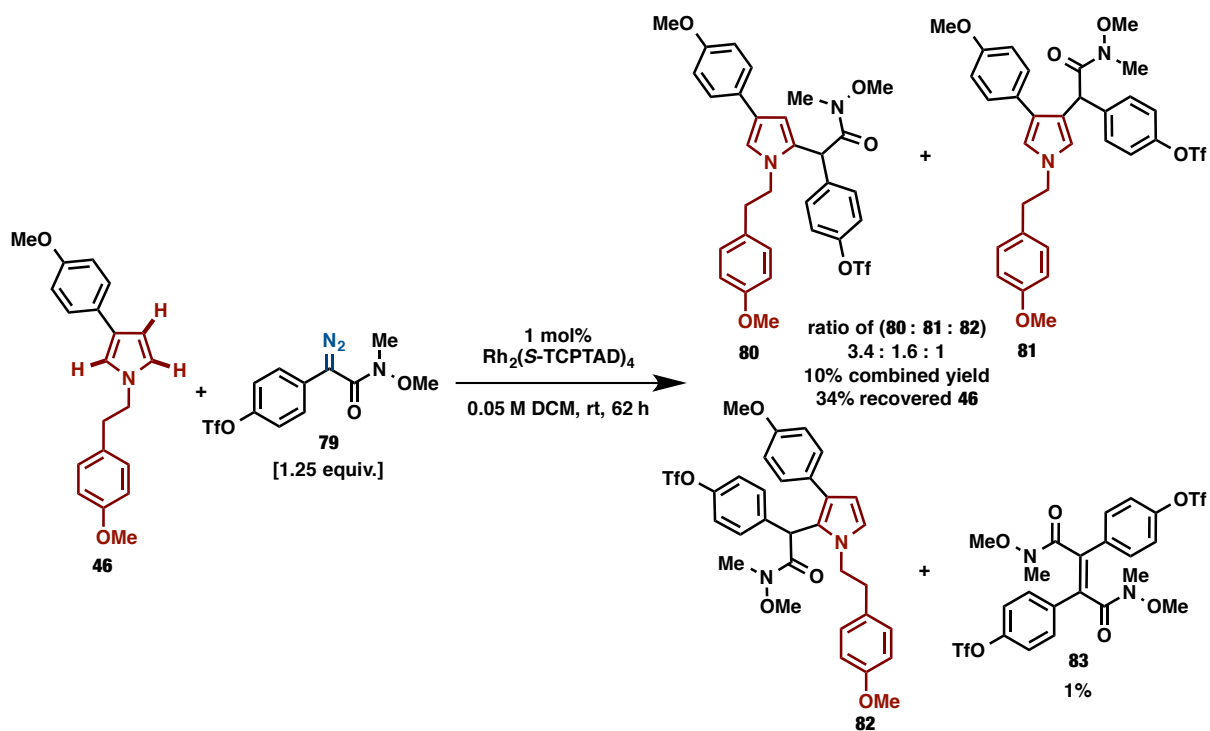
Weinreb amide-substituted aryldiazo **79** was synthesized. First, conversion of the trichloroethyl ester of **66** to the Weinreb amide **78** proceeded in 74% yield and proved to be scalable to a 10 mmol scale. The Weinreb amide-substituted aryldiazo **79** was then synthesized in moderate yield (44%) by diazo transfer to **78** (Scheme 5.20).

Scheme 5.20 Synthesis of Weinreb amide-substituted aryldiazo



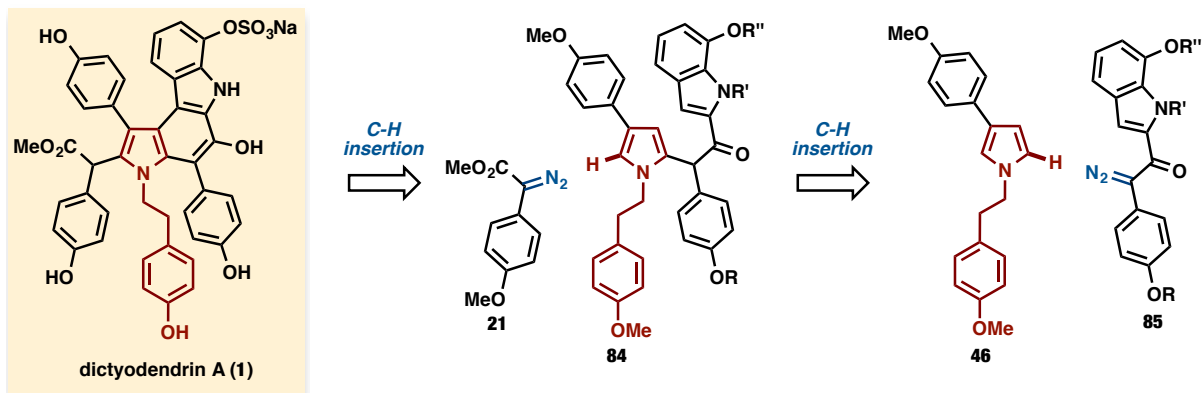
The functionalization of **46** with Weinreb amide-substituted aryldiazo **79** gave a complex mixture of products and 34% recovered starting pyrrole **46**. An inseparable regioisomeric mixture of **80**, **81**, and **82** was obtained in 10% combined yield along with a small amount of the product of carbene dimerization (**83**) (Scheme 5.21).

Scheme 5.21 Pyrrole C–H functionalization with Weinreb amide-substituted aryldiazo



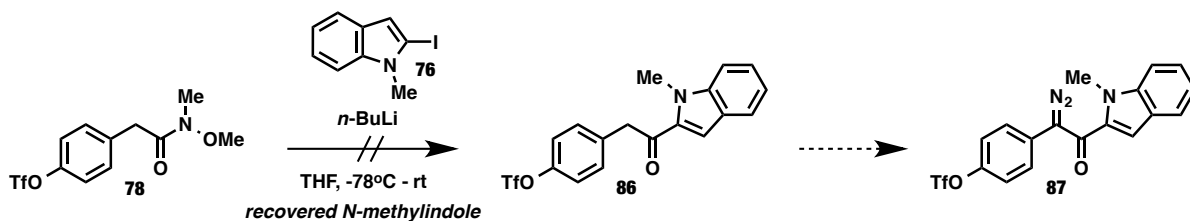
Another reaction that proved troublesome in Dr. Atsushi Yamaguchi's studies had been the conversion of the Weinreb amide of **75** to the indole moiety of **77** (Scheme 5.19). We envisioned that one plausible way to circumvent this problem would be with the use of an α -keto indole aryldiazo (**85**) in the first functionalization of **46** (Scheme 5.22). This would ideally simplify and shorten the synthesis of dictyodendrin A from the previously proposed retro-synthetic route.

Scheme 5.22 Modified retro-synthetic route to dictyodendrin A featuring an α -selective carbenoid insertion with an α -ketoindole aryldiazo



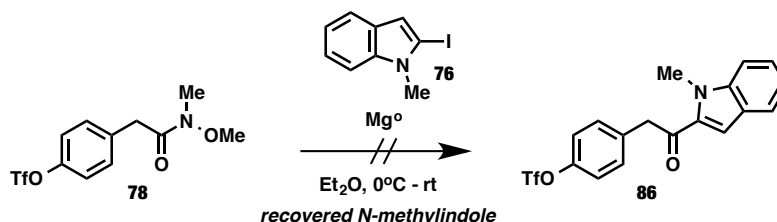
Initial attempts to convert Weinreb amide of **78** into the α -keto indole of **86** were unsuccessful. Lithiation of 2-iodo-1-methyl-1H-indole (**76**) followed by alkylation of **78** failed and the only product observed from the reaction was *N*-methylindole (Scheme 5.23). This could be due in part to slow reactivity of **78** with (1-methyl-1H-indol-2-yl)lithium.

Scheme 5.23 Attempted conversion of the Weinreb amide to an α -ketoindole functionality for installation of the indole moiety of dictyodendrin A



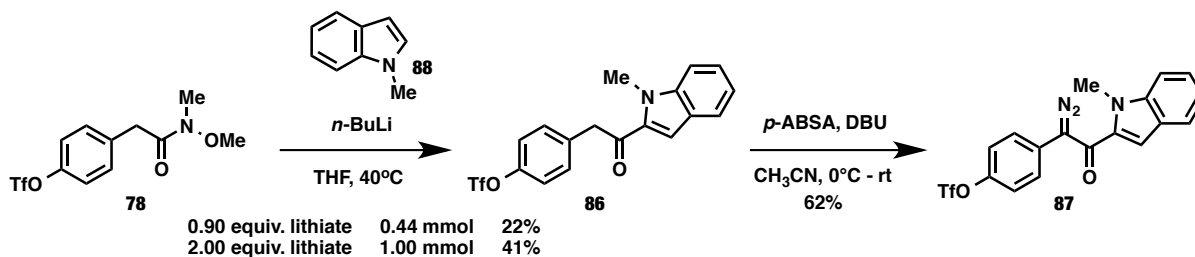
Since lithiation of **76** followed by alkylation of **78** proved problematic, the conversion of **76** into a Grignard reagent followed by alkylation of **78** was attempted. This reaction also failed primarily providing recovered *N*-methylindole (Scheme 5.24).

Scheme 5.24 Attempted synthesis of precursor to an electron-poor α -ketoindole-substituted donor/acceptor-diazo compound



After much optimization, synthesis of electron-poor α -ketoindole-substituted donor/acceptor-diazo compound **87** could be achieved in two steps from Weinreb amide-substituted starting material **78**. Direct lithiation of *N*-methylindole (**88**) followed immediately by direct alkylation of Weinreb amide **78** provided **86** in 22% yield. When the equivalents of the resulting (1-methyl-1H-indol-2-yl)lithium post-lithiation were increased from 0.9 to 2 equiv, **86** could be obtained in better yield (41%). Diazotization of **86** proceeded in 62% yield on a 0.1 mmol scale (Scheme 5.25). This reaction is particularly promising as it cuts out two steps (conversion of *N*-methylindole (**88**) into 2-iodo-1-methyl-1H-indole (**76**) which had proceeded in low yield) from the initially attempted synthesis of **87** shown in Scheme 5.23.

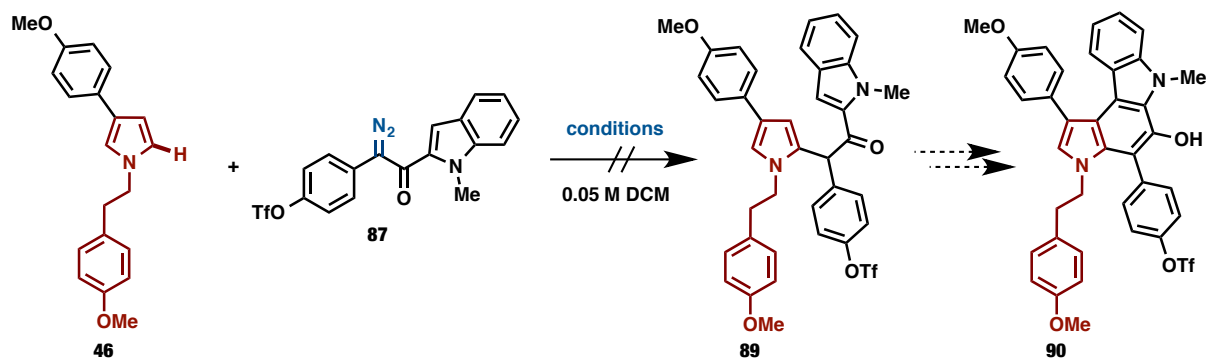
Scheme 5.25 Synthesis of an electron-poor α -ketoindole-substituted donor/acceptor-diazo compound



The functionalization of arylated pyrrole **46** was then screened with to α -keto indole arylidiazos **78**. The reaction of **78** with **44** to give **79** failed to proceed under dirhodium catalysis.

Similarly, thermal reaction of free carbene derived from **78** with **44** failed to proceed even under microwave conditions (Table 5.8).

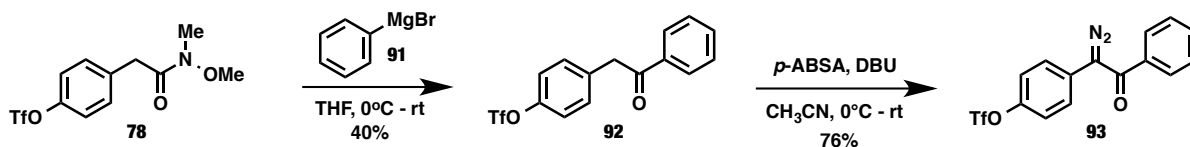
Table 5.8 Attempted pyrrole C–H functionalization with an electron-poor α -ketoindole aryldiazo



entry	catalyst	temperature	solvent	product
1	1 mol% $\text{Rh}_2(\text{S-TCPTAD})_4$	rt	DCM	recovered SM
2	1 mol% $\text{Rh}_2(\text{S-DOSP})_4$	rt	DCM	recovered SM
3	1 mol% $\text{Rh}_2(\text{OAc})_4$	rt	DCM	recovered SM
4	1 mol% $\text{Rh}_2(\text{R-BNP})_4$	rt	DCM	recovered SM
5	1 mol% $\text{Rh}_2(\text{R-BNP})_4$	85°C	1,2-DCE	recovered SM
6	none	85°C	1,2-DCE	recovered SM
7	none	μW , 85°C	1,2-DCE	recovered SM

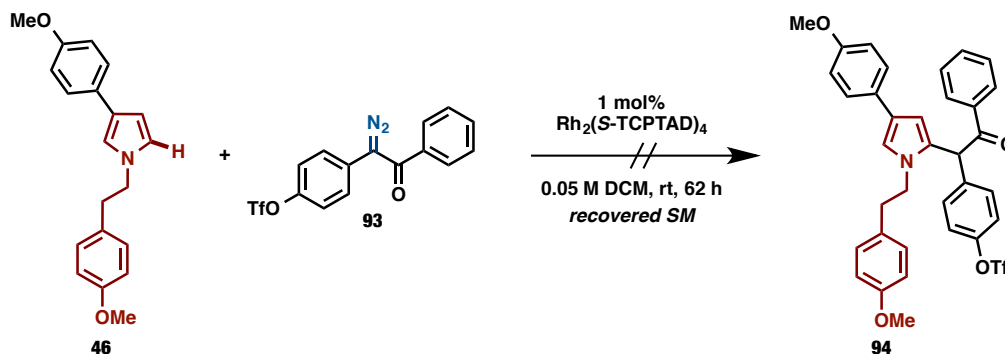
To determine if any α -ketoaryl-substituted aryldiazos could be employed in 5-functionalization of arylated pyrrole **46**, the α -ketophenyl aryldiazo derivative of **87**, diazo **93**, was synthesized and tested in pyrrole functionalization. Diazo **93** was readily synthesized in 2-steps from **78** with the Grignard addition of phenylmagnesium bromide (**91**) to Weinreb amide **78** proceeding in 40% yield followed by diazotization of **92** using standard diazo transfer conditions to provide **93** in 76% yield (Scheme 5.26).

Scheme 5.26 Synthesis of an electron-poor α -ketophenyl-substituted donor/acceptor-diazo compound



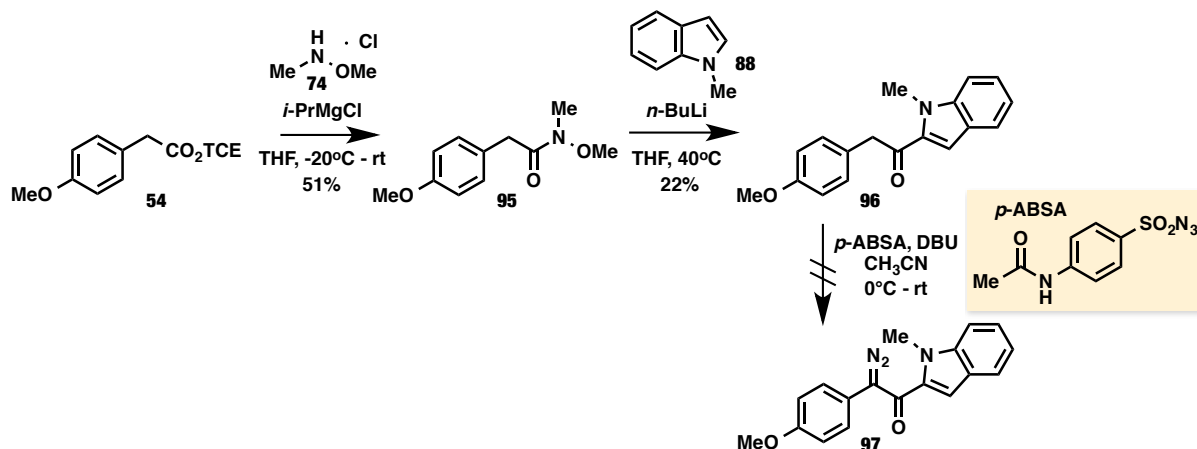
The 5-functionalization of arylated pyrrole **46** was screened with α -ketoaryldiazoacetate **93**. The reaction of **93** with **46** failed to provide the desired C–H functionalization product **94**. Only starting materials **46** and **93** were recovered after 62 hours (Scheme 5.27).

Scheme 5.27 Attempted pyrrole C–H functionalization with an electron-poor α -ketophenyl-substituted donor/acceptor-diazo compound



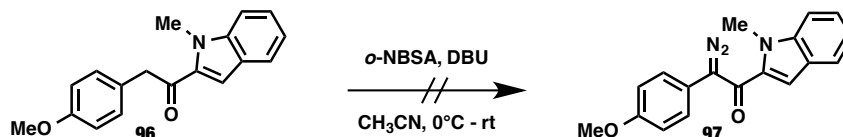
As the *para*-trifluoromethane sulfonate substitution on the aryldiazo was shown to reduce the regioselectivity of the C–H functionalization (Table 5.7 vs. Scheme 5.17), synthesis of the *para*-methoxy substituted derivative **97** was attempted. Similar to the problem encountered in the synthesis of the 2,2,2-trichloroethyl 2-diazo-2-(4-methoxyphenyl)acetate (Scheme 5.13, **47a**), subsection of **96** to the standard diazo transfer conditions with *p*-ABSA as the diazo transfer reagent failed to yield the desired diazo compound **97** (Scheme 5.28).

Scheme 5.28 Attempted synthesis of an electron-rich α -ketoindole-substituted donor/acceptor-diazo compound



Unfortunately, employing *o*-NBSA in diazo transfer to **96** also failed to provide the desired diazotization product **97** (Scheme 5.29).

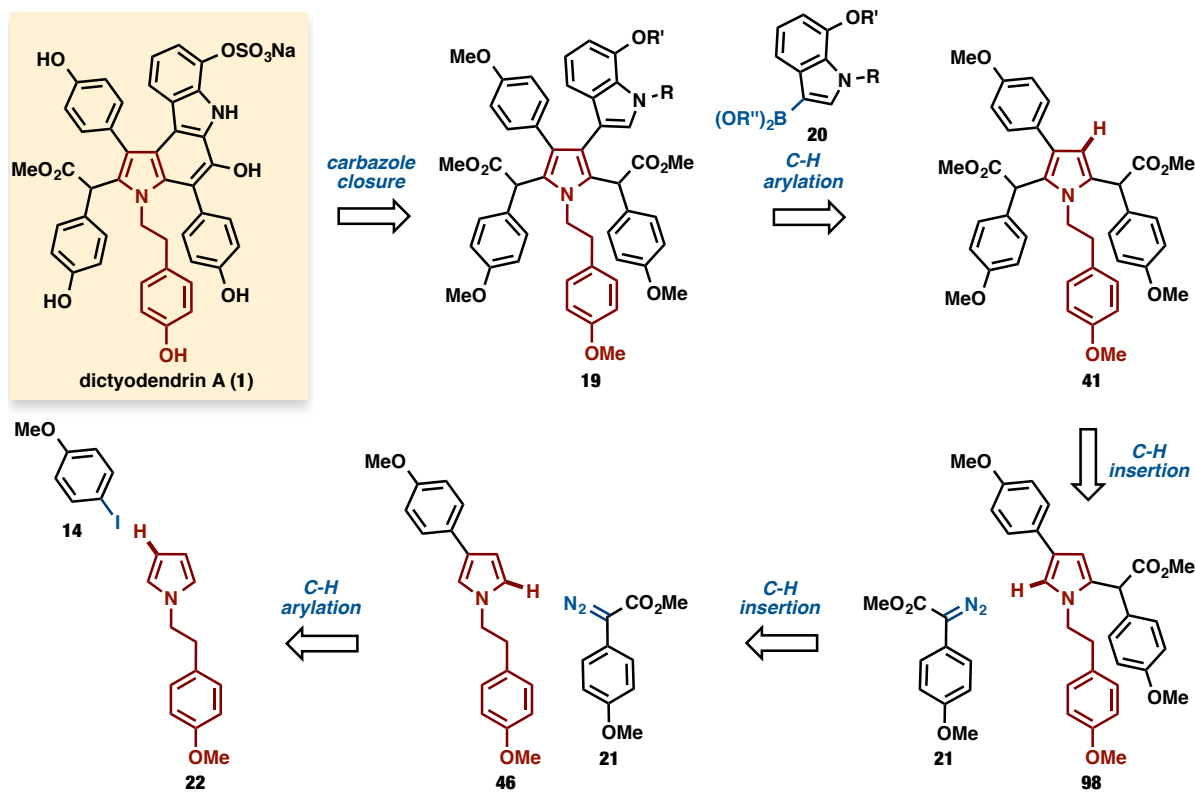
Scheme 5.29 Attempted *o*-NBSA-mediated diazo transfer to electron-rich α -ketoindole



5.4 Formal Synthesis of Dictyodendrin A

After extensive screening of aryldiazo carbonyls featuring elaborate electron withdrawing groups in pyrrole C–H functionalization, we decided to return our focus to the use of the simple aryldiazoacetate **21** in α -selective pyrrole functionalization. We envisioned beginning this attempt toward the synthesis of dictyodendrin A with β -selective arylation of **22** followed by sequential α -selective carbenoid insertions employing **21** as the rhodium carbenoid precursor (Scheme 5.30).

Scheme 5.30 Davies / Itami retro-synthetic route to dictyodendrin A via β -selective arylation followed by sequential α -selective carbenoid insertions



The reaction of the *para*-methoxy substituted aryldiazoacetate (**21**) with arylated pyrrole (**46**) was then explored. Although the initial screening of Davies' dirhodium catalysts previously conducted by Dr. Atsushi Yamaguchi had revealed that $Rh_2(S\text{-TCPTAD})_4$ was the best catalyst for the double C–H insertion of **21** into unsubstituted *N*-alkylpyrrole **22** (Scheme 5.7), we realized that a more extensive investigation may be necessary in order to determine the ideal catalyst for the C–H functionalization of the 3-arylpyrrole **46** with aryldiazoacetate **21**. For this reason, a variety of dirhodium(II) complexes (Figure 5.4) were then screened in for their ability to catalyze α -selective pyrrole functionalization.⁹

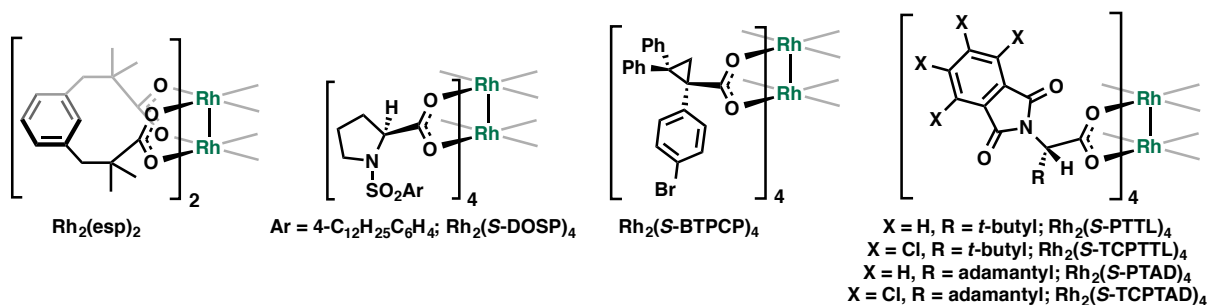
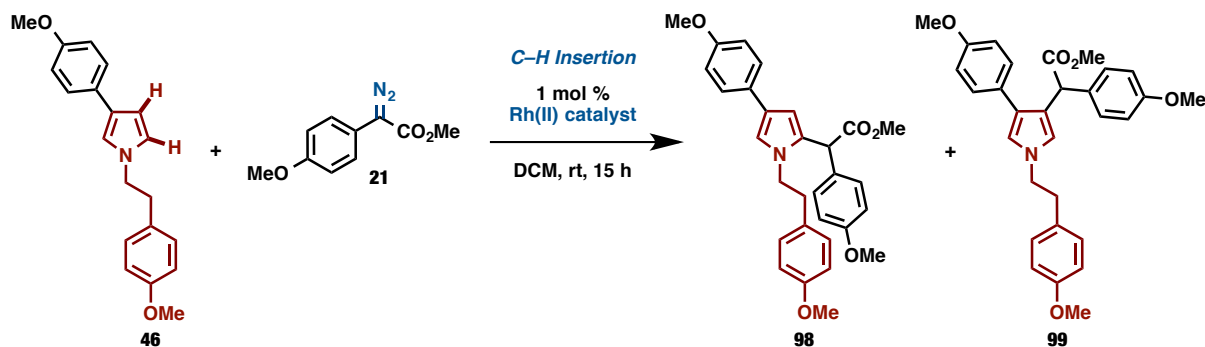


Figure 5.4 Dirhodium(II) catalysts screened in the α -selective pyrrole functionalization

$\text{Rh}_2(\text{OAc})_4$ and $\text{Rh}_2(\text{S-DOSP})_4$ failed in this reaction (Table 5.9, entries 1 and 2). $\text{Rh}_2(\text{esp})_2$, $\text{Rh}_2(\text{S-PTAD})_4$, and $\text{Rh}_2(\text{S-PTTL})_4$, on the other hand, all proceeded to give the desired alkylated product **98** along with the undesired regioisomer **99** as an inseparable mixture with low to moderate selectivities (entries 3–5). In an effort to improve the regioselectivity, other rhodium catalysts possessing more sterically encumbered ligands including $\text{Rh}_2(\text{S-BTPCP})_4$, $\text{Rh}_2(\text{S-TCPTTL})_4$ and $\text{Rh}_2(\text{S-TCPTAD})_4$ were screened (entries 6–8). Of these catalysts, $\text{Rh}_2(\text{S-TCPTAD})_4$ gave the highest regioselectivity (entry 8, 90 : 10 ratio of **98** : **99**). Further optimization of the reaction conditions with $\text{Rh}_2(\text{S-TCPTAD})_4$ allowed for the catalyst loading to be decreased by scaling up the reaction and reducing the number of equivalents of the diazoester. The optimized conditions afforded the alkylated products in 78% yield with high regioselectivity (entry 9, 92 : 8 ratio of **98** : **99**).⁹

Table 5.9 Optimization of the α -selective rhodium carbenoid-mediated pyrrole mono-functionalization



entry ^a	Rh(II) catalyst	ratio (98 : 99)	yield of 98 and 99 (%)
1 ^b	Rh ₂ (OAc) ₄	–	< 1
2 ^b	Rh ₂ (S-DOSP) ₄	–	< 1
3	Rh ₂ (esp) ₂	76 : 24	53
4	Rh ₂ (S-PTAD) ₄	55 : 45	33
5	Rh ₂ (S-PTTL) ₄	61 : 39	54
6	Rh ₂ (S-BTPCP) ₄	53 : 47	12
7	Rh ₂ (S-TCPTTL) ₄	54 : 46	23
8	Rh ₂ (S-TCPTAD) ₄	90 : 10	36
9 ^c	Rh ₂ (S-TCPTAD) ₄	92 : 8	78

^a reaction conditions: pyrrole (0.1 mmol), diazo (2.0 equiv) and Rh(II) catalyst (1 mol%) in DCM (0.05 M), rt, 15 h.

^b reaction conducted by Dr. Atsushi D. Yamaguchi

^c Rh(II) cat. (0.1 mol%), pyrrole (3.0 mmol), and diazo (1.3 equiv) were used.

Regioselective 5-functionalization of 3-arylpyrrole **46** to provide **98** (Table 5.9) followed by 2-functionalization of difunctionalized pyrrole **98** in various ways could potentially enable access to other dictyodendrins. Dictyodendrins possessing a pyrrolocarbazole core have been classified into four types (**types I–IV**) according to their oxidation state and their substituent at the C2 position of the central pyrrole ring (Figure 5.5). The C2 substituent of **type I** could potentially be transformed into an acyl group (**type II**) or a benzyl group (**type III**) via hydrolysis of the ester group followed by decarboxylation. Also, fragmentation of the substituent of **type I** could potentially provide the core structure of **type IV**.

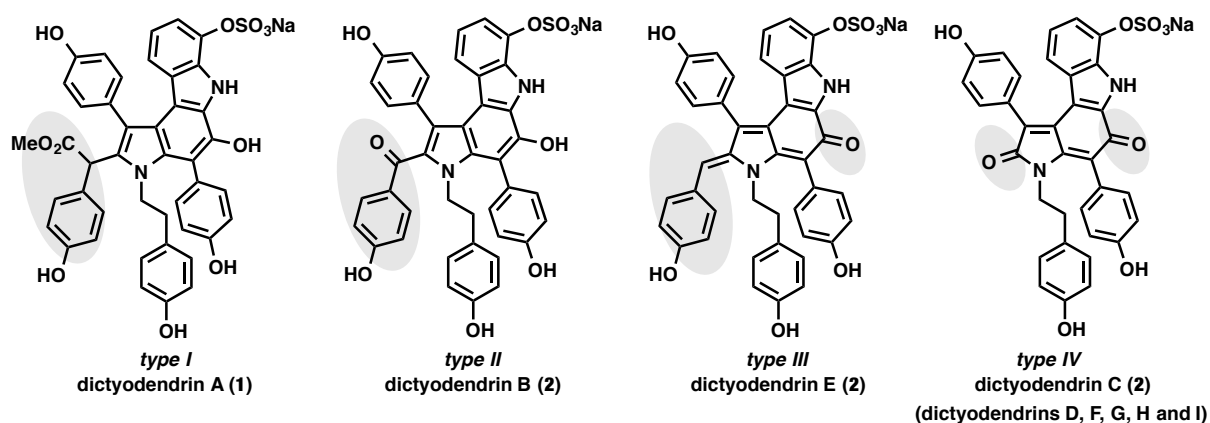
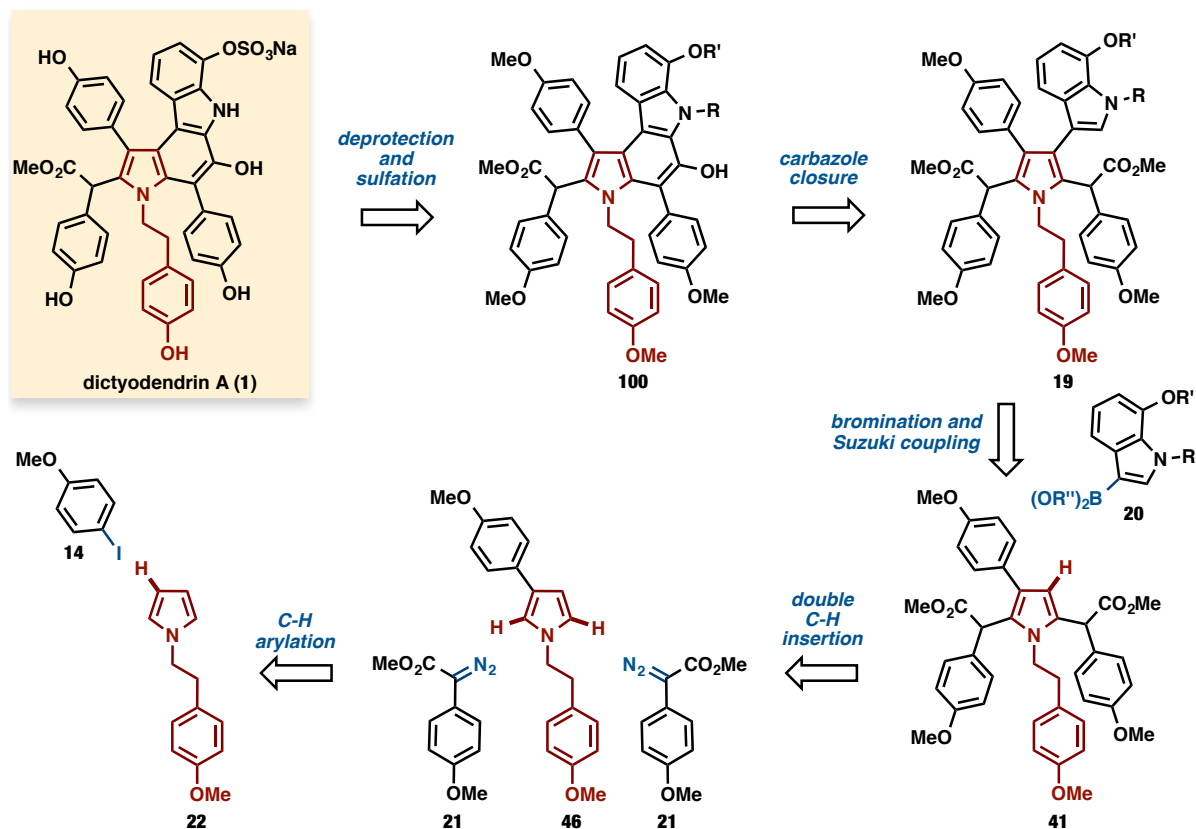


Figure 5.5 The four types of dictyodendrins:

classification according to oxidation state and the C2 substituent of the central pyrrole

Finally, the optimal route to dictyodendrin A via sequential C–H functionalizations was discovered commencing with Itami’s β -selective C–H arylation methodology followed by a double carbenoid functionalization of the arylated pyrrole **46** at the 2- and 5-positions as well as a late-stage pyrrole/indole coupling, closure of the final ring of the pyrrolocarbazole core, and global deprotection of the methoxy groups and the *N*-alkyl group (Scheme 5.31).⁹

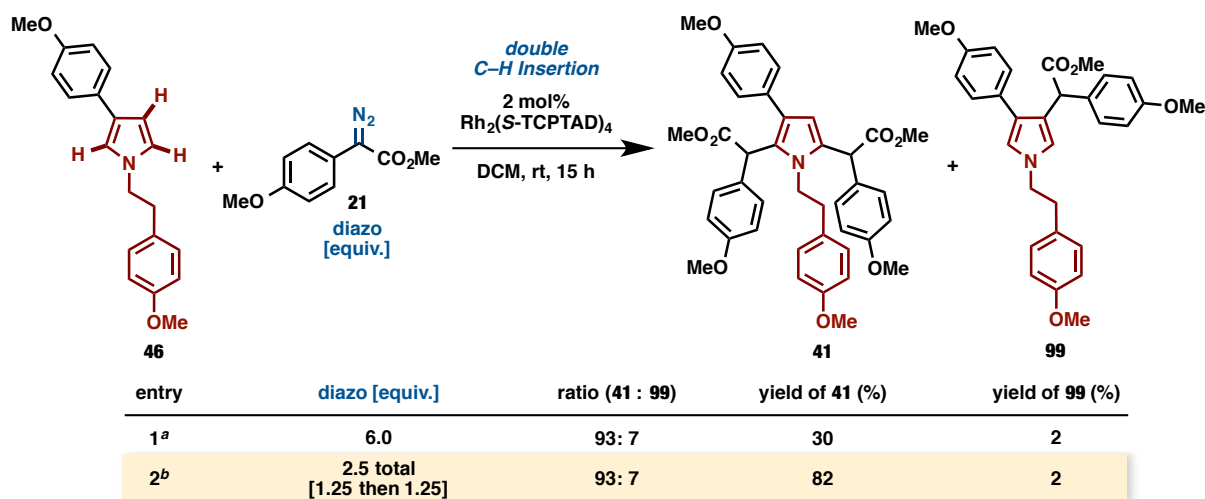
Scheme 5.31 Davies / Itami retro-synthetic route to dictyodendrin A via β -selective arylation followed by an α -selective double carbenoid insertion



In attempting to accomplish the synthesis of dictyodendrin A by the original synthetic route shown in Scheme 5.6, Dr. Atsushi Yamaguchi screened various conditions for an initial double C–H functionalization at the 2- and 5- positions of the unsubstituted *N*-alkyl pyrrole **22** and found that the yields of this transformation were low and gave a mixture of products (Scheme 5.7). However, the arylated pyrrole **46** had not been previously screened in this transformation. The difunctionalization of arylated *N*-alkylpyrrole **46** proceeded in low yield when 6 equiv. of diazo was employed to give 2,5-dialkylated product **41** as an inseparable diastereomeric mixture in 30% yield (Table 5.10, entry 1). The moderate yield was presumed to be due to the further alkylation of **41** although by-products could not be identified. When the two C–H functionalizations were carried out sequentially but in one pot, however, a high isolated yield of

the desired product was obtained (entry 2, 82%). Treatment of **46** with 1 mol% of Rh₂(S-TCPTAD)₄ and 1.25 equiv of diazoester **21** initially provided predominantly **98**. After 8 h, further treatment of the reaction mixture with an additional 1 mol% of Rh₂(S-TCPTAD)₄ and 1.25 equiv of diazoester **21** resulted in the production of **41** in 82% yield. This reaction was scalable to a 2 mmol scale.⁹

Table 5.10 Optimization of the α -selective rhodium carbenoid-mediated pyrrole di-functionalization

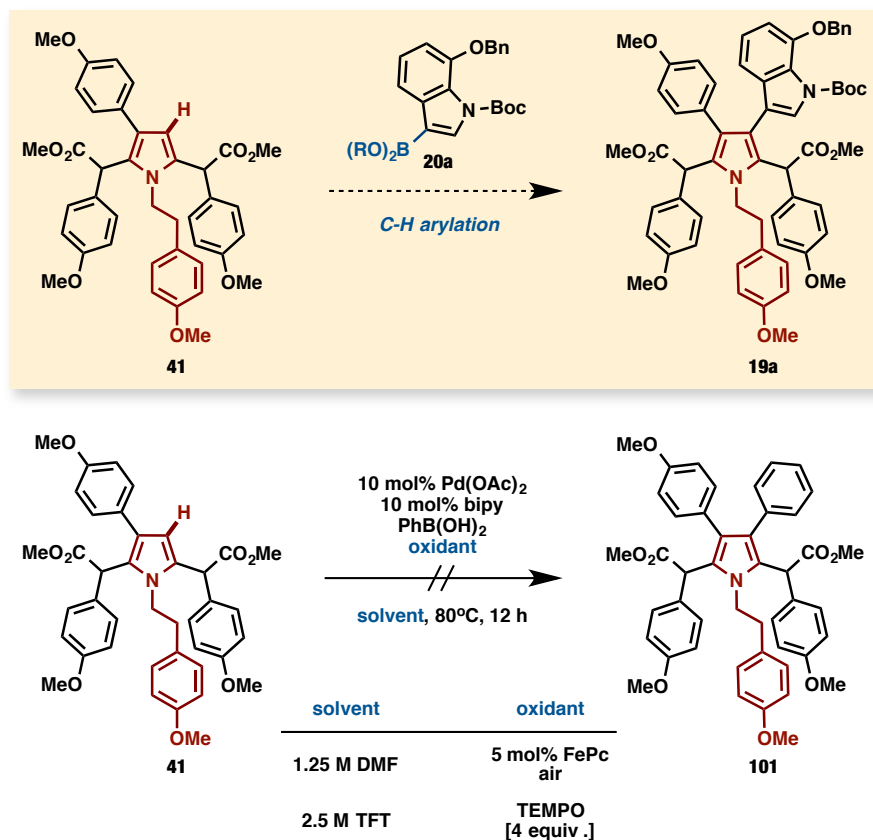


^a Rh(II) cat. (2 mol%), pyrrole (0.1 mmol), diazo (6.0 equiv) were used.

^b Rh(II) cat. (1 mol%) and diazo (1.25 equiv) were added initially, but a second portion of Rh(II) cat. (1 mol%) and diazo (1.25 equiv) were added after 8 h.

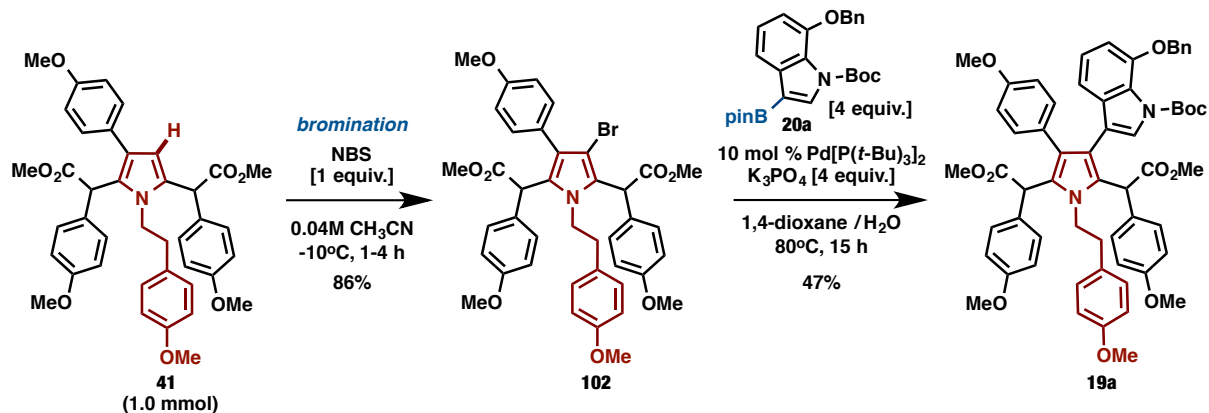
In an attempt to functionalize all four C–H bonds around the pyrrole core of dictyodendrin A using a combination of Davies and Itami C–H coupling methodologies, two different sets of Itami C–H arylation conditions were screened for the arylation of trifunctionalized pyrrole intermediate **41**, but both failed to provide the diarylated/tetrafunctionalized product **101** in a simple model reaction with phenylboronic acid as the substrate in place of the benzoylated indole boronic acid **20a** (Table 5.11).

Table 5.11 Attempted C–H arylation of the 4-position of trifunctionalized *N*-alkylpyrrole



In place of C–H arylation, direct bromination followed by Suzuki coupling was attempted on substrate **41**. Dr. Atsushi Yamaguchi achieved the direct bromination of intermediate **41** with the use of *N*-bromosuccinimide on a 1 mmol scale to provide **102** in high yield (86%). Suzuki–Miyaura coupling of **102** with indole pinacol boronate **20a** could be achieved with the use of bis(*tri-tert*-butylphosphine)palladium(0) to give **19a** in moderate yield (Scheme 5.32, 47%).

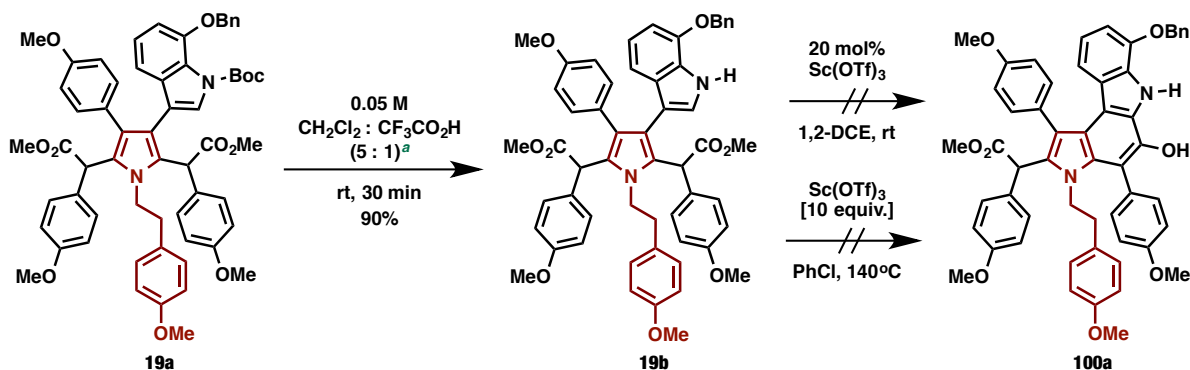
Scheme 5.32 Direct bromination and Suzuki coupling of the 4-position of the trifunctionalized *N*-alkylpyrrole



reactions conducted by Dr. Atsushi D. Yamaguchi

Attempts at intra-molecular Friedel–Crafts type cyclization were unsuccessful with the deprotected indole of **19b**. Both catalytic and stoichiometric $\text{Sc}(\text{OTf})_3$ -mediated cyclizations were attempted, but neither set of conditions provided the desired pyrrolo[2,3-*c*]carbazole **100a** (Scheme 5.33).

Scheme 5.33 Attempted $\text{Sc}(\text{OTf})_3$ -mediated cyclization to form the pyrrolo[2,3-*c*]carbazole core of dictyodendrin A

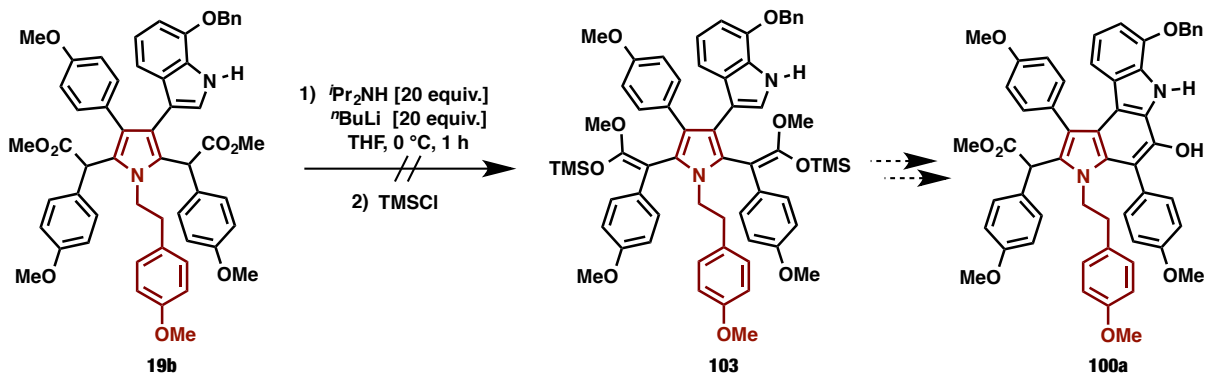


^a deprotection reaction conducted by Dr. Atsushi D. Yamaguchi

Similarly, initial attempts to generate the pyrrolo[2,3-*c*]carbazole structure via a 6π -electrocyclization by converting intermediate **19b** into (trimethylsilyl)ketene acetal intermediate **103** were unsuccessful. This reaction was attempted with the use of lithium diisopropylamide at

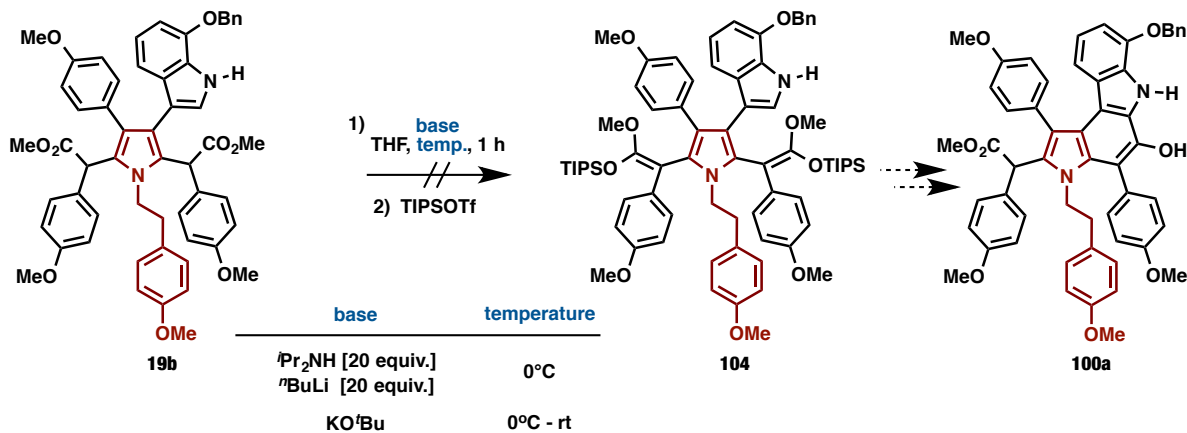
0 °C (Scheme 5.34).

Scheme 5.34 Attempted 6π -electrocyclization to form the pyrrolo[2,3-*c*]carbazole core of dictyodendrin A via a (trimethylsilyl)ketene acetal intermediate



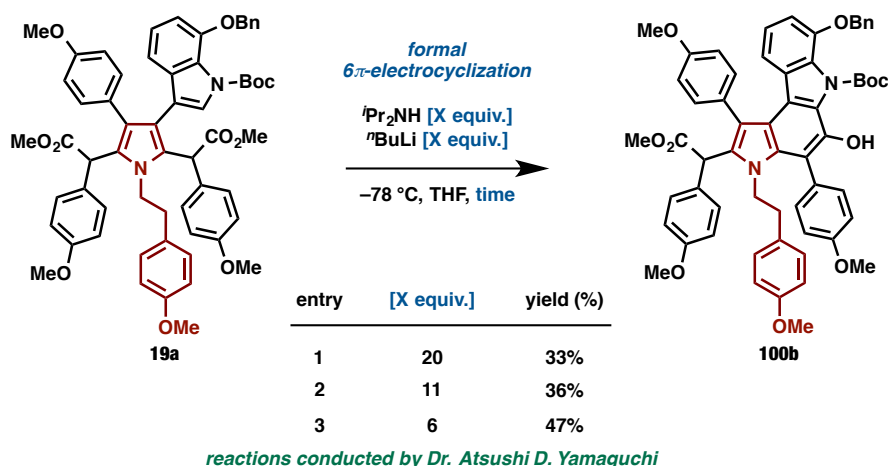
Attempted conversion of intermediate **19b** into (triisopropylsilyl)ketene acetal intermediate **104** also failed with the use of lithium diisopropylamide at 0 °C. Modifying the base used in this reaction from lithium diisopropylamide to KO^tBu had no effect on the reactivity, and, one again, none of the desired intermediate **104** or product **100a** was obtained from the reaction (Table 5.12).

Table 5.12 Attempted 6π -electrocyclization to form the pyrrolo[2,3-*c*]carbazole core of dictyodendrin A via a (triisopropylsilyl)ketene acetal intermediate



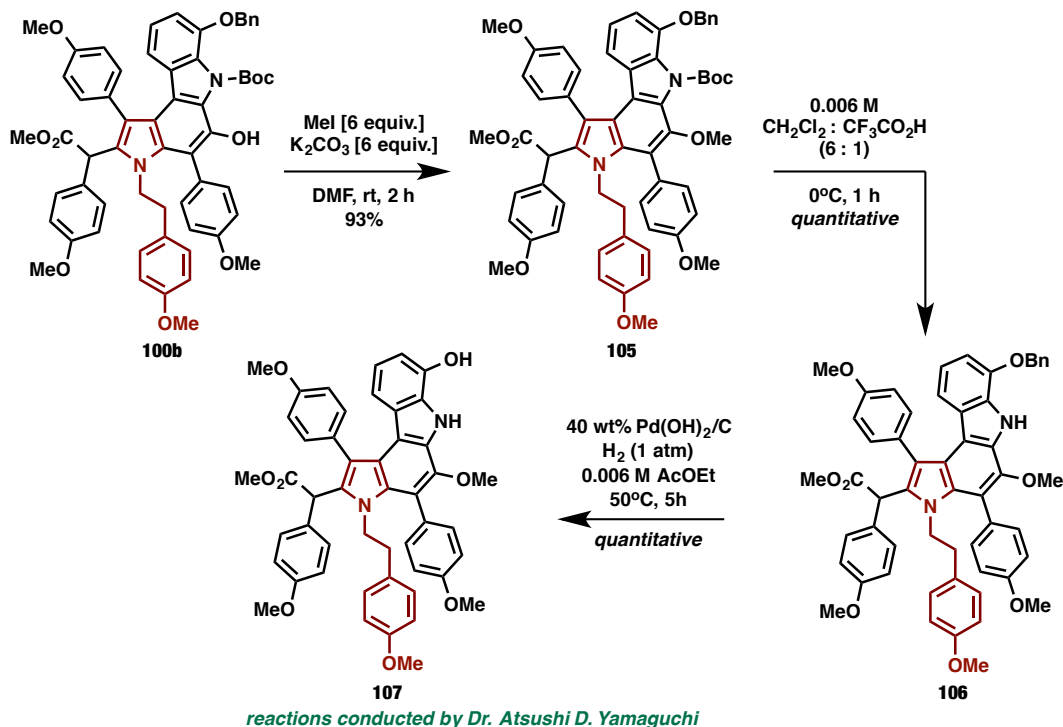
Dr. Atsushi Yamaguchi found that formal 6π -electrocyclization of *N*-Boc indole-containing intermediate **19a** could be achieved with the use of lithium diisopropylamide at $-78\text{ }^{\circ}\text{C}$ to close the pyrrolo[2,3-*c*]carbazole core of dictyodendrin A and provide **100b** in moderate yield with the use of six equivalents of lithium diisopropylamide (Table 5.13, 47%).

Table 5.13 6π -electrocyclization to form the pyrrolo[2,3-*c*]carbazole core of dictyodendrin A



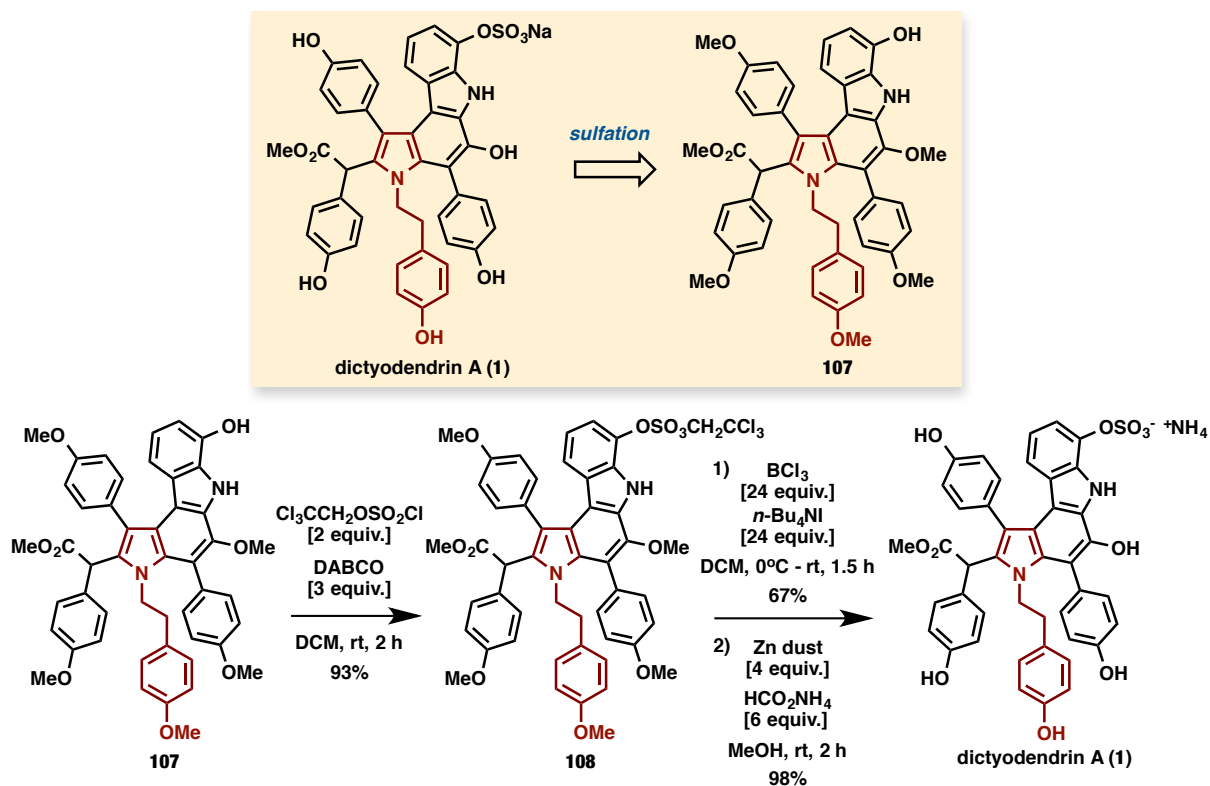
Formal synthesis of the Tokuyama intermediate (**107**) to dictyodendrin A was achieved by Dr. Atsushi Yamaguchi via a series of protections and deprotections. Methylation of **100b** to give **105**, followed by *N*-Boc deprotection of the indole moiety with trifluoroacetic acid, and finally removal of the benzyl group of **106** by hydrogenation under palladium(II) hydroxide catalysis provided the Tokuyama intermediate (**107**)^{7a} to dictyodendrin A in 23% yield over the three protection/deprotection steps (Scheme 5.35).

Scheme 5.35 Completion of the formal synthesis of dictyodendrin A:
protection / deprotection sequence to Tokuyama intermediate



Tokuyama reported the conversion of **107** to dictyodendrin A in three steps by sulfonation, followed by trichloroethyl removal and finally salt formation to provide the natural product (**1**) (Scheme 5.36).^{7a} Specifically, exposure of the phenol of **97** to trichloroethyl chlorosulfate furnished arylsulfate **98** in 93% yield. Then, removal of the methyl groups, followed by removal of the trichloroethyl group proceeded in 98% yield to complete the synthesis of dictyodendrin A (**1**).^{7a}

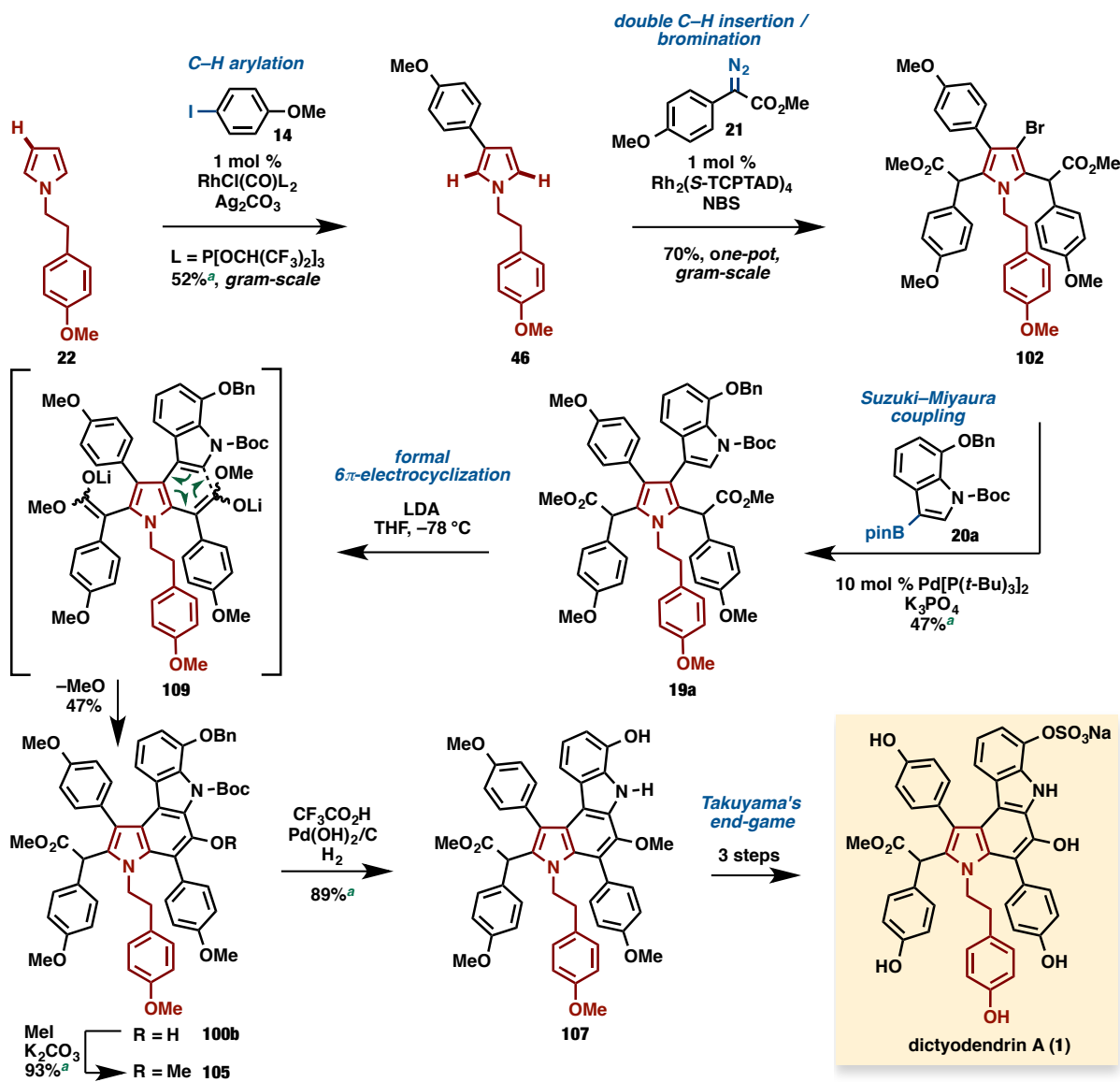
Scheme 5.36 Conversion of Tokuyama's intermediate to dictyodendrin A



In summary, the synthesis commenced with synthesis of alkyl pyrrole **22** from dimethoxytetrahydrofuran and corresponding alkyl amine via Paal-Knorr synthesis.²⁸ 1-substituted pyrrole **22** then underwent selective C–H arylation at the 3-position with electron donating *p*-iodoanisole **14** to provide 3-arylpyrrole **46** in 52% on gram-scale. A one-pot double carbenoid C–H functionalization / bromination was successfully employed to functionalize the 2-, 4- and 5-positions of pyrrole **46** and provide tetra-substituted pyrrole **102** in 70% on gram-scale. A formal synthesis of dictyodendrin A was then completed using Suzuki-Miyaura coupling to tether the indole (**20a**) and pyrrole (**102**) moieties followed by formal 6π -electrocyclization to close the pyrrolo[2,3-*c*]carbazole core (**100b**). Methylation (93%) followed by *N*-Boc and benzyl deprotection (89%) provided the Tokuyama intermediate to dictyodendrin A (**107**). This represents the most efficient total synthesis of dictyodendrin A to date with 12

longest linear steps, 15 total steps (Scheme 5.37).⁹ (In addition to the sequence mentioned above, two steps were needed for the preparation of boronate ester).

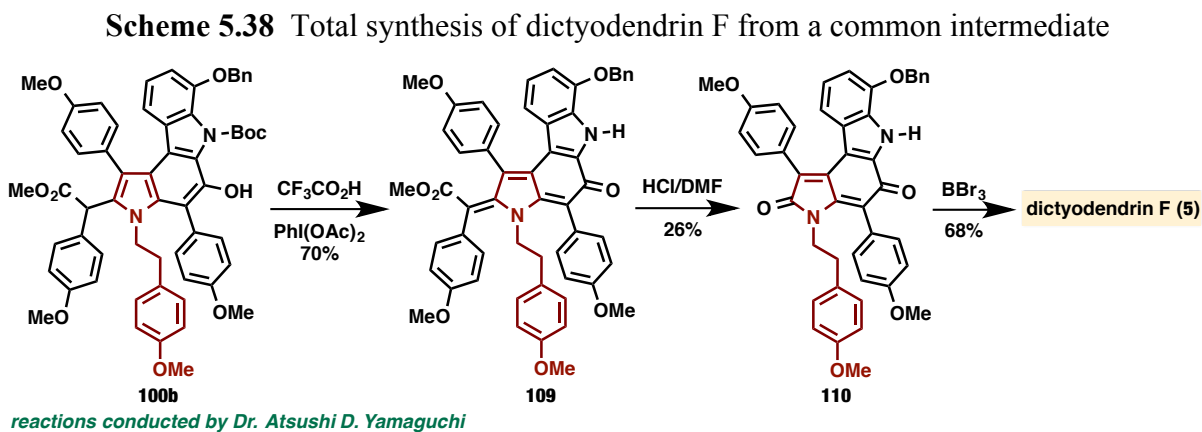
Scheme 5.37 Formal synthesis of dictyodendrin A by sequential C–H functionalization strategy



^a reactions conducted by Dr. Atsushi D. Yamaguchi

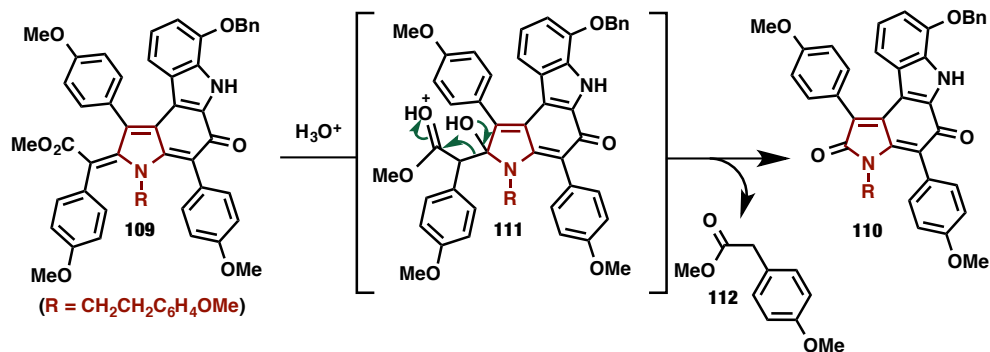
5.5 Total Synthesis of Dictyodendrin F

Following the completion of the concise synthesis of dictyodendrin A (**1**), Dr. Atsushi Yamaguchi completed the total synthesis of dictyodendrin F (**5**) in three steps from intermediate **100b** by removal of the substituent at the C2 position and adjusting the oxidation state. The removal of Boc group from **100b** with $\text{CF}_3\text{CO}_2\text{H}$, followed by treatment with $\text{PhI}(\text{OAc})_2$, provided quinone **109** in 70% yield through oxidation of the pyrrolocarbazole core. Next, hydrolysis for the cleavage of the C2 side chain was investigated. An acidic mixture with DMF afforded **110** in 26% yield. Finally, removal of methyl and benzyl ethers completed the total synthesis of dictyodendrin F (**5**). Treatment of **110** with an excess amount of BBr_3 at $-78\text{ }^\circ\text{C}$ to room temperature furnished dictyodendrin F (**5**) in 68% yield (Scheme 5.38). This synthetic route only required 10 longest linear steps.⁹



The proposed mechanism of the formation of **110** is shown in Scheme 5.39. Hydration of **109** followed by the retro-aldol condensation gave diketone **110**.

Scheme 5.39 Proposed mechanism of the hydration/ retro-aldol condensation to give dictyodendrin F



5.6 Conclusion

In this chapter, the concise synthesis of natural alkaloids dictyodendrins A and F was reported utilizing several direct C–H functionalization reactions of pyrroles. Many things were learned through the explorations of the different synthetic routes attempted to dictyodendrin A. The reaction sequence of β -selective C–H arylation and double C–H insertion followed by Suzuki–Miyaura cross-coupling reaction commenced with a simple *N*-alkylpyrrole, to construct a fully functionalized pyrrole, which was the key intermediate toward both natural products. Completion of the total syntheses was achieved by direct pyrrolo[2,3-*c*]carbazole formation via a formal 6π -electrocyclization of the highly substituted pyrrole. The synthesis of dictyodendrin A was accomplished by a longest linear sequence of 12 steps and the route for the synthesis of dictyodendrin F only needed 10 longest linear steps.

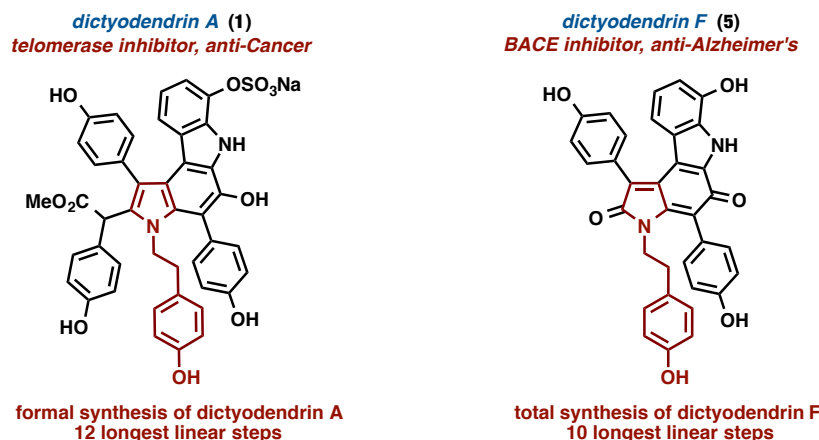
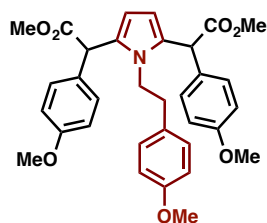


Figure 5.6 Summary of the formal synthesis of dictyodendrin A and total synthesis of dictyodendrin F

5.7 Experimental Section

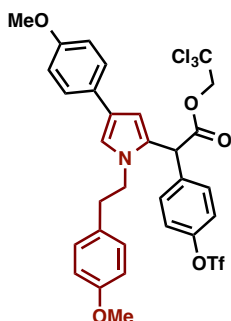
General: Unless otherwise noted, all materials including dry solvents were obtained from commercial suppliers and used without further purification. $\text{P}[\text{OCH}(\text{CF}_3)_2]_3$,³⁰ $\text{RhCl}(\text{CO})\{\text{P}[\text{OCH}(\text{CF}_3)_2]_3\}_2$,^{18a} $\text{Rh}_2(\text{S-TCPTAD})_4$,²⁶ $\text{Rh}_2(\text{S-BTPCP})_4$,³¹ $\text{Rh}_2(\text{S-PTTL})_4$,³² $\text{Rh}_2(\text{S-TCPTTL})_4$,³³ methyl 4-methoxyphenyldiazoacetate (**21**)³⁴ were prepared according to procedures reported in the literature. Unless otherwise noted, all reactions were performed with dry solvents under an atmosphere of nitrogen in heat-gun-dried glassware using standard vacuum-line techniques. All work-up and purification procedures were carried out with reagent-grade solvents in air. Analytical thin-layer chromatography (TLC) was performed using E. Merck silica gel 60 F_{254} pre-coated plates (0.25 mm). The developed chromatogram was analyzed by UV lamp (254 nm) and ethanolic phosphomolybdic acid/sulfuric acid. Flash column chromatography was performed with E. Merck silica gel 60 (230–400 mesh). Preparative high performance liquid chromatography (preparative HPLC) was performed with a Biotage Isolera One equipped with Biotage[®] SNAP Cartridge KP-C18-HS columns using acetonitrile/water as an eluent. Preparative recycling gel permeation chromatography (GPC) was performed with a JAI LC-9204

instrument equipped with JAIGEL-1H/JAIGEL-2H columns using chloroform as an eluent. The high-resolution mass spectra were conducted on Thermo Fisher Scientific Exactive. Nuclear magnetic resonance (NMR) spectra were recorded on a JEOL JNM-ECA-600 (^1H 600 MHz, ^{13}C 150 MHz) spectrometer. Chemical shifts for ^1H NMR are expressed in parts per million (ppm) relative to tetramethylsilane (d 0.00 ppm), $\text{DMSO-}d_6$ (d 2.50 ppm) or CD_3OD (d 3.31 ppm). Chemical shifts for ^{13}C NMR are expressed in ppm relative to CDCl_3 (d 77.0 ppm), $\text{DMSO-}d_6$ (d 39.5 ppm) or CD_3OD (d 49.0 ppm). Data are reported as follows: chemical shift, multiplicity (s = singlet, d = doublet, dd = doublet of doublets, t = triplet, q = quartet, p = pentet, m = multiplet, brs = broad singlet), coupling constant (Hz), and integration. Coupling constants (J values) were calculated directly from the spectra. $\text{Rh}_2(\text{OAc})_4$, $\text{Rh}_2(\text{esp})_2$, *N*-methylpyrrole, phenylmagnesium bromide, 4-(dimethylamino)pyridine (DMAP), *N,N'*-dicyclohexylcarbodiimide (DCC), 2,2,2-trichloroethanol, 1,8-diazabicycloundec-7-ene (DBU), *p*-ABSA, *N*, *O*-dimethylhydroxylamine hydrochloride, and 4-iodoanisole (**14**) were all commercially available and used without further purification. Since the compounds **43**, **44**, **68**, **69**, **70**, **71**, **72**, **80**, **81**, and **82** were formed as inseparable mixtures, authentic samples of the products from C–H functionalization could not be fully characterized. The results reported in Schemes 5.8, 5.17, 5.18, 5.21 and Table 5.7, are based upon ^1H NMR shifts of structural analogs as well as from LCMS data on product mixture. Compounds **1**, **5**, **20a**, **22**, **19b**, **46**, **73**, **75**, **105**, **106**, **107**, **109**, and **110** were synthesized by Dr. Atsushi D. Yamaguchi. The characterization data for all intermediates in the syntheses of dictyodendrins A and F by sequential the C–H functionalization strategy can be found in the supplementary information of the published work.⁹



Dimethyl 2,2'-(1-(4-methoxyphenethyl)-1H-pyrrole-2,5-diyl)bis(2-(4-methoxyphenyl)acetate) (42):

A 25-mL round-bottomed flask, containing a magnetic stirring bar, was dried and filled with nitrogen after cooling to 23 °C. To this vessel were added 1-[2-(4-methoxyphenyl)ethyl]pyrrole (**22**) (40.2 mg, 0.20 mmol, 1.0 equiv), Rh₂(S-PTAD)₄ (3.1 mg, 2.0 mmol, 1 mol%) and CH₂Cl₂ (500 mL). In a separate vial, diazoester **21** (82.5 mg, 0.40 mmol, 2.0 equiv) was dissolved in CH₂Cl₂ (1.5 mL) and then added to the reaction mixture by syringe pump over 1 h. After 14 h of additional stirring, CH₂Cl₂ was removed *in vacuo* and the remaining residue was purified by silica-gel flash column chromatography (hexane/EtOAc = 5:1) to afford the title compound **42** (mixture of diastereomers, 37.9 mg, 30% yield) as a yellow solid. ¹H NMR (600 MHz, CDCl₃) δ 7.19–7.15 (m, 8H), 6.86–6.79 (m, 16H), 6.11 (s, 2H), 6.09 (s, 2H), 4.77 (s, 2H), 4.77 (s, 2H), 3.82–3.66 (m, 34H), 2.58–2.53 (m, 1H), 2.45 (t, *J* = 7.2 Hz, 2H), 2.27–2.22 (m, 1H); ¹³C NMR (150 MHz, CDCl₃) δ 172.17, 172.13, 159.1, 159.0, 158.5, 158.4, 130.0, 129.7, 129.6, 129.5, 129.42, 129.38, 114.07, 114.05, 114.03, 107.9, 107.8, 55.3, 55.2, 52.4, 49.2, 49.1, 45.71, 45.67, 36.33, 36.30; HRMS (ESI) *m/z* calcd for C₃₃H₃₄NO₇ [M–H][−]: 556.2330 found: 556.2322.⁹



2,2,2-trichloroethyl 2-(1-(4-methoxyphenethyl)-4-(4-methoxyphenyl)-1H-pyrrol-2-yl)-2-

(4-(((trifluoromethyl)sulfonyl)oxy)phenyl)acetate (67), Procedure 1:

A 30 mL flask was charged with 1-(4-methoxyphenethyl)-3-(4-methoxyphenyl)-1H-pyrrole (**46**) (66.3 mg, 0.2156 mmol, 1.00 equiv) and Rh₂(S-TCPTAD)₄ (4.5 mg, 0.0021 mmol, 0.01 equiv) dissolved in 2 mL of dichloromethane.

2,2,2-trichloroethyl 2-diazo-2-(4-

(((trifluoromethyl)sulfonyl)oxy)phenyl)acetate (**47b**) (190.4 mg, 0.4312 mmol, 2.00 equiv)

dissolved in 8 mL of dichloromethane was then slowly added over the course of three hours by syringe pump. The resulting was allowed to stir for 12 hours and then concentrated in vacuo. The

resulting crude product was purified on silica gel eluting with hexanes : ethyl acetate (4:1) to

afford combined yield of **67** and **68** as a yellow oil (1.4:1, 160.4 mg, 99 % yield).

Characterization of 1: *R_f* = 0.38 (hexane : ethyl acetate 3:1); ¹H NMR of **67** (400 MHz, CDCl₃) δ

7.38 (d, *J* = 8.0 Hz, 4H), 7.25 (s, 1H), 6.88 (d, *J* = 12.0 Hz, 4H), 6.85-6.84 (m, 2H), 6.80 (d, *J* =

8.0 Hz, 2H), 6.42 (s, 1H), 4.84 (s, 1H), 4.78 (dd, *J* = 12.0, 16.0 Hz, 2H), 3.91-3.87 (m, 2H), 3.82

(s, 3H), 3.78 (s, 3H), 2.87 (p, *J* = 8.0 Hz, 1H), 2.74 (p, *J* = 8.0 Hz, 1H); ¹³C NMR of **67** (100

MHz, CDCl₃) δ 169.3, 158.8, 158.0, 149.3, 137.2, 130.8, 130.0, 129.9, 128.3, 127.5, 126.2,

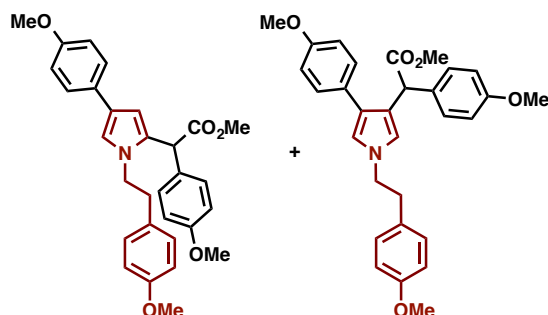
124.0, 121.8, 118.1, 114.4, 114.3, 107.3, 94.7, 74.7, 55.5, 55.4, 48.9, 48.8, 37.5; IR (film): 2956,

1706, 1608, 1512, 1421, 1248, 1209, 1136, 1031, 885, 833, 718; HRMS (p NSI) calcd for

C₃₁H₂₈O₈NCl₃F₃S (M+H)⁺ 736.0548 found 736.0560.

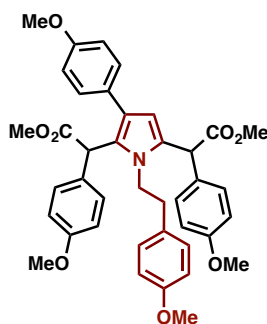
Procedure 2: A 30 mL flask was charged with 1-(4-methoxyphenethyl)-3-(4-methoxyphenyl)-

1H-pyrrole (153.7 mg, 0.5000 mmol, 1.00 equiv) and Rh₂(S-TCPTAD)₄ (10.6 mg, 0.0050 mmol, 0.01 equiv) dissolved in 2 mL of dichloromethane. 2,2,2-trichloroethyl 2-diazo-2-(4-(((trifluoromethyl)sulfonyl)oxy)phenyl)acetate (220.8 mg, 0.5000 mmol, 1.00 equiv) dissolved in 8 mL of dichloromethane was then slowly added over the course of three hours by syringe pump. The resulting was allowed to stir for 12 hours and then concentrated in vacuo. The resulting crude product was purified on silica gel eluting with hexanes : ethyl acetate (4:1). R_f = 0.38 (hexane: ethyl acetate 3:1).



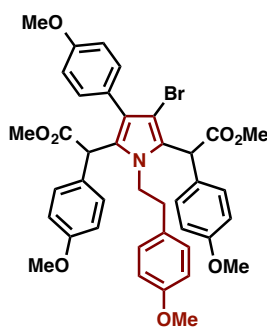
Methyl 2-(1-(4-methoxyphenethyl)-4-(4-methoxyphenyl)-1H-pyrrol-2-yl)-2-(4-methoxyphenyl)acetate (98) and methyl 2-(1-(4-methoxyphenethyl)-4-(4-methoxyphenyl)-1H-pyrrol-3-yl)-2-(4-methoxyphenyl)acetate (99): A 100-mL round-bottomed flask, containing a magnetic stirring bar, was dried and filled with nitrogen after cooling to 23 °C. To this vessel were added 3-arylpyrrole **46** (922 mg, 3.0 mmol, 1.0 equiv), Rh₂(S-TCPTAD)₄ (6.0 mg, 3.0 mmol, 0.1 mol%) and CH₂Cl₂ (7.4 mL). In a separate 50 mL round-bottomed flask, diazoester **21** (804 mg, 3.9 mmol, 1.3 equiv) was dissolved in CH₂Cl₂ (22.5 mL) and then added to the reaction mixture by syringe pump over 1 h. After 14 h of additional stirring, CH₂Cl₂ was removed *in vacuo* and the remaining residue was purified by silica-gel flash column chromatography (hexane/EtOAc = 4:1) to afford **98** and **99** (inseparable mixture of **98** and **99**, 1.10 g, 78% combined yield, **98** : **99** = 11.7 : 1 = 92 : 8) as a yellow solid. ¹H NMR of **98** (600

MHz, CDCl₃) δ 7.38 (d, *J* = 8.7 Hz, 2H), 7.20 (d, *J* = 8.7 Hz, 2H), 6.90 (d, *J* = 8.7 Hz, 2H), 6.87–6.85 (m, 4H), 6.81 (s, 1H), 6.79 (d, *J* = 2.0 Hz, 2H), 6.32 (d, *J* = 1.4 Hz, 1H), 4.75 (s, 1H), 3.85 (t, *J* = 7.6 Hz, 2H), 3.80 (s, 3H), 3.78 (s, 3H), 3.77 (s, 3H), 3.73 (s, 3H), 2.81–2.76 (m, 1H), 2.70–2.65 (m, 1H); ¹H NMR of **99** (600 MHz, CDCl₃) δ 7.18 (d, *J* = 8.7 Hz, 2H), 7.08 (d, *J* = 8.7 Hz, 2H), 6.99 (d, *J* = 8.7 Hz, 2H), 6.83–6.79 (m, 6H), 6.62 (d, *J* = 2.5 Hz, 1H), 6.57 (d, *J* = 2.5 Hz, 1H), 4.91 (s, 1H), 4.06–3.97 (m, 2H), 3.78 (s, 3H), 3.78 (s, 6H), 3.57 (s, 3H), 2.99 (t, *J* = 7.5 Hz, 2H); ¹³C NMR of **98** (150 MHz, CDCl₃) δ 172.4, 159.2, 158.6, 157.8, 130.3, 129.94, 129.88, 129.85, 129.4, 128.7, 126.1, 123.5, 117.5, 114.3, 114.25, 114.20, 106.4, 55.48, 55.46, 55.44, 52.7, 49.0, 48.8, 37.4; HRMS (ESI) *m/z* calcd for C₃₀H₃₁NO₅Na [M+Na]⁺: 508.2094 found: 508.2081.⁹



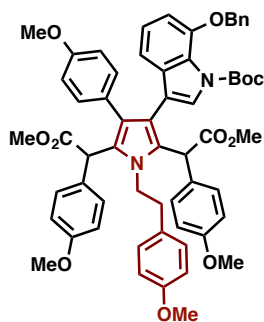
Dimethyl 2,2'-(1-(4-methoxyphenethyl)-3-(4-methoxyphenyl)-1*H*-pyrrole-2,5-diyl)bis(2-(4-methoxyphenyl)acetate) (41**):** A 50-mL round-bottomed flask, containing a magnetic stirring bar, was dried and filled with nitrogen after cooling to 23 °C. To this vessel were added 3-arylpyrrole **46** (615 mg, 2.0 mmol, 1.0 equiv), Rh₂(*S*-TCPTAD)₄ (42.2 mg, 20.0 mmol, 1 mol%) and CH₂Cl₂ (4.0 mL). In a separate vial, diazoester **21** (516 mg, 2.5 mmol, 1.25 equiv) was dissolved in CH₂Cl₂ (8.0 mL) and then added to the reaction mixture by syringe pump over 3 h. After 5 h of additional stirring, Rh₂(*S*-TCPTAD)₄ (42.2 mg, 20.0 mmol, 1 mol%) was added to the reaction mixture, and then CH₂Cl₂ solution of diazoester (516 mg, 2.5 mmol, 1.25 equiv) was

added by syringe pump over 3 h. After 5 h of additional stirring, CH₂Cl₂ was removed *in vacuo* and the remaining residue was purified by silica-gel flash column chromatography (hexane/EtOAc = 3:1) to afford the title compound **41** (mixture of diastereomers, 1.09 g, 82% yield) as a yellow solid. ¹H NMR (600 MHz, CDCl₃) δ 7.31–7.25 (m, 8H), 7.04 (d, *J* = 8.4 Hz, 2H), 6.96 (d, *J* = 8.4 Hz, 2H), 6.91–6.83 (m, 14H), 6.80–6.76 (m, 6H), 6.31 (s, 1H), 6.23 (s, 1H), 5.36 (s, 1H), 5.34 (s, 1H), 4.96 (s, 1H), 4.95 (s, 1H), 3.81–3.67 (m, 34H), 3.63 (s, 3H), 3.57 (s, 3H), 2.54–2.44 (m, 3H), 2.32–2.28 (m, 1H); ¹³C NMR (150 MHz, CDCl₃) δ 172.4, 172.3, 172.1, 172.0, 159.03, 159.01, 158.5, 158.4, 158.2, 158.0, 157.9, 130.0, 129.81, 129.76, 129.54, 129.48, 129.41, 129.33, 129.30, 129.2, 129.12, 129.06, 124.5, 124.3, 124.24, 124.20, 114.0, 113.9, 113.8, 113.7, 113.55, 113.52, 109.9, 109.7, 55.1, 52.4, 52.2, 52.1, 49.02, 49.00, 46.8, 46.7, 46.6, 36.2, 36.1; HRMS (ESI) *m/z* calcd for C₂₆H₄₀NO₈ [M–H][–]: 662.2748 found: 662.2752.⁹



Dimethyl 2,2'-(3-bromo-1-(4-methoxyphenethyl)-4-(4-methoxyphenyl)-1H-pyrrole-2,5-diyl)bis(2-(4-methoxyphenyl)acetate) (102):⁹ A 100-mL round-bottomed flask, containing a magnetic stirring bar, was dried and filled with nitrogen after cooling to 23 °C. To this vessel were added 3-arylpyrrole **46** (1.00 g, 3.25 mmol, 1.0 equiv), Rh₂(S-TCPTAD)₄ (34.2 mg, 16.3 mmol, 0.5 mol%) and CH₂Cl₂ (6.5 mL). In a separate vial, diazoester **21** (839 mg, 4.06 mmol, 1.25 equiv) was dissolved in CH₂Cl₂ (13 mL) and then added to the reaction mixture by syringe pump over 3 h. After 5 h of additional stirring, Rh₂(S-TCPTAD)₄ (34.2 mg, 16.3 mmol, 0.5

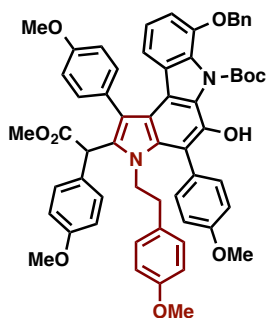
mol%) was added to the reaction mixture. Then CH₂Cl₂ solution of diazoester (839 mg, 4.06 mmol, 1.25 equiv) was added by syringe pump over 3 h. After 2 h of additional stirring, dichloromethane was removed *in vacuo* and the residue was dissolved to dry CH₃CN (24 mL). The flask was cooled to -10 °C and *N*-bromosuccinimide (NBS; 579 mg, 3.25 mmol, 1.0 equiv) was added to the reaction mixture. After stirring for 5 min, the reaction mixture was quenched with saturated aqueous Na₂S₂O₃. It was extracted with ethyl acetate (12 mL x 3), dried over Na₂SO₄ and concentrated *in vacuo*. The crude residue was purified by silica-gel flash column chromatography (hexane/EtOAc = 3:1 to 2:1) to afford title compound bromopyrrole **102** (mixture of diastereomers, 1.70 g, 70% yield) as an orange solid. ¹H NMR (600 MHz, CDCl₃) δ 7.30–7.23 (m, 4H), 7.19 (d, *J* = 8.4 Hz, 2H), 7.15 (d, *J* = 9.0 Hz, 2H), 7.01 (d, *J* = 8.4 Hz, 2H), 6.94 (d, *J* = 7.8 Hz, 2H), 6.91–6.85 (m, 12H), 6.83–6.73 (m, 8H), 5.27 (s, 2H), 5.20 (s, 1H), 5.17 (s, 1H), 3.86–3.67 (m, 34H), 3.56 (s, 3H), 3.47 (s, 3H), 2.48–2.20 (m, 4H); ¹³C NMR (150 MHz, CDCl₃) δ 171.7, 171.47, 171.42, 171.35, 158.7, 158.51, 158.48, 158.1, 131.72, 131.67, 129.6, 129.5, 129.4, 129.3, 129.1, 129.0, 128.8, 128.7, 127.99, 127.96, 126.5, 126.4, 126.2, 126.1, 125.4, 125.3, 124.3, 124.0, 113.84, 113.76, 113.74, 113.2, 113.1, 99.1, 99.0, 55.00, 54.96, 54.92, 52.51, 52.48, 52.1, 52.0, 47.6, 47.3, 47.2, 35.9, 35.7; HRMS (ESI) *m/z* calcd for C₄₀H₃₉BrNO₈ [M-H]⁻: 740.1854 found: 740.1870.⁹



Dimethyl 2,2'-(3-(7-(benzyloxy)-1-(tert-butoxycarbonyl)-1H-indol-3-yl)-1-(4-methoxyphenethyl)-4-(4-methoxyphenyl)-1H-pyrrole-2,5-diyl)bis(2-(4-

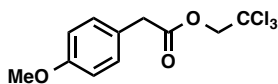
methoxyphenyl)acetate) (19a):⁹ A 20-mL glass vessel equipped with screw cap, containing a magnetic stirring bar, was dried and filled with nitrogen after cooling to 23 °C. To this vessel were added bromopyrrole **102** (74.1 mg, 0.10 mmol, 1.0 equiv), Pd[P(*t*-Bu)₃]₂ (5.2 mg, 10 mmol, 10 mol%), and K₃PO₄ (85.2 mg, 0.40 mmol, 4.0 equiv) under a stream of nitrogen. Then to the reaction mixture were added the solution of boronate **20a** (180 mg, 0.40 mmol, 4.0 equiv) in 1,4-dioxane (1.0 mL) and degassed H₂O (100 mL). After capped, the vessel was heated at 80 °C for 15 h in an oil bath with stirring. After cooling the reaction mixture to 23 °C, it was passed through a pad of silica gel (EtOAc) and the filtrate was concentrated *in vacuo*. The residue was purified by GPC to afford title compound **19a** (mixture of diastereomers, 46.3 mg, 47% yield) as an orange solid. ¹H NMR (600 MHz, DMSO-*d*₆, 100 °C) δ 7.50 (d, *J* = 7.8 Hz, 2H), 7.50 (d, *J* = 7.8 Hz, 2H), 7.34 (t, *J* = 7.8 Hz, 2H), 7.34 (t, *J* = 7.8 Hz, 2H), 7.29 (t, *J* = 7.8 Hz, 1H), 7.29 (t, *J* = 7.8 Hz, 1H), 7.24 (brs, 1H), 7.19 (brs, 1H), 7.12–7.01 (m, 12H), 6.97–6.72 (m, 22H), 6.64 (d, *J* = 9.0 Hz, 2H), 6.62 (d, *J* = 9.0 Hz, 2H), 5.33 (s, 1H), 5.31 (s, 1H), 5.26 (s, 1H), 5.26 (s, 1H), 5.15 (s, 2H), 5.15 (s, 2H), 3.83–3.69 (m, 22H), 3.63 (s, 3H), 3.62 (s, 3H), 3.54 (s, 3H), 3.53 (s, 3H), 2.98 (s, 3H), 2.98 (s, 3H), 2.51–2.41 (m, 4H), 1.48 (s, 9H), 1.47 (s, 9H); ¹³C NMR (150 MHz, DMSO-*d*₆, 100 °C) δ 170.92, 170.88, 170.75, 170.68, 157.9, 157.84, 157.78, 157.65, 157.2, 147.8, 146.3, 136.9, 133.7, 133.5, 130.56, 130.48, 129.40, 129.37, 129.10, 129.06, 128.84,

128.79, 127.6, 127.5, 127.3, 127.0, 126.9, 126.8, 125.0, 124.5, 124.4, 124.05, 123.97, 122.39, 122.35, 114.1, 114.0, 113.7, 113.6, 113.5, 113.4, 113.2, 113.1, 112.9, 112.62, 112.57, 108.2, 82.2, 70.1, 54.7, 54.6, 54.4, 51.3, 51.2, 50.94, 50.88, 46.8, 46.7, 46.6, 46.5, 46.0, 45.9, 34.8, 27.1, 26.9; HRMS (ESI) m/z calcd for $C_{60}H_{60}N_2O_{11}Na$ $[M+Na]^+$: 1007.4089 found: 1007.4055.⁹



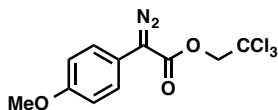
Methyl 2-(7-(benzyloxy)-6-(tert-butoxycarbonyl)-5-hydroxy-3-(4-methoxyphenethyl)-1,4-bis(4-methoxyphenyl)-3,6-dihydropyrrolo[2,3-c]carbazol-2-yl)-2-(4-methoxyphenyl)acetate (100b):⁹ A 20-mL Schlenk flask, containing a magnetic stirring bar, was dried and filled with nitrogen after cooling to 23 °C. To this vessel were added diisopropylamine (75.0 mL, 530 mmol, 6.0 equiv) and THF (0.70 mL). After cooled to 0 °C, 1.6 M *n*-hexane solution of *n*-butyllithium (330 mL, 530 mmol, 6.0 equiv) was added and the reaction mixture was stirred for 30 min at 0 °C. After the reaction mixture was cooled to –78 °C, the solution of pyrrole **19a** (87.1 mg, 88.0 mmol, 1.0 equiv) in THF (1.2 mL) was added dropwise. After stirring for 1 h at –78 °C, the reaction mixture was quenched by saturated aqueous NH_4Cl (2.0 mL) and extracted with EtOAc (5.0 mL x 3). The combined organic layer was dried over Na_2SO_4 and the solvent was evaporated *in vacuo*. The crude residue was purified by preparative HPLC to afford pyrrolocarbazole **100b** (39.4 mg, 47% yield) as a brown solid. 1H NMR (600 MHz, $CDCl_3$) δ 10.83 (s, 1H), 7.55–7.53 (m, 3H), 7.41 (d, $J = 7.2$ Hz, 2H), 7.38 (dd, $J = 7.8, 1.8$ Hz, 1H), 7.34 (t, $J = 7.2$ Hz, 2H), 7.29 (t, $J = 7.8$ Hz, 1H), 7.11 (d, $J = 9.0$ Hz, 2H), 7.06–7.01 (m, 3H), 6.97

(dd, $J = 8.4, 2.4$ Hz, 1H), 6.82–6.77 (m, 4H), 6.60 (t, $J = 7.8$ Hz, 2H), 6.33 (d, $J = 9.0$ Hz, 2H), 5.79 (d, $J = 8.4$ Hz, 1H), 5.35 (s, 1H), 5.12 (s, 2H), 3.89 (s, 3H), 3.87 (s, 3H), 3.80–3.72 (m, 2H) 3.76 (s, 3H), 3.71 (s, 3H), 3.63 (s, 3H), 2.34–2.22 (m, 2H) 1.32 (s, 9H); ^{13}C NMR (150 MHz, CDCl_3) δ 171.8, 159.2, 159.0, 158.5, 157.9, 156.1, 148.6, 141.2, 136.7, 133.4, 133.3, 133.0, 132.92, 132.87, 130.5, 130.3, 130.1, 129.7, 129.5, 129.3, 128.8, 128.5, 128.1, 127.9, 127.6, 124.5, 120.5, 117.9, 117.1, 116.6, 113.9, 113.80, 113.75, 113.70, 113.68, 113.3, 112.9, 110.1, 85.4, 71.2, 55.4, 55.3, 55.24, 55.15, 52.2, 47.0, 46.9, 35.1, 27.4; HRMS (ESI) m/z calcd for $\text{C}_{59}\text{H}_{55}\text{N}_2\text{O}_{10}$ $[\text{M}-\text{H}]^-$: 951.3851 found: 951.3869.⁹

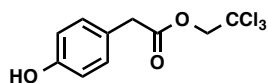


2,2,2-trichloroethyl 2-(4-methoxyphenyl)acetate (54): A 1 L flask was charged with 4-methoxyphenylacetic acid (**52**) (30.0 g, 180.5 mmol, 1.0 equiv), 4-(dimethylamino)pyridine (DMAP: 2.2 g, 18.1 mmol, 0.1 equiv), and 2,2,2-trichloroethanol (20.7 mL, 216.6 mmol, 1.2 equiv) and dissolved in 370 mL dichloromethane. The reaction mixture was then cooled to 0°C in an ice bath. Once cool, a solution of *N,N'*-dicyclohexylcarbodiimide (DCC: 41.0 g, 198.6 mmol, 1.1 equiv) in dichloromethane (92 mL) was added to the reaction mixture. The mixture was slowly allowed to warm to room temperature and stirred overnight. The resulting white precipitate was removed by filtration and washed with copious diethyl ether. The filtrate was then concentrated *in vacuo* and the remaining residue was purified on silica gel eluting with hexane:ethyl acetate (20:1) to afford the title compound **54** as a clear oil (53.6 g, 99% yield). $R_f = 0.28$ (hexane:ethyl acetate 20:1); ^1H NMR (400 MHz, CDCl_3) δ 7.24 (d, $J = 8.4$ Hz, 2H), 6.88 (d, $J = 8.4$ Hz, 2H), 4.74 (s, 2H), 3.78 (s, 3H), 3.70 (s, 2H); ^{13}C NMR (100 MHz, CDCl_3) δ 170.4, 159.1, 130.6, 125.1, 114.2, 95.0, 74.3, 55.5, 40.2; IR (film): 2935, 2836, 2117, 1752,

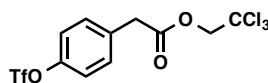
1613, 1512, 1463, 1301, 1247, 1178, 1125, 1032, 820, 785, 765, 729, 713; HRMS (ESI) calcd for C₁₁H₁₂O₃Cl₃ (M+H)⁺ 296.98483 found 296.98465.



2,2,2-trichloroethyl 2-diazo-2-(4-methoxyphenyl)acetate (47a): This diazo compound **47a** was prepared using *o*-nitrobenzenesulfonyl azide (*o*-NBSA) as the diazo transfer reagent. This reagent was prepared according to a literature protocol.³⁵ According to the known literature procedure,³⁴ a 30 mL flask was charged with 2,2,2-trichloroethyl 2-(4-methoxyphenyl)acetate (**54**) (297.6 mg, 1.000 mmol, 1.000 equiv) and *o*-NBSA (342.3 mg, 1.500 mmol, 1.500 equiv) dissolved in 8 mL acetonitrile and cooled to 0 °C in an ice bath. 1,8-diazabicycloundec-7-ene (DBU: 0.33 mL, 2.20 mmol, 2.20 equiv) was then slowly added. The reaction mixture was then allowed to slowly warm to room temperature overnight. The resulting orange solution was quenched with saturated 10 mL NH₄Cl and the aqueous layer was extracted with diethyl ether (3 x 20 mL). The combined organic layers were dried over MgSO₄, filtered, and concentrated *in vacuo*. The remaining residue was purified on silica gel eluting with hexane : ethyl acetate (20 : 1) to afford the title compound **47a** as a light orange solid (88.5 mg, 27 % yield). *R*_f = 0.30 (hexane: ethyl acetate 20:1); ¹H NMR (600 MHz, CDCl₃) δ 7.38 (d, 2H, *J* = 8.7 Hz), 6.94 (d, 2H, *J* = 8.7 Hz), 4.88 (s, 2H), 3.08 (s, 3H); ¹³C NMR (150 MHz, CDCl₃) 164.0, 158.6, 126.3, 116.2, 114.9, 95.3, 74.0, 55.6; IR (neat): 2953, 2935, 2090, 1690, 1234 cm⁻¹; ¹H NMR (600 MHz, CDCl₃) δ 7.38 (d, *J* = 9.0 Hz, 1H), 6.95 (d, *J* = 9.0 Hz, 1H), 4.88 (s, 2H), 3.80 (s, 3H); ¹³C NMR (150 MHz, CDCl₃) δ 158.67, 128.40, 126.37, 116.21, 114.97, 114.52, 95.32, 74.07, 55.58; HRMS (APCI) *m/z*: [M+H-N₂]⁺ calcd for C₁₁H₁₀O₃Cl₃ 294.9690, found 294.9688.

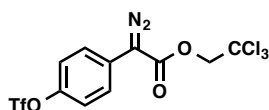


2,2,2-trichloroethyl 2-(4-hydroxyphenyl)acetate (65): A 1 L flask was charged with 4-hydroxyphenylacetic acid (**64**) (25.4 g, 166.9 mmol, 1.0 equiv), 4-(dimethylamino)pyridine (DMAP: 2.0 g, 16.7 mmol, 0.1 equiv), and 2,2,2-trichloroethanol (19.2 mL, 200.3 mmol, 1.2 equiv) and dissolved in 370 mL dichloromethane. The reaction mixture was then cooled to 0 °C in an ice bath. Once cool, a solution of *N,N'*-dicyclohexylcarbodiimide (DCC: 41.0 g, 198.6 mmol, 1.1 equiv) in dichloromethane (92 mL) was added to the reaction mixture. The mixture was slowly allowed to warm to room temperature and stirred overnight. The resulting white precipitate was removed by filtration and washed with copious diethyl ether. The filtrate was then concentrated *in vacuo* and the remaining residue was purified on silica gel eluting with hexane:ethyl acetate (5:1) to afford the title compound **65** as a yellow oil (47.3 g, quantitative yield). $R_f = 0.35$ (hexane: ethyl acetate 5:1); $^1\text{H NMR}$ (400 MHz, CDCl_3) δ 7.14 (d, $J = 8.6$ Hz, 2H), 6.77 (d, $J = 8.6$ Hz, 2H), 6.03 (bs, 1H), 4.73 (s, 2H), 3.68 (s, 2H); $^{13}\text{C NMR}$ (100 MHz, CDCl_3) δ 171.2, 155.4, 130.7, 124.6, 115.8, 94.8, 74.3, 40.1; IR (film): 3403, 2935, 1748, 1614, 1514, 1216, 1127, 835, 783, 713; HRMS (ESI) calcd for $\text{C}_{10}\text{H}_{10}\text{O}_3\text{Cl}_3$ ($\text{M}+\text{H}$) $^+$ 282.96924 found 282.96900.



2,2,2-trichloroethyl 2-(4-((trifluoromethyl)sulfonyl)oxy)phenyl)acetate (66): A 500 mL flask was charged with 2,2,2-trichloroethyl 2-(4-hydroxyphenyl)acetate (**65**) (25.0 g, 88.2 mmol, 1.0 equiv) dissolved in 187 mL dichloromethane. The reaction mixture was then cooled to -15 °C in an ethylene glycol/ $\text{CO}_2(\text{s})$ bath. Once cool, *N,N*-diisopropylethylamine (18.3 mL, 104.9 mmol, 1.2 equiv) was added dropwise to the reaction mixture over 10 minutes. The reaction mixture

was then allowed to stir at -15 °C for an additional 30 minutes. Trifluoromethanesulfonic anhydride (16.0 mL, 95.2 mmol, 1.1 equiv) was then added and the mixture was slowly allowed to warm to room temperature and stirred overnight. The reaction mixture was then washed with 1 N hydrochloric acid (2 x 100 mL), followed by 1 N aqueous sodium hydroxide (2 x 100 mL), followed by deionized water (2 x 100 mL) and then dried over sodium sulfate, filtered, and concentrated *in vacuo*. The remaining residue was purified on silica gel eluting with hexanes : ethyl acetate (20 : 1) to afford the title compound **66** as a yellow oil (30.0 g, 69 % yield). $R_f = 0.26$ (hexane: ethyl acetate 20:1); $^1\text{H NMR}$ (400 MHz, CDCl_3) δ 7.44 (d, $J = 8.6$ Hz, 2H), 7.27 (d, $J = 8.6$ Hz, 2H), 4.76 (s, 2H), 3.81 (s, 2H); $^{13}\text{C NMR}$ (100 MHz, CDCl_3) δ 169.3, 149.1, 133.7, 131.6, 123.7, 121.8, 120.5, 117.3, 114.1, 94.8, 74.4, 40.3; IR (film): 1756, 1503, 1418, 1207, 1128, 1019, 884, 815, 722; HRMS (ESI) calcd for $\text{C}_{17}\text{H}_{19}\text{O}_5\text{N}_3\text{F}$ ($\text{M}+\text{H}$) $^+$ 364.13043 found 364.13033.

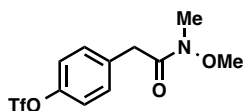


2,2,2-trichloroethyl 2-diazo-2-(4-((trifluoromethyl)sulfonyl)oxy)phenyl)acetate (47b):

According to the known literature procedure,³⁴ a 30 mL flask was charged with 2,2,2-trichloroethyl 2-(4-((trifluoromethyl)sulfonyl)oxy)phenyl)acetate (**66**) (250.0 mg, 0.6016 mmol, 1.000 equiv) and *p*-ABSA (216.6 mg, 0.9023 mmol, 1.500 equiv) dissolved in 5 mL acetonitrile and cooled to -40 °C in an acetonitrile/ $\text{CO}_2(\text{s})$ bath. 1,8-diazabicycloundec-7-ene (DBU: 0.13 mL, 0.9023 mmol, 1.5 equiv) was then slowly added. The reaction mixture was then allowed to slowly warm to room temperature overnight. The resulting orange solution was quenched with saturated 10 mL NH_4Cl and the aqueous layer was extracted with diethyl ether (3 x 20 mL). The combined organic layers were dried over MgSO_4 , filtered, and concentrated *in vacuo*. The

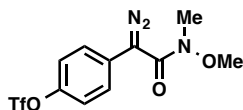
remaining residue was purified on silica gel eluting with hexane:ethyl acetate (20:1) to afford the title compound **47b** as a light yellow solid (190.4 mg, 72 % yield). $R_f = 0.33$ (hexane: ethyl acetate 20:1); $^1\text{H NMR}$ (400 MHz, CDCl_3) δ 7.61 (d, $J = 9.2$ Hz, 2H), 7.34 (d, $J = 9.2$ Hz, 2H), 4.93 (s, 2H); $^{13}\text{C NMR}$ (100 MHz, CDCl_3) δ 162.9, 147.6, 126.0, 125.5, 122.3, 120.6, 117.3, 95.0, 74.1; IR (film): 2910, 2098, 1713, 1504, 1424, 1207, 1135, 883, 838, 717; HRMS (p NSI) calcd for $\text{C}_{11}\text{H}_7\text{Cl}_3\text{F}_3\text{N}_2\text{O}_5\text{S}$ ($\text{M}+\text{H}$) $^+$ 440.9094 found 441.5832.

Procedure 2: A 100 mL flask was charged with 2,2,2-trichloroethyl 2-(4-(((trifluoromethyl)sulfonyl)oxy)phenyl)acetate (8.09 g, 19.46 mmol, 1.000 equiv) and *p*-ABSA (7.01 g, 29.20 mmol, 1.500 equiv) dissolved in 162 mL acetonitrile and cooled to -40°C in an acetonitrile/ $\text{CO}_2(\text{s})$ bath. 1,8-Diazabicycloundec-7-ene (DBU, 4.36 mL, 29.2 mmol, 1.50 equiv) was then slowly added. The reaction mixture was then allowed to slowly warm to room temperature overnight. The resulting orange solution was quenched with saturated 100 mL NH_4Cl and the aqueous layer was extracted with diethyl ether (3 x 100 mL). The combined organic layers were dried over MgSO_4 , filtered, and concentrated *in vacuo*. The remaining residue was purified on silica gel eluting with hexane:ethyl acetate (20:1) to afford light yellow solid (4.51 g, 53% yield). $R_f = 0.33$ (hexane: ethyl acetate 20:1).



4-(2-(methoxy(methyl)amino)-2-oxoethyl)phenyl trifluoromethanesulfonate (78): According to the known literature procedure,³⁶ to a dry and nitrogen-purged 30 mL round bottom flask was added a slurry of 2,2,2-trichloroethyl 2-(4-(((trifluoromethyl)sulfonyl)oxy)phenyl)acetate (**66**) (831.2 mg, 2.000 mmol, 1.000 equiv) and *N, O*-dimethylhydroxylamine hydrochloride (302.4 mg, 3.100 mmol, 1.550 equiv) in 4 mL of tetrahydrofuran. The reaction mixture was then cooled

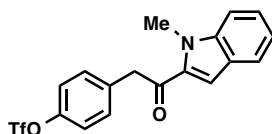
to -20 °C. A 2.0 M solution of isopropylmagnesium chloride solution in tetrahydrofuran (3 mL) was then added over 15 minutes while maintaining a reaction temperature below -5 °C by keeping the external temperature at -20 °C. The reaction mixture was then allowed to stir for an additional hour at -10 °C (reaction monitored by thin layer chromatography). Once complete, the reaction was quenched with saturated aqueous ammonium chloride. The product was then extracted using tetrahydrofuran and the organic solution was dried over sodium sulfate and concentrated. The crude residue was purified on silica eluting hexanes : ethyl acetate (5 : 1) increasing to hexanes : ethyl acetate (2 : 1) to afford the title compound **78** as a light brown oil (352.0 mg, 74% yield). $R_f = 0.36$ (hexane: ethyl acetate 2 : 1); $^1\text{H NMR}$ (400 MHz, CDCl_3) δ 7.37 (d, $J = 7.3$ Hz, 2H), 7.22 (d, $J = 7.3$ Hz, 2H), 3.79 (s, 2H), 3.66 (s, 3H), 3.20 (s, 3H); $^{13}\text{C NMR}$ (100 MHz, CDCl_3) δ 171.6, 148.6, 135.7, 131.4, 122.1, 121.4, 117.8, 115.7, 61.5, 38.5, 32.3; IR (film): 2941, 1666, 1502, 1419, 1249, 1208, 1137, 1019, 888; HRMS (p NSI) calcd for $\text{C}_{11}\text{H}_{13}\text{O}_5\text{NF}_3\text{S}$ (M+H) $^+$ 328.0461 found 328.0454.



4-(1-diazo-2-(methoxy(methyl)amino)-2-oxoethyl)phenyl trifluoromethanesulfonate (79):

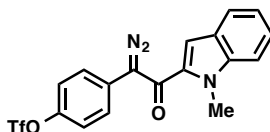
According to the known literature procedure,³⁴ to a dry and nitrogen-purged 5 mL round bottom flask was added 4-(2-(methoxy(methyl)amino)-2-oxoethyl)phenyl trifluoromethanesulfonate (**78**) (69.0 mg, 0.200 mmol, 1.00 equiv) and *p*-ABSA (72.1 mg, 0.301 mmol, 1.50 equiv) in dry acetonitrile (3 mL). The reaction mixture was cooled to 0 °C and 1,8-diazabicycloundec-7-ene (DBU, 0.045 mL, 0.301 mmol, 1.50 equiv) was slowly added. The reaction was then allowed to slowly warm to room temperature and stirred overnight. The reaction was then quenched with saturated aqueous ammonium chloride, extracted with diethyl ether, dried over magnesium

sulfate, filtered and concentrated. The crude residue was purified on silica eluting hexanes : ethyl acetate (10 : 1) to afford the title compound **79** as a yellow oil (56.0 mg, 76%). mp 36-39 °C; R_f = 0.23 in hexanes : ethyl acetate (10 : 1); ^1H NMR (400 MHz, CDCl_3) δ 7.55 (d, J = 9.0 Hz, 2H), 7.27 (d, J = 9.0 Hz, 2H), 3.71 (s, 3H), 3.28 (s, 3H); ^{13}C NMR (100 MHz, CDCl_3) δ 165.8, 147.5, 128.6, 126.9, 121.9, 120.6, 117.4, 61.4, 34.2; IR (film): 2945, 2076, 1624, 1501, 1423, 1362, 1207, 1134, 883, 846, 749; HRMS (p NSI) calcd for $\text{C}_{11}\text{H}_{11}\text{O}_5\text{N}_3\text{F}_3\text{S}$ ($\text{M}+\text{H}$) $^+$ 354.0366 found 354.0362.



4-(2-(1-methyl-1H-indol-2-yl)-2-oxoethyl)phenyl trifluoromethanesulfonate (86): According to the known literature procedure,³⁷ to a 50 mL dried and nitrogen-purged Schlenk flask equipped with a stir bar was added *N*-methylindole (**88**: 0.95 mL, 7.39 mmol, 15.30 equiv) and diethyl ether (14 mL). *n*-Butyllithium (1.6 M in hexanes, 4.84 mL, 7.75 mmol, 1.05 equiv) was then added dropwise over 10 minutes and an additional 3 mL diethyl ether was added. The solution was heated at reflux (40 °C) and monitored by TLC. After five hours, the reaction had gone to completion and was equilibrated to room temperature. To a separate 30 mL round bottom flask equipped with a stir bar was added 4-(2-(methoxy(methyl)amino)-2-oxoethyl)phenyl trifluoromethanesulfonate (**78**) (327.3 mg, 1.000 mmol, 1.000 equiv with respect to the 4.85 mL, 2.00 mmol, 2.00 equiv. of (1-methyl-1H-indol-2-yl)lithium) and diethyl ether (2 mL). The solution was cooled to 0 °C, then the contents of the Schlenk flask (5.34 mL, 0.3384 M in diethyl ether) were added over 5 minutes. It was stirred at 0 °C for one hour before quenching with saturated aqueous ammonium chloride (30 mL) and diluted with diethyl ether (30 mL). The organic layer was separated and washed with a saturated aqueous sodium chloride

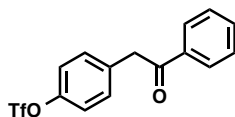
(30 mL). The reaction mixture was dried over magnesium sulfate, filtered and concentrated. The crude residue was purified on silica eluting hexanes : ethyl acetate (20 : 1) increasing to (10 : 1) to afford the title compound **86** as a white solid (163.1 mg, 41% yield). mp 88-91°C; R_f = 0.22 (hexane: ethyl acetate 10:1); ^1H NMR (400 MHz, CDCl_3) δ 7.71 (d, J = 8.4 Hz, 1H), 7.40 (s, 1H), 7.37 (m, 2H), 7.24 (m, 2H), 7.16 (m, 1H), 6.87 (d, J = 8.4 Hz, 2H), 4.19 (s, 2H), 4.04 (s, 3H), 3.77 (s, 3H); ^{13}C NMR (150 MHz, CDCl_3) δ 192.1, 158.8, 140.5, 134.6, 130.7, 127.3, 126.2, 126.0, 123.2, 121.0, 114.3, 112.2, 110.6, 55.5, 46.1, 32.4.; IR (film): 2947, 1660, 1501, 1418, 1209, 1137, 887, 752, 735; HRMS (p NSI) calcd for $\text{C}_{18}\text{H}_{15}\text{O}_4\text{NF}_3\text{S}$ ($\text{M}+\text{H}$) $^+$ 398.0668 found 398.0665.



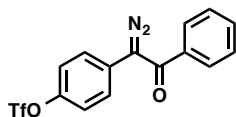
4-(1-diazo-2-(1-methyl-1H-indol-2-yl)-2-oxoethyl)phenyl trifluoromethanesulfonate (87):

According to the known literature procedure,³⁴ to a 5 mL dry and nitrogen-purged round bottom flask was added 4-(2-(1-methyl-1H-indol-2-yl)-2-oxoethyl)phenyl trifluoromethanesulfonate (**86**) (39.0 mg, 0.098 mmol, 1.00 equiv) and *p*-ABSA (35.3 mg, 0.147 mmol, 1.50 equiv) in 2 mL dry acetonitrile. The reaction mixture was then cooled to 0 °C and 1,8-diazabicycloundec-7-ene (DBU, 0.045 mL, 0.301 mmol, 1.50 equiv) was slowly added. The reaction was then allowed to slowly warm to room temperature and stirred overnight. The reaction was then quenched with saturated aqueous ammonium chloride, extracted with diethyl ether, dried over magnesium sulfate, filtered and concentrated. The crude residue was purified on silica eluting hexanes : ethyl acetate (10 : 1) to afford the title compound **87** as a light orange oil (22.0 mg, 62%) R_f = 0.22 in (hexanes : ethyl acetate 10 : 1); ^1H NMR (400 MHz, CDCl_3) δ 7.71-7.66 (m, 2H), 7.45-7.36 (m, 4H), 7.22-7.17 (m, 2H), 7.02 (s, 1H), 3.99 (s, 3H); ^{13}C NMR (150 MHz,

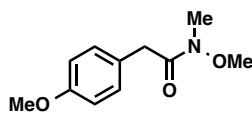
CDCl₃) δ 148.1, 139.6, 132.7, 130.5, 127.3, 125.8, 122.8, 122.3, 121.7, 121.5, 121.2, 120.4, 119.8, 110.5, 109.1; IR (film): 2925, 2077, 1614, 1501, 1425, 1286, 1213, 1140, 887, 741; HRMS (p NSI) calcd for C₁₈H₁₂O₄N₃F₃NaS (M+Na)⁺ 446.0393 found 446.0394.



4-(2-oxo-2-phenylethyl)phenyl trifluoromethanesulfonate (92): According to the known literature procedure,³⁸ to a dry and nitrogen-purged 30 mL round bottom flask was added a solution of 4-(2-(methoxy(methyl)amino)-2-oxoethyl)phenyl trifluoromethanesulfonate (**78**) (163.6 mg, 0.500 mmol, 1.000 equiv) in tetrahydrofuran (3.5 mL). The solution was cooled to 0 °C. Phenylmagnesium bromide (1.0 M in tetrahydrofuran, 0.60 mL, 0.597 mmol, 1.194 equiv) was then added dropwise to the reaction mixture. The reaction was slowly warmed to room temperature and monitored by thin layer chromatography. After allowing the reaction to stir for three hours, the reaction mixture was poured into 1 N HCl (aq.) and extracted with three portions of ethyl acetate. The combined organic layers were washed with saturated aqueous sodium bicarbonate followed by saturated aqueous sodium chloride. The organic layers were dried over magnesium sulfate and concentrated *in vacuo*. The crude residue was purified on silica eluting hexanes : ethyl acetate (10 : 1) to afford the title compound **92** as a white powder (69.0 mg, 40%). R_f = 0.24 in hexanes : ethyl acetate (10 : 1). R_f = 0.24 in 10 : 1 (hexanes : ethyl acetate) ¹H NMR (400 MHz, CDCl₃) δ 8.07 – 7.93 (m, 2H), 7.69 – 7.56 (m, 1H), 7.51 (t, J = 7.6 Hz, 2H), 7.36 (d, J = 9.0 Hz, 2H), 7.26 (d, J = 9.0 Hz, 2H), 4.34 (s, 2H). Data are consistent with the literature.³⁹

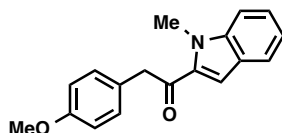


4-(1-diazo-2-oxo-2-phenylethyl)phenyl trifluoromethanesulfonate (93): According to the known literature procedure,³⁴ to a dry and nitrogen-purged 5 mL round bottom flask was added 4-(2-oxo-2-phenylethyl)phenyl trifluoromethanesulfonate (**92**) (69.0 mg, 0.200 mmol, 1.00 equiv) and *p*-ABSA (72.1 mg, 0.301 mmol, 1.50 equiv) in dry acetonitrile (3 mL). The reaction mixture was cooled to 0 °C and 1,8-diazabicycloundec-7-ene (DBU, 0.045 mL, 0.301 mmol, 1.50 equiv) was slowly added. The reaction was then allowed to slowly warm to room temperature and stirred overnight. The reaction was then quenched with saturated aqueous ammonium chloride, extracted with diethyl ether, dried over magnesium sulfate, filtered and concentrated. The crude residue was purified on silica eluting hexanes : ethyl acetate (10 : 1) to afford the title compound **93** as a yellow oil (56.0 mg, 76%) $R_f = 0.23$ in hexanes : ethyl acetate (10 : 1); ¹H NMR (400 MHz, CDCl₃) δ 7.91 (ddd, $J = 7.4, 3.2, 1.7$ Hz, 1H), 7.65 (d, $J = 9.0$ Hz, 2H), 7.60 - 7.52 (m, 1H), 7.51 - 7.39 (m, 2H), 7.35 (d, $J = 9.0$ Hz, 2H), 7.26 - 7.19 (m, 1H); ¹³C NMR (100 MHz, CDCl₃) δ 150.1, 148.0, 137.7, 132.3, 131.0, 130.8, 130.5, 129.0, 127.8, 127.2, 122.2; IR (film): 3050, 2081, 1742, 1627, 1501, 1424, 1250, 1210, 1138, 886; HRMS (p NSI) calcd for C₁₅H₉F₃LiN₂O₄S (M+Li)⁺ 377.0395 found 377.1190.



***N*-methoxy-2-(4-methoxyphenyl)-*N*-methylacetamide (95):** According to the known literature procedure,³⁶ to a dry and nitrogen-purged 100 mL round bottom flask was added a slurry of 2,2,2-trichloroethyl 2-(4-methoxyphenyl)acetate (**54**) (2.9756 g, 10.000 mmol, 1.000 equiv) and *N*, *O*-dimethylhydroxylamine hydrochloride (1.5119 g, 15.500 mmol, 1.550 equiv) in 20 mL of

tetrahydrofuran. The reaction mixture was then cooled to -20 °C. A 2.0 M solution of isopropylmagnesium chloride solution in tetrahydrofuran (15 mL) was then added over 15 minutes while maintaining a reaction temperature below -5 °C by keeping the external temperature at -20 °C. The reaction mixture was then allowed to stir for an additional hour at -10 °C (reaction monitored by thin layer chromatography). Once complete, the reaction was quenched with saturated aqueous ammonium chloride. The product was then extracted using diethyl ether and the organic solution was dried over sodium sulfate and concentrated. The crude residue was purified on silica eluting hexanes : ethyl acetate (2 : 1) increasing to hexanes : ethyl acetate (1 : 1) to afford the title compound **95** as a clear oil (2.0925 mg, 51% yield). $R_f = 0.23$ (hexane: ethyl acetate 2 : 1); $^1\text{H NMR}$ (600 MHz, CDCl_3) δ 7.20 (d, $J = 8.6$ Hz, 2H), 6.84 (d, $J = 8.6$ Hz, 2H), 3.78 (s, 3H), 3.70 (s, 2H), 3.60 (s, 3H), 3.18 (s, 3H); $^{13}\text{C NMR}$ (150 MHz, CDCl_3) δ 158.6, 130.5, 127.1, 118.3, 114.1, 100.1, 77.5, 77.2, 77.0, 61.5, 55.4, 38.6; IR (film): 2937, 2836, 1659, 1512, 1442, 1246, 1177, 1033, 1004, 789; HRMS (p NSI) calcd for $\text{C}_{11}\text{H}_{16}\text{O}_3\text{N}$ ($\text{M}+\text{H}$) $^+$ 210.1125 found 210.1122.



2-(4-methoxyphenyl)-1-(1-methyl-1H-indol-2-yl)ethan-1-one (96): According to the known literature procedure,³⁷ to a 50 mL dried and nitrogen-purged Schlenk flask equipped with a stir bar was added *N*-methylindole (**88**: 0.95 mL, 7.39 mmol, 15.30 equiv) and diethyl ether (14 mL). *n*-Butyllithium (1.6 M in hexanes, 4.84 mL, 7.75 mmol, 1.05 equiv) was then added dropwise over 10 minutes and an additional 3 mL diethyl ether was added. The solution was heated at reflux (40 °C) and monitored by TLC. After five hours, the reaction had gone to completion and was equilibrated to room temperature. To a separate 30 mL round bottom flask equipped with a

stir bar was added *N*-methoxy-2-(4-methoxyphenyl)-*N*-methylacetamide (**84**) (991.0 mg, 4.740 mmol, 1.000 equiv with respect to the 27.90 mL, 9.47 mmol, 2.00 equiv. of (1-methyl-1*H*-indol-2-yl)lithium) and diethyl ether (1 mL). The solution was cooled to 0 °C, then the contents of the Schlenk flask (27.90 mL, 0.3384 M in diethyl ether) were added over 5 minutes. It was stirred at 0 °C for one hour before quenching with saturated aqueous ammonium chloride (20 mL) and diluted with diethyl ether (20 mL). The organic layer was separated and washed with a saturated aqueous sodium chloride (20 mL). The reaction mixture was dried over magnesium sulfate, filtered and concentrated. The crude residue was purified on silica eluting hexanes : ethyl acetate (15 : 1) increasing to (10 : 1) to afford the title compound **96** as a white solid (286.6 mg, 22% yield). mp 101-104°C; R_f = 0.29 (hexane: ethyl acetate 20:1); $^1\text{H NMR}$ (600 MHz, CDCl_3) δ 7.70 (d, J = 8.1 Hz, 1H), 7.40 (s, 6H), 7.37 (d, J = 11.7 Hz, 0H), 7.24 (d, J = 8.9 Hz, 3H), 7.15 (ddd, J = 8.0, 5.2, 2.7 Hz, 1H), 6.87 (d, J = 8.7 Hz, 2H), 4.19 (s, 3H), 4.05 (s, 8H), 3.78 (s, 3H); $^{13}\text{C NMR}$ (150 MHz, CDCl_3) δ 192.1, 158.8, 140.5, 134.7, 130.7, 127.3, 126.2, 126.0, 123.2, 121.0, 114.3, 112.2, 110.6, 55.5, 46.1, 32.4; IR (film): 2936, 1665, 1510, 1462, 1388, 1301, 1177, 1161, 1027, 991, 812, 778, 763, 735; HRMS (p NSI) calcd for $\text{C}_{18}\text{H}_{18}\text{O}_2\text{N}$ ($\text{M}+\text{H}$) $^+$ 280.1332 found 280.1328.

References:

1. Warabi, K.; Matsunaga, S.; van Soest, R. W. M.; Fusetani, N. *J. Org. Chem.* **2003**, *68*, 2765.
2. Parkinson, E. K. *Ann. Med.* **2003**, *35*, 466.
3. Zhang, H.; Conte, M. M.; Khalil, Z.; Huang, X.-C.; Capon, R. J. *RSC Adv.* **2012**, *2*, 4209.
4. Ayats, C.; Soley, R.; Albericio, F.; Alvarez, M. *Org. Biomol. Chem.* **2009**, *7*, 860.
5. (a) Fürstner, A.; Domostoj, M. M.; Scheiper, B. *J. Am. Chem. Soc.* **2005**, *127*, 11620;
(b) Fürstner, A.; Domostoj, M. M.; Scheiper, B. *J. Am. Chem. Soc.* **2006**, *128*, 8087;
(c) Buchgraber, P.; Domostoj, M. M.; Scheiper, B.; Wirtz, C.; Mynott, R.; Rust, J.; Fuerstner, A. *Tetrahedron* **2009**, *65*, 6519.
6. (a) Hirao, S.; Yoshinaga, Y.; Iwao, M.; Ishibashi, F. *Tetrahedron Lett.* **2010**, *51*, 533;
(b) Hirao, S.; Sugiyama, Y.; Iwao, M.; Ishibashi, F. *Biosci., Biotechnol., Biochem.* **2009**, *73*,

1764.

7. (a) Okano, K.; Fujiwara, H.; Noji, T.; Fukuyama, T.; Tokuyama, H. *Angew. Chem., Int. Ed.* **2010**, *49*, 5925; (b) Tokuyama, H.; Okano, K.; Fujiwara, H.; Noji, T.; Fukuyama, T. *Chem. - Asian J.* **2011**, *6*, 560.
8. (a) Liang, J.; Hu, W.; Tao, P.; Jia, Y. *J. Org. Chem.* **2013**, *78*, 5810; (b) Tao, P.; Liang, J.; Jia, Y. *Eur. J. Org. Chem.* **2014**, *26*, 5735.
9. Yamaguchi, A. D.; Chepiga, K. M.; Yamaguchi, J.; Itami, K.; Davies, H. M. L. *J. Am. Chem. Soc.* **2015**, *137*, 644.
10. Davies, H. M. L.; Hedley, S. J. *Chem. Soc. Rev.* **2007**, *36*, 1109.
11. (a) Maryanoff, B. E. *J. Org. Chem.* **1979**, *44*, 4410; (b) Maryanoff, B. E. *J. Heterocycl. Chem.* **1977**, *14*, 177.
12. Maryanoff, B. E. *J. Org. Chem.* **1982**, *47*, 3000.
13. (a) Davies, H. M. L.; Saikali, E.; Young, W. B. *J. Org. Chem.* **1991**, *56*, 5696; (b) Davies, H. M. L.; Matasi, J. J.; Hodges, L. M.; Huby, N. J. S.; Thornley, C.; Kong, N.; Houser, J. H. *J. Org. Chem.* **1997**, *62*, 1095; (c) Reddy, R. P.; Davies, H. M. L. *J. Am. Chem. Soc.* **2007**, *129*, 10312.
14. Lian, Y.; Davies, H. M. L. *Org. Lett.* **2010**, *12*, 924.
15. Hedley, S. J.; Ventura, D. L.; Dominiak, P. M.; Nygren, C. L.; Davies, H. M. L. *J. Org. Chem.* **2006**, *71*, 5349.
16. Peschko, C.; Steglich, W. *Tetrahedron Lett.* **2000**, *41*, 9477.
17. Davies, H. M. L.; Hansen, T.; Hopper, D. W.; Panaro, S. A. *J. Am. Chem. Soc.* **1999**, *121*, 6509.
18. (a) Yanagisawa, S.; Sudo, T.; Noyori, R.; Itami, K. *J. Am. Chem. Soc.* **2006**, *128*, 11748; (b) Yanagisawa, S.; Sudo, T.; Noyori, R.; Itami, K. *Tetrahedron* **2008**, *64*, 6073.
19. Ueda, K.; Yanagisawa, S.; Yamaguchi, J.; Itami, K. *Angew. Chem., Int. Ed.* **2010**, *49*, 8946.
20. Yanagisawa, S.; Ueda, K.; Sekizawa, H.; Itami, K. *J. Am. Chem. Soc.* **2009**, *131*, 14622.
21. Kirchberg, S.; Tani, S.; Ueda, K.; Yamaguchi, J.; Studer, A.; Itami, K. *Angew. Chem., Int. Ed.* **2011**, *50*, 2387.
22. (a) Liegault, B.; Lapointe, D.; Caron, L.; Vlassova, A.; Fagnou, K. *J. Org. Chem.* **2009**, *74*, 1826; (b) Roger, J.; Doucet, H. *Adv. Synth. Catal.* **2009**, *351*, 1977; (c) Gryko, D. T.; Vakuliuk, O.; Gryko, D.; Koszarna, B. *J. Org. Chem.* **2009**, *74*, 9517; (d) Rene, O.; Fagnou, K. *Adv. Synth. Catal.* **2010**, *352*, 2116; (e) Jafarpour, F.; Rahiminejadan, S.; Hazrati, H. *J. Org. Chem.* **2010**, *75*, 3109; (f) Nadres, E. T.; Lazareva, A.; Daugulis, O. *J. Org. Chem.* **2011**, *76*, 471.
23. Yanagisawa, S.; Sudo, T.; Noyori, R.; Itami, K. *J. Am. Chem. Soc.* **2006**, *128*, 11748.
24. Ueda, K.; Amaiike, K.; Maceiczky, R. M.; Itami, K.; Yamaguchi, J. *J. Am. Chem. Soc.* **2014**, *136*, 13226.
25. Guptill, D. M.; Davies, H. M. L. *J. Am. Chem. Soc.* **2014**, *136*, 17718.
26. Reddy, R. P.; Davies, H. M. L. *Org. Lett.* **2006**, *8*, 5013.
27. Brodsky, B. H.; Du Bois, J. *Org. Lett.* **2004**, *6*, 2619.
28. Axford, L. C.; Holden, K. E.; Hasse, K.; Banwell, M. G.; Steglich, W.; Wagler, J.; Willis, A. *C. Aust. J. Chem.* **2008**, *61*, 80.
29. Zhu, M.; Jalalian, N.; Olofsson, B. *Synlett* **2008**, *4*, 592.
30. Van Leeuwen, P. W. N. M.; Roobeek, C. F. *Tetrahedron* **1981**, *37*, 1973.
31. Qin, C.; Boyarskikh, V.; Hansen, J. H.; Hardcastle, K. I.; Musaev, D. G.; Davies, H. M. L. *J. Am. Chem. Soc.* **2011**, *133*, 19198.

32. Watanabe, N.; Ogawa, T.; Ohtake, Y.; Ikegami, S.; Hashimoto, S.-i. *Synlett* **1996**, *1*, 85.
33. Yamawaki, M.; Tanaka, M.; Abe, T.; Anada, M.; Hashimoto, S. *Heterocycles* **2007**, *72*, 709.
34. Davies, H. M. L.; Hansen, T.; Churchill, M. R. *J. Am. Chem. Soc.* **2000**, *122*, 3063.
35. (a) Goldsmith, D. *o-Nitrobenzenesulfonyl Azide, e-EROS*, **2001**; (b) Brodsky, B. H.; Du Bois, J. *Org. Lett.* **2004**, *6*, 2619.
36. Williams, J. M.; Jobson, R. B.; Yasuda, N.; Marchesini, G.; Dolling, U.-H. *Tetrahedron Lett.* **1995**, *36*, 5461.
37. Marcus, A. P.; Lee, A. S.; Davis, R. L.; Tantillo, D. J.; Sarpong, R. *Angew. Chem., Int. Ed.* **2008**, *47*, 6379.
38. Jones, D. G.; Liang, X.; Stewart, E. L.; Noe, R. A.; Kallander, L. S.; Madauss, K. P.; Williams, S. P.; Thompson, S. K.; Gray, D. W.; Hoekstra, W. J. *Bioorg. Med. Chem. Lett.* **2005**, *15*, 3203.
39. Giles, D. P.; Willis, R. J. *Pyrazoline insecticides*. Patent Application EP113213A2, **1984**.